# Visual perception and attention and their neurochemical and microstructural brain correlates in healthy and pathological ageing


A thesis submitted for the degree of Doctor of Philosophy

School of Psychology, Cardiff University

October 2021

Lauren Revie

**Word count: 76,738**

# Thesis summary

Visual perception and attention declines with normal ageing, however their neural and cognitive mechanisms in healthy and pathological ageing are yet to be fully understood. This thesis aimed to provide a characterisation of normal age-related differences across the visual perception and attention hierarchy, identify their underlying neural correlates, and assess how normal ageing contrasts with pathological ageing in Dementia with Lewy bodies (DLB).

**Chapter 1** introduces the perception and attention hierarchy, and its related brain structures in ageing. **Chapter 2** outlines applications of quantitative macro- and microstructural MRI and MR Spectroscopy used in this thesis. **Chapter 3** investigated visual perceptual and attentional performance in younger and older adults, and DLB patients. Results showed some impairment in lower and mid-level visual tasks and greater speed-accuracy trade-off (SAT) in higher-level tasks in older adults. DLB patients showed impairments in most tasks from mid-level, and varied response times (RT). **Chapter 4** characterised brain differences using multi-modal MRI in young, old and DLB patients. Older adults showed reductions in: general cortical thickness, microstructural integrity in the fornix, optic radiations and superior longitudinal fasciculus (SLF), and metabolite concentrations in the anterior cingulate cortex (ACC) and posterior parietal cortex (PPC). DLB patients showed elevated PPC metabolites. **Chapter 5** revealed that these brain differences predicted age-related compensation and a shift to longer SATs. **Chapter 6** investigated older adults' RT slowing using a drift diffusion model and assessed related brain differences. Findings showed age-related deficits in sensory accumulation, predicted by lower SLF and ILF microstructure and metabolic differences in the ACC. Finally, **Chapter 7** applied this model to DLB patients. Results showed impaired lower-level perception, which was related to visual hallucinations. These results provide a characterisation of the neural substrates underlying perceptual performance in both older adults, and how these findings may be applied to investigate pathological ageing.

# Acknowledgements

I would like to acknowledge the unwavering support I have received from the following people, without whom this body of work would never have been possible:

To my family - for supporting my curiosity and feeding my enthusiasm.

To my friends - you have been there from the very beginning and have always kept me grounded and listened when I needed you. Thank you for always lending a helping hand, letting me think out loud, and keeping me smiling when things weren't going to plan.

To Claudia – my thanks for your supervision, patience and expertise. Thank you for taking a chance on me. Without your help this project would never have come to fruition, and I am truly grateful.

To Ben - your understanding, support and interest has been so valuable to me. Thank you for never letting me give up.

To all those providing academic support and guidance – my thanks go to Prof Tony Bayer, Dr Liz Coulthard and Dr Amrita Varanasi for help with patient recruitment and clinical support. My thanks also extend to Dr Christoph Teufel for his useful discussions concerning visual perception, Dr Chris Jenkins, Dr John Evans and Dr Mohamed Tachrount for their MRS guidance, and Allison Cooper and Peter Hobden for their patience and training in data acquisition. Special thanks also go to Dr George Lovell at Abertay University for help in developing the contour integration task and psychophysics advice, and to Dr Craig Hedge for help with drift diffusion modelling and kind provision of custom scripts. Thanks also go to Prof Alan Thomas, Dr Paul Donaghy, Dr Joanna Ciafone and Dr Calum Hamilton at Newcastle University for kindly sharing LewyPro patient data and contributing to its eventual publication.

To all patients and their families, and all participants – my thanks go to you for your time, energy and often determination and resilience during testing. This would not be possible without your generosity and devotion to the cause. It is my hope that this work can contribute to our ever-growing understanding of the dementia syndrome.

I would finally like to acknowledge my incredible fortune to have been provided the opportunity to work towards this PhD thesis. I see this as a privilege - one which has been denied to so many women and girls.

With that, this thesis is wholly dedicated to my wonderful grandmother, Rita – the strongest woman I ever knew.

# Preface

The structure across parts of Chapter 1 is in line with a literature review in pre-print:

**Revie, L.**, Bayer, A., Teufel, C., & Metzler-Baddeley, C. (2019, December 19). A review of the perceptual and attentional-executive characteristics of dementia with Lewy bodies relative to Alzheimer's and Parkinson's disease.

The results of Chapter 7 are available as a published article:

**Revie, L.**, Hamilton, C. A., Ciafone, J., Donaghy, P. C., Thomas, A., & Metzler-Baddeley, C. (2020). Visuo-Perceptual and Decision-Making Contributions to Visual Hallucinations in Mild Cognitive Impairment in Lewy Body Disease: Insights from a Drift Diffusion Analysis. *Brain Sciences*, *10*(8), 540.

The results of Chapter 6 were presented as a poster at the *Organisation for Human Brain Mapping International conference (OHBM, June 2020),* and are in the process of being compiled into a manuscript for publication.

# Table of contents

# List of Figures

# List of Tables

# List of Abbreviations

ACC – anterior cingulate cortex
AD – Alzheimer's disease
ANT – attention network test
BOLD – blood oxygen level dependent
CHARMED – composite hindered and restricted model of diffusion
CSF – corticospinal fluid
DDM – drift diffusion model
DLB – dementia with Lewy bodies
DLPFC – dorsolateral prefrontal cortex
DWI – diffusion weighted imaging
FA – fractional anisotropy
GABA – gamma amino-butyric acid
GM – grey matter
fMRI – functional magnetic resonance imaging
ILF – inferior longitudinal fasciculus
FR – restricted fraction
L1 – axial diffusivity
LGN - lateral geniculate nucleus
MCI – mild cognitive impairment
MD – mean diffusivity
MEGA-PRESS – Meschler-Garwood Point-Resolved Spectroscopy Sequence
MOCA – Montreal cognitive assessment
MRI – magnetic resonance imaging
MRS – magnetic resonance spectroscopy
NAA – N-acetyl aspartate
OCC – occipital cortex
PD – Parkinson's disease
PDD – Parkinson's disease dementia
PFC – prefrontal cortex
PPC – posterior parietal cortex
PPM – parts per million
RBD – REM sleep behaviour disorder
RD – radial diffusivity
REM – rapid eye movement sleep
ROI – region of interest
RF – radio frequency
RT – reaction time
SAT – speed-accuracy trade-off
SLF – superior longitudinal fasciculus
V1 – primary visual cortex
V2 – secondary visual cortex
V3 – tertiary visual cortex
V4 – visual cortex 4
V5 – visual cortex 5
WAIS – Weschler adult intelligence scale
WMH – white matter hyperintensities

# Chapter 1 : General introduction

## 1.1 Ageing

Advances in medical care and modern lifestyle changes mean that people are currently living longer than any period in history, resulting in an ageing global population. According to the Office for National Statistics it is predicted that by 2066 the number of UK residents over the age of 65 will rise to 20.4 million – which is 26% of the total population (Coates, Tanna & Scott-Allen, 2019).

With population ageing comes the increasing need to understand more about physical, mental and social changes that impact the growing proportion of older adults. It is particularly important that cognitive and neural changes in normal ageing are understood, as they can have a sizeable effect on an older adult's day-to-day functioning. Effective cognition is crucial for independence particularly as people get older, as impaired or altered cognition will impact the ability to live independently, drive and take medications effectively (Murman, 2015). A more comprehensive understanding of these changes is also imperative as they can develop into more serious age-related and pathological cognitive decline. Effectively understanding cognitive systems and how they are altered with normal ageing provides a basis from which we can more readily identify non-normal cognitive changes.

### 1.1.1 Normal cognitive ageing

Normal ageing in the literature typically refers to ageing in the absence of disease, with research generally focusing on populations above the age of retirement (60-65 years) as this is considered to be the beginning of 'old age' (Amarya et al., 2018). Normal ageing encompasses a variety of changes in physiology such as stiffening of arteries and bone shrinkage, but also important changes in memory and cognition such as slowing of response time and difficulty with multitasking (Amarya et al., 2018).

Cognitive ageing refers to the changes in cognitive processing that occur as people get older (Harada et al., 2013). It is well established that with healthy ageing many physiological changes in the brain occur, which can impact some aspects of cognitive function – in particular some perceptual processes, working memory, attention and speed of processing are vulnerable to decline with age (Joubert & Chainay, 2018; Roberts & Allen, 2016; Verhaeghen & Basak, 2005). However in normal cognitive ageing these changes are not severe enough to interfere significantly with daily life (Joubert & Chainay, 2018).

In the ageing literature, cognitive processes that change with age are often referred to as fluid abilities and those which remain stable are often referred to as crystallized abilities (Baltes et al., 1980). Fluid abilities require manipulation and transformation of information, requiring attention and speed of processing, which is seen to steadily decline from age 20 to age 80 (Murman, 2015). In contrast crystallized abilities which

require acquired knowledge, such as reading comprehension or vocabulary, actually improve until age 60 after which a plateau is reached (Salthouse, 2010).

Some aspects of memory are maintained with normal ageing, such as immediate memory, but tasks requiring the manipulation of information or short-term storage in working memory and source memories are often impaired (Murman, 2015). This is also reflected in age-related impairments on episodic memory tasks which require more free recall in comparison to, for instance, recognition tasks requiring a forced choice response that relies less on episodic retrieval (Nyberg & Pudas, 2019).

Memory impairments in ageing have been extensively studied in the context of pathological ageing (Bishop et al., 2010) and the neural correlates of these impairments have been well established. In contrast perceptual abilities, attention and processing speed in healthy ageing have typically received less attention, although they may provide an equally valuable insight into cognitive changes that occur with pathological ageing (Murman, 2015). Changes in some visual perceptual functions are considered to be markers for discriminating normal from pathological ageing (Risacher & Saykin, 2013) and have even been highlighted as targets for interventions which can slow cognitive decline (Lin et al., 2016). Moreover, it is important to understand perceptual changes in ageing as this affects everyday functions such as driving (Wagner & Nef, 2011), balance and gait (Osoba et al., 2019) and the incidence of falls (Saftari & Kwon, 2018).

In light of this, I discuss evidence from the domains of perception, attention and processing speed in normal ageing in the current chapter. I will also discuss how investigating these domains may aid the understanding of pathological ageing. More specifically, I will highlight perceptual changes that occur in older adults at different stages of the visual processing system as well as how attention and processing speed are altered in older age.

## 1.2 Cognition in older adults

### 1.2.1 Perception

Perception is the individual interpretation and awareness of information via our fundamental senses. It refers to both the unconscious receiving of these signals and information, and the shaping of this information via prior knowledge, memory and experience. Perception consists of specific functions which can be attributed to different stages in the hierarchically structured human visual system. Within this, specific cortical regions are specialised in order to process elements of a visual object, from simple or basic processing to more complex functions (Hubel & Wiesel, 1962) (see Figure 1.1).

Neurons in different cortical areas are 'tuned to' different types of features, increasing in complexity as information is passed along the hierarchy. Neurons in primary visual cortex (V1) mainly process oriented edges with information then progressing to V2 which processes lines, angles and contour, V3 which is

associated with segregation of foreground from background features, V4 which is associated with shape processing, and V5/MT which is concerned largely with the processing of motion (Allman et al., 1985) (Figure 1.1). Considering these stages, visual perceptual processing can be grouped into three more general categories: low-level vision associated with simple features, mid-level vision that integrates simple feature processing into more complex functions and high-level vision, which is largely concerned with whole object processing. It has been proposed that each region of the cortical visual pathway is specialised to process different visual information and is organized hierarchically, with information being processed serially from simple to complex features (Maunsell & van Essen, 1983). That is, following light information being transduced by photoreceptors in the retina, information travels via the optic nerve - which is comprised of retinal ganglion cell axons - to the lateral geniculate nucleus (LGN) of the thalamus. Information is then transmitted to the primary visual cortex (V1) where ascending visual information is sent to one of two extra-striate pathways (Erskine et al., 2019). In V1, neurons code simple stimulus features such as orientation, with information requiring more complex feature-processing occurring in the extra-striate cortices, i.e., V2 processes information consisting of lines, stripes and contours, V3 information for segregating foreground from background features, V4 for shape processing, and V5/MT processes motion features (Figure 1.1). More broadly, the visual system is thought to be organized into two processing pathways, a ventral stream for object vision/recognition ("what" pathway) and a dorsal stream for spatial vision ("where" pathway) (Mishkin & Ungerleider, 1982). The ventral stream includes regions in the temporal cortex and lateral occipital areas while the dorsal stream includes areas of the parietal and frontal cortices (Mishkin, Ungerleider & Macko, 1983). More recent research has suggested that basic object information may be represented in a similar manner in both pathways but that higher-order information may be processed more selectively by each stream (Konen & Kastner, 2008; Figure 1.1).

Perceptual processing is also related to individual expectations and mechanisms of attention, which ultimately influence the final percept. Within visual perception, the concept of different streams of information processing posits that perception is a product of the interaction between bottom-up and top-down processing. Bottom-up processing refers to basic sensory information that is processed automatically, whereas top-down processing refers to more complex higher order cognitive functions related to our knowledge of the world as well as expectations and goals that control the allocation of attention and hence shape our perception. Although top-down processing was initially thought to be a modulatory process influencing the allocation of attention, it is now thought to interact with bottom-up information in order to 'optimise' processing using higher level object representations to shape the percept (Teufel et al., 2015). Thus, although the visual system may be referred to as hierarchically structured in some instances, visual processing does not occur in a truly 'hierarchical' manner as feedforward and feedback systems between lower and higher processing act to support mutual processes. Recent non-human primate research has also investigated this further, suggesting that low-level visual information can also be decoded at mid-to-higher level cortical areas depending on feature processing (Lu et al., 2018). Considering this, this thesis aims to

assess not only performance at each visual 'level' but also assess neural functioning related to this performance to assess changes in recruited mechanism that may arise as a result of healthy or pathological ageing. Furthermore, I assessed vision alongside attentional functions and response times in order to investigate how the structure of the visual network may alter in healthy ageing and DLB. As such, this will be considered in the interpretation of the results reported in this thesis, as assumptions cannot be made that impaired visual processing at one level will impact processes 'up stream' and vice versa.

In the following section, evidence regarding age-related changes in low, mid and higher-level perception and attention functions will be discussed. Most notably, ageing appears to affect mid-level processing stages while sparing lower-level functioning as supported by work in aged non-human primates (Liang et al., 2012).

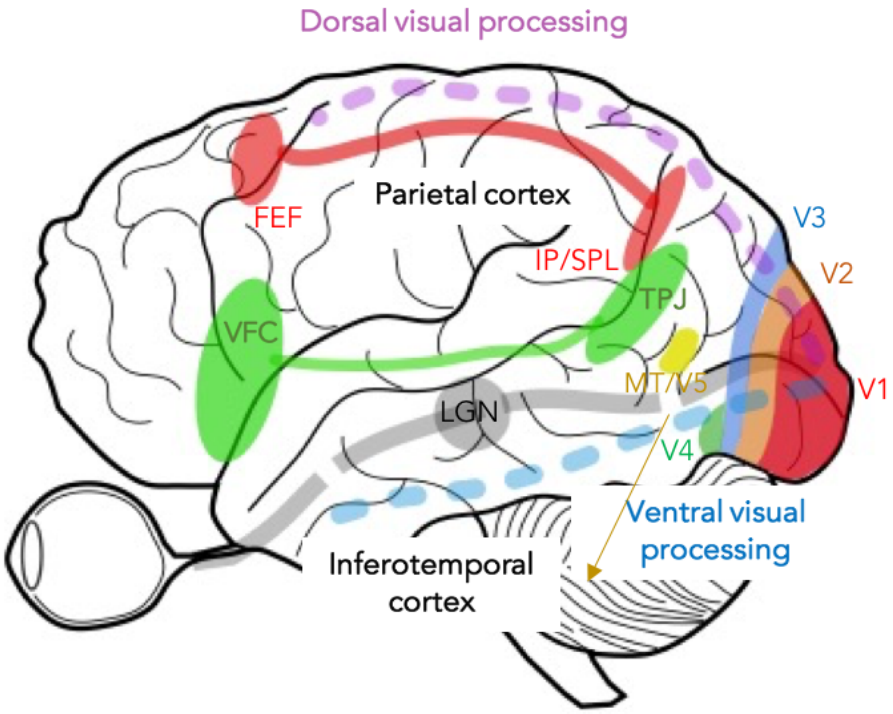


Figure 1.1 Visual cortices and dorsal and ventral processing pathways within the cortex. IP/SPL = intraparietal/ superior parietal lobule, FEF = frontal eye fields, TPJ = temporoparietal junction, VFC = ventral frontal cortex, LGN = lateral geniculate nucleus. V1 = primary visual cortex, V2 = secondary cortex, V3 = tertiary visual cortex, V4= visual cortex 4, and MT/V5 = motor cortex, visual cortex 5.

#### 1.2.1.1 Low-level vision in older adults

Characterising normal vision in older adults is challenging as ageing is often associated with eye conditions such as glaucoma or cataract, which can go undiagnosed (McGwin et al., 2010). In addition, optical problems associated with age such as decreased retinal illumination may impact low-level perceptual functions (Billino & Pilz, 2019). However accumulating evidence suggests there are also perceptual changes occurring at multiple levels of the visual system that are distinct from retinal changes or eye disease (Andersen, 2012). Furthermore, these perceptual changes cannot always be explained in terms of systemic

changes in brain functions, such as the generalized slowing hypothesis described later in this chapter (Birren, 1974).

Low-level vision refers to early visual processing stages, including visual acuity, but also early cortical processing of simple visual features such as orienting ability. With regards to lower-level visual functions the ageing literature remains relatively conflicting. Some older adults show impairments in contrast sensitivity in comparison to younger adults at certain spatial frequencies (Elliott et al., 1990). However, it has been proposed that this may be largely due to changes in optical factors as opposed to changes in cortical visual processing (Owsley, 2011). For example, it has been shown that functions such as orientation discrimination remain constant despite age with older adults requiring adjustment of stimuli to account for optic changes in contrast (Delahunt et al., 2008; Govenlock et al., 2009).

Some research suggests that age-related differences in orientation discrimination cannot be explained by a reduction in retinal illumination in older age alone. For example, it has been shown that older relative to younger adults showed poorer sensitivity to the orientation of Gabor patches in noise while retinal illumination was held constant (Betts et al., 2007). Gabor patches are grating stimuli consisting of white and black bars that allow the controlled manipulation of orientation, contrast and scaling features to study early visual processing activity. Previous studies have shown an age-dependent impairment in orientation discrimination of stimuli embedded in external noise, (Casco et al., 2017), which has been attributed to reduced visual cortical inhibition (Smith & Ratcliff, 2004). In addition, signal amplitude in the visual cortex was found lower for older than younger adults, suggesting an age-related decline of activation in these regions during early stages of perceptual processing (Madden, Whiting & Huettel, 2004). However, this does not necessarily impact lower-level functions, but instead may affect functions further 'upstream' in cortical processing. Moreover, animal models have demonstrated a reduction in orientation tuning in cells within the primary visual cortex in ageing monkeys (Leventhal et al., 2003). However, when GABA – the brain's major inhibitory neurotransmitter – was applied to these cells, orientation tuning was restored. This indicates a primary lower-level deficit in perceptual functioning in ageing and suggests that neurochemical mechanisms may be directly related to orientation impairment in ageing. Conversely, antagonistic blocking of GABA has been showing to interrupt orientation tuning (Wolf et al., 1986)

#### 1.2.1.2 Mid-level vision in older adults

Mid-level visual perceptual functions are lesser studied and more challenging to define. There is some controversy around what constitutes mid-level visual processing (Peirce, 2015). Mid-level vision may include the processing of visual regions which are not included in the primary visual cortex but are prior processing stages to the dorsal and ventral systems. This would be V3 and V4 for form or contour integration and colour processing, and V5 for motion (Li et al., 2002).

A number of studies have focused on motion processing impairments in older adults, in which reduced sensitivity to motion and reduced ability in identifying motion direction have been reported (Snowden & Kavanagh, 2006). Most notably, motion perception changes with age appear to be specific to certain patterns of motion information (Billino et al., 2008) which are not accounted for by changes in retinal illumination. For example, whilst older adults have poorer performance in speed detection of motion, some studies have reported no ageing effects in horizontal planar motion coherence (Kavcic et al., 2011). In addition, mechanisms of reduced inhibition in the visual cortex have also been reported to reduce surround-motion performance (Betts et al., 2005) again suggesting possible age-related reductions in mid-level visual functioning.

With regards to other mid-level visual changes, contour integration is often assessed which involves linking elements in order to perceive a complete contour and relies on functions from low level orienting and contrast perception to more complex mid-level functions requiring integration of shapes (Field et al., 1993). Contour integration can be assessed using Gabor task 'snake' stimuli which requires the ability to perceive a circular outline by integrating the orientation aligned Gabor patches into one shape, in which older adults show significant impairment (Roudaia et al., 2008). Moreover, age-related declines in spatial integration when observing moving contours have been observed (Andersen, 2012; Andersen & Ni, 2008) indicating an age-related decline in contour integration abilities. Finally, colour perception has also been reported to decline with age. The ability to discriminate colour hue also declines from around age 20 into old age, however these changes have also been attributed to changes in retinal illuminance rather than cortical processing (Werner, Schefrin & Bradley, 2010).

#### 1.2.1.3 Higher-level vision in older adults

High-level visual processing concerns the representation of objects, faces and scenes amongst others. Higher-level processing requires the interaction with attentional networks in the brain, but also interaction with basic 'bottom-up' sensory information to effectively shape and process stimuli. Second order visual stimuli – those thought to require the involvement of multiple detection mechanisms in the visual cortex – are more severely affected by ageing than simple stimuli requiring only basic sensory processes (Dagnelie, 2013).

Some evidence indicates that older adults may show a decline in higher-level visual processing in comparison to younger adults, such as diminished object perception (Goh et al., 2007), pattern separation (Toner et al., 2009), shape perception and discrimination, whilst the ability to judge depth does not decline with age (Norman et al., 2004). Despite this, visual search task accuracy performance was reported to be relatively stable with age (Madden, 2007) aside from age-related slowing. As visual search has been shown to be based on prior expectations (Berggren & Eimer, 2019) this suggests that this aspect of top-down processing can be spared in older adults. This in turn may suggest that bottom-up aspects of processing

contribute to some of the age-related slowing or inaccuracy in higher-level visual tasks such as the ones mentioned above.

An alternative view proposes that these higher level visual task impairments in older adults reflect a switch in the neural strategies which are recruited to complete these processes between older and younger adults (Grady, 2000). For instance, reduced functional magnetic resonance imaging (fMRI) activation of the ventral pathway during age-related slowing in performance on an object processing task was reported in older compared with younger adults (Grady et al., 1994, as cited by Madden, Whiting & Huettel, 2005). Despite age-related slowing, accuracy did not differ between groups, suggesting the reduced activation was related to age-related changes in speed of processing of object information. Moreover task-related fMRI activation occurred outside the ventral stream, primarily in the parietal cortex in older but not in younger adults. Conversely, in tasks requiring dorsal pathway processing, older adults tended to activate cortical regions outside the dorsal pathway – primarily prefrontal regions. As such, functional differentiation of the ventral and dorsal processing pathways from task-specific activation was less evident for older adults than for younger adults (Grady et al., 1994). However, the cause of this more diffuse activation pattern observed in older adults remains unknown. It could be the case that age-related decline in lower-level vision impacts on the neural strategies being employed in higher-level processing. On the other hand, higher-level visual functions are also more complex and require effective attentional processing which can also be affected by age as will be detailed in the following section.

### 1.2.2 Attentional functions

Attention is a complex function which involves multiple cognitive domains and processes with the ultimate goal of focusing resources, processing incoming information and optimising receptivity (Lezak et al., 2004). Attentional processes are often measured by tasks of focal, covert and sustained attention, and is necessary for almost all cognitive domains. Executive functions also contribute to effective attentional performance, and can be narrowed down to three core domains: inhibition, working memory updating and cognitive flexibility (Diamond, 2013). Executive functions are often referred to as 'frontal' processes as they are mediated by anterior brain areas including the prefrontal cortex and anterior cingulate cortex (Zelazo & Cunningham, 2007). Attention and executive processes are largely interlinked as executive functions control the 'top-down' voluntary aspect of attention and interact with other ongoing cognitive processing to direct behaviour.

One framework of attention suggests that bottom-up stimulus-driven processes such as alerting, and top-down goal-directed selection work together towards effective attentional processing (Corbetta & Shulman, 2002). This model is closely related to the dual-stream model of visual processing (Mishkin, Ungerleider & Macko, 1983), and proposes that bottom-up processing is carried out by the ventral attention network, and top-down processing by the dorsal attention network. The ventral attention network, located in the

temporoparietal and inferior frontal cortices, is specialised for the detection of relevant stimuli, and directs attention to salient events. The dorsal attention network, involving the intraparietal and superior frontal cortices is responsible for goal-directed allocation of resources. Both pathways work in collaboration in order to respond to the environment appropriately in a goal directed manner, which requires executive functions including prioritising and judgement (Robbins, 1996). Another influential model of attention, proposed by Posner & Petersen, (1990), posits that attention involves three serial networks: alerting, orienting and executive functioning. The alerting network, responsible for the modulation of arousal and maintenance of optimal vigilance, is thought to be located in the right parietal and frontal cortices. The orienting network, which prioritizes incoming information by identifying relevant spatial locations, involves the superior colliculus, frontal, posterior parietal and thalamic regions. The executive network enables target detection, focus and consciousness and is said to involve regions in the anterior cingulate cortex and prefrontal cortex.

#### 1.2.2.1 Attention and executive functions in older adults

There is evidence that attention and executive functions may decline as a result of ageing, dependent on individual differences in perceptual load, processing capacity and inhibitory ability (Kramer & Kray, 2006). It has been suggested that the main component of cognitive ageing is a reduction in the efficiency of executive functions (Lustig & Jantz, 2015) notably that of inhibition, attention switching and updating abilities which have been shown to decline both cross-sectionally (Hasher & Zacks, 1988) and longitudinally in older adults (Fjell et al., 2016; Madden, 2007). Hsieh et al (2012) showed that older adults had larger switching costs than younger adults but maintained the ability to prepare for a perceptual judgement task switch. The authors concluded that older adults may demonstrate impairments in advanced preparation even over a longer interval, in comparison to younger adults. Moreover, age-related impairments are present in tasks which present a switch cost -i.e. alternating between tasks – or mixing cost – i.e. intermixing one task with another. These have been investigated in work by Whitson et al (2014), where it was reported that poorer performance in tasks involving a mixing cost was related to response mapping and response programming, which suggested that older adults attempt to recruit greater proactive control in a bid to mitigate their vulnerability to interference following stimulus presentation. The authors also concluded that this may be consistent with age-related compensation in this domain specifically.

There is evidence for specific age-related deficits in tasks of divided attention such as global set-shifting, suggesting that executive functions involved in switching may be compromised with age (Grönholm-Nyman et al., 2017). Age differences are found in processes involving the maintenance of two distinct mental task sets, whereas no age differences are identified in local switching (Dorbath et al., 2011). Such executive deficits with age may arise from a slowing of overall processing speed, they may be influenced by the stimuli itself or by the time given to process information, which typically differs between studies (de Bruin & Sala, 2018). However, some research has reported no age-related deficits in executive processes

which involve active selection or inhibition of stimuli (Dorbath et al., 2011) or set-shifting (Basak & Verhaeghen, 2011).

Age-related reductions in executive control have been linked to changes in the prefrontal cortex (Denburg & Hedgcock, 2015, MacPherson, Phillips & Della Sala, 2002) as well as the anterior cingulate cortex (Korsch et al., 2014) (see section 2.3, 2.4). The latter is thought to form an anterior salience network together with the insula cortex, which is important for attention maintenance and switching between cognitive resources (Touroutoglou et al., 2012). It has also been suggested that changes to these cognitive functions in older age may in turn have a detrimental effect on central executive network connectivity, resulting in more general cognitive decline (Chand et al., 2017).

Besides evidence for an age-related decline in anterior executive networks, research has also found evidence for ageing effect on posterior attention networks. For instance, age-related decline has been reported in the alerting attention network using the Attention Network Task (ANT; see section 3.2), which is expressed in the ability to use warning signs in speed responding (Mahoney et al., 2010). Mahoney et al., (2010) reported diminished alerting effects but enhanced orienting effects in older adults. In addition, it has been shown that older adults demonstrated difficulties in sustaining attention in the absence of an alerting stimuli in comparison to younger adults suggesting that they may rely more heavily on external alerts to maintain attention function (Fernandez-Duque, 2006; van der Leeuw et al., 2017). With regards to the potential neural correlates of these attention deficits, some studies have reported age-related cortical atrophy in parietal regions, as well as loss of white matter volume in the inferior parietal region. As parietal regions are thought to be responsible for orienting attention age-related atrophy in these regions is likely to contribute to a decline in orienting functioning (Crivello et al., 2014; Raz et al., 2005). Indeed, atrophy in the parietal region has been reported to be related to slower visual search (Bennett et al., 2012), suggesting a decline in ventral attentional functioning.

As ageing may affect both bottom-up visual processing at the sensory level, and top-down attention due to the decline in the executive processing, older relative to younger adults appear to be particularly impaired in tasks requiring the combination of bottom-up and top-down neural processing (Li et al., 2013, Li et al., 2015). Moreover evidence has suggested that age-related impairments in performance on visual tasks which predict functional outcomes (such as safe driving) are the product of age-related reductions in contrast sensitivity, and deployment of visual attention, as assessed using a cueing stimulus (Power et al., 2017). These findings indicated that the combination of both bottom-up sensory impairments and top-down guiding of attentional resources may underlie a decline in overall performance in perceptual tasks with ageing. A decline in executive processing resources with age may also present as attentional distractibility. One study indicated that older adults had increased distractibility on a competitive attention task, altered top-down mechanisms and resulting in poorer suppression of task-irrelevant information (ElShafei et al.,

2020). These findings were supported by findings from magnetoencephalography (MEG) outcomes, which indicated reduced synchronisation in oscillations associated with top-down activation, reduced activation in lateral prefrontal regions responsible for inhibition, and over-enhancement signal in systems of bottom-up attention in response to attentional activation (ElShafei et al., 2020). Together, these findings point to the possibility that age-related attentional decline may be due to a problem with the integration of bottom-up and top-down streams of information.

### 1.2.3 Processing speed in ageing

Processing speed refers to the speed with which cognitive processes are performed, most often measured by response times (RTs) (Harada et al., 2013). It is well established that in healthy ageing older adults show slower RTs than younger adults in many cognitive tasks (Salthouse, 1996). Older adults show consistently slower response times (Salthouse, 1996) and greater variability in responses times (Hultsch et al., 2002) in comparison to younger adults, but often maintain accuracy levels thus they show a shift in the speed-accuracy trade off compared with younger adults. This suggests that a slower and more cautious response strategy is adopted to mitigate inaccuracies in ageing. However there is some variability in the literature, with investigations reporting contrasting findings; for instance, slowing of simple RT (SRT) performance in older adults but preserved choice RT (CRT) performance (Vaportzis et al., 2013), or slower performance in both SRT and CRT in older compared to younger groups (Anstey et al., 2005). Moreover, it is suggested that age-related slowing on simple and choice RT tasks may be related to impaired executive function (Bugg et al., 2006) in addition to age-related changes in white matter microstructure, particularly in the frontal and parietal connections (Jackson et al., 2012). There is some evidence that these slower RTs as well as age-related decline in various cognitive abilities are a product of generalized slowing with age (Salthouse, 1996, 2001). However, more recently others have argued this response slowing with age may be domain specific – for example, the product of a decline in response inhibition (Sebastian et al., 2016). This concept has been investigated further in recent ageing research by applying models which allow the estimation of the different elements thought to be encapsulated by RT (Hedge et al., 2018). Most prominently, the drift diffusion model of RT which allows the estimation of perceptual, motor, information threshold and quality of processing has been applied in ageing research to further clarify the nature of response time slowing in older adults (Ratcliff & Stern, 2010). Findings have generally demonstrated longer perceptual encoding and evidence accumulation times, leading to overall RT lengthening and variability (Ratcliff & Stern, 2010), which also reflects the more cautious response strategy often seen in older adults. This has often been assessed by calculating speed accuracy trade-off (SAT) values. The SAT refers to the balance that is struck by an individual when completing a task or making a decision and can be influenced by numerous factors such as direct task instruction and most importantly age (Standage et al., 2015). Older adults are most often reported to have lengthened SAT as they tend to sacrifice speed in favour of maintaining accuracy (Ratcliff & Stern, 2010). Therefore in addition to measuring RT performance on visual tasks, SAT was also calculated, to assess the cognitive strategy of older adults during perceptual processing. and I also applied

a drift diffusion model of RTs in my current empirical work to investigate the elements of the SAT in older adults further and will discuss this in detail in Chapter 6.

An age-related slowing in processing speed is likely to affect performance in cognitive tests. On one hand, a 'slowing' with age does not necessarily correlate with poorer performance in terms of response accuracy but on the other hand may negatively impact scores on tests which do not reflect the actual age-related change (or no change) in cognition. Furthermore, slowing at perceptual level in older age shares a portion of age-related variance in higher order cognitive measures such as memory and reasoning, suggesting that a more generalized slowing of information processing may underlie many of the observed age-related changes in perceptual and cognitive performance.

### 1.2.4 Summary of cognitive ageing

Older relative to younger adults show some notable changes in perceptual and attentional functions. Vision is seen to change at multiple processing stages with age, however, a decline in lower-level function appears to be the product of poorer retinal function, as opposed to perceptual deficits. Investigations suggest a general decline in executive function and top-down attentional functioning in older age, which impacts performance in tests of multiple domains. As such, it is pertinent to gain a better understanding of the specific changes in the visual and attentional systems in ageing, and how these may interact. Generally the literature so far supports a theme of slowing in responses with older age, which may be the product of either perceptual and/or attentional changes. Modelling response and processing speed in ageing may also help to illuminate the mechanisms contributing to cognitive changes in older adults. For example, an age-related slowing of RTs typically accompanies a maintenance in response accuracy. As such the aim of this thesis was to investigate, in a systematic and comprehensive manner, different stages of visual perception functioning in older adults and attempt to answer the question at which stage of visual perceptual processing age-related decline becomes apparent. Moreover this thesis will aim to address which attentional networks show decline with age, and the nature of processing speed changes with age. This was done by compiling a novel task battery designed to assess different stages of the visual perceptual and attention processing hierarchy. Some of the tasks in this battery incorporated psychophysical stair-case methods to measure performance thresholds (see Chapter 3) in addition to speed-accuracy trade-offs to provide sensitive measures of perceptual performance. Once the cognitive profile of older adults was established, the aim of the work in this thesis was then to explore multi-modal neural differences that may underlie patterns of age-related cognitive differences.

## 1.3 Brain changes in normal ageing

Normal brain ageing is typically characterised by generalised grey and white matter volume loss, declining at a rate of approximately 5% per decade after the age of 40 (Peters, 2006). As individuals age, a number of changes to the brain occur such as grey matter (GM) and white matter (WM) volume loss in anterior

(Chen et al. 2019) and dorsolateral brain regions (Bergfield et al., 2010). Frontal regions of the brain most typically experience shrinkage in normal ageing, with the prefrontal cortex most notably affected followed by the striatum, neostriatum temporal lobe and most widely reported, the hippocampus (Raz et al., 2005). Moreover, widespread decline in white matter volume, notably affecting temporal and frontal regions have also been reported with ageing (Chen et al., 2019).

The research described in this thesis employed grey matter (GM) volume and metabolic measurements as well as white matter (WM) microstructural indices from magnetic resonance imaging (MRI, see Chapter 2) to characterise age-related brain differences that may underpin perceptual and attention differences with age. More specifically, the study focused on grey matter regions of visual and attention networks as well as their white matter connections. White matter connections are important for information transfer in the brain (Penke et al., 2012), and hence may provide the structural correlates of age-related decline in response speed (Madden et al., 2009; Penke et al., 2010). Furthermore, while accumulating evidence suggests a close link between white matter microstructure and brain metabolites (Palombo et al., 2018), metabolic studies employing magnetic resonance spectroscopy (MRS, see Chapter 2) are still relatively limited in ageing. This is despite the combination of grey matter metabolites and white matter microstructural measurements promising to provide further insights into age-related brain changes at a cellular level and how these may relate to cognitive and structural brain changes (Gao et al., 2013, Simmonite et al., 2019). For these reasons, these methods were employed in this thesis and current evidence regarding age-related changes in these modalities are discussed below.

### 1.3.1 Morphological brain changes in ageing

Brain morphology can be assessed with grey and white matter volume and cortical thickness and age-related changes in these measurements have been widely studied. Anterior regions of the brain tend to be the first to show age-related reductions in cortical thickness and volume, notably the prefrontal and the anterior cingulate cortex (Chen et al., 2019) as well as dorsolateral and medial frontal regions (Bergfield et al., 2010). In contrast posterior regions such as the visual and auditory cortex are thought to be less vulnerable to atrophy (Sowell et al., 2004). This pattern has been coined the anterior-posterior gradient of ageing (Davis et al., 2008). Some brain structures decline in a linear manner with age such as subcortical structures as the thalamus and nucleus accumbens, whereas other structures for instance the hippocampus and other medial temporal lobe show a non-uniform, non-linear pattern of grey matter reduction which appear to be more susceptible to individual differences (Walhovd et al., 2011). In healthy ageing, frontal lobe grey and white matter atrophy is a major contributor to age-related cognitive decline (Fjell & Walhovd, 2010; Pichet Binette et al., 2020), as is temporal and parietal lobe atrophy (Fjell et al., 2013) (Bartzokis et al., 2001; Raz et al., 2005).

While the occipital cortex is generally thought to be preserved in ageing (Gardener et al., 2021, Lee et al., 2018), there are however some reports of age-related reductions in primary visual cortical thickness (Lee et al., 2019), which are also correlated with a reduction in retinal thickness (Jorge et al., 2020). Evidence from the Lothian birth cohort has also suggested that right medial occipital surface area is reduced with age (Cox et al., 2018). This was also related to cognitive ageing, as indicated by a composite measure of intelligence and the Mini-mental state exam, however the strength of this correlation was relatively weak. As such there is some evidence that age-related reductions in the cortical thickness of visual regions may occur, but results are largely mixed.

### 1.3.2 Microstructural changes in the brain in normal ageing

Age-related changes in white matter microstructure have most commonly been investigated with diffusion tensor imaging (DTI) (see Chapter 2). DTI yields a number of metrics including diffusivity measures and fractional anisotropy (FA), an index of fibre coherence that will be introduced in more detail in Chapter 2. DTI studies have typically reported increases in mean diffusivity (MD) and decreases in FA, suggestive of compromised white matter microstructure in ageing. These changes were predominantly but not exclusively observed in temporal and frontal regions, including the forceps major (Chen et al., 2019). Results from longitudinal modelling across the lifespan reported that microstructural indices such as FA, plateau around the third decade of life and subsequently begin a steady decline from approximately 40 years of age, accelerating in later years (Beck et al., 2021). MD, axial diffusivity (L1) and radial diffusivity (RD) decrease until around 40 years, then show a steady period, and then begin to increase in later years, also representing age-related impairment (Beck et al., 2021). However, FA is persistently negatively associated with age (Bennett & Madden, 2014), with large age differences in FA being reported in frontal white matter (Bennett et al., 2010), fornix, parahippocampal cingulum and uncinate fasciculus (Metzler-Baddeley et al., 2011), which are regions associated with fronto-temporal connectivity and episodic working memory function. Even more recently, FA has been reported to decrease annually from the age of 50, with increases in diffusivity measures occurring mainly in superior regions (Sexton et al., 2014). RD is also found to be significantly altered in older adults in the cingulum bundle in comparison to younger adults (Borghesani et al., 2013), and both axial and radial diffusivity in found to increase with age in the fornix, SLF, CST and uncinate (Sala et al., 2012).

This pattern of change is thought to reflect the lifespan of myelination which begins with maturation of myelin in childhood and adolescence, and then subsequent myelin loss during later stages of adulthood (Bartzokis et al., 2004). For instance, age-related differences in fornix microstructure were reported to be related to apparent white matter myelin loss – estimated with quantitative magnetization transfer imaging - as opposed to neurite density from multi-shell diffusion imaging (Coad et al., 2020; Claudia Metzler-Baddeley et al., 2019). This was also associated with hippocampal grey matter damage during ageing, suggesting that microstructural impairments may have a subsequent impact on other brain changes

occurring in the ageing process. On the other hand, other studies have linked reductions in frontal lobe FA with ageing to increased axonal dispersion rather than markers of demyelination, as shown using multi-shell diffusion imaging (Billiet et al., 2015).

With regards to age-related microstructural changes in the visual system, some studies report little to no significant changes in occipital and visual regions (Jacobs et al., 2013). However, microstructural integrity of tracts and regions associated with the occipital lobe and visual functioning, such as the fronto-occipital fasciculus have been shown to decline in older adults and were related to poorer cognitive control (Hinault et al., 2020). Similar findings also indicated that age-related reductions in FA specifically in the fronto-occipital fasciculus were apparent, and mediated executive function performance (Santiago et al., 2015). Finally, it was also shown that reductions in microstructural integrity in connections between the posterior thalamus and occipital cortex may underlie a decline in visual short term memory performance (Menegaux et al., 2020). In summary, specific reductions in microstructural integrity in tracts related to visual function, rather than the wider occipital cortex, are seen to be present in older adults and may mediate both visual and executive performance.

### 1.3.3 Metabolic changes in the brain in normal ageing

Changes in key brain metabolites have been reported in normal ageing, albeit to a lesser extent than other modalities. There is an emerging profile of metabolic changes in older people, which has also been associated with changes in cognitive processing (Charlton et al., 2007). Age-related changes in key brain metabolites are discussed below, and the exact functions of these metabolites are discussed in more detail in Chapter 2.

Most notably, N-acetyl-aspartate (NAA) – one of the most prolific brain metabolites – is found to be reduced in frontal (Haga et al., 2009) and parietal (Gruber et al., 2008) brain regions in normal ageing. NAA is also reduced in a wide range of neuropathologies and is more broadly associated with neuronal health and brain energy metabolism (Moffett et al., 2013). Reductions of NAA in older adults have been found to differ between white and grey matter but have been interpreted as a marker of reduction in neuronal volume or neuronal metabolic activity (Minati et al., 2010). Significant relationships between reductions in white matter NAA and processing speed in tasks of attention in older adults have also been reported (Ross et al., 2005) suggesting potential links between NAA and cognitive speed.

Decreases in choline and creatine in the parietal lobe are also reported in older adults (Haga et al., 2009). Conversely, higher creatine and choline is present in the anterior cingulate cortex (ACC) and hippocampus in older adults (Lind et al., 2020). Higher choline and creatine in the posterior cingulate cortex has also been associated with poorer verbal learning, performance on the trail-making task and the Wechsler Adult Intelligence Scale (WAIS) in older adults (Kantarci et al., 2011). These changes in choline and creatine were

correlated with higher Pittsburgh compound B marked levels of pathological amyloid ß – the key pathological marker of Alzheimer's disease (AD) – in normal older adults (Kantarci et al., 2011).

Myoinositol is found to be altered in the healthy ageing brain, with raised levels in the dorsolateral prefrontal cortex (DLPFC) observed in mid-life, which then increases in the hippocampus and thalamus in older age (Lind et al., 2020). Myoinositol changes have also been related to visuospatial working memory performance in healthy ageing, with a negative correlation observed between metabolite level and cognitive performance (Lind et al., 2020).

Glutamine and glutamate have also been shown to exhibit regionally specific changes in concentration with ageing. Glutamine levels are raised in the corona radiata in older adults, and reduced in the motor cortex, which is reported to be consistent with neuronal loss and neuronal shrinkage with age (Kaiser et al., 2005). Lower glutamate in the striatum is related to poorer performance on tests of visuomotor skills in older adults, and higher blood pressure, suggesting brain glutamate may underlie neural and physiological motor performance in healthy ageing (Zahr et al., 2013).

Finally, the brain's primary inhibitory neurotransmitter, GABA, has been shown to decline with age throughout adulthood in both anterior, posterior, and particularly the frontal cortices (Gao et al., 2013). Recent ageing studies have postulated a link between GABA and cognitive processing, due to its role in conflict resolution and perceptual processing (Hermans et al., 2018; Simmonite et al., 2019). Fluid processing has recently been shown to correlate with GABA in older adults, as evidenced by a decline in fluid processing being related to a decline in GABA in the occipital cortex (Simmonite et al., 2019). However, it is unclear whether fluid processing may result in a generalized slowing of RT in older age, or may refer to a specific cognitive domain, such as response inhibition or information processing. Similar to glutamine, motor inhibition changes in older age have been related to changes in GABA with ageing. Older adults with lower GABA levels in pre-supplementary motor area had longer stop-signal RT, suggesting a role for GABA in inhibitory deficits observed in older age (Hermans et al., 2018). Furthermore, increased visual cortical GABA and reduced glutamine/glutamate were also reported in older adults. Visual cortical GABA was correlated with perceptual performance in tasks of spatial suppression of motion and binocular rivalry (Pitchaimuthu et al., 2017), and neural distinctiveness in the auditory cortex is also related to age related declines in GABA (Lalwani et al., 2019). As such, GABA poses as an important marker for cognitive changes in both attentional, visual and processing speed in older adults.

As such, a number of studies report reductions in GABA in older adults in the occipital cortex (Gao et al., 2013, Pitchaimuthu et al., 2017, Simmonite et al., 2019), however the study of other metabolites of interest in the occipital lobe has been very limited. NAA and choline have been reported to largely show no change with age in the occipital cortex (Saunders et al., 1999, Christensen et al., 1993), but some more recent studies have shown decreases (Eylers et al., 2016, Marjanska et al., 2017). Myoinositol has been shown to increase with age in the occipital cortex (Saunders et al., 1999), however to the best of my knowledge no other

studies focus on quantifying metabolic changes in the occipital lobe in older adults. As such, evidence to aid in the characterisation of the metabolic profile of the ageing visual system is limited to both few and outdated studies.

### 1.3.4 Summary of brain changes

In summary, GM volume shows a global reduction in the whole cortex with age, with anterior regions showing more substantial and earlier decline in normal ageing. Frontal, temporal and parietal white matter volume is also reduced with age, with medial temporal structures being particularly vulnerable. Reductions in microstructural integrity are also reported in temporal and frontal tracts, particularly in the fronto-parietal connections and cingulum, and also in the fornix. Finally, frontal and parietal reductions in NAA, choline and creatine, and increased myoinositol in the frontal cortex are reported in older adults, which have been related to poorer executive functioning. GABA is seen to decline in the frontal and posterior cortex in older adults, with some evidence that reductions in occipital GABA may be related to a decline in perceptual and fluid processing in age. This evidence suggests that predominantly frontal regions show declines in morphology, microstructure and metabolites with normal ageing. Some evidence though also suggest that metabolic and microstructural changes occur in the parietal and occipital lobes. However, these require further investigation as it still remains to be fully understood how they relate to age-related changes in visual perceptual and attentional functioning. This thesis therefore aimed to address this gap in the literature by characterising age-related brain differences in visual perceptual and attentional networks, using multi-modal imaging to capture morphological, microstructural and metabolic changes and by relating these to differences in perceptual and attentional performance. This approach is novel, as metabolic changes in the brain in the anterior cingulate, posterior parietal and occipital cortices have not previously been assessed in relation to a hierarchy of perceptual and attentional functions in older age. In addition, this thesis applied advanced multi-shell diffusion imaging to provide a potentially more sensitive measure of white matter microstructure with age in tracts relating to visual and attentional function (see Chapter 3 for a more detailed discussion).

## 1.4 Theories of ageing in cognitive neuroscience

Several theories have been derived which aim to link cognitive and brain changes in older adults and explain why cognitive decline occurs with age and why it may be subject to individual differences.

### 1.4.1 The frontal ageing hypothesis

One theory of cognitive ageing is the frontal ageing hypothesis (Dempster, 1992). This hypothesis claims that impairments in the frontal – particularly prefrontal – cortex are disproportionally affected by the ageing process, and hence lead to a decline in cognitive functions supported by this region at an earlier age than other functions (Dempster, 1992; West, 1996). As outlined in section 1.3 there is substantial neuroimaging evidence for an anterior-posterior gradient in age-related brain changes with normal ageing having a marked

impact on the structure and function of the prefrontal cortex (PFC) (Lövdén et al., 2007; Nordahl et al., 2006). Consistent with this, age-related effects in measures of fractional anisotropy and diffusivities are greater in the anterior corpus callosum, and frontal matter in comparison to temporal, parietal and occipital white matter (Head et al., 2004; Madden et al., 2007), and age-related deterioration of white matter is more prominent in fibres connecting to the frontal lobe (Kennedy & Raz, 2009). From middle age myelin becomes more vulnerable to decline in later myelinating regions such as the frontal lobe, in contrast to less vulnerable regions such as the visual cortex (Bartzokis et al., 2004; Flechsig, 1901). This has been related to age-related impairment in tasks associated with PFC functioning including executive function, attention, working memory and inhibitory functions (Bucur et al., 2008; Nordahl et al., 2006). It has also been posited that age-related decline in processing speed are caused by impairments in the frontal lobe – specifically white matter decline in the PFC is related to increased RT (Bucur et al., 2008). It is suggested that age-related slowing becomes more pronounced as the complexity of processing demands increases, also known as the complexity hypothesis (Birren et al., 1974; Bashore et al., 1997) which is consistent with the role for the frontal lobe in age-related increases in RT. That is, with age PFC grey matter is seen to be selectively reduced in volume with volume loss affecting the anterior cingulate and middle frontal gyri disproportionately (Bartzokis et al., 2001; Cowell et al., 2007; Good et al., 2001). Similarly, age-related loss in PFC white matter volume is also reported (Bartzokis et al., 2001; Salat et al., 2001), declining slowly until later in life during which time white matter hyperintensities and vascular abnormalities become more prevalent in the frontal lobe (Jernigan et al., 2001, Nordhal et al., 2006). These findings would support the concept that PFC structure and function is vulnerable to decline in ageing, resulting in a decline in associated cognition.

However, the frontal ageing hypothesis has received some criticism, namely in the lack of empirical evidence which examines frontal decline and related functions over time in comparison to other regions (Greenwood, 2000). Moreover, age-related decline is evident in a broad range of functions particularly visuospatial abilities which are not solely reliant on the functioning of the frontal lobes. More recent research has suggested that the brain may be capable of plasticity resulting in preservation of cognitive performance in domains which may otherwise experience decline. The functional plasticity hypothesis posits that more severe age-related decline is avoided by brain network re-organisation (Cabeza et al., 2003; Greenwood, 2007; Zarahn et al., 2007). Specifically, whilst there is evidence that declines in age-related processing speed, microstructural integrity and brain volume are present, many studies which assess higher cognitive abilities show only a relatively small loss of function or even maintained performance with age (Greenwood et al., 2007)

In addition, the frontal ageing hypothesis considers the PFC to be the vulnerable site of marked age-related decline, however the PFC consists of many subregions including the ACC, dorsolateral prefrontal cortex and orbitofrontal cortex (Happaney et al., 2004). As these regions are associated with different cognitive

functions, it is possible that normal ageing impacts certain regions of the PFC and therefore certain functions differently. For example, lateral prefrontal regions are associated with primarily set shifting and inhibition (Yochim et al., 2009), whereas medial and orbitofrontal regions relate to emotional and social processing (Hornak et al., 2003). For instance, Kievit et al., (2014) identified specific relationships between subregions of the PFC and subtypes of executive function processes such as inhibition. They also showed that age-related differences in PFC grey and white matter integrity contributed to inter-individual differences in the effective executive performance. This again supports the view that the frontal ageing hypothesis may be too simplified, however it is still evident that frontal regions remain selectively vulnerable to change with age.

#### 1.4.1.1 Compensation, maintenance and reserve

Functional magnetic resonance (fMRI) evidence has suggested that the brain is capable of reorganising cognitive processing as a consequence of age-relate changes in the brain (Cabeza, 2001). The Hemispheric Asymmetry Reduction in Older adults (HAROLD; Cabeza, 2002) model was formed in response to these findings, and suggests that older adults do not show the 'typical pattern' observed in younger adults in which the left hemisphere is activated during encoding and the right hemisphere during retrieval (Tulving et al., 1994). This hypothesis attempts to explain age-related changes as a result of regional and network changes involving both compensatory and differentiation processes (Cabeza et al., 2002; Greenwood et al., 2007).

In a further attempt to explain the effects of ageing, Cabeza (2002, 2018) proposed that age-related cognitive decline may be mediated by three interacting mechanisms: reserve, maintenance and compensation. This theory is not limited to one cognitive domain or brain region but may aid in the understanding of all cognitive and brain changes occurring with age.

Reserve refers to the cumulative improvement of neural resources that mitigate the effects of neural decline in ageing. Reserve occurs before the brain is affected by ageing and takes place over a number of years, for example, education level may boost reserve by increasing synaptic density (Cabeza et al., 2002). Research focusing on brain activity in those with higher versus lower education as proxy for reserve have found that reserve is limited to superior temporal and parietal cortical activation measured by fMRI during visual processing, concluding that perhaps higher reserve results in more effective use of cerebral networks in age (Solé-Padullés et al., 2009). This has been supported by findings suggesting that higher memory task-related connectivity in the left frontal cortex was related to higher network efficiency and enhanced memory reserve in ageing (Franzmeier et al., 2018).

Maintenance refers to preservation of neural resources and depends on the magnitude and rate of decline and efficiency of repair (Cabeza et al., 2018). Examples of maintenance include findings of cognitive and

neural benefits of physical exercise that allow older individuals to sustain their performance. More generally, maintenance refers to those older adults who maintain their cognitive performance and show little brain decline. For example, longitudinal research found older individuals with preserved episodic memory demonstrated less hippocampal atrophy over time than those with episodic memory decline (Persson et al., 2018). Similarly, another longitudinal study following individuals over 65 years of age also reported less hippocampal atrophy in individuals who exhibited little to no episodic memory decline over a four-year period (Cabeza et al., 2018). However, the underlying mechanisms by which maintenance occurs in older age is of great debate and ranges from preventative practices such as exercise (Stillman et al., 2020), yoga (Gothe et al., 2016) or weight maintenance (Dye et al., 2017) to genetic factors (Harris & Deary, 2011).

Compensation refers to the recruitment of alternative neural resources in response to high cognitive demand. Observing fMRI correlates, compensation describes a situation where brain activity or functional connectivity is more widespread in older adults than younger adults, coupled with maintained cognitive performance (Dennis et al., 2008). There are 3 proposed mechanisms of compensation: 1) compensation by upregulation which refers to the enhancement of cognitive performance by boosting a neural process in response to task demands. This could explain the finding that some age-related activity increases are evident in brain regions that younger adults also recruit to do the same task. 2) compensation by selection, which refers to the recruitment by older adults of neural circuitry associated with cognitive processes that are not engaged by younger adults under the same objective task conditions. 3) compensation by reorganization, meaning that older adults use neural mechanisms to respond to ageing-induced losses that would not otherwise be used by younger adults during the same cognitive process. There is some empirical evidence to support the concept that compensation occurs with age. Gutchess et al., (2005) showed less blood-oxygen-level-dependent (BOLD) signal on fMRI in the parahippocampus in older adults who performed at the same level as younger adults during scene encoding, but more activation in the middle frontal cortex than in younger adults. They suggested that these older adults who showed lower hippocampal activity showed more compensatory activation frontal areas. Similar findings were demonstrated in work by Cox et al., (2015) showing that the dorsolateral PFC volume was related to task performance, which they suggest indicated a compensatory mechanism for the frontal lobe in memory performance with age. In addition, the authors suggested that age related memory decline is related to an inefficient use of neural resources, mediated by the inability of the left PFC to inhibit non-task related activity in the right PFC via the anterior corpus callosum. However, the study reported no evidence of anterior corpus callosum integrity being related to task performance, suggesting that the evidence supports the compensatory theory of ageing as opposed to a disconnect or failure to inhibit irrelevant information. Episodic memory maintenance in normal ageing has been related to preservation of hippocampal volume, and greater hippocampal BOLD signal change (Cabeza et al., 2018). Moreover, older adults who had greater episodic memory retrieval performance showed bilateral frontal activity, in comparison to low performing older adults who showed unilateral frontal activity (Cabeza et al., 2018). In addition, during working memory tasks older adults show

greater BOLD signal change in the right dorsolateral PFC than younger adults at lower levels of task demands, but less signal change at higher levels of working memory load. This suggests compensatory changes in neural mechanisms for cognitive functions that experience age related decline. Compensatory recruitment of the prefrontal regions in older age has also been widely reported (Eyler et al., 2011; Spreng & Turner, 2019), as the responsiveness of the executive system decreases with ageing (Cappell et al., 2010; Kennedy & Raz, 2015; Schneider-Garces et al., 2009). Responses also show a corresponding age-related shift to posterior brain activity which may reflect a shift from proactive to reactive cognitive control (Davis & Cabeza, 2015).

Finally, functional plasticity is also suggested as an extension and explanation for the idea of neural compensation in older age (Greenwood et al., 2007). Plasticity involves cellular and synaptic mechanisms, referring to the capability of neuronal circuitry to respond to atrophy, dysconnectivity or shrinkage. Those cortical regions showing most consistent atrophy and change in older age – predominantly PFC and parietal cortex – also show increase regional activation in age. In a similar way to compensation, it is suggested that losses in brain integrity in certain areas drive functional reorganization and processing strategy change (Greenwood et al., 2007). However, to the best of my knowledge there have not been investigations which have focused on these differences specifically in the visual system.

#### 1.4.1.2 Dedifferentiation in ageing

The concept of ageing and neural dedifferentiation refers to the notion that neural representations of perceptual and conceptual information may be less distinctive with age (Koen & Rugg, 2019). Neural resource allocation is thought to compromise the clarity of neural representations with older age. Previous studies found more widespread neural activity during task engagement in older adults where cognitive performance is poorer than in younger adults, potentially driven by a reduction in regional response to a certain stimulus (Park et al., 2012). Rodent research has noted the importance of GABA as a mechanism for neural dedifferentiation, suggesting that reductions in GABA mediate age-related neural dedifferentiation in perceptual tasks and in the functioning of large-scale brain networks (Koen et al., 2020). Recent work has also shown that reductions of GABA in the ventral visual cortex predicted age-related differences in neural distinctiveness in response to faces and objects (Chamberlain et al., 2019).

Neural dedifferentiation in particular has been linked to the decline in episodic memory typically witnessed in older age (Yassa et al., 2011). Other research has emphasised the importance of network segregation in the brain for effective processing speed and fluid intelligence performance, a loss of which may then contribute to the age-related decline reported in these domains (Chan et al., 2014).

Importantly, recent work has shown that the ability to maintain good performance in visuo-motor tasks in older age is related to the modulation of separate functional networks - or functional connectivity

dedifferentiation – in the whole brain (Monteiro et al., 2020). Age-related reductions in fMRI activation in visual-attentional regions including the superior parietal and premotor cortex have been reported in response to visual task demands (Roski et al., 2013). Moreover, lower functional connectivity between sensorimotor and visual attention related regions were also reported, indicating age-related deficits in top-down control, which the authors attribute to neural dedifferentiation (Roski et al., 2013).

These concepts are relevant to the current research, as I look to establish the neural differences that are present between younger and older age in response to visual and attentional tasks. As discussed, age-related brain changes are typically reported to be more prominent in anterior regions, and corresponding functions are often found to experience greater decline in older adults. However, it is unclear which brain mechanisms may change in the visual perceptual and attentional networks in older-age, and whether corresponding cognition is maintained as a result of neural compensation, whether cognitive strategy changes occur due to neural changes, or whether cognitive decline due to neural changes is in line with theories of dedifferentiation. In contrast to most previous neuroimaging research into these questions the current thesis does not employ functional but multimodal structural neuroimaging to characterise age-related differences in macro- and microstructural as well as neurochemical properties of visual perception and attention networks. This approach assumes that the ageing process affects structural and chemical properties of brain networks which in turn will affect their functioning. Thus, this thesis aimed to further our understanding into the age-related differences in these properties and how they may relate to the decline, maintenance, or compensation of functions within the visual perception and attention processing hierarchy.

## 1.5 Pathological ageing

### 1.5.1 Dementia

Understanding the cognitive and neural changes in healthy ageing is crucial to provide a baseline for investigating pathological ageing. This is particularly important in the current health climate, as we see a rise in age-related disorders, most notably dementia related disorders (Prince, 2015). In the current thesis, normal ageing was contrasted with pathological ageing in individuals with a clinical diagnosis of dementia with Lewy bodies (DLB), as the hallmark features of DLB are visual perception and attention deficits.

Dementia refers to a syndrome characterised by a progressive decline in memory, behaviour and ability to perform everyday activities (World Health Organisation, 2019). One in three people will develop dementia within their lifetime, with an estimated 850,000 people living with dementia in the UK alone (Prince, 2015), with this number now projected to reach 131.5 million people living with dementia globally by 2050 (Prince, 2015). Moreover, the impact of dementia concerns not only the economy - in which it is estimated that the disease has a worldwide cost of $948 billion - but also families, individuals and caregivers emotionally, psychologically and socially (Xu et al., 2017). Dementia can be the result of numerous conditions, with the

two most common age-related neurodegenerative diseases being AD and Lewy body disease (McKeith et al., 2017).

#### 1.5.1.1 Core clinical features in dementia with Lewy bodies

DLB is the second most common neurodegenerative dementia disorder following AD, and accounts for approximately 20% of all dementia cases at post-mortem (Vann Jones & O'Brien, 2014). Ultimately, a definite diagnosis of DLB requires histopathological verification, but a clinical diagnosis of possible or probable DLB is provided based on diagnostic criteria, which were formed by the DLB consortium (McKeith et al., 2017). The consensus diagnostic criteria have high levels of specificity for DLB (approximately 95%), and list core clinical features, in addition to several suggestive and supportive features to aid diagnosis (McKeith et al., 2017).

DLB is characterised by four core clinical features: cognitive fluctuations, Parkinsonism, visual hallucinations and rapid eye movement (REM) sleep behaviour disorder (RBD; McKeith et al., 2017), in addition to a progressive decline in functioning which significantly affects activities of daily living (ADLs). A diagnosis of probable DLB is made if two or more core features, or one core feature plus a suggestive feature, are present. Possible DLB is diagnosed if one core or suggestive feature is present alone.

##### 1.5.1.1.1 Cognitive fluctuations

Cognitive fluctuations are the most prevalent core symptom in DLB, occurring in approximately 90% of patients (McKeith et al., 2017). These fluctuations present as marked and severe variations in level of arousal and alertness, ranging from episodes of confusion to periods of responsiveness (O'Dowd et al., 2019). Cognitive fluctuations in DLB are characterised by periods of reduced attentiveness and awareness to external stimuli (McKeith, 2006), but are not necessarily a product of environmental factors. Whilst cognitive fluctuations are not unique to DLB, they are one of the most frequently reported and specific diagnostic features in the disease (Bradshaw, 2004). Qualitative descriptions of DLB suggest an interruption in awareness and attention, in association with confusion, difficulty in conversation and incoherent speech, followed by return to alertness, clarity and normal conversation (Bradshaw et al., 2004).

##### 1.5.1.1.2 Visual hallucinations

The second core clinical feature of DLB is complex visual hallucinations. These occur in around 60-80% of patients (Burghaus et al., 2012), and are more severe and likely to persist over time than in other dementias (Ballard et al., 2001). Hallucinations in DLB are complex and typically consist of people, animals and objects (Mosimann et al., 2006; Onofri et al., 2015), as opposed to simple hallucinations of colours, lines, flashes or light. Complex hallucinations in DLB are commonly associated with apathy and anxiety and are reported by patients as unpleasant (Mosimann et al., 2006) or frightening experiences (Burghaus et al., 2012). Other symptoms such as pupil reactivity impairments, saccadic and pursuit eye movements are

also present in DLB patients (Armstrong, 2012). Visual hallucinations in DLB are also associated with cognitive and perceptual impairments.

Reduced GABAergic transmission in the visual cortex in DLB patients may also contribute to the incidence of visual hallucinations (Khundakar et al., 2016). Visual hallucinations are also associated with the reduced perfusion in the anterior cingulate and orbitofrontal cortices in DLB (Heitz et al., 2016).

#### 1.5.1.1.3 Parkinsonism

Patients with DLB may also experience extra-pyramidal parkinsonism symptoms, which can occur in up to 68% of cases (Aarsland et al., 2001). Parkinsonism is defined as bradykinesia (slowness of movement), tremor, stooped posture, shuffling gait and/or rigidity in patients and does not occur due to medication or stroke (McKeith et al., 2017). DLB patients are varied in their motor presentation, in which some patients shown clear extra-pyramidal symptoms such as a pill-rolling tremor, and others may have no apparent motor problems (Gomperts, 2016). Patients who are diagnosed with Parkinson's disease (PD) and later develop dementia resulting in Parkinson's disease dementia (PDD), tend to have more severe motor symptoms than in DLB (Petrova et al., 2016). In DLB, motor symptoms may follow the development of dementia symptoms more than one year from onset. In contrast, a diagnosis of PDD is made when motor symptoms are present and are followed by the onset of cognitive impairments (Gomperts, 2016).

#### 1.5.1.1.4 REM sleep behaviour disorder

Rapid eye movement (REM) sleep behaviour disorder (RBD) is a parasomnia, in which the patient loses normal muscle atonia during REM sleep, resulting in prominent motor activity and dreams (Boeve et al., 2004; McKeith et al., 2017). Patients with RBD often experience vocalizations and behaviour during sleep which can be violent. Behaviours such as limb jerking, punching, kicking, running, jumping out of bed are common, and can be dangerous for both patients and bed partners (Boeve et al., 2004; Ferman et al., 2011). The conversion rate from RBD to DLB is between 29-55%, and RBD patients are often seen to have cognitive impairment, in particular attentional and executive deficits (Marchand et al., 2017).

### 1.5.1.2 Pathology

Like many neurodegenerative disorders, DLB is pathologically characterised by aberrant misfolding of tissue proteins. Cases diagnosed with DLB have an aggregation of α-synuclein containing cytoplasmic inclusions named Lewy bodies and Lewy neurites, which are located in high concentrations in the neurons of the midbrain, limbic system and neocortex (Perry et al., 1990; Figure 1.2). Limbic and neocortical Lewy body pathology is also associated with cognitive impairments, therefore Lewy body pathology in these regions is necessary for a pathological diagnosis of DLB. It is hypothesised that the spread of Lewy body pathology occurs via propagation by recruiting endogenously expressed α-synuclein, in a prion like manner throughout the nervous system (Masuda-Suzukake et al., 2013). However, mild Lewy body pathology may also be present in individuals without cognitive or motor impairments.

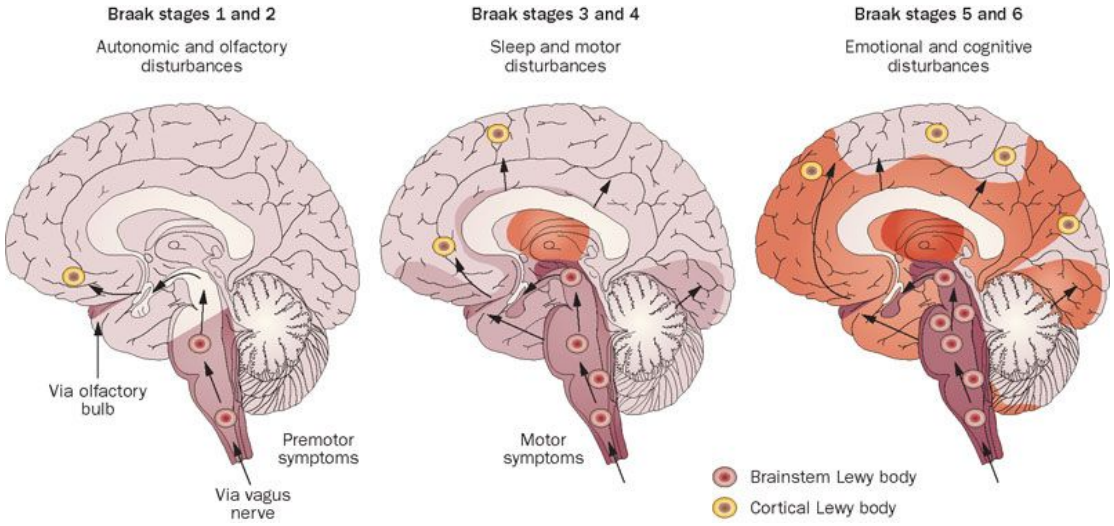


Figure 1.2 Braak staging guidelines outlining the spread of Lewy body pathology in Lewy body disorders. Patients with PD typically show pathology in stages 1 and 2, and progress to later stages, whereas DLB patients will more often show cortical Lewy bodies earlier in the disorder (adapted from Halliday et al., 2011).

Microglial activation, a marker of neuroinflammation, is often present in neurodegenerative diseases, and is observed in early DLB (Iannaccone et al., 2013). Activated microglia can also result in the release of iron from its storage protein, ferritin (Yoshida et al., 1995). The over-expression of α-synuclein has also been reported to increase iron accumulation (Ortega et al., 2015). Iron is an important metal in many processes within the brain such as myelin production and synthesis of neurotransmitters. However, excessive iron accumulation has also been linked to neurodegeneration and accelerated cognitive decline (Penke et al., 2012).

Amyloid β-peptide (Aβ) is the primary component of neuritic plaques often present in neurodegenerative disease (Hardy, 2002) - most notably AD - and may also be present in DLB cases. However, the presence of amyloid-β is not required for a DLB diagnosis. Whilst not as prolific in the cortex as Lewy bodies, it is hypothesised that striatal Amyloid-β may also underlie clinical symptoms of cognitive impairments in DLB. Findings have demonstrated that Amyloid-β immunoreactive plaque deposition in the striatum can reliably distinguish DLB cases from PDD cases, suggesting that this deposition contributes to early dementia (Halliday et al., 2011). Moreover, a relationship between the deposition of amyloid plaques and cortical Lewy bodies in DLB has also been observed (Pletnikova et al., 2005).

Neurofibrillary tangles and neuropil threads consist of the protein tau. In neurodegenerative conditions, tau becomes phosphorylated in an abnormal manner, and accumulates in neurons, resulting in a destabilisation of the microtuble network and axonal structure.

#### 1.5.1.3 Cognition in DLB

Many studies investigating perceptual deficits in DLB have focused on visual functioning, which is markedly impaired in DLB patients, in comparison to AD and PD. However, these studies generally recruit neuropsychological tasks which are not specific to different functions of vision and often require additional cognitive resources such as working memory to successfully complete. Only a couple of recent studies have focused on specific stages of visual processing and have generally found that DLB patients show impairments in mid to high-level visual processing stages (Landy et al., 2015; Metzler-Baddeley et al., 2010).

##### 1.5.1.3.1 Visual perception in DLB

Functions such as acuity and orientation have been reported to be preserved in DLB patients, in comparison to AD patients (Metzler-Baddeley et al., 2010). However, some research has reported impaired performance on orientation tasks in both mild cognitive impairment (MCI) DLB and RBD patients who were at greater risk of developing DLB (Donaghy et al., 2018; Chahine et al., 2016). Furthermore, a study by Wood et al. (2013) assessed DLB patient's performance on a battery of visual tasks, in which patients showed poorer angle discrimination performance in comparison to AD patients. Impairments in low level visual functions in DLB patients may also be linked to the incidence of visual hallucinations. DLB patients who experience hallucinations may adopt a more 'liberal' threshold for detection of bottom-up sensory information, as these patients appear to have deficits in separating visual signals from noise when presented with a prime (Bowman, 2017).

DLB patients are reported to have impaired visual texture recognition, a mid-level perceptual function (Oishi et al., 2018a). Patients were required to recognise images of materials, such as wood and metal, and were found to be significantly worse than control participants, however this is the only assessment of this nature at present in DLB patients. Other mid-level perceptual processes such as colour discrimination are reported to be impaired in DLB patients in comparison to AD and control patients, in a task associated with ventral visual pathway activation (Woods et al., 2013). Moreover, DLB patients experience greater impairment in colour identification in comparison to AD patients (Flanigan et al., 2018), which has also been related to the incidence of visual hallucinations and visuospatial functions (Matar et al., 2019). DLB patients also showed significant impairment in motion tasks on the same task battery, which remains constant over a 12-month period. In addition, reduced functional activation in the V5 motion area in response to motion stimuli was found in DLB patients (Taylor et al., 2012). In comparison to AD and PD patients, DLB and PDD patients show significantly impaired performance on tasks of dot motion discrimination (Landy et al., 2015). DLB patients also demonstrate impairments in perceiving contours and

have a lower perceptual threshold for contour integration (Metzler-Baddeley et al., 2010; Ota et al., 2015). Similar tasks in the Hooper Visual Organisation Test requiring contour detection in fragmented stimuli also showed disproportionate impairments in DLB patients in comparison to AD patients (Mitolo et al., 2016).

Higher-level visual functions, such as space and object perception are disproportionately impaired in DLB, as evidenced by the Visual Object and Space Perception battery (VOSP) performance (Pal et al., 2016), which may indicate a primary dorsal stream processing impairment. Moreover, DLB patients show decreased functional connectivity between left and right components of the fronto-parietal executive networks which was related to the spatially oriented subtasks of the VOSP task battery, in comparison to controls (Chabran et al., 2018; Uddin et al., 2009). DLB patients show lower processing efficiency of stimuli when completing the Rorschach test – a test in which participants are presented with inkblots and asked to verbally describe what they can see (Kimoto et al., 2017). The Rorschach performance is measured by a derived score called the 'perception and thinking index' (PTI), which reflects cognitive and perceptual distortion. DLB patients show lower PTI, in addition to reporting more unusual details in the stimuli than AD patients, indicating that integrating and organizing incoming information may be problematic. DLB patients also perceive a greater number of meaningful stimuli in ambiguous visual scenes in comparison to AD and controls, indicating a potential over-activation of top-down input to the visual percept (Yokoi et al., 2014; Uchiyama et al., 2012). This phenomenon is also present in idiopathic RBD patients, who report seeing figures, objects or faces when they are not present in stimuli (Sasai-Sakuma et al., 2017). As there is a high conversion of idiopathic RBD to DLB, and RBD is highly predictive of DLB, this may indicate that a perceptual impairment in integrating and organizing information is present in very early DLB. Performance when viewing ambiguous stimuli is also influenced by a primed mood manipulation, with DLB patients reporting significantly more objects that were not present in the stimulus, in comparison to control and AD patients (Watanabe et al., 2018). This indicates that impairment may be abnormal perceptual bias, modulated by mood, as opposed to lower-level sensory deterioration. Findings have also shown a difference in performance between lower and higher level visual perceptual functions, with DLB patients performing worse in the Rey Osterrieth – a complex figure-background segregation task – but with unimpaired performance on the Benton judgement of line orientation task (Robertson et al., 2016). The impaired performance on Rey Osterrieth task was also related to lower occipital-parietal perfusion in comparison to control participants.

#### 1.5.1.3.2 Attention in DLB

Marked impairments in attention and executive functions are present in DLB from very early disease stages (Ciafone et al., 2020) and are related to faster disease progression. More recent evidence suggests that dysfunction in attentional networks responsible for alerting may result in impaired attentional processes, and that a potential disconnection and desynchronization between attentional networks may underpin DLB patients' attention deficits (Firbank et al., 2016; Fuentes et al., 2010). Evidence also suggests that DLB

patients may have executive impairments in the form of a reduction in working memory capacity but may have intact short-term binding abilities (Scullin et al., 2012). Investigations have shown neural correlates for attentional and executive impairments in DLB patients, using the Attention Network Task (ANT; Fan et al., 2002), which was designed to assess the functioning of the alerting, orienting and executive attentional networks (Posner & Petersen, 1990). DLB patients show a reduction in sustained alertness and showed neither orienting or executive network effects without an alerting cue, in comparison to AD and control participants (Fuentes et al., 2010). This suggests that, without external cueing or alerting, patients experience difficulties in allocating attentional resources to stimuli. DLB patients also show higher error rates and longer RT on the ANT, in comparison to controls and AD patients (Kobleva et al., 2017). These findings were related to hypo-connectivity of the dorsal and ventral attention networks, and a reduction in connectivity between these networks and frontal regions in DLB patients, using fMRI. DLB patients also have a reduction in white matter volume in the lateral occipital cortex, which was correlated with an impairment in orienting network activation (Cromarty et al., 2018). This suggests that impaired orienting may be in part due to impairments in visual functioning.

In summary, there is evidence that attention and perceptual functions are impaired in DLB patients, but that these may be specific to certain functions within the processing hierarchy rather than general impairment. Previous tasks have typically used less sensitive measures of assessment, such as clinical task batteries than may not provide a detailed characterisation of decline in specific visuo-perception and attention functions. Therefore, this thesis aimed to design a task battery which was suitable for DLB patients to complete and assessed perceptual function at different stages of the hierarchy in a sensitive manner by using when possible adaptive stair-case procedures (see Chapter 3). Moreover, some results suggest that perceptual and attentional functions could be related to clinical symptoms, which this thesis also aimed to address by measuring cognitive fluctuations and visual hallucinations.

#### 1.5.1.4 Brain changes in DLB

Brain changes have been reported in DLB, typically in comparison to patients with AD, PD, or normal ageing. Limited studies have investigated the microstructural changes that occur in DLB, and even fewer have reported metabolic brain changes. These studies are discussed below.

##### 1.5.1.4.1 Structural changes in the brain in DLB

Whole brain atrophy at early stages is not as diffuse in DLB as in other dementia disorders notably AD with preservation of medial temporal lobe structures being a defining clinical feature in the DLB profile (Burton et al. 2009). However, further findings have suggested that changes in the hippocampus may still be present in DLB, but are more specific, showing preservation of the cornu ammonis and subiculum, but atrophy in the perirhinal and parahippocampal cortex (Delli Pizzi et al., 2015). Less specific structural changes in the cortex are also present in DLB, such as reduction in GM volume in the posterior and parietal

regions (Watson et al., 2017), superior temporo-occipital and lateral orbito-frontal regions (Lebedev et al., 2013), and the substantia inominata and dorsal mesopontine area (Whitwell et al., 2007). Moreover, greater occipital and striatal GM reductions (Lee et al., 2010) and temporo-parietal GM reductions (Beyer et al., 2007) in DLB have been reported in comparison to patients with PDD, showing specificity of these volumetric changes. Reductions in precuneus and inferior frontal lobe GM volume have also been correlated with visual hallucinations in DLB (Sanchez-Castaneda et al., 2009), but not in PDD.

#### 1.5.1.4.2 Microstructural changes in the brain in DLB

In contrast to AD, there is only limited evidence with regards to white matter microstructural changes in DLB. Some studies have found DLB related changes in microstructural parameters in parieto-occipital white matter in comparison to AD patients (Watson et al., 2009, 2012) and lower FA in the insula and posterior cingulate cortex (Lee et al., 2010). White matter alterations in the inferior longitudinal fasciculus have also been observed (Kantarci et al., 2010; Mak et al., 2014; Ota et al., 2009). These whole brain analysis findings have been supported by tractography based analyses, which have reported reduced FA in the inferior longitudinal fasciculus (ILF), posterior thalamic radiation (Watson et al., 2012) and occipito-frontal fasciculus (Kiuchi et al., 2011), suggesting tracts related to visual functioning experience particular degeneration in DLB.

Subcortical white matter changes are also present in DLB patients in the left thalamus and pons (Mak et al., 2014; Watson et al., 2012), in addition to reductions in FA in the precuneus (Firbank et al., 2007). Widespread cortical MD has also been reported in DLB in the brainstem, thalamus, frontal, parietal, temporal and occipital lobes, which showed a similar pattern to patients with AD (Watson et al., 2012). MD in the parahippocampal and cingulate regions also showed correlation between episodic memory impairment in DLB patients, and MD in the subcortical regions and tracts in the parietal lobes showed a correlation with poorer letter fluency in DLB (Watson et al., 2012). In contrast, alterations in frontal and parietal FA showed a relationship with letter fluency performance and FA in the subcortical structures showed a relationship with parkinsonism in DLB patients (Watson et al., 2012).

#### 1.5.1.4.3 Metabolic changes in the brain in DLB

Variable and very limited findings have been reported in DLB patients' metabolic brain changes in vivo. NAA levels were reported to be comparable to healthy older adults in some instances (Kantarci et al., 2004; Mak et al., 2014), but were also reportedly lower in the thalamus in comparison to AD (Delli Pizzi et al., 2015), and reduced in the posterior cingulate and hippocampus in MCI-DLB (Tumati et al., 2013). Normal myoinositol levels in DLB patients have also been reported (Kantarci et al., 2004), however more recent investigations show raised myoinositol in the posterior cingulate cortex (Tumati et al., 2013). Finally, choline and creatine are higher in patients with DLB (Mak et al., 2014), with increases found in the right thalamus in comparison to AD patients, which has also been linked to severity of cognitive fluctuations.

## 1.6 Research questions

The main objective of this research was to establish the profile of attention and perception differences that occur in healthy ageing compared to young adults and how these relate to macrostructural, microstructural and neurochemical changes in the brain. More specifically, in the following empirical work I will characterise which cognitive processes, brain regions and modalities experience age-related decline or maintenance and how this informs theories of cognitive ageing. My research then aims to extend this approach to DLB patients, which provides a comparison with pathological ageing in which specific perceptual and attentional impairments are present. With an increasingly ageing global population it is important to gain further insights into the underpinning mechanisms of such changes. On one hand because such insights may help inform the development of interventions to optimising cognitive resources in older age, and on the other because they may aid our understanding of early warning signs of neurodegenerative processes such as those associated with DLB. By characterising perceptual and attentional processing decline and related brain changes in normal ageing, this research may then aid early differential diagnosis of the pathological processes affecting the brain and cognition that are witnessed in DLB. Moreover, the neural underpinnings of age-related changes in vision and attention have not been assessed using both advanced diffusion imaging and MR spectroscopy including GABA. Whilst much research has focused on age-related changes in memory and processing speed, accumulating evidence suggests that older adults are also susceptible to changes in visual perception and attention, but the neural underpinnings of these changes are not well understood. Age-related changes in standard MRI measures of white and grey matter morphology and microstructure based on DTI are well-documented. However, these measurements are limited with regards to the inferences about biological processes underpinning age-related brain changes. More advanced magnetic resonance imaging and magnetic resonance spectroscopy techniques that allow the quantification of brain metabolites and microstructural properties beyond DTI-based indices promise to provide further insights into the nature of age-related brain changes.

Initially, this study was designed to focus on perceptual and attentional decline and associated neural correlates in DLB patients in comparison to healthy older adults, which had not previously been done in one detailed psychophysical and MRI study. As such, elements of the study design such as MRI protocol and visual and attention tasks were tailored to consider the ability of patients. However, as the recruitment of suitable DLB patients turned out to be very challenging, a substantial portion of the thesis will be devoted to age-related differences in visual perception and attention and their neural underpinnings. The novel aspects of this thesis lie in a comprehensive assessment of age-related differences in perceptual and attentional functions at different levels of the visual hierarchy (Chapter 3) as well as by studying their neural correlates with advanced spectroscopy and diffusion MRI methods (see Chapter 4). In addition, I investigated whether age-related differences in different brain modalities could predict performance differences between younger and older adults, the results of which are reported in Chapter 5. Moreover,

both cognitive and brain differences in the same regions were assessed in a small number of DLB patients and are compared with healthy ageing in Chapters 3 and 4.

I also aimed to investigate the nature of age-related differences in processing speed and decision-making in further detail using diffusion drift model approaches in Chapter 6. Such model-based approaches have suggested that cognitive changes in healthy ageing follow a profile, in which older adults become slower and more cautious in their responses, and also experience difficulty in perceptual processing. However, it remains unknown how these changes in processing speed parameters relate to changes in the ageing brain, specifically metabolic changes. The work in this thesis therefore aimed to establish how decision-model parameters of healthy ageing relate to changes in the brains of older adults. By doing so, I hope to achieve a more specific understanding of how declines in processing speed in older age occur, and how this may be related to brain ageing. In addition, this may highlight neural changes which are susceptible to particular decline, which may be relevant both clinically, and in the understanding of healthy ageing. To the best of my knowledge, the drift diffusion model has not been applied to investigate the nature of RT changes in DLB patients, despite evidence which has related decision model parameters to visual hallucinations in other disorders (O'Callaghan et al., 2017). To address this, in Chapter 7 I applied the drift diffusion model to RTs from DLB patients from the LewyPro cohort (Donaghy et al., 2018) and investigate how the outcome parameters may be related, or underlie, clinical symptoms such as complex visual hallucinations. By doing so, I hope to further understand specifics of cognitive decline in DLB and how they may relate to clinical symptoms notably visual hallucinations.

# Chapter 2 : Magnetic Resonance Imaging methods in the study of ageing

## 2.1 Chapter overview

Despite the large body of literature investigating neural changes that occur in ageing, research which considers multiple modalities of neuroanatomical changes within one study are limited. Notably, evidence regarding the relationship between neurochemical and cognitive changes in ageing is sparse. Given that normal ageing is a multifaceted phenomenon and is therefore supported by distributed brain networks, in order to gain a more complete understanding of the processes underlying cognitive ageing ideally one would seek to characterise age-related changes using multimodal techniques. As ageing is typically associated with widespread reductions in white matter microstructural integrity (Bartzokis et al., 2004), and some studies suggest that microstructure may be related to metabolic changes (Chiappelli et al., 2015; Reid et al., 2016) but little is known about these changes with age, I chose to employ these two main modalities. The present research focused on studying age and disease-related differences in structural and metabolic properties of brain networks underpinning visual perception and attention with magnetic resonance imaging (MRI) at 3 Tesla. This consisted of high-resolution T1 weighted anatomical images for morphological measurements (cortical thickness, volume), multi-shell diffusion-weighted imaging (DWI) to quantify white matter microstructure and magnetic resonance spectroscopy (MRS) to investigate neurochemical changes in key brain metabolites. This chapter will provide a brief introduction into the basic concept of MRI, and the more advanced applications of multi-shell DWI and MRS which were employed in this thesis to achieve a comprehensive characterisation of the macro and microstructural, and bio-metabolic profile of normal ageing.

## 2.2 MRI overview

MRI is a non-invasive medical imaging technique that allows the collection of three-dimensional anatomical images as well as the quantification of estimates of biophysical tissue properties. It uses magnetic fields and radiofrequencies, as opposed to ionising radiation used in other forms of clinical imaging. MRI capitalizes on the magnetic property of hydrogen atoms - the spin of a charged hydrogen particle – to induce a magnetic moment known as nuclear magnetic resonance (NMR). By applying a strong external magnetic field ($B_0$), the atomic hydrogen nuclei are aligned parallel with, or perpendicular to, the external field (Grover et al., 2015). The hydrogen protons spin around the long axis of $B_0$, which the greatest proportion of nuclei align parallel to. This is referred to as precession, the rate of which is the Larmor frequency described below (Equation 2.1).

$$\omega_0 = \gamma B_0 \tag{2.1}$$

Where $\omega_0$ = precessional or Larmor frequency (MHz), $\gamma$ = gyro-magnetic ratio (MHz/Tesla), and B0 = magnetic field strength (Tesla). When protons precess together, they are said to be 'in phase', and Larmor frequency changes in proportion to magnetic field strength.

Gradient coils generate secondary magnetic fields in the x, y and z axis of the bore, and eventually allow for spatial encoding of images, or localisation. Nuclei can then be excited within this external field by applying a radiofrequency (RF) pulse ($B_1$) with the same precession frequency. This causes some protons to flip to a higher energy state, decreasing longitudinal magnetisation and synchronises the protons to be 'in phase'. In turn, this induces transverse magnetisation in which the net magnetisation vector of the protons becomes perpendicular to B0. The RF coil then measures the time taken for relaxation of the protons to their equilibrium state. Relaxation is measured either in the longitudinal (T1) direction on the z-axis, parallel to B0 or in the transverse direction (T2), perpendicular to B0 on the x-y axis. Relaxation time varies dependent on tissue composition and relaxation direction, with water molecules taking longer to relax in T1 and T2. The absorption of energy during this process causes a transition between higher and lower energy states, inducing a voltage which is detected by a tuned coil of wire. This is known as the 'free-induction decay' (FID) and is variable depending on the tissue type containing the nuclei, the strength of $B_0$, and the application of the RF pulse(s). The amplitude and duration of these gradients then determine how information is read in the frequency domain. Multiple echoes or FIDs are typically obtained, depending on scan acquisition, which are then signal averaged and converted into k-space, the temporary space for storage of digitised MR signals. K-space is then translated into a spatial domain using Fourier transform to display an image or the frequency domain to display a spectrum in the case of magnetic resonance spectroscopy (Grover et al., 2015) (Figure 2.1).

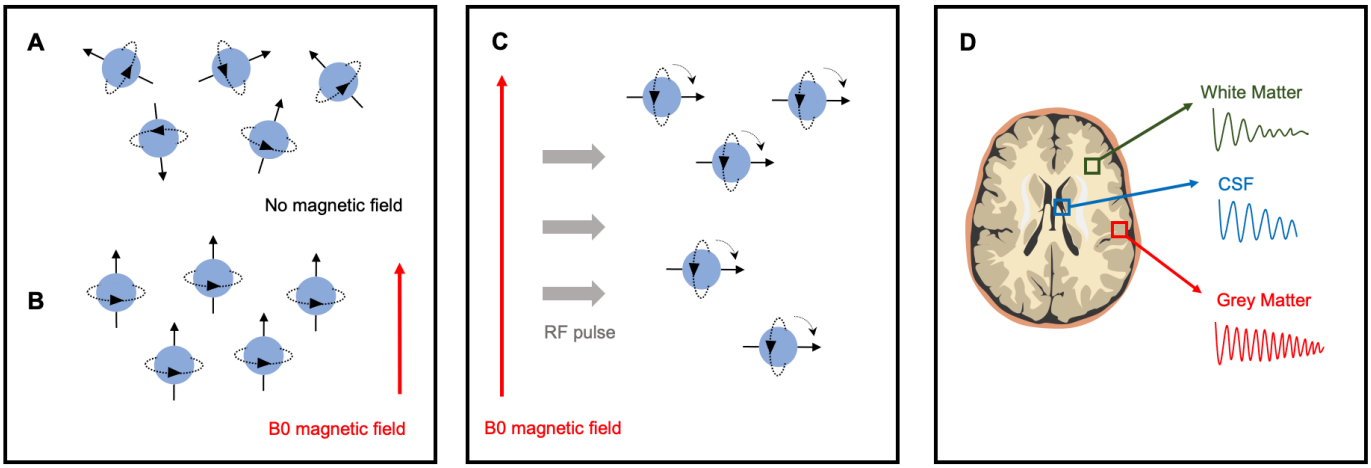


Figure 2.1 Molecular representation of the acquisition of MR images (A) protons in the body go from randomly precessing to aligning with the B0 magnetic field (B). (C) protons absorb radio-frequency (RF) energy and 'flip' their orientation away from the B0 field. (D) Signals from different tissues have different properties which can be quantified based on their relaxation properties.

MRI can be utilized in several ways in order to measure different metrics within the brain. These include measuring diffusion of water in the brain as a proxy estimate of microstructural integrity, measurement of neurochemistry in the brain, measurement of oxygenated blood flow as a proxy of neural activity, in addition to estimating structural thickness and volume. For the purpose of the current thesis, I chose to focus on grey matter thickness and volume, white matter microstructure and neurochemistry. These metrics were selected on the basis of previous literature which suggests changes or depletion of certain microstructural, neurochemical and grey matter elements are present in age in regions which are typically involved in visual perception and attention.

## 2.3 MR Spectroscopy

MR Spectroscopy (MRS) is a non-invasive MR technique which is employed to quantify metabolites in the brain in vivo. Where MRI is predominantly concerned with the collection of tissue data to form anatomical images and quantify tissue properties, MRS refers to the techniques employed to acquire frequency spectra to assess the biochemical composition of tissues in a selected brain region. Each MR-visible metabolite in the brain produces a unique signal in the MRS spectrum due to the differences in the environment of the individual spins. Metabolites can produce several resonances at different frequencies based on their nuclear structure and can be characterised by the degree of frequency separation from one another or chemical environment (Jansen et al., 2006). Water nuclei are ~10,000 times more abundant than those of metabolites of interest in MRS, meaning that the water signal dominates the frequency spectrum. By suppressing signals typically obtained from water within the tissue, MRS allows us to determine a quantifiable spectrum which illustrates the concentration of a number of smaller metabolites naturally present in tissue. As the metabolite signals are plotted on the spectrum with the y-axis indicating the amplitude of the signal and the x-axis indicating the frequency, metabolites can be easily identified at higher field strengths and quantified by calculating the area-under its peak as a measure of abundance in the voxel (Stagg & Rothman, 2013, Figure 2.2.).

### 2.3.1 MRS methodology

MRS is based on the principle that there is a variation in the frequency of hydrogen protons depending on their chemical environment. This occurs due to J-coupling and chemical shift (Stagg & Rothman, 2013). As each molecule has a different structure, they are able to be distinguished from each other based on these unique frequencies. Chemical shift occurs when protons experience differing electron shielding (i.e. either electrons are drawn closer to or pushed further from the hydrogen proton) within a molecule, causing the frequency of the spin to alter. The electrons shield protons from the external B-field, reducing the 'effectiveness' of the field. This reduces the frequency of precession, which is proportional to $B_0$. The chemical shift is expressed in units of parts per million (PPM), which also allows the identification of metabolites based on their ppm position on the x-axis of the MRS spectra. J-coupling is an interaction

between a molecule's hydrogen atoms, mediated through chemical bonds and can cause peak splitting and modulation (Stagg & Rothman, 2013).

As spatial frequency-encoding is reserved for identifying chemical shifts between different metabolites, there are several techniques which are available to determine the location of signal during MRS. Most commonly employed is the single voxel spectroscopy (SVS) technique, which uses RF pulses in addition to gradients in three planes, defining a three-dimensional cuboid voxel encapsulating an anatomical region as the source of the signal. RF pulses applied during acquisition select a single slice in each plane and the intersection of these planes is where the signal from the spin frequencies of protons is measured (Stagg & Rothman, 2013).

As water is the source with the greatest volume of hydrogen protons within the brain, water suppression is required to visualise an MRS spectrum containing other metabolites which are present at much lower concentrations (at millimolar level). This typically involves applying an RF pulse at the same resonance frequency as water to excite these protons, and a strong B-field gradient to minimize the water signal during visualisation (Stagg & Rothman, 2013).

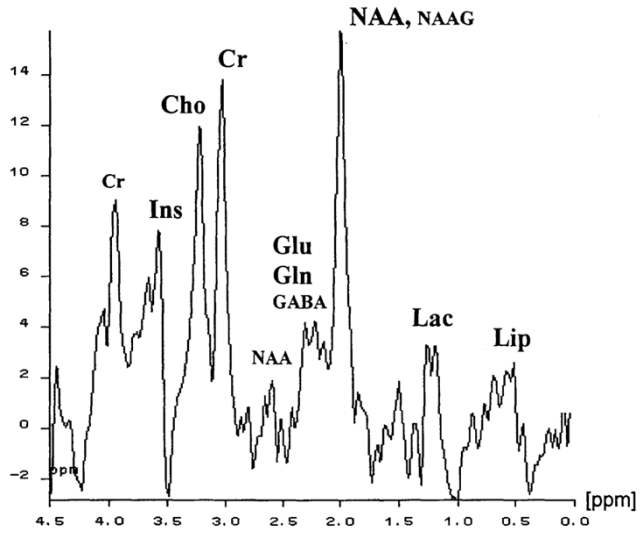


Figure 2.2 Chemical spectra acquired during MRS. Frequency position (x-axis) of the metabolic peaks on the spectra identifies different metabolites of interest reliably and can be quantified in millimolar (y-axis) (adapted from Hájek et al., 1998). Cr = creatine, Ins = myoinositol, Cho = choline, NAA = N-acetyl-aspartate, Glu = glutamate, Gln = glutamine, GABA = gamma amino-butyric acid, Lac = lactate, Lip =lipid.

### 2.3.2 Metabolites

Within the MRS obtained spectra, three major peaks are often identified, representing the concentrations of N-acetyl-aspartate (NAA), creatine (Cr) and choline (Cho), in addition to smaller peaks of myo-inositol (mI) and neurotransmitters glutamate/glutamine (Glx) and γ- aminobutyric acid (GABA), amongst some others (Figure 2.2).

To quantify metabolites the area under the spectral peak is used (Figure 2.2). However, the area under the peak is not a direct measure of metabolite concentration, and is influenced by relaxation values of each metabolite, type of pulse sequence and inhomogeneities in the $B_0$ and $B_1$ field. In addition, as MRS resonance overlap and have complex splitting patterns, quantifying area under the peak does not provide metabolite concentration. Therefore, the spectral curve fitting to quantify metabolites must involve applying a model which contains advanced prior knowledge regarding spectral location and line shape of expected metabolites. These algorithms can provide only relative metabolite concentrations, therefore an internal reference standard from another concentration such as tissue water can be used to estimate brain metabolites by comparing their peak area ratios to the area of water or other reference chemicals which are relatively stable (Jansen et al., 2006). In clinical applications of MRS, often the ratios of metabolites are used as opposed to absolute metabolite concentrations (Safriel, 2005), in order to establish a range of relatively stable values from which other metabolic concentrations can then be compared. Creatine is often used as a reference value from which to provide a ratio, as it is relatively stable in many clinical populations, however in AD and PD, creatine levels have been reported to be significantly different to normal controls (Firbank et al., 2002). Moreover, other studies have used brain water as a reference value in AD and PD populations (Huang et al., 2001, Schuff et al., 1998) successfully, thus I selected brain water as a more stable reference for comparing healthy younger, older and DLB patients.

Moreover, due to comparisons between healthy and patient samples, relative concentrations on metabolites were variable, which would hinder any conclusions made from reported pure ratios such as GABA/Cr. Considering this, the concentration of metabolites (M) were calculated using Equation 2.2, where R= known concentration of brain water, Sr = signal of reference, Sm = signal from metabolite and C = correction factor. This allowed me to determine an amplitude of each metabolite using brain water as a reference signal, which are the final metabolic concentration values reported throughout this thesis.

$$M = R \times C\ (Sm/Sr) \tag{2.2}$$

Specific pipelines used in peak fitting will be discussed in experimental methods (Chapter 4). Brain metabolites of interest which were quantified in this thesis are discussed in the following sections.

#### 2.3.2.1 N-acetyl-aspartate (NAA)

NAA, the largest peak in the MRS spectrum, is a compound present in neurons. NAA is the acetylated form of aspartate, typically occurring in concentrations between 10 – 20 Mm (Rae, 2014). The exact role of NAA in the brain is somewhat disputed. It is often viewed as a marker of neuronal density or viability, due to its apparent role in energy metabolism in neuronal mitochondria (Lu et al., 2004). However, other hypotheses consider NAA to be involved in regulating the release of neurotransmitters (Rae, 2014) and also in myelin synthesis in oligodendrocytes (Rae, 2014). In general, NAA is considered to be a marker of

neuronal health, which arises from the former hypotheses, as well as from observations of an inverse relationship between NAA and atrophy, and NAA reductions in disorders such as dementia, stroke and multiple sclerosis (Moffett et al., 2013). Lower NAA has been linked to generalized cognitive dysfunction (Mathiesen et al.,2006), while increased concentrations of NAA in frontal regions were shown to be related to improved executive performance (Grachev et al., 2001).

#### 2.3.2.2 Creatine

Creatine, involved in energy metabolism, is relatively abundant in the brain and on the MRS spectrum represents the creatine kinase/ phosphocreatine energy shuttle, a way in which a cell generates ATP (Stagg & Rothman, 2013). In fact, the synthesis of ATP is not possible without creatine, which in turn allows immediate energy release and/or resynthesis of ATP when required (Turner & Gant, 2013 in Stagg & Rothman, 2013). Creatine also acts as a buffer to maintain intracellular ATP at the required level and is higher in glia than neurons suggesting a role in glial function (Urenjak et al., 1993). Creatine supplementation has been seen to improve performance on tasks requiring working memory and long-term memory particularly in the elderly (McMorris et al., 2007), however this has not been shown in younger adults (Rawson et al., 2008). In contrast, elevated regional creatine in the hippocampus and frontal regions in older adults predicted poorer visuospatial working memory performance (Lind et al., 2020), suggesting a complex relationship between glial-related biochemistry in older age and cognitive outcomes.

#### 2.3.2.3 Choline

Choline often occurs in low concentrations in the healthy brain, however can be elevated in disease involving both inflammation and demyelination due to its role in cell-membrane signalling (Zeisel & da Costa, 2009). Choline has a complex role in several important neural processes. Most notably, it is the precursor for acetylcholine which is one of the most abundant neurotransmitters in the brain primarily concerned with maintaining homeostasis and governing necessary autonomic functions. In addition, choline is present in the metabolism of some cancers and acute neurological degeneration such as stroke (Stagg & Rothman, 2014). The choline peak on MRS at 3.2 ppm represents choline containing compounds, free choline and phosphorylated choline which are markers of cellular density, cell wall turnover and cellular metabolism (Miller et al., 1996; Lin & Gant, 2014 in Stagg & Rothman, 2014). As such, choline represents structural integrity and efficient signalling of cells, however pathological states may lead to unusually elevated choline levels and cognitive impairment. Raised choline in frontal brain regions is also related to poorer working memory performance (Lind et al., 2020).

#### 2.3.2.4 Myoinositol

Myoinositol is often viewed as a marker of astrocytic health, with decreased myoinositol occurring in chronic processes such as ischemia. Myoinositol has been proposed as a marker of glial cell proliferation as it tends to be contained within glia and has been demonstrated to be selectively taken up by glial cells in

comparison to neurons (Glanville et al., 1989). Elevated myoinositol levels have been observed in conditions such as AD and Huntington's disease, also presenting the hypothesis that myoinositol is an early MRS marker for neurodegenerative disease. To this end, it has also been suggested that myoinositol could be recruited in the monitoring of disease progression or response to treatment in mild cognitive impairments (Stagg & Rothman, 2014). Increases in myoinositol are also related to generalised cognitive decline in age or mild cognitive impairment, and are thus of interest in this thesis (Kantarci et al., 2013).

#### 2.3.2.5 Glutamate/ Glutamine (Glx)

Glx is the combined signal of glutamate, the brain's major excitatory neurotransmitter, and glutamine which is the product of glutamate reuptake by astrocytes. Glutamate and glutamine are combined into Glx due to difficulties in separating the peaks at lower field strengths. Glx is often found to be raised in acute brain diseases, such as epilepsy (Stagg & Rothman, 2014). The Glx peak has been used as a marker of glutamatergic neurotransmission. Any changes to the Glx peak may reflect a dysregulation in neurotransmitter functioning, and thus metabolic dysfunction in neurons or astrocytes (Stagg & Rothman, 2014). Moreover, as glutaminase – the enzyme which catalyzes the breakdown of glutamine to form glutamate - is present in the mitochondria it is purported that a change in the Glx peak may also reflect mitochondrial dysfunction. Related to cognition, higher Glx in the prefrontal cortex is related to improved task learning (Lacreuse et al., 2018) in non-human primates, and increased generation of mental representations (Huang et al., 2015). Furthermore, Glx in the posterior cingulate is positively correlated with performance in a word learning task (Riese et al., 2015). Taken together these findings suggest a role for Glx in mitochondrial functioning and in effective cognition including learning and mental imagery.

#### 2.3.2.6 GABA

GABA is the major inhibitory neurotransmitter in the brain present in interneurons. GABA in the brain is involved in synaptic vesicles and neurotransmission, and also in the cytoplasm in metabolic processes. It is difficult to distinguish the different GABA signals in the whole MRS voxel and rather GABA on MRS is interpreted as a measure of tonic inhibition (Harris et al., 2015). As well as acting as a key neurotransmitter, GABA plays a role in influencing synaptic plasticity and it has also been seen to underlie interindividual differences in behaviour. GABA acts as a 'shunt' in the metabolic cycle, but also as a neurotransmitter and a neuromodulator via two major families of GABA receptors; $GABA_A$ and $GABA_B$. GABA is involved in motor control and has been observed to increase in levels in the motor cortex during motor task learning (Floyer-Lea et al., 2006). Activation of GABAergic interneurons in the rodent visual cortex have also been shown to sharpen feature selectivity and enhance visual perceptual discrimination (Lee et al., 2014). Furthermore, higher concentrations of somatosensory GABA has been associated with enhanced perception and more selective cortical tuning, emphasising the importance of GABA in effective visual perception (Kolasinski et al., 2017).

GABA has also been widely linked to cognitive functioning, particularly occipital GABA in the encoding of sensory information (Schmidt-Wilcke et al., 2018) orientation and size (Song et al., 2017) visuospatial intelligence and surround suppression (Cook et al., 2016). Moreover, frontal cortical GABA is also related to working memory (Yoon et al., 2016) and impulsivity (Boy et al., 2011). Interestingly, individual differences in baseline GABA have also been seen to predict behavioural performance (Duncan et al., 2014).

Evidence has also demonstrated the role of frontal cortical GABA in attentional processing (Pehrson et al., 2013) and PFC GABA in impulse control (Paine et al., 2015) and sensitivity to distractors during attention tasks in rodents (Auger et al., 2017). A number of studies also investigate the role of GABA in attentional function in patients with impulsivity disorders (Edden et al., 2012; Ende et al., 2016) and visual attentional function in patients with schizophrenia (Wassef et al., 2003; Yoon et al., 2010). However, to date this relationship has not been measured in healthy older adults in vivo.

### 2.3.3 PRESS and MEGA-PRESS

The concentration of these metabolites is determined by the amplitude of the peak and identified by their position along the spectrum. For example, NAA can be reliably identified at a chemical shift of 2.0. The most popular method for MRS is a single voxel spectroscopy (SVS) method, point resolved spectroscopy (PRESS), which utilises 3 RF-pulses applied in conjunction with a magnetic field gradient at x, y and z direction and generates a spin echo signal (Jansen et al., 2006). The PRESS method, developed by Bottomley (1987), involves a double spin-echo sequence, consisting of 90-degree excitation RF pulse, and two 180 degree refocusing RF pulses. These are applied in conjunction with magnetic field gradients which restrict pulse effects to a localised volume (voxel) to allow for in vivo acquisition of the chemical spectra. However, metabolite signals often overlap meaning that some more abundant metabolites may obscure signals from more limited metabolites, or some metabolites are difficult to quantify (Puts & Edden, 2012). In particular GABA, the brain's major inhibitory neurotransmitter can be obscured due to its lower peak and appearance at three locations along the chemical shift axis. As such, the standard PRESS method is not able to optimally quantify GABA. It is possible to compensate for these phenomena, by applying two frequency selective pulses which affect one of the signal peaks arising from J-coupling. If two sequences are acquired, one with the editing pulse and one with a pulse applied elsewhere on the spectrum, the difference between these two spectra will give a measurement of only signals which are affected by this selective pulse. This removes the strong overlapping signals from the spectrum and allows us to observe GABA concentrations, and thus provides the basis for popular MRS acquisition sequences such as Mescher-Garwood PRESS (MEGA-PRESS; Mescher et al., 1998, Figure 2.3).

The MEGA-PRESS acquisition involves two scans which are interleaved (Fig 2.4). Firstly the 'ON' scan is acquired which applies a frequency-selective RF pulse to GABA at 1.9ppm, affecting the GABA spins at

3.0ppm. Secondly the 'OFF' scan is acquired which applies an RF pulse at a frequency which does not affect the GABA signal (Mullins et al., 2014). The ON spectrum is subtracted from the OFF spectrum to result in an edited spectrum consisting of GABA signal at 3.0ppm, signals close to 1.9ppm and Glx at 3.75ppm from which GABA at 3.0ppm can be isolated and quantified (Mullins et al., 2014). This peak is referred to as GABA+, as there are other signals included in the measurement from macro-molecules and glutathione which are co-edited. However, throughout this thesis this will be referred to as GABA when referencing GABA measured using MRS in the literature, and GABA/$H_20$ when referencing the results from this work. However, it should also be noted that the presence of macro-molecules in the GABA signal may be a significant confound in the interpretation of GABA/$H_20$ concentrations in both ageing and in relation to cognitive performance within this thesis. As there are clear benefits in employing MEGA-PRESS in the acquisition of a GABA signal, I used MEGA-PRESS to quantify GABA and PRESS to acquire a signal from other metabolites of interest.

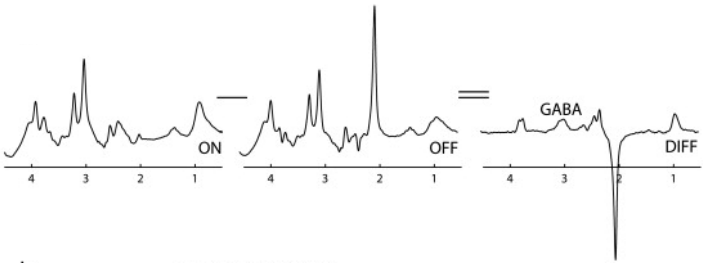


Figure 2.3 MEGA-PRESS editing technique for the acquisition of GABA. Subtracting 'OFF' scans from edited pulse 'ON' scans removes any overlying signal, providing a gamma-amino butyric acid (GABA) signal in the difference 'DIFF' spectrum (adapted from Mullins et al., 2014)

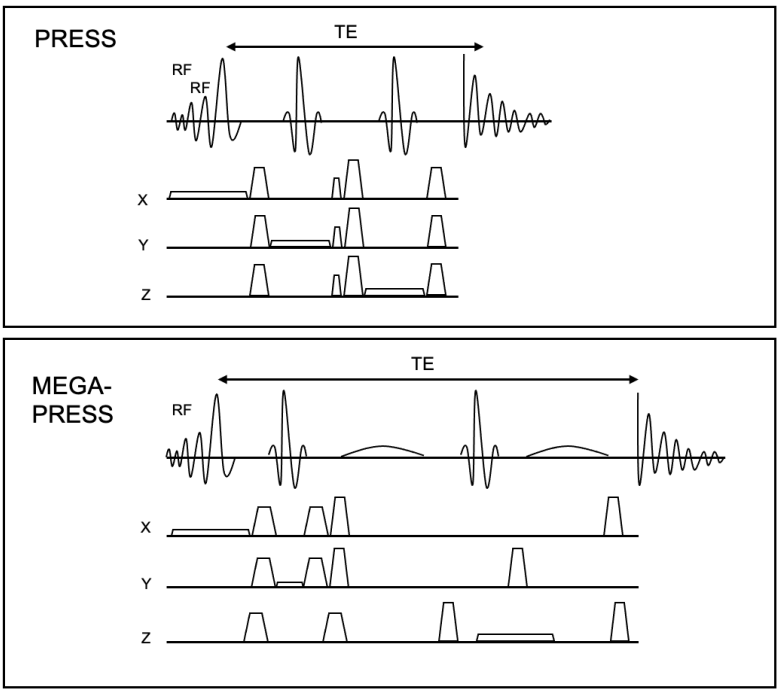


Figure 2.4 PRESS and MEGA-PRESS pulse sequences for the MR acquisition of metabolic spectra and GABA signal. X, y and z represent magnetic field gradients. MEGA-PRESS shows addition of edited pulses around the second 180-degree pulse. TE= echo time, RF = radio-frequency. Adapted from Mullins et al. (2014).

Previous research has used one voxel when employing MRS methods, most often in the occipital cortex due to long scan times. For this research, I sought to characterise the metabolic profile of visual perception and attentional systems in older age. As such, I selected three regions which would enable an estimation of metabolites in these networks. These were; the occipital cortex involved in visual function, the posterior parietal cortex involved in higher vision and attention and the anterior cingulate cortex involved in attention and executive functioning.

These regions have previously been selected in the characterisation of GABA using MEGA-PRESS (Bai et al., 2015; Bhagwagar et al., 2008; Duncan et al., 2019; Simmonite et al., 2019) and allowed us to acquire sufficient signal from ON/OFF spectra which can be challenging in some cortical regions due to presence of cerebrospinal fluid (CSF), proximity to scalp or depth of subcortical region. I also chose to use larger voxels, which allows for improved signal to noise ratio but in turn compromises on some anatomical specificity (for example, the occipital voxel largely includes the visual cortices 1-3). Voxel size and anatomical location were piloted, with the original sequence including voxels in the thalamus and PFC. Unfortunately, poor signal was acquired from the thalamic voxel due to its' subcortical location and number of head coil channels meaning this voxel was not included. Similarly, due to time constraints in the acquisition of GABA coupled with multi-shell diffusion imaging, the PFC voxel was also omitted from the sequence. Time was important in acquisition, as the sequence was designed to be manageable for patients, therefore this compromise was reached.

## 2.4 Diffusion MR

### 2.4.1 Diffusion-weighted magnetic resonance imaging

Diffusion-weighted imaging (DWI) is a widely used MRI technique that exploits the random thermal motion of water molecules (Brownian motion or diffusion) in the brain. DWI techniques apply magnetic field gradients of different orientations to measure apparent water displacement in three dimensions (Jones et al., 1999). Diffusion of water molecules along a gradient causes the MR signal to be lost in that direction. By measuring signal attenuation along gradients of different orientations, it is possible to characterise diffusion processes along those gradient directions. As the diffusion process of water molecules is influenced by the surrounding tissue properties and architecture, DWI allows the probing of tissue microstructure and the visualisation of white matter pathways. For instance, in CSF filled spaces, water molecules can move freely in all directions and will hence display isotropic diffusion during the time of a typical DWI experiment. In contrast, in highly organised structures such as tightly packed white matter bundles, diffusion of water molecules will be hindered perpendicular to the bundle by axonal membranes and myelin sheaths while diffusion will be relatively unhindered along the bundle's length, resulting in anisotropic diffusion. Thus, diffusion anisotropy can be estimated by observing the degree of loss in the MRI signal when the orientation, strength (G), duration (d) and separation time (D) of gradient pulses are

manipulated. Together, these parameters combine to the b-value (s/mm$^2$) that is described by the following equation (Equation 2.3) (Stejskal & Tanner, 1965).

$$b = g^2d^2G^2(D-d^3) \quad (2.3)$$

With g representing the gyromagnetic ratio of hydrogen protons. The larger the b-value the larger the degree of signal loss in DWI and the lower the Signal to Noise Ratio (SNR) on standard 3T MRI systems. Higher b-values allow probing water displacements in highly restricted compartments such as intra-axonal/cellular spaces (Assaf & Basser, 2005).

As images acquired with linear tensor encoding only capture the water displacement along the direction of the applied gradient, it is important to sample multiple different gradient directions to obtain sufficient information about the directionality of fibres (Jones, 2004). For instance, it has been shown that at least 30 unique and evenly distributed gradient orientations are required for a robust estimation of diffusion tensor-based indices of fractional anisotropy and diffusivities and to ensure that the variance in these measurements is independent of the gradient orientations (Jones, 2004). Furthermore, the directional information of the diffusion process gained in this way can be used to reconstruct diffusion streamlines that create visual displays of the underlying white matter fibre bundles. This approach is called tractography and is further detailed below.

### 2.4.2 Analysis of DWI data: The diffusion tensor model

The diffusion tensor imaging (DTI) model has been the most influential and widely employed model to analyse DWI data (Basser et al., 2000; Catani et al., 2002; Conturo et al., 1999). DTI assumes a Gaussian displacement of diffusion with a set of tensor eigenvalues reflecting the magnitude and their eigenvectors reflecting the direction of diffusion (see Figure 2.5). The shape of the tensor represents the degree of diffusion anisotropy in a given region of interest. For instance, it's shape will be sphere-like when diffusion is isotropic and cigar-shaped when it is anisotropic (Basser, 1995; Basser & Jones, 2002; Basser et al., 1994). The diffusion tensor can be described by a 3 x 3 symmetric matrix (D) that describes the diffusion displacement in the three-dimensional space (Equation 2.4).

$$D = \begin{matrix} Dxx & Dxy & Dxz \\ Dxy & Dyy & Dyz \\ Dxz & Dyz & Dyy \end{matrix} \quad (2.4)$$

Based on the diffusion tensor matrix, a number of indices can be derived that describe the underlying diffusion properties (Basser et al., 1994). Notably, these include the "mean square displacement" of diffusion that can be estimated by averaging the three diffusion tensor eigenvalues, giving the mean diffusivity (MD). Lambda 1 ($\lambda 1$) or axial diffusivity as it is referred to in this thesis (L1) (Figure 2.5) describes

the diffusivity along the principal orientation of the tensor whilst radial diffusivity (RD) the average of Lambda 2 and 3 refers to the diffusivity perpendicular to the principal orientation. Fractional anisotropy (FA) is a metric thought to reflect the degree of fibre coherence or directionality and can be described as the relative ratio between L1 and RD (Acosta-Cabronero & Nestor, 2014). FA approaches 0 in isotropic and 1 in anisotropic conditions.

When making inferences about white matter microstructural properties from DTI indices, it is important to consider that these indices are not only influenced by biological properties of white matter such as axon density, diameter and myelin but also by the orientational complexity and organisation of the fibre architecture (Beaulieu & Allen, 1994). Thus, it is not possible to interpret differences in FA and diffusivity metrics in terms of any specific biophysical property of white matter (Jones, 2010; Wheeler-Kingshott & Cercignani, 2009). Furthermore, the DTI model makes the assumption of Gaussian diffusion, and only defines a single tensor for each voxel, while a typical MRI voxel contains several thousands of axon fibres with multiple fibre orientations (Jeurissen et al., 2011). The fibre architecture in most voxels in the brain is hence highly complex and contains crossing, kissing or fanning fibres that result in non-Gaussian diffusion, so that the DWI signal cannot be accurately described with just one tensor. Thus, the DTI framework is too simple to resolve highly complex WM structures and hence may result in inaccurate results, exemplified by a marked reduction in FA in the centre semiovale, a brain area with a highly complex WM architecture. More recently, novel methods have been proposed to derive more biologically plausible microstructural information from DWI data. One such models is the Composite Hindered and Restricted Model of Diffusion (CHARMED) (Assaf & Basser, 2005) employed in the current thesis overcomes some of the limitations of the tensor model.

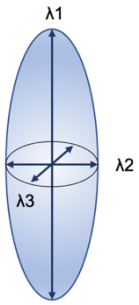


Figure 2.5 Diffusion ellipsoid demonstrating the traditional diffusion tensor model fit to diffusion weighted images acquired by MRI. λ1 shows diffusion along the principal diffusion direction (longitudinal), λ2 and λ3 show diffusion along orthogonal directions.

### 2.4.3 The Composite Hindered and Restricted Model of Diffusion (CHARMED)

CHARMED is a multi-compartment model that assumes two sources of the DWI signal: first, a Gaussian contribution from hindered diffusion in the extra-axonal compartment described by the standard DTI model fit to DWI data acquired with lower b-values. Second, a non-Gaussian contribution from restricted diffusion in the intra-axonal compartment described by diffusion in impermeable cylinders and fit to DWI

data acquired at higher b-values (up to approx. 8500 s/mm² in Assaf & Basser, 2005) (Figure 2.6). Thus, in addition to the standard DTI measurements, CHARMED provides a number of microstructural metrics including fibre orientation and intra-axonal signal fractions. In the present work the intra-axonal signal fraction, or FR, estimated from CHARMED was employed as this measure has been proposed as an index of axonal density (Santis et al., 2014). FR has also been shown to be more sensitive than DTI indices and has been suggested as a potential biomarker for axonal microstructural changes (De Santis et al., 2017). The application of the CHARMED model to multi-shell diffusion data has shown to result in increased accuracy and precision on estimated parameters (Santis et al., 2014). This is particularly beneficial, as although DTI allows estimation of brain tissue alterations these indices are nonspecific, in that FA and MD may appear to be the same but consist of different levels of alteration in axonal density and myelination (Santis et al., 2014). This is because, as discussed, DTI indices are strongly affected by the geometric property of fibres. CHARMED addresses this limitation by modelling extra and intra-axonal volume fraction, allowing estimates to be more sensitive in characterising microstructural alterations in white matter.

However, the acquisition of DWI data to fit the CHARMED model requires multiple shells resulting in longer acquisition times. CHARMED also requires an a priori decision about the assumed number of restricted compartments (1,2 or 3) and model fitting can be computationally expensive (Parker, 2014). Despite this, the acquisition time was still deemed to be feasible in the current thesis.

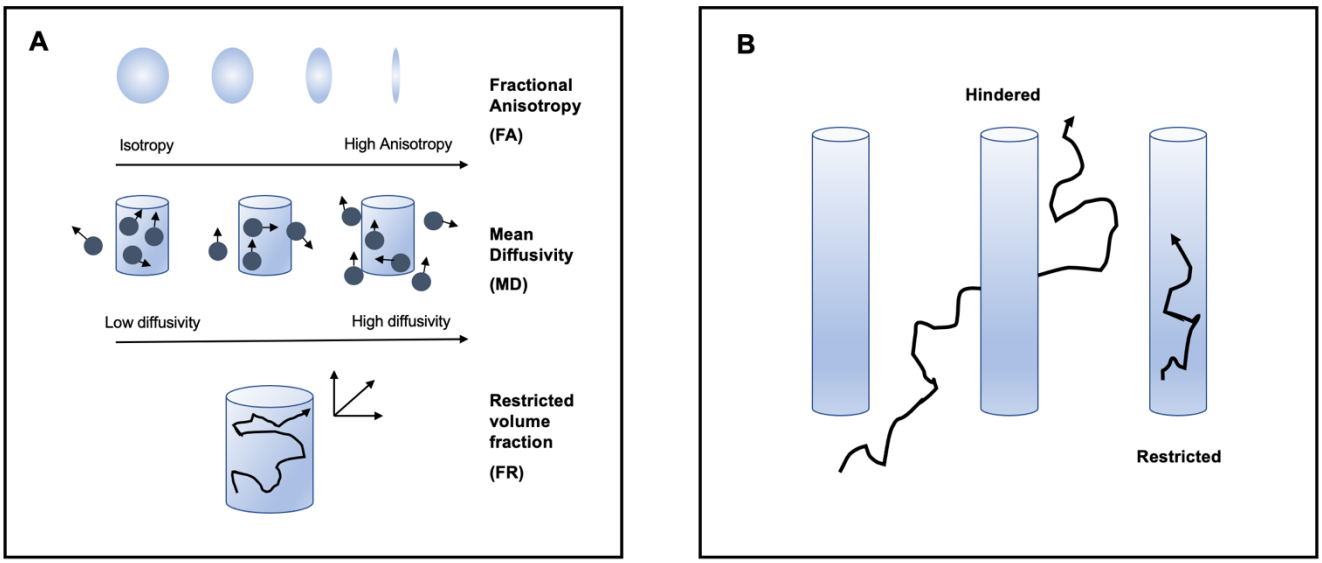


Figure 2.6 Schematic diagram representing measurements of diffusion in vivo often acquired by applying a diffusion model to diffusion weighted MRI. (A) Metrics referring to directionality, level and movement of diffusion in intra-axonal water. (B) Hindered vs restricted fraction of diffusion.

### 2.4.4 Tractography

DWI allows for the three-dimensional reconstruction of white matter pathways using tractography (Wakana et al., 2007). Given the limitation of using DTI as a tractography algorithm outlined above, recent research

efforts have focused on improving fibre tracking techniques. This has been done firstly by optimising dMRI data acquisition, for example with high angular resolution diffusion imaging (HARDI) (Tuch et al., 2002) and secondly by employing fibre tracking algorithms with spherical deconvolution-based techniques that allow the resolution of peaks in fibre orientation functions (Dell'Acqua & Tournier, 2019; Tournier et al., 2004).

The traditional tensor model of diffusion weighted imaging measures the diffusion in the brain based on the eigenstructure of the diffusion tensor (Figure 2.5). However, the tensor model is not capable of estimating multiple fibre orientations within a voxel as it only incorporates a single orientation maximum value (L1). HARDI sequences have been employed to address these limitations of the tensor model. HARDI acquisition involves high b-value diffusion gradient sampling to establish sufficient contrast between components of diffusion in crossing fibres (Tuch et al., 2002). Moreover, HARDI allows for the detection of diffusion signal within maxima and minima as a function of gradient orientation, allowing the identification of multiple fibre orientations (Tuch et al., 2002). Given the advantages of employing HARDI in the accurate identification and reconstruction of white matter tracts, I chose to use HARDI sequences in this thesis. Data were then fit to the CHARMED model, and tracts were delineated, as described below.

By measuring the signal for each voxel in different orientations, white matter fibre tract orientation and integrity can be assessed throughout the brain and reconstructed, which forms the basic process of tractography. In this way tractography allows the visualisation of white matter connections as well as the quantification of their microstructural properties.

To reconstruct fibres, tractography assumes that each voxel is characterised by a fibre orientation, which is estimated by measuring the diffusion signal along several non-collinear orientations. These local fibre orientations are then pieced these together to form global fibre trajectories or streamlines (Jeurissen et al., 2019). This is done by assuming the local fibre orientations are a three-dimensional vector field and the streamline is a curve which has a trajectory which just touches the vector field. To manually estimate tracts of interest, first seeding is carried out which involves defining regions of interest (ROIs) and placing seeds at each voxel within a region thus provides the basis from which tracking can occur. Streamlines are then generated in a probabilistic or deterministic manner. Probabilistic tractography encompasses an algorithm which considers fibre orientation estimates at each voxel, from which the next propagation direction for the tract is selected, generating multiple streamlines through one seed (Jones, 2010). Deterministic tractography refers to the algorithm which propagates tracts based on the principal eigenvector of the tensor for each voxel throughout the brain (Jones, 2010). Deterministic tractography has methodological advantages in that calculations are relatively simple and clear and fast delineation of fibre tracts is usually achieved (Lilja & Nilsson, 2015). This contrasts with probabilistic techniques which may address uncertainty of diffusion orientation within the voxel but require a priori thresholding of the uncertainty

estimates, long calculation times and may exclude voxels with low FA (Lilja & Nilsson, 2015). As the MRI acquisition was primarily designed for the assessment of white matter connections (and metabolic function) in the attention and perception networks in an older adult and patient sample, it was anticipated that fibre tracts may be altered or non-uniform between participants (Huang et al., 2012). It was therefore decided that streamlines would be reconstructed manually on colour-coded FA maps (Pierpaoli & Basser, 1996) using regions of interest for each participant and assessed visually for errors, for example where streamlines were not consistent with expected anatomy of the tract of interest. The coloured fractional anisotropy map (otherwise known as the principal diffusion direction map) is a standard format for tract reconstruction which assigns colours to voxels based on a combination of anisotropy and direction. Typical convention is that the orientation of the principal eigenvector controls hue, and FA controls brightness. Red, green and blue represent angle deviations of diffusion from the principal eigenvector in three directions, and based on the diffusion direction within a voxel, colour combinations are generated (Tournier et al., 2011). In the interests of processing time deterministic tractography was more appropriate. Detail of exact acquisition parameters and processing procedures used in this thesis are provided in Chapter 4.

Finally, a defined termination criterion such as fibre orientation density function (fODF) peak amplitude and turning angle threshold is placed to terminate the tracking procedure and define anatomical pathways (Soares et al., 2013). In this thesis, whole brain tractography was performed with the damped Richardson-Lucy (dRL) spherical deconvolution method for the purpose of subsequent manual delineation of white matter pathways of interest (Dell'Acqua et al., 2010). Deconvolution methods characterise a response function for a fibre orientation which is then deconvolved (Lipp et al., 2020). The dRL was formulated as an approach to reduce instabilities and spurious orientations (Dell'Acqua et al., 2010), and therefore is appropriate in the assessment of patient populations in which these instabilities are highly likely. This family of algorithms allow accurate tracking through kissing and crossing fibres by extracting multiple peaks in the fibre orientation density function (fODF) in voxels with more complicated fibre structure. The dRL method was adopted in this thesis, as in contrast to standard deconvolution methods, the algorithm reduces isotropic partial volume effects and may not consider spurious fibre orientations. For dRL based tracking in this thesis, from the seed points streamlines were propagated in 0.5mm steps, with a length constraint of 30-500mm (Jeurissen et al., 2011). At each location, fODF were resolved and the FOD peak direction that was closest to the previous direction was extracted (Jeurissen et al., 2011). Tracking was then terminated if the fODF peak amplitude fell below 0.05 or if directionality of the path changed by more than 45 degrees between successive steps.

### 2.4.5 Whole brain white matter assessment

I also sought to assess the microstructural properties of white matter in the whole brain, in addition to specifically delineating tracts of interest. As several brain regions demonstrate an age-related decline in the microstructural integrity of white matter, particularly in the frontal and prefrontal lobes (Cabeza & Dennis,

2012), it was of interest to conduct whole brain exploratory assessments for these measures as a sense-check.

One of the most common and relatively simple to implement approaches uses voxel-wise statistics on diffusion metrics and allows the comparison of these metrics between specified groups. The tract-based spatial statistics (TBSS) method encompasses this approach in a fully automated package (Smith et al., 2006) and has been used widely to assess changes in diffusion metrics across the whole brain in a number of different groups including older adults (Barrick et al., 2010). In addition, TBSS can account for the limitation of voxelwise statistical analysis which occurs with standard registration algorithms by conducting non-linear registration followed by projecting diffusion metric measurements onto a 'mean skeleton' (Smith et al., 2006).

TBSS briefly comprises of the following stages; firstly, alignment of the subjects' diffusion metric images to a registration target in a non-linear manner and creating an average of these aligned images. Thinning is then applied by suppressing voxels perpendicular to the tract structure to eventually form the skeletonised image. Each subjects' image is then projected onto the skeleton voxel by voxel by identifying the maximum value in each image perpendicular to the local skeleton structure. The voxel which has the highest value during this search is identified as the centre of the tract. These high values are compared with neighbouring values in the assumed direction of the tract perpendicular and, if they are higher than their neighbouring values, they are assumed to be lying on the skeleton. Finally, TBSS thresholds mean values to exclude voxels which are predominantly CSF or grey matter. Once these steps have been completed, voxel-wise statistics are then carried out across subjects on the data in the common skeleton space. Further details of TBSS and voxel-wise statistical parameters used in thesis can be found in Chapter 4.

### 2.4.6 MRI morphology assessment and segmentation

The morphology of cortical grey matter is most commonly assessed using T1-weighted MRI, in conjunction with automated computerised methods (Hutton et al., 2009). The most common analysis strategies for investigating grey matter in the cortex include volumetric and/or cortical thickness comparisons of regions of interest which are delineated either manually or automatically, whole-brain voxel-based comparisons and surface-based comparisons of thickness.

One of the most prominent packages for processing MR data is FreeSurfer (Fischl & Dale, 2000), however voxel-based morphometry (VBM; Ashburner & Friston, 2000) is also a popular software. FreeSurfer provides an automated pipeline to produce models of cortical thickness and volume, by inputting T1-weighted images and fitting these to either a standardized or custom template. In brief, FreeSurfer automatic segmentation includes motion correction, skull stripping, transformation to Talairach space, normalization of intensity, topology correction and the follows intensity gradients on the cortical surface in order to optimally place grey and white matter or CSF boundaries to segment the cortex. In contrast, in VBM each image is spatially normalized and segmented into tissue class based on the DARTEL algorithm

(Ashburner, 2007). To segment tissue types, a Random Field model uses prior information of spatial distribution of tissue types, and a subsequent clean up procedure is implemented particularly at borders of tissue types. Comparisons of the two programs have yielded relatively similar results, with FreeSurfer relying more on a priori data to segment, whereas VBM uses hidden Markov random fields (Grimm et al., 2015). It has been shown that both pipelines perform at a comparable level of accuracy to manual segmentation (Grimm et al., 2015).

Moreover, both FreeSurfer (Liem et al., 2015) and VBM (Pareek et al., 2018) have been found to be reliable in the quantification of morphological properties in healthy ageing, and dementia (Blanc et al., 2015; Colloby et al., 2017). FreeSurfer in particular has been validated using histological measurements (Rosas et al., 2002) and found to be reliable in estimation of cortical thickness (Cardinale et al., 2014). Given the comparable performance of both methods, this thesis employed FreeSurfer methods due to ease of access and validation with histology and use in patient datasets. Further details of cortical thickness and volume processing can be found in Chapter 4.

### 2.4.7 Approach to MR analyses in this thesis

To characterise age-related differences in neural correlates underlying perception and attention, key brain regions and tracts involved in visual and attention networks were identified for each modality. These key brain regions formed the basis of the a priori anatomically guided MR analyses, in which only these regions were assessed as a primary outcome. Following this, exploratory whole brain analyses in cortical thickness and microstructure were conducted. The purpose of this was two-fold, 1) to understand the context of results from a priori analysis, e.g., whether impairments were widespread, or were largely limited to only regions involved in the initial analysis, and 2) to replicate findings from the ageing in the literature to ensure that the pattern of age-related differences observed in the sample here were consistent with the well-established anterior-posterior gradient pattern reported in older age.

Conducting both a priori analysis and exploratory analyses was important in the current empirical work. In neuroimaging research the number of variables is often high, meaning a hypothesis driven a priori approach is required to ensure the research question is addressed and avoid 'p-hacking'. With the possibility to include a vast number of brain regions as predictors of cognitive behaviour therefore also comes a risk that the influence of these predictors becomes inflated. As such, it was necessary to employ theoretically and anatomically guided a priori analyses to address specific research questions. On the other hand, approaching data with a rigid hypothesis may overlook questions and findings that may not otherwise be addressed (Haueis, 2014). In order to ensure that findings were consistent with previous literature and a priori results did not overlook any general age-related differences which would be important in the conclusions of more specific analyses, exploratory analyses were therefore also conducted as a sanity check following a priori analyses.

For a priori analysis, neuroanatomical regions and tracts that are known to play a key role in visual perception and attention were selected. For metabolites these regions were the occipital cortex (OCC), anterior cingulate cortex (ACC) and the posterior parietal cortex (PPC). For microstructural assessment these tracts were the superior longitudinal fasciculus (SLF 1, 2 and 3), inferior longitudinal fasciculi (ILF), optic radiation and fornix. For assessments of cortical thickness and volume, regions selected were located in the visual, parietal and frontal cortices (Figure 2.7). As discussed in Chapter 1, these regions are known to play a key role in perception and attention functioning and were therefore assumed to contribute most to the understanding of age-related differences in the cognitive outcome measures. To summarise briefly, the rational for the ROI selection was based on the following considerations.

Voxels for MRS were placed in the OCC, ACC and PCC as they are thought to be key hubs in the visual perceptual and attentional networks. Metabolites in the OCC have been reported to be related to visual functioning (Pitchaimuthu et al., 2017; Simmonite et al., 2019) in older age, and metabolites in the ACC have been related to inhibitory and attentional functioning in older adults (Chiu et al., 2014). Whilst posterior parietal metabolites have not been investigated in detail, more general parietal metabolites have been related to inhibitory mechanisms in visual and attentional function (Weerasekera et al., 2020).

To assess age-related differences in the strength of connections between these key hubs and throughout the perceptual and attention networks, white matter microstructure was assessed in relevant visual association fibres. First, microstructure of the optic radiations, projecting from the lateral geniculate nucleus to the visual cortex, were assessed. The optic radiations are studied to a lesser extent in the literature but white matter microstructure of these tracts have been implicated in lower-level visual functioning such as visual acuity (de Blank et al., 2013).

Next, white matter microstructure in the inferior longitudinal fasciculus (ILF) - a long visual association fibre connecting the occipital and temporal-occipital regions of the brain to the anterior temporal lobe regions (Herbet et al., 2018) - was assessed. The ILF is the key white matter pathway that contributes to effective functioning of the ventral visual processing stream, particularly in object recognition (Herbet et al., 2018).

White matter microstructure of the superior longitudinal fasciculus (SLF) - a large intrahemispheric fibre bundle that connects parietal with frontal cortices - was also assessed. The SLF was chosen as the major connection of parieto-frontal attention and executive function networks. Relationships between microstructural changes in the SLF and attentional, visual and processing speed functions have been previously reported (D'Andrea et al., 2019; Kim et al., 2020; Turken et al., 2008). The SLF can be subdivided into three components (SLF1, 2, 3). The SLF 1 originates in the dorsal parietal cortex and reaches the medial regions of the frontal lobe, the SLF 2 begins at the inferior parietal lobe, spans through the angular

gyrus and terminates in the dorsolateral frontal cortex, and the SLF 3 begins in the supramarginal gyrus and reaches to the PFC (Nakajima et al., 2019). These subdivisions of the SLF each are thought to have the following unique functions: SLF 1 is associated with spatial functions and goal-directed attention (De Schotten et al., 2011; Parlatini et al., 2017), the SLF 2 is considered to be the major dorsal pathway of orienting attention and integrating dorsal and ventral networks (Nakajima et al., 2019), and the SLF3 is associated with reorienting of spatial attention (De Schotten et al., 2011; Nakajima et al., 2019). These tracts were therefore delineated separately in this thesis.

Next, the fornix is a white matter tract bundle which spans either side of the midsagittal plane, and extends from the hippocampus, around the thalamus in an arc, connecting the hippocampus to other midbrain cortical regions (Thomas et al., 2011). The fornix is key in episodic memory functioning, particularly visual-spatial memory required for navigation (Murray, Wise & Graham, 2017) and was included as a control limbic pathway that was expected to be relatively preserved in DLB. However, it should be noted that fornix microstructural alterations are reported reliably in ageing (Christiansen et al., 2016), therefore this region also provided a sanity check or control to assess white matter microstructural differences that would typically occur in older participants.

Finally, cortical thickness was measured in regions related to visual and attentional functioning including the parietal, frontal, temporal, occipital and cuneus (Gaetz et al., 2012; Schilling et al., 2013; Zhou et al., 2013). The optic chiasm volume was also included due to its relationship with effective visual functioning.

For the secondary exploratory whole-brain analyses, metabolic measurements could not be included, as single rather than whole-brain voxel spectroscopy data were acquired. White matter microstructure in the whole-brain was assessed using Tract-Based Spatial Statistics (TBSS; Smith et al., 2006) and whole-brain cortical thickness was assessed using the Qdec function in FreeSurfer. Further details of these procedures can be found in Chapter 4.

### 2.4.8 General Statistical approach

Prior to participant recruitment, the sample size for the present study was determined using a power analysis conducted in G*Power (v3.1.9.7; Bach, 1996) in which the effect sizes from similar studies in relevant literature were used to calculate an appropriate sample size which would provide sufficient power (0.8) for an MRI and cognitive imaging study in ageing. The power calculation showed that a sample of 25 younger and 25 older participants would provide adequate power for MR scanning, based on relevant literature in the assessment of microstructure and metabolites comparing healthy younger and healthy older adults (healthy young healthy young - 1-$\beta$ = 0.83, $d$=1.10, n = 24; healthy old - 1-$\beta$=0.76, $d$=0.72, n = 22) (Davis et al., 2009; Pitchaimuthu et al., 2017; Simmonite et al., 2019). However, it should be noted that despite the calculation demonstrating adequate power for the current sample size, this should be interpreted with

caution. Firstly, only a limited number of studies exist which assess both microstructure and metabolites in an ageing context thus limiting the current power calculation to those studies with relatively small samples. In addition, the above calculation provides the minimum sample size required to give a high effect size (> 0.8). However if the effect being tested exists within the data (i.e. distributions of older and younger adults are significantly different in the context of the research questions asked), a small sample may prevent that effect being detected at a given alpha level, even if the effect is large. As such, by estimating a sample size based on high effect sizes from previous work it is possible that a non-significant result found in this thesis may not be fully reflective of an actual non-significant effect in the population and should be interpreted with caution. Despite this, the studies used in the calculation did find significant effects and return high effect sizes with similar sample sizes, indicating the power calculation is sufficient for the present thesis. Throughout Chapters 3, 4, 5 and 6, data analysed were from the same two participant groups (younger and older) and the same DLB cases, unless otherwise stated. No power analysis for sample size was conducted for DLB patients, due to the challenging nature of recruitment.

In Chapter 7, the DLB data were from the LewyPro study (Donaghy et al., 2018), and the control group were the older adults from the previous empirical chapters.

The following general statistical approach was adopted for all data and statistical analyses in this thesis, unless otherwise stated. All data were first inspected for the assumptions of parametric statistical testing, i.e. normal distribution, homogeneity of variance, and data independence. Datasets were assessed for normality by plotting data and visually assessing for skew. The assumption of normality was also assessed using the Shapiro-Wilk test. In the instance of non-normality, data were log-transformed, or data were subject to non-parametric testing as stated. Data were then checked for outliers as ±2 standard deviations from the mean, within each age group and patients and outliers were removed as stated in empirical chapters. Homogeneity of variance was assessed using Levene's test where required.

All statistical hypothesis testing was two-tailed, including pairwise comparisons unless otherwise stated. In all instances multiple comparisons were corrected for False Discover Rate (FDR) to mitigate the likelihood of Type 1 error by employing the Benjamini-Hochberg procedure at 5% (Benjamini & Hochberg, 1995), unless otherwise stated. This procedure was selected as it has been shown to be more liberal in the control of FDR and yields greater power than comparative methods such as Bonferroni correction (Thissen et al., 2002).

Throughout the empirical work in this thesis, a number of statistical tests were used. Group differences in demographic information were assessed using one-way Analysis of Variance (ANOVA)s and chi-square tests where appropriate. For assessing group differences in multiple variables (Chapters 3 and 4) where the assumptions of parametric testing were met, a Multivariate analysis of variance (MANOVA) with post hoc

comparisons was conducted, and where the assumptions were not met Mann-Whitney U tests were conducted. In Chapter 4, relationships between brain measures were also assessed using Spearman's Rho correlations, due to non-normally distributed data. Throughout Chapters 3 and 4, DLB patient data were too limited to conduct formal statistical testing, but data were plotted visually and 95% confidence intervals from older adult data were presented as a comparison.

In Chapter 5, stepwise linear hierarchical regressions were used to determine significant predictors of cognitive functioning from brain measurements, in addition to z-score correlation coefficient comparisons to compare group differences, and Pearson correlations to establish relationships between brain and cognitive outcomes. Group differences in DDM measures in younger and older adults were also assessed using one-way ANOVAs in Chapter 6, followed by linear regression models to assess their relationship with brain measurements. Spearman's Rho correlations were employed to assess the directionality and group-specificity of these predictors. Finally in Chapter 7, group differences in DDM measures in DLB patients and older adults were assessed using one-way ANOVAs and hierarchical regressions were used to determine which clinical and cognitive measures best predicted DDM outcomes.

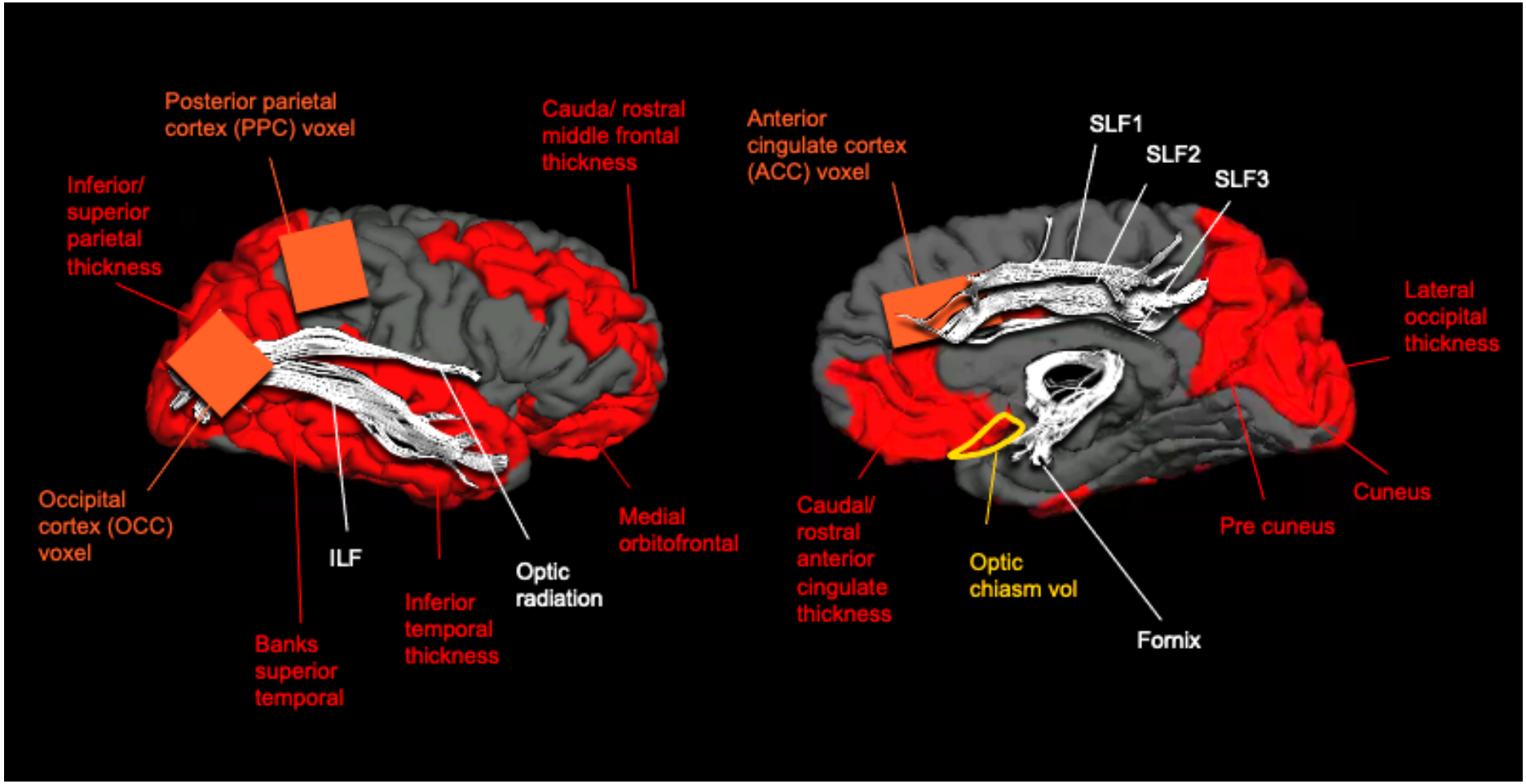


Figure 2.7 Regions selected for a priori regression models in this thesis study. Red values indicate regions included in cortical thickness analysis, white values indicate tracts included in microstructural measurement (FA/MD/FR/RD/L1), orange values indicate metabolic voxels (GABA/ Glx/ Cho/Cr/ Ins), yellow indicates the region included in volume analysis. SLF = superior longitudinal fasciculus. ILF = inferior longitudinal fasciculus.

# Chapter 3 : Development of a task battery to assess the processing stages across the hierarchy of visual perception and attentional functions: effects of ageing

## 3.1 Introduction

The objective of this chapter was to compile a battery of tests known to target the different processing stages across the hierarchy of visual perception and attention functions, as described in Chapter 1. The purpose of this task battery was to achieve a detailed and comprehensive assessment of normal age-related performance differences and disease-related differences in DLB across the perceptual hierarchy. The importance of assessing these functions in the context of normal and pathological ageing has been highlighted, particularly as perceptual functions may be used as an early marker for dementia. Moreover, age-related perceptual impairments may lead to hindered independence, poor gait and falls in older age (Osoba et al., 2019). Despite the importance of this investigation, widely employed standard neuropsychological test batteries used to assess perception and attention in memory clinics have some limitations. Most of these tests such as the Visual Object and Space Perception (VOSP) battery (Warrington & James, 1991) rely on accuracy - in terms of the number of correct responses - as the primary outcome measure for performance. Moreover, many of these neuropsychological tests do not allow the isolation of specific perceptual and attentional abilities. However, there are more sensitive measures which can be employed to mitigate these limitations, such as the implementation of psychophysical staircase methods. This chapter describes a visual perception and attention test battery that was designed to measure different functions at low, mid and higher levels of processing along the visual perception and attention hierarchy as described in Chapter 1. Adaptive psycho-physical methods to determine performance thresholds were implemented when possible, to provide more sensitive outcome measures than the number of correct responses alone (see below). Furthermore, the battery was designed whilst considering the abilities and requirements of older adults with DLB. As DLB patients have severe difficulties in visual perception and attention, the tasks needed to be presented at a range of difficulty levels that allowed patients to be able to perform the tasks. In addition, the duration of the stimulus presentations needed to be sufficiently long to ensure that patients could meaningfully encode the information whilst keeping the task duration brief enough to avoid fatigue effects. These considerations were balanced with the need to collect a sufficient amount of data to determine performance thresholds reliably. All these aspects were piloted carefully prior to starting experimental assessments in younger and older age groups aged between 18-30 and 50-90 years. Details of the pilot study can be found in Appendix 1. The present chapter will focus on presenting the results with regards to healthy ageing by comparing performance on the task battery from a group of older with a group of younger participants in Section 3.3, and the same healthy older adults will be compared with four DLB patients as single cases in Section 3.4.

### 3.1.1 Psychophysical approach to measuring visual perception

Psychophysical principles refer to a set of assessment techniques which can be integrated into a stimulus task in order to determine a threshold – or level of perceptual sensitivity - at which an individual is able to perceive a particular element (Kingdom & Prins, 2016). Adaptive psychophysical procedures provide methods to adjust the stimulus values based on performance in previous responses. As the task continues, the algorithm selects stimuli to 'narrow down' on the range of perceptual sensitivity of the observer and achieve a more sensitive threshold of performance. This provides increasingly sensitive assessments of perceptual functioning and mitigates the need for extensive trial numbers. One such method, the 'up-down staircase', is designed to estimate thresholds at certain probabilities of correct responses by altering the stimulus (either up or down in perceptual 'difficulty') and converges on a certain percentage for 'correct' scores. Staircases begin at a starting value specified by the researcher and increase or decrease the value of the following stimulus based on a pre-determined 'step size' (i.e. how many 'levels' of difficulty can be stepped up or down depending on a correct or incorrect answer). For example, in a 3-up 1-down staircase, the signal is increased after 3 consecutive correct responses or decreased after each error. Typically, staircases also include 'reversals', which occur when the stimulus value moves down at a signal value where it last moved up. Stopping rules of staircases may be based on a certain number of reversals, or less commonly a certain number of trials. Other more complex staircase procedures also exist which may provide highly sensitive measurements of perceptual sensitivity, but often require greater computational power or a larger number of trials.

Due to its' ease of implementation and requirement of lower trial numbers, a simple up-down staircase was employed in visual tasks in this thesis to provide measures of sensitivity in tasks. Visual perceptual functions to be assessed were selected according to the processing hierarchy as previously described (see Figure 1.1 and section 1.2).

Visual acuity and contrast were measured to establish basic visual ability, in addition to visual orientation as measures of low-level visual perceptual function. These functions were thought to correspond to visual processing in the early visual cortices and primary visual pathway. Assessments of visual acuity and contrast sensitivity are shown to be related to fMRI activation in the primary and secondary visual cortices, particularly using population receptive field mapping (Silva et al., 2018) and modulation of primary visual cortex activity using transcranial electrical stimulation has been shown to influence performance on Landolt 'C' tasks of acuity and contrast, as used and described in this thesis (section 3.2.2, Donkor et al., 2021). Greater cortical thickness in V1 has also been shown to be related to better visual acuity performance (Bridge et al., 2014). Moreover, damage to the microstructure of the optic radiation has also been shown to result in poorer performance in similar assessments of visual acuity (Reich et al., 2009).

Next, contour integration and motion coherence perception were measured to assess mid-level visual functioning. Contour integration – the process of establishing the outline of a shape by integrating individual elements – was assessed using a Gabor patch 'snake' task in which individuals were required to perceive and identify a contour by integrating and linking the patches at varying levels of orientation (Lovell, 2005). Contour integration tasks have been evidenced to recruit lower to mid-level cortical regions V1 to V4, using neuronal recordings in non-human primates viewing these stimuli (Chen et al., 2014). Evidence from fMRI also supports this, with contour integration task performance showing relationships with activity in V1 to V4 (Kourtzi & Huberle, 2005; Altmann, Deubelius & Kourtzi, 2004). Next, motion coherence was assessed using a random dot kinetogram as has been previously employed (Landy et al., 2015). Performance in this task has been shown to correspond to fMRI activation in the medial superior temporal area consistent with the neuroanatomical location of V5/MT (Hessellman et al., 2008; Larcombe et al., 2018), but also FA in the projections of white matter tracts from the V5/MT area to fronto-parietal lobes (Csete et al., 2014).

Finally, higher-level processing in the visual association areas (dorsal and ventral streams) were assessed using three tasks. As the dorsal visual processing stream is associated with visuo-spatial abilities, a task of mental rotation was used to assess these functions. Greater mental rotation performance has been associated with widespread fMRI activation in the dorsal stream, encompassing fronto-parietal regions (Podzebenko et al., 2002) but also parietal lobe cortical thickness (Koscik et al., 2009). The embedded figures test (EFT) performance was also assessed as it involves perceiving information which is integrated into a background, and involves the parieto-occipital and frontal cortical regions of the brain (Ring et al., 1999) as compassed by the dorsal processing stream. Embedded figures task performance has been shown to be associated with inferior parietal grey matter volume, but also prefrontal cortical volume, suggesting that the dorsal processing stream plays a key role in embedded figure task performance (Hao et al., 2013). To assess ventral stream functioning a change blindness paradigm was employed to measure object and scene processing. Change blindness paradigms including objects and scenes have been shown to relate to single neuron recording in the human medial temporal lobe (Reddy et al., 2006), which is encompassed in the visual ventral stream.

Functioning of the attention networks (alerting, orienting and executive functions, as described in Chapter 1) were also assessed using the Attention Network Task (ANT; Fan et al., 2002). Event-related fMRI has indicated that these networks are located in the thalamus and posterior cortex for the alerting network, the parietal cortex for the orienting network, and the anterior cingulate and frontal lobe in the executive network (Fan et al., 2005). Furthermore, accuracy and RTs from all tasks were recorded and speed accuracy trade-off (SAT) calculations were generated. As previously discussed, it is well established that older adults exhibit 'general slowing' of RT (Kerchner et al., 2012) leading to SATs that are longer in older adults, but reflect a trade-off of slower RTs in the interest of maintaining accuracy. The reason these tasks were selected

was to assess functioning at all major stages of visual processing including the contribution of the attentional networks. In particular, the executive network and activity within the prefrontal cortex has been shown to mediate reaction time (Rypma et al., 2007) and SAT may be mediated by increases in baseline activity in cortical areas related to decision, such as the dorsolateral prefrontal cortex (Van Veen et al., 2008) but may also involve regions responsible for inhibition (Lo & Wang, 2006).

However, despite these tasks being selected based on their relationship and assessment of different functionalities of the visual system, it should be noted that the visual system is not always truly hierarchical. For example, functioning and performance at a mid or higher-level task requires an element of lower-level functioning and performance on some lower-level tasks require input from higher-level visual functions. Whilst the stimuli and methods recruited for each of these tasks (described in section 3.23) were designed to be specific to each stage of visual processing, it should be noted that performance on each task may reflect an element of processing from a different hierarchical stage.

### 3.1.2 Age effects on visual perception and attention functions

As outlined in Chapter 1 previous research suggests that older adults exhibit some impairments in the visual and attentional systems. With regards to lower level visual function there is evidence for age-related changes in visual contrast and orientation sensitivity (Greene & Madden, 1987, Madden et al., 2004, Richards, 1977). In contrast, impairments in visual acuity appear to occur primarily due to eye disease such as macular degeneration (Salonen & Kivelä, 2012; Sarks, 1976). Such visual disturbances are often reported to be a major risk factor for falls in older age (Lord et al., 1991), and are even associated with an increased mortality risk (Freeman et al., 2005).

With regards to mid-level visual functions age-related changes in motion perception have been reported (Betts et al., 2007). For instance, an age-related decline in performance on global dot motion coherence has been found in a number of studies (Ward et al., 2018, Pilz et al., 2017). Similarly, age-related decline in contour integration performance on tasks using Gabor patch contour stimuli have been shown (Casco et al., 2017; Roudaia et al., 2008).

Finally, age-related impairments in tasks requiring higher visual functions such as scene perception (Porter et al., 2012) have been reported. Specifically, in tasks requiring ventral stream processing of scenes and objects, older adults showed lower levels of performance in comparison to younger adults (Bergmann et al., 2016). Age-related decline was also apparent in functions requiring dorsal stream functioning, for instance spatial visual processing (Hatta et al., 2015). One such ability, mental rotation, has been reported to decline throughout the lifespan but performance is particularly poor in older age (Cerella et al., 1981). However, the severity of this decline is dependent on the task stimulus with greater age-related impairments being reported in object-based tasks as opposed to egocentric rotation tasks involving rotation of human

figures (Jansen & Kaltner, 2014). Finally, a decline in perceptual integration has been reported in older adults (Mahoney et al., 2014). Impairments in figure-ground segregation performance are reported to be present with normal ageing (Markus & Nielsen, 1973), however there have been no recent studies which have assessed age-related performance on this task.

Attention is closely linked to visual perception in older age, and is also often reported to be altered in normal ageing (Hartley et al., 1992). The relationship is notable, as visual perception is affected by alertness but is also influenced by the ability to inhibit or suppress irrelevant environmental stimuli (Gaspelin & Luck, 2018, Maksimenko et al., 2017). Moreover, it has been suggested that both changes in general visual perception with age may be influenced by the ability to suppress 'background' information, or vice versa (Agathos et al., 2015). Madden et al (2007) also posited that changes in visual attentional performance may be due to an over-engagement in top-down influences in comparison to occipital activation for younger adults. Age-related changes in performance on the ANT have also been reported (Ishigami et al., 2016; Mahoney et al., 2010). Findings have shown that whilst the ANT can be reliably completed by older adults and network activations are present (Ishigami et al., 2016), reductions in alerting effect are observed in comparison to younger adults but not in orienting or executive network effects (Jennings et al., 2007).

Finally, older adults often reliably show changes in SAT. SAT - the relationship between making a fast response and making an accurate response - is typically seen to be longer with ageing. This is thought to reflect an age-related strategy change where older adults make decisions slowly in a bid to avoid errors, where younger adults make faster responses and accept a greater number of errors (Rabbitt, 1979, Salthouse, 1979, Starns & Ratcliff, 2010). Whilst there have been several explanations for this phenomenon posited in the literature, it has been proposed that a greater SAT in older adults may be due to a decline in bottom-up sensory processing, leading to more exhaustive top-down processes, thus slowing the decision and RT (Madden et al., 2007). Moreover, it has been reported that an age-related decline in white matter microstructure between frontal top-down processing and lower-level cortical processing, meaning older adults are unable to shortcut more exhaustive information accumulation (Forstmann et al., 2011). As such, I also assess SAT in visual tasks, with a view to establishing potential neural mechanisms for this change in response style.

### 3.1.3 Visual perceptual and attentional impairments in Dementia with Lewy bodies

Age-related impairment in some lower and higher-level visual functions have also been linked to the progression of pathological ageing (Mapstone et al., 2006), particularly in DLB (Van der Beek, 2021). As described in Chapter 1, visual perceptual abilities in DLB are more severely impaired than in healthy older people and AD patients. Perceptual impairments also present earlier in DLB than in AD, and often in conjunction with attentional and executive impairments (Collerton et al., 2003, Metzler-Baddeley, 2007, Ralph, 2001, Simard, 2000). In clinical settings, typical tasks to assess visual functions in DLB include

pentagon copying, the drawing of a clock face (Agrell & Dehlin, 1998) and the trail-making test (Reitan & Wolfson, 1985), in which DLB patients are impaired in comparison to AD patients (Ala, 2001; Cormack, Aarsland, et al., 2004). In addition, DLB patients exhibit a significant impairment in visual search task performance (Cormack et al., 2004) and trail-making task performance in comparison to AD patients (Breitve et al., 2018). However as discussed, these tasks are cognitively complex and considering the cortical organisation and framework of visual perception, it is difficult to distinguish details of the processing stages which may be affected in DLB through performance on these tasks.

Metzler-Baddeley et al (2010) assessed DLB patients' performance using tasks designed to assess different levels of visual perceptual processing from acuity and contrast to orientation, contour integration, and object rotation in increasing complexity. Findings indicated that DLB patients have a preservation of performance in lower-level visual functions, and impairments begin to show around mid to higher level (contour integration to object rotation). These results suggest that deficits in visual perceptual performance in DLB patients are more complex and detailed than previous tasks have demonstrated. However, evidence with regards to lower-level visual functions in DLB remain mixed. Some studies reported preserved visual acuity and orientation (Metzler-Baddeley et al., 2010) while others have reported impaired performance on orientation tasks in both mild cognitive impairment (MCI) DLB and RBD patients who were at greater risk of developing DLB (Chahine et al., 2016; Donaghy et al., 2018). Given that the latter was observed at early MCI DLB stages these discrepancies may only be partly driven by disease stage and/or severity.

Mid-level perceptual processes such as motion coherence are also impaired in DLB patients, who showed poor performance on a motion coherence task over a 12-month period (Wood et al.,2013). Impairments in dot motion discrimination are also apparent in DLB in comparison to both AD and PD patients (Landy, Salmon, Galasko, et al., 2015). In addition, reduced functional activation in the V5 motion area in response to motion stimuli was found in DLB patients (Taylor et al., 2012). With regards to contour integration performance, DLB patients show impairments on tasks requiring the detection of contours in shapes and letters, in comparison to AD patients (Ota et al., 2015). DLB patients also demonstrate impairments in perceiving contours and have a lower perceptual threshold for contour integration (Metzler-Baddeley et al., 2010).

Space and object perception are disproportionately impaired in DLB, as evidenced by VOSP performance (Pal et al., 2016). DLB patients have shown decreased functional connectivity between left and right components of the fronto-parietal executive networks which was related to the spatially oriented subtasks of the VOSP task battery, in comparison to controls (Chabran et al., 2018; Uddin et al., 2009). However, no studies attempt to investigate more complex visual perceptual processing in tasks such as mental rotation, embedded figures or change blindness.

Finally, DLB patients show a reduction in sustained alertness and showed neither orienting or executive network effects without an alerting cue in the ANT in comparison to AD and control participants (Fuentes et al., 2010). This suggests that, without external cueing or alerting, patients experience difficulties in allocating attentional resources to stimuli using top-down processing. DLB patients also show longer RT on the ANT (Kobeleva et al., 2017) and choice RT tasks (Ballard et al., 2001) in comparison to controls. Based on the discussed evidence, one of the prominent theories of visual hallucination incidence, the Perception Attention Deficit (PAD model; Collerton et al., 2005) states that visual disturbances in DLB occur as a result of poor bottom-up sensory processing, leading to an over reliance in top-down attentional processes. According to both evidence which suggests that lower-level vision is relatively preserved in DLB, but higher-level processing requiring greater top-down resources is impaired, and the PAD model, it is hypothesized that integration between top-down attentional and bottom-up sensory processing is impaired in DLB patients.

### 3.1.4 Aims and hypotheses

The aim of the research in this chapter was therefore to compile a battery of tasks which would assess the functioning of the different levels of visual processing described above in order to characterise the processing hierarchy in healthy and pathological ageing. I aimed to assess these differences in a more sensitive manner than has previously been achieved by employing simple psychophysical methods where appropriate, and by calculating SATs and attentional network activations in younger, older and DLB patients. Based on the evidence summarised above, it was hypothesised that older adults would show some level of impairment in all visual tasks in comparison to younger adults, excluding visual acuity. Despite reports of impaired visual acuity with older age, it was anticipated that visual acuity would not differ between groups, as exclusion criteria for eye disease was in place and corrected-to-normal vision was allowed. Moreover, it was hypothesised that more marked impairment may be present in those tasks requiring higher level visual processing, due to the greater attentional and executive requirements of participants that are thought to underpin the complexity effect of ageing. It was anticipated that this would be reflected in longer RTs in older adults, however it was expected that older adults may be slower but no less accurate as reflected by longer SATs. It was also hypothesised that older adults would show reductions in alerting network effect but not orienting or executive network effects in the ANT.

Finally, it was hypothesised that DLB patients compared to healthy older adults would demonstrate maintained lower-level vision, such as acuity and orientation, but that impairments would become apparent at mid to higher levels of visual processing. Based on the empirical evidence summarised above, and the PAD model of visual impairment in DLB (Collerton et al. 2005), it was hypothesised that lower-level functions would show no great difference in comparison to healthy older adults, but that impairments would become apparent around the level of contour integration and above.

## 3.2 Methods

### 3.2.1 Pilot study

Prior to the main study with the cohort described in this chapter and Chapters 4 and 5, all tasks were piloted in younger and older age groups, to assess feasibility of the task battery. Participants in the pilot group (n=41 consisting of 10 older adults and 31 younger adults) were either in a younger adult (aged between 18-30 years, M=20.89, SD=3.37, 10 male, 21 female) or an older adult group (aged between 50-90 years, M=67.2, SD=8.59, 3 male, 7 female), all of which had normal or corrected to normal vision and were free from eye disease. Participants were recruited using the Cardiff University Experimental Management System (EMS) or from the Cardiff University community panel. Participants completed the task battery outlined below, with the addition of a computerised Stroop task (Stroop, 1935), verbal fluency F-A-S task (see Machado et al., 2009) and visual search task (Wolfe et al., 2002), and Doors and People task (Baddeley, Emslie & Nimmo-Smith, 1994), which were subsequently removed from the battery due to time constraints, reducing total behavioural testing time from ~3 hours to ~2 hours. Further details of the methods and results of the pilot study can be found in Appendix 1.

### 3.2.2. Main study

### 3.2.2 Participants

Participants aged 18-30 years (n=26) were recruited from a student sample at Cardiff University via the EMS. A second group of participants aged between 60-90 years (n=26) were recruited from Cardiff and surrounding areas via the Cardiff University community panel (see Table 3.1 for demographic information). Participants were invited to take part in the study if they had normal or corrected-to-normal vision, were fluent English speakers and had no history of psychiatric or neurological disorders excluding depression. Individuals with visual impairments, such as visual field loss or glaucoma were excluded from the study by answering self-reported questions regarding medical issues including vision via email or phone prior to testing.

Table 3.1 Demographic and baseline cognitive scores for younger and older adults' mean and standard deviation (SD) performance. MOCA = Montreal cognitive assessment, TOPF = test of premorbid functioning.

| | **Younger Mean (SD)** | **Older Mean (SD)** |
|---|---|---|
| Age | 21.65 (2.76) | 68.46 (5.91) |
| Gender | Male (12) Female (14) | Male (9) Female (17) |
| Handedness | Left (1) Right (28) | Left (3) Right (22) |
| Years of education | 14.95 (1.89) | 15.12 (2.40) |
| MOCA score | 28.89 (1.25) | 29.04 (1.14) |
| TOPF-UK score | 60 (6.43) | 62.52 (13.3) |
| Visual acuity (Snellen fraction) | 1.91 (0.18) | 1.66 (0.48) |
| Visual contrast (LogMAR) | 1.12 (0.49) | 1.68 (0.58) |

DLB patients (n=4, male=4) were compared as individual cases to older adults in order to assess their performance on visual tasks. Patients were recruited from three healthcare trusts (Cardiff and Vale University Health Board, Aneurin Bevan University Health Board, and North Bristol NHS trust) from specialist memory clinics, and were aged 63-73 years. Patients were invited to take part in the study if they were of capacity to consent for themselves (as assessed by a clinician), and had probable or possible DLB, as diagnosed by the consortium guidelines (McKeith et al., 2017). Patients were otherwise neurologically healthy and free from psychiatric illness (excluding mild depression). All patients had normal or corrected to normal vision. Profiles for each patient are shown in Table 3.1.

Table 3.2 Demographic and baseline cognitive scores for DLB cases and older adults' mean and standard deviation (SD) performance. MOCA = MOntreal Cognitive Assessment, NEVHI = North East Visual Hallucinations Inventory, CAF = Cognitive Assessment for Fluctuations, TOPF = Test Of Premorbid Functioning.

| | **DLB 1** | **DLB 2** | **DLB 3** | **DLB 4** | **Older Control Mean (SD)** |
|---|---|---|---|---|---|
| Age | 73 | 67 | 63 | 72 | 68.84 (5.9) |
| MOCA | 23 | 21 | 24 | 25 | 28.57(2.02) |
| NEVHI | 3 | 10 | 12 | 4 | 0.19(0.49) |
| CAF | 8 | 6 | 4 | 5 | 0.34(0.62) |
| Years of education | 16 | 21 | 16 | 15 | 20.76(5.22) |
| TOPF UK score | 63 | 54 | 66 | 67 | 64.92(4.65) |

### 3.2.3 Materials & Procedure

This study received ethical approval from the Cardiff University School of Psychology Ethics Committee (EC 18.06.12.5313) and from the National Health Service Research Ethics committee (NHS REC) Wales 1 (REC reference: 18/WA/0153) for the patient recruitment of the study. All participants provided informed written consent prior to taking part in the study in accordance with the Declaration of Helsinki. Participants completed baseline assessments, including the test of premorbid intelligence (Wechsler, 2011; TOPF UK, Pearson Corporation), the clinical assessment for fluctuations (CAF; Walker et al., 2000), Montreal Cognitive assessment (MOCA; Nasreddine et al., 2005) and the North East Visual Hallucinations Inventory (NEVHI) (Mosimann et al., 2008). Participants then completed computerised testing as described below. Participants also completed MRI scanning, as detailed in Chapter 4.

Testing was conducted at Cardiff University Brain Research Imaging Centre (CUBRIC), during one visit lasting approximately 2 hours. Participants first completed baseline assessments as described. Next, participants completed the computerised visual and attention test battery described in detail below which was presented on a MacBook Pro (macOS Mojave v 10.14, 2.3GHz, Intel Core i7, Apple Inc., CA) with a 15" screen (1440 x 900 native resolution). Responses were recorded using a wireless keypad for macOS (BKB-Apple-PM, Cateck Inc., Tokyo) which was adapted for tasks using coloured and arrow response

buttons. All tasks were written by myself using PsychoPy psychophysics software (Peirce, 2009) for Python (v1.85.6) with the exception of the Freiburg Visual Acuity and Contrast Test (FRACT). Participants viewed the screen at a distance of 400mm adjusted to eye level, unless otherwise stated. DLB patients completed visual tasks following the same procedure, however patients were provided greater breaks between tasks where required, resulting in longer overall testing sessions (approximately 2.5 hours).

#### 3.2.3.1 Low-level visual perceptual tasks

Visual acuity and contrast sensitivity were assessed by the Freiburg Visual Acuity and Contrast Test (FRACT, v 3.10.0) (Bach, 1996) which is a stand-alone software to test visual function. The task presents Landolt 'C' shapes on the screen and varies either in their size (acuity) or their contrast to the background (contrast). Participants viewed the screen seated at a distance of 2m as recommended by task manufacturers and were asked to respond to the direction of the 'gap' in the C using the wireless response pad. Stimuli were displayed until a response, and the task was self-paced. Participants completed the standard 24 trials per task, resulting in an automatically generated measurement of Snellen fraction for visual acuity and logMAR (logarithm of the minimum angle of resolution) for visual contrast (Figure 3.1A, 3.1B).

To assess visual orientation, two Gabor patches were presented on the screen, positioned to the left and right of the central fixation point (spatial frequency =1 cycles/degrees, diameter = 40mm, subtending visual angle 5.7 degrees; See Figure 3.1C) (Gabor, 1946). The task was a 2 alternative forced choice task built on a simple 1-up 3-down adaptive staircase, in which 3 correct responses resulted in a single level of signal change to a more 'difficult' stimuli (Kingdom & Prins, 2016). The first trial presented showed one Gabor patch at an exactly vertical orientation, and the other Gabor patch at 20° orientation. Participants responded using arrow keys to determine which of the two stimuli are presented at vertical orientation. Based on the response, the task adapted the 'difficulty' of trials by decreasing the angle of orientation of one of the two Gabor patches between 20° and 0° (vertical 'stripe') orientation on a linear scale (step sizes 6,4,2,1°; trials = ~30, number of reversals = 6). One Gabor patch always remained vertical (0°), and the target side presentation was selected randomly, with a stimulus duration of 2000ms. Participants were prompted to make a response that was as quick and accurate as possible, however the next trial was not presented unless a response was made. The sensitivity value at the first two reversals were discarded (Kingdom & Prins, 2016), and an average of the remaining reversals calculated to provide an estimate of perceptual threshold.

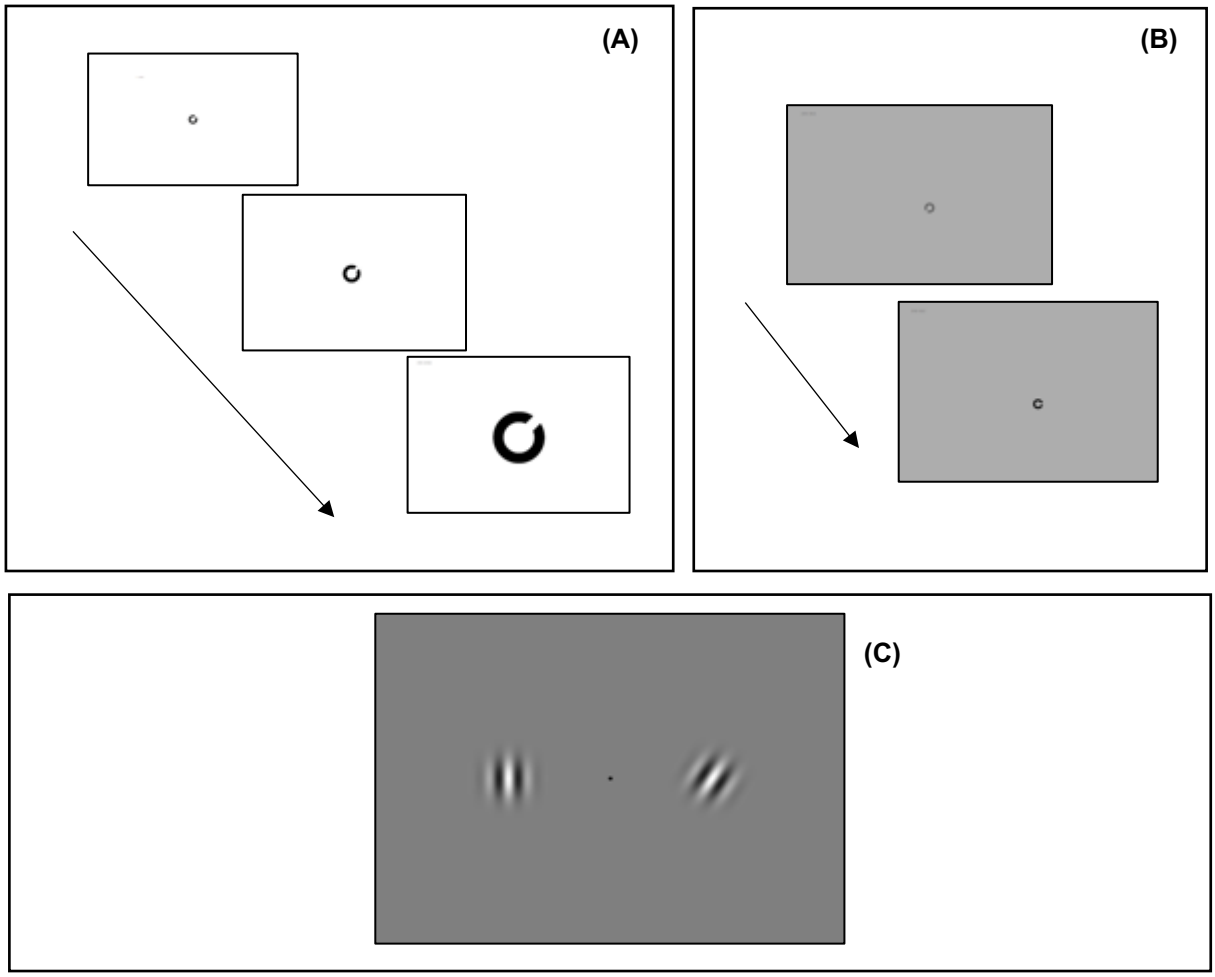


Figure 3.1 Lower-level visual perceptual task stimuli used in the assessment of visual perception in younger adults, older adults and DLB patients. Freiburg Acuity and Contrast Test (FRACT) stimuli for visual acuity (A), and contrast (B), and (C) Gabor patch stimuli for 2-alternative forced choice visual orientation task. (A) Participants must respond to the direction of the gaps in the 'C', generating a Snellen Fraction for measuring visual acuity and the same task with altered contrasts in (B) to measure visual orientation. (C) To measure visual orientation ability, participants must decide which Gabor patch is exactly 'vertical' (0 degrees rotation) and response left or right. 'Difficulty' is altered as the target becomes closer to 0 degrees orientation.

#### 3.2.3.2 Mid-level visual perceptual tasks

To assess contour integration, participants viewed a seemingly random array of Gabor patches on a screen, in which a circular shape was present, consisting of aligned Gabor patches (Figure 3.2A) (path angle = 0.1°, spatial frequency = 1cycles/degrees). The contour task was a 4-alternative forced choice task based on a simple 1-up-3 down adaptive staircase. The target shape was presented at the top, bottom, left and right of the screen, and varied between 0° of jitter (rotation either clockwise or anticlockwise), in which the shape outline is fully visible, and 40° of jitter, in 2° increments. Participants were asked to respond to the location of the shape on the screen using the four arrow keys, with three correct responses resulting in a level 'up' in difficulty on a linear scale (step sizes: 12, 8, 4, 2, 1°; trials = ~30, number of reversals = 6). Stimuli were presented for a maximum of 1600ms, however participants were instructed to provide a response as quickly and accurately as possible, and the following trial was not presented until a response was provided. Original

Gabor patch stimuli were generated and provided by George Lovell (Lovell, 2005) using a bespoke automated script in MATLAB.

Motion coherence perception was measured using a random dot kinetogram stimuli built with a simple adaptive staircase as previously described, which resulted in the alteration of 'coherence', or ratio of signal dots moving in one direction to noise dots moving in a random direction. The dot stimuli contained 200 white dots on a black screen, with signal dots moving in one direction (left or right), which was randomly assigned at the beginning of each trial (field = 90mm diameter, circular; dot size = 7 pixels). Participants responded to the direction in which the signal dots were travelling, with three correct responses resulting in a level 'down' in coherence, making recognition more challenging, on a logarithmic scale (step sizes: 0.8, 0.4, 0.2, 0.1, 0.05; trials = 50, number of reversals = 6; Figure 3.2B). Stimuli were presented for a maximum of 5000ms and participants were required to make a response before the next trial was presented. Perceptual thresholds were calculated as previously described.

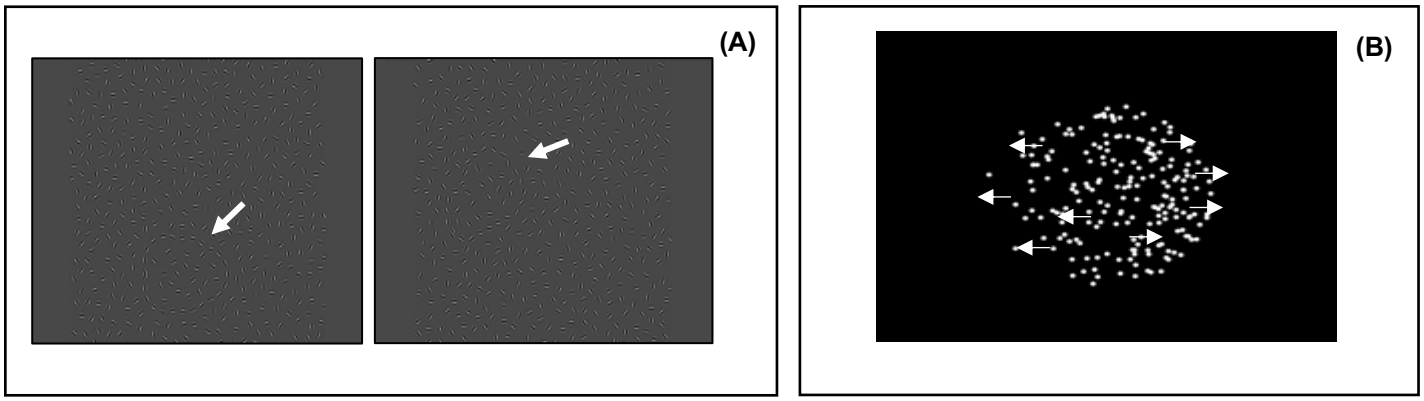


Figure 3.2 Mid-level visual perceptual task stimuli. (A) Contour integration stimuli showing multiple Gabor patches, of which some form the target shape, indicated by arrow. Task difficulty is altered by increasing 'jitter' of Gabor patches to make the contour more difficult to perceive. (B) Motion coherence task in which animated white signal and noise dots are presented on a black background. Arrows indicate direction of dot movement, where the participant must decide the direction of global movement. Difficulty is increased by reducing the coherence of signal and noise dots.

#### 3.2.3.3 High-level visual perceptual tasks

Higher-level perception including rotation ability, change blindness function and figure-ground segregation were assessed. As these tasks were more cognitively complex, psychophysical staircases were not incorporated but accuracy and RT were measured. Mental rotation is a high-level visual perceptual function which typically involves the dorsal stream regions of visual perception including the parieto-occipital areas (Tagaris et al., 1996). The mental rotation task in this thesis was based on a task by Ganis & Kievit (2015), in which 3-dimensional objects built from varying numbers of cubes were displayed in pairs on the screen (see Figure 3.3A). Object stimuli (Shepard & Metzler, 1988) were presented simultaneously, and were either in the same position, or with the right-hand stimuli rotated at 50, 100 or 150°. Participants were asked to make a 'same' or 'different' judgement for each object pair. The object pairs were presented for an indefinite

amount of time until participants responded and participants were requested to make a response as quickly and accurately as possible. Participants were given two practice trials and 30 main task trials and were instructed to respond using colour coded keys (trials = 30).

Change blindness – the phenomenon in which seemingly large changes in a scene, such as the removal of an object, can be missed due to absence of attentional processing to the particular element - was assessed in the present study by presenting participants with coloured photographs of household scenes (see Figure 3.3C) accessed from the 'SCEGRAM' image database (Öhlschläger & Võ, 2017) with permission. Each trial consisted of the presentation of one photograph on the screen (6000ms), followed by a blank screen interval with a central fixation cross (1000ms), and the subsequent presentation of a second photograph. The second photograph shown was identical to the first, however an element of the image was altered from the first photograph. Following the presentation of images, participants were shown three choices on screen (for example 'plant', 'chair', 'newspaper'), and were prompted to select which of the items they believed had changed (either appeared or disappeared) between the images. The next trial was not presented until a response had been made. Images and items were altered for difficulty by manipulating the size and location of the target in the scene. Participants were given two practice trials before completing main trials (trials = 20) (Figure 3.3B).

For the embedded figures task, the observer was required to separate the figure from the background in order to perceive the embedded target (de-Wit et al., 2017). The EFT uses stimuli from the Leuven Embedded figures test (L-EFT). Participants viewed one target line shape at the top of the screen (e.g. triangle) and three line drawings at the bottom of the screen (see Figure 3.3D). Participants were asked to identify which of the three-line drawings contained the target shape embedded into the lines. Trials were presented for an indefinite amount of time until response, but participants were requested to respond as quickly and accurately as possible. The number of lines in the target shape, number of lines in the line drawing options and symmetry of the target shape were manipulated to make the trials more difficult. Participants were given three practice trials, then moved onto main trials which were each presented until response (trials = 62).

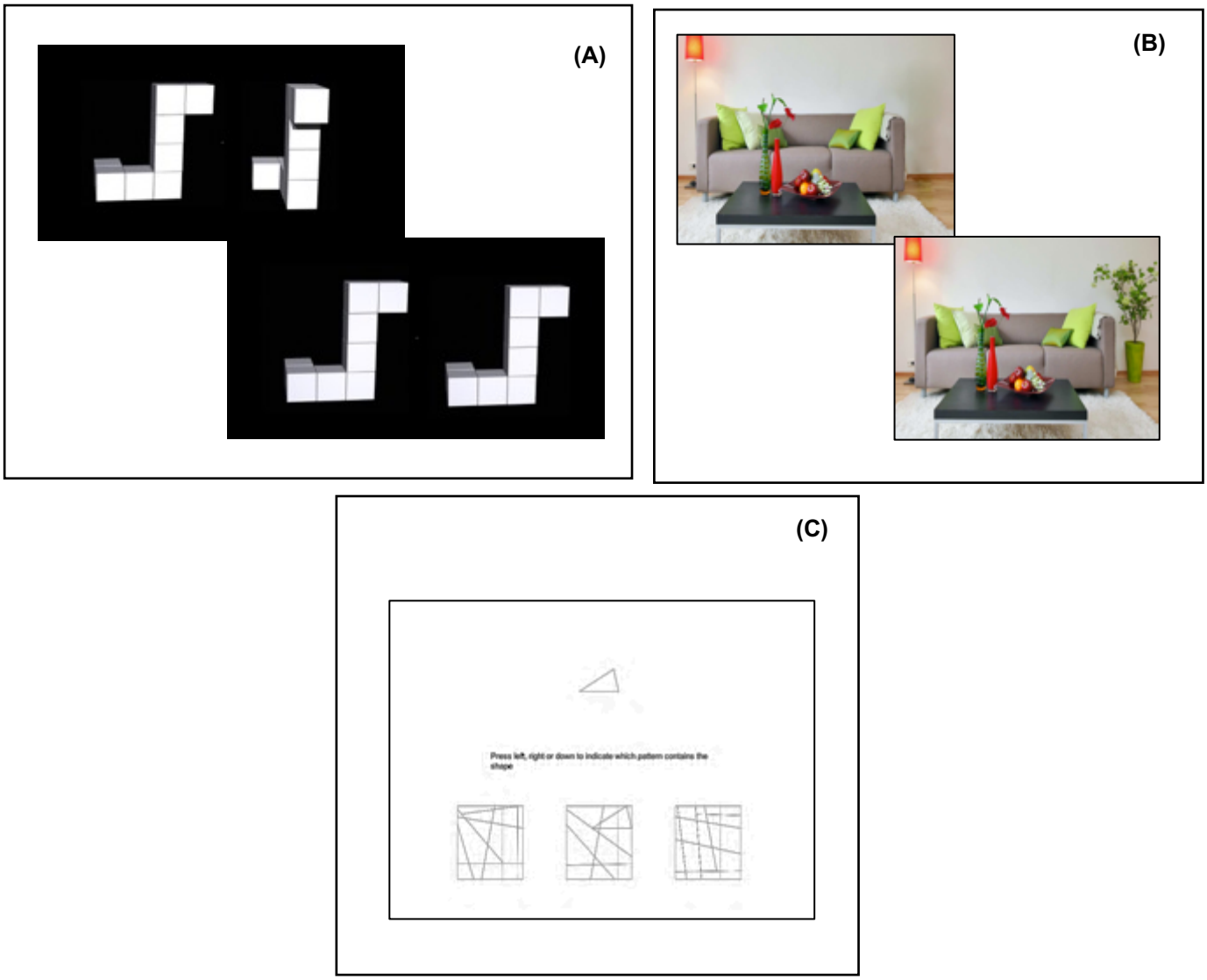


Figure 3.3 Higher level visual perceptual stimuli. (A) Mental rotation stimuli, showing pairs of 3D shapes, which participants must judge if these are the same shape (but one has potentially been rotated) or different shapes, requiring mental rotation. Difficulty is altered by increasing the number of blocks in the shape. (B) Change blindness stimuli, showing 'spot the difference scenario', where participants are shown one image after the other and asked to identify the item that differed (either added or removed) between scenes. (C) Embedded figures task, where participants are asked to identify which of the bottom three grids contains the shape (triangle) at the top.

### 3.2.3.4 Attention Network task

Attention functions were assessed with the ANT (Fan et al., 2002) which combines the Posner cueing task (Posner, 1980) with the Eriksen flanker task (Eriksen & Eriksen, 1974) and provides measures of the three attentional networks proposed by Posner and Petersen (alerting, orienting and executive), (Petersen & Posner, 2012; Posner & Petersen, 1990). The task consisted of a 'cueing' element – a white asterisk on a grey background - in which participants were shown no cue, a central cue, a spatial cue (either at the top or bottom of the screen corresponding to the proceeding trial location), or a double cue (asterisk is presented at the top and bottom of the screen simultaneously) (Figure 3.4). Each cue was displayed for 100ms,

followed by a fixation cross in the centre of the screen for 400ms. The second 'flanker' element was then displayed, in which participants are presented with five horizontal stimuli. These stimuli were: (1) congruent arrows, in which all five horizontal arrows pointed in one direction (left or right), (2) incongruent arrows, in which the central arrow pointed in a different direction to flanker arrows, and (3) neutral stimuli, in which the central stimulus was an arrow, and flankers are horizontal lines. Flanker stimuli are presented either centrally, at the top or at the bottom of the screen. For trials with spatial cues, the flankers are presented in the location corresponding to the cue. Participants were asked to respond to the direction of the central arrow only, using left and right arrow keys. The target was presented for a maximum of 1700ms, or until the participant made a response (trials = 65). Outcome measures were the three network effects. An alerting network effect is calculated by subtracting mean RT of double cue trials from no cue trials, the orienting effect is calculated by subtracting mean RT of spatial cue trials from centre cue trials, and the executive network effect is calculated by subtracting mean RT of congruent trials from mean RT of incongruent trials.

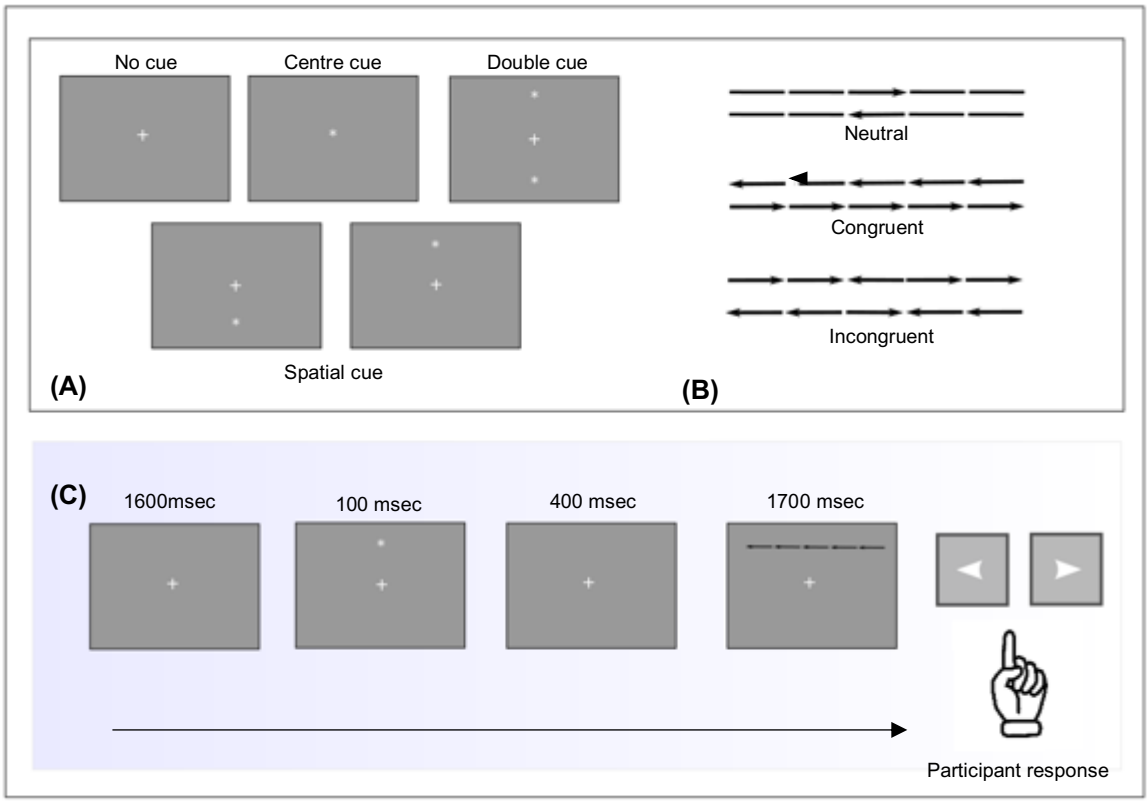


Figure 3.4 Attention Network Task as originally devised by Fan et al., (2002). (A) Participants are initially presented with one of four cues, which then disappears. (B) Arrow stimuli are then presented, in which the target arrow (centre) is either surrounded by neutral flankers, congruent or incongruent flankers. This stimulus is presented either in the centre, top or bottom of the screen according to 'spatial' cue conditions (C) Participants must then provide a response to direction of target.

### 3.2.4 Statistical Analysis

Outcome measures for all tasks are listed in Table 3.2. For tasks where RT was an outcome measure (contour integration, motion coherence, embedded figures, mental rotation task and change blindness task)

the SAT was calculated using the linear integrated speed accuracy score (LISAS; Vandierendonck, 2017) method, which combines RT and proportion of error in a linear manner, according to the formula (Equation 3.1).

$$RTj + \frac{SRT}{SPE} \text{ x } PEj \quad (3.1)$$

Where RTj is the mean RT, PEj is the proportion of errors, SRT is the participants' overall RT standard deviation, and SPE is the participants' overall standard deviation for the proportion of errors.

3.2.3.1 Older and younger group comparisons

Demographic group differences were assessed using one-way ANOVAs and Chi-square tests where appropriate. To compare cognitive test outcomes between younger and older groups, a Multivariate analysis of variance (MANOVA) was conducted on all 13 variables, using group as a fixed factor with simple contrasts. RT data were log-transformed to address the skewed distribution. Attention network task group differences were assessed with separate MANOVA using log transformed RT data.

3.2.3.2 Patient and older control group comparisons

Due to the low number of DLB patients, it was statistically inappropriate to conduct formal group comparisons. Instead, each DLB patient was visually plotted in comparison to the 95% confidence intervals of the older adult group, that was calculated according to the formula (Equation 3.2):

$$X \pm 1.96 \frac{s}{\sqrt{(n)}} \quad (3.2)$$

Where X is the mean, s is the standard deviation and n is the number of observations for one cognitive outcome (i.e. visual orientation threshold). DLB patients' performance scores that fell outside the 95% confidence interval were considered as deviating from the healthy control group.

## 3.3 Results: Perceptual and attention differences in healthy older and younger adults

Group differences in demographic factors are listed in Table 3.3. A full list of tasks, outcome measures and group differences are listed in Table 3.4. Significant group-differences in age ($F(1,49)=1325.9$, $p<.001$) and TOPF score ($F(1,59)=9.658$, $p=.003$) were present. However, no significant group differences were shown in gender ($\chi^2=1.388$, $p=.239$), handedness ($\chi^2=2.388$, $p=.122$), education ($F(1,49)=.320$, $p=.574$) or the MOCA score ($F(1,49)=.196$, $p=.660$).

Table 3.3 Demographic information for younger and older participants and group comparisons. TOPF-UK = Test Of Premorbid Functioning (UK version), MOCA = MOntreal Cognitive Assessment. One way ANOVA and chi-square test results for group comparisons are reported.

| | **Younger M (SD)** | **Older M (SD)** | **Statistical group comparison** |
|---|---|---|---|
| Age | 21.65 (2.76) | 68.46 (5.91) | $F(1,49)=1325.9$, $p<.001$ |
| Gender | Male (12) Female (14) | Male (9) Female (17) | $\chi^2=1.388$, $p=.239$ |
| Handedness | Left (1) Right (28) | Left (3) Right (22) | $\chi^2=2.388$, $p=.122$ |
| Years of education | 14.95 (1.89) | 15.12 (2.40) | $F(1,49)=.320$, $p=.574$ |
| MOCA score | 28.89 (1.25) | 29.04 (1.14) | $F(1,49)=.196$, $p=.660$ |
| TOPF-UK score | 60 (6.43) | 62.52 (13.3) | $F(1,59)=9.658$, $p=.003$ |
| Visual acuity (Snellen fraction) | 1.91 (0.18) | 1.66 (0.48) | |
| Visual contrast (LogMAR) | 1.12 (0.49) | 1.68 (0.58) | |

Table 3.4 List of tasks assessing different functions in the visual hierarchy, their stimuli used in the task, outcome measures of the task, and result of group comparisons *indicating older controls had poorer performance than younger controls ($p<.05$). FRACT= Freiburg Visual Acuity and Contrast Test, OCO = Older Controls, RDK = Random dot kinetogram, RT = Reaction Time, YOC = Younger Controls.

| *Low-level vision* | | | | | |
|---|---|---|---|---|---|
| **Function** | **Stimuli/ task** | **Outcome measures** | **Group comparison** | **Stimuli duration** | **Adaptive staircase** |
| Visual Acuity | FRACT – Landolt C | Snellen Fraction | YCO = OCO | - | Yes |
| Visual Contrast | FRACT – Landolt C | logMAR | YCOC<OCO* | - | Yes |
| Orientation | Gabor patch | Threshold (degrees orientation) | YCO<OCO* | 600ms | Yes |
| *Mid-level vision* | | | | | |
| Motion coherence | RDK | Threshold (% coherence) | YCO<OCO* | 1000ms | Yes |
| | | RT | YCO=OCO | | |
| | | SAT | YCO=OCO | | |
| Contour integration | Gabor patch contours | Threshold (degrees jitter) | YCO=OCO | 10000ms | Yes |
| | | RT | YCO<OCO* | | |
| | | SAT | YCO<OCO | | |
| *Higher-level vision* | | | | | |
| Mental Rotation | 3-D block shapes | Accuracy | YCO=OCO | - | No |
| | | RT | YCO<OCO* | | |
| | | SAT | YCO<OCO* | | |
| Change blindness | Scenes and objects | Accuracy | YCO=OCO | 1st stimuli=6000ms | No |
| | | RT | YCO<OCO | 2nd stimuli = no limit | |
| | | SAT | YCO<OCO* | | |
| Embedded Figures | Line patterns | Accuracy | YCO=OCO | - | No |
| | | RT | YCO<OCO | | |
| | | SAT | YCO<OCO* | | |

Overall, there was a statistically significant difference in visual performance between older and younger adults as shown in the omnibus group effect for all dependent variables, $F(13,13)=3.646$, $p=.013$; Wilk's $\Lambda = 0.215$, partial $\eta^2=.785$. Results are displayed as low-level, mid-level or high-level vision and ANT. The

results are displayed in Figure 3.5 with the older adult group (old control; OCO) shown in red, and younger adults (young control; YCO) are shown in grey. Data are displayed as a violin plot, in which the distribution of data in each group is shaded, each data point represents one observer, and a median and inter-quartile range (IQR) are shown overlaid as a boxplot.

### 3.3.1 Low level vision

Post-hoc effects from the MANOVA indicated some group differences between younger and older groups in low level visual performance (Figure 3.5). No significant differences were found in visual acuity between younger and older groups ($F(1,49)=1.239$, $p=.276$; partial $\eta^2=.047$), however visual contrast (Weber contrast %) was significantly poorer in older adults ($F(1,49)=27.903$, $p<.001$, partial $\eta^2=.527$). Orienting threshold was significantly higher – therefore showing poorer discrimination ability – in older adults in comparison to younger adults ($F(1,49)=6.201$, $p=.020$; partial $\eta^2=.199$).


Figure 3.5 Lower-level visual task performance in younger (grey) and older (red) adults. MANOVA results indicate significantly poorer performance in visual contrast (higher % contrast = poorer performance and orientation tasks (higher threshold = poorer performance) in older adult group, but visual acuity performance (higher Snellen fraction = better performance) shows no group difference. *p<.005, **p<.001, YCO= young adults in grey OCO= older adults in red.

### 3.3.2 Mid-level vision

No difference in contour integration threshold ($F(1,49)=.048$, $p=.829$; partial $\eta^2=.002$), but a significant group difference in motion coherence threshold ($F(1,49)=3.496$, $p=.043$; partial $\eta^2=.123$) were observed with older adults showing higher threshold scores and therefore worse performance than younger adults (Figure 3.6).

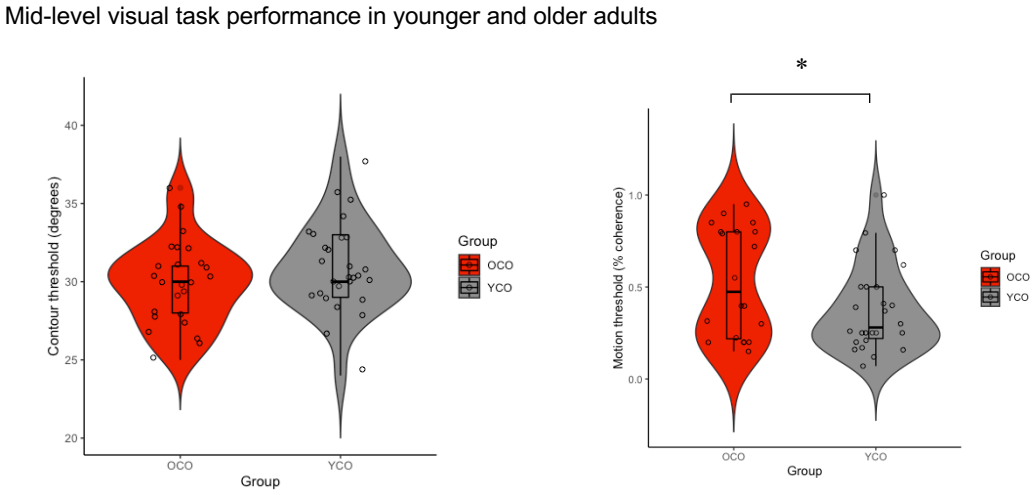


Figure 3.6 Mid-level visual task performance in younger (grey) and older (red) adults. MANOVA results indicated significantly poorer performance in motion coherence in the older control group in comparison to younger participant. No group differences in contour integration were shown. *p<.005, **p<.001, YCO= young adults OCO= older adults.

### 3.3.3 High level vision

No significant group differences were detected in embedded figures task accuracy ($F(1,49)=.119$, $p=.733$; partial $\eta^2=.005$), rotation accuracy ($F(1,49)=2.291$, $p=.143$ partial $\eta^2=.084$), or change blindness ($F(1,49)=.020$, $p=.890$; partial $\eta^2=.001$) (Figure 3.7).

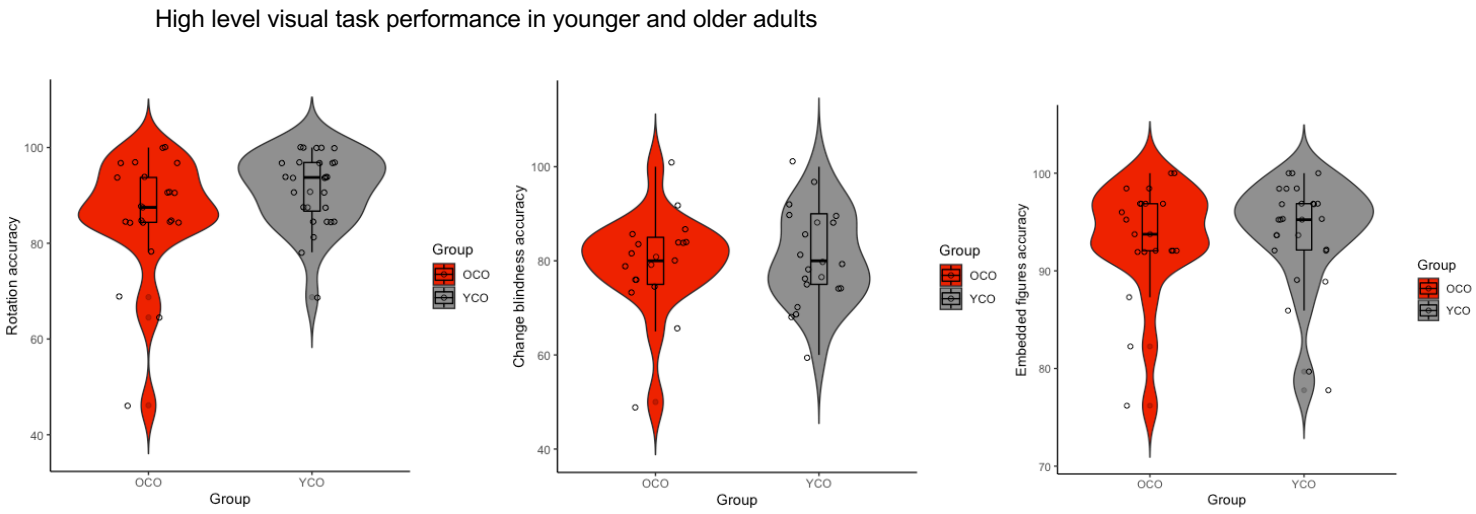


Figure 3.7 High-level visual task performance (accuracy %) in younger (grey) and older (red) adults. MANOVA results showed no significant group differences were observed in rotation, change blindness or embedded figures accuracy. *p<.005, **p<.001, YCO= young adults OCO= older adults.

### 3.3.4 Reaction time (RT)

Older adults had significantly slower RT in contour integration ($F(1,49)=3.496$, $p=.043$; partial $\eta^2=.163$), embedded figures ($F(1,49)=5.470$, $p=.028$; partial $\eta^2=.180$), change blindness ($F(1,49)=23.295$, $p<.001$; partial $\eta^2=.482$) and mental rotation ($F(1,49)=4.694$, $p=.040$; partial $\eta^2=.158$), but not in RT for motion threshold ($F=.357$, $p=.556$; partial $\eta^2=.014$) (Figure 3.8).

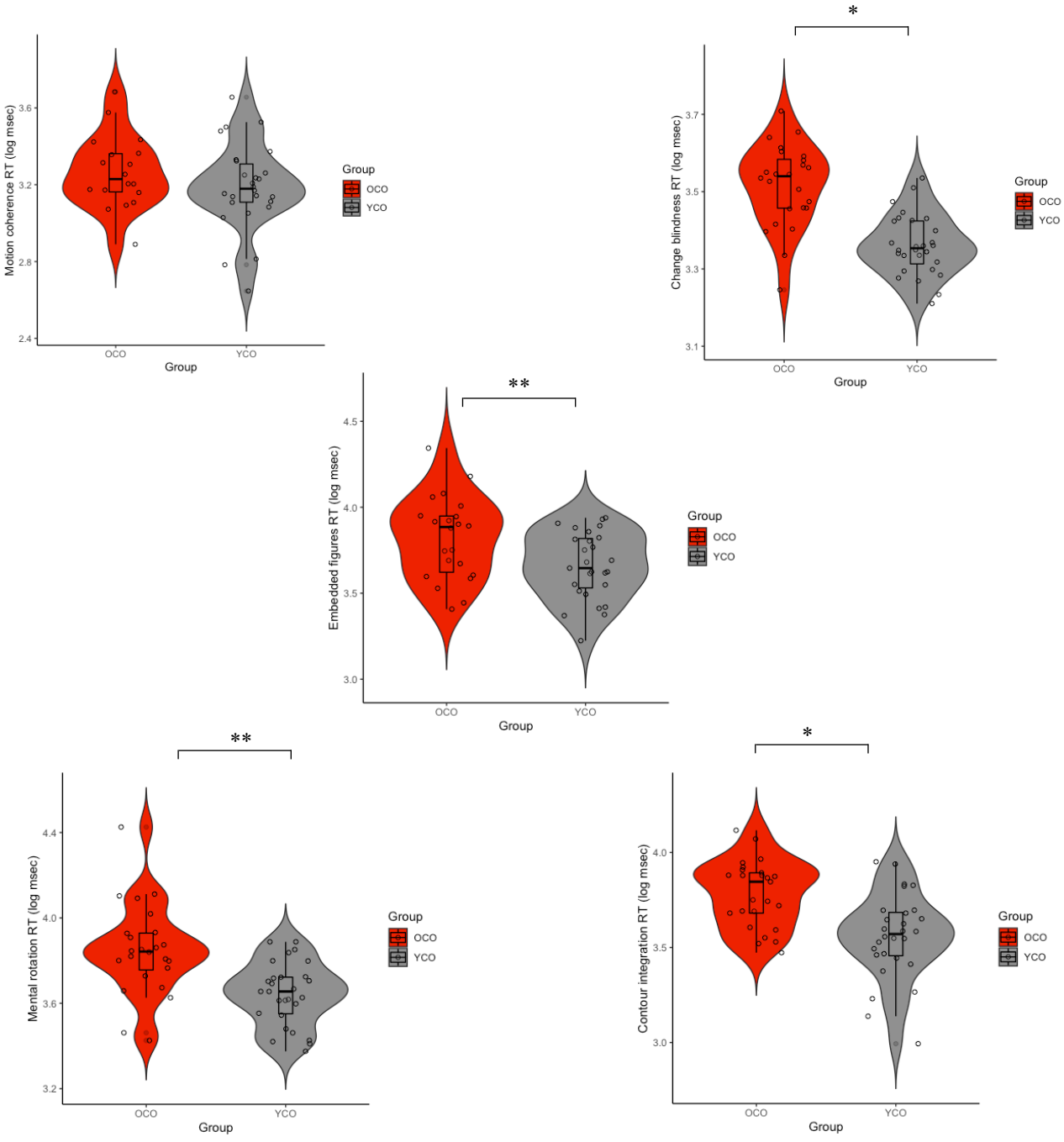


Figure 3.8 Mid-to high-level visual task reaction time (RT) in younger (grey) vs older (red) adults. MANOVA results showed that older adults have significantly greater average RT in rotation, embedded figures and contour integration tasks, in comparison to younger adults. No significant difference was shown in average RT in motion or change blindness tasks. *p<.005, **p<.001, YCO= young adults OCO= older adults.

### 3.3.5 Speed accuracy trade-off (SAT)

SAT was significantly greater in older adults in comparison to younger adults in contour integration ($F(1,49)=8.72$, $p=.006$; partial $\eta^2=.195$), embedded figures ($F(1,49)=4.247$, $p=.047$; partial $\eta^2=.106$),

mental rotation (F(1,49)=4.976, p=.032; partial $\eta^2$=.121) and change blindness (F(1,49)=8.72, p=.006; partial $\eta^2$=.256), but not motion coherence (F(1,49)=.875, p=.356; partial $\eta^2$=.024).

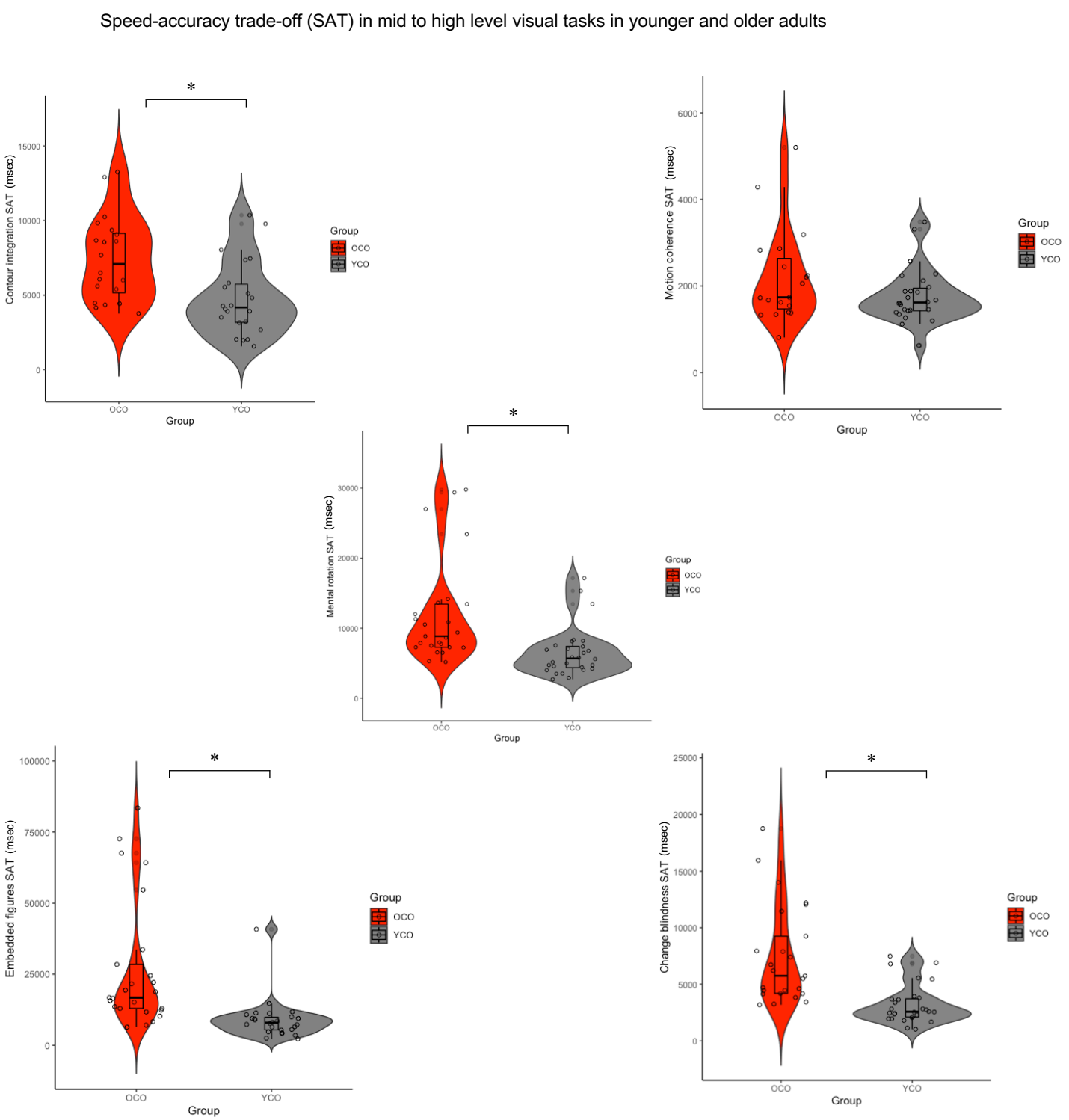


Figure 3.9 Speed accuracy trade-off (SAT) in mid-to high-level visual tasks in younger (grey) and older (red) adults. MANOVA results indicated that older adults have significantly greater SAT in contour integration, mental rotation, embedded figures and change blindness. No significant difference was shown in motion coherence SAT between younger and older adults. *p<.005, **p<.001, YCO= young adults OCO= older adults.

### 3.3.6 Attention Network task performance

A significant effect of group on ANT conditions and network activations was observed overall; $F(9,39)=3.722$, $p=.002$ Wilk's $\Lambda = 0.538$, partial $\eta^2=.462$. Older adults showed significantly longer average RT in no cue ($F(1,49)=24.741$, $p<.001$; partial $\eta^2=.345$), double cue ($F(1,49)=14.992$, $p<.001$; partial $\eta^2=.242$), spatial cue ($F(1,49)=12.227$, $p=.001$; partial $\eta^2=.206$) and centre cue ($F(1,49)=29.718$, $p<.001$; partial $\eta^2=.387$) trials. In addition, older adults had significantly greater average RT in incongruent ($F(1,49)=19.409$, $p<.001$; partial $\eta^2=.292$) and congruent ($F(1,49)=22.941$, $p<.001$; partial $\eta^2=.328$) trials. However, significant group differences only approached significance in the overall orienting effect (centre cue mean RT – spatial cue mean RT) ($F(1,49)=3.702$, $p=.060$; partial $\eta^2=.073$), with no significant group differences in alerting ($F(1,49)=2.351$, $p=.132$; partial $\eta^2=.048$) or executive effects ($F(1,49)=.230$, $p=.634$; partial $\eta^2=.005$) (Figure 3.9).

Attention Network Task performance in younger and older adults

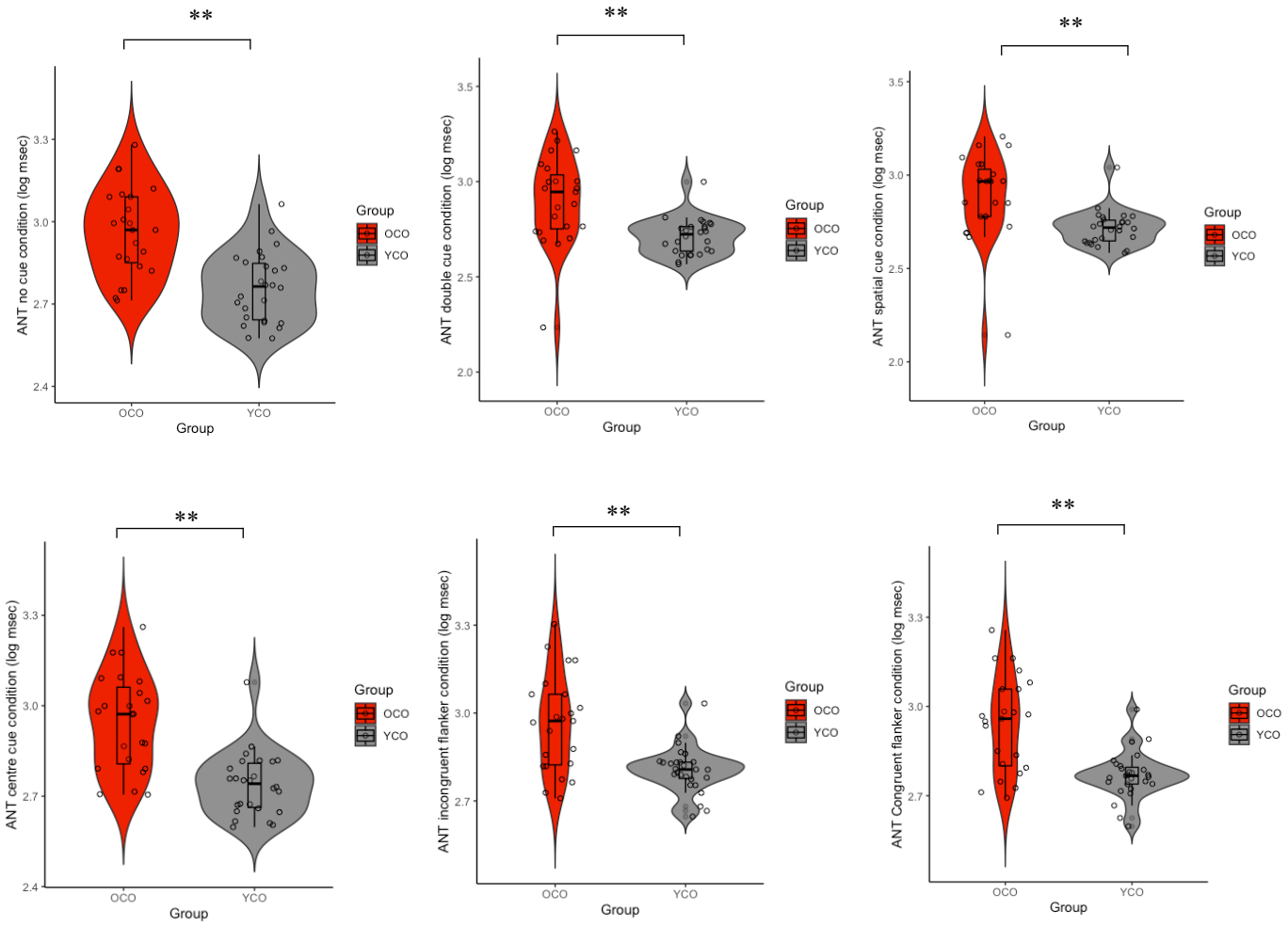

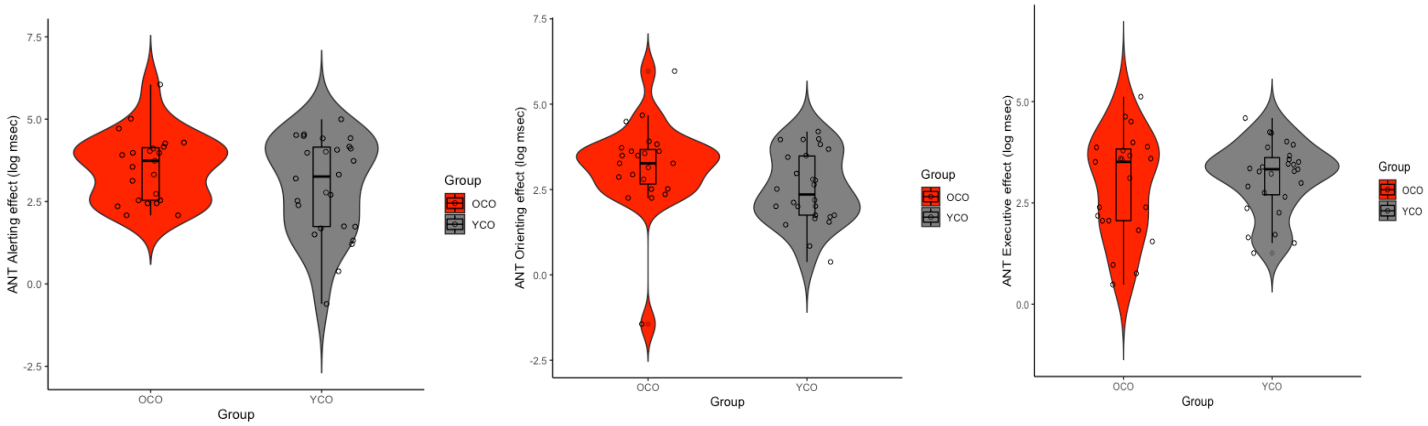


Figure 3.10 Attention Network Task (ANT) performance in younger (grey) and older (red) adults. Reaction time (RT) in log milliseconds is shown for flanker conditions (neutral, congruent or incongruent) and all cueing conditions (cue presented prior to flanker either in the centre, corresponding location to the target, double cue above and below the target or no cue). ANT network activations are also shown, calculated by obtaining the difference between two condition RTs (alerting = double cue RT – no cue RT, orienting = spatial cue RT – centre cue RT, executive = incongruent flanker RT – congruent flanker RT). MANOVA results indicated that older adults showed significantly longer RTs in all cue and flanker conditions in comparison to younger adults. Alerting, orienting and executive effects were not significantly different between groups. *p<.05, **p<.001, YCO= young adults OCO= older adults.

## 3.4 Results: DLB case comparisons

### 3.4.1 Demographics

DLB patients' individual performance were then compared descriptively with older participants (n=4). Patients' ages, years of education and TOPF-UK performance (excluding one DLB patient) fell within the 1 standard deviations of older adults' years of education suggesting that they were comparable to the healthy older adult group in these variables. However, consistent with their DLB diagnosis all patients had lower MOCA scores in comparison to average and standard deviations of older adults' performance. In addition, patients' NEVHI scores were higher than older adults and fell outside of the standard deviations of older adults' performance (see Table 3.5).

Table 3.5 DLB patients and older adults' demographic information and performance on clinical and baseline assessments (Mean and standard deviation (SD) performance). * indicates values which fell outside the older adult group SD.

| | **DLB 1** | **DLB 2** | **DLB 3** | **DLB 4** | **Older Control Mean (SD)** |
|---|---|---|---|---|---|
| Age | 73 | 67 | 63 | 72 | 68.84 (5.9) |
| MOCA | 23* | 21* | 24* | 24* | 28.57(2.02) |
| NEVHI | 3* | 10* | 12* | 4* | 0.19(0.49) |
| CAF | 8* | 6* | 4* | 5* | 0.34(0.62) |
| Years education | 16 | 21 | 16 | 15 | 20.76(5.22) |
| TOPF-UK score | 63 | 54* | 66 | 67 | 64.92(4.65) |

### 3.4.2 Lower-level vision

95% confidence intervals (CI) for each dependent variable were calculated for the older adult group for the purpose of comparing the DLB individuals with their control group. Older control participants' visual acuity performance fell within a 95% CI of older controls for DLB patients 1 and 2 performing within this range, and DLB patients 3 and 4 performing at a higher (and therefore better) level. In contrast, almost all DLB patients performed at a higher (and therefore poorer) level of visual contrast, with patients DLB1, 2 and 3 performing above the 95% CI of older controls (Table 3.6, Figure 3.10). All patients showed normal performance within the control 95% CI for orientation.

Table 3.6 DLB patient mean performance on lower-level visual tasks, in comparison to 95% confidence interval (CI) upper and lower bounds for older control participants. * indicates scores deviating from 95% CI.

| | **Lower control CI** | **Upper control CI** | **DLB 1** | **DLB 2** | **DLB 3** | **DLB 4** |
|---|---|---|---|---|---|---|
| *Visual Acuity* | 1.25 | 1.954 | 1.53 | 1.30 | 2.0* | 2.0* |
| *Visual Contrast* | 1.216 | 2.019 | 3.24* | 4.34* | 2.26* | 1.90 |
| *Orientation* | 1.362 | 2.112 | 1.95 | 1.39 | 1.79 | 1.70 |

Low-level visual task performance in DLB patients and older adults

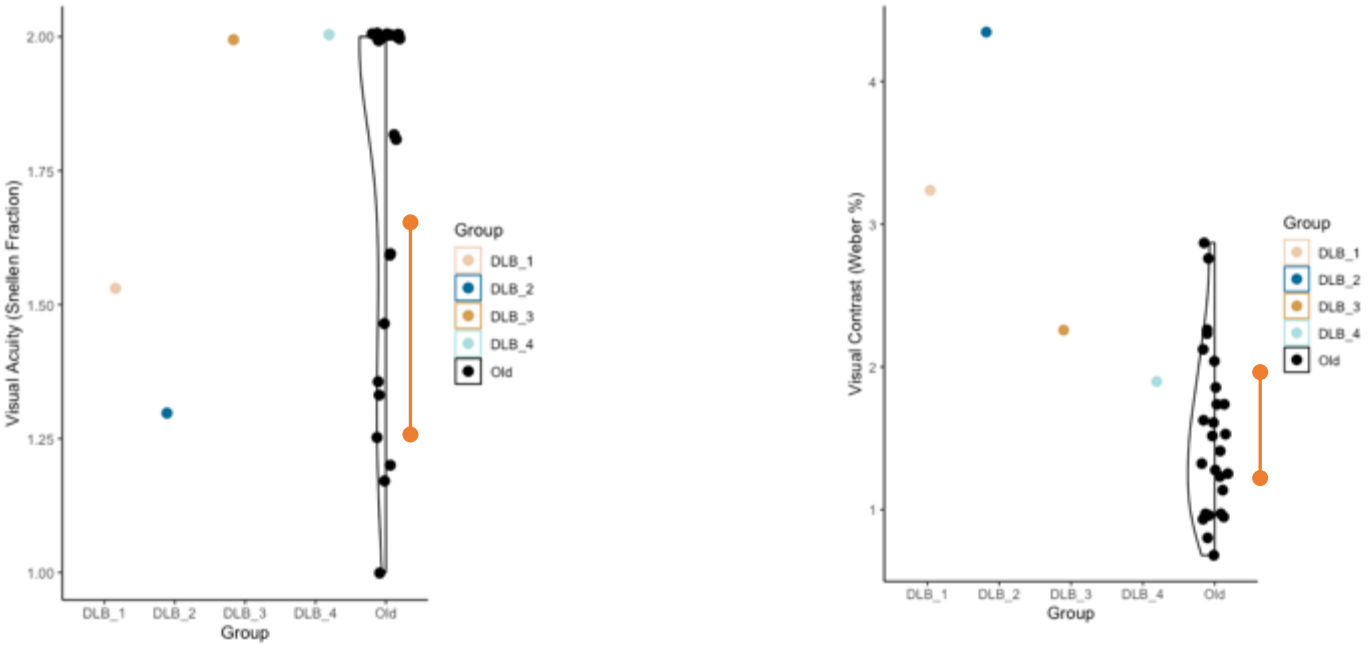

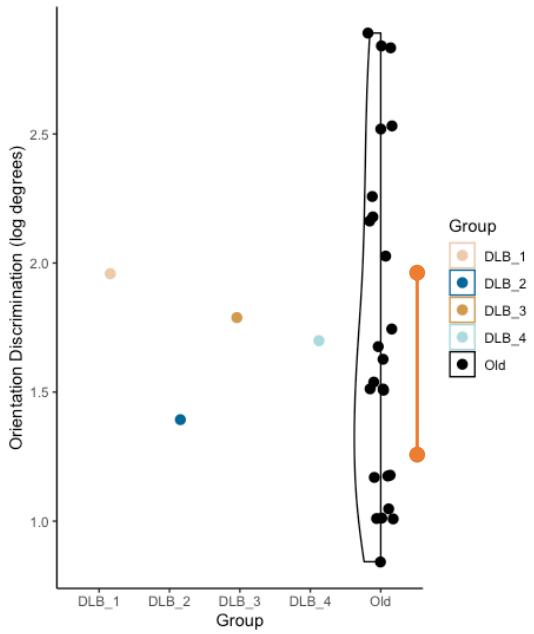


Figure 3.11 Low-level visual task performance in DLB patients and older adults. Visual acuity performance for DLB patients was within or exceeded 95% confidence interval (CI) for the older adult control group (CI = mean +/- 1.96 x √n). Visual contrast was poorer in three (DLB1, DLB2, DLB3) DLB patients in comparison to CI in older adults. Visual orientation for all DLB patients was within the 95% CIs. Orange bar represents older adults' 95% CI.

### 3.4.3 Mid-level vision

For mid-level vision tasks, DLB patients' contour integration threshold was lower than the 95% CI, indicating poorer integration performance in DLB1, 2 and 4. Furthermore, motion coherence thresholds for patients 1 and 3 were greater than the 95% CI for older adults, indicating poorer motion performance (Table 3.7, Figure 3.11).

Table 3.7 DLB patient mean performance on mid-level visual tasks, in comparison to 95% confidence interval (CI) upper and lower bounds for older control participants. * indicates scores deviating from 95% CI.

| | Lower control CI | Upper control CI | DLB 1 | DLB 2 | DLB 3 | DLB 4 |
|---|---|---|---|---|---|---|
| *Contour threshold* | 26.92 | 31.38 | 20* | 20* | 32* | 24* |
| *Motion coherence threshold* | 0.43 | 0.75 | 0.91* | 0.5 | 0.83* | 0.48 |

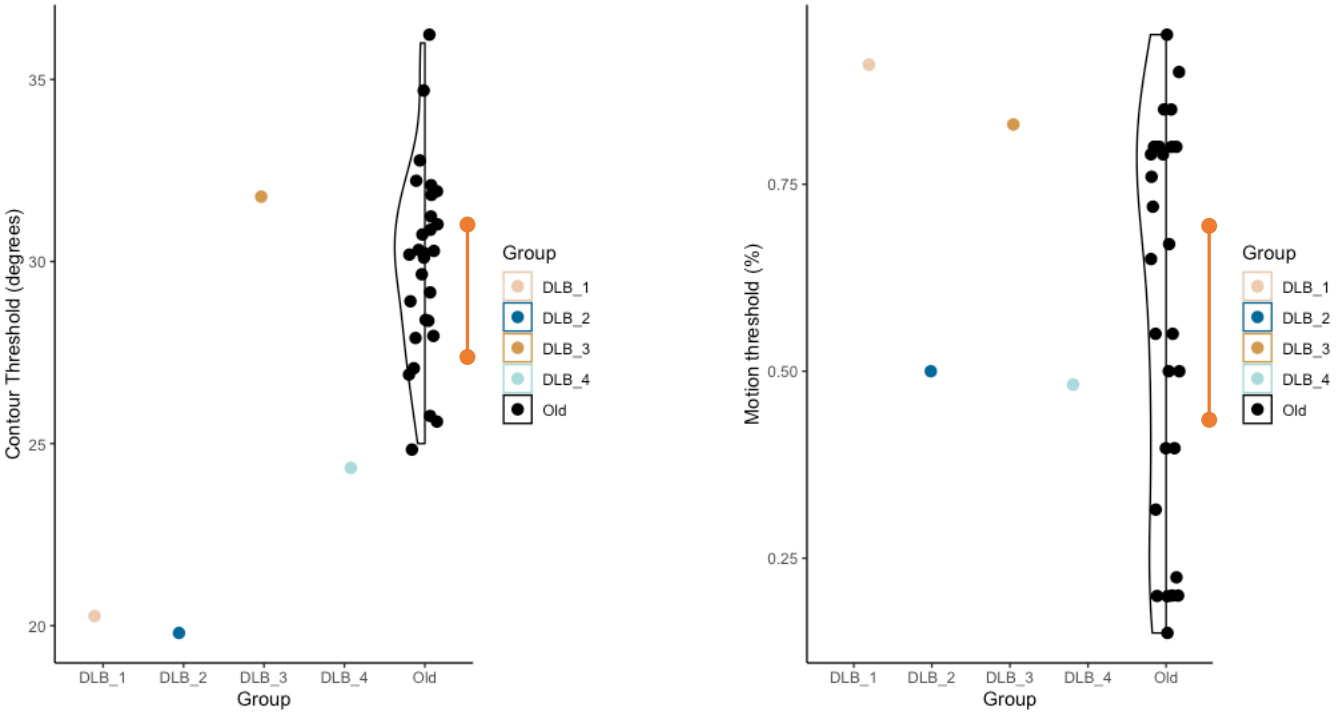


Figure 3.12 Mid-level visual task performance in DLB patients and older adults. Contour threshold performance for DLB patients was higher than 95% confidence interval (CI) for the older adult control group (CI = mean +/- 1.96 x √n) in one case (DLB 3), and lower in the other three cases. Motion coherence was higher than 95% CIs (and thus poorer) in two cases (DLB1, DLB3) and within CIs for two DLB patients (DLB2 and DLB4). Orange bar represents older adults' 95% CI.

### 3.4.4 High-level vision

Embedded figures accuracy was lower for DLB patients 1, 2 and 4 in comparison to 95% CI for older adults, and rotation accuracy was lower in patients 1 and 2 in comparison to 95% CI for older adults. In addition, patients 1, 2 and 3 performed at a lower level than the 95% CI for older adults in change blindness accuracy (Table 3.8, Figure 3.12).

Table 3.8 DLB patient mean performance on high level visual tasks, in comparison to 95% confidence interval (CI) upper and lower bounds for older control participants. * indicates scores deviating from 95% CI.

| | Lower control CI | Upper control CI | DLB 1 | DLB 2 | DLB 3 | DLB 4 |
|---|---|---|---|---|---|---|
| *Embedded figures accuracy* | 86.65 | 96.02 | 73.17* | 85.18* | 96 | 72.72* |
| *Change blindness accuracy* | 72.61 | 79.97 | 50* | 40* | 50* | 75 |
| *Rotation accuracy* | 72.02 | 92.34 | 51.61* | 48.37* | 100* | 90.63 |

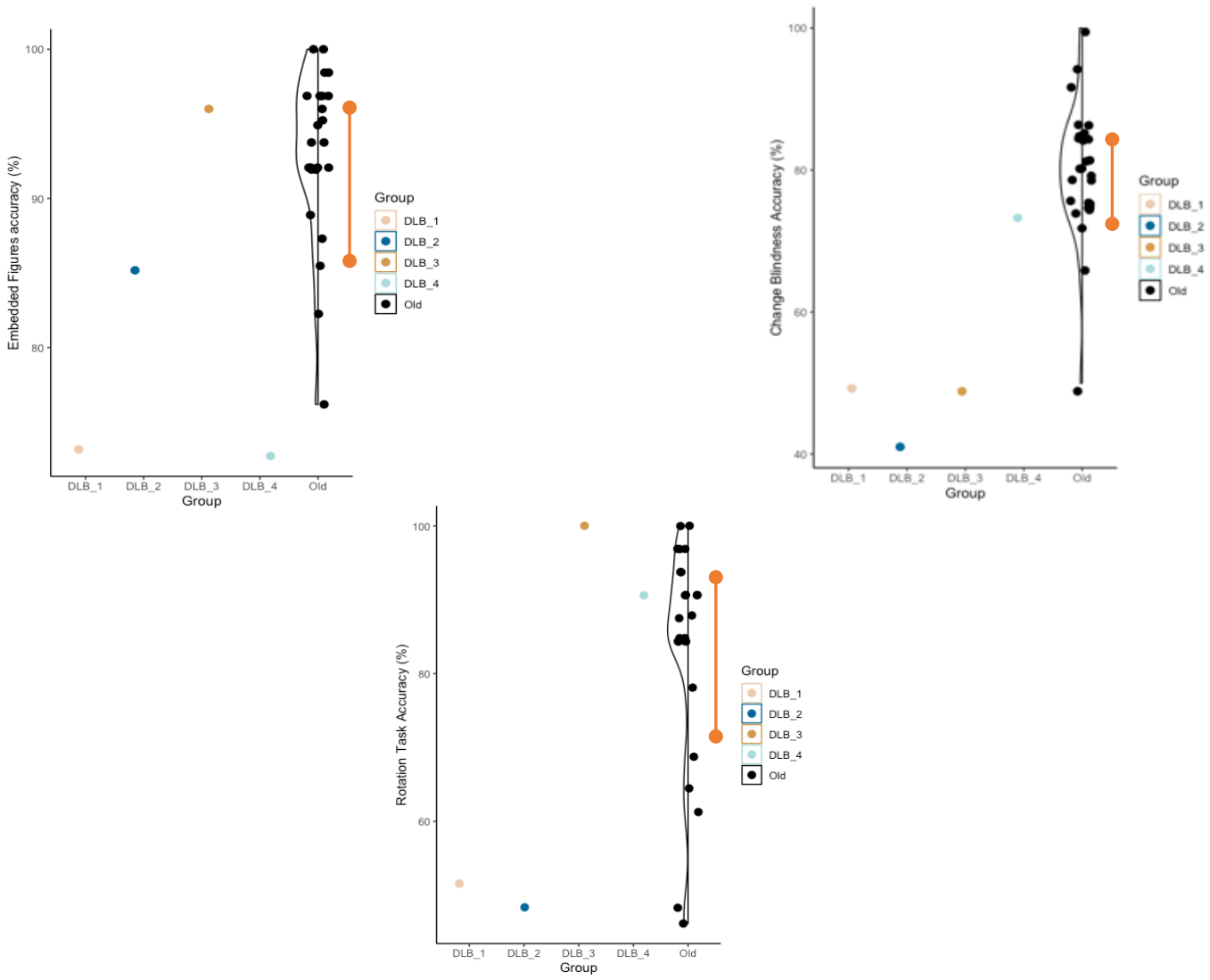


Figure 3.13 High-level visual task performance (accuracy %) in DLB patients and older adults. For Embedded figures accuracy, 3 DLB patients showed lower performance than 95% confidence interval (CI) for the older adult control group (CI = mean +/- 1.96 x √n) and in one case (DLB 3), performance was within CIs. For change blindness accuracy, three patients (DLB1, DLB2, DLB3) showed lower than 95% CIs performance, and DLB4 showed performance within CIs. For rotation accuracy, DLB3 and 4 showed performance within or exceeding 95% CIs, and DLB 1 and DLB 2 showed lower rotation accuracy than 95% CIs. Orange bar represents older adults' 95% CI.

### 3.4.5 Reaction times (RT)

DLB patient 1 showed RTs lower than the older adults 95% CIs in all tasks, except for motion coherence, in which they showed greater RTs. In addition to predominantly lower RTs outside the 95% CI in all tasks, DLB1 also showed RTs outside the 95% CI, indicating both impaired RT and accuracy. For DLB3, RT which was greater than the 95% CI was also related to poorer task performance, however for DLB2 and DLB4, 'poorer' task accuracy (outside the 95% CI) did not seem to relate to altered RT outside of the 95% CI (Table 3.9, Figure 3.13).

Table 3.9 DLB patient mean reaction time on all visual tasks, in comparison to 95% confidence interval (CI) upper and lower bounds for older control participants. * indicates scores deviating from 95% CI.

| | Lower control CI | Upper control CI | DLB 1 | DLB 2 | DLB 3 | DLB 4 |
|---|---|---|---|---|---|---|
| *Contour RT* | 4454.61 | 7607.32 | 3731.54* | 4367.89* | 6303.07 | 3199.568* |
| *Motion RT* | 1540.25 | 2676.76 | 3974.34* | 1515.55* | 2728.87* | 1600.87 |
| *Embedded figures RT* | 6719.45 | 12691.91 | 4812.64* | 17536.95* | 7428.78 | 12215.75 |
| *Change blindness RT* | 2854.22 | 7519.54 | 1423.78* | 6933.77 | 4190.28 | 12135.8* |
| *Rotation RT* | 5722.64 | 11297.39 | 5361.17* | 9054.87 | 7557.74 | 4113.86* |

RT performance in mid to high level visual tasks in DLB patients and older adults

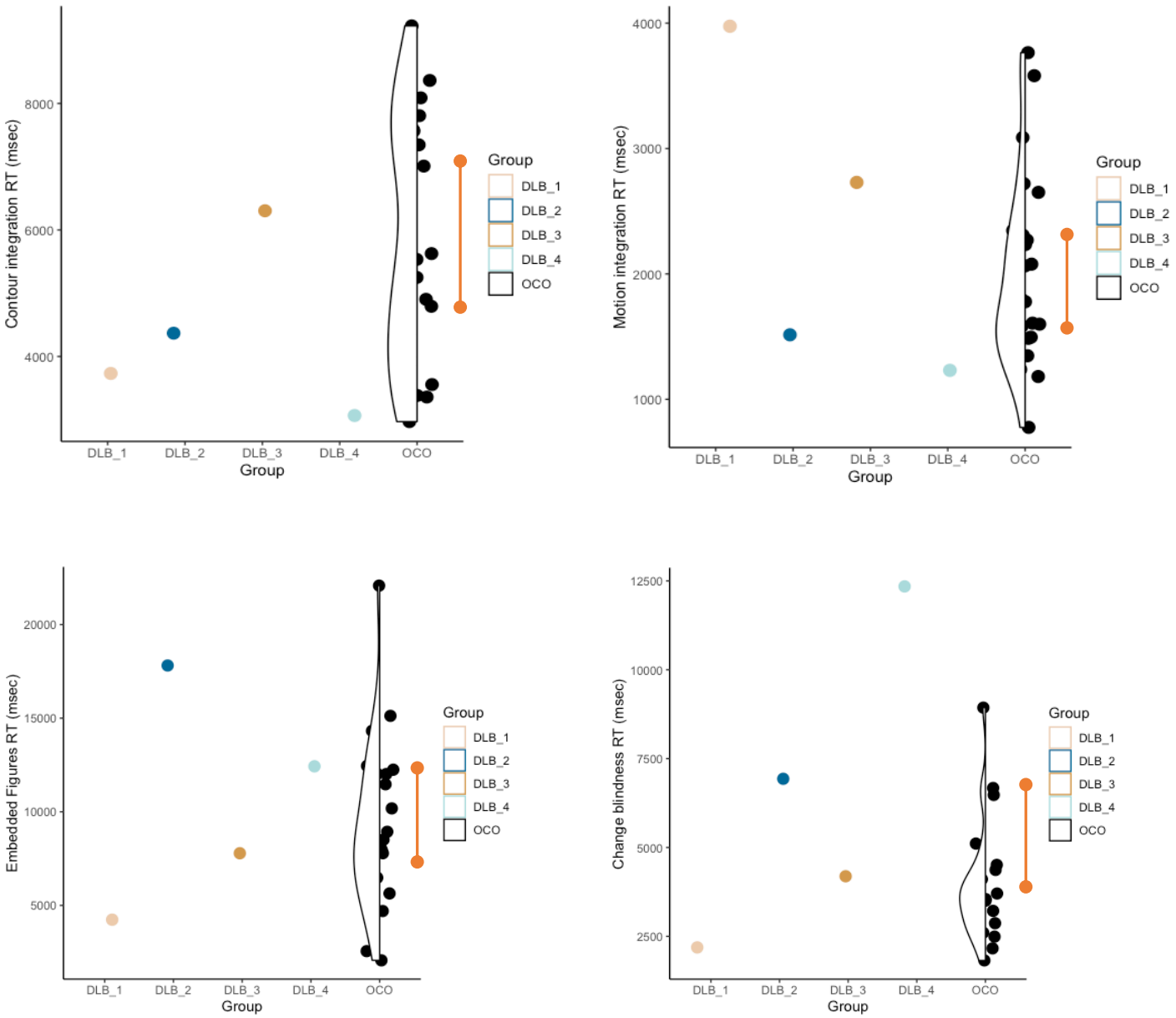

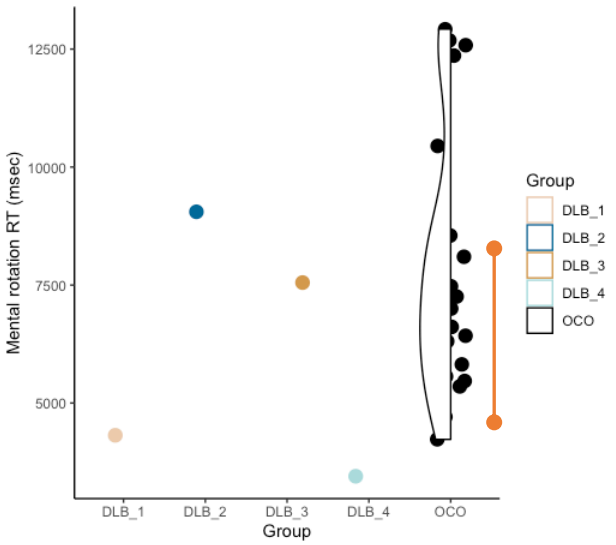


Figure 3.14 Reaction time (RT) performance in mid- to high-level visual tasks in DLB patients and older adults. RTs are varied in DLB patients, in comparison to older adults' 95% confidence interval (CI = mean +/- 1.96 x √n). Lower and mid-level visual task RT appear to be lower and greater with complexity of task in some cases, with the opposite pattern in some DLB cases. Many cases fell outside of older CI. Orange bar represents older adults' 95% CI.

### 3.4.6 Speed accuracy trade-off (SAT)

DLB patient 1 showed a higher SAT performance for contour integration and motion tasks, but SAT were within the normal ranges for other higher-level tasks (Table 3.10). For DLB 2, the opposite pattern was observed, with contour and motion task performance within CIs for older controls but higher SAT in embedded figures and change blindness, and SAT towards the higher end of CI for mental rotation. DLB 3 and 4 showed similar performance patterns for contour and motion tasks, with higher SAT for both tasks and for embedded figures task. DLB 3 was in the SAT CI for change blindness, but DLB 4 was much higher, and DLB 3 showed much higher SAT for mental rotation, but DLB 4 showed much lower SAT for the same task (Figure 3.15).

Table 3.10 DLB patient mean SAT on mid and higher-level visual tasks, in comparison to 95% confidence interval (CI) upper and lower bounds for older control participants. * indicates scores deviating from 95% CI.

| | Lower control CI | Upper control CI | DLB 1 | DLB 2 | DLB 3 | DLB 4 |
|---|---|---|---|---|---|---|
| *Contour SAT* | 6449.51 | 8650.62 | 14092.70* | 7923.57 | 11186.54* | 13546.65* |
| *Motion SAT* | 1576.96 | 2523.83 | 5864.34* | 2375.06 | 3856.69* | 2885.03* |
| *Embedded figures SAT* | 15896.54 | 34225.89 | 25898.29 | 46362.87* | 43655.87* | 33925.63* |
| *Change blindness SAT* | 5710.71 | 9456.86 | 8902.43 | 9585.07* | 7654.37 | 16359.65* |
| *Rotation SAT* | 8775.38 | 13518.21 | 10982.89 | 12081.34 | 13606.59* | 6841.95* |

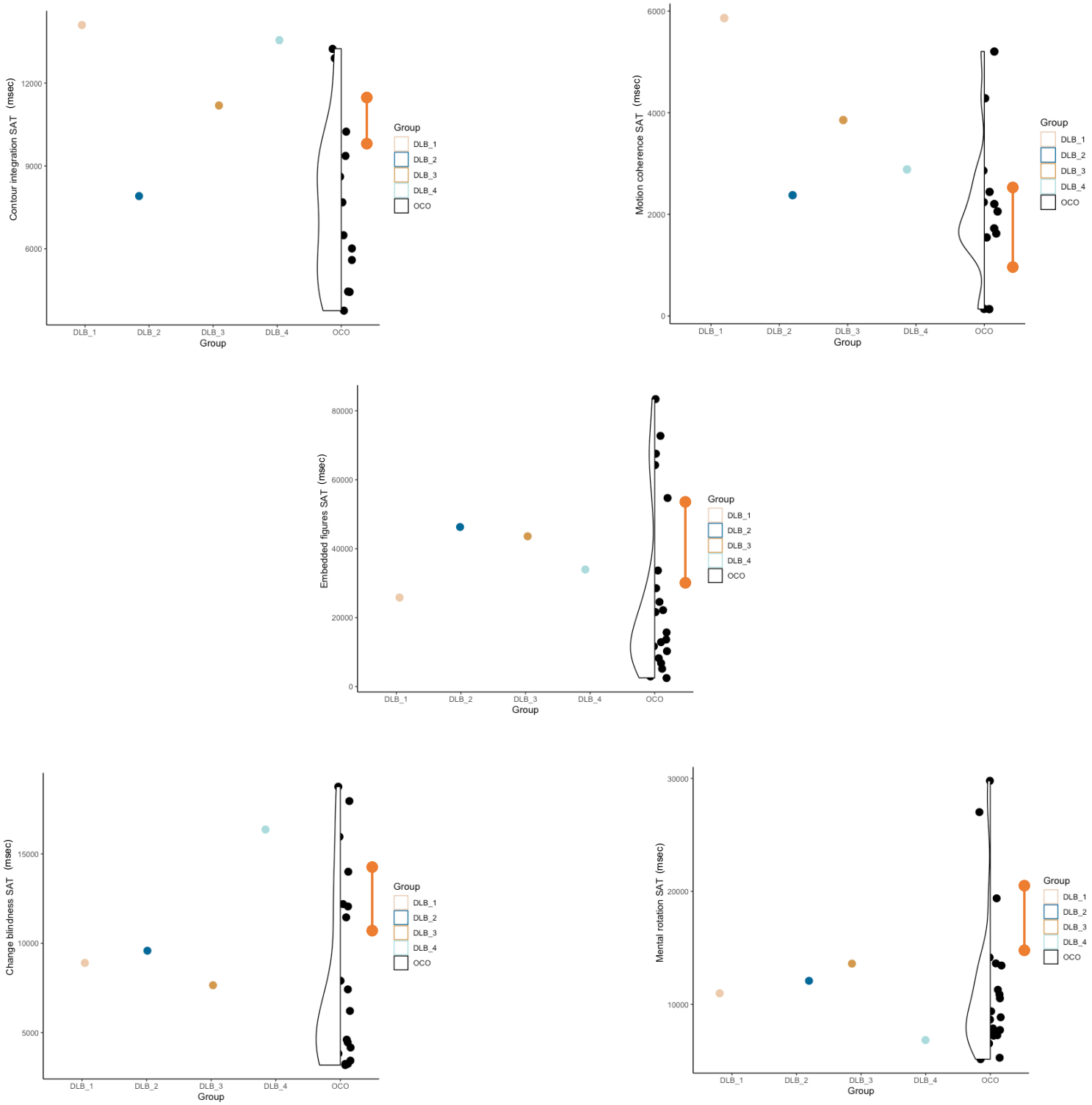


Figure 3.15 Speed accuracy trade-off (SAT) in mid- to high-level tasks in DLB patients and older adults. SATs are varied in DLB patients, in comparison to older adults' 95% confidence interval (CI) for the older adult control group (CI = mean +/- 1.96 x √n ). Many cases fell outside of older CI, with most DLB patients showing higher SAT than older adults, except for during mental rotation task performance. Orange bar represents older adults' 95% CI.

### 3.4.7 Attention Network Task performance

ANT task performance was highly varied, with DLB 1 and 2 showing significantly longer RTs in all conditions. DLB patients 2, 3 and 4 showed alerting effects while DLB1 did not. For DLB 1, 2, ad 3 orienting and executive effects were within, if not exceeding performance in older adults. This is with the exception of DLB 4, who showed greater alerting effect, but a negative or impaired orienting effect which then also limited the executive network effect. (Table 3.8, Figure 3.14).

Table 3.11 DLB patient mean performance in cue and flanker conditions and network effects in the Attention Network task, in comparison to 95% confidence interval (CI) upper and lower bounds for older control participants. * indicates scores deviating from 95% CI.

| | Lower control CI | Upper control CI | DLB 1 | DLB 2 | DLB 3 | DLB 4 |
|---|---|---|---|---|---|---|
| *ANT no cue RT* | 802.39 | 1293.13 | 1670.36* | 1650.70* | 1274.57 | 1035.81 |
| *ANT double cue RT* | 685.41 | 1238.83 | 1698.19* | 1602.36* | 1238.44 | 858.51 |
| *ANT spatial cue RT* | 686.34 | 1175.15 | 1638.87* | 1616.76* | 1225.34* | 913.65 |
| *ANT centre cue RT* | 762.73 | 1240.27 | 1670.13* | 1755.57* | 1267.02* | 840.51 |
| *ANT incongruent RT* | 793.40 | 1307.45 | 1687.59* | 1857.72* | 1201.51 | 934.188 |
| *ANT congruent RT* | 754.87 | 1194.65 | 1533.18* | 1530.48* | 1160.75 | 928.52 |
| *ANT alerting effect* | 5.58 | 100.27 | 0.23* | 95.13 | 7.55 | 195.31* |
| *ANT orienting effect* | -1.13 | 61.27 | 31.26 | 38.81 | 41.68 | -73.147* |
| *ANT executive effect* | 11.09 | 131.23 | 154.41* | 327.24* | 40.76 | 5.67* |

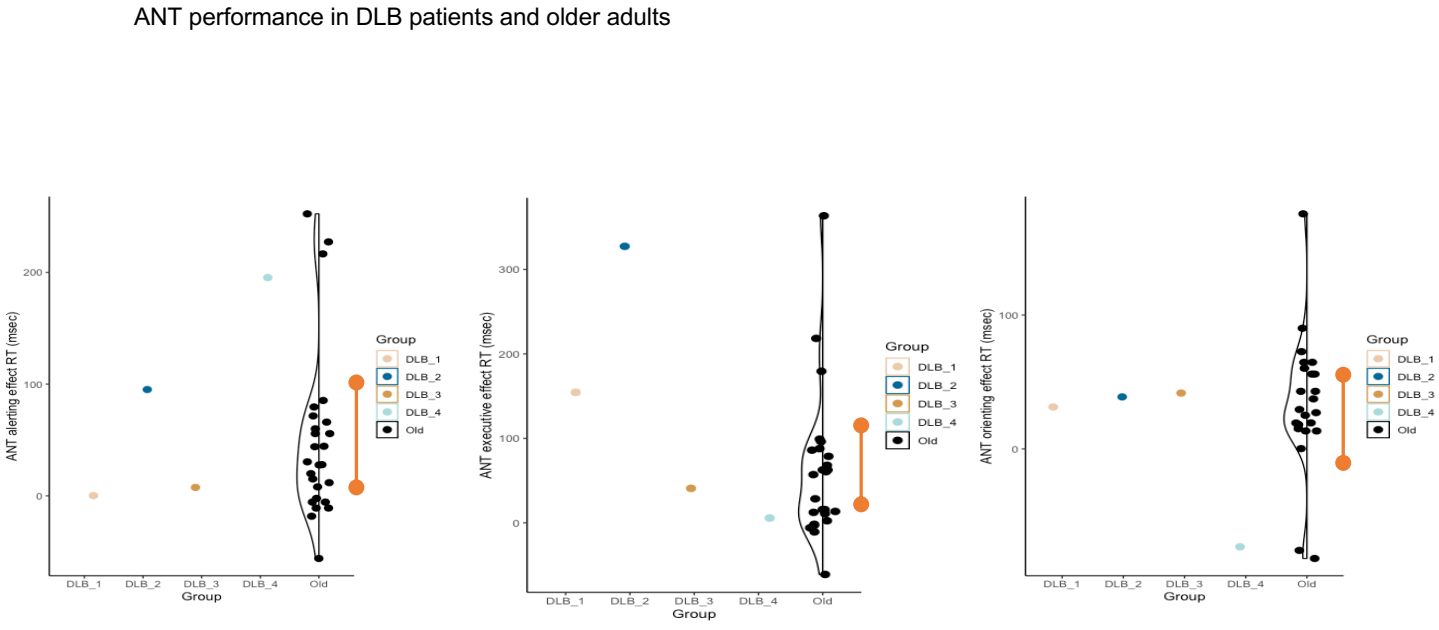


Figure 3.16 Attention Network Task (ANT) performance in DLB patients and older adults. ANT network activations are shown, calculated by obtaining the difference between two condition RTs (alerting = double cue RT – no cue RT, orienting = spatial cue RT – centre cue RT, executive = incongruent flanker RT – congruent flanker RT). Most DLB patients' fell within CI of older adults for alerting and orienting effect. Those DLB patients demonstrating an alerting effect appeared to also demonstrate a orienting and executive effect. DLB 4 showed higher alerting, lower orienting effect. Orange bar represents older adults' 95% CI.

## 3.5 Discussion

The present chapter investigated age and DLB-related differences in visual perception and attention functions across a hierarchy of low, mid and higher-level tasks. While older adults tended to respond slower in most tasks in comparison to younger adults, they only showed reduced abilities in visual contrast, orientation and motion discrimination tasks while more complex, higher order visual perception and attention including orienting, alerting and executive functioning were relatively preserved, albeit at the cost of a slower RTs. In contrast, there was evidence for DLB affecting visual perceptual and attention function across the whole hierarchy with the exception of low-level visual acuity. In the following section I will discuss these results in more detail within the context of the existing literature as well as in terms of their implications for our understanding of age and disease-related changes in visual perception and attention.

### 3.5.1 Low-level visual functions in ageing

As hypothesised my analysis revealed that visual acuity did not show any significant age-related decline. Previous research suggests that visual acuity impairments in ageing may occur due to age-related diseases that can lead to visual impairments such as Type II diabetes, cataracts or macular degeneration (Sinclair, 2000). Furthermore, it has been observed that age-related dynamic visual acuity impairments can be mitigated by adjustment of luminance (Long & Crambert, 1990). In this thesis all participants were carefully screened for any diseases that may affect their vision and only older adults free from eye disease or other visual impairment were recruited and assessed using vision correction (i.e. spectacles or contact lenses). Thus, no visual acuity impairments were observed in older versus younger adults. Together these results suggest that previously reported declines in age-related visual acuity (Freeman et al., 2005) may be a product of age-related decline in visual health rather than a primary function of older age.

However, as hypothesised and in line with previous research (Casco et al., 2017, Greene & Madden, 1987 Betts, Sekuler & Bennett, 2007), visual contrast and visual orientation performance did show decline in the older group. Indeed, age-related decline in contrast sensitivity has previously been proposed as a reliable and useful measure for the identification of age-related visual function (Green & Madden, 1987). Moreover, a decline in contrast sensitivity in older adults is thought to account for increased orientation discrimination thresholds (Delhahunt, Hardy & Werner, 2008). Both impairments have been attributed to age-related neuronal loss within the lower-level visual pathways (Elliot et al., 1990), but also age-related damage to cells in the parvocellular pathway (Schiller et al., 1990). Age-related changes to the morphology of retinal ganglion cells such as reduced dendrites (Nadal-Nicolas, 2019), may therefore lead to particular impairments in contrast sensitivity and orientation, resulting in hindered bottom-up sensory processing in older adults.

### 3.5.2 Mid-level visual functions in ageing

In contrast to previous reports (Roudaia et al., 2008), no age-related differences in contour integration were found at mid-level visual functioning. Recently it has been shown that ageing does not affect sensitivity in

certain elements of a Gabor patch contour stimuli such as their collinearity or proximity (Roudaia et al., 2013). Notably, accuracy in a Gabor contour integration task showed no age-related effects when contour and distracter elements had equal spacing. As equal spacing was implemented in the current study this may explain why no age-related effects were shown. In addition, older adults are known to require longer stimulus durations (1 second minimum) for the successful discrimination of contours. As the current tasks were set up to be suitable for DLB patients stimuli presentation was restively long in duration (16000ms) for older adults' to process the information. Thus, the type of Gabor stimuli and the length of stimulus presentation in my task battery very likely provided conditions which allowed older adults to perform at an equal level with younger adults (Roudaia et al., 2011). This suggests that in the present context the requirement of the tasks to be feasible for DLB patients may have 'simplified' the task for older adults, resulting in no significant age-related differences in performance.

However, in contrast to contour integration and consistent with a number of previous studies (eg Pilz et al., 2017), an age-related performance decline was observed in motion coherence threshold. In contrast to previous reports though (Snowden & Kavanagh, 2006), this reduced threshold was observed in the absence of any age-related slowing in response speed. In contrast to the contour integration task the motion coherence tasks was written with a fixed rather than a self-paced stimulus duration of 5000ms. The choice for the stimulus duration was based on previous reports of robust age-related motion perception with these specific task parameters (Bennett, Sekuler & Sekuler, 2007). Therefore, my results may reflect the reverse of the usually observed speed-accuracy trade off in ageing of slower responses in favour of accuracy, suggesting that when older adults have to respond as fast as younger adults and are given no option of longer stimulus duration, they were not able to detect motion coherence as reliably as younger adults. Motion coherence also involves an element of dorsal stream functioning, recruiting regions for attentional control (Billino & Pilz, 2019) which older adults often exhibit impairments in, which would also account for poorer motion threshold performance.

### 3.5.3 Higher level visual functions in ageing

No differences in accuracy in higher-level visual tasks such as embedded figures task, mental rotation task or change blindness accuracy were found consistent with reports in the literature (Endrass et al., 2012). Preserved accuracy was accompanied by slower response latencies in older adults in contour integration, embedded figures, change blindness and mental rotation tasks. This pattern of results is consistent with the pattern of SAT typically observed in ageing, where responses are slower in a bid to maintain accuracy. One of the reasons for this may have been that older adults were reluctant to commit to errors, potentially due to a distrust in sensory processing (as was shown to be impaired), meaning they adopt a cautious attitude and accumulate more evidence before making a decision (Forstmann et al., 2011; Rabbitt, 1979). These results are interesting as they replicate previous findings suggesting a complexity effect in older adults, in that RT slows with age and with increasing task demands and/or neural processing complexity (Bashore et

al., 1997). However, it should be noted that as the motion task in the current study was not self-paced, older adults may show a more typical profile of increased RT to mitigate accuracy during a longer stimuli duration. As such, these findings also warrant further investigation of the elements within RT which may show decline and brain regions associated with this (Chapter 6).

### 3.5.4 Speed accuracy trade-off in ageing

SAT was significantly greater in contour integration, embedded figures, mental rotation and change blindness tasks in older adults in comparison to younger adults. This was due to older relative to younger adults showing longer RTs but preserved accuracy in these tasks and hence these findings are consistent with the typical pattern of SAT, reflecting slower and more cautious decision making in older adults (Starns & Ratcliff, 2010). For contour integration, threshold did not differ between groups, but SAT was longer in older adults, suggesting that any age-related impairments in mid-level contour abilities (or centre surround suppression) may be mitigated by longer processing time or more cautious decision making. When completing higher-level tasks it is also evident that any lower-level age-related visual impairments (such as impairments in visual contrast or orientation) may have also been mitigated in the same way by a slower and thus more cautious approach.

In contrast, motion coherence SAT did not differ between groups. This was most likely as a result of stimuli duration being shorter in this task, leading to no significant group difference in RTs. Although threshold levels were lower in older adults in comparison to younger adults, accuracy levels did not differ between groups. This was due to the staircase adjustments of stimuli within the task, where thresholds were lowered in older adults, allowing them to remain highly accurate, resulting in no difference in SAT. Therefore, older adults were able to respond as fast and accurately as younger adults but at a lower level of coherence, suggesting that perceptual factors may contribute significantly to age-related lengthening of SAT.

### 3.5.5 Attentional functions in ageing

There were no group differences in my results in any ANT network effects, with orientation network effect only approaching significance. This is inconsistent with previous literature, describing age-related impairment in executive network functioning (Mahoney et al., 2010). One explanation of this may be due to the order of the tasks. A previous study has reported that there was a significant influence of presenting object and scenery stimuli in boosting executive network performance in the ANT in older adults (Gamble et al., 2014). The authors suggest that this attenuation effect may be due to a reduction in fixations, and thus effortful attention occurs when viewing scenes as opposed to other stimuli, mitigating the fatigue effect of prior task completion that is typically prominent in healthy older adults (Hess & Ennis, 2011). In this empirical work, as participants completed the cognitive battery in one sitting, with the ANT task following the visual hierarchical tasks it may be that completing the change blindness task in which scenes were

presented and responded to by participants may have provided a restorative effect on executive attention, and attenuated performance in the ANT.

An alternative explanation may be that the age-related theory of executive decline, or frontal ageing, is not as prominent in older adults as previous anticipated. It has been reported that although older adults showed impairments in using top-down attentional control for the suppression of task irrelevant information, some forms of top-down attention are not susceptible to the decline in age-related executive control (Madden, 2007). Moreover, executive functions such as sorting (Zelazo, Craik & Booth, 2004), task initiation (Bedard et al., 2002) and task switching (Cepeda et al., 2001) have been shown to have a U-shaped function of age, increasing from younger adulthood into later life (Zelazo, Craik & Booth, 2004). Older adults have been shown to be successful in recruiting top-down attention for target-relevant information in search tasks which are more complex and involve the guiding of attention (Madden et al., 2007). In my study older adults exhibited comparable alerting, orienting and executive effects as younger adults. This suggests that anterior and posterior attention mechanisms were relatively preserved in older adults. It may, however, be the case that older adults were able to recruit top-down attention by attending to target-relevant information rather than focusing on suppressing task-irrelevant stimuli.

### 3.5.6 Unimpaired, impaired and shift performance in older adults

Taken together, this pattern of results does not seem to be consistent with the view that lower-level visual functions are preserved, and that ageing affects higher order, more complex tasks disproportionately. Thus, these results appear to contradict the frontal ageing hypothesis, as tasks which require greater executive function expenditure were relatively preserved in older adults. On the basis of performance in these tasks, I categorized outcomes in to three categories: impaired, unimpaired and shift. First, 'impaired' tasks in which group comparisons showed that older adults had poorer performance, with no indication of compensation in other outcome measures of the task (i.e. speed vs accuracy) including visual contrast, visual orientation and motion performance. For 'unimpaired' tasks, group comparisons showed no significant differences, indicating that older adults' performance was comparable to that of younger adults including visual acuity, contour threshold and ANT tasks. Finally, tasks which showed a 'shift' includes SATs, where older adults showed poorer RT in order to mitigate accuracy, which was unimpaired, indicating a 'shift' in strategy including SAT performances. This 'shift' did not necessarily mean older adults had impaired performance but adopted a more cautious strategy in their response.

Older adults performed at a comparable level in higher-level tasks and attention tasks with regards to threshold and congruency effects and were thus categorised as 'unimpaired'. This suggests that older adults are in fact able to recruit top-down executive attention mechanisms when required, potentially to mitigate lower-level perceptual impairments, but at the costs of response slowing. Previous research has shown that older adults are able to orient attention, ignore intermodal distraction and perform local task-switching,

when taking bottom-up sensory deficits into account (Zanto & Gazzaley, 2014). In contrast, those in the 'impaired' category were typically tasks where cognitive demand on global attentional functioning was higher, with the exception of visual contrast. My observation of age-related impairments in motion coherence performance appear consistent with this pattern as although the task was not cognitively complex in terms of processing resource it did require enhanced attentional function due to the speeded nature of the stimulus delivery.

Altogether the pattern of the observed findings suggests that ageing may be associated with hampered bottom-up sensory processes, notably contrast sensitivity and orientation but not visual acuity. It is assumed that such bottom-up processes feed into mid to higher level visual functions and hence that any impairments will affect the processing in higher order tasks. In the current results, such lower-level visual impairments appeared to be compensated for in mid to higher level tasks when older adults had sufficient time to process the information, i.e. in tasks with sufficiently long stimulus duration. This was reflected in the age-related SAT differences with preserved accuracies at the cost of longer RTs, or those in the 'shift' category. The more complex and attentionally demanding the task the longer the required processing time for older adults, for instance RTs tended to be longer in the Embedded figures task than in the orientation task. However, when older adults are not able to apply a more cautious but slower strategy and were forced to perform at the same speed as younger adults, they exhibited a poorer level of accuracy in the motion task.

Thus bottom-up deficits in ageing can be mitigated to a certain extent by top-down processing, but that this requires greater stimulus duration in ageing, potentially due to greater age-related limitations in top-down attentional mechanisms (Zanto & Gazzaley, 2014). Degraded sensory input with age has been shown to lead to a higher 'load' on cognitive processes, reducing resources available and increasing the 'cognitive difficulty' of tasks for older adults, and may lead to (in some cases) inefficient compensatory mechanisms (Roberts & Allen, 2016).

### 3.5.7 Visual perception and attention in DLB

The current DLB results were only based on four patients, and therefore their interpretation requires caution. However, DLB patients compared with their age-matched healthy controls showed poorer contrast performance while visual acuity or visual orienting performance appeared to remain preserved, suggesting a relative sparing of lower-level visual functions. In addition, there was evidence of poorer contour threshold and motion coherence performance (for two patients) reflecting difficulties in mid-level vision. Finally, all higher visual tasks appeared affected by DLB. For change blindness and embedded figures performance, the majority of DLB patients performed worse than the 95% CI for older adults. Interestingly, mental rotation performance was higher than 95% CI in one DLB patient but lower in others. However, this may be a product of long stimulus duration. These results suggest a widespread decline throughout all

levels of the visual hierarchy which becomes more apparent in more complex, higher-level tasks. Moreover, results were subject to interindividual variation, which likely reflects both disease stage of the patient and location of deposition of Lewy body pathology in the brain in individual patients. These results therefore require replication in a larger sample size of DLB patients.

ANT task performance for DLB patients was again varied. Two patients showed significantly longer RTs in all conditions of the task, which is consistent with previous findings reporting overall slowing in DLB (Ballard et al., 2001). One of the DLB cases showed a very limited alerting effect, suggesting that this participant was unable to effectively attend to and focus on the stimuli. However, contrary to previous findings (Fuentes et al., 2010) which have shown that when DLB have limited alerting ability they also show diminished performance in other ANT networks, this participant showed orienting and executive effects which were either within or above the performance level of older adults. These results suggest that despite their general alerting impairment, the individual was able to orient to the relevant stimuli and inhibit irrelevant stimuli during incongruent trials, potentially reflecting a compensatory cognitive mechanism for completing the task. Two DLB patients were able to show alerting, orienting and executive effects that were within the control group's 95% CIs, if not exceeding, performance in older adults. Finally, one of the DLB patients showed an opposite profile, in that they had a greater alerting effect, but a negative orienting effect and a limited the executive network effect. These findings are somewhat consistent with previous results showing that if DLB patients are able to demonstrate an alerting effect, then they are able to successfully show activation in other attention networks (Firbank et al., 2016). This also indicates that top-down attentional systems can be recruited effectively to orient attention and suppress irrelevant information if the stimulus is alerted to.

RT performance was also varied in DLB patients, with some tasks showing much lower RT – therefore faster performance – and some showing much longer RT than 95% CIs in older adults. These results were also supported by SAT, showing some but not all DLB patients experienced lengthened SATs. These findings are interesting, as it would typically be anticipated that RT would be slower in DLB patients due to difficulty focusing and maintaining attention, or difficulty in visual processing (Ballard et al., 2001). This is somewhat evident in higher level visual tasks in which DLB patients were slower than older adults. As with attention networks, it may be the case that DLB patients struggle to perceptually process stimuli therefore make fast responses as engagement with the task and cognitive processing is not actually occurring. The current varied findings and potential methodological limitations of using mean RTs and their difference as outcome measures suggest that it would be more informative to investigate the different processing elements that contribute to the overall RT. Drift diffusion modelling assumes that perceptual processing elements, information processing quality, and level of information are all required to make a response and hence contribute to the overall RT. Such modelling may provide greater detail to aid in the understanding of which specific elements of cognitive processing are underlying variation in RTs in DLB

patients. In addition, identifying impairments in RT decision-making elements may provide insight into the basis for clinical symptoms of visual hallucinations and cognitive fluctuations. This line of enquiry is explored more thoroughly in Chapter 7.

### 3.5.8 Limitations

In my assessment of visual and attentional functions in younger and older adults there are several limitations. Most notably, as the tasks were designed to be accessible by older adults with dementia as well as younger and older adults, some compromises had to be made in the number of trials and stimuli duration included in the tasks. Whilst these tasks still endeavour to assess different functions of the visual processing system in a sensitive manner, there was some simplification necessary which may limit validity. Subsequent work focusing on healthy ageing only should increase trial numbers to provide a more valid assessment of these functions.

In addition, it should be acknowledged that whilst psychophysical principles were incorporated into tasks where appropriate, this could not be easily applied to all tasks such as higher-level vision in which multiple visual variables were altered in the stimuli. In addition, the tasks which did incorporate psychophysical principles used an adaptive staircase method as opposed to a more classical method of adjustment. This is an advantage; as it addresses the challenge of selecting the 'correct' stimulus values to assess a participant and provides a more sensitive estimate of performance threshold. However, the staircase method relies on the 'correct' or appropriate starting point to be selected. Whilst this limitation was mediated by thorough pilot testing, it may still influence the results in a detrimental manner by over or under inflating performance. In addition, staircase procedures typically require a larger number of trials to estimate an accurate threshold. Whilst an experienced psychophysicist (G.Lovell) was consulted for guidance with regards to the minimum number of acceptable trials for all tasks employing a staircase, it should be considered that a greater trial number may provide more accurate estimations of performance. It is also noteworthy that more 'precise' adaptive methods can be employed such as the maximum-likelihood adaptive procedures of QUEST (Watson, 1983), or interleaving staircases. This was no selected due to the complexity and number of trials required, however implementing a more complex Bayesian staircase would also improve the accuracy of threshold estimates in subsequent research.

Specifically with regards to the current orientation stimuli, the oblique effect was not considered in the design of the task. The oblique effect refers to a phenomenon in which orientation detection is related to a strong response in V1 (Koelewijn et al., 2011) and significantly negatively correlated with visual cortex GABA (Edden et al., 2009), which is not as apparent with vertical stimuli. Considering this evidence, it is possible that the current stimuli which compared oblique to a vertical orientation gabor patch may not evoke a visual response in such a way that the oblique effect shows for orientation ability. Therefore, this

may have resulted in greater variance in performance within the sample and thus resulted in a greater effect being reported in the present results. As such, the results should be interpreted in light of this.

Moreover, one potential limitation regards the sample of older adults assessed in the current chapter. Older adults were excluded on the basis of visual impairments and had normal or corrected to normal vision. However, visual impairments such as cataract or glaucoma are common in the normal ageing population with a vast proportion of older adults experiencing some form of visual impairment or visual loss to an extent (Swenor et al., 2020). It should then be considered that the exclusion criteria for the current study may then limit the generalisability of the results to the wider healthy ageing population. Moreover, relatively few older adults who expressed interest in taking part in the current study were excluded on the basis of visual impairment again highlighting that the current sample may be less representative of the general population, possibly as a result of the method of recruitment. That is, older adults who are more likely to readily partake in psychological studies may be of generally good health as has been previously reported (Gao et al., 2015).

With regards to the behavioural assessment of DLB patients, it may be that the methodology of these tasks is not suitable to capture DLB differences in processing speed reliably and robustly due to the high variation in their performance. As RTs were very long and variable in these particular DLB patients, it may highlight that observing the difference between RTs as a measure of these visual functions is not appropriate. As such, future investigations should consider focusing on obtaining and assessing accuracy or threshold as a measure of visual function and assessing RT alone as a measure of response speed to a relatively low-level attentional task.

Finally, due to the practical logistics of the entire testing procedure (including MRI scanning), the time at which cognitive testing was conducted was variable, meaning some participants took part during evening sessions or early morning sessions. Age differences in cognitive performance are reported to be modulated by the time of day at which the testing takes place (Anderson et al., 2014), suggesting that this may play a role in participant fatigue and subsequent performance. However, this was difficult to control due to participant and researchers' schedules and all other controllable factors were kept constant across participants, such as order of task administration, instructions from the experimenter and order in which cognitive testing and MRI scanning was conducted to reduce this effect. Due to the length of testing sessions, participants were also given the opportunity to take short breaks which may also have impacted performance variability between participants. Despite this, participants took part in the same number of practice trials and tasks were only commenced when confirmation was received that the participant was ready to begin to help mitigate the effects of any additional or limited preparedness. With regards to DLB patients, all behavioural testing was conducted during a mid-morning session to ensure the effects of fatigue were minimised as much as practically possible.

### 3.5.9 Chapter summary

Previous research has noted impairments in a number of attentional and visual tasks in older adults, but rarely have these functions been assessed sequentially along to the visual processing hierarchy in one study. I addressed this gap in the literature by first establishing the behavioural profile of older adults' vision and attention from visual acuity through to higher level vision and attention. In summary, my results show that whilst visual acuity showed no age-related decline, low-level functions of contrast sensitivity and orientation discrimination did. In mid-level vision, older adults were poorer in a motion coherence perception task but did not show performance differences in contour integration. In higher-level visual tasks, no differences in accuracy performance were found between younger and older adults, but older adults showed longer RTs and SAT. Finally, in the ANT I saw no differences in alerting, orienting or executive network performance between older and younger adults. The results above support the ageing-complexity and also typical SAT patterns in ageing but contrast typical theories of age-related executive decline. Four individuals with DLB were also assessed using this task battery and showed preservation of low-level visual functions (excluding visual contrast) but a decline in performance in mid to higher-level functions in comparison to heathy older adults. These findings suggest a more widespread impairment in perceptual and attentional functioning than anticipated. This pattern of age-related performance differences in tasks designed to assess processing stages across the visual perception and attention hierarchy allowed me to further explore i. the neural correlates of age-related decline, maintenance and compensation (Chapter 5) and ii. modelling of the components that may contribute to the slowing of reaction times in older age (Chapter 6).

# Chapter 4 : Metabolic, microstructural and macrostructural changes in ageing

## 4.1 Introduction

Following characterisation of the cognitive profile of older adults and DLB patients in Chapter 3, the objective of the research in the present chapter was to characterise age- and disease-related differences in the microstructural, neurochemical and morphological properties of brain networks underpinning visual perception and attention performance. Neuropathological evidence suggests that rather than being associated with significant cortical neuronal loss, healthy ageing may be associated with a decline in synaptic markers (Hatanpää et al., 1999), reductions in dendritic trees (Flood et al., 1985, Morrison & Hof, 2007) and small myelinated axons (Tang et al., 1997). Furthermore, healthy ageing is also known to be associated with metabolic slowing of mitochondria (Zhang et al., 2018). Whilst there is some evidence regarding these microstructural and metabolic differences associated with ageing (see below), very little is known about such changes in DLB. Given the distinct perceptual and attentional impairments associated with DLB, studying the microstructural and metabolic changes that occur in perceptual and attention networks may aid in our understanding of the biological mechanisms that lead to the cognitive and clinical profile of the disease. As discussed in Chapter 2, MR techniques can be employed to gain estimates of some of these brain tissue properties that are vulnerable to ageing and disease. In the present chapter cortical thickness measures were employed to gain estimates of age- and DLB-related cortical grey matter loss while multi-shell DWI techniques were applied to probe these differences in white matter microstructure. In addition, neurochemical differences in cortical grey matter regions were measured with MR spectroscopy. Mean measurements were extracted from the cortical grey matter regions of interest and the white matter pathways of the visual perception and attention networks discussed in Chapter 2. These were then compared between young and older adults as well as between the older adult controls and the four DLB cases (by comparing their individual scores with the control group's 95% CI) to assess age and DLB-related differences in these properties of the vision and attention network regions.

Finally, the relationship between brain metabolites and white matter microstructure is not well understood. Age-related between-subject variation in these measurements provide the opportunity to study their relationship and to probe the question whether age-related differences in brain metabolites may underpin microstructural changes or vice versa. For instance, age-related reductions in neuronal activity estimated with NAA may be accompanied by reductions in white matter microstructure due to Wallerian degeneration and/or reduced information transfer due to white matter damage. The present chapter therefore explored correlations between metabolites and microstructural indices that demonstrated significant differences with age.

As explained in Chapter 2, a priori ROI analyses for healthy age effects on white matter microstructure and cortical thickness were followed up by whole brain exploratory analyses. These analyses acted as sanity checks for the anatomical specificity of the age effects from the a priori analysis and to assess them within the context of whole brain changes notably the frontal-posterior gradient pattern reported in the literature. The following sections provide an overview of the empirical evidence regarding age and DLB-related changes in metabolic, microstructural and morphological properties of the visual and attention networks of interest.

### 4.1.1 Age-related changes in visual and attentional brain regions

#### 4.1.1.1 Brain metabolites

As discussed in Chapter 2, MRS provides the best non-invasive in vivo technique of investigating age and disease-related differences in brain metabolites. According to a review of the literature by Haga et al. (2009), healthy ageing is generally associated with a global increase in choline and creatine and a reduction in NAA in the brain, although there are some inconsistencies in the literature with regards to the direction of the effects and where these changes may occur anatomically.

With regards to the occipital lobe (OCC), concentrations of NAA and Glutamine (Glx) were reported to be lower and concentrations of choline to be higher in healthy older compared with younger adults (Christiansen et al., 1993; Marjańska et al., 2017). As NAA is a marker of neuronal health and energy metabolism, reduced NAA may reflect impaired mitochondrial activity in older adults. However, NAA has also been found to show no change in concentration in the OCC in older age (Ross et al., 2005). Furthermore, concentrations of both GABA and Glx show a decline in the OCC in older adults (Pitchaimuthu et al., 2017; Simmonite et al., 2019), suggesting reductions of key inhibitory (GABA) and excitatory (Glx) neurotransmitters with ageing. Finally, only one study investigated age-related differences in OCC myoinositol and found no significant change (Marjańska et al., 2017).

In the frontal lobe, cholinergic receptors are reported to be reduced in older adults (Raz, 2001) and this has been linked to an age-related increase in total choline (Haga et al., 2009). Such age-related increases in choline have been linked to greater levels of inflammation and demyelination in this region (Lind et al., 2020). In addition, increases in creatine and myoinositol have also been reported in the frontal lobe and in the posterior cingulate cortex (Gruber et al., 2008; Haga et al., 2009). These changes were proposed to reflect gliosis in the ageing brain as an increase in myoinositol signifies glial cell proliferation and may be consistent with post-mortem evidence that showed evidence of gliosis in patients with elevated myoinositol (Dichgans et al., 2005, Gruber et al., 2008; Reyngoudt et al., 2012). With regards to NAA, findings are again inconclusive in older age. Some studies reported reduced NAA in the frontal lobe (Gruber et al., 2008), while others found no age-related differences (Harada et al., 2001). Only very few studies have investigated age-related metabolic differences in the ACC. Those that did reported results that largely mirror the general

findings in the frontal lobes; increased choline and creatine and increases in NAA were present in the ACC in older adults, suggesting both glial proliferation and neuronal hypertrophy as a result of healthy ageing (Chiu et al., 2014). Evidence also suggests that GABA declines with age in the frontal cortex (Gao et al., 2013; Porges et al., 2017) and specifically in the ACC (Marenco et al., 2018), although other studies report no change or increased levels (Huang et al., 2017; Pitchaimuthu et al., 2017).

Finally, age-related changes in NAA in the parietal lobe were also mixed with some studies reporting reduced (Gruber et al., 2008) and others preserved levels (Ferguson et al., 2002). Moreover, increases in choline and creatine occur in the parietal lobe with ageing, but no apparent changes in myoinositol are reported (Haga et al., 2009). Glutamine is also shown to be lower in older age in the parietal cortex (Zahr et al., 2013). Finally, a limited number of studies have also reported that GABA in parietal and sensorimotor brain regions decreases with age (Gao et al., 2013; Porges et al., 2013) which has been associated with inhibitory control performance (Hermans et al., 2018) and motor learning (King et al., 2020).

Taken together, these preliminarily findings suggest that reductions in metabolites related to neuronal energy metabolism may be a key age-related change in the OCC. In contrast, metabolic changes in the ACC were more suggestive of age-related increases in inflammation and glial proliferation. This distinction potentially highlights the vulnerability of frontal white matter to decline with age, as inflammatory and glial changes are likely to be associated with white matter impairments. This is somewhat supported by the unclear pattern of metabolic changes in the parietal lobe and highlights the important of investigating the microstructural changes that may occur in white matter connective tracts within the ageing brain and how these relate to metabolite measurements.

#### 4.1.1.2 White matter microstructure

As discussed in Chapter 1, many studies have provided evidence for age-related changes in white matter microstructure across the brain. These are thought to occur primarily due to a damage and loss of myelination (Bartzokis et al., 2010) notably in small, myelinated fibres rather than axonal loss (Tang et al., 1997). These myelination changes may also be reflected by changes in restricted fraction (FR). Evidence for this comes from De Santis et al. (2014) who showed that the anterior to posterior gradient of white matter degeneration in FR may reflect the thinner myelin in the frontal lobes. Moreover, the same study highlighted sex differences in FR to be consistent with sex differences in myelin protein synthesis, suggesting that FR may also be a strong proxy myelin measurement. As discussed earlier, widespread age-related reductions in fractional anisotropy (FA) and increases in diffusivities have been reported in frontal, temporal and parietal white matter including the corpus callosum and fornix (Inano et al., 2011) but also within posterior visual cortices (Giorgio et al., 2010; Madden et al., 2010).

More specifically with regards to the visual perceptual and attention systems, age-related reductions in white matter microstructure have been reported in the optic radiation and have been linked to longer visual processing speed, suggesting less efficient local low-level processing in older adults (Price et al., 2017). Similarly, integrity of connective fibres between the posterior thalamus to the occipital cortex have been reported to decline as a function of age (Menegaux et al., 2020). FA/MD, axial and radial diffusivity are also altered with age in the anterior thalamic radiation (Cox et al., 2015). Furthermore widespread decline in estimates of WM microstructure have been reported in the visual association fibres with age (de Groot et al., 2013), most specifically in the fronto-parietal white matter tracts of the SLF (Bennett et al., 2012, Kennedy & Raz, 2009 Veldsman et al., 2020). In particular, FA/MD are also reported to be decreased and increased respectively in the SLF in normal ageing (Cox et al., 2016). Similar patterns of FA and MD alterations were seen to be impaired with older age in the ILF association fibres (Cox et al., 2016).

However, most of this previous evidence regarding age-related microstructural changes in the visual and attentional regions was based on standard DTI measurements. As previously discussed, DTI methods are not sensitive to the different contributions of underlying microstructure to the diffusion signal. Moreover, standard DTI methods are often less sensitive in their estimation of microstructure in regions where white matter tracts cross or kiss. Multi-shell models of diffusion such as NODDI (Zhang et al., 2012) or CHARMED (Assaf & Basser, 2004) aim to address these shortcomings by modelling neurite/axonal density and orientation in the case of NODDI, and intra and extra-axonal diffusion in the case of CHARMED. Both NODDI and CHARMED estimates have been shown to be more sensitive in the estimation of underlying microstructure. Evidence has shown that NODDI provides higher contrast in white matter pathology than standard DTI and provides metrics more specific to neurite morphology as assessed in specific pathology observed in patients with multiple sclerosis (By et al., 2017). In a similar assessment, CHARMED has been shown to be more sensitive than standard DTI, with FR showing greater effect sizes than other DTI parameters for discerning lesions in patients (De Santis et al., 2019). Furthermore, advanced diffusion models have been shown to provide the most sensitive measures of age-related microstructural changes in white matter in the brain in comparison to standard DTI alone (Beck et al., 2021).

In this thesis, CHARMED is employed as it provides the restricted fraction (FR) which measures diffusion within the restricted compartment which is proposed to estimate axonal density. In addition, FR has been shown to be related to myelination in the brain, in the context of myelin changes with ageing (De Santis et al., 2014).

These advanced multi-shell diffusion weighted imaging techniques have been employed to investigate age-related changes in white matter (Billiet et al., 2015, Toschi et al., 2020). These studies reported increased neurite dispersion in frontal white matter with age (Billiet et al., 2015, Toschi et al. 2020), and declines in

hindered and free diffusion in hippocampal grey matter which captured the greatest level of age-related variance (Venkatesh et al., 2020).

In the visual tracts of interest, FR is also reported to be significantly reduced in older adults in the posterior thalamic radiation (Toschi et al., 2020). Age-related reductions in FR have also been evidence in the SLF (Toschi et al., 2020), and in the temporal lobes, a significant linear decline in OD in the temporal lobes has been reported with age (Nazeri et al., 2015).

However, whilst many studies have shown declines in standard DTI estimates with age in the visual tracts of interest in this thesis, very few have employed more sensitive multishell imaging to characterise these tracts. On this basis, I chose to employ multi-shell diffusion imaging as opposed to standard DTI to provide a more sensitive estimate of microstructural differences in older adults. As discussed in Chapter 2, I will employ CHARMED to achieve a more sensitive axon microstructural measure to provide a more informative estimate of the changes in the brain microstructure underlying perception and attention in older age.

Importantly none of the above studies have investigated the potential relationships between white matter microstructure and grey matter metabolites. Only very few studies have previously investigated this link, and none has studied age-related differences in these relationships. Eylers et al., (2016) for instance reported that T2 transverse relaxation time in the occipital lobe was negatively related to NAA and creatine levels in younger adults, suggesting decreased neuronal function or attenuation with age in this region (Eylers et al., 2016). Furthermore, negative relationships between frontal white matter FA on one hand and Glx and myoinositol on the other was found in younger adults, suggesting that a decrease in FA may be related to an increase in glial activity and/or inflammation (Chiappelli et al., 2015; Reid et al., 2016).

Furthermore, studying how metabolites are related to microstructure may provide further clarity as to the nature of age-related differences at the cellular level and how these may affect information transfer at the network level. It is known that some metabolites, such as myoinositol are thought to be related to glial function. As glia are integral in myelination of axons, it is possible that imbalances if myoinositol with ageing may underlie reductions in diffusion estimates (FR) related to myelin (Nave et al., 2010), however to my knowledge this has not been established in the context of ageing. In addition, NAA is thought to be related to neuronal attenuation and functioning, thus a reduction in NAA theoretically may underlie white matter integrity at a cellular level. Again, to my knowledge this relationship is yet to be established in the context of ageing and the visual system.

As such, I aimed to address gaps in the literature identified by employing multishell diffusion imaging in the visual and attentional system to characterise age-related differences in a sensitive manner, and I also aimed to observe the relationships between microstructure and metabolites in older age.

#### 4.1.1.3 Cortical thickness

Cortical thickness has been shown to decline globally with age, with notable exceptions of the entorhinal cortex and ACC (Frangou et al., 2020). Considerable inter-individual variability is also reported in the temporal and frontal regions in age (Frangou et al., 2020), and thinning in older age is also prominent in the parietal cortices (McGinnis et al., 2011), most specifically the temporoparietal, inferior and superior parietal cortices, in addition to the superior temporal gyrus and precuneus (Fjell & Walhovd, 2010). Whilst examining these differences in older adults was not of direct interest in this chapter – as these patterns of decline are well established in ageing - it may aid in the interpretation of results and provide context for brain differences in the ageing brain.

Based on current limited evidence, I hypothesised that both NAA and myoinositol may be altered to different levels in different voxels and would be higher in the frontal cortex and reduced towards the posterior voxels in older adults. I also hypothesised that my results would show reductions in GABA and Glx in the OCC and increases in choline and creatine in the ACC with age.

I also hypothesised that microstructural measurements would be reduced in all regions in older adults, but that FR may be show specific decline in frontal regions and connections, due to the vulnerability of myelin in the frontal lobe with age.

Finally, I anticipated that older adults would show reductions in cortical thickness, with the frontal, parietal, temporal and cuneus regions showing the greatest age-related thinning, sparing the occipital cortex. This was hypothesised as the frontal cortex is observed to be more vulnerable to age-related change, with this vulnerability being reduced in more posterior regions.

### 4.1.2 Brain changes in visual and attentional regions in DLB

Only very few studies have investigated differences in brain metabolites in DLB (Kantarci et al., 2013). Preliminary findings from whole-brain MRS showed reductions in most brain metabolites particularly in NAA, choline and myoinositol in the frontotemporal and posterior cingulate regions while increases in NAA, choline and myoinositol were observed in occipital regions in DLB patients (Su et al., 2016; Zhang et al., 2015). However, another study showed decreased NAA in the occipital lobe but normal NAA in the frontal lobe in DLB patients when compared to AD (Graff-Radford et al., 2014). This may contrast with healthy older adults and demonstrates a more widespread decline in neuronal metabolism and mitochondrial function, but further investigation is required to clarify this pattern of metabolic change.

Further to this, no study to date has investigated GABA in the brain of DLB patients using spectroscopy in vivo. However, this relationship is important to investigate due to both the integral inhibitory role of GABA in the visual system (Song et al., 2017) and findings from a post-mortem study, which indicated reductions in GABA in the primary visual cortex in DLB which were also related to the incidence of visual hallucinations (Khundakar et al., 2016). In summary there is only very limited evidence with regards to the metabolic profile in DLB and the present study will thus address this gap in the literature.

With regards to white matter microstructure, the progression of microstructural changes in DLB patients does not appear to occur more rapidly than in older adults over time but has been shown to be more severe in some regions (Firbank et al., 2016). Parieto-occipital white matter tracts show reduced FA in early stages of DLB (Watson et al., 2012) and significant reductions in microstructural integrity have been reported in visual association areas, particularly the temporal and parietal lobes and precuneus (Su et al., 2015). One study reported decreased FA in the ILF in DLB patients, which was also found to be related to visual hallucinations (Kantarci et al., 2010; Kiuchi et al., 2011).

Some advanced microstructural imaging studies employing NODDI (Kamagata et al., 2018, Mitchell et al., 2019) and CHARMED (Nilsson et al., 2015) have been conducted in other Lewy body disorders - PDD and PD. These studies suggested that microstructural integrity (as evidenced by FR) was reduced in the cingulum and the anterior thalamic projections in PDD patients (Nilsson et al., 2015) as well as OD in the basal ganglia (Kamagata et al., 2018) and striatum, thalamus and midbrain (Mitchell et al., 2019) in PD patients. However, to the best of my knowledge there has been no application of advanced diffusion imaging methods, such as CHARMED, in the study of DLB. As previously discussed, multishell diffusion imaging provides a more sensitive estimate of the microstructural properties of tissue and may provide more sensitive insight into the nature of white matter pathology in disease groups (De Santis et al., 2019). On this basis, it is therefore timely to investigate the nature of white matter impairments to a greater degree of sensitivity in DLB by employing this method.

Cortical thinning has been shown to be relatively localized to the superior temporo-occipital and lateral orbito-frontal regions in addition to the middle and posterior cingulate gyri in DLB patients (Lebedev et al., 2013). Moreover, reduced volume in the occipital lobe and striatum (Lee et al., 2010) in addition to the precuneus and frontal lobe is also shown to be present in DLB and is associated with visual hallucinations (Sanchez-Castaneda et al., 2010). Finally, a large-scale patient study confirmed atrophy is more prominent in the posterior cortex but spares the medial temporal lobes in DLB patients (Oppedal et al., 2019).

### 4.1.2 Aims and hypotheses

Based on the studies summarised above, it is apparent that there is only very limited and somewhat contradictory evidence available regarding the metabolic and microstructural profile of visual and attentional brain regions in ageing and particularly in DLB. Thus, the aim of the present chapter was to

shed further light on the metabolic and microstructural underpinnings of age-and DLB related differences in visual perception and attention networks by employing advanced MRS and multi-shell diffusion weighted imaging techniques.

- Hypotheses regarding age-related differences in grey matter metabolites:

Based on the empirical evidence summarised above and evidence suggesting age-related metabolic slowing of mitochondria, reduced synaptic activity, reductions of dendritic trees and loss of small, myelinated axons it was hypothesised that NAA, myoinositol, GABA/$H_20$ and Glx would be overall reduced in ACC, PPC and OCC in older compared with younger adults. The largest reduction in GABA/$H_20$ and Glx was expected to be present in OCC. With regards to choline and creatine an overall increase in the measurements was expected in older relative to younger adults. This was anticipated due to the central role of choline in cell-membrane signalling and thus both inflammatory and demyelination processes (Zeisel & da Costa, 2009), and the role of creatine in effective glial functioning (Urenjak et al., 1993). This increase was expected to be largest in the ACC, again due to the vulnerability of the frontal cortex to these processes with ageing.

- Hypotheses regarding age-related differences in white matter microstructure:

It was hypothesised that in older compared to younger adults FA and FR would be reduced and MD, RD and AD increased in all white matter pathways i.e. the optic radiation, SLF (1,2,3), ILF and fornix. I hypothesised that the SLF would be particularly vulnerable to declines in FR and DTI indices with age, based on its anatomical connectivity with the frontal lobes.

- Hypothesis regarding age-related differences in grey matter morphology:

It was hypothesised that older versus younger adults would show reduced cortical thickness in frontal, anterior cingulate, temporal, parietal and occipital cortices.

- Hypotheses regarding the relationship between grey matter metabolites and white matter microstructure

Given the evidence discussed, it was anticipated that alterations in metabolites, particularly NAA, choline and myoinositol would be related to microstructural measurements in particular FA and FR. This was anticipated as NAA, choline and myoinositol have been related to neuronal health, cell membrane integrity and glial function, which may all impact white-matter integrity at a cellular level. As FR and FA estimate axonal structure at both crude and more sensitive levels, it was anticipated that these measurements would be most strongly related to changes in metabolites related to cellular integrity and health.

- Hypotheses regarding whole brain grey and white matter analysis in ageing

It was hypothesised that a replication of anterior-posterior gradient in age-related differences would be apparent – thus it was anticipated that more prominent differences in frontal than posterior brain regions including OCC would be present in older adults.

- Hypotheses regarding DLB-related differences in cortical metabolites

In DLB patients I hypothesised that GABA/$H_20$ would be reduced particularly in the OCC, due to the role of GABA in visual functions and hallucinations. I anticipated that NAA and myoinositol reductions would be widespread and choline may be elevated, indicating inflammatory response.

- Hypotheses regarding DLB-related differences in white matter microstructure

It was also hypothesised that specifically ILF microstructural estimates would be impaired, and reduced FR would be seen in the SLF in DLB patients, in comparison to older adults. With regards to the optic radiations, I anticipated that some microstructural impairment may be present, but that this would not significantly differ in comparison to older adults, as low-level visual function was not seen to be greatly impaired.

- Hypotheses regarding DLB-related differences in grey matter morphology

Finally, reductions in anterior cortical thickness were also anticipated in DLB patients, but it was hypothesised that occipital cortical thickness would not be significantly reduced. This was hypothesised based on evidence supporting the diagnostic guidelines for DLB, which show relative preservation of grey matter structure in the occipital lobes.

## 4.2 Part 1: A priori analysis

### 4.2.1 Methods

#### 4.2.1.1 Participants

The same participants as described in Chapter 3 took part in the procedure described in the current chapter. Participants were screened for MR contraindications according to Cardiff University Brain Research Imaging Centre (CUBRIC) policy. This excluded any participants with metallic or electronic bodily implants, some dental work and some tattoos, subject to radiographer assessment. Sample size (younger n=28, older n=26), procedure and demographics are reported in Chapter 3 (section 3.21).

DLB patients were also the same patients as described in Chapter 3, however one patient (DLB 4) was physically unable to take part in MRI scanning, therefore the data from only 3 patients are included in this chapter. DLB patients' demographics are also reported in Chapter 3 and followed the same procedure as younger and older participants with the exception that some MRI sessions (n=2) were scheduled on

different days to the cognitive testing sessions to address issues with patient fatigue. One patient (DLB 2) required a break during a scanning session, terminating the first session before the acquisition of DWI data. This resulted in two T1 images being acquired for this participant, one which was used in the structural analysis and co-registration for MRS processing, and one which was used to co-register subsequent DWI.

#### 4.2.1.2 MRI acquisition

All MR data were acquired on a Siemens 3 Tesla (T) Magnetom Prisma MR system (Siemens Healthcare GmbH, Erlangen) fitted with a 32-channel receiver head coil (Siemens Healthcare GmbH, Erlangen) at CUBRIC. A 3D, T1-weighted magnetization prepared rapid gradient-echo (MP-RAGE) structural scan was acquired for each participant (TE/TR = 3.06/2250ms, TI = 850ms, flip angle = 9deg, FOV = 256mm, 1 x 1 x 1mm resolution, acquisition time = ~6min). The MPRAGE was used as anatomical reference for the placement of MRS region of interest voxels as well as for morphological brain analyses (cortical thickness, volume).

MRS was used to measure metabolites of Glx, GABA/$H_20$, NAA, choline, creatine and myoinositol in the brain in vivo. Single voxel proton spectra were obtained from voxels of interest placed in the OCC (voxel measuring 30 x 30 x30 $mm^3$), the PPC (voxel measuring 30 x 30 x 30 $mm^3$) and the ACC (voxel measuring 27 x 30 x 45mm) using a PRESS acquisition (TE/TR = 68/2000ms, 8 averages, flip angles = 90/180deg, acquisition time = ~ 2 min. See Figure 4.1 for voxel placement. The OCC voxel was placed above the tentorium cerebelli, avoiding scalp tissue in order to prevent lipid contamination to the spectra. The PPC voxel was placed with the posterior edge against the parieto-occipital sulcus, and the ventral edge of the voxel above and parallel to the splenium. Finally, the ACC was placed directly dorsal and parallel to the genu of the corpus callosum. In each voxel, a spectral editing acquisition (MEGA-PRESS, Mescher et al., 1998) was performed. MEGA-PRESS was selected above non-spectral edited sequences due to difficulties of traditional point-resolved spectroscopy techniques in the quantification of GABA. This is because GABA concentrations are very low in comparison to other spectral metabolites, and GABA spectral peaks are often hidden by other metabolites due to the phenomenon of J-coupling, as described in Chapter 2.

GABA editing was achieved by applying an additional pulse symmetrically about water resonance, providing 'on' and 'off' editing pulses which allow for the subtraction of peaks which may mask GABA in the spectra (MEGA-PRESS; TE/TR = 68/2000ms, 16 averages, editing pulse frequency = 7.50/1.90ppm, acquisition time = ~12 min per voxel). Manual shimming was performed before all MRS scans to ensure water-line width of 20Hz or lower, in order to obtain accurate peaks in the spectra (Figure 4.1).

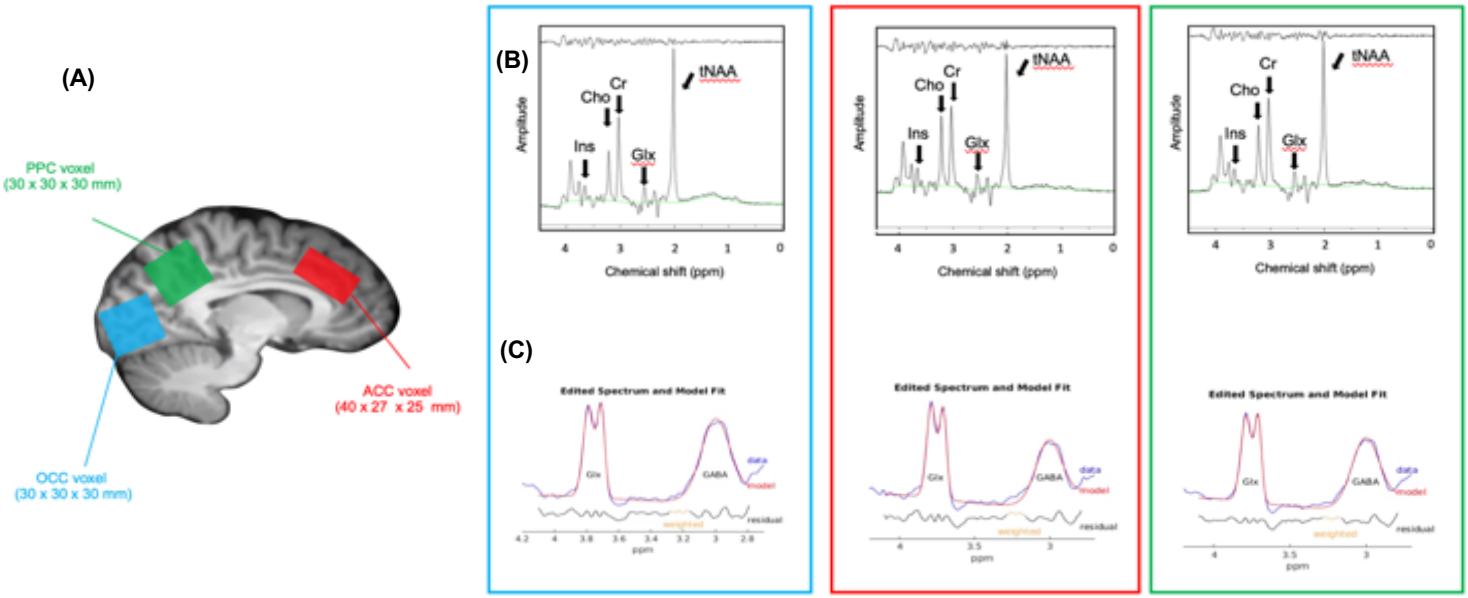


Figure 4.1 MRS voxel placement (A) MRS voxel placement: red = anterior cingulate cortex (ACC), blue = occipital cortex (OCC), green = posterior parietal cortex (PPC) (B) Spectra for each voxel showing location of metabolites of interest: Ins = myoinositol, Cho = choline, Cr = creatine, Glx = glutamate/ glutamine, tNAA = total N-Acetyl Aspartate (C) GABA edited spectra retrieved following ON-OFF spectral editing.

A multi-shell diffusion MRI sequence was also conducted using a high angular resolution diffusion (HARDI) weighted echo-planar imaging (EPI) sequence (TE/TR = 73/ 4100ms, FOV = 220x220mm, isotropic voxel size 2mm$^3$, 66 slices, slice thickness 2mm, acquisition time ~15 min, 2 x 2 x 2mm resolution). Five diffusion weightings were applied along gradient directions: b = 200 s/mm$^2$ (20 directions), b= 500 s/mm$^2$ (20 directions) b = 1200 s/mm$^2$ (30 directions), b=2400 s/mm$^2$ (61 directions), b =4000 s/mm$^2$ (61 directions). 12 unweighted (b0) volumes were acquired, interspersed throughout diffusion-weighted scans. In addition, a diffusion reference sequence was acquired for later blip-up blip-down analysis to correct for EPI distortion (Bodammer et al., 2004) in which a diffusion weighting of b=1200 s/mm$^2$, and 12 un-weighted (b0) images were acquired interspersed throughout the sequence.

### 4.2.1.3 A priori MR data analysis

The primary aim of this chapter was to characterise age and DLB-related metabolic, microstructural and morphological differences in brain regions involved in perception and attention. Grey matter ROIs and white matter tracts are summarised in Table 4.1. Grey matter cortical and subcortical region of interests were segmented using the FreeSurfer pipeline (Fischl, 2012) and cortical thickness and subcortical volume measures were extracted for these ROIs. White matter pathways were reconstructed with deterministic tractography, and mean values of microstructural indices were extracted for each tract (see Table 4.1). Finally, MRS metabolites were extracted from voxels in the OCC, ACC and PPC (Table 4.1).

#### 4.2.1.3.1 Cortical thickness and grey matter volume

Cortical thickness and grey matter volume were processed using FreeSurfer software (Fischl, 2012) [FreeSurfer, version 6.0, https://surfer.nmr.mgh.harvard.edu/]. T1 weighted images were corrected for motion (Reuter et al., 2010) and images were averaged. Images were skull-stripped by using a watershed and surface deformation procedure (Ségonne et al., 2004) and transformed automatically into Talairach space (Talairach, 1988). FreeSurfer segmented the subcortical white matter and deep grey matter volumetric structures (Fischl et al., 2004), normalised intensity (Sled et al., 1998), and conducted automated topology correction (Fischl et al., 2001). Surface deformation was performed in order to place grey and white matter, and grey and CSF fluid borders optimally on the T1 image (Fischl & Dale, 2000). These processed data are then registered to a spherical atlas to calculate cortical folding patterns (Fischl et al., 1999), and the cortex is parcellated according to gyri and sulci (Desikan et al., 2006; Fischl et al., 2004). Information from the segmentation and deformation procedures is then used to create maps of representations of cortical thickness and volume (Fischl & Dale, 2000). Average thickness and volumetric values for surface regions involved in perception and attention were calculated for each participant for a priori analyses (Table 4.1).

Table 4.1 Regions of interest associated with visual and attention function selected as primary outcome measures of cortical thickness and volume in the current study. FA = fractional anisotropy, MD = mean diffusivity, L1 = axial diffusivity, RD = radial diffusivity, FR = restricted fraction.

| **Anatomical region** | **Metric** |
|---|---|
| Occipital cortex (OCC) | GABA/Glx/ NAA/ Myoinositol/ Choline/ Creatine |
| Anterior cingulate cortex (ACC) | GABA/Glx/ NAA/ Myoinositol/ Choline/ Creatine |
| Posterior parietal cortex (PPC) | GABA/Glx/ NAA/ Myoinositol/ Choline/ Creatine |
| SLF1 | FA/MD/L1/RD/FR |
| SLF2 | FA/MD/L1/RD/FR |
| SLF3 | FA/MD/L1/RD/FR |
| ILF | FA/MD/L1/RD/FR |
| Optic radiation | FA/MD/L1/RD/FR |
| Optic-Chiasm | Volume |
| Banks of the superior temporal sulcus | Cortical thickness |
| Caudal anterior cingulate (L/R) | Cortical thickness |
| Caudal middle frontal (L/R) | Cortical thickness |
| Cuneus | Cortical thickness |
| Pericalcarine | Cortical thickness |
| Inferior frontal (L/R) | Cortical thickness |
| Inferior parietal (L/R) | Cortical thickness |
| Inferior temporal (L/R) | Cortical thickness |
| Lateral occipital (L/R) | Cortical thickness |
| Medial orbitofrontal (L/R) | Cortical thickness |
| Middle temporal gyrus (L/R) | Cortical thickness |
| Rostral anterior cingulate (L/R) | Cortical thickness |
| Rostral middle frontal (L/R) | Cortical thickness |
| Superior frontal gyrus | Cortical thickness |
| Superior parietal (L/R) | Cortical thickness |
| Superior temporal gyrus | Cortical thickness |

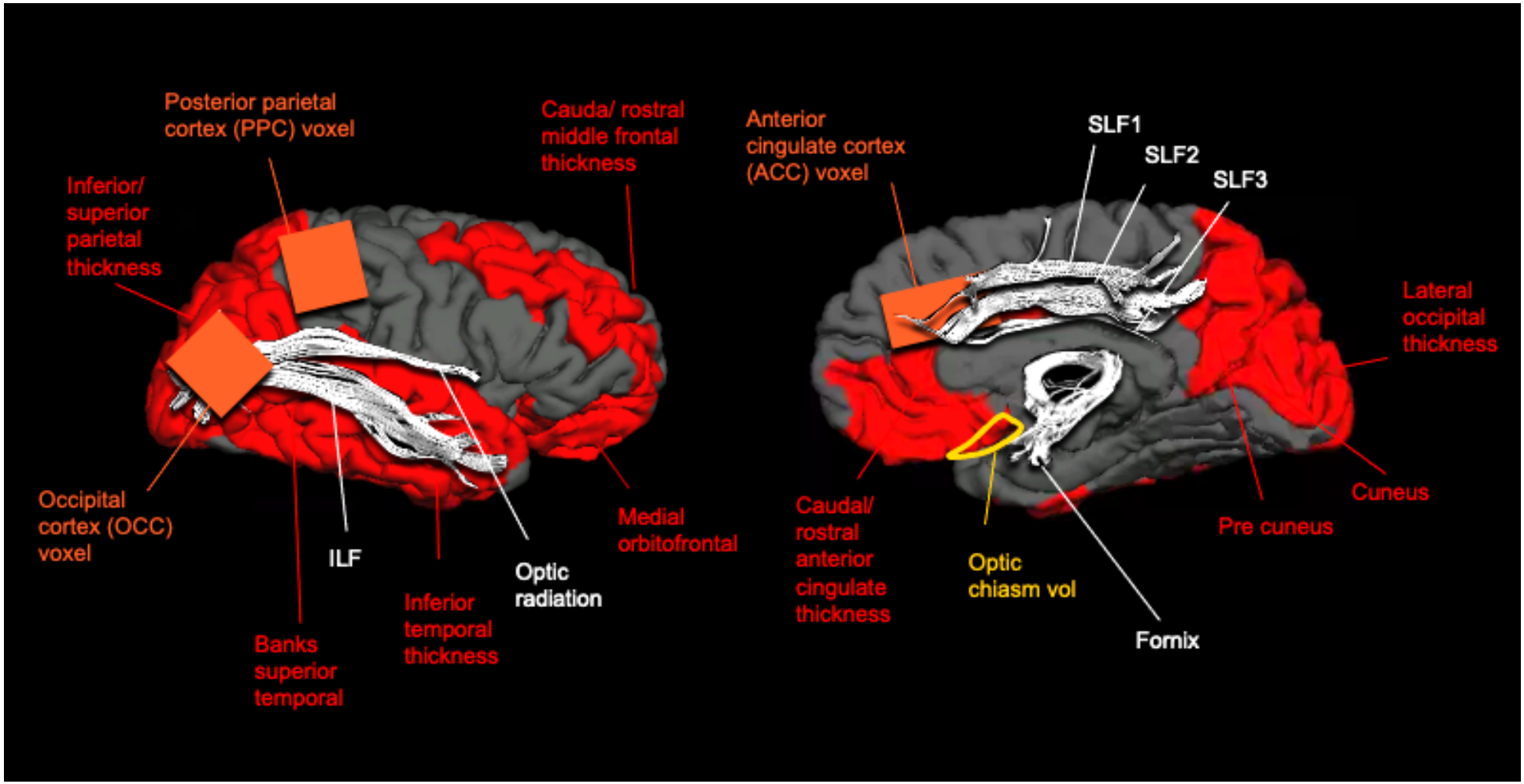


Figure 4.2 Visual perceptual regions of interest assessed in the current chapter. Areas highlighted in red are regions assessed for cortical thickness, areas highlighted in yellow are regions assessed for grey matter volume, tracts highlighted in white are tracts assessed for restricted fraction (FR), fractional anisotropy (FA), mean diffusivity (MD), radial diffusivity (RD) and axial diffusivity (L1). Voxels highlighted in orange are regions assessed for metabolites of interest (N-acetyl aspartate, choline, creatine, myoinositol, GABA, Glx). SLF = superior longitudinal fasciculus, ILF = inferior longitudinal fasciculus

#### 4.2.1.3.2 1H-MRS data analysis

Data were also analysed using Totally Automatic Robust Quantification in NMR (TARQUIN) version 4.3.11 (Reynolds, Wilson, Peet & Arvanitis, 2006) in order to determine estimated concentrations of other metabolites of interest (Choline, NAA, Glx, Creatine, Myoinositol). To ensure data quality, metabolites were excluded if the Cramer Rao Lower Bound (CRLB) was above 20% as recommended in literature (Stagg & Rothman, 2013). OFF spectra were subject to pre-processing in which residual water is removed, phase is adjusted, basis set simulation and nonlinear least-squares is fit, in order to estimate metabolite concentrations. Due to difficulty in the separation of NAA and N-acetyl-aspartyl-glutamate peaks, the total NAA was measured, which combined the two concentrations. Moreover, as glutamine and glutamate peaks overlap these are combined as 'Glx' as conducted in previous literature (see Figure 4.7).

MEGA-PRESS data were analysed using GANNET (GABA-MRS Analysis Tool) version 3.0 (Edden et al., 2014). GABA data were visually assessed by two experienced researchers, which resulted in 8 participants from the younger adult group being invited back for re-scanning of the OCC voxel, due to lipid contamination. Metabolite concentrations were corrected for the composition of tissue within each voxel. In native space, voxels were segmented to obtain proportion of grey matter, white matter and CSF using FAST (FMRIB's Automated Segmentation Tool) in FSL (Zhang et al., 2001). Estimated metabolite values were corrected to account for CSF voxel fraction, and water reference signal was corrected to account for differing water content of CSF, grey matter and white matter. All metabolites were quantified using water as a concentration reference, as described in Chapter 2, and were expressed as concentration in millimoles per unit (mM).

#### 4.2.1.3.3 Diffusion pre-processing

Two-shell HARDI data were split by b-value (b=1200, and b=2400 s/mm$^2$) and were corrected for distortions and artifacts using a custom in-house pipeline in MATLAB and Explore DTI (Leemans et al., 2009). Correction for echo planar imaging distortions was carried out by using interleaved blip-up, blip-down images. Tensor fitting was conducted on the b=1200 s/mm$^2$ data, and the two compartment 'free water elimination' (FWE) procedure was applied to improve reconstruction of white matter tracts close to ventricles (Pasternak et al., 2009) and to account for partial volume contamination due to CSF which is particularly apparent in older age (Metzler-Baddeley et al., 2012). Data were fit to the CHARMED model (Assaf & Basser, 2005) which involved the correction of motion and distortion artifacts with the extrapolation method of Ben-Amitay et al., (2012). The number of distinct fibre populations in each voxel (1, 2 or 3) was determined using a model selection approach (De Santis et al., 2014) and FR maps (Assaf & Basser, 2005) were then extracted by fitting the CHARMED model to the DWI data, with an in-house analysis coded in MATLAB (The MathWorks, Natick, MA). This resulted in maps of fractional anisotropy (FA), mean diffusivity (MD), radial diffusivity (RD), axial diffusivity (L1) and restricted signal fraction (FR).

#### 4.2.1.3.4 Tractography analysis

Whole brain tractography was performed with the dampened Richardson-Lucy (dRL) spherical deconvolution method (Dell'Acqua et al., 2010), as detailed in Chapter 2. Tractography was performed on the b=2400 s/mm² data to provide better estimation of fibre orientation (Vettel et al., 2001). The dRL algorithm extracted peaks in the fibre orientation density function (fODF) in each voxel using a step size of 0.5mm. Streamlines were terminated if directionality of the path changed by more than 45 degrees, as per default deterministic dRL parameters used by the standardised in-house processing pipeline at CUBRIC provided with permission by G.Parker.

Manual fibre reconstructions were performed in ExploreDTI v4.8.3 (Leemans et al., 2009). Tracts of interest were the left and right superior longitudinal fasciculus (SLF; segmented into SLF1, 2 and 3), inferior longitudinal fasciculi (ILF) and optic radiations were obtained by applying region of interest (ROI) Boolean logic AND, OR and NOT gates to isolate specific tracts. These were manually drawn on direction encoded colour FA maps (Pierpaoli & Basser, 1996) in native space, according to the anatomical landmarks as described below (see Figure 4.2).

##### 4.2.1.3.4.1 ILF reconstruction

ILF reconstruction was obtained by identifying the posterior edge of the cingulum bundle on the sagittal plane, and then placing a seed region in one hemisphere in the coronal slice at this position. An AND region was drawn around the temporal lobe in the coronal plane, which was at the level of the most posterior coronal slice in which the temporal lobe was not connected to the frontal lobe (Hodgetts et al., 2015; Wakana et al., 2007). Any fibres which were inconsistent with the known anatomy of the ILF were excluded by placing further NOT ROIs in the axial plane above the level of the corpus callosum; in the sagittal plane at the level of the longitudinal fissure or in the coronal plane at the level of the genu of the corpus callosum to exclude fibres extending to the frontal cortex (Figure 4.2, Figure 4.3A). This procedure was repeated for both the left and right ILF.

##### 4.2.1.3.4.2 SLF reconstruction

SLF reconstruction involved drawing a seed region around one hemisphere on the coronal plane, excluding the temporal lobe just anterior to the posterior commissure, and a NOT region anterior to the posterior commissure in the axial slice below the level of the splenium of the corpus callosum (Wakana et al., 2007). In addition, AND gates were placed in the coronal slice at the level of the anterior commissure in one of three regions corresponding to the SLF 1,2 or 3, using the MD map to determine anatomical references (Figure 4.3). The SLF1 was delineated according to protocol by Thiebaut de Schotton et al., (2011) by placing an AND gate on the coronal plane at the level with the anterior commissure around the superior frontal gyrus, the SLF 2 was located by placing the AND gate around the middle frontal gyrus, and the SLF3 was located by drawing the ROI around the inferior frontal gyrus. Manual correction was then

conducted by placing further NOT gates to exclude fibres projecting to the opposite hemisphere, or those belonging to the cingulum bundle, arcuate fasciculus or those not consistent with SLF anatomy.

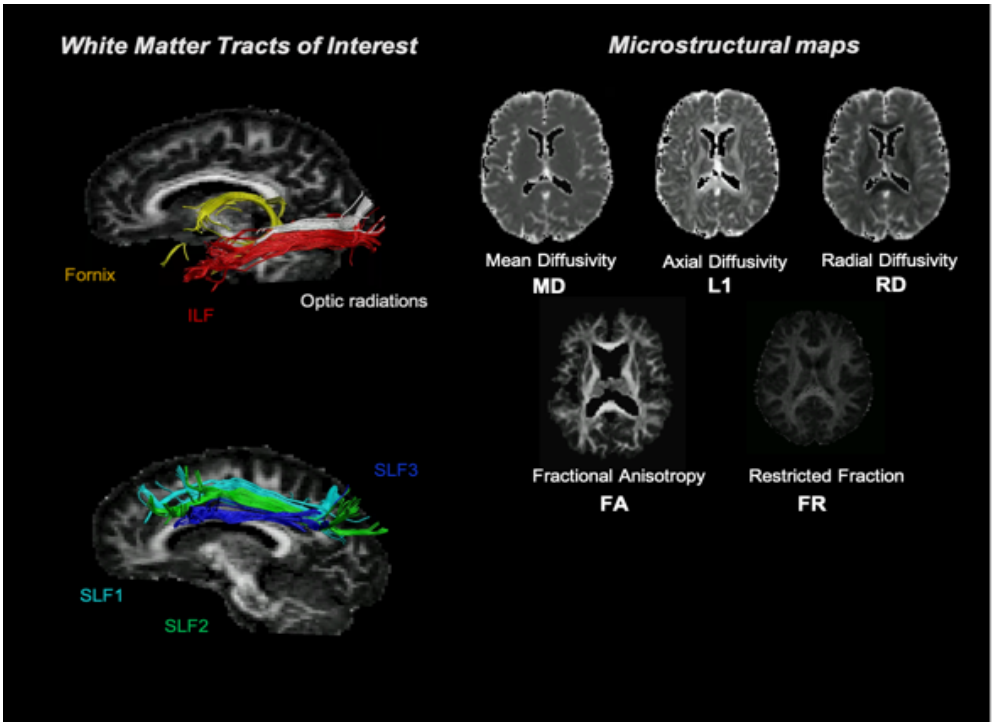


Figure 4.3 White matter tracts assessed in the current study. These tracts were selected based on their role in the visual and attentional networks. From each tract, microstructural maps were extracted for diffusion measurements of interest. ILF= inferior longitudinal fasciculus, SLF = superior longitudinal fasciculus

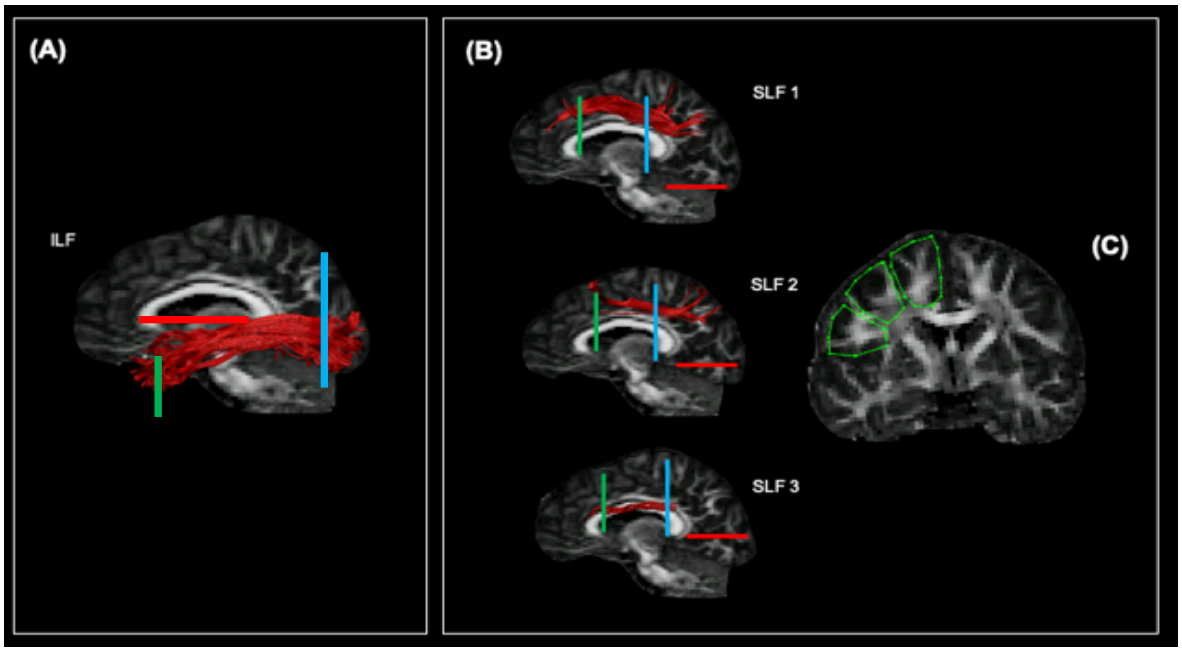


Figure 4.4 (A) Demonstration of tractography gate placement to delineate the superior longitudinal fasciculus (SLF) using ExploreDTI. Images are an average subject presented in their native space. (B) Red shows NOT gate, blue shows SEED gate, and green shows AND gate. (C) Delineation of 'AND' gates for SLF1, 2 and 3. SLF = superior longitudinal fasciculus.

#### 4.2.1.3.4.3 Optic radiation reconstruction

The optic radiation was delineated by placing a seed region on the white matter of the optic radiation lateral to the lateral geniculate nucleus in the axial plane (Thompson et al., 2014). A second 'AND' gate was placed on the coronal plane at the anterior edge of the primary visual cortex. Fibres crossing to the opposite hemisphere, or into the frontal lobe were excluded by placing further NOT gates in the sagittal and axial planes (see Figure 4.4).

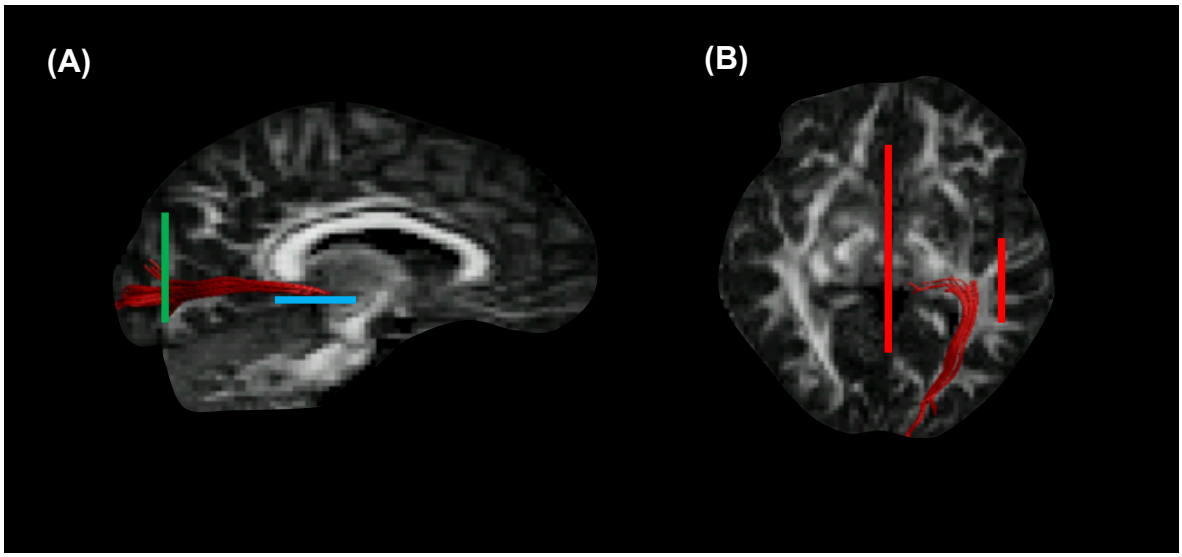


Figure 4.5 Optic radiation tractography gate placement. (A) blue shows SEED gate, and green shows AND gate on the sagittal plane. (B) Red shows NOT gate placement on the axial plane.

#### 4.2.1.3.4.4 Fornix reconstruction

The fornix was reconstructed by locating the body of the fornix bundle, located by identifying the posterior body of the corpus callosum on a sagittal plane (Figure 4.5). A SEED gate was placed medially on the coronal slice to encompass the fornix bundle at the entry point of the anterior pillars into the body of the fornix (Metzler-Baddeley et al., 2011).

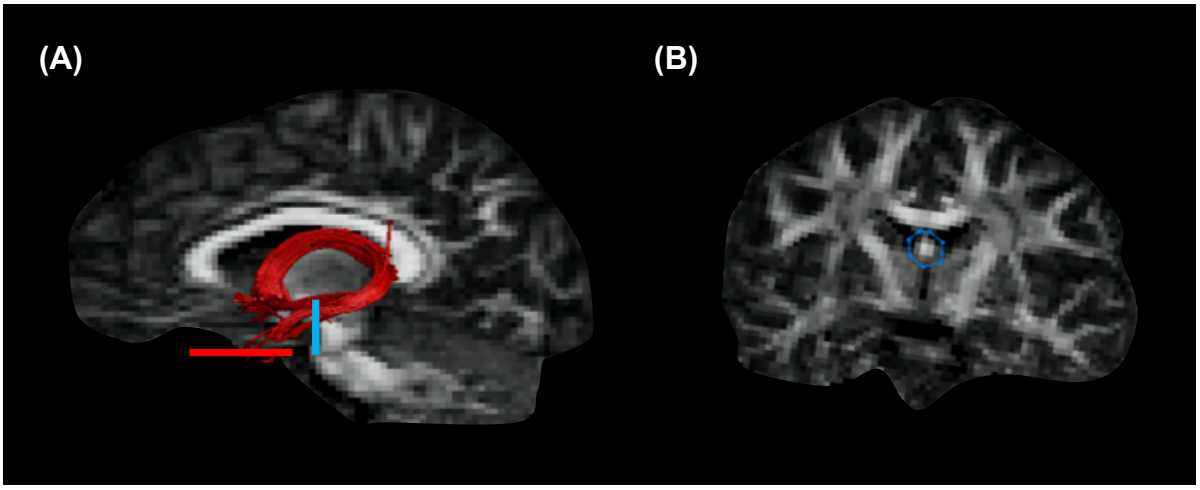


Figure 4.6 Fornix gate placement. (A) Red shows NOT gate, blue shows SEED gate on the sagittal plane. (B) Coronal plane shows SEED gate placement in blue.

#### 4.2.1.4 Statistical analyses

Tractography outcome measures (FA, MD, RD, L1, FR) and metabolite outcome measures (GABA/$H_20$, NAA, Glx, Myoinositol, Choline, Creatine) were compared between older and younger control groups by conducting non-parametric Mann Whitney U tests. Non-parametric tests were employed on the basis of results from Kolmogorov-Smirnov testing, which revealed non-normal data distributions of metabolites and microstructural values. Group differences in cortical thickness and volume were determined using MANOVA. Metabolites which showed significant group differences were also correlated using non-parametric Spearman's rho correlations with metrics from white matter tracts which showed significant group differences. Finally, to explore the direction of the relationships between microstructure and metabolites, and their relationship with age, linear mediation analyses were conducted. Linear mediation analyses were conducted using the logarithmic transformation of age, due to its non-normal distribution, metabolites and microstructure (MacKinnon et al., 2018). Two mediations were conducted for each age-metabolite-microstructure relationship, one which assessed whether inclusion of microstructure mediated the direct effect on metabolites, and one which assessed whether inclusion of metabolites mediated the direct effect on microstructure. Effect sizes and 95% confidence intervals were based on bootstrapping with 5000 replacements. Mediation model 1 tested for the indirect effects of metabolites on the direct effect of age on FR (path c'). The indirect was calculated as a product of a*b of the correlations between age and metabolites (path a) and the partial correlation between metabolites and FR accounting for age (path b). Model 2 tests for the indirect effect of FR on the direct effect of age on metabolites (Figure 4.7).

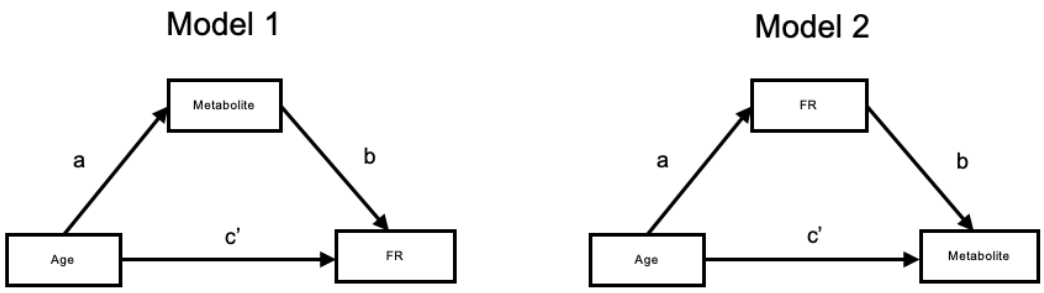


Figure 4.7 Mediation models used to assess the relationship between age, FR and metabolites. Model 1 tests for the indirect effects of metabolites on the direct effect of age on FR (path c'). The indirect = a*b of correlations between age and metabolites (path a) and metabolites and FR accounting for age (path b). Model 2 tests indirect effects of FR on direct effect of age on metabolites.

#### 4.2.1.5 Analysis of brain imaging data in DLB patients

All MRI acquisition and data processing followed an identical procedure to those outlined in previous sections of this chapter (section 4.3). This was with the exception of one post-processing stage during structural MR data analysis, in which a study specific template (SST) was created for DLB patients prior to the calculation of cortical thickness and volume values. This SST was created due to anticipated differences in grey matter volume between groups. The SST was initialized in FreeSurfer (Fischl, 2012) by creating a

template using an average of all DLB patients' brains and registering each subject to the new template. Thickness and volume values were then extracted in the new template space. DLB patients' data followed the same a priori analysis pipeline as conducted with healthy younger and older adults in this chapter.

### 4.2.2 Results: younger vs older adults

#### 4.2.2.1 Metabolic differences between older and younger adults

Descriptive statistics for GABA/$H_20$ and metabolites in older and younger groups are reported in Appendix 2. Full results are displayed in Table 4.1. Group comparisons between older and younger control groups showed no significant differences in GABA/$H_20$ levels in the ACC, OCC or the PPC. (Figure 4.8).

GABA in occipital, anterior cingulate and posterior parietal cortices in younger vs older adults

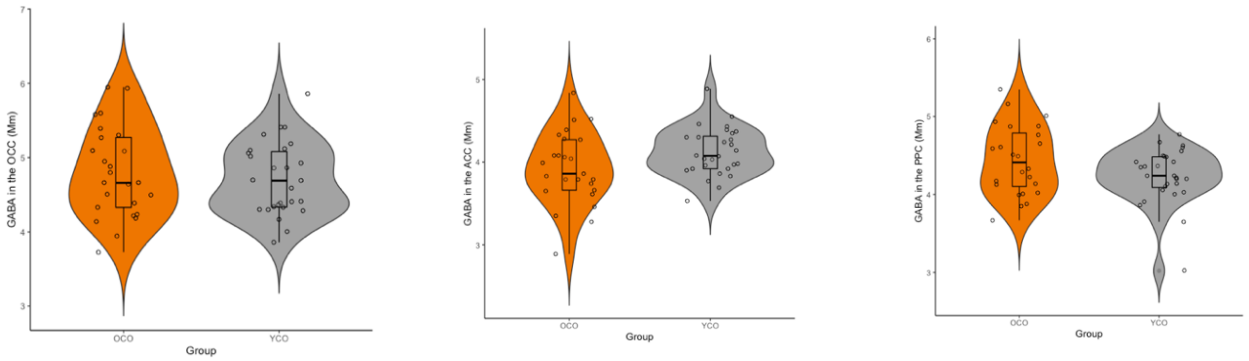


NAA in occipital, anterior cingulate and posterior parietal cortices in younger vs older adults

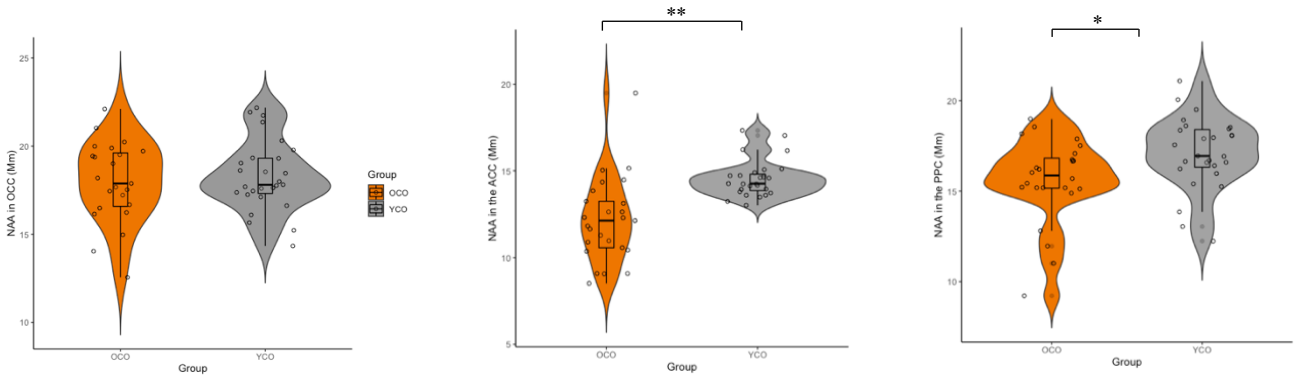


Glx in occipital, anterior cingulate and posterior parietal cortices in younger vs older adults

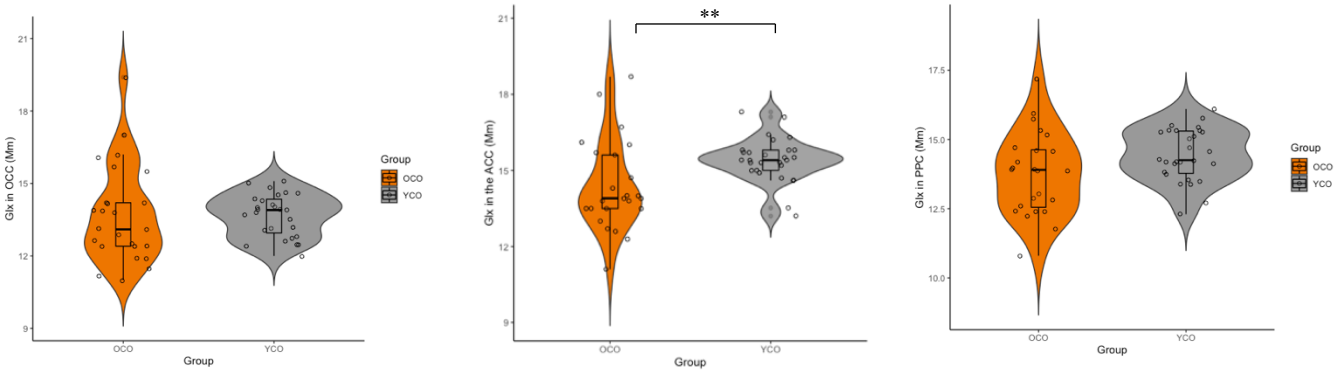

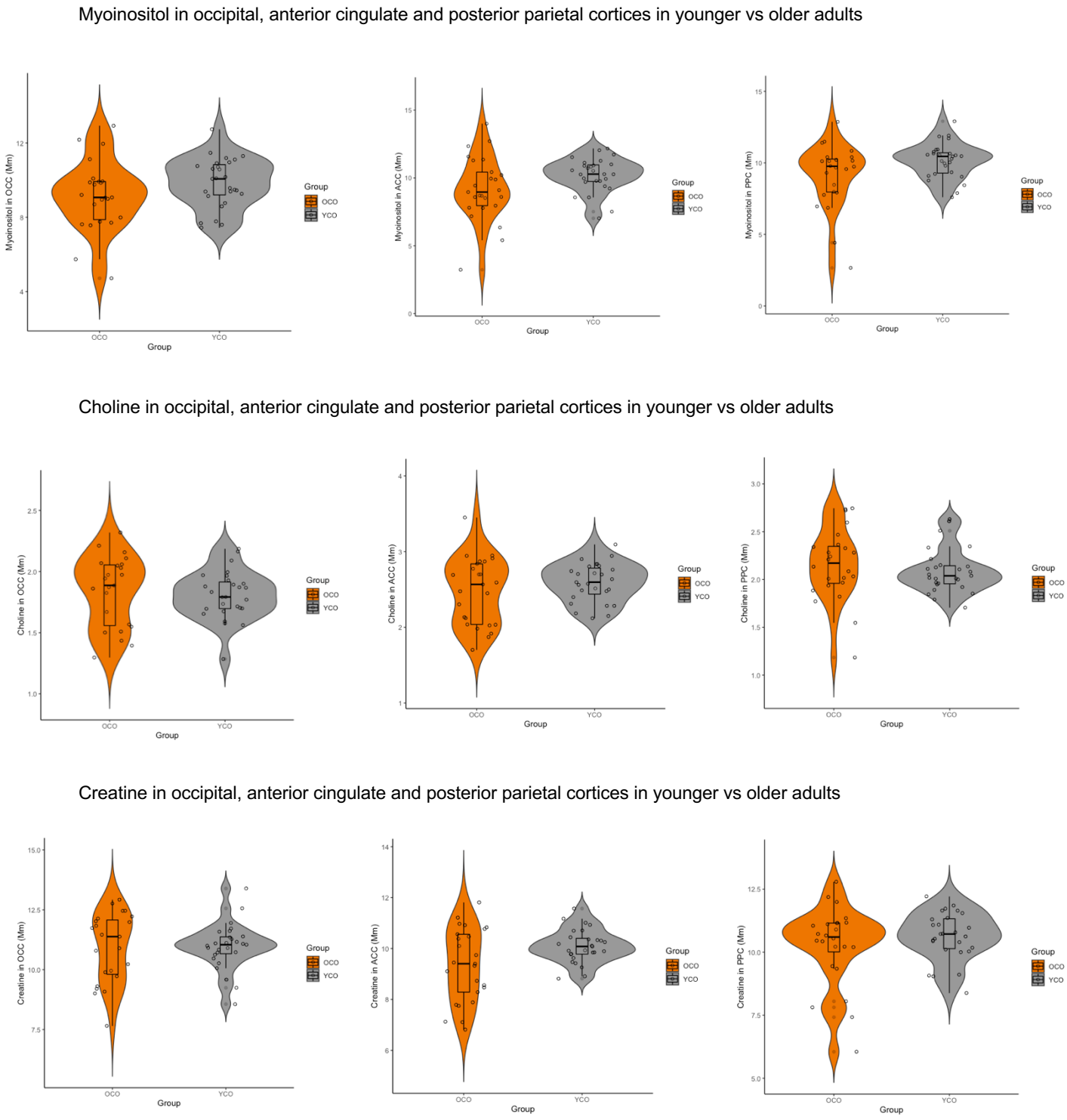


Figure 4.8 MRS metabolites in older (orange) and younger (grey) participants. Mann-Whitney U tests showed Glx in the ACC, NAA in the ACC and NAA in the PPC were significantly lower in the older adults than younger adults. All other metabolites of interest showed no significant group differences. OCO = older adults, YCO = younger adults **p<.001, *p<.0.05

Older control participants had significantly lower Glx (U=189, p=.004) and NAA (U=109, p<.001) in the ACC than younger adults. A trend towards significantly lower myoinositol in older adults in comparison to younger adults in the ACC was also observed (U=234, p=.058). In the PPC, older adults showed

significantly lower NAA (U=190, p=.011), and a trend towards lower Glx (U=231, p=.054) than younger adults (Figure 4.9, Table 4.2).

Table 4.2 Full results for Mann-Whitney group comparisons in metabolites in younger and older adults OCC=occipital voxel, ACC=anterior cingulate cortex voxel, PPC=posterior parietal cortex voxel

| | OCC | | | ACC | | | PPC | | |
|---|---|---|---|---|---|---|---|---|---|
| | **Mann-Whitney U** | **Significance (corrected)** | **Z value** | **Mann-Whitney U** | **Significance (corrected)** | **Z value** | **Mann-Whitney U** | **Significance (corrected)** | **Z value** |
| *GABA/H20* | 318 | .721 | -.35 | 249 | .072 | -1.80 | 265 | .196 | -1.29 |
| *Glx* | 295 | .441 | -.77 | 189 | .004* | -2.87 | 231 | .054 | -1.93 |
| *NAA* | 298 | .808 | -.24 | 109 | <.001** | -4.19 | 190 | .011* | -2.53 |
| *Myoinositol* | 230 | .117 | -1.57 | 234 | .058 | -1.89 | 224.5 | .060 | -1.87 |
| *Choline* | 277 | .514 | -.65 | 289 | .374 | -.88 | 270.5 | .313 | -1.01 |
| *Creatine* | 292 | .726 | -.35 | 240 | .074 | -1.78 | 298 | .624 | -.491 |

### 4.2.2.2 Differences in Restricted Fraction between older and younger adults

Significantly lower restricted fraction was shown in the older control group in the fornix (U=75, p<.001), right optic radiation (U=154, p=.001), left SLF1 (U=152, p=.001), left SLF2 (U=170, p=.002) and right SLF3 (U=169, p=.002) (Figure 4.10).

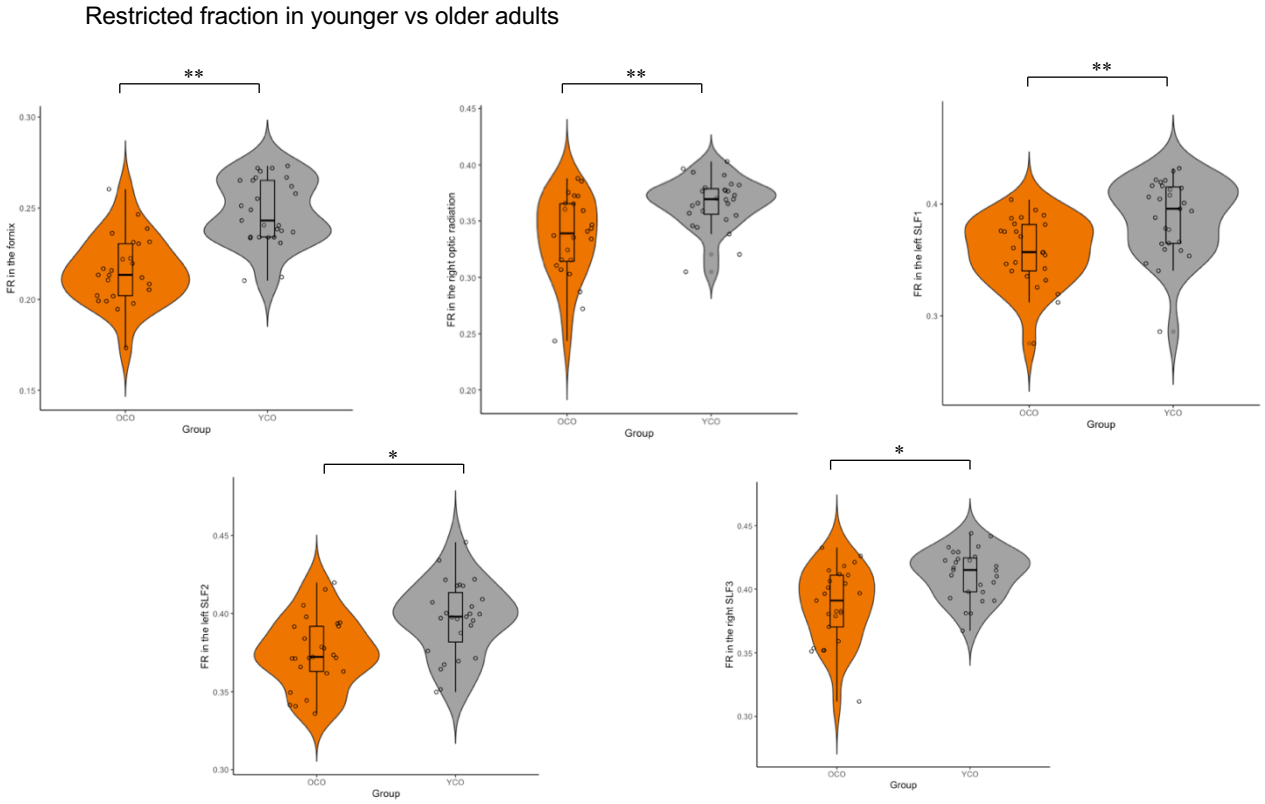


Figure 4.9 Restricted fraction (FR) in visual and attentional tracts of interest between older (orange) controls and younger (grey) controls. Mann-Whitney U tests showed FR was significantly lower in the fornix, optic radiation, SLF1, 2 and 3 in older adults in comparison to younger adults. OCO = older adults, YCO = younger adults **p<.001, *p<.0.05

### 4.2.2.3 Differences in DTI indices between older and younger adults

#### 4.2.2.3.1 Fractional anisotropy

Full statistics for tractography in older and younger groups are reported in Appendix 3. Significantly higher FA in the fornix (U=22, p<.001), right optic radiation (U=207, p=.027), left ILF (U=203, p=.014), right ILF (U=157, p=.001), left SLF1 (U=131.5, p<.001), left SLF2 (U=195, p=.009), and right SLF2 (U=218, p=.029), and right SLF3 (U=163, p=.001) was found in younger adults in comparison to older adults (Fig 4.10).

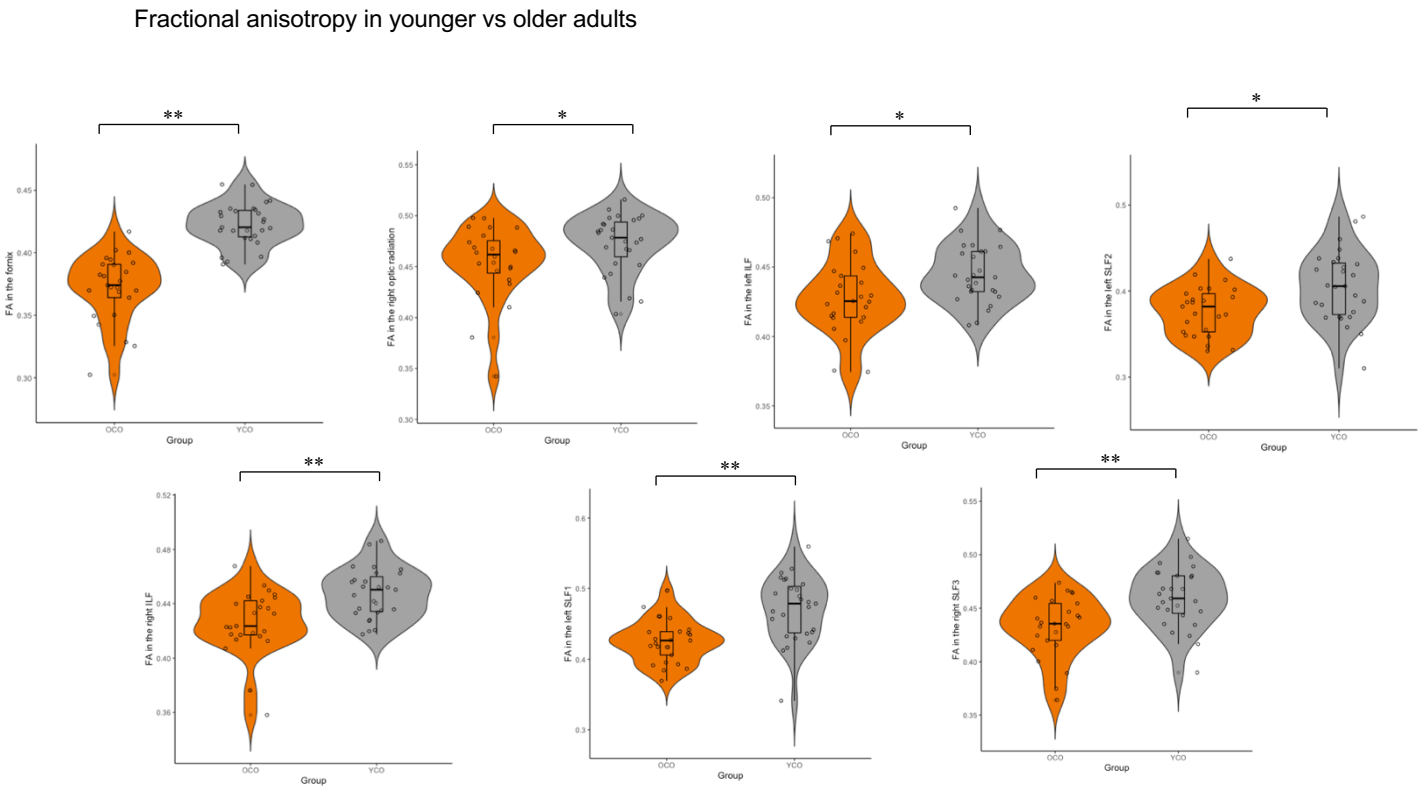


Figure 4.10 Fractional anisotropy (FA) in visual and attentional tracts of interest between older (orange) controls and younger (grey) controls. Mann-Whitney U tests showed FA in the fornix, optic radiation, SLF 1, 2 and 3 was significantly lower in older adults than younger adults. OCO = older adults, YCO = younger adults **p<.001, *p<.0.05

#### 4.2.2.3.2 Mean Diffusivity

Significantly higher MD in the older group in comparison to the younger control group was found in: fornix (U=84, p<.001), left optic radiation (U=78, p<.001), right optic radiation (U=131, p<.001), right ILF (U=203, p=.014), right SLF1 (U=175, p=.003), right SLF3 (U=175, p=.003) (Figure 4.11).

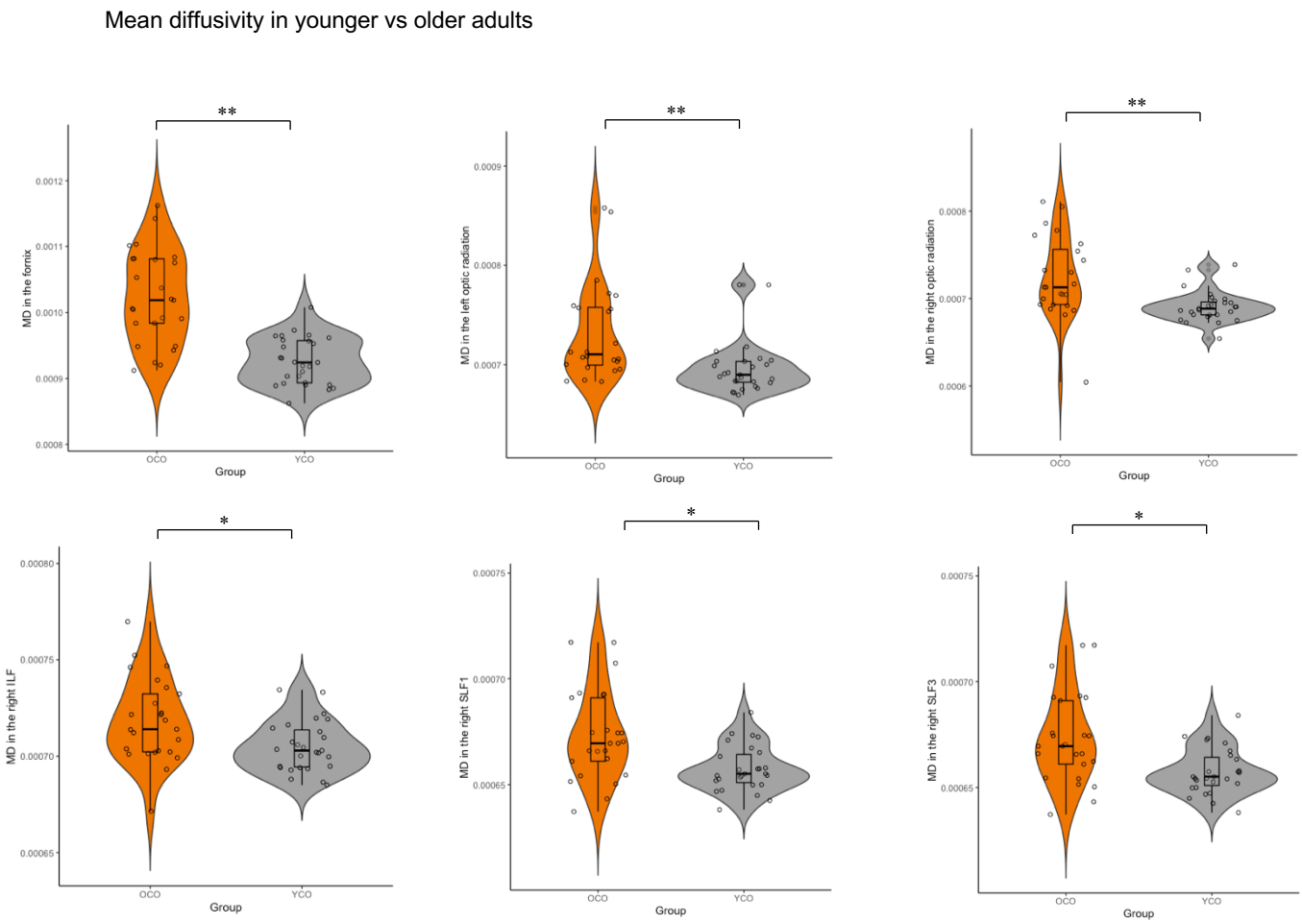


Figure 4.11 Mean diffusivity (MD) in visual and attentional tracts of interest between older (orange) controls and younger (grey) controls. Mann-Whitney U tests showed MD was significantly higher in the fornix, optic radiation, ILF, SLF1 and SLF 3 in comparison to younger adults, OCO = older adults, YCO = younger adults **p<.001, *p<.0.05.

#### 4.2.2.3.3 Radial Diffusivity

Radial diffusivity was significantly higher in the older control group in all tracts of interest except the right SLF1: fornix (U=39, p<.001), left optic radiation (U=145, p=.001), right optic radiation (U=139, p<.001), left ILF (U=189, p=.007), right ILF (U=143, p<.001), left SLF1 (U=130, p<.001), left SLF2 (U=256, p=.199), right SLF2 (U=178, p=.003), left SLF3 (U=197.5, p=.010), right SLF3 (U=135.5, <.001) (Figure 4.12).

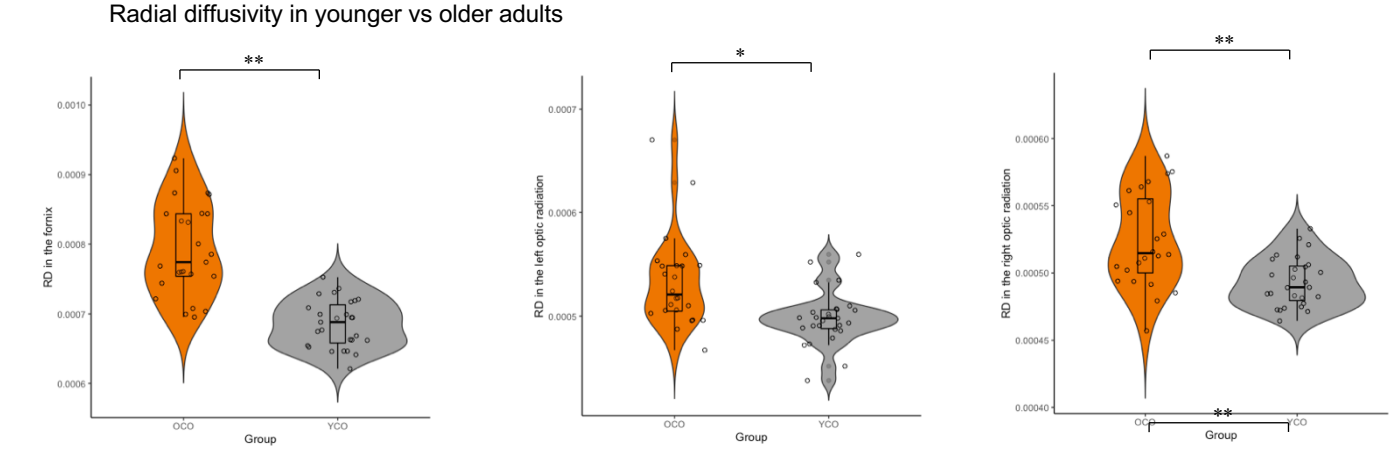

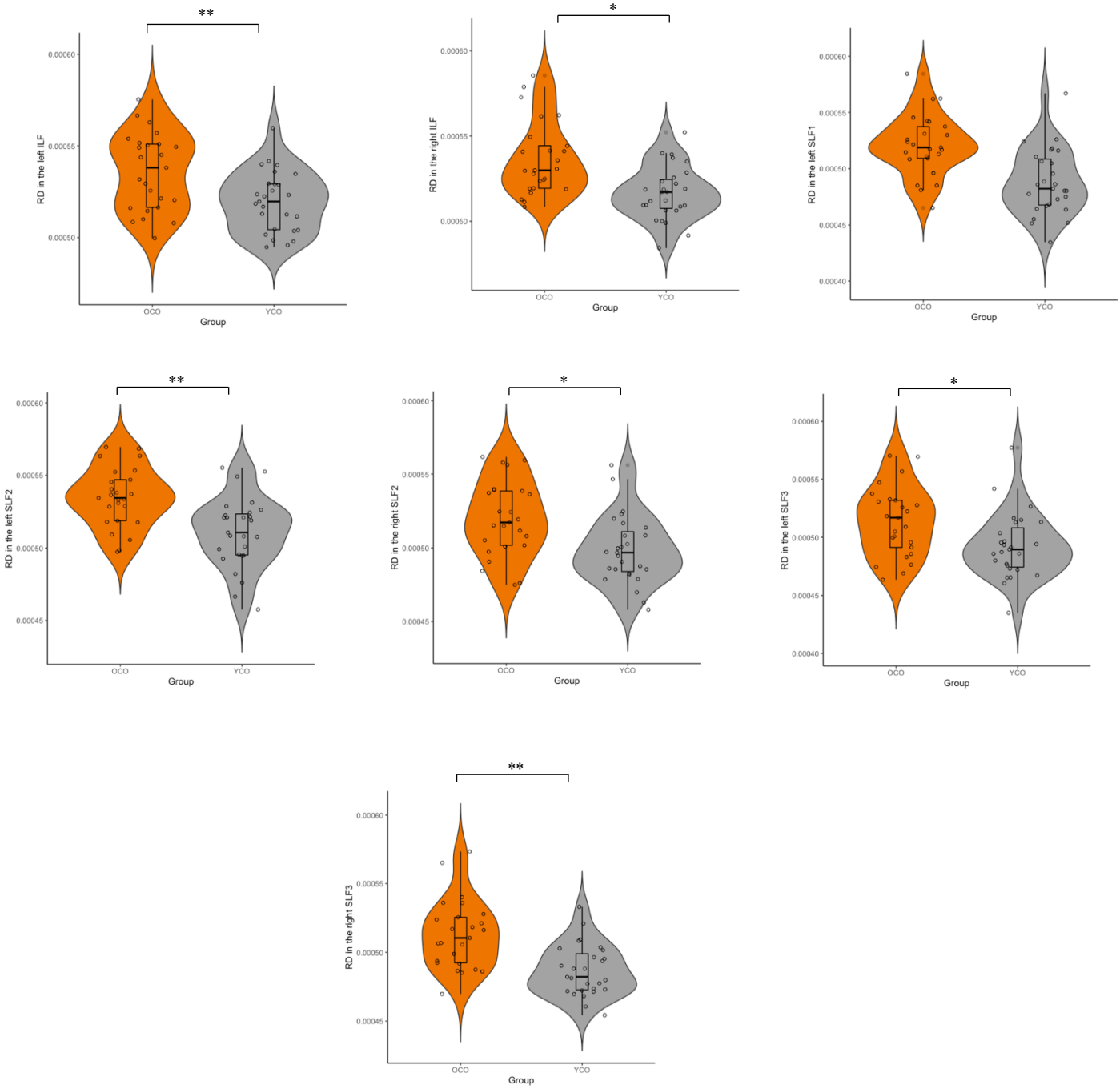


Figure 4.12 Radial diffusivity (RD) in visual and attentional tracts of interest between older controls and younger controls. Mann-Whitney U tests showed RD in the fornix, optic radiations, ILF, SLF1, 2 and 3 were significantly higher in older adults than younger adults. OCO = older adults, YCO = younger adults **p<.001, *p<.0.05.

#### 4.2.2.3.4 Axial diffusivity (L1)

Significantly greater axial diffusivity in older adults was found in the fornix (U=529, p<0.001), and significantly lower axial diffusivity in older adults was found in the SLF1 left (U=178, p=0.003) (Figure 4.13).


Figure 4.13 Axial diffusivity (L1) in visual and attentional tracts of interest between older (orange) controls and younger (grey) controls. Mann-Whitney U tests showed L1 was significantly higher in older adults in the fornix, but lower in SLF1 in older adults. OCO = older adults, YCO = younger adults **p<.001, *p<.0.05.

Table 4.3 Full results for Mann-Whitney group comparisons in white matter tracts for left and right hemispheres. WM=white matter, GM=grey matter. SLF = superior longitudinal fasciculus, ILF = inferior longitudinal fasciculus.

| | | *Left* | | | *Right* | |
|---|---|---|---|---|---|---|
| | **Mann-Whitney U** | **Significance (corrected)** | **Z value** | **Mann-Whitney U** | **Significance (corrected)** | **Z value** |
| *FA fornix* | 22 | <.001** | -5.77 | | | |
| *FA optic radiation* | 232 | .083 | -1.74 | 207 | .027* | -2.21 |
| *FA ILF* | 203 | .014* | -2.46 | 157 | .001* | -3.31 |
| *FA SLF 1* | 131.5 | <.001** | -3.77 | 262 | .167 | -1.38 |
| *FA SLF 2* | 195 | .009* | -2.61 | 218 | .029* | -2.19 |
| *FA SLF 3* | 229 | .050 | -1.98 | 163 | .001* | -3.19 |
| *MD fornix* | 78 | <.001** | -4.75 | | | |
| *MD optic radiation* | 143 | .001** | -3.42 | 131 | <.001** | -3.64 |
| *MD ILF* | 232 | .053 | -1.93 | 203 | .014* | -2.46 |
| *MD SLF 1* | 214 | .052 | -2.26 | 175 | .003* | -2.97 |
| *MD SLF 2* | 222 | .064 | -2.12 | 218 | .059 | -2.18 |
| *MD SLF 3* | 201 | .067 | -2.50 | 175 | .003* | -2.97 |
| *FR fornix* | 75 | <.001** | -4.81 | | | |
| *FR optic radiation* | 213 | .036* | -2.09 | 154 | .001* | -3.21 |
| *FR ILF* | 283 | .318 | -.998 | 191 | .087 | -2.68 |
| *FR SLF 1* | 152 | .001** | -3.39 | 301 | .504 | -.668 |
| *FR SLF 2* | 170 | .002* | -3.07 | 199 | .052 | -.307 |
| *FR SLF 3* | 197.5 | .05 | -2.78 | 169 | .002* | -3.07 |
| *RD fornix* | 39 | <.001** | -5.47 | | | |
| *RD optic radiation* | 145 | .001* | -3.37 | 139 | <.001** | -3.49 |
| *RD ILF* | 189 | .007* | -2.72 | 143 | <.001** | -3.56 |
| *RD SLF 1* | 130 | <.001** | -3.8 | 205 | .191 | -1.31 |
| *RD SLF 2* | 151 | .001* | -3.42 | 178 | .003* | -2.92 |
| *RD SLF 3* | 197.5 | .010* | -2.57 | 135.5 | <.001** | -3.7 |
| *L1 fornix* | 136 | <.001** | -3.55 | | | |
| *L1 optic radiation* | 217.5 | .070 | -1.81 | 217 | .069 | -1.82 |
| *L1 ILF* | 305 | .892 | -.13 | 291.5 | .691 | -.398 |
| *L1 SLF 1* | 176 | .005* | -2.79 | 248.5 | .12 | -3.31 |
| *L1 SLF 2* | 256 | .199 | -1.28 | 308 | .763 | -.30 |
| *L1 SLF 3* | 307 | .748 | -.32 | 295 | .584 | -.547 |

### 4.2.2.4 Relationship between metabolic and microstructural measurements

A non-parametric correlation matrix was conducted to assess relationships between all metabolites and microstructural outcome measures (Figure 4.14). The most significant correlations were present between FR measures in SLF 1,2, and 3 and the ILF, and NAA and Myoinositol in all MRS voxels. Cohen's d effect sizes were also generated for group comparisons for all microstructural measurements, which indicated the greatest effect sizes were present for FR measurements (all correlation p-values and effect sizes are reported

in Appendix 4). As such, non-parametric Spearman's rho correlations were conducted between FR measurements and metabolites which were shown to be significant in the correlation matrix after FDR correction. These were between FR in the SLF1 (left) and NAA in ACC (rho=0.516, p<.001), NAA in PPC (rho=0.341, p=.001), and myoinositol in ACC (rho=.346, p=.012). A significant correlation was also found between the FR in the SLF2 (left) and NAA in ACC (rho=0.527, p=<.001) and NAA in PPC (rho=.273, p=.043). Finally, a significant correlation was present between the FR in SLF 3 (right) and NAA in ACC (rho=0.380, p=.005), and FR in ILF (rho=.367, p=.009) (Figure 4.15).

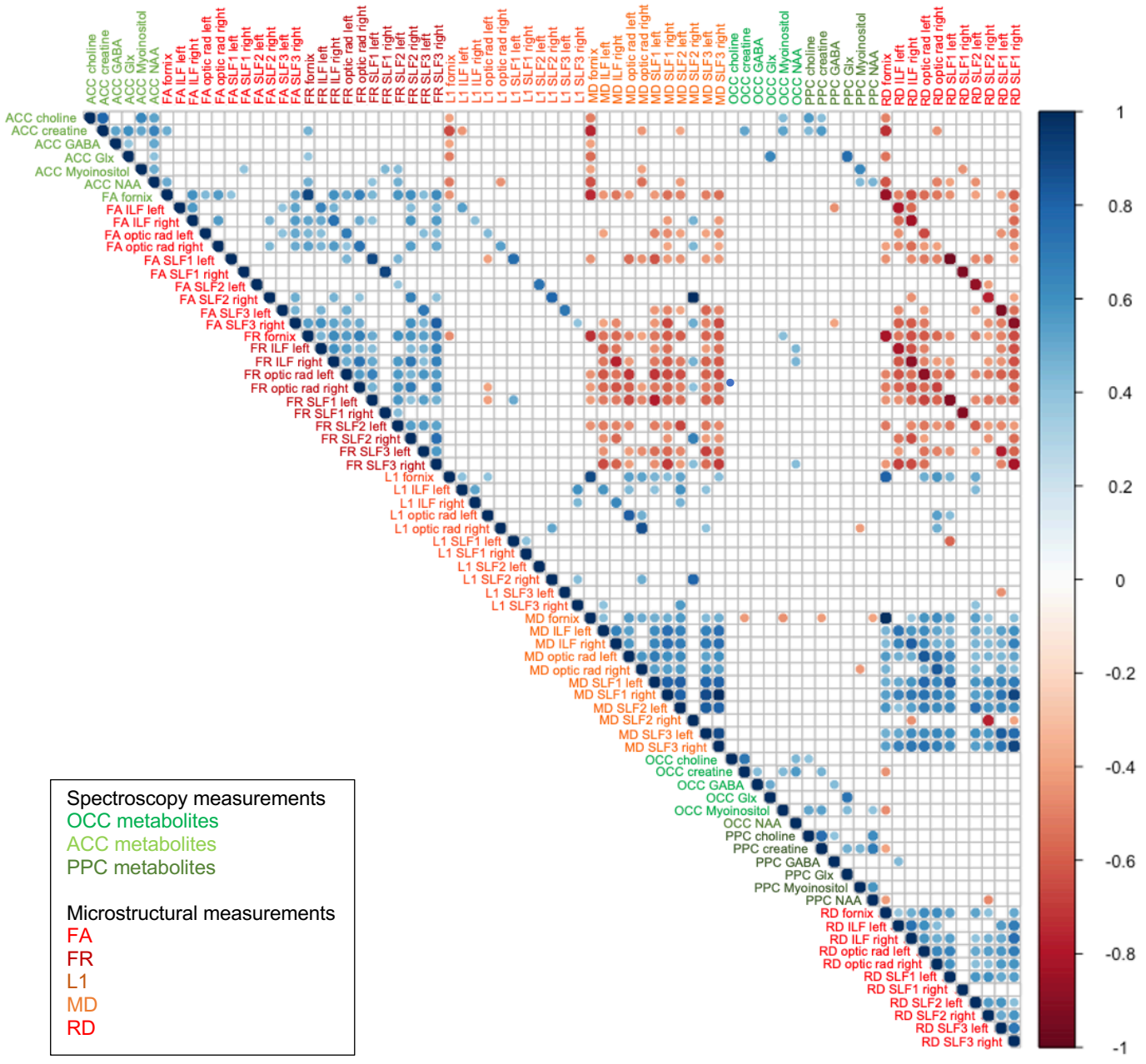


Figure 4.14 Correlation matrix between all metabolites and all microstructural measurements in all tracts. Significance threshold = p<.001. Scale bar demonstrates rho value and direction of relationship. Cho = choline, Cr = creatine, ins = myoinositol, Glx = glutamate/glutamine. FA = fractional anisotropy, MD = mean diffusivity, RD = radial diffusivity, L1 = axial diffusivity, FR = restricted fraction, oprad = optic radiations, SLF = superior longitudinal fasciculus, ILF = inferior longitudinal fasciculus,

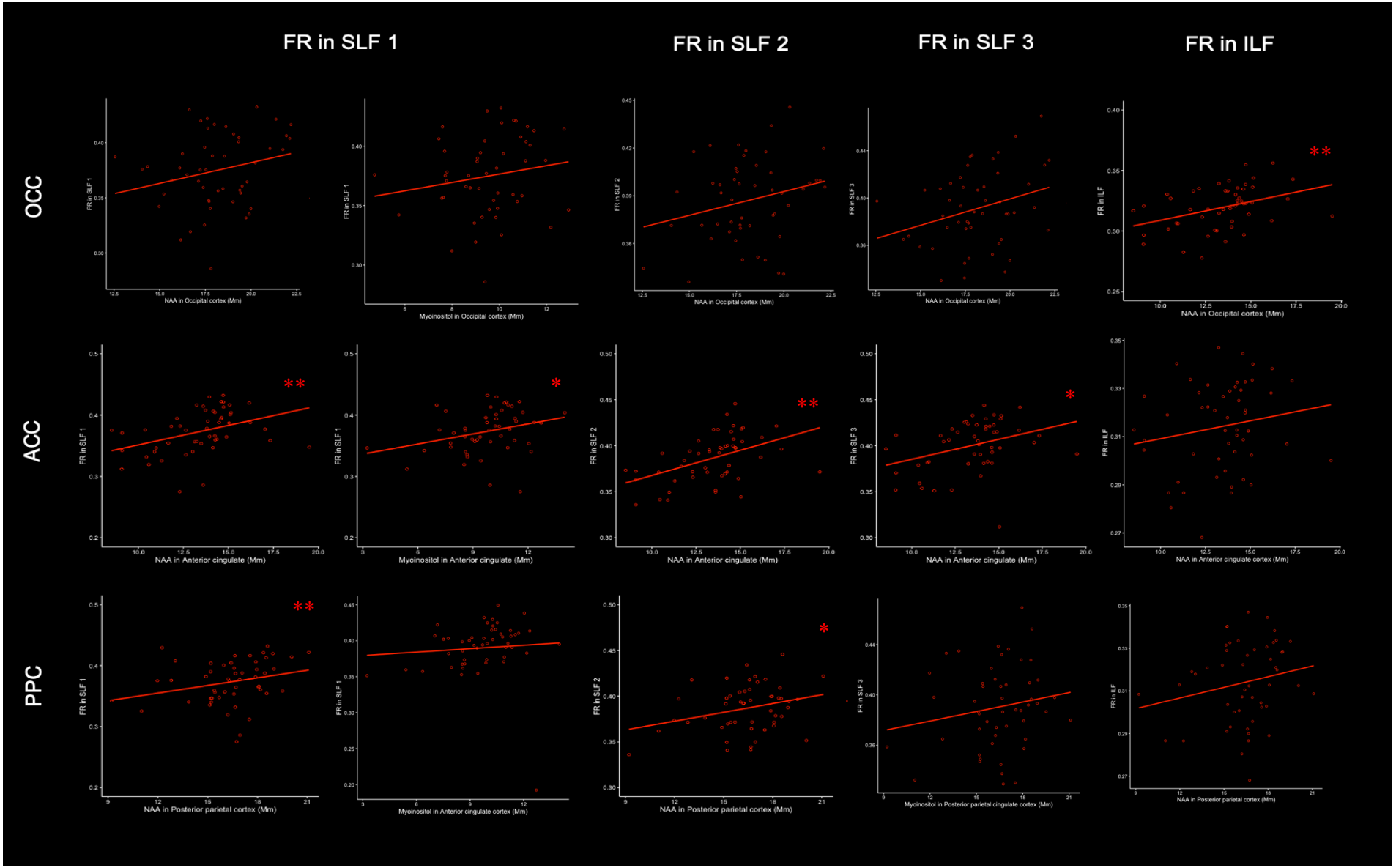


Figure 4.15 Correlations between metabolites showing age-related differences in the ACC and PPC and restricted fraction in the SLF in both younger and older adults together. Significant positive correlations were present between NAA in the ACC and FR in SLF 1, 2 and 3, NAA in the PPC and FR in SLF 1 and 2, Myoinositol in the ACC and FR in SLF 1, and NAA in OCC and FR in ILF **=p<.001, *=p<.05

Finally, mediation analyses were conducted between those metabolite and FR variables which were identified as significantly correlated above. Mediations were conducted to examine the direction of the metabolite-microstructure relationship when observing age as a predictor. In the first model, where metabolites were entered as a mediator, I observed a full mediation of NAA in ACC in the relationship between age and FR in SLF 1, 2 and 3 (Figure 4.16 highlighted in red). In the first model, significant relationships between age and NAA in PPC and the direct relationship between age and FR in SLF 1 were present, but the indirect relationship between NAA in PPC and FR in SLF 1 was not significant, indicating the mediational hypothesis was not supported. In the second model, only relationships between age and FR in SLF 1, and the indirect relationship between FR in SLF 1 and Myoinositol were significant, but inclusion of FR in SLF 1 did not mediate the direct effect between age and myoinositol in ACC. All other models failed to show a significant indirect or direct effect indicating that the mediational hypothesis was not supported.

As such, full mediation of age effects on metabolites were observed in the first model, indicating that age-related differences in NAA in ACC mediated age differences in FR in SLF 1, but not vice versa.

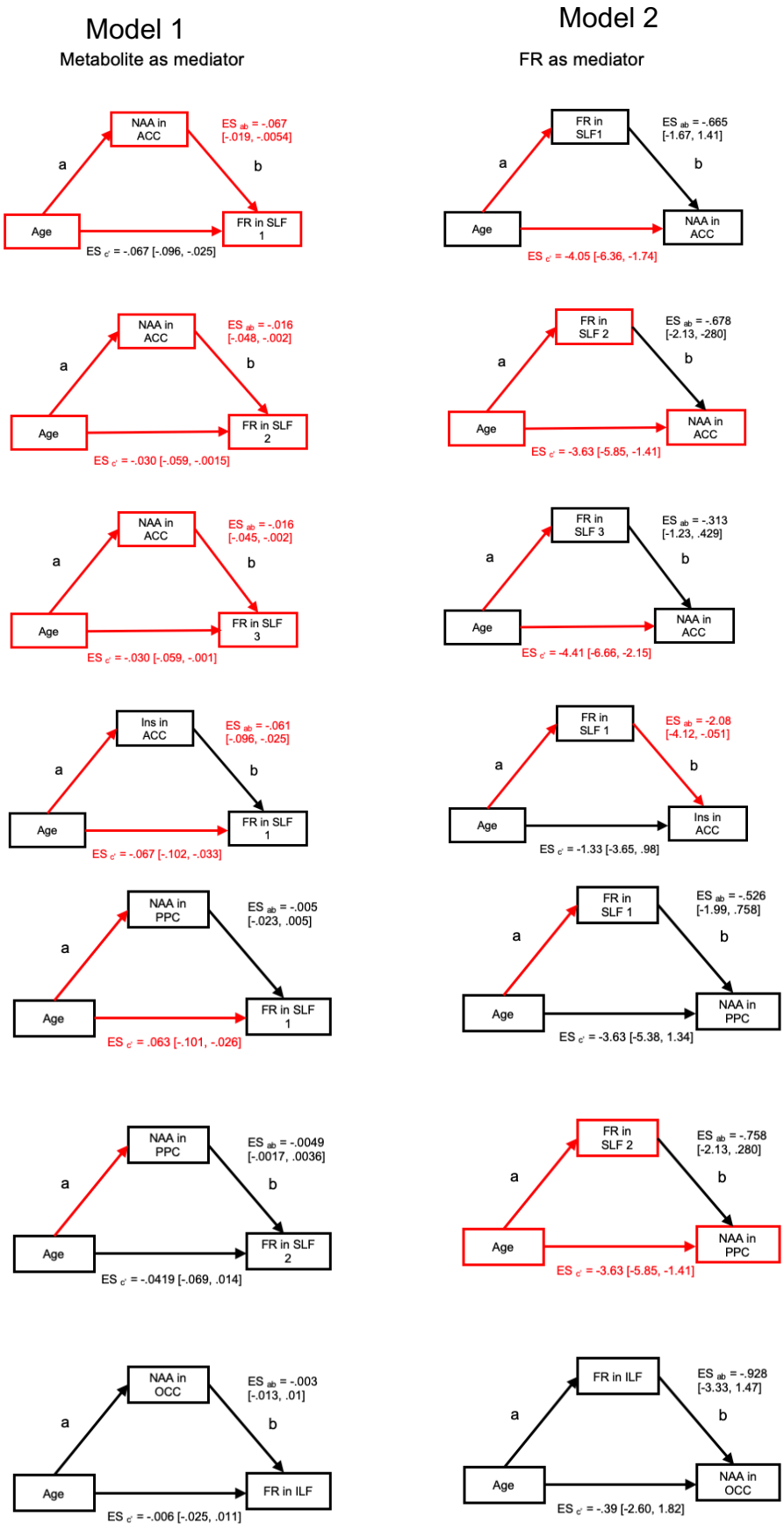


Figure 4.16 Linear models observing the mediation of metabolites on the relationship between age and restricted fraction (FR; model 1) and the mediation of FR on the relationship between age and metabolites (model 2). NAA = N-acetyl aspartate, OCC = occipital cortex, ACC = anterior cingulate cortex, PPC = posterior parietal cortex, FR = restricted fraction, ES = effect size [95% confidence intervals of effect sizes (ES x $10^{-1}$)]. Significant relationships highlighted in red.

### 4.2.2.5 Cortical thickness

Descriptive statistics for cortical thickness in older and younger groups are reported in Appendix 5. MANOVA results from cortical thickness group comparisons showed significant differences between older and younger groups, as indicated by the omnibus effect F(50,1)=4.449, p=<.001; Wilk's $\Lambda = 0.151$, partial $\eta^2$=.849. Univariate F tests showed lower cortical thickness in all regions of interest in older adults compared to younger adults (Table 4.4; Figures 4.17 and 4.18). In contrast, no significant difference was present in optic chiasm volume between groups.

Table 4.4 Full MANOVA group comparisons for cortical thickness in the left and right hemisphere. ACC=anterior cingulate cortex

| | *Left* | | | *Right* | | |
|---|---|---|---|---|---|---|
| | **F value** | **Significance** | **Partial $\eta^2$** | **F value** | **Significance** | **Partial $\eta^2$** |
| *Bank superior temporal sulcus* | 37.24 | <.001 | .422 | 29.25 | <.001 | .364 |
| *Caudal ACC* | 22.15 | <.001 | .303 | 17.61 | <.001 | .257 |
| *Caudal middle frontal* | 12.97 | .001 | .203 | 17.65 | <.001 | .257 |
| *Cuneus* | 5.14 | .028 | .092 | 6.771 | .012 | .117 |
| *Inferior parietal* | 36.74 | <.001 | .419 | 26.03 | <.001 | .338 |
| *Inferior temporal* | 11.92 | .001 | .189 | 23.65 | <.001 | .317 |
| *Lateral occipital* | 6.65 | .013 | .115 | 11.70 | .001 | .187 |
| *Medial orbitofrontal* | 28.30 | <.001 | .357 | 29.66 | <.001 | .368 |
| *Middle temporal* | 43.97 | <.001 | .463 | 30.92 | <.001 | .377 |
| *Rostral ACC* | 15.96 | <.001 | .238 | 7.29 | .009 | .125 |
| *Rostral middle frontal* | 47.97 | <.001 | .485 | 22.81 | <.001 | .309 |
| *Superior frontal* | 31.07 | <.001 | .379 | 49.75 | <.001 | .494 |
| *Superior parietal* | 12.25 | .001 | .194 | 24.05 | <.001 | .320 |
| *Superior temporal* | 49.22 | <.001 | .491 | 63.18 | <.001 | .553 |
| *Optic Chiasm volume* | 1.94 | .170 | .553 | | | |

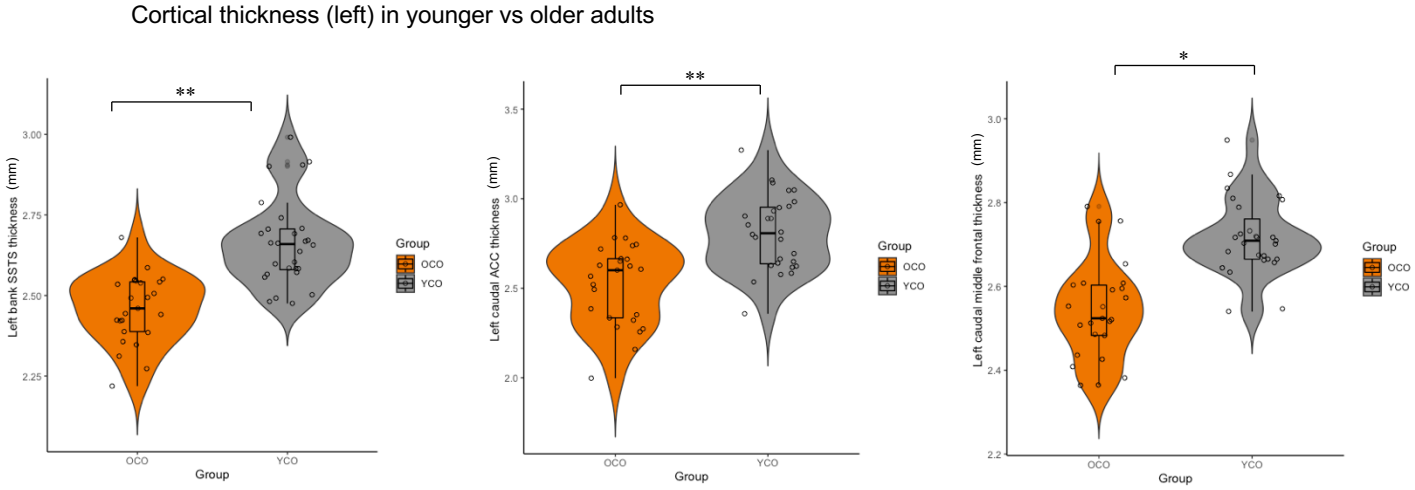

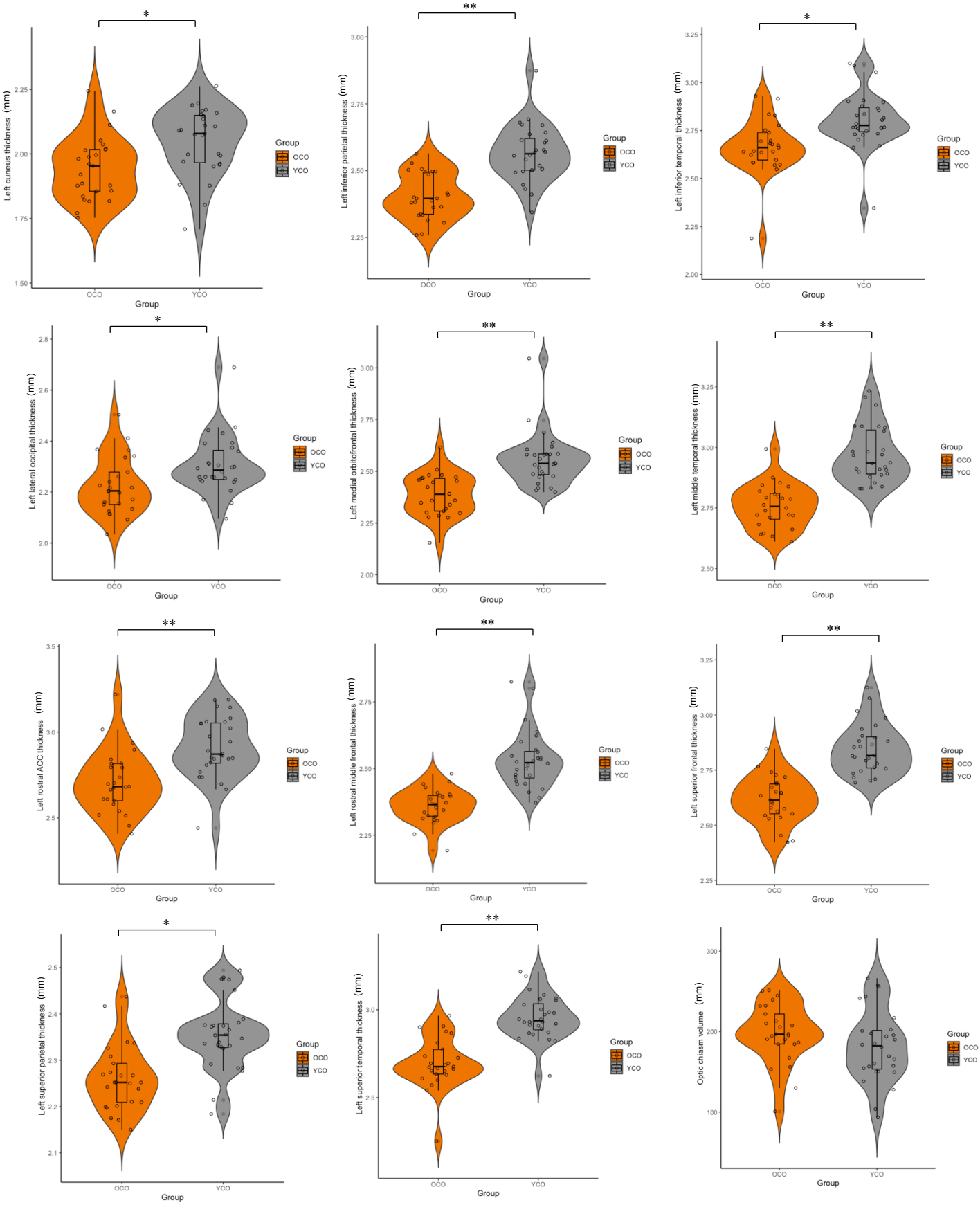


Figure 4.17 Cortical thickness (left hemisphere) in older (orange) and younger (grey) adults. MANOVA results indicate that left cortical thickness was significantly lower in older adults in the bank STS, caudal/rostral ACC, caudal/rostral frontal, cuneus, inferior/superior parietal, inferior/superior temporal, lateral occipital, medial orbitofrontal, superior /inferior /middle temporal, optic chiasm in comparison to younger adults. OCO = older adults, YCO = younger adults **p<.001, *p<.0.05.

Cortical thickness (right) in younger vs older adults

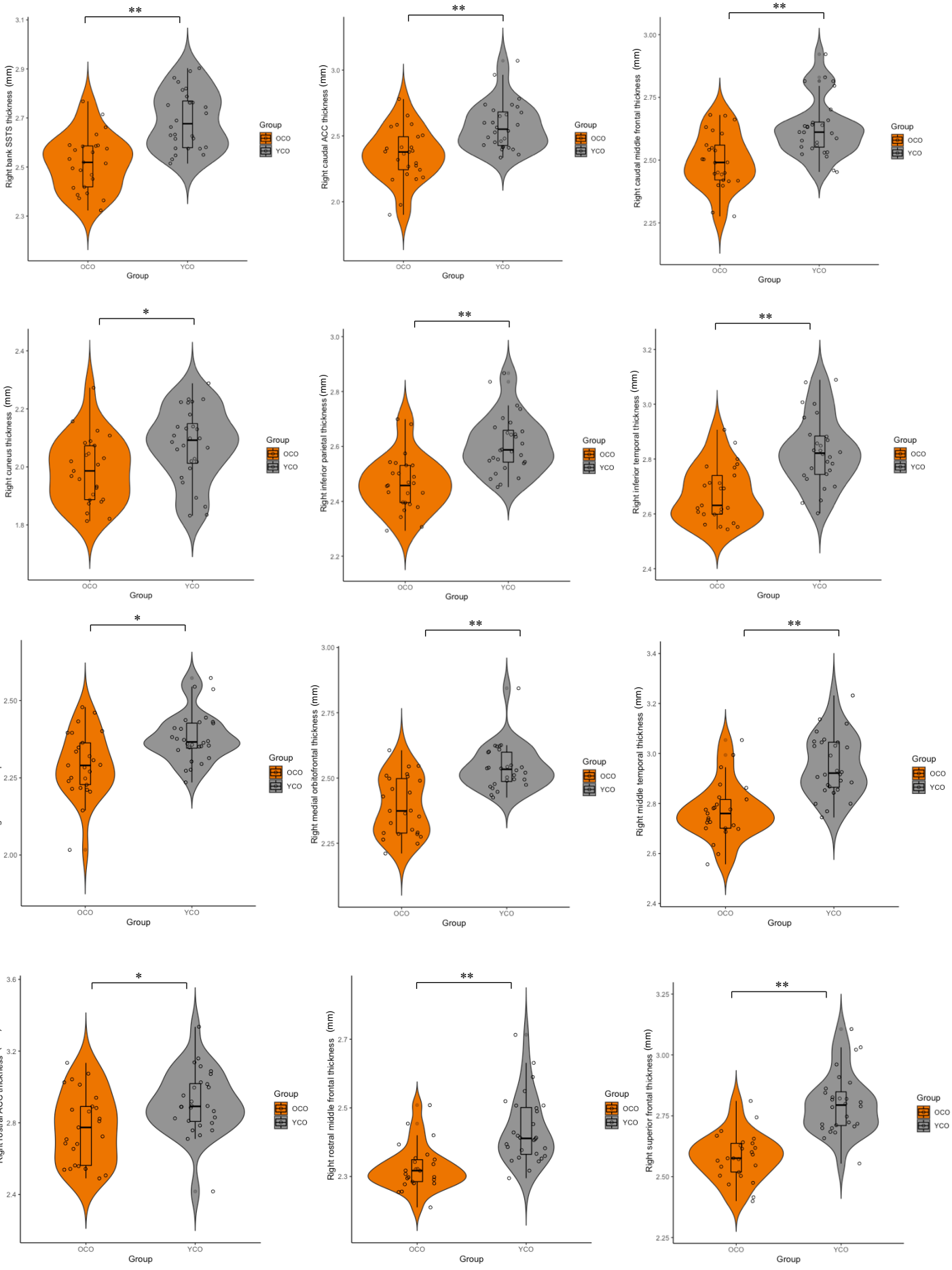

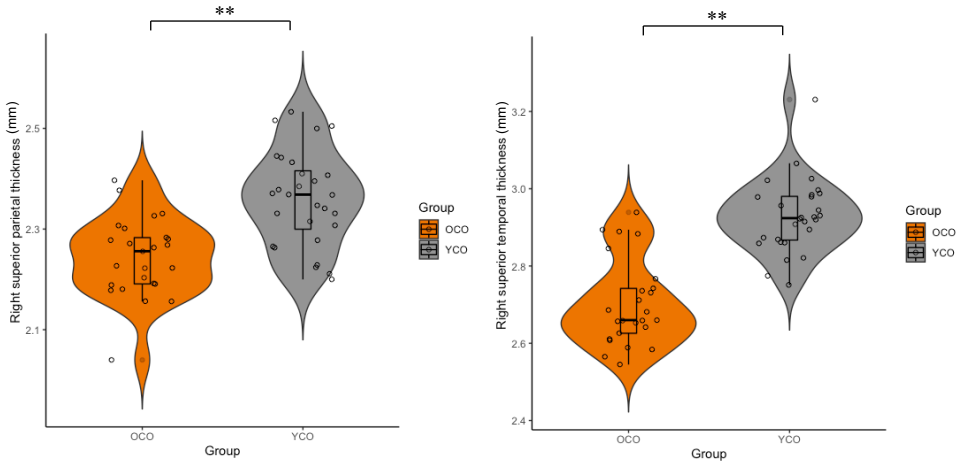


Figure 4.18 Cortical thickness (right hemisphere) in older (orange) and younger (grey) adults. MANOVA results indicate that cortical thickness was significantly lower in older adults in the banks STS, caudal/rostral ACC, superior/ caudal/rostral frontal, cuneus, inferior/superior parietal, inferior/superior temporal, lateral occipital, medial orbitofrontal, superior /inferior /middle temporal, optic chiasm in comparison to younger adults. OCO = older adults, YCO = younger adults **p<.001, *p<.0.05

### 4.2.3 Results: DLB patients' brain differences

As previously described in Chapter 3, 95% CIs were calculated for the older adult control group and are displayed below in section 4.7. DLB patients were then observed against this interval as individual cases. DLB patients were observed against older participants (n=3), as in previous comparisons. 95% confidence intervals were calculated for older control participants, and those metabolites and microstructural findings in which DLB patients' results fell outside of the confidence interval are reported. All values for DLB patients and CIs are listed in Appendix 6.

#### 4.2.3.1 DLB patient metabolite comparisons

DLB patients have variable GABA/$H_20$ in the OCC and ACC, however all DLB patients' have raised GABA/$H_20$ in the PPC, which is higher than the healthy older control 95% CI. DLB patients were visually compared with healthy older control participants. A 95% CI was calculated for the healthy older control group, indicated in orange. Those parameters in which DLB patients fell outside the confidence interval are visualised. Metabolites in which at least 1 DLB patient showed results outside of the 95% CI of healthy controls are displayed (Figure 4.19, 4.20). 2 DLB patients showed lower GABA/$H_20$ in the OCC, whilst 1 DLB patient showed higher GABA/$H_20$ in OCC. All DLB patients showed higher GABA/$H_20$ in the PPC than the 95% confidence interval for healthy older controls.

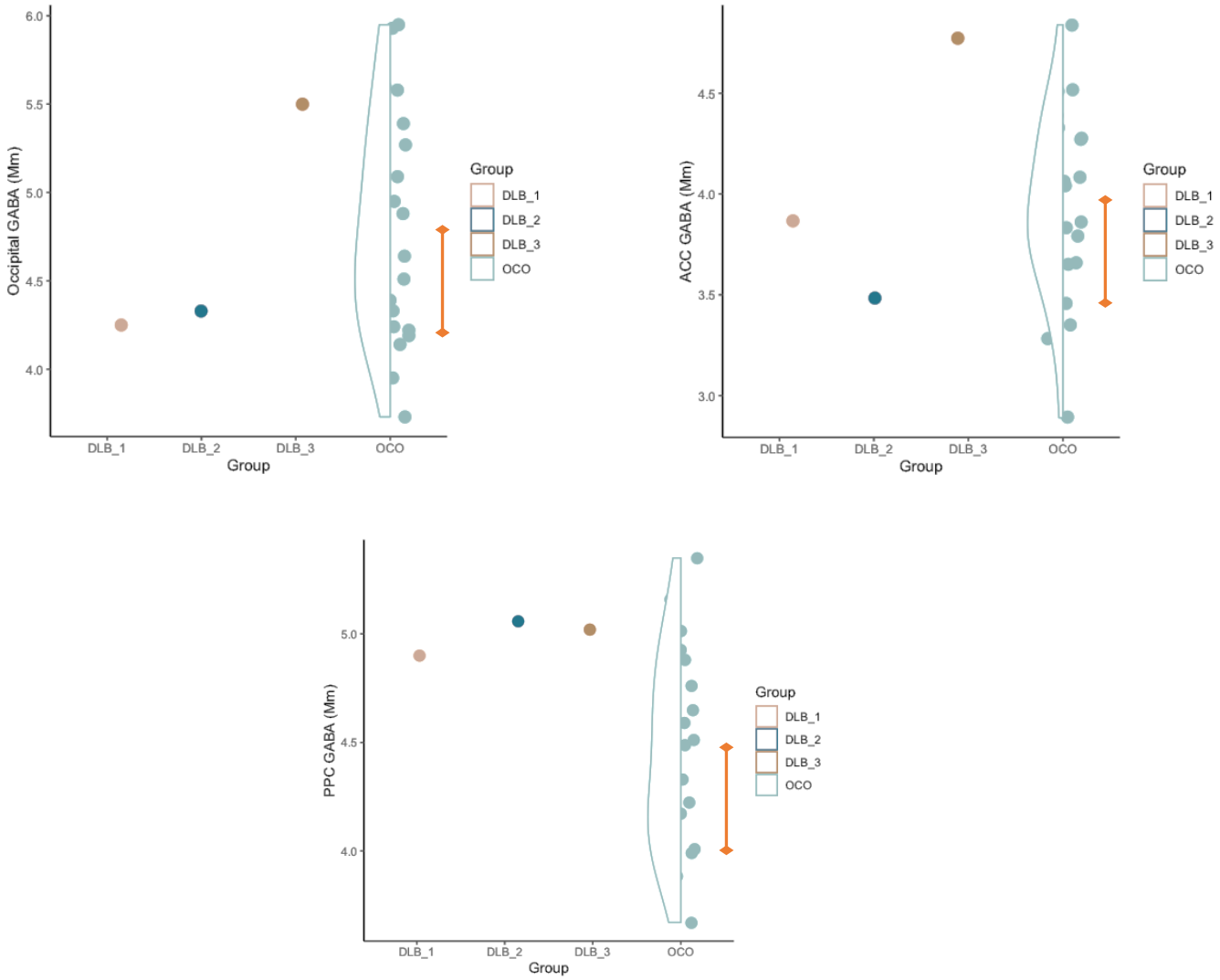


Figure 4.19 Dementia with Lewy bodies (DLB) patient GABA/$H_20$ plotted against older controls (OCO). Orange band indicates 95% confidence intervals calculated for older control groups. ACC = anterior cingulate cortex, PPC = posterior parietal cortex.

Metabolites showing differences between DLB patients vs older adults

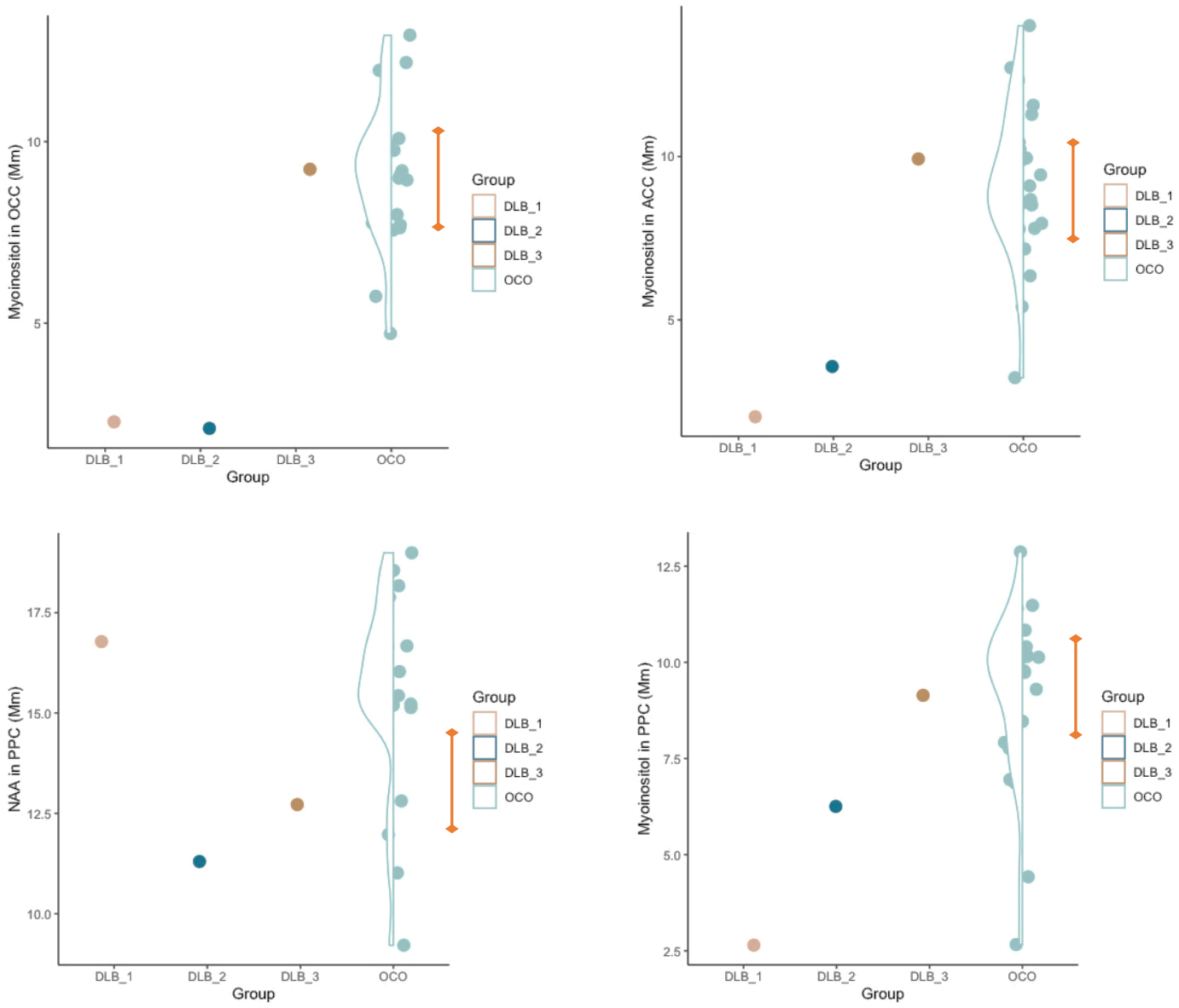


Figure 4.20 Dementia with Lewy bodies (DLB) patient brain metabolic differences plotted against older controls (OCO). Orange band indicates 95% confidence intervals calculated for older control groups. OCC = occipital cortex, ACC = anterior cingulate cortex, PPC = posterior parietal cortex.

### 4.2.3.2 DLB patient microstructural comparisons

Microstructural metrics and tracts in which DLB patients show discrepancy from 95% confidence intervals in healthy controls are displayed (Figure 4.21). DLB patients show variable results, however all DLB patients show lower FA in the right ILF, lower FR in the right SLF 3 and higher RD and L1 in the Fornix in comparison to 95% confidence intervals from healthy older control participants.

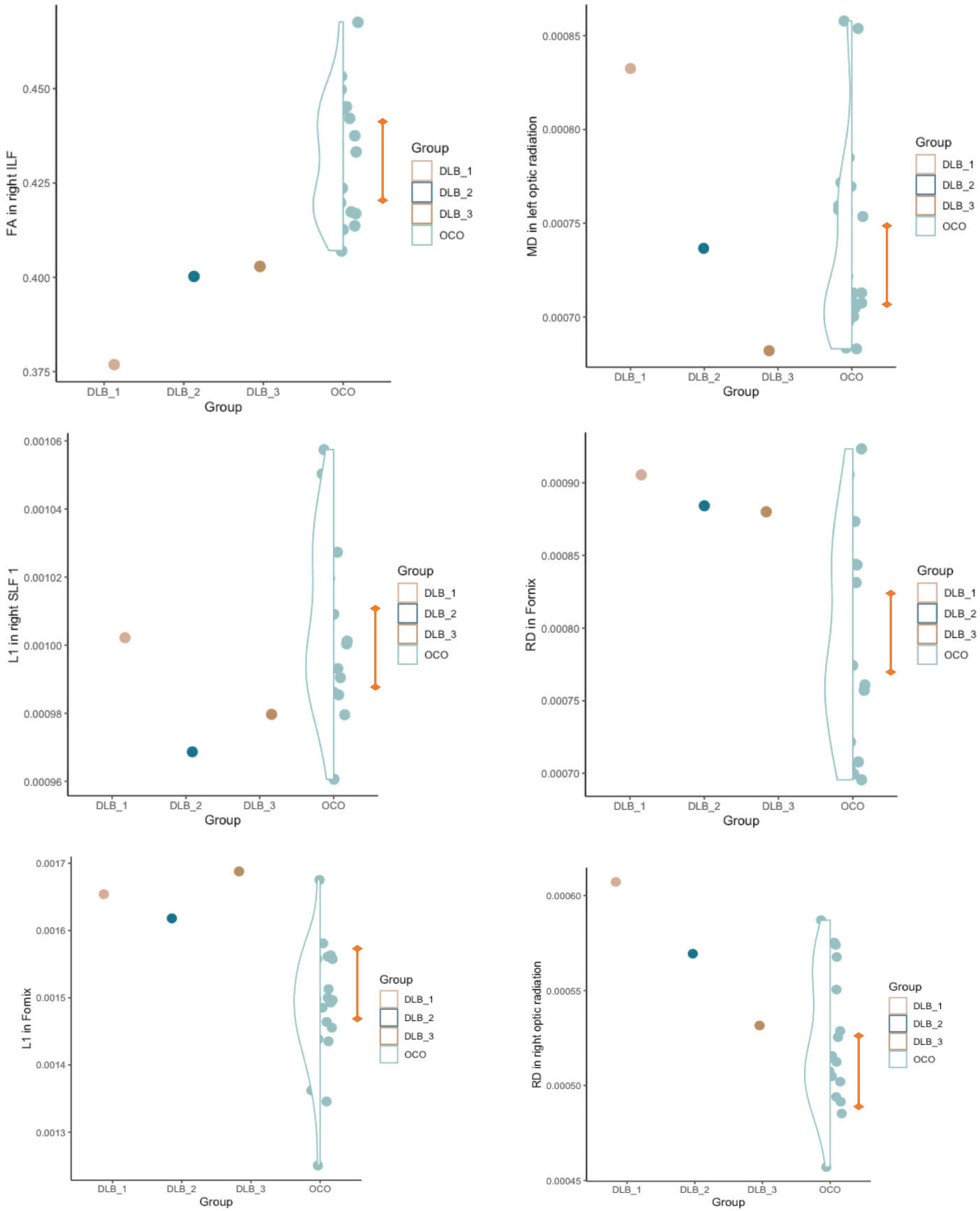


Figure 4.21 Dementia with Lewy bodies (DLB) patient microstructural differences in visual and attentional tracts of interest plotted against older controls (OCO). Orange band indicates 95% confidence intervals calculated for older control groups. FA = fractional anisotropy, MD = mean diffusivity, RD = radial diffusivity, L1 = axial diffusivity

### 4.2.3.3 DLB patient cortical thickness comparisons

DLB patients show variable results; right medial orbitofrontal cortex thickness was higher in all DLB patients than control participants, and some DLB patients showed lower left precuneus thickness and higher rostral ACC thickness (Figure 4.22).

Cortical thickness in both hemispheres (left and right) in DLB patients

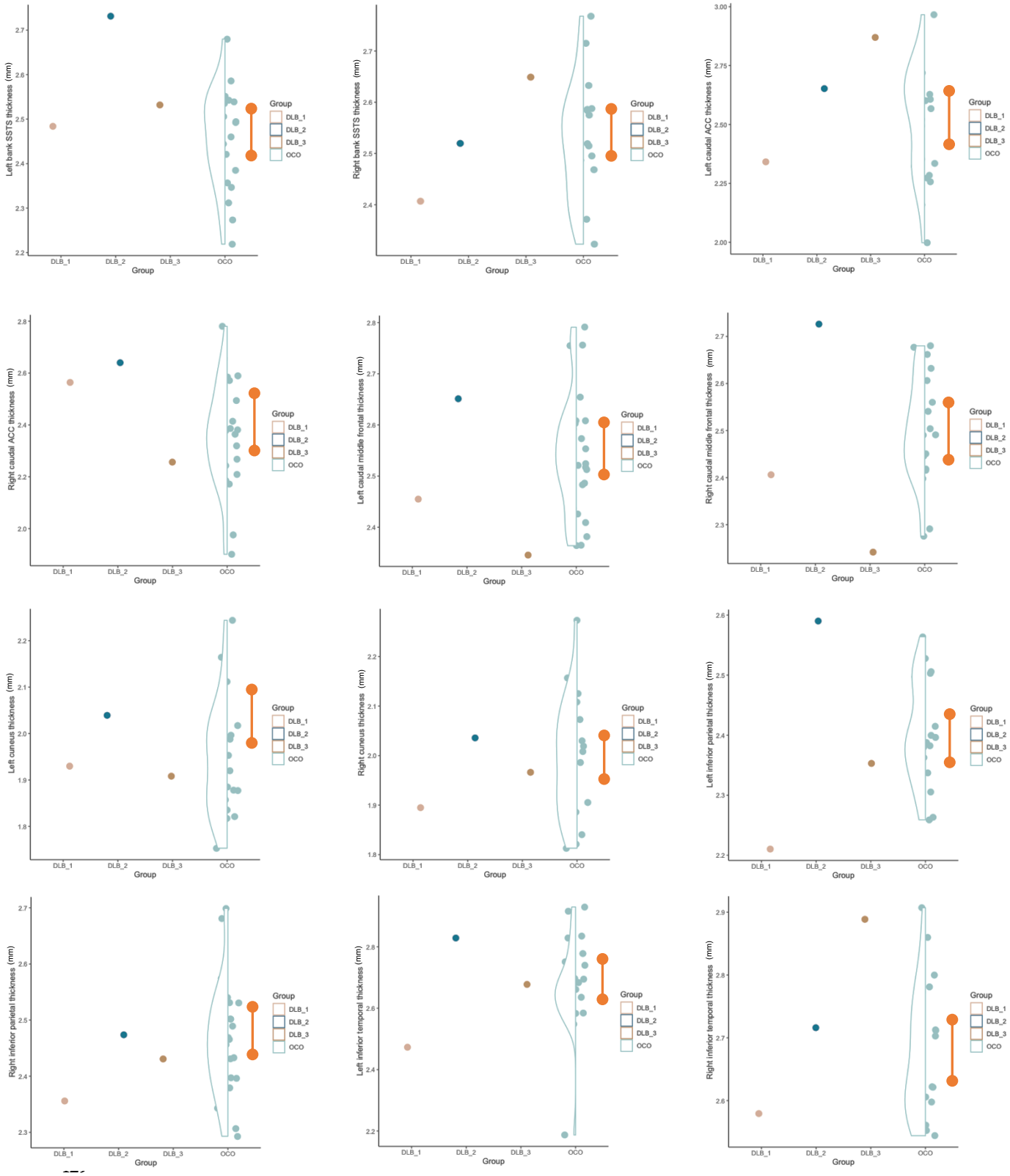

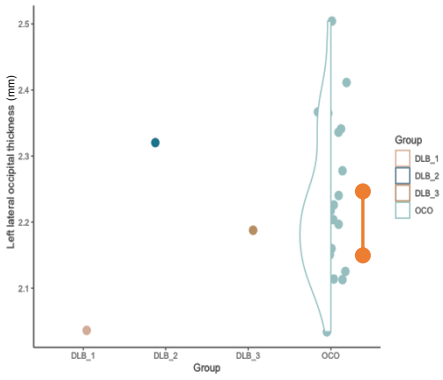
Left lateral occipital thickness (mm)
2.5
2.4
2.3
2.2
2.1
DLB_1
DLB_2
DLB_3
OCO
Group
Group
DLB_1
DLB_2
DLB_3
OCO

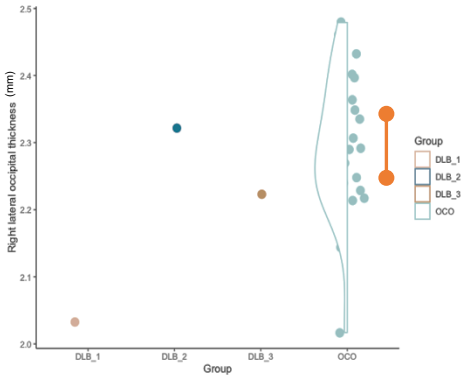
Right lateral occipital thickness (mm)
2.5
2.4
2.3
2.2
2.1
2.0
DLB_1
DLB_2
DLB_3
OCO
Group
Group
DLB_1
DLB_2
DLB_3
OCO

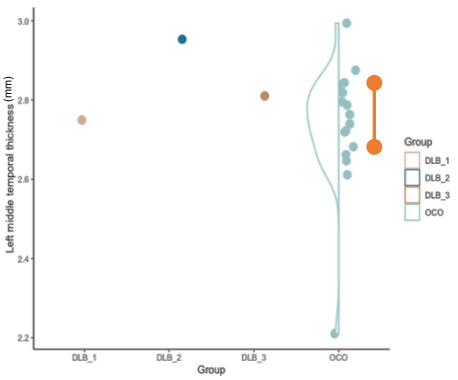
Left middle temporal thickness (mm)
3.0
2.8
2.6
2.4
2.2
DLB_1
DLB_2
DLB_3
OCO
Group
Group
DLB_1
DLB_2
DLB_3
OCO

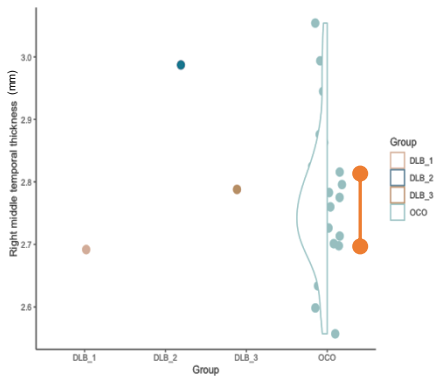
Right middle temporal thickness (mm)
3.0
2.9
2.8
2.7
2.6
DLB_1
DLB_2
DLB_3
OCO
Group
Group
DLB_1
DLB_2
DLB_3
OCO

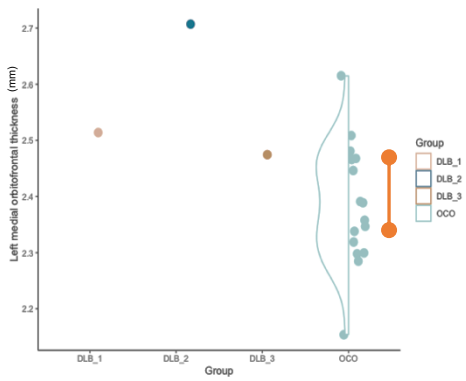
Left medial orbitofrontal thickness (mm)
2.7
2.6
2.5
2.4
2.3
2.2
DLB_1
DLB_2
DLB_3
OCO
Group
Group
DLB_1
DLB_2
DLB_3
OCO

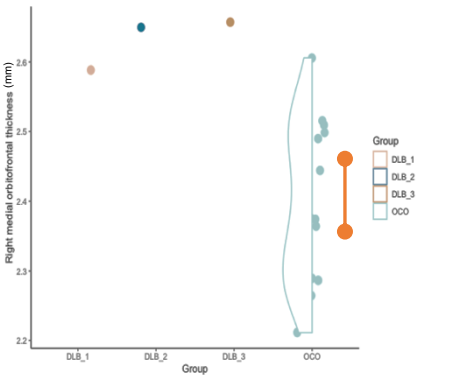
Right medial orbitofrontal thickness (mm)
2.6
2.5
2.4
2.3
2.2
DLB_1
DLB_2
DLB_3
OCO
Group
Group
DLB_1
DLB_2
DLB_3
OCO

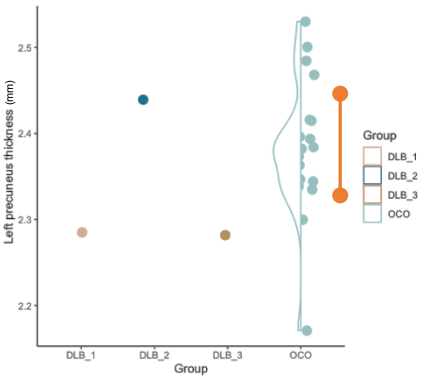
Left precuneus thickness (mm)
2.5
2.4
2.3
2.2
DLB_1
DLB_2
DLB_3
OCO
Group
Group
DLB_1
DLB_2
DLB_3
OCO

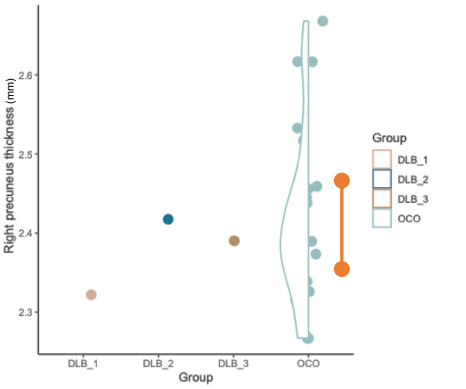
Right precuneus thickness (mm)
2.6
2.5
2.4
2.3
DLB_1
DLB_2
DLB_3
OCO
Group
Group
DLB_1
DLB_2
DLB_3
OCO

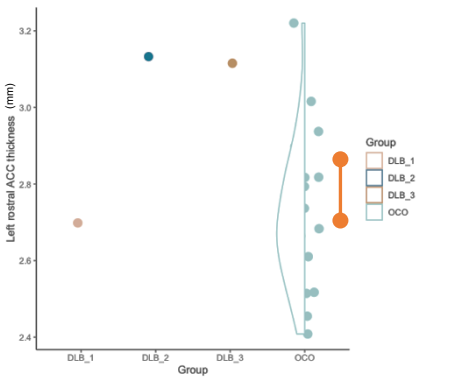
Left rostral ACC thickness (mm)
3.2
3.0
2.8
2.6
2.4
DLB_1
DLB_2
DLB_3
OCO
Group
Group
DLB_1
DLB_2
DLB_3
OCO

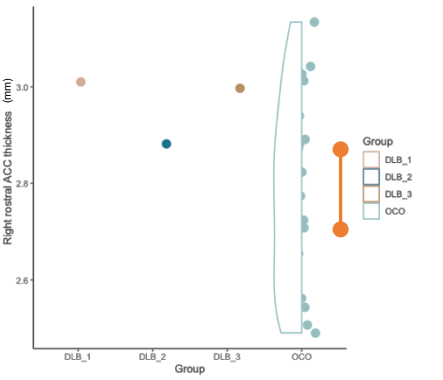
Right rostral ACC thickness (mm)
3.0
2.8
2.6
DLB_1
DLB_2
DLB_3
OCO
Group
Group
DLB_1
DLB_2
DLB_3
OCO

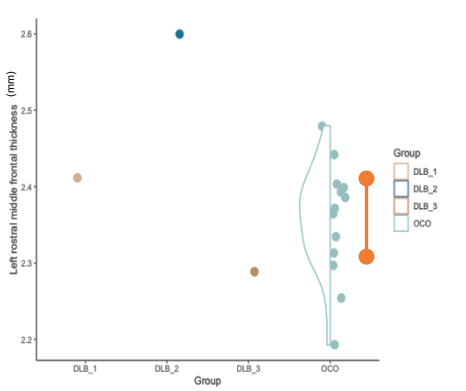
Left rostral middle frontal thickness (mm)
2.6
2.5
2.4
2.3
2.2
DLB_1
DLB_2
DLB_3
OCO
Group
Group
DLB_1
DLB_2
DLB_3
OCO

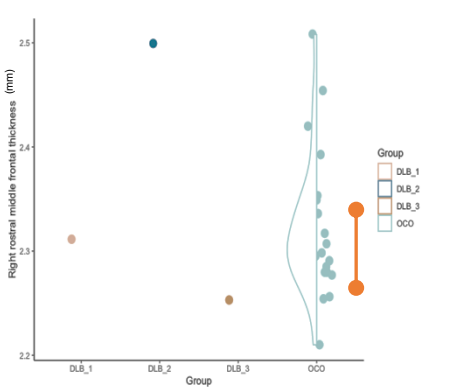
Right rostral middle frontal thickness (mm)
2.5
2.4
2.3
2.2
DLB_1
DLB_2
DLB_3
OCO
Group
Group
DLB_1
DLB_2
DLB_3
OCO

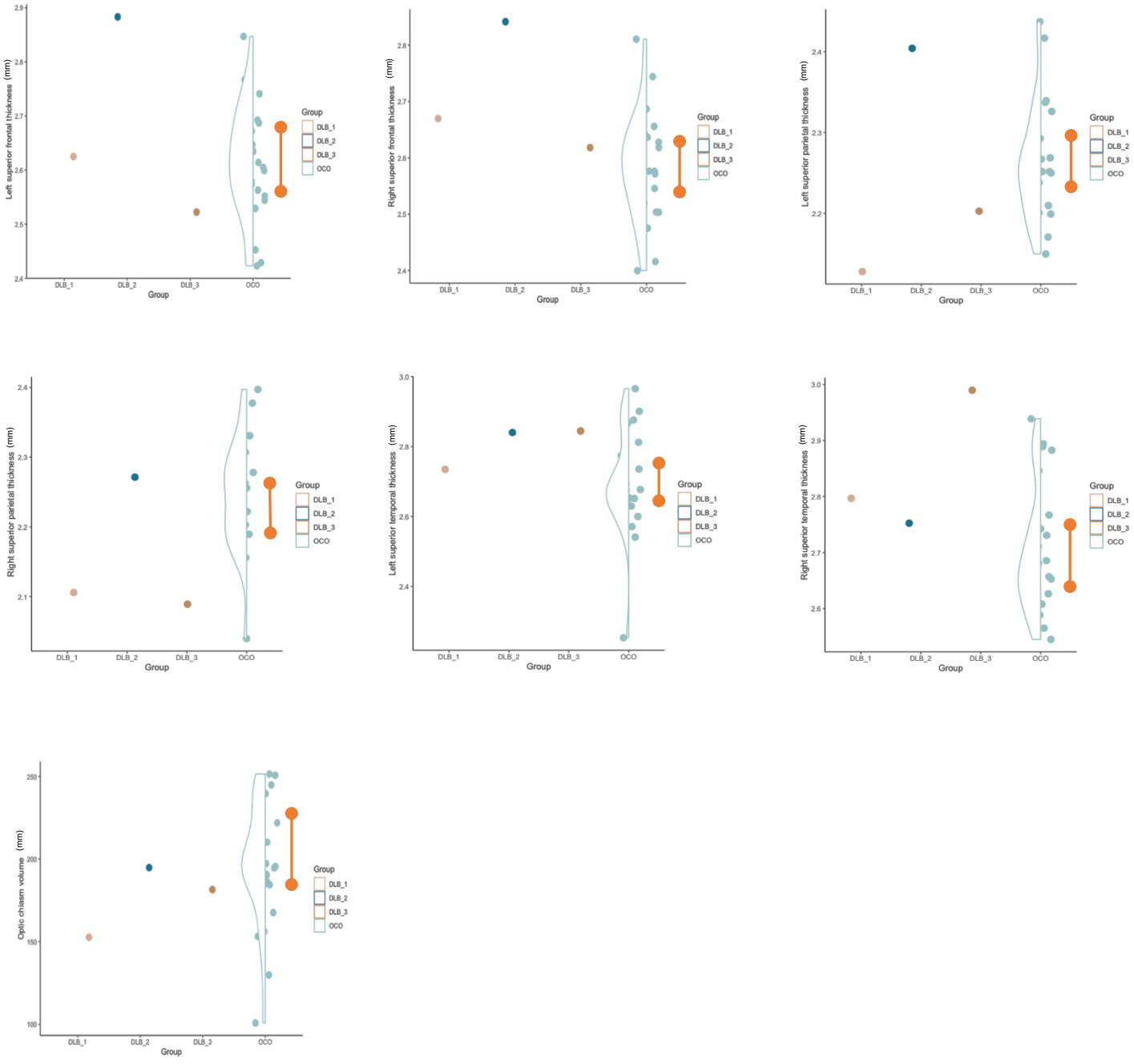


Figure 4.22 Dementia with Lewy bodies (DLB) patient cortical thickness in left and right hemispheres plotted against older controls (OCO). Orange band indicates 95% confidence intervals calculated for older control group. SSTS = bank of the superior temporal sulcus, ACC = anterior cingulate cortex.

## 4.3 Part 1 Discussion

One of the main objectives of this chapter was to characterise the differences between younger and older adults in brain metabolites, white matter microstructure and grey matter morphology in regions and tracts involved in visual perception and attention. This was done by assessing differences in a priori selected ROIs and white matter tracts of the visual perceptual and attentional networks and was followed by exploratory whole brain analyses of grey matter macrostructure and white matter microstructure. With regards to age-

related differences in metabolites, I hypothesised that choline and creatine would show an increase with age, particularly in the frontal voxel (ACC), while GABA/$H_20$ and Glx would be lower in older adults particularly in the OCC. I also hypothesised that these NAA and myoinositol would be raised in frontal regions and reduced in more posterior voxels, consistent with previous literature (Gruber et al., 2008; Harada et al., 2013). With regards to white matter microstructure, I hypothesised that white matter integrity measured with FR and FA would be generally lower, while diffusivity measures were expected to be generally higher in older adults and that these differences would be specifically pronounced in fronto-parietal networks Finally, widespread reductions in grey matter cortical thickness and volume was expected in older compared with younger adults, particularly in frontal, superior parietal and superior temporal regions involved in multi-sensory perception, attention and executive functions. In the following section I will be discussing the age-related results I observed for these different modalities and then with regards to the relationships between brain metabolites and microstructure.

### 4.5.1 Metabolite differences between younger and older adults

Older adults show reduced levels of Glx and NAA in the ACC compared with younger adults. In addition, they also exhibited lower levels of NAA in the PPC. No other metabolites showed age-related differences although a trend for lower levels of myoinositol in the ACC in older adults was observed. This was contrary to my hypothesis and previous research which has shown NAA to be most consistently reduced in posterior regions, and metabolites associated with inflammation to be raised in the frontal lobe in older adults. However, the frontal lobes are vulnerable to age-related decline. NAA and Glx are both markers of neuronal metabolism (Newsholme et al., 2003) and are considered to play a key role in energy metabolism in neural mitochondria (Lu et al., 2004). With normal ageing, the accumulation of biological 'imperfections' such as protein aggregation is thought to lead to both low-level inflammation and impaired mitochondrial function, resulting in reduced total glucose uptake, synaptic deterioration and gliosis (Currais, 2015). My results showing reductions in NAA and Glx in the ACC in older adults may reflect a reduction in neuronal metabolism due to the accumulation of these biological 'imperfections'. Taken together, this indicates that NAA and Glx may be reduced, impairing effective mitochondrial function in the frontal and parietal cortex in the healthy ageing brain. Thus, my findings suggest that ageing affects neuronal metabolism in frontal and parietal attention regions but not the OCC. These findings are consistent with some accumulating evidence from several studies suggesting that healthy ageing is associated with a reduction in mitochondrial energy metabolism (Reddy & Beal, 2008, Reutzel et al., 2020, Yin et al., 2014). Moreover, these findings support the anterior-posterior gradient evident in ageing research and support the theory of selective vulnerability of the anterior brain structures and mechanisms in healthy ageing.

In contrast to this, and unexpectedly, no significant age-related differences were observed for GABA/$H_20$. This finding is inconsistent with previous albeit limited reports of age-related GABA/$H_20$ reductions particularly in the OCC (Pitchaimuthu et al., 2017, Simmonite et al., 2019). While it remains unclear why

these discrepancies between studies were observed, they might be accountable by methodological differences in the techniques used to measure GABA/$H_20$ concentrations. GABA is particularly difficult to extract from a chemical spectrum due to its relative lower concentration to other metabolites. The processing of GABA concentrations is particularly susceptible to individual differences in voxel placement, for example placing a voxel too close to subarachnoid space or may result in lipid contamination. Whilst this was controlled for as much as possible during GABA acquisition and by post-processing adjustments in the current study, it is possible that due to losses in cortical thickness or atrophy this was a factor particularly in the older group in the assessment of GABA.

### 4.5.2 Microstructural differences between younger and older adults

Consistent with my hypotheses, tractography analyses provided evidence for lower white matter FR and FA and greater MD, RD and L1 in older compared to younger adults. Microstructural differences were observed in all white matter pathways of interest i.e. the optic radiation, the ILF, the SLF and the fornix Overall this pattern of widespread age-related differences in white matter microstructure is consistent with the literature and suggests that all of the studied white matter connections of visual perception and attention networks are detrimentally affected by age. While previous studies into age-related differences in white matter microstructure have primarily focused on DTI measurements and have for instanced reported reduced FA, increased MD and RD for the ILF (Inano et al., 2011), SLF (Lai & Wu, 2014) and the fornix (Metzler-Baddeley et al., 2011; Chen et al., 2015), not many studies have applied advanced diffusion-based metrics from multi-shell imaging.

Here I observed reductions in FR with age in the SLF, optic radiation and the fornix. I also showed greater effect sizes for group comparisons of FR in most of the observed tracts. These findings suggest firstly that FR may be a more sensitive estimate of age-related changes to tract microstructure, as has been indicated by the studies discussed above (Billiet et al., 2015, Toschi et al., 2020). As FR is proposed as an index of axonal density (Santis et al., 2014) as it provides an estimate of restricted vs hindered diffusion, these findings suggest an age-related reduction in axonal density in the fornix, optic radiation and the SLF. This may reflect a selective reduction in myelination in fronto-parietal, low-level visual and striatal tract bundles, supporting the theory that these regions are particularly vulnerable to degeneration in healthy ageing. However, this is caveated as although all DWI measures will reflect myelin structure to some extent, none of the measures employed in the current study are specific to myelin. A myelin specific acquisition was not included due to time constraints in the current study, however these findings suggest that future extensions of this work should consider examining myelin in the SLF, fornix and optic radiations in the context of visual performance in ageing.

### 4.5.3 Relationships between age-related differences in brain metabolites and white matter microstructure

A correlation matrix exploring the relationships between microstructural and metabolic measures showed a greater number of significant relationships between FR and metabolites of interest. Moreover, there was a much greater number of higher effect sizes for FR group differences comparison to standard DTI measures. On this basis, I explored the relationship between measures of FR in all tracts of interest and metabolites. This was explored in all participants to investigate the direction and strength of the relationship between metabolites and microstructure. Results indicated that positive relationships were present between FR measures in all subtracts of the SLF and the ILF, and NAA and Myoinositol in all MRS voxels. Specifically, FR in the SLF 1, SLF 2 and SLF 3 were positively related to NAA in the ACC and. These findings indicate that reduced neural metabolism, as indicated by NAA is associated with reductions in axonal density, as estimated by FR. Further mediation analyses also showed full mediating effects of NAA in ACC in the relationship between age and FR, but not vice versa, suggesting that metabolite changes in age may drive age-related FR changes.

Recent findings have highlighted the relationship between NAA and diffusion tensor outcome measures (Wong et al., 2020), and advanced diffusion outcome measures (Grossman et al., 2015), therefore my results are in line with the previous literature. Whilst a causal relationship cannot be inferred from the current investigation, it has been evidenced that mitochondrial impairment activates the Wallerian pathway, resulting in age-related axonal degeneration (Loreto et al., 2020), suggesting that metabolic changes may drive microstructural changes in age. This was also supported in results from my mediation analyses which showed a significant mediating effect of NAA specifically on the relationship between age and FR in SLF. With regards to the anatomical changes underlying these results, reductions in neuronal and mitochondrial functioning in the anterior cingulate and posterior parietal cortex may lead to degeneration of connective tracts between these regions – the SLF – thus limiting fronto-parietal connectivity in older adults. This indicates communication in this network – responsible for 'top-down' attentional control – may be compromised in age, which may lead to response slowing as will be investigated in the following chapter. A positive relationship was shown between NAA in the OCC and FR in the ILF, which I posit supports the direction of the metabolic-microstructural degenerative process as information processing typically occurs in the primary visual cortex and continues to the ILF. Thus reduced neuronal integrity in the occipital lobe may result in reduced microstructural integrity in the ILF, as described above. However, as metabolic levels were not assessed in the temporal lobe this cannot be definitively determined and requires further supportive evidence. Mediation analyses also did not show any significant effect thus this requires further investigation.

Moreover, FR in the SLF 1 was also positively related to myoinositol levels. As myoinositol is key in the generation of myelin (Glanville et al., 1989) this relationship may reflect patterns of age-related changes in

myelination. Whilst I did not employ methodology to specifically quantify myelin, FR does provide a specific proxy measure of axon density changes (De Santis et al., 2014), allowing for some inference to be drawn from my current results. This also further supports the potential role of metabolic reductions in age-related Wallerian degeneration, which warrants future investigation, however this was not fully supported by mediation analyses.

### 4.5.4 Metabolic, microstructural and morphological differences in DLB patients

GABA/$H_20$ in the OCC and ACC showed variable results with some values lower and some higher than 95% CI in older adults. GABA/$H_20$ in the PPC for DLB patients was higher than 95% CI for all cases. These findings are inconsistent with my hypotheses that GABA/$H_20$ would be reduced in the OCC, however these results suggesting a disproportionately large amount of the inhibitory neurotransmitter was present in the PPC in DLB patients. GABA in the PPC is largely responsible for the efficient inhibition of attentional and higher visual processes, with parietal GABA being correlated with size illusion, but not orientation ability (Song et al., 2017). These findings suggest a new avenue of interest in DLB patients which could potentially be important in DLB. They indicate that levels of inhibitory neurotransmitter which have been linked to the incidence of visual hallucinations are not limited to alterations in the occipital cortex but are also altered in the parietal cortex. This suggests that occipito-parietal attentional mechanisms may play a role in the aetiology of hallucinations in DLB, supporting cognitive theories such as the PAD (Collerton et al., 2005). This warrants further investigation to establish the role of GABA in the top-down processing stream in DLB and its relationship to hallucination incidence.

For two DLB patients, myoinositol in the OCC, ACC and PPC was consistently lower than 95% CI, and NAA in PPC was lower in two DLB cases. As such, patterns of other metabolites remain unclear in DLB patients due to the limited sample, however as myoinositol and NAA are important in glial and neuronal functioning respectively, these findings warrant further investigation.

All patients showed lower FA in the ILF than 95% CI, and for RD and L1 in the fornix, and RD in optic radiation all DLB cases showed higher values than 95% CI, which was consistent with my hypotheses. These results indicate microstructural impairment in tracts relating to object recognition, low level vision and memory processes. Object recognition as a higher-level visual task, is markedly impaired in DLB and previous findings have evidenced microstructural impairments in ILF (Kantarci et al., 2010), therefore this supports well established work. However, no studies investigating DLB have shown microstructural impairments in optic radiations. This is interesting particularly as previous studies have shown relative preservation of very low-level vision (Metzler-Baddeley et al., 2010). I also found relative preservation of visual acuity and orientation ability in DLB patients, therefore this finding is unexpected. However, it is possible that this result is due to generalised white matter infarcts with DLB, or slightly older age of patients. As such, this finding may warrant further clarification from more detailed investigation.

Patients showed relatively preserved cortical thickness, with only higher right medial orbitofrontal cortex thickness and lower precuneus appearing outside the 95% CI in DLB patients. In contrast to findings in DLB patients which have shown reduced cortical thickness in the insula, anterior cingulate, orbitofrontal and later occipital lobes, DLB patients in the current sample did not show marked reductions in cortical thickness (Blanc et al., 2015). One reason for this is potentially disease progression. In order to meet the demands of the study, only patients who showed mild cognitive impairment took part in MRI scanning. As such, these patients are likely to show less cortical thinning than their peers who experiment greater progression. Blanc et al (2015) also showed only thinning in the pars opercularis, insula and right medial orbitofrontal regions in prodromal DLB patients, none of which survived correction for FDR. Therefore, consistent with previous literature, the current results do not show marked cortical thickness differences in earlier stage DLB patients compared to healthy older adults. In contrast, a number of regions showed volumetric reductions in DLB patients, most notably subcortical grey matter, caudate and overall cortex volume which is also consistent in previous findings (Watson et al., 2012).

## 4.4 Part 2: Exploratory analysis

In addition to conducting specific comparisons of microstructure, metabolites and cortical thickness between younger and older adults, I also conducted exploratory analyses comparing the two groups for microstructure and cortical thickness in the whole brain. Older adults shown reliable reductions in white matter microstructure throughout the cortex but particularly in frontal regions (Barrick et al., 2010), and also widespread reductions in cortical thickness, particularly in frontal and medial temporal regions (Frangou et al., 2021). On this basis, I conducted exploratory analyses (1) to establish the context of brain changes in the perceptual and attention networks, i.e. if these differences were specific, or were amongst more widespread age-related decline, and (2) as a 'sanity check' to confirm the results from a priori analyses were replicated in whole brain analysis. It was hypothesised that older adults would show greater microstructural differences and cortical thickness reductions in the frontal lobes, in concordance with the frontal ageing hypothesis (MacPherson & Cox, 2017)

### 4.4.1 Methods

#### 4.4.1.1 Tract based spatial statistics (TBSS)

Following a priori analysis, exploratory whole brain analyses were carried out on cortical thickness, volume and diffusion-weighted data. Tract based spatial statistics (TBSS) was conducted to assess microstructural measurements in the whole brain, and FreeSurfer was used to assess cortical surface and subcortical data.

To assess group comparisons between older and younger groups, voxel wise statistical analysis of CHARMED data was carried out using TBSS (Smith et al., (2006), part of FSL (the Analysis Group at the Oxford Centre for Functional MRI of the Brain [FMRIB] Software Library [FSL]; Smith et al., 2004). First, FA images were created by fitting a tensor model to raw diffusion data using FDT – an FSL function which

applies a probabilistic framework for estimating local probability density functions in a model of diffusion (Behrens et al., 2003) - and then brain-extracted using FSL's Brain Extraction Tool (BET; (Smith, 2002). All subjects' FA data were then aligned to MNI152 standard-space using the nonlinear registration tool FNIRT (FMRIB's Non-Linear Registration Tool; Andersson, 2007), which uses a b-spline representation (a more flexible function to deal with more irregular or complex data) of the registration warp field (Ruekert, 2000). Next, the mean FA image was created and thinned, by using a default threshold of FA <0.2, to create the mean FA skeleton which represents the centres of all tracts common to the group. Each subject's aligned FA data were then projected onto this skeleton and the resulting data were fed into voxel-wise cross-subject statistics using randomise – FSL's tool for nonparametric permutation inference (Winkler et al., 2014). Threshold-free cluster enhancement (TFCE) was used to identify significant clusters thresholded at .95 to give clusters significant at $p<0.05$ level. TBSS allowed an inference into white matter microstructure within the whole brain and was conducted as a secondary analysis following the a priori tractography analysis to explore the anatomical specificity of the age-related differences in the ROI analyses. Figures 4.23 – 4.27 display the results of the TBSS analyses.

#### 4.4.1.2 Whole brain cortical thickness and volume analyses

Cortical thickness and volume were assessed using FreeSurfer, as previously described. For exploring whole-brain group differences in cortical thickness, FreeSurfer's interactive statistical analysis tool 'Qdec' was employed. Qdec stands for Query, Design, Estimate and Contrast, and performs statistical inference on cortical surface data produced by FreesSurfer, based on the general linear model (GLM). Pre-processed cortical thickness data (as previously described) were entered into Qdec, along with a design matrix containing details of group membership for each subject. All cortical thickness data were fit to the GLM, with group as the discrete independent variable. Finally, multiple comparisons were corrected by running Monte Carlo cluster-wise simulations to determine significant clusters at a threshold of 5%.

### 4.4.2 Results

#### 4.4.2.1 Restricted Fraction (FR)

Restricted fraction (FR) was greater in younger control participants than older control participants in the left and right optic tract (Fig 4.23, 2i), right ILF and the inferior cerebellar regions (Fig 4.23, 2ii), and medial temporal, and corticospinal tracts (Fig 4.23, 2iii).

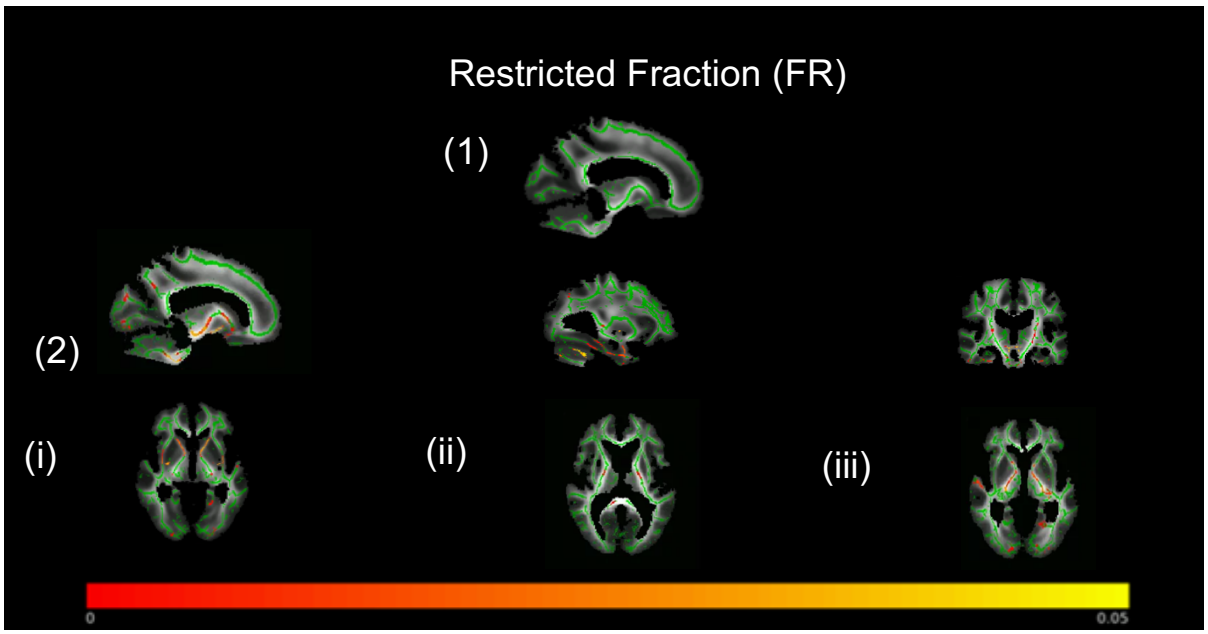


Figure 4.23 Whole brain tract based spatial statistics (TBSS) in younger and older adults. Restricted fraction (FR) group comparisons – tracts highlighted in red indicates regions where p-values where FR is significantly greater in younger controls (YCO) than older controls (OCO). (1) Mean FR skeleton (2) [i] Higher FR (red) in younger adults in the left and right optic tracts [ii] higher FR in the anterior temporal region and ILF [iii] higher FR in medial and inferior temporal region.

### 4.4.2.2 Diffusion tensor indices

#### 4.4.2.2.1 Fractional Anisotropy

Results of TBSS using FA maps indicated that the younger control group had greater FA in the left ILF (Fig 4.24, 2i) and anterior fornix regions (Fig 4.24, 2ii). In addition, greater FA in younger adults was observed in the right optic tract (Fig 4.24, 2iii).

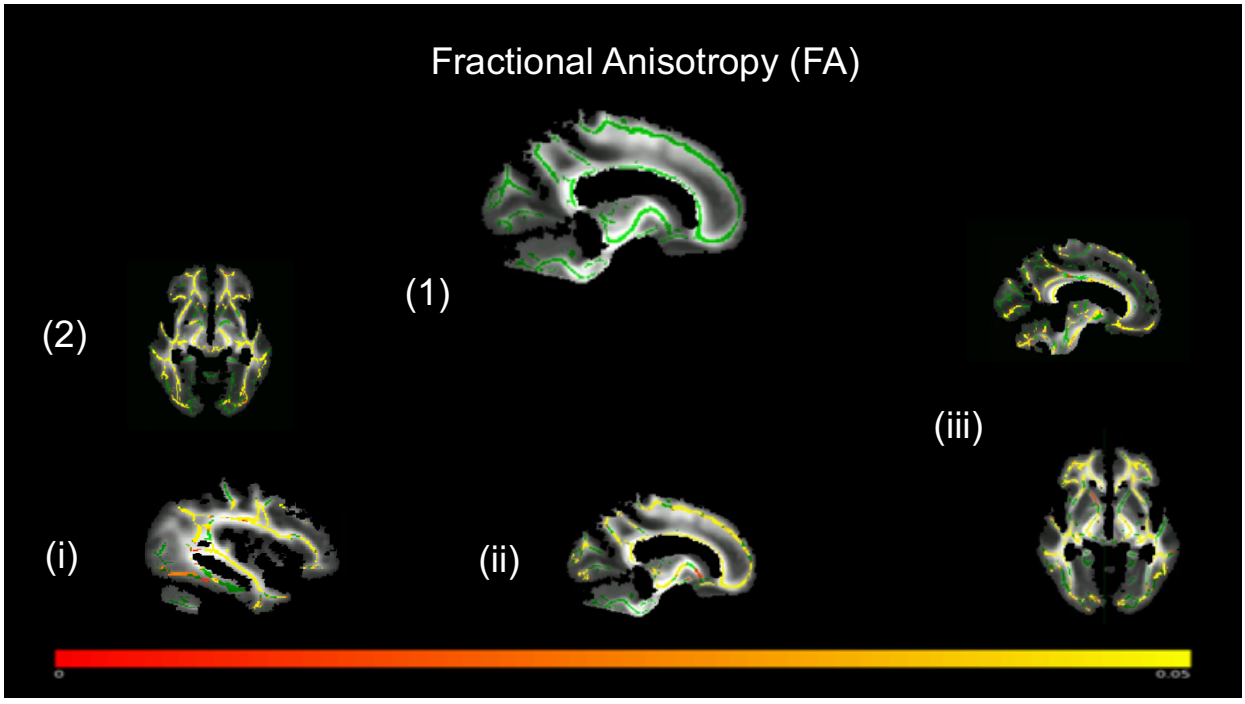


Figure 4.24 Whole brain tract based spatial statistics (TBSS) in younger and older adults. Fractional anisotropy (FA) group comparisons – tracts highlighted in red indicates regions where p-values where FA is significantly greater in younger controls (YCO) than older controls (OCO). (1) Mean FA skeleton (2) [i] Higher FA in younger adults in the ILF (red) and temporal region. [ii]. Higher FA in younger adults in the anterior fornix. [iii] Higher FA in younger adults in the right optic tract and left temporal region. Red indicate TFCE correct p-values at significance level of 5%

#### 4.4.2.2.2 Mean Diffusivity (MD)

Mean diffusivity was greater in older control participants than younger control participants in the left and right optic tracts (Fig 4.25, 2i), the medial temporal region (Figure 4.18, 2ii), the central sulcus and left temporal lobe (Figure 4.25, 2iii) the left visual cortex, left posterior parietal region and anterior commissure (Figure 4.25, 2iv).

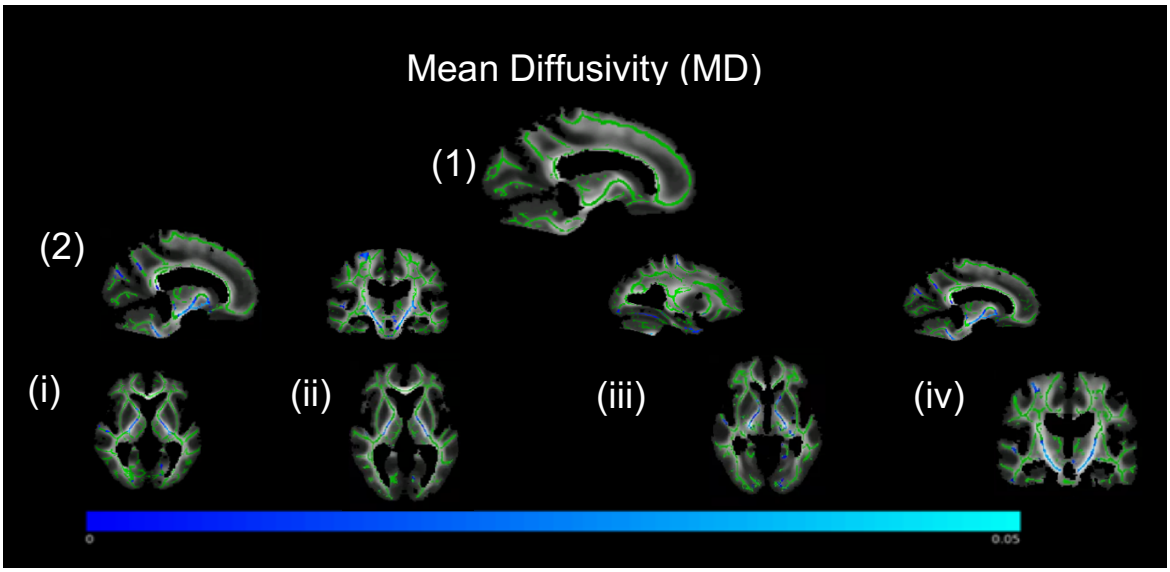


Figure 4.25 Whole brain tract based spatial statistics (TBSS) in younger and older adults. Mean Diffusivity (MD) group comparisons – tracts highlighted in blue indicates regions where p-values where MD is significantly greater in older controls (OCO) than younger controls (YCO). (1) Mean diffusivity skeleton (2) [i] Higher MD in older adults (blue) in optic tracts, [ii] higher MD in older adults in central sulcus, medial temporal and corticospinal [iii] left temporal and central sulcus [iv] higher MD in OCC and PPC

#### 4.4.2.2.3 Radial Diffusivity (RD)

Results indicate that radial diffusivity is greater in the older control group in the internal capsule participants (Fig 4.26, i and iii) and the cerebellum (Figure 4.26, ii). No differences were present in which younger control groups had higher radial diffusivity than older control groups.

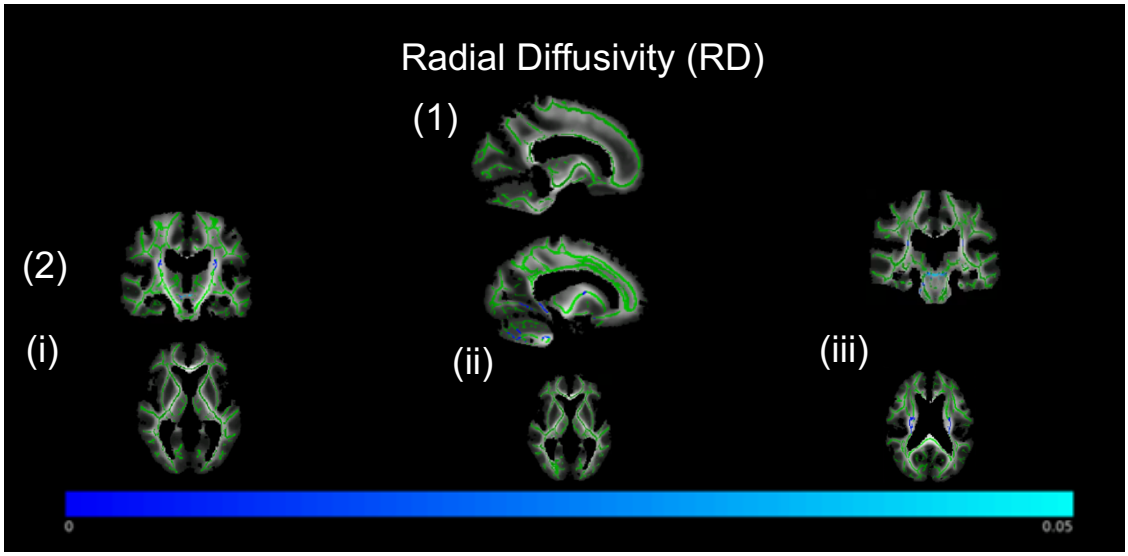


Figure 4.26 Whole brain tract based spatial statistics (TBSS) in younger and older adults. Radial Diffusivity (RD) group comparisons – tracts highlighted in blue indicates regions where p-values where RD is significantly greater in older controls (OCO) than younger controls (YCO). (1) Mean radial diffusivity skeleton (2) [I, iii] Higher RD in older adults (blue) in the internal capsule, [ii] higher RD in the older adults in the cerebellum.

#### 4.4.2.2.4 Axial Diffusivity (L1)

Results from TBSS indicated greater axial diffusivity in older adults in the insular cortex (bilateral), medial temporal cortex (bilateral), anterior thalamus and cingulate gyrus in comparison to younger control participants (Figure 4.27).

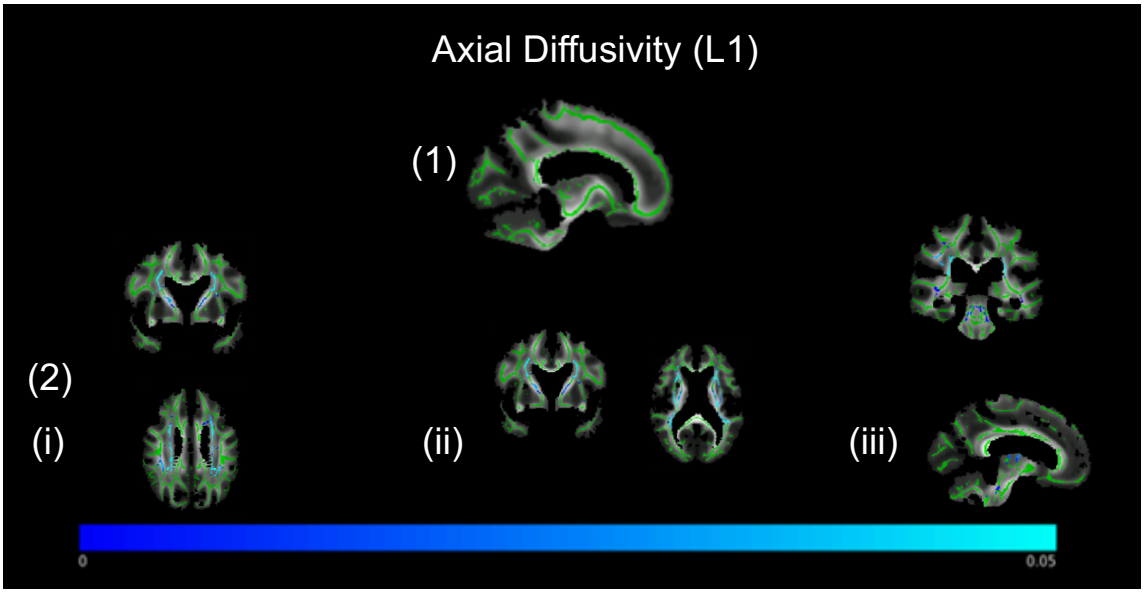


Figure 4.27 Whole brain tract based spatial statistics (TBSS) in younger and older adults. Axial Diffusivity (L1) group comparisons – tracts highlighted in blue indicates regions where p-values where L1 is significantly greater in older controls (OCO) than younger controls (YCO). (1) Mean L1 skeleton (2) [i, ii] Higher L1 in older adults in the internal capsule, extending to the caudate nucleus [iii] higher MD in older adults in the internal capsule, arcuate fibres and anterior cerebellum.

#### 4.4.2.2.5 Cortical thickness

Qdec analyses showed significant widespread differences in cortical thickness in a number of regions. Cortical thickness was reduced in older adults in all listed regions (Table 4.5) including the lateral occipital, superior temporal and parietal gyri and lingual gyrus which showed reductions in both hemispheres (Figure 4.28, 4.29).

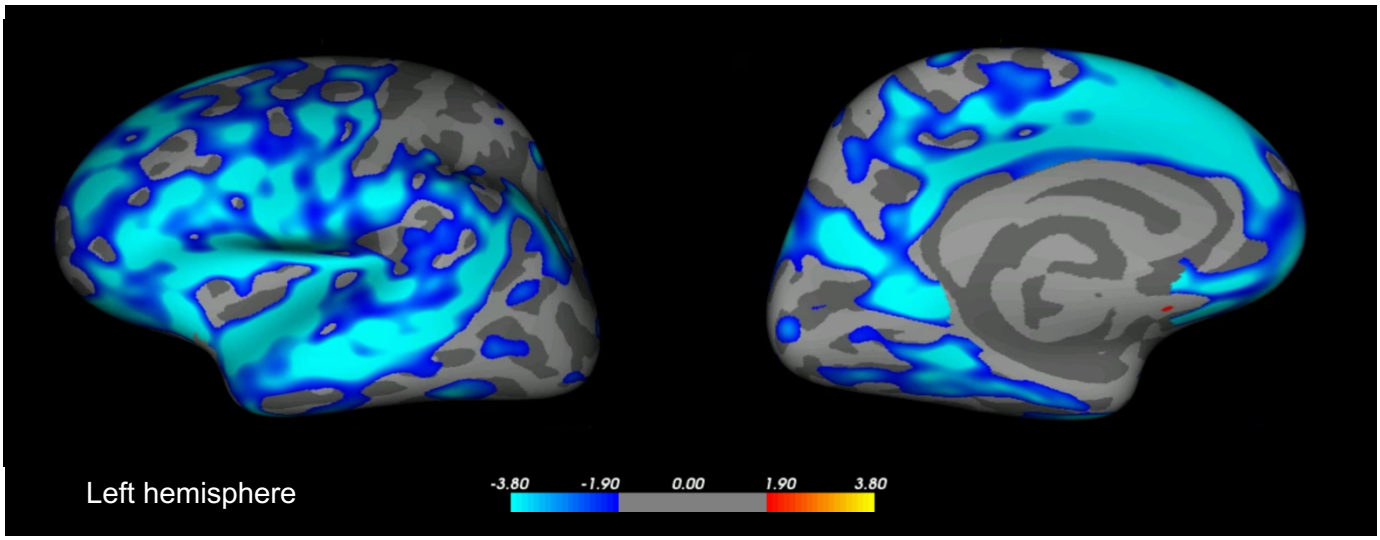


Figure 4.28 Left hemisphere cortical thickness comparisons between younger and older adults using Qdec. Lighter blue highlighted areas show regions where group comparisons indicate older adults have reduced cortical thickness ($p<.001$). Results show widespread reductions in cortical thickness largely in left temporal, frontal and superior parietal regions in older adults. Threshold correction to $p=.001$.

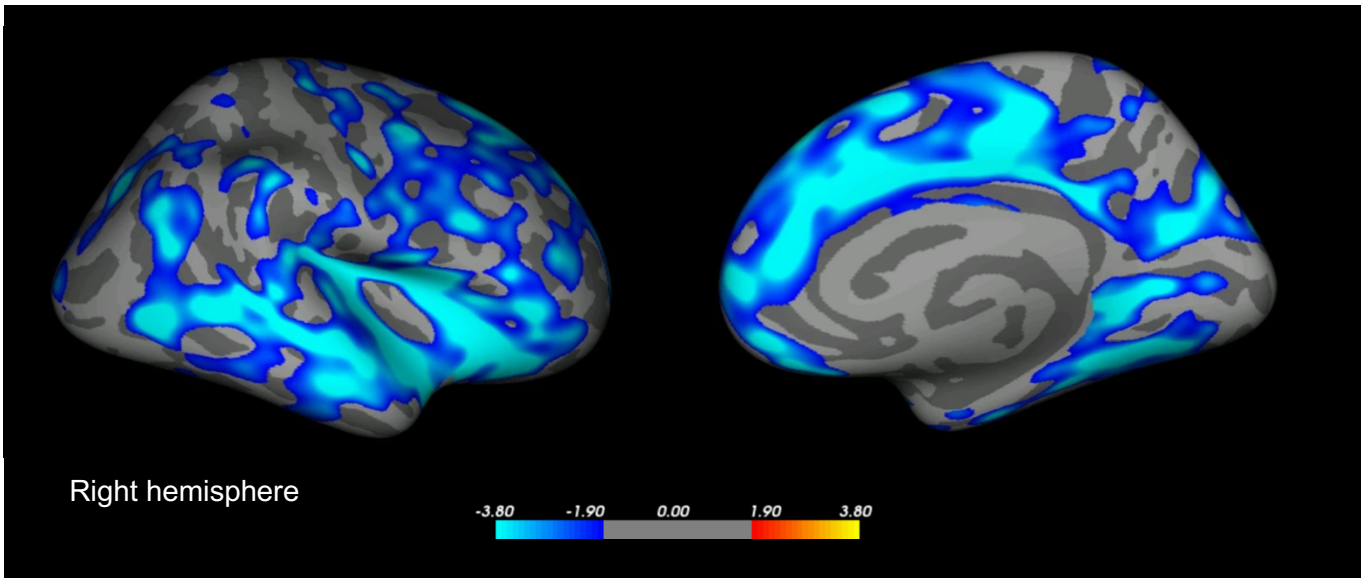


Figure 4.29 Right hemisphere cortical thickness comparisons between younger and older adults using Qdec. Lighter blue highlighted areas show regions where group comparisons indicate older adults have reduced cortical thickness ($p<.001$). Results show widespread reductions in cortical thickness largely in right temporal, and frontal regions in older adults. Threshold correction to $p=.001$.

Table 4.5 Clusters which show significant reductions in cortical thickness in older adults from Qdec cortical thickness group comparisons

| | *Left* | | | *Right* | |
|---|---|---|---|---|---|
| | **Sig (-log(10))** | **P Value** | | **Sig (-log(10))** | **P Value** |
| *Superior temporal* | -10.03 | *<.001* | *Superior temporal* | -9.23 | <.001 |
| *Lingual* | -6.97 | *<.001* | *Lingual* | -5.74 | <.001 |
| *Inferior parietal* | -4.69 | *<.001* | *Supramarginal* | -4.10 | <.001 |
| *Superior parietal* | -4.26 | *<.001* | *Superior parietal* | -5.88 | <.001 |
| *Inferior temporal* | -3.88 | *<.001* | *Precentral* | -4.04 | <.001 |
| *Paracentral* | -3.59 | *<.001* | *Posterior cingulate* | -2.52 | <.001 |
| *Pericalcarine* | -2.83 | *0.001* | *Precuneus* | -2.76 | <.001 |
| *Middle temporal* | -2.48 | *0.003* | *Entorhinal* | -2.40 | <.001 |
| *Lateral occipital* | -2.11 | *0.007* | *Lateral occipital* | -3.06 | <.001 |
| *Temporal pole* | -1.99 | *0.010* | *Fusiform* | -2.16 | 0.006 |
| *Medial orbitofrontal* | -1.76 | *0.017* | | | |

#### 4.4.2.3 Grey matter volume

The omnibus result was significant for group, $F(34,18)=7.095$, $p=<.001$; Wilk's $\Lambda = 0.069$, partial $\eta^2=.931$. Univariate F tests showed there was a significantly lower grey matter volume in older adults compared to younger adults in all regions in both left and right hemispheres, with full results reported in Table 4.6 (Figure 4.30, 4.31).

Table 4.6 Full MANOVA results for group comparisons of grey matter volume in left and right hemisphere. WM= white matter, GM=grey matter

| | *Left* | | | *Right* | | |
|---|---|---|---|---|---|---|
| | **F value** | **Significance (corrected)** | **Partial $\eta^2$** | **F value** | **Significance (corrected)** | **Partial $\eta^2$** |
| *Accumbens* | 14.94 | <.001** | .227 | 15.822 | <.001* | .237 |
| *Amygdala* | 11.99 | .001* | .190 | 6.420 | .014* | .112 |
| *Caudate* | 8.931 | .004* | .149 | 6.09 | .017* | .107 |
| *Cerebellum* | 21.18 | <.001** | .293 | 14.70 | <.001** | .224 |
| *Choroid plexus* | 28.70 | <.001** | .360 | 26.65 | <.001** | .343 |
| *Hippocampus* | 12.30 | .001* | .194 | 9.39 | .003* | .156 |
| *Lateral ventricle* | 34.21 | <.001** | .401 | 38.889 | <.001** | .433 |
| *Putamen* | 13.65 | .001* | .211 | 7.96 | .007* | .135 |
| *Thalamus* | 25.1 | <.001** | .329 | 20.76 | <.001** | .289 |
| *WM hypointensities* | 9.72 | .003* | .160 | | | |
| *Subcortical GM* | 16.37 | <.001** | .243 | | | |
| *Total GM* | 19.13 | <.001** | .273 | | | |

Grey matter volume (left) in younger vs older adults

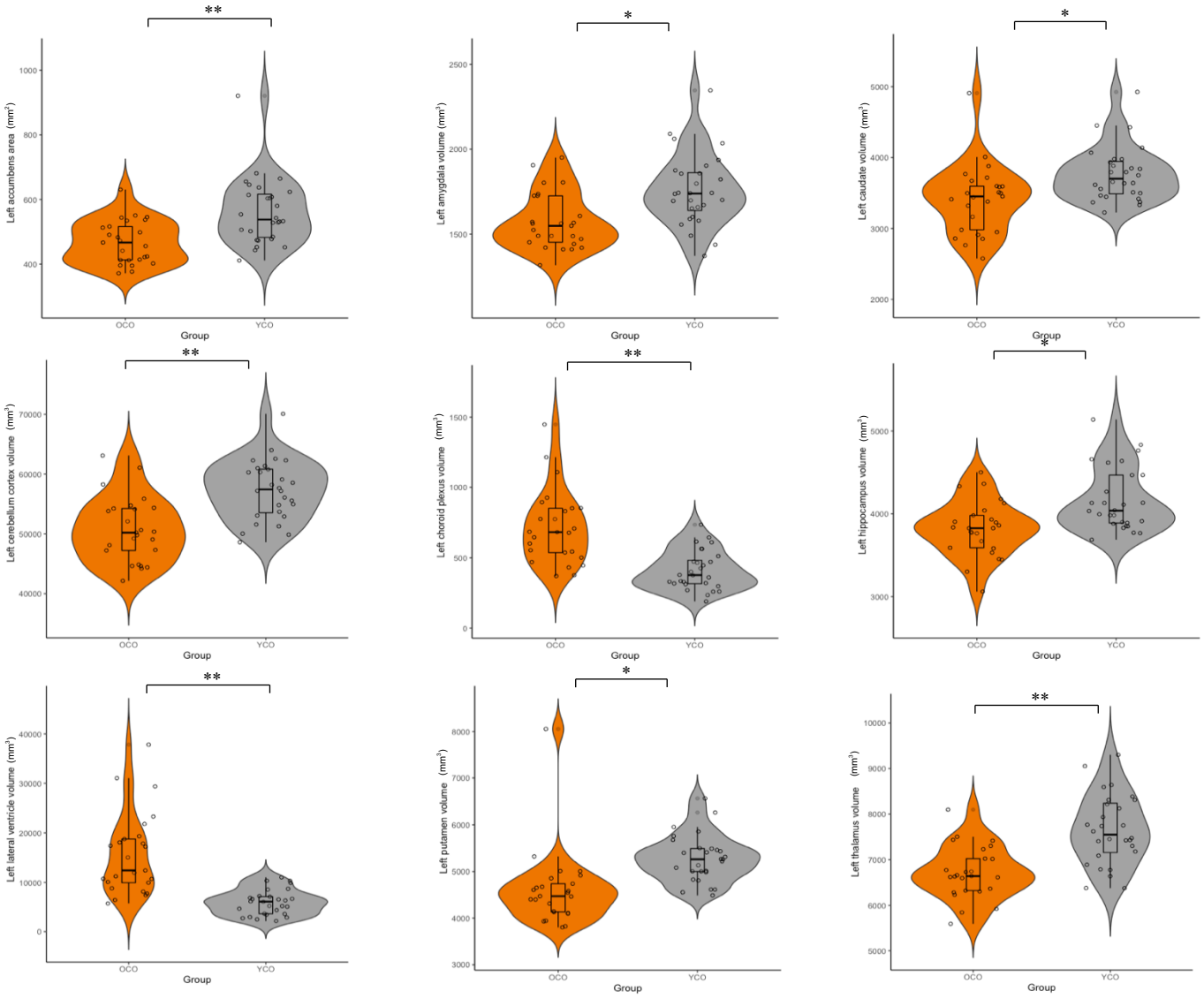


Figure 4.30 Left hemisphere grey matter volume group differences between younger and older adults. MANOVA results indicate that grey matter volume was significantly lower in older adults in the accumbens, amygdala, caudate, cerebellum, choroid plexus, hippocampus, lateral ventricle, putamen and thalamus in comparison to younger adults OCO = older adults, YCO = younger adults **p<.001, *p<.0.05

Grey matter volume (right) in younger vs older adults

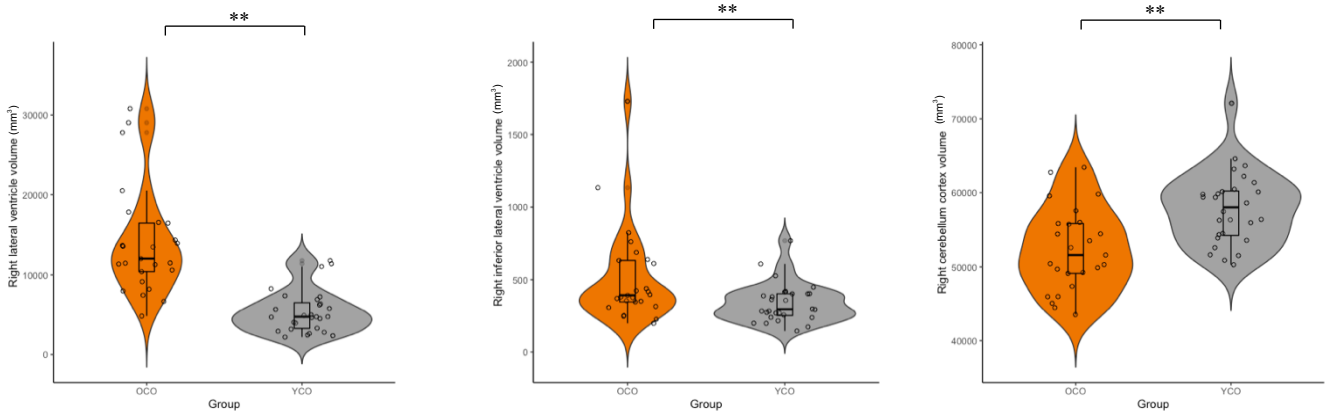

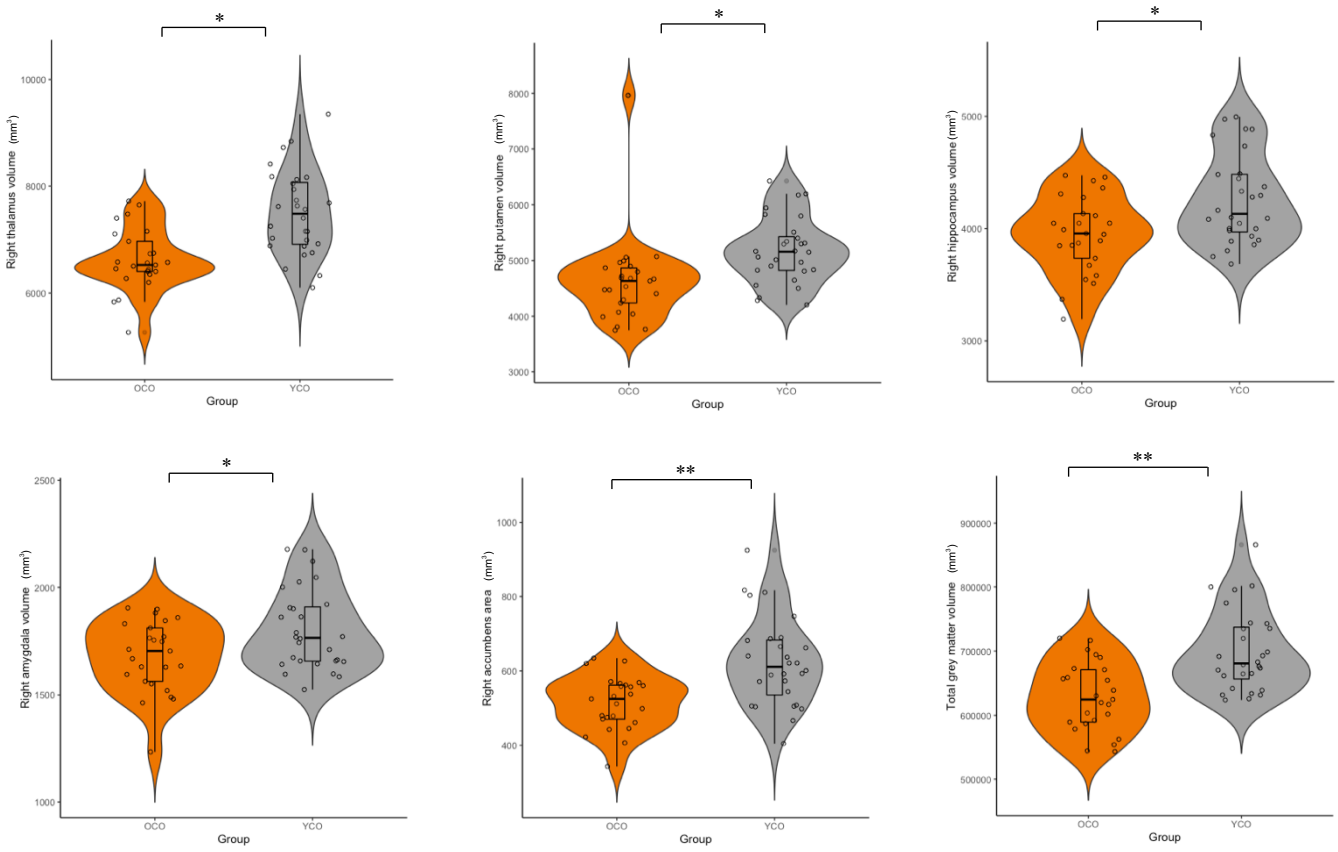


Figure 4.31 Left hemisphere grey matter volume group differences between younger and older adults. MANOVA results suggest that grey matter volume was significantly lower in older adults in lateral and inferior lateral ventricles, cerebellum, thalamus, putamen, hippocampus, amygdala, accumbens and total grey matter. OCO = older adults, YCO = younger adults **p<.001, *p<.0.05

## 4.5 Part 2 Discussion

In Part 2, I assessed whole-brain differences in white matter microstructure and cortical thickness in younger and older adults. It was anticipated that older adults would show more widespread reductions in these measures, and that reductions in cortical thickness and microstructure would be more pronounced in frontal regions. My results supported these hypotheses but also highlighted greater white matter microstructure differences in older adults in posterior regions, and reductions in cortical thickness in subcortical regions, as discussed below.

### 4.5.1 TBSS comparisons

The exploratory TBSS whole brain analysis showed age-related reductions in FA in the ILF, fornix and optic radiation, higher MD in the optic tracts, corticospinal region and occipito-parietal lobe, higher RD in the cerebellum and higher L1 in the internal capsule, arcuate and cerebellum. These findings primarily indicate a reduction in microstructural integrity in standard DTI measures in the fornix, lower-level optic regions, corticospinal and medial temporal regions in older adults which is consistent with previous findings (Kochunov et al., 2012, Jang et al., 2011, Sala et al., 2012). For FR, greater loss of microstructural integrity with age in visual regions including the optic tract and visual association fibres was shown. This evidence

contrasts the typically reported vulnerability of anterior white matter in older adults (Head et al., 2004), highlighting the importance of examining microstructural changes in visual regions in normal ageing. Moreover, taken together, these findings may contrast the typical age-related anterior-posterior gradient of impairment and suggest that white matter integrity in the elements of these tracts connecting to the visual cortex may show age-related decline. This is important, as the anterior-poster gradient is also thought to underlie a primary frontal executive function impairment in ageing. As results from Chapter 3 indicated that executive functioning in these older adults where relatively intact, and frontal white matter also appears to be less affected with age in this sample, these results may provide evidence against these hypotheses. Furthermore, these findings are notable, as FR was shown to have greater effect sizes than standard DTI measures and may then be a more sensitive estimate of age-related microstructural changes. As such, the TBSS findings may reflect age-related changes in microstructure in the visual system that are otherwise not captured by standard DTI, which has important considerations for future studies estimating microstructural changes in the brain with age.

### 4.5.2 Grey matter volume and cortical thickness differences

Cortical thickness and grey matter volume group comparisons showed lower thickness in older adults in all regions selected for a priori analysis, excluding the optic chiasm which showed no significant group difference in volume. Regions which showed reduced cortical thickness in older adults included the banks of the superior temporal sulcus, inferior and superior temporal cortex, anterior cingulate cortex, inferior and superior parietal cortex, superior and middle frontal cortex, and the cuneus and lateral occipital cortex. These findings are generally consistent with previous findings which report age-related cortical thinning particularly in the temporal, parietal and visual cortices (Fjell et al., 2010). The current results highlight the relevance of investigating age-related changes in both cortical thickness in combination with other modalities in the perceptual and attentional network. However, these cortical thickness results also act as validation for the metabolic and microstructural analyses. Replicating previous widely reported findings in the ageing literature allows for greater reassurance that results from other modalities may provide an insight into the typical brain changes observed in older age.

Whole brain cortical thickness analyses with Qdec showed age-related reductions in parietal, temporal and occipital regions with significant clusters largely overlapping those regions shown to be significant in perceptual and attentional regions. These results both supports the findings reported from a priori tractography and cortical thickness analyses, indicating that these regions show reliable age-related microstructural alterations with ageing. In addition, as results from exploratory and a priori analyses largely align, and microstructural and cortical thickness changes are not apparent throughout the whole brain, a priori results may indicate specific age-related brain changes rather than being elements in more widespread decline. Despite this, grey matter volume loss in older adults was relatively widespread, in subcortical regions such as the bilateral accumbens and amygdala, thalamus and caudate, and structures such as the

hippocampus and bilateral cerebellum. Moreover, increased volume in the lateral ventricles was also present in older adults in comparison to younger adults. These findings are consistent with previous literature (Thambisetty et al., 2010) and again provide validation for the reliability of a priori results.

### 4.5.3 Overall limitations

There are some limitations with regards to the MR methodology employed in this chapter that should be considered. Firstly, MRS can be subject to several methodological problems. One limitation may be the manual placement of voxels. This was done according to anatomical landmarks and was conducted by the same researcher for each subject; however, these voxels may capture other brain structures such as ventricles because of individual anatomical variation. In addition, MRS metabolites may be subject to menstrual variation in females or caffeine levels, which were not controlled for due to the extensive length of the testing and scanning sessions, limited access to participants who otherwise met inclusion criteria, and largely older adult sample, but may influence results in the younger adult group.

Furthermore, advanced diffusion imaging was used, which accounted for some of the typically issues accounted for in traditional diffusion tensor imaging as described in Chapter 2. However, it should be noted that whilst the diffusion model provided more sensitive estimates of microstructural integrity, it did not account for more advanced estimates of myelin, for example macromolecular proton fraction which provides an index of white matter neuroglia, that can be obtained from methods such as quantitative magnetisation transfer (qMT) imaging (Smith et al. 2009, Sled, 2018). CHARMED was selected in this thesis due to its ease of fitting to multi-shell data, superior estimation of microstructural measurements in comparison to standard diffusion tensor imaging, and my interest in acquiring FR measurements and limiting the number of overall indices from brain measures. However, adopting methods such as qMT to quantify myelin in subsequent research may be of interest with regards to exploring relationships with metabolites, which may provide greater insight into the mechanism of age-related decline across brain networks involved in visual perception and attention.

### 4.5.4 Overall chapter summary

In summary, the older adult cohort appeared to show differences generally consistent with previous literature and hypotheses, supporting the reliability of the sample for further analyses with cognitive data. Age-related reductions in frontal and parietal NAA and Glx were present, in addition to reductions in FR and FA, and increases in MD, RD and L1 in the SLF, ILF, optic radiation and fornix. NAA and myoinositol in ACC and PPC were also positively correlated with FR in the SLF. Age-related differences in GABA/$H_20$ were not present in contrast to my hypothesis. Reductions in cortical thickness in older adults were present in all regions within the networks of interest. These results were also supported by findings from the exploratory analyses, which showed age-related cortical thickness and microstructural integrity reductions in the posterior and temporal regions. These results are of interest primarily as they provide further clarity

to the limited literature examining metabolic differences in the brain in healthy ageing. These results also provide novel insight into the relationships between metabolites and sensitive estimates of white-matter microstructure, and how this may translate to changes observed in the healthy ageing brain. Secondly, my results suggest that age-related differences in metabolites related to mitochondrial function may be more pronounced in the anterior regions, but that microstructural and cortical thickness changes are not limited to frontal areas of the brain as typically reported. Instead, this thesis provides evidence which may go against the typical frontal ageing or anterior vulnerability hypothesis for all brain measurements in older age. It is then pertinent to examine the brain changes which corresponding to changes in perception and attention, which will be examined in the following chapter.

In DLB patients, my results demonstrate novel findings including a decrease in estimates of white matter microstructural integrity in the optic radiation, and a consistent increase in GABA/$H_20$ in the PPC in comparison to healthy older adults. I posit that these findings highlight new lines of enquiry in a larger sample of DLB patients, as they may provide further clarity and insight into the brain mechanisms underlying perceptual decline in DLB patients.

# Chapter 5 : Neural differences underlying visual perceptual and attentional changes in older adults

## 5.1 Introduction

Having characterised age-related differences in visual perception and attention as well as in brain microstructural and neurochemistry in the previous two chapters, the objective of Chapter 5 was to find out which brain differences would predict performance differences with ageing. More specifically, I sought to determine which brain measurements would predict age-related performance in visual perception and attention tasks where age-related impairments were shown, as well as metrics that were predictive of age-related strategy shift or cognitive maintenance. Previous research has indicated that there are relationships between some of the brain measures assessed in this study and perceptual and attentional performance. However, no study has provided a detailed and systematic characterisation of age-related differences across the hierarchy of visual perception and attention functions. This is important, as a detailed characterisation of age-related differences in perceptual and attentional performance and their neural correlates may allow a greater understanding of changes that occur with healthy ageing, and pathological ageing. To the best of my knowledge, no study has linked performance differences across the visual hierarchy to age-related differences in both metabolic and microstructural metrics in perception and attention networks using both advanced diffusion and spectroscopy MR methods. This is also important, as a more in depth and advanced understanding of neural substrates underlying cognitive changes may provide new lines of enquiry for ageing research and guide the focus of the cognitive neuroscience of ageing, where this may otherwise have been overlooked.

### 5.1.1 Metabolites and microstructure underlying perceptual functions in older adults

In lower-level vision, visual orientation changes have been reported in adults in relation to occipital GABA, with lower GABA resulting in poorer performance (Edden et al., 2009; Pitchaimuthu et al., 2017). Occipital GABA reductions have also been associated with reduced fluid processing in older adults, including measures of visual perception such as contour detection and dot speed discrimination (Simmonite et al., 2019). In addition, white matter microstructural alterations particularly in posterior regions have been shown to underlie changes in visual perceptual function (Madden et al., 2009). For instance, associations between age-related reductions in FA and perceptual performance have been demonstrated (Toepper, 2017) particularly in the optic radiation, which has been reported to mediate sensory function in aged macaques (Gray et al., 2020). Moreover, reduced T2 intensities in the occipital lobe in older adults which are associated with age-related impairments in lower-level visual function have also been shown, in addition to reduced white matter integrity in the occipital central field (Beer et al., 2020).

In mid-level vision, interindividual variability in motion perception was reported to be related to Glx concentration in the prefrontal cortex on MR spectroscopy in healthy younger adults (Takeuchi et al., 2017)

and Glx signal in the V5/MT (Schallmo et al., 2019). However, no evidence exists to support this within the context of ageing despite a reliable decline in motion perception in older adults. Moreover, no studies quantify the underlying neurochemical markers of contour perception at present. Further, investigation of the neural substrates of contour integration have typically used a functional MRI or EEG approach, reporting that activity in the lateral occipital, parietal and primary visual areas underlie contour processing (Mijović, 2014; Volberg & Greenlee, 2014). However, to the best of my knowledge no study has specifically attempted to link contour integration or motion coherence performance with microstructural changes in ageing. Long range connectivity between cells of similar spatial and orientation tuning in the early visual cortex is required for effective contour integration (Hess et al., 2003). Considering this and evidence suggesting that neural populations in the lateral occipital cortex represent contour (Kourtzi & Kanwisher, 2001), it seems possible that age-related differences in lateral occipital white matter micro- and macrostructure would be related to differences in contour integration function. Moreover, recent post-mortem investigations have outlined the ILF and optic radiations amongst other white matter tracts as key in the complex connectivity of the lateral occipital lobe (Palejwala et al., 2020). The authors also speculated that the microstructural integrity of these tracts may likely to be related to motion perception and object recognition.

With regards to higher-level vision, concentrations of visual cortical GABA have been reported to predict visual intelligence and perceptual surround suppression with higher cortical GABA resulting in more successful performance in these tasks (Cook et al., 2016). Dorsal stream visual performance is also related to metabolic concentrations, with evidence showing that visuospatial performance correlated negatively with total choline and creatine in the ACC (Lind et al., 2020). In the ventral visual stream, age-related reductions in GABA were also related to less distinct fMRI activation patterns for faces and objects which was also mediated by age (Chamberlain et al., 2019). The authors proposed that age-related reductions of GABA may contribute to age-related reductions in neural distinctiveness. With regards to attention performance, posterior parietal GABA has been linked to perceptual task switching and integrated control ability (Kondo et al., 2018). Moreover, GABA in the frontal eye fields is relevant for resolving visual distractions (Sumner et al., 2010), and GABA in the dorsolateral prefrontal cortex predicts impulsivity (Boy et al., 2011). Lower GABA in the ACC in particular has been related to greater impulsivity and poorer response inhibition (Silveri et al., 2013), suggesting it plays a key role in visual-related executive and attention functions. More specifically a reduction in ACC GABA was reported to mediate the relationship between age and a decline in performance on a test of executive functioning requiring set shifting (Marenco et al., 2018). However, it should be noted that very few studies observe the role of other metabolites in higher-level vision both in younger and older samples, therefore it is unclear what the pattern of age-related differences in metabolites that underlie these functions may be.

In contrast, it has been well established that white matter tract integrity in the ILF is important in effective ventral stream object processing (Herbet et al., 2018), and SLF function has been related to set shifting and inhibitory control (Urger et al., 2015), spatial neglect (Shinoura et al., 2009). Significant relationships between poorer executive function and impaired white matter microstructure of the left anterior thalamic radiation and right uncinate have been reported in older adults (MacPherson et al., 2017). In addition, microstructural changes in the fronto-parietal tracts have been reported in relation to RT performance, underlying increased SAT (Kerchner et al., 2012) and visuospatial attention in healthy ageing (Monge et al., 2017).

Taken together, this evidence suggests that low-level vision in older adults is related to GABA in the OCC and white matter microstructure in the occipital lobe and optic radiations. Mid-level vision in older adults is related to Glx in the frontal lobe and V5, but findings are very limited therefore the metabolic and microstructural underpinnings of age-related mid-level visual performance is unclear. Finally, higher-level vision is seen to be related to choline in the frontal lobe, GABA in the temporal and parietal lobes and microstructural integrity in the ILF and SLF in older adults. Moreover, microstructure in the SLF appears to be related to RT and SAT performance in older adults. However, again these investigations are limited and have not examined the role of other metabolites such as NAA or myoinositol, or advanced microstructural estimates in higher-level vision and attention in ageing. This chapter therefore aims to address these gaps by assessing the relationship between age-related performance differences in visual and attentional tasks as characterised in Chapter 3 and those metabolic, microstructural and morphological brain measurements of visual perception and attention networks characterised in Chapter 4. Such an investigation may help clarify our understanding of which neural mechanisms may contribute to age-related impairments and maintenance of visual perception and attention functions.

Moreover, in Chapter 3, I found that older adults displayed a decline in performance in some visual tasks (visual contrast, visual orientation, motion threshold) and lengthened SAT for all higher visual tasks and contour integration. But not all tasks showed age-related impairments in performance. On this basis, I approached the analysis in this chapter accordingly, to determine which brain measurements predicted performance at different levels of the hierarchy but also to compare if these predictors differed depending on age-related cognitive performance. This was done by observing the results of group comparisons in Chapter 3, and categorising tasks based on whether older adults showed 'impaired', 'unimpaired' or a 'shift' in their cognitive outcomes. For 'unimpaired' tasks, group comparisons showed no significant differences in cognitive outcomes, indicating that older adults' performance was comparable to that of younger adults either through maintenance or compensatory mechanisms. For 'impaired' tasks, group comparisons showed that older adults had poorer performance in these cognitive outcomes, with no indication of compensation in other outcome measures of the task (i.e. speed vs accuracy). Finally, tasks which showed a 'shift' included all SAT outcomes for mid to higher level tasks. These tasks were labelled 'shift', as older

adults showed lengthened RT in order to mitigate accuracy, which was unimpaired, indicating a 'shift' in strategy. This 'shift' did not necessarily mean older adults had impaired performance but adopted a more cautious strategy in their response. In these tasks only SAT was assessed as a dependent variable, as opposed to accuracy and RT. This was done as older adults clearly showed a lengthening in SAT in comparison to younger adults, which represented longer RTs in order to maintain accuracy. Using SAT therefore provides a composite measure of this 'shift' in cognitive strategy as opposed to accuracy and RT individually which would be less informative. This was with the exception of Motion SAT, which was excluded in the current chapter due to methodological constraints of the task which forced all participants to answer quickly. As it is evident that older adults benefit in terms of maintained accuracy from longer response times, it was concluded that Motion SAT may not reliably represent the observed shift effect recorded in all other tasks. Moreover, due to my results in Chapter 4 highlighting novel relationships between microstructure and metabolite, I focused on these modalities only in the current chapter. This was done both due to limited previous research examining the relationship between cognition and microstructure/metabolites, but also with a view to reducing predictors in regression to ensure robustness of statistical procedures.

### 5.1.2 Hypotheses

- Hypotheses regarding neural predictors of 'impaired' outcomes (visual contrast, orientation and motion threshold)

Given that cognitive performance showed age-related decline, it was hypothesised that I would see relationships between different predictors of the same cognitive function in older and younger groups. I anticipated that occipital metabolites and optic radiation microstructure, in addition to SLF and ILF would predict these outcomes, and that the direction of the relationship would be opposite between groups.

- Hypotheses regarding neural predictors of 'unimpaired' outcomes (visual acuity, contour threshold, ANT network effects)

It was hypothesised that predictors mediating each cognitive function would be the same in both younger and older adults or highlight potential effective compensatory neural mechanisms in older adults. Specifically, I anticipated microstructural parameters in the ILF may underlie contour integration, as the ILF was relatively spared in ageing in Chapter 4. In addition, I hypothesised that ANT network effects would show predictors consistent with those shown in previous research (Fan et al., 2010) (alerting effect predicted by occipito-parietal microstructure and metabolites, orienting effect predicted by temporo-parietal microstructure and metabolites, and executive effect predicted by frontal and temporal microstructure and metabolites).

- Hypotheses regarding neural predictors of 'shift' outcomes (Embedded figures SAT, Change blindness SAT, Contour SAT, Rotation SAT)

It was hypothesised that this 'shift' in cognitive strategy in older adults may be correlated with more frontal and parietal predictors in older rather than younger participants, as older adults adopt a more cautious top-down strategy of processing. As such, it was anticipated that younger adults may show predictors which were related to lower-level vision, such as the optic radiations and occipital cortex, but that older adults may show greater reliance on fronto-parietal regions and tracts for the same cognitive outcome.

To identify significant brain predictors, I used linear stepwise regression analyses for the young and old groups separately using brain measurements as independent predictors and performance measurements as dependent variables. Given the number of brain measurements for the different ROIs and the challenges associated with overfitting of the regression models, these analyses were first conducted for each brain modality, i.e. microstructural and metabolites, separately. The correlation coefficients between each significant predictor and performance measure were then standardized and compared between the two age groups to determine whether ageing was associated with a shift in the contribution of brain areas and measurements to performance. In the case of a significant z-test, correlations were conducted for brain measurement predictors and dependent variable in both age groups separately to determine the directionality of relationship. In addition, partial correlations between significant brain predictors and performance measures were conducted for older adults to account for the potential effects of generalised age-related brain atrophy by controlling for total grey matter volume.

## 5.2 Methods

### 5.2.1 Participants

Data analysed in the current chapter is identical to the data reported in Chapters 3 and 4 and involved the same participants in younger (n=28) and older (n=26) groups. Demographic information is reported in Chapter 3 (section 3.2.1).

### 5.2.2 Visual and attentional tasks

Participants completed a visual task battery as previously described in Chapter 3. Visual acuity, visual contrast, orientation, contour integration threshold, contour SAT, motion coherence threshold, motion SAT, Embedded figures SAT, change blindness SAT, ANT alerting, ANT orienting, and ANT executive effects were selected as dependent variables, as the research question focused on explaining group differences in performance and their underlying neural substrates. For the purpose of this chapter, outcome measures from Chapter 3 were selected and categorised into 'unimpaired', 'impaired' and 'shift' depending on results of group comparisons as previously described (Table 5.1). Full regression and z-test statistics are reported in Appendix 7.

Table 5.1 Categorisation of cognitive tasks based on group comparison outcome. Unimpaired indicates younger and older adults' performance was not significantly different. Impaired indicates older adults' performance was poorer than younger adults. Shift indicates a change in response strategy to a slower more cautious process in older adults. ANT = attention network test, SAT = speed accuracy trade-off.

| Performance | Task |
|---|---|
| Unimpaired | Visual Acuity |
| | Contour threshold |
| | ANT alerting |
| | ANT orienting |
| | ANT executive |
| Impaired | Visual contrast |
| | Visual orientation |
| | Motion threshold |
| Shift | Embedded figures SAT |
| | Mental rotation SAT |
| | Change blindness SAT |
| | Contour integration SAT |

### 5.2.3 MRI and behavioural comparisons

MRS data and diffusion-weighted images were acquired, pre-processed and analysed as previously described in Chapter 4. Outcome variables were mean fractional anisotropy (FA), mean diffusivity (MD), restricted fraction (FR), radial diffusivity (RD) and axial diffusivity (L1) for SLF 1, 2, 3, the ILF, the optic radiations and the fornix (all left and right), GABA/$H_20$, Glx, Choline, Myoinositol, N-Acetyl aspartate and creatine for Occipital (OCC), anterior cingulate cortex (ACC) and posterior parietal cortex (PPC) voxels. For linear regressions, I sought to address which of the regions in neural networks involved in visual perception and attention would best predict cognitive functioning in older and younger adults. Therefore, I selected metrics which had direct neuroanatomical involvement in these networks only as previously described in Chapter 2 (Table 5.2).

Table 5.2 Microstructure and Magnetic Resonance Spectroscopy (MRS) variables entered initial regression models. SLF = superior longitudinal fasciculus, ILF = inferior longitudinal fasciculus, FA= fractional anisotropy, MD = mean diffusivity, L1 = axial diffusivity, RD = radial diffusivity, FR = restricted fraction, GABA = gamma amino-butyric acid, Glx = glutamate/ glutamine, NAA = N-acetyl aspartate.

| **Anatomical region** | **Metric** |
|---|---|
| Occipital cortex | GABA/Glx/ NAA/ Myoinositol/ Choline/ Creatine |
| Anterior cingulate cortex | GABA/Glx/ NAA/ Myoinositol/ Choline/ Creatine |
| Posterior parietal cortex | GABA/Glx/ NAA/ Myoinositol/ Choline/ Creatine |
| SLF1 | FA/MD/L1/RD/FR |
| SLF2 | FA/MD/L1/RD/FR |
| SLF3 | FA/MD/L1/RD/FR |
| ILF | FA/MD/L1/RD/FR |
| Optic radiation | FA/MD/L1/RD/FR |

### 5.2.4 Statistical analyses

The purpose of the present statistical analyses was three-fold. First, I aimed to assess which visual perceptual and attentional related brain measurements (selected a priori, Table 5.2) were involved in predicting cognitive scores for those tasks that showed a group difference between younger and older adults. Second, I aimed to determine if the two groups differed significantly in the size and the direction of the relationships between these predictors and cognitive performance. Third, I studied whether brain-function relationships in older adults were influenced by more general effects of healthy ageing on the brain by conducting partial correlations controlling for overall grey matter volume as proxy measures of brain atrophy and generalized WMH as a proxy measure of age-related vascular and/or inflammatory events that may damage the white matter. The impact of multiple comparisons was corrected using FDR across both younger and older adults' regression models for each cognitive task.

#### 5.2.4.1 A priori analysis: Analytical pipeline

To address these questions, the following analyses pipeline was employed for tasks in which age-related impairment, maintenance and shift in strategy was apparent (Figure 5.2).

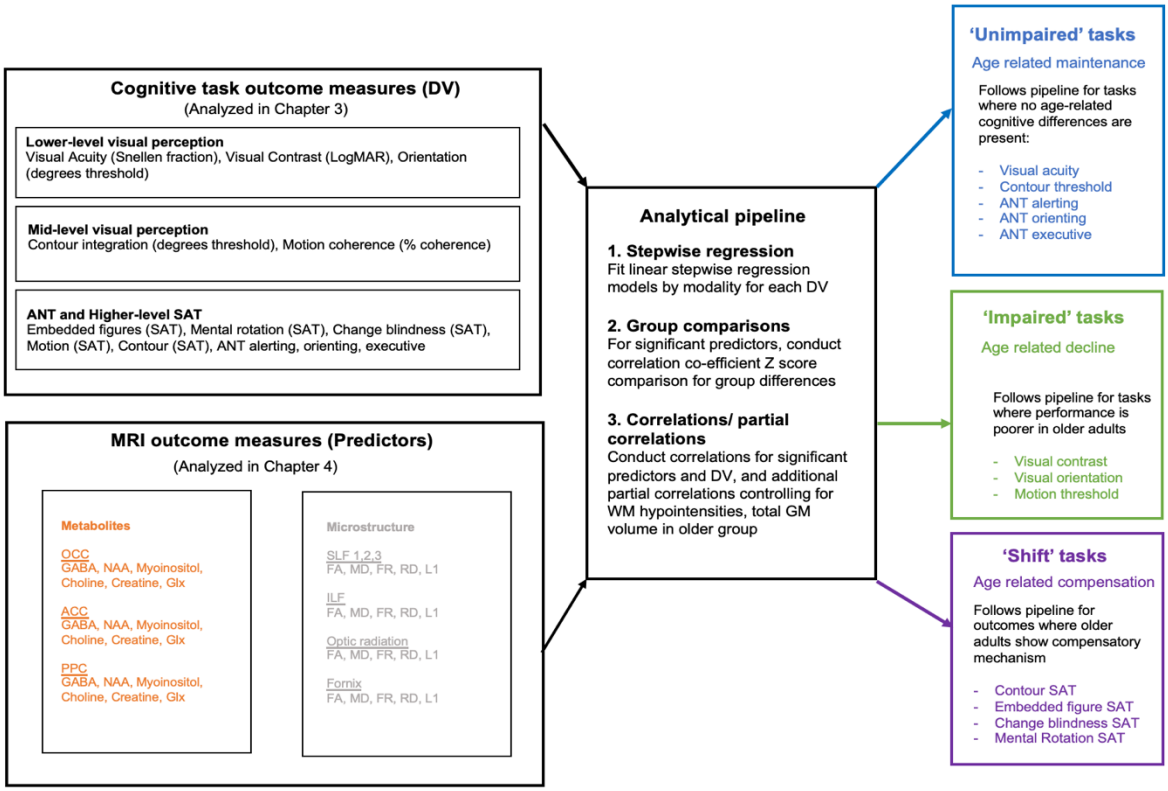


Figure 5.1 Methodological flowchart demonstrating dependent variables and pipeline for statistical analysis in Chapter 5. Cognitive task outcome measures were entered as dependent variables, and MRI outcome measures as predictors into stepwise regression models by modality. Group comparisons were conducted for significant predictors by assessing Z-scores for group differences. For older adults, partial correlations controlling for the effects of white matter hypointensities and total grey matter volume were also conducted. DV = dependent variable, ANT = attention network task, SAT = speed-accuracy threshold, OCC = occipital cortex, ACC = anterior cingulate cortex, PPC = posterior parietal cortex, FA= fractional anisotropy, MD = mean diffusivity, L1 = axial diffusivity, RD = radial diffusivity, FR = restricted fraction.

Firstly, I constructed linear stepwise regressions models by modality i.e. separate analyses were conducted in which predictors were white matter microstructural or metabolite measurements as listed in Table 5.1. These models were run separately for young and old participants; hence age was not included as a predictor. This was done as the large number of predictors fit to one regression model would have presented the problem of overfitting. Education was also included as a predictor, but sex was not as I reported no significant difference between the sexes in older or younger groups (see Table 3.5 in Chapter 3). Due to the high number of variables entered into the regression models, significant predictors were reported after 1% FDR correction across all predictors for all cognitive tasks for both groups.

Where significant predictors of cognitive performance were identified in models, Pearson R correlation coefficients were calculated for each group and converted to Fisher Z scores using the transformation: $z = .5[\ln(1+r) - \ln(1-r)]$ (Fisher, 1925). This allowed me to compute the z-score of the difference between the two groups and use an independent z-test to determine whether there was a significant difference in the correlation coefficients between young and older participants. Those significant predictors which also showed a significant z-test suggested that the predictor was influential in only one group but not the other. For these predictors I explored whether an age effect was due to age-related brain differences by conducting partial correlations between these predictors and cognitive performance controlling for WMH and total grey matter volume.

## 5.3 Results

Results are presented in three different categories: unimpaired, impaired, or shift. These categories refer to the results of group comparisons for the cognitive tests in Chapter 3.

'Unimpaired' tasks were visual acuity, contour threshold, motion SAT and all ANT network effects. 'Impaired' tasks were visual contrast, orientation and motion threshold, and 'Shift' tasks were mental rotation SAT, Embedded figures SAT, change blindness SAT and contour integration SAT (Table 5.1). Brain predictors which were shown to be significant in linear regression modelling and showed a significant Z-test for comparing independence of these predictors to either younger or older adults, are reported. Predictors which appeared in linear regression but did not show significant Z-test are shown in Appendix 7.

### 5.3.1 Unimpaired performance

Following FDR correction across all predictors, no significant predictors of unimpaired task performance were apparent in either the younger or the older group. This suggests that no clear relationships between neural predictors and cognitive performance were present in the current sample.

### 5.3.2 Impaired performance

#### 5.3.2.1 Visual Contrast performance

In younger adults, visual contrast was not shown to be predicted by any of the variables in the model. In older adults, visual contrast was predicted by FA in the right optic radiation ($R^2$=.557, adj $R^2$=.509, beta=-.509, p=.001), which was unique to older adults (Z=2.49, p=.01) and showed a significant negative partial correlation (r=.544, p=.016) (Figure 5.2).

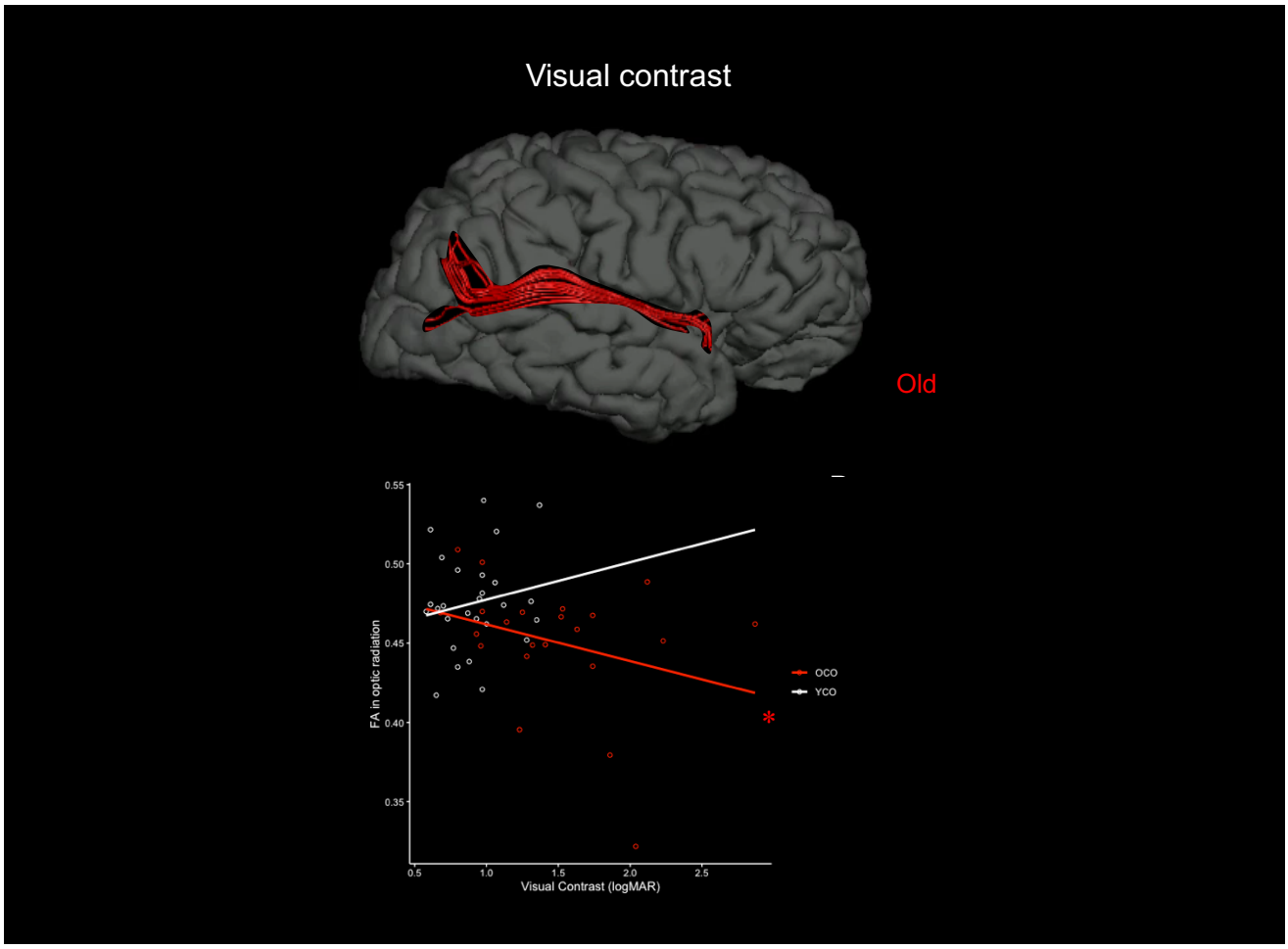


Figure 5.2 Microstructural and metabolic predictors of tasks where older adults show poorer performance than younger adults. Neural predictors of visual contrast which showed a significant Z-difference between younger and older adults following linear regression: only FA in the optic radiation in older adults was a significant predictor of visual contrast performance. No significant predictors of Partial correlations between visual contrast performance and significant predictors are shown *p=.05, **p=<.001

#### 5.3.2.2 Visual orientation performance

Visual orientation was significantly predicted by FR in SLF1 in younger adults ($R^2$=.288, adj $R^2$=.252, beta=-.767, p=<.001) (Z=2.1, p=.013), and GABA/$H_20$ in PPC (r2=.629, adj $R^2$=.567, beta=.204, p=.009) (Z=1.5, p=.04). Several predictors were shown to predict visual orientation in older adults, including Glx in ACC ($R^2$= .552, adj $R^2$=.515, beta=.417, p<.001) (Z=1.8, p=.03) which showed significant partial correlation, (r=.632, p=.004), and FA in SLF2 right ($R^2$=.916, adj $R^2$=.890, beta=-.641, p<.001) (Z=1.10, p=.03) which also showed significant partial correlation (r=-.473, p=.041). RD in the left optic radiation

also predicted older adults' orientation performance ($R^2$=.778, adj $R^2$=.738, .303, p=.000) but this did not show a significant partial correlation (r=.091, p=.710) (Figure 5.3).

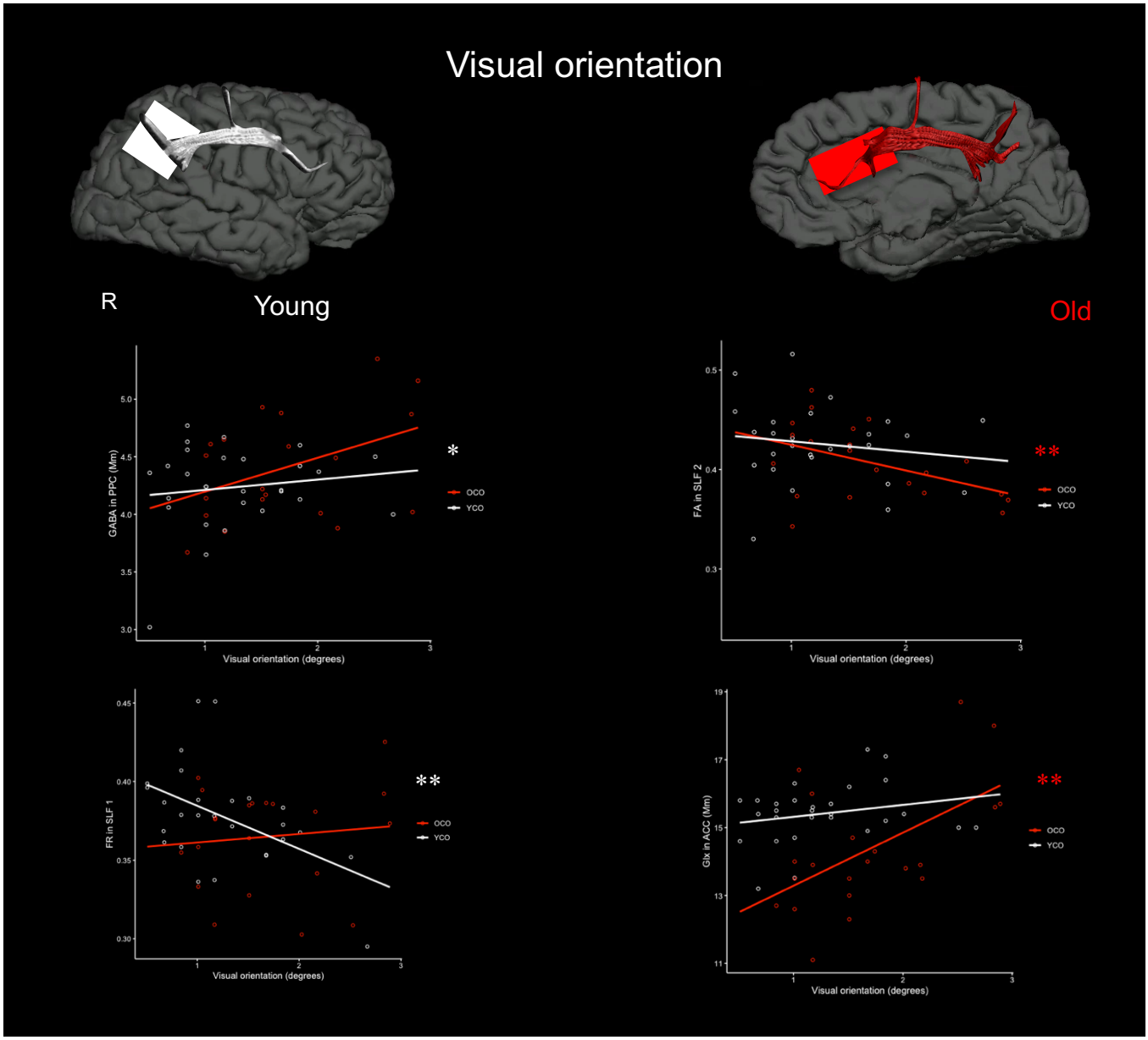


Figure 5.3 Microstructural and metabolic predictors of tasks where older adults show poorer performance than younger adults. Neural predictors of visual orientation which showed a significant Z-difference between younger and older adults: GABA/$H_20$ in PPC and FR in SLF1 in younger adults, FA in SLF2 and Glx in ACC in older adults. Partial correlations between visual orientation performance and significant predictors are shown *p=.05, **p=<.001

### 5.3.2.3 Motion threshold performance

Motion threshold showed no significant predictors in younger adults. In older adults, performance was predicted by GABA/$H_20$ in OCC ($R^2$=.344, adj $R^2$=.294, beta=.777, p<.001) (Z=1.85, p=.03) which showed significant partial correlation (r=.538, p=.017), and L1 right SLF 2 ($R^2$=.591, adj $R^2$=.522, beta=.768, p<.001), however this did not show significant correlation (r=.352, p=.139) (Figure 5.4).

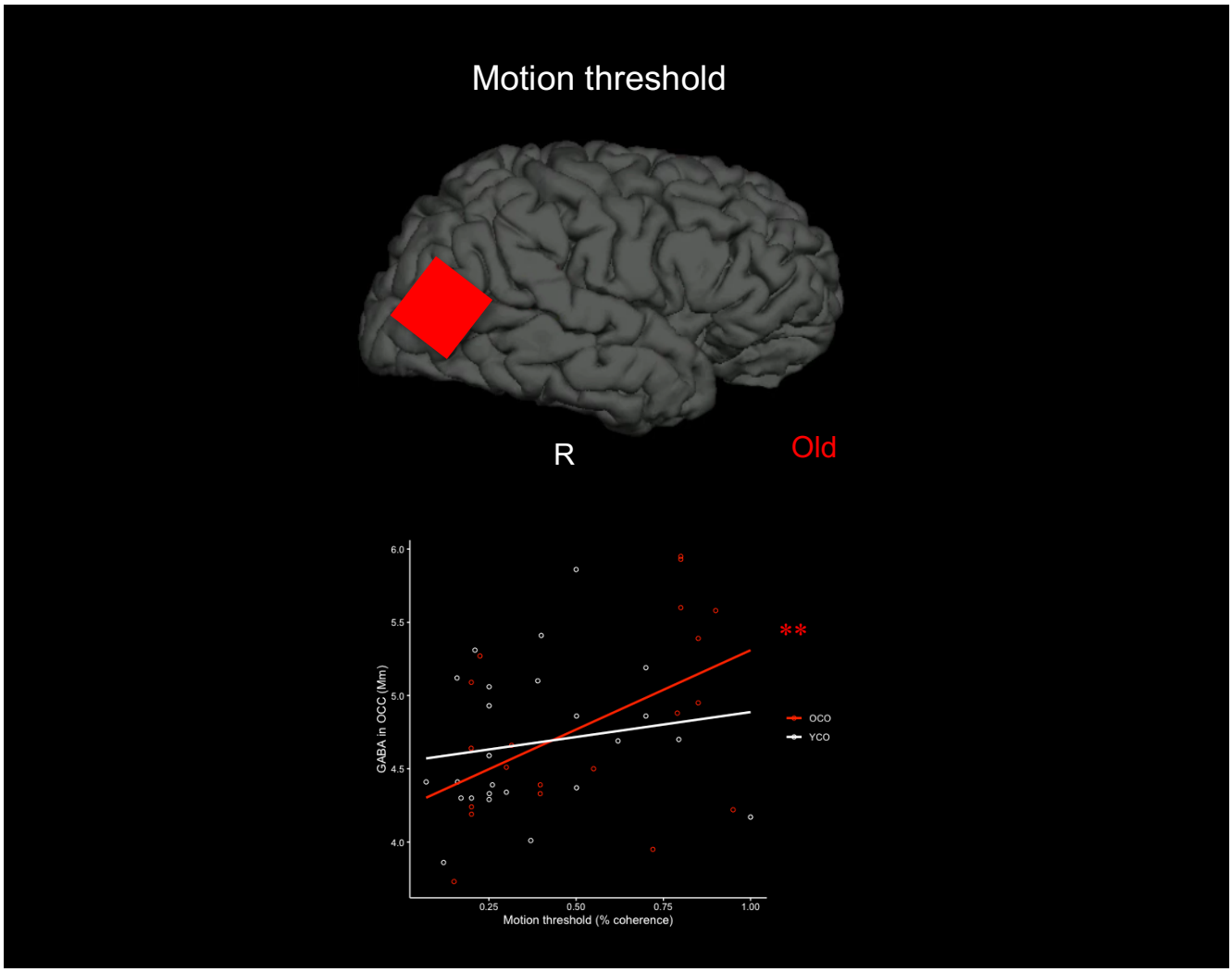


Figure 5.4 Microstructural and metabolic predictors of tasks where older adults show poorer performance than younger adults. Neural predictors of motion threshold which showed a significant Z-difference between younger and older adults: GABA/$H_20$ in OCC in older adults, but no significant predictors in younger adults. Partial correlations between motion threshold performance and significant predictors are shown *p=.05, **p=<.001

### 5.3.3 Shift performance

#### 5.3.3.1 Contour SAT

Contour SAT was predicted by MD in the fornix ($R^2$=.267, adj $R^2$=.230, beta=-.517, p=.009) (Z=2.44, p=.007) in younger adults. In addition, younger adults' performance was predicted by FR in right optic radiation ($R^2$=.224, adj $R^2$=.185, beta=.473, p=.002) (Z=1.77, p=.04) and FA in right SLF1 ($R^2$=.881, adj $R^2$=.830, beta=-1.248, p=.003) Z=1.87, p=.032).

In older adults, contour SAT was predicted by GABA/$H_20$ in the PPC ($R^2$=.253, adj $R^2$=.204, beta=-.503, p=.039) (Z=2.40, p=.008) which survived partial correlation (r=-.450, p=.009) (Figure 5.5).

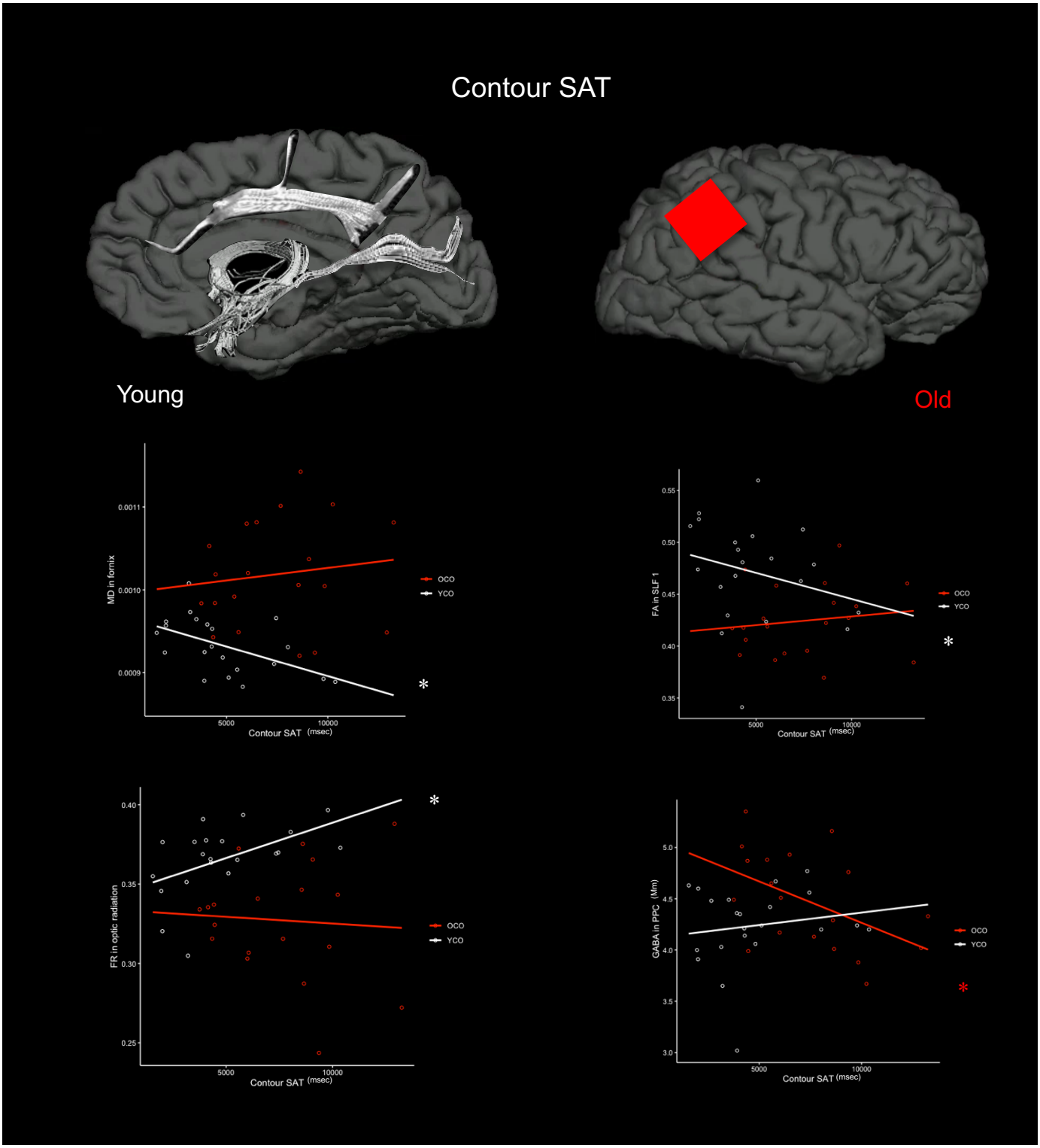


Figure 5.5 Microstructural and metabolic predictors of tasks where older adults demonstrated a shift to slower response time to maintain accuracy. Neural predictors of contour integration speed accuracy trade-off (SAT) which showed a significant Z-difference between younger and older adults: MD in fornix and FR in optic radiation in younger adults, GABA/$H_20$ in PPC and FA in SLF 1 in older adults. Partial correlations between contour SAT performance and significant predictors are shown *p=.05, **p=<.001.

### 5.3.3.2 Embedded SAT

Embedded figures SAT was predicted by FA in the left optic radiation ($R^2$=.367, adj $R^2$=.337, beta=-.606, p=.002) (Z=2.106, p=.018) in younger adults (Figure 5.6).

Embedded figures SAT was predicted by FR in SLF 1 in older adults ($R^2$=.19, adj $R^2$=.157, beta=.446, p=.003) but this was not found to be significant following partial correlation (r=.277, p=.224), indicating that this may be a product of more generalised age-related atrophy.

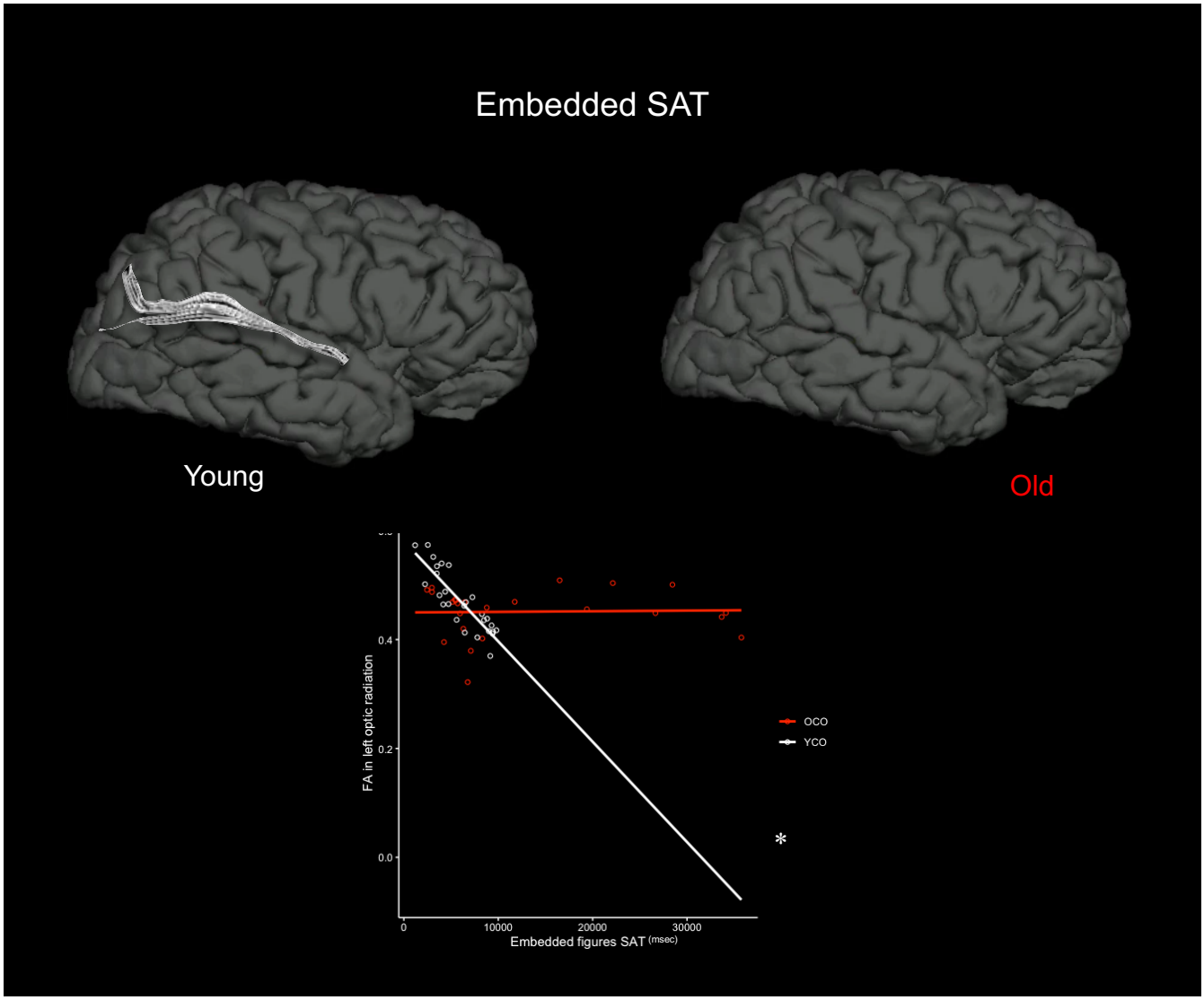


Figure 5.6 Microstructural and metabolic predictors of tasks where older adults demonstrated a shift to slower response time to maintain accuracy. Neural predictors of embedded figures SAT which showed a significant Z-difference between younger and older adults: FA in left optic radiation in younger adults. Partial correlations between embedded figures SAT and significant predictors are shown *p=.05, **p=<.001

### 5.3.3.3 Mental rotation SAT

Rotation SAT was shown to be significantly predicted by L1 in the left optic radiation ($R^2$=.241, adj $R^2$=.205, beta=-.491, p=.007) (Z=1.86, p=.03), in younger adults. FR in the left SLF2 ($R^2$=.491, sdj

$R^2$=.465, beta=-.244, p=.004) (Z=1.99, p=.022) also predicted performance in younger adults (Figure 5.12). In older adults, mental rotation SAT was predicted by NAA in ACC ($R^2$=.364, adj $R^2$=.330, beta=.603, p=.004) (Z=1.67, p=.046) and showed a significant positive correlation (r=.598, p=.002). Choline in the ACC ($R^2$=.806, adj $R^2$=.785, beta=-.859, p<.001), L1 in SLF1 ($R^2$=.206, adj $R^2$=.164, beta=-.478, p=.003), FA in right optic radiation ($R^2$=.391, adj $R^2$=.323, beta=-.883, p<.001) and FR in SLF 3 ($R^2$=.668, adj $R^2$=.609, beta=.695, p=.002) were also predictors of mental rotation SAT in older adults, but these predictors did not show any significant partial correlations (Figure 5.7).

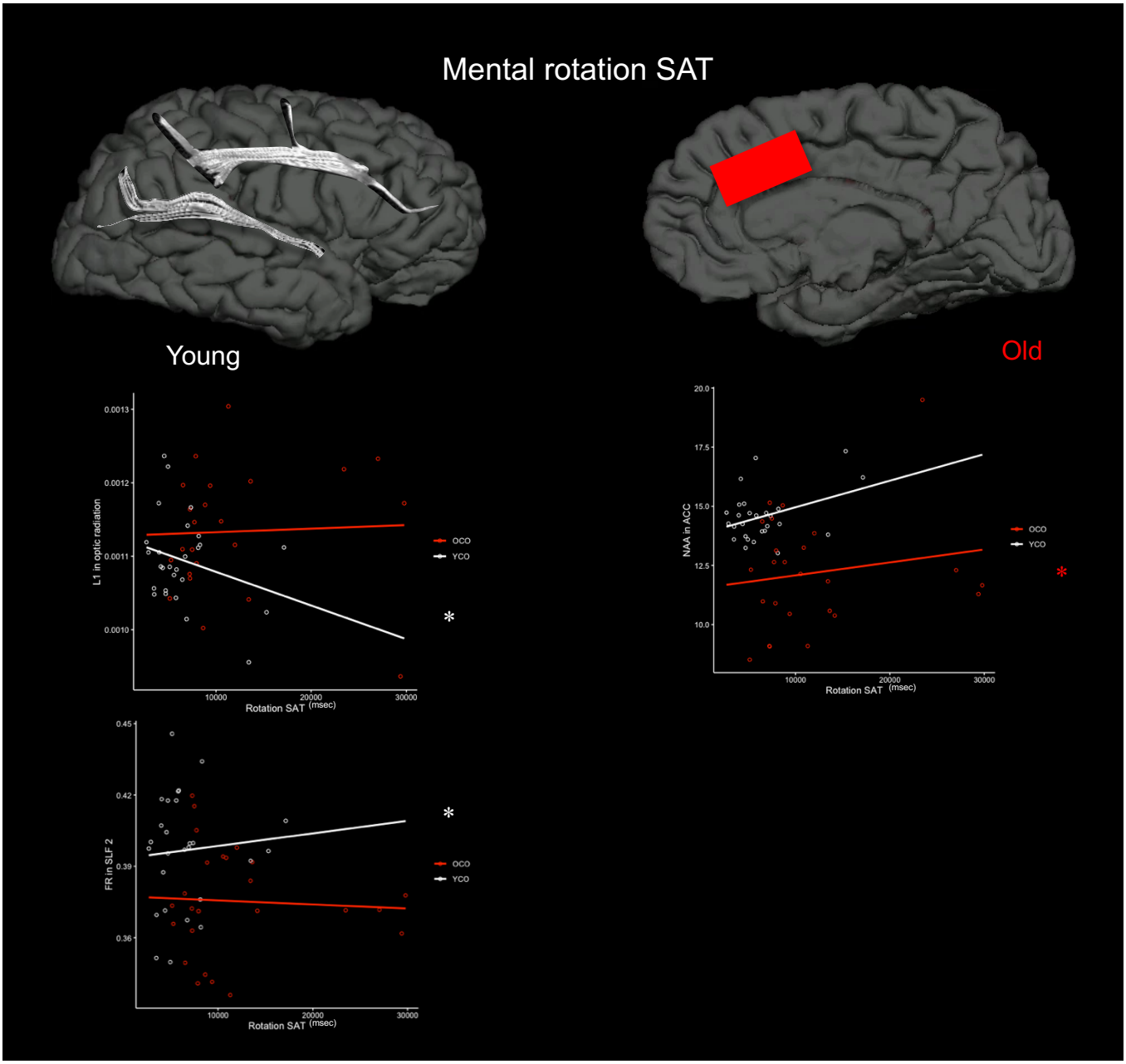


Figure 5.7 Microstructural and metabolic predictors of tasks where older adults demonstrated a shift to slower response time to maintain accuracy. Neural predictors of mental rotation SAT which showed a significant Z-difference between younger and older adults: L1 in optic radiation and FR in SLF 2 in younger adults, NAA in ACC in older adults. Partial correlations between mental rotation SAT performance and significant predictors are shown *p=.05, **p=<.001

### 5.3.3.4 Change blindness SAT

Change blindness SAT was shown to be predicted by FA in the left optic radiation in younger adults ($R^2$=.299, adj $R^2$=.265, beta=-.547, p=.007) (Z=1.82, p=.034). In older adults, change blindness SAT was significantly predicted by GABA/$H_20$ in ACC ($R^2$=.284, adj $R^2$=-.246, beta=-.533, p=.002) (Z=2.91, p=.002), which also showed significant negative partial correlation (r=-.461, p=.020) (Figure 5.8).

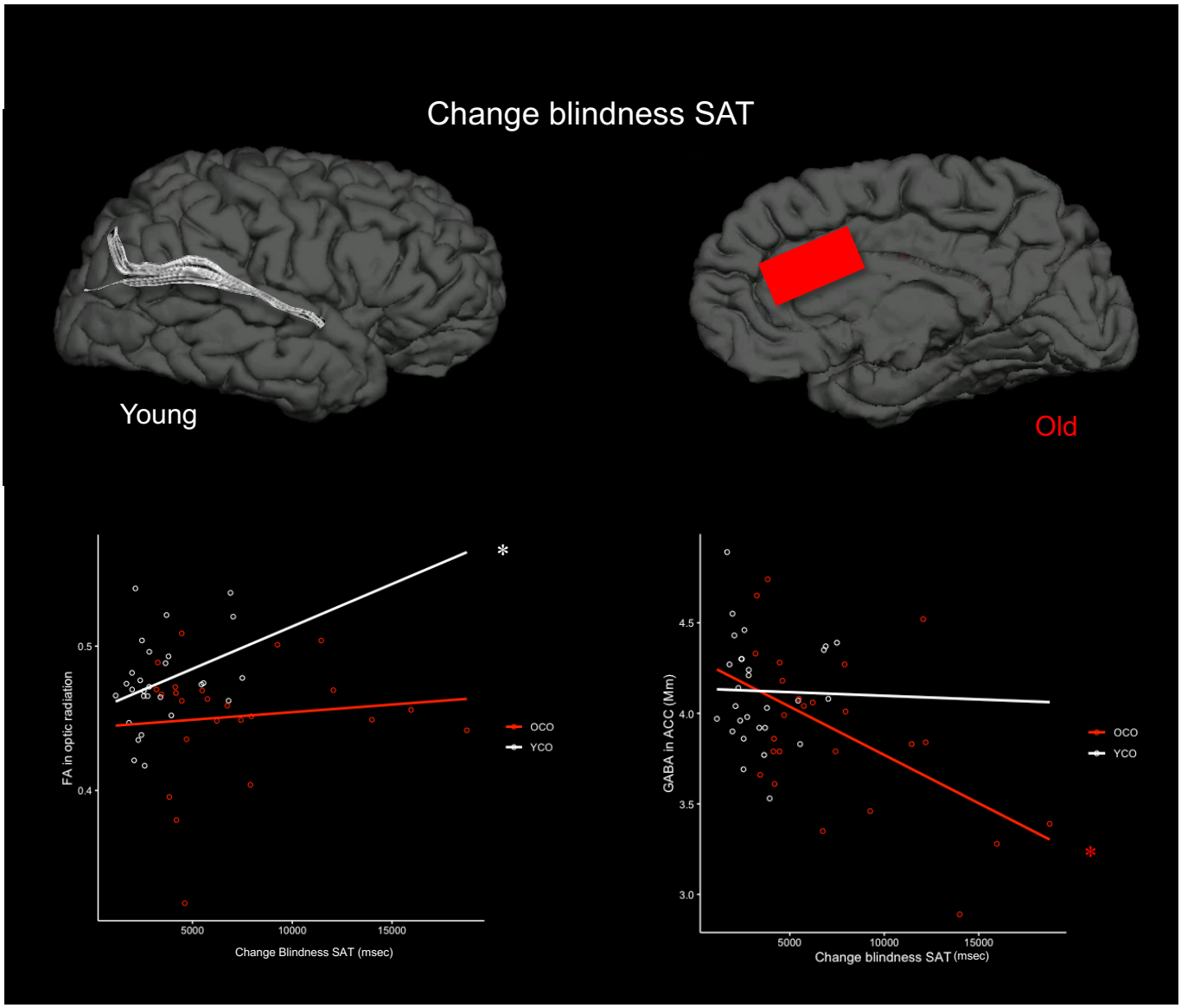


Figure 5.8 Microstructural and metabolic predictors of tasks where older adults demonstrated a shift to slower response time to maintain accuracy. Neural predictors of change blindness SAT which showed a significant Z-difference between younger and older adults: FA in optic radiation in younger adults, GABA/$H_20$ in ACC in older adults. Partial correlations between change blindness SAT performance and significant predictors are shown *p=.05, **p=<.001

Neural predictors for all groups and all tasks are summarised in the table below (Table 5.3), and direction of relationship is indicated. All predictors for each group and each cognitive task category are further visualised in a summary in Figure 5.9.

Table 5.3 Summary table illustrating the significant neural predictors of cognitive performance in tasks where age-related performance was impaired or showed a shift in strategy. YCO = younger adults, OCO = older adults, SAT=speed-accuracy trade-off, ANT=attention network task, FA=fractional anisotropy, RD = radial diffusivity, FR = restricted fraction, L1 =axial diffusivity, ILF=inferior longitudinal fasciculus, SLF = superior longitudinal fasciculus, NAA = N-acetyl aspartate, OCC = occipital cortex, ACC = anterior cingulate cortex, PPC = posterior parietal cortex.

| Performance | Task | Neural predictors YCO | Neural predictors OCO |
|---|---|---|---|
| Impaired | Visual contrast | - | FA in right optic radiation (-) |
| | Visual orientation | GABA/$H_20$ in PPC (+)<br>FR in SLF 1 (-) | Glx in ACC (+)<br>FA in SLF 2 (-) |
| | Motion threshold | | GABA/$H_20$ in OCC (+) |
| Shift | Embedded figures SAT | FA in optic radiation (-) | - |
| | Mental rotation SAT | L1 in optic radiation (-)<br>FR in SLF 2 (+) | NAA in ACC (+) |
| | Change blindness SAT | FA in optic radiation (+) | GABA/$H_20$ in ACC (-) |
| | Contour integration SAT | MD fornix (-)<br>FR optic radiation (+)<br>FA in SLF 1 (-) | GABA/$H_20$ in PPC (-) |

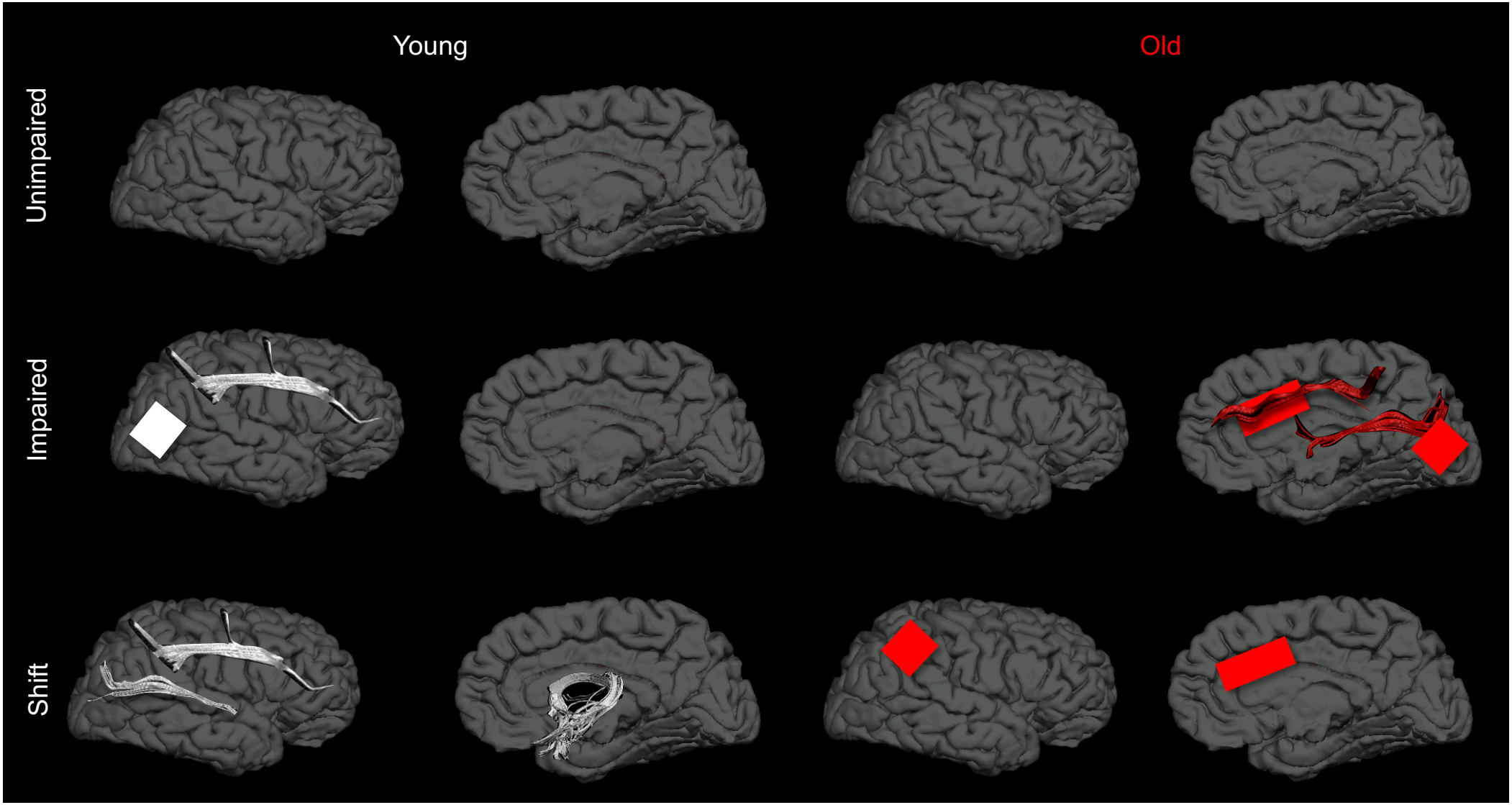


Figure 5.9 Figure illustrating neural predictors for each category of task (unimpaired, impaired and shift) and each group (younger adults in white, and older adults in red). For 'impaired' tasks, predictors in younger adults are GABA/$H_20$ in PPC, and FR in SLF 1 and for older adults' predictors are FA in right optic radiation, Glx in ACC, FA in SLF 2 and GABA/$H_20$ in OCC. For 'shift' category, predictors in younger adults are FA, FR and L1 in optic radiation, MD in fornix, and FA and FR in SLF 1, and for older adults' predictors are NAA and GABA/$H_20$ in ACC and GABA/$H_20$ in PPC.

## 5.4 Discussion

### 5.4.1 Overview

In this chapter I aimed to firstly establish which metabolic and microstructural variables in relevant brain networks best predicted perceptual and attentional functioning throughout the visual hierarchy in younger and older adults, and which of these predictors were unique to either respective group. Secondly, I aimed to determine which of these predictors may be related to more general age-related changes, such as overall reduction in grey matter, or whether these were independent changes. These predictors were assessed in relation to cognitive outcome measures where older adults showed impaired performance, unimpaired performance or evidence of a 'shift' in neural strategy as indicated in SATs for older adults. Results showed different patterns of predictors between these different categories of cognitive outcome measures, with older adults showing some maintenance of neural mechanisms underlying performance and some indication of alternative neural strategies to compensate for cognitive outcome. Notably, for those cognitive tasks where older adults demonstrated a shift to a slower response strategy, predictors were largely metabolic whereas for the same tasks in younger adults, microstructural variables predicted faster response times. Results are discussed below and compared between unimpaired, impaired and shift categories of cognitive outcome.

### 5.4.2 Neural predictors of unimpaired task performance

As established in Chapter 3, cognitive outcomes which were unimpaired between younger and older adults were: visual acuity, contour threshold, ANT alerting, ANT orienting and ANT executive network effects. I hypothesised that predictors would be the same for both groups, and potentially show additional supportive compensatory predictors in older adults. However, after adjusting for multiple comparisons, no predictors of unimpaired cognitive performance were found to meet the accepted threshold for significance in either younger or older groups. I posit that this is likely due to methodological limitations, both in the size of the sample and wider age ranges of the older group. As such, it is possible that the select and/or hypothesised brain regions may be related to unimpaired perceptual performance however due to the limited sample, and the variance of performance within the older group, this data is limited and noisy, thus clear patterns are unable to emerge.

### 5.4.3 Neural predictors of impaired task performance

In contrast, the predictors found for impaired tasks are significant at a very high threshold, and thus suggest that these relationships are stable, despite the above limitations. Cognitive outcomes for which older adults showed more impaired performance in comparison to younger adults were: visual contrast, visual orientation and motion threshold. Visual contrast performance was predicted by FA in optic radiation in old participants, but no predictors were present in the younger adults. This is consistent with my hypothesis that lower-level visual function would be predicted by age-related decline in lower-level visual regions and suggests a clear mechanism for the consistent finding that older adults show impaired contrast ability in

comparison to younger adults. However, this finding does also support the notion that the visual system may not be truly hierarchical. Whilst visual contrast is considered to be a lower-level visual function and the optic radiations transmit information from the retina to the early visual cortex, it would be anticipated that visual contrast impairments would be related to primary visual cortex changes. Moreover, if age-related declines in optic radiation are apparent, it would also be expected that visual acuity would be impaired, due to a disruption in information transmission from retina to cortex – which is not demonstrated in the present results. Considering this, it may be that age-related disruptions feedforward and/or feedback connections along the optic radiation (Alvarez et al.,2015) underlie the relationship seen here between visual contrast and optic radiation microstructure. This suggests that the visual system does not necessarily process information in a linear, hierarchical manner and that this may be altered in age.

I also hypothesised that age-related depletions in GABA/$H_20$ and NAA in visual regions may be related to changes in orientation ability. However, it was Glx in the ACC and FA in SLF that were significant predictors of older adults' performance in the current results. FR in SLF1 and Glx in ACC were also predictors of orientation performance in younger adults, however GABA/ $_20$ in PPC was also a significant predictor of performance in younger adults. GABA has been reliably shown to be involved in visual orientation perception, as it plays a key role in inhibitory processes required to effectively discriminate different orientation (Song et al., 2017). Moreover, GABA specifically in the PPC suggests that inhibitory processes in parietal regions responsible for attentional functions supplement frontal and fronto-parietal predictors in younger adults during visual orientation performance. Although GABA/$H_20$ in the PPC alone was not seen to be significantly reduced in older adults, it is possible that these results reflect an age-related impairment within the inhibitory mechanisms of GABA in the parietal region age-related impairment within the mechanism between inhibitory GABA in the parietal region, excitatory Glx in the frontal ACC region and SLF connecting fronto-parietal region. It is possible that as the orientation task required a level of perceptual decision-making and as the ACC is involved in decision confidence (Stolyarova et al., 2019), and older adults' decisions are more cautious (Bossaerts & Murawski, 2016), age-related changes in metabolites in the ACC (as shown in Chapter 4) may underlie impaired performance in this task. In addition, reductions in microstructural integrity in the SLF connecting frontal and parietal regions involved in decision making which were shown to predict orientation performance in this chapter may also be involved in age-related impairments in this mechanism. As such, the neural correlates of perceptual decision making in older adults warrants further investigation and will be explored in the following chapter.

Finally, motion performance showed no significant predictors in younger adults, but increased GABA/$H_20$ in OCC was a predictor of performance in older adults. Previous findings have also demonstrated that increased GABA/$H_20$ in the OCC is related to decreased spatial suppression in a motion perception task in older adults (Pitchaimuthu et al. 2017). Primate evidence has shown that increased GABA in the visual cortex is correlated with decreased noise activity, leading to reduced spatial suppression of motion (Thiele

et al., 2012). As my results have evidenced both lower-level perceptual impairments and reductions in white matter microstructural integrity in visual tracts, it is possible that older adults experience reduced efficiency of perceptual processing, and thus have increased GABA in the OCC in a bid to reduce perceptual noise. This in turn would result in reductions in spatial suppression during motion perception in older adults.

### 5.4.4 Neural predictors of strategy shift in performance

I hypothesised that lower-level visual regions underlying bottom-up processing would be significant predictors of SAT performance in younger adults, but that the 'shift' in strategy may be reflected in predictors being related to top-down processing in older adults. Consistent with my hypothesis, for all tasks where older adults show longer SATs - due to increased RT but maintained accuracy - predictors in older adults are GABA/$H_20$ and NAA in the posterior parietal and anterior cingulate cortices. In contrast, predictors in younger adults were largely microstructural measurements and metabolites in the occipital cortex, indicating a potential shift between alterations in sensory visual regions, and fronto-parietal regions involved in top-down processing.

NAA in the ACC was shown to be a predictor of Mental rotation SAT for older adults, which has been previously shown in Chapter 4 to show age-related reductions. This relationship indicates that for longer SATs, NAA in ACC is higher, suggesting that poorer age-related SAT is a product of too much NAA in ACC. As such, it is possible that an imbalance in ACC NAA – either too much or too little - may underlie SAT slowing in older adults. In contrast, L1 in optic radiation was shown to be a significant predictor of mental rotation SAT in younger adults, but not older adults. I posit then, that it is possible that this pattern of neural predictors represents an over-compensation of top-down processing to account for age-related short comings in engaging bottom-up mechanisms. These results suggest a compensatory role for the dorsal stream of processing, conflict monitoring and inhibition via the ACC in older adults, whilst younger adults may recruit more basic visual functions and object processing to complete the task. Previous results confirm a slowing of RT in older adults during mental rotation tasks which, coupled with these results, perhaps suggests a more careful and object-oriented approach to task completion, utilising elements of the stimuli. These results may indicate that whilst younger adults are able to respond to this visual information in a more immediate manner, older adults require greater time to recruit the ACC as support in this process. (Duma et al., 2019).

Embedded figures SAT was predicted by FA in the optic radiations which do show age-related reductions in Chapter 4. No significant predictors were present in older adults, therefore it is possible that this combination of microstructural and metabolic predictors in bottom-up processing is key in shorter SATs, but no clear shift in neural strategy is apparent with the switch to longer SATs in older adults. Previous research has indicated that individual cognitive style in adopting greater field dependence or independence influences the approach to embedded figures task (Hao et al., 2013). More successful task completion

requires field independence, such that individuals can suppress environmental information that is not relevant. The fronto-parietal network was found to mediate feature identification in those with a more field independent cognitive style (Hao et al., 2013). However, age-related changes in field dependence-independence have been reported, in which a general shift in cognitive style toward field dependence is observed with older age (Chan & Yan, 2018). Older adults show a tendency to relay on environmental information which is posited to be a result of compensatory mechanisms in reducing top-down control and relying on bottom-up processing. This may be reflected in the current results, leading to older adults recruiting ventral processing streams to compensate in successfully completing the task.

For change blindness SAT, FA in optic radiation predicts younger adults' performance, which is reduced in older adults, but is compensated by GABA/$H_20$ in the ACC. Again, this supports the theory that age-related lengthening in SATs is due to a switch between bottom-up processing in younger adults and more reliance on processing in top-down mechanisms in older adults. For this task involving object and scene perception, it would initially be anticipated that adults would recruit ventral processing stream regions. However, the nature of the task required participants to 'spot the difference' which is known to require a significant level of executive functioning and inhibitory processing. This may explain the presence of fronto-parietal connectivity governing spatial attention and perception of visual space (SLF 2) as a predictor in younger adults. In addition, this may also explain the presence of metabolites in the ACC in older adults in predicting change blindness performance. It may seem counterintuitive that lower NAA concentrations in the ACC are responsible for inhibition and conflict monitoring aspects of executive functioning in older adults. However, NAA in the ACC is shown to be related to cognitive interference, with lower NAA being present in those participants able to process information in higher interference conditions, thus indicating more effective cognitive control (Grachev et al., 2001). This poses an interesting contrast, with metabolic ACC processes being greater predictor of task success in older adults than microstructural integrity of SLF in younger adults. This result clearly highlights the importance of investigating the role of biometabolites in cognitive ageing, which may present as novel markers of higher-level perception.

Faster contour integration SAT was predicted by greater diffusivity in the fornix younger adults in addition to greater microstructural integrity in FR in optic radiation and FA in SLF 1. Conversely, older adults' better SAT performance was predicted by higher GABA/$H_20$ in the PPC, suggesting a switch to parietal, top-down processing mechanisms to better complete the task. GABAergic inhibition in the visual cortex has also been related to centre surround suppression (Yoon et al., 2010), which is reduced in older adults. The present results may then represent a switch to more attentional suppression, and less of a response to orientation of Gabor patches, but a change in strategy from orientation specific suppression usually conducted in the visual cortex in response to Gabor patch contours (Song et al., 2017), however this is also speculatory at present.

In addition, although higher-level tasks showed evidence of a shift in strategy in older adults, it should be noted that there are functions earlier in visual processing which have shown some impairment in older age (i.e. visual contrast). These processes cannot be compensated for and may be impacting the results of higher order processing. As such, a 'shift' in response strategy is still present in older adults but it may be as a result of earlier visual processing impairment.

### 5.4.5 Comparison of findings

Where age-related impairment in cognitive performance was apparent, predictors which showed age-related impairments in microstructural integrity were apparent, indicating that impaired white matter microstructure may underlie impaired lower-level perceptual performance in age. I also observed that in impaired tasks, older adults' performance was predicted by metabolites and white matter microstructure in connections the same fronto-parietal network as younger adults suggesting that older adults are able to engage this neural processes in response to the same task, but that it shows some physical age-related decline leading to impaired performance. More specifically, downregulation in metabolites coupled with poorer white matter microstructure contributed to impaired cognitive performance, which is consistent with the results of mediation analyses in the previous chapter. However, as the design of these particular tasks did not allow for adults to have a longer response time and thus adopt more cautious strategy, it is possible that older adults attempt to compensate for poor sensory input by recruiting top-down processing, but that insufficient time is allowed for this processing thus the strategy fails in these instances.

In 'shift' tasks where older adults-maintained accuracy but could make a slower response, I also saw effective recruitment of fronto-parietal predictors, which was in contrast to the occipital bottom-up predictors underlying faster SAT in younger adults. Interestingly, these predictors were specific to metabolic changes in the PPC and ACC in older adults and microstructural and/or metabolic measurements in the OCC in younger adults. In Chapter 4, I investigated the relationship between metabolic declines in the ACC and PPC and reductions in FR in the SLF. As discussed, I observed a significant decline in NAA in the ACC and PPC in older adults thought to reflect hampered mitochondrial function. This age-related reduction in NAA in the ACC and PPC was correlated with a reduction in FR in the SLF. The relationship between age-related mitochondrial decline and subsequent Wallerian generation was also discussed (Loreto et al., 2020). My results in this Chapter may show this mechanism to be related to age-related changes in SAT – or lengthened RTs - in an attempt to respond cautiously and spare accuracy levels. As shown in Chapter 4, it is possible that NAA changes in the ACC and PPC may mediate subsequent age-related microstructural decline in the SLF. Reductions in fronto-parietal white matter has previously been shown to be related to age-related slowing (Gold et al., 2010), suggesting that slower, more cautious response time in older adults may be the result of this metabolite and microstructural relationship. This is notable as lengthened SAT in ageing has been shown to be a 'voluntary' choice or strategy (Forstmann et al., 2011),

suggesting that older adults may voluntarily recruit greater top-down attentional control, but that this may be impaired by reductions in NAA and subsequent SLF decline in white matter integrity.

GABA/$H_20$ was seen to be a predictor of two measures of SAT in older adults. This is surprising, as GABA has been related to the variability of cognitive performance in adults (Simmonite et al., 2019) and also visual functioning (Edden et al., 2009). However, I do report relationships between other metabolites and cognitive functioning in older adults which were independent of more general GM thickness reductions and volume loss. This provides support for the study of the role of brain metabolites in cognition in older age which requires further investigation.

### 5.4.6 Limitations

There are several limitations to the current study which may have influenced the outcome of results. It should be noted that some of the predictors correlated with more general measures of ageing such as WMH and total grey matter volume. The basis for these findings may be two-fold. Firstly, it may be that the initial predictors may contribute significantly to observed cognitive differences between younger and older adults. If this is true, the contribution of these predictors to ageing cognition in previous research may then have been overlooked or outweighed by more general age-related changes. As such, it may be that these predictors are valuable in the explaining age-related differences in perception and attention but require more sensitive evaluation. In contrast, it may be that these predictors initially appear to underlie cognitive and perceptual differences in older adults but are the product of more general differences in ageing, such as reduced grey matter. Metabolites in these analyses are quantified by correcting for grey, white and CSF volume in voxels, correcting for this latter interpretation. However, it would be expected that microstructural measurements would be influenced by total WMH and any loss of grey matter. As such, this is a potential caveat to the current results.

Moreover, it should also be noted that the current chapter attempted to assess relationships between metabolites and microstructure, and different aspects of age-related cognitive functioning and/or changes which are highly complex in nature. As the participants included in the current analysis were originally recruited as control participants for the study of DLB, it is possible that the analysis has limited power. The repercussions of this are that the current results may be partly the product of spurious correlations due to noisy data. If the study were to be replicated, these limitations should be considered, and a larger sample size recruited.

In addition, the role of brain and cognitive reserve in these results should be noted. Cognitive reserve (as discussed in chapter 1) refers to the individual differences in how people perform a task, and how some may be more flexible or efficient with brain resources than others (Stern et al.,2012). In the context of ageing, those individuals with higher cognitive reserve are more able to engage compensatory mechanisms

than those with lower cognitive reserve and can maximise performance through recruiting alternative neural networks or strategies. This may be apparent as I report that most older adults engage a shift in their response strategy, potentially demonstrating relatively high cognitive reserve. As such, it should be noted that this shift may not be apparent in all older adults and results may not be generalisable to the older adult population.

Finally, speed-accuracy trade-off is shown in this chapter to evidence a shift in strategy for older adults however there are numerous other factors that my influence RT in the context of ageing in addition to the SAT such as motor speed (Woods et al.,2015). It is possible then that the 'shift' observed in older adults is a product of other factors and not primarily a change in SAT behaviour. In addition, motor speed and the contribution of visual noise in ageing may influence the SAT, in which case a 'shift' in strategy may be the product of faulty perceptual input or limited motor speed as opposed to an alternative neural or cognitive strategy being adopted.

### 5.4.7 Future directions

To support the potential conclusion that older adults experience a shift in cognitive strategy in response to visual stimuli, future investigations would benefit from rigorous assessment of executive and inhibitory cognitive processes. More specifically, tasks associated with ACC functioning such as inhibition, effective suppression of non-relevant stimuli and task switching would help to establish whether the observed results are a product of age-related decline in these functions.

Future directions in which greater a sample size was to be recruited, or larger trial numbers collected, may benefit from employing data dimension reduction methods, such as principal components analysis (PCA), to clarify the clustering of both cognitive and brain variables and establish a clearer pattern of results. A PCA was initially conducted for the current analysis, however this did not add further clarity for the analyses, and therefore was not included in the main analysis.

In addition, as discussed, greater sample size may clarify some relationships and trends which appear at present. This would be particularly useful, given the dispute in the literature regarding strategies which best support successful cognitive ageing. It would be pertinent to explore the contrasting relationships between younger and older adults' successful RT performance. Indeed, I also sought to investigate this relationship in the current project, by assessing which neural changes underlie different aspects of RT in older adults. This was done as several tasks in the present study including RT scores were seen to be predicted by changes in neurochemistry. Relatively little is known about the cognitive correlates of age-related changes in neurochemistry in comparison to the far wider literature concerning changes in white matter connectivity and cortical thickness or volume changes with age. As such, it is recommended that future research

considers the role of neurochemical fluctuation in cognitive changes with age in addition to other neural measurements.

### 5.4.8 Chapter summary

This chapter analysed results from Chapters 3 and 4 in order to determine which neural correlates best predicted perceptual and attentional performance differences in ageing. My results indicated that where cognitive performance was poorer in older adults, ACC metabolites and reductions in microstructural integrity in optic radiation and SLF predicted lower-level vision, and GABA/$H_20$ in OCC predicted mid-level vision. Furthermore, my findings indicate that for SAT's which show a 'shift' in cognitive strategy with age, lower-level sensory tracts and occipital regions underlie faster SAT in younger adults, but anterior and parietal regions underlie slower SAT in older adults. This further provides support for both the frontal ageing hypothesis in that older adults show slower response times related to frontal regions (Dempster, 1992), but also demonstrates the reliance of older adults on top-down processing and a more cautious strategy as a possible consequence of impaired optic radiation microstructure and reduced occipital metabolites. Where performance was unimpaired between younger and older adults, no significant predictors were present suggesting that limitations of the sample may have prevented a clear pattern of results in this instance.

# Chapter 6 : Relationships between elements of processing speed and brain differences in ageing: a drift diffusion and MRI analysis

## 6.1 Introduction

In Chapter 3, I found that older adults had slower response times than younger adults in most visual perception and attention tasks. These observations were consistent with numerous reports of age-related slowing in the literature (Haynes, Bunce, et al., 2017; Kerchner et al., 2012). I also observed age-related shifts in the SATs as older adults tended to make slower decisions to mitigate the likelihood of errors (Starns & Ratcliff, 2010). In other words, older adults adopt a more cautious approach and tend to accumulate more information before making a decision (Rabbitt, 1979). This contrasts with younger adults who attempt to balance speed and accuracy (Starns & Ratcliffe, 2010). In Chapter 5, my results also showed that age-related lengthening of SATs may be related to a switch between bottom-up and top-down processing streams and a switch between predominantly microstructural predictors of performance in lower-level visual regions in younger adults, to metabolite predictors of performance in the fronto-parietal network of the brain in older adults. As lengthened SAT is a reliable finding in the study of cognition in older adults, understanding the nature of age-related brain changes and how they may differ depending on processing strategy is important in clarifying key brain changes in healthy ageing. However, studying SAT alone presents issues in the comparison of performance between individuals or groups, as this measure does not distinguish between different decision-making contributions to overall RTs. Thus, while participants may exhibit comparable SAT levels, it is possible that they may differ in their underlying trade-offs in decision making processes. Based on the analyses of raw response speed and accuracies alone it is not possible to infer about the decision-making components that may lead to the observed shifts in older adults' speed-accuracy trade-offs. Similarly, it remains a matter of debate whether age-related RT changes arise due to a general slowing of cognitive processes (Salthouse, 1979), or due to impairments in specific elements of the response process (Verhaeghen, 2011). Again, the latter cannot be measured by observing raw RTs alone (Verhaeghen, 2011) but requires the modelling of response latencies. Drift diffusion models (DDM; see below) have been influential in characterising different elements of response processing that contribute to overall RT, and how they may be differentially affected by age (Noorani & Carpenter, 2011).

In Chapter 5, I demonstrated that the observed perceptual and attentional differences in normal ageing were related to age-related microstructural and metabolic differences in the brain networks that are known to mediate these functions. These analyses suggest that older adults adopt different strategies and recruit different brain regions to mediate SAT performance. Some studies have now also started to investigate the neural correlates of the elements of response processing using DDMs but these have been primarily limited to structural and DTI-based microstructural domains (Monge et al., 2017). To the best of my knowledge, no study has yet focused on linking RT modelling in older adults to their metabolic and advanced microstructural correlates with the MR methods employed here. As previously discussed, recent work has

demonstrated the sensitivity of employing advanced diffusion imaging over standard DTI in the estimation of age-related microstructural changes (Billiet et al., 2015, Toschi et al., 2020). My own research observed significant relationships between FR in SLF and NAA in ACC and PPC in older adults. Based on these findings, in this chapter I will apply a DDM to data from a simple choice RT task in younger and older adults, compare group outcomes and explore relationships between group differences in RT model and microstructural and metabolic differences.

It has been proposed that despite older adults showing longer RTs and thus 'cognitive slowing', there may be further elements involved in a decision-making process associated with RT that could be subject to change with age. According to this view, ageing does not lead to a global deficit, or general slowing but to a switch in domain specific strategies (Hedge et al., 2018). This view assumes that a number of cognitive processes are encompassed within an RT and that any of these may be subject to age-related changes. This is important in the context of studying visual perception and attention, as RTs are thought to involve perceptual, inhibitory and information processing elements which are indistinct when measuring RT alone. Applying more complex cognitive models to RT, such as the DDM, can help tease apart these processing elements allowing for a more detailed analyses of the relationship between age, cognitive processing, and brain measurements. Such cognitive modelling has been applied to data from choice RT tasks in an effort to examine differences in specific processes between older and younger adults that may underpin the overall slowing effect that occurs with age (Dutilh et al., 2013; Spaniol et al., 2006; Starns & Ratcliff, 2012).

Traditionally, decision researchers have employed recursive models which focus on performance, as opposed to feedforward models which incorporate an aspect of learning from experience (Busemeyer & Johnson, 2004). More specifically, the dominant category for computational models of decision-making is 'sequential sampling', in which an 'evidence accumulation' approach is adopted in order to explain the speed accuracy trade-off. This states that the changes in the amount of evidence necessary to form a response selection underlie overall decision processes (Cassey et al., 2014). Accumulator theories state that a decision is reached by gradually accumulating evidence which favours one of two choices in the decision; when a high threshold for evidence is set, the decision process is slower but more cautious, and when a low threshold for evidence is set, decisions are made quickly, and are often less accurate (Cassey et al., 2014). A number of sequential sampling models exist, which differ based on whether evidence is assumed to be sampled at equally spaced time intervals or random intervals; whether evidence is sampled in varying or fixed amounts, and the rule at which sampling ceases and a decision is eventually reached (Ratcliff & Smith, 2004).

The DDM (Ratcliff, 1978; Ratcliff & Rouder, 1998) is a sequential-sampling model which assumes that information that drives a decision is accumulated over time, until it reaches one of two response boundaries and then forms the final response (for example, 'left' or 'right' would be response boundaries in one model;

Figure 6.1). According to the DDM, overall processing is segmented into several components which contribute to ultimate performance: first, components of processing which do not include active decision, such as perceptual encoding and response execution, represented by 'non-decision time (t)', second, a criteria threshold that information accumulates to, represented by 'boundary separation (a)', and third the rate at which information accumulates towards a decision, represented by 'drift rate (v)'. The DDM assumes that the accumulation of information (drift rate) during a decision process is not constant but varies over time, represented by (s). This variability also contributes to error responses, where the accumulation of information can reach the incorrect boundary. In the context of a flanker task, for example, in which stimuli are either congruent, thus 'easy', or incongruent thus 'harder', drift rates will be more prone to variation in harder conditions, and therefore response times are slower and have a higher probability of reaching an incorrect response boundary. In the context of a flanker task, for example, in which stimuli are either congruent, thus 'easy', or incongruent thus 'harder', drift rates will tend to be more prone to variation in harder conditions, and therefore response times are slower and have a higher probability of reaching an incorrect response boundary (Figure 6.1). DDMs are built on the assumption that total RT is the sum of non-decision and decision components (Luce, 1986) in accordance with the following equation (6.1)

$$RT = DT + T_{er'} \tag{6.1}$$

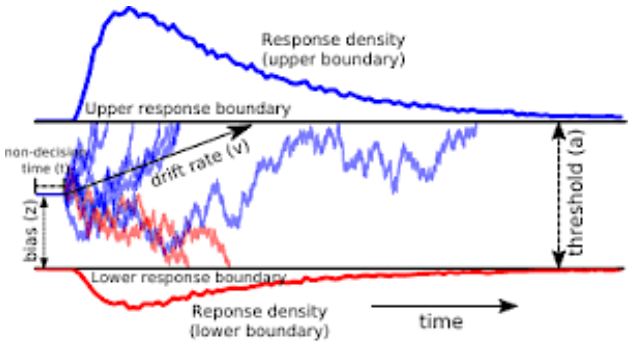


Figure 6.1 The drift diffusion model (DDM) of response time. Red and blue lines denote different responses in a 2-choice task (for example, left or right). Reaction times (RT) are fit to the DDM to return an estimate of non-decision time (t) reflecting perceptual and motor processing time, boundary separation value or threshold (a), representing the level at which information must reach to trigger a response and drift rate (v), representing the efficiency of the drift process. Adapted from Zhang & Rowe (2014)

The data required to fit the DDM are error rate and RT distributions for correct and incorrect responses. The model is fit according to one of several models (Ratcliff & Tuerlinckx, 2002), which vary depending on the implementation of the DDM.

The DDM is often selected in the study of older adults due to its' methodological strengths in comparison to other models such as the linear ballistic accumulator (LBA) model of decision making (Ratcliff et al., 2004). LBA is a simple model, based on the concept that independent accumulators of the decision compete towards a common response threshold (Brown & Heathcote, 2008). The LBA uses linear deterministic accumulation and also belongs to the family of sequential sampling models. However, in comparison to the diffusion model the LBA simplifies the decision-making process by omitting within trial variation, and response competition in the decision process, assuming that evidence is accumulated in a linear manner towards either response option. In addition, the LBA assumes that evidence is accumulated at discrete, equally spaced time steps (Ratcliff & Smith, 2004) with an absolute stopping rule. As such, I chose to employ the DDM in the current chapter based on its' methodological appropriateness and wealth of literature supporting it as a method of investigating RT in older adults.

One implementation of the DDM is the EZ model (Wagenmakers et al., 2007); a simplified version of the original diffusion model which is designed to estimate three primary outcome variables (drift rate [v], boundary separation [a], and non-decision time [t]) from mean RT, accuracy (proportion correct), and variance of response times for correct decisions (Figure 6.2).

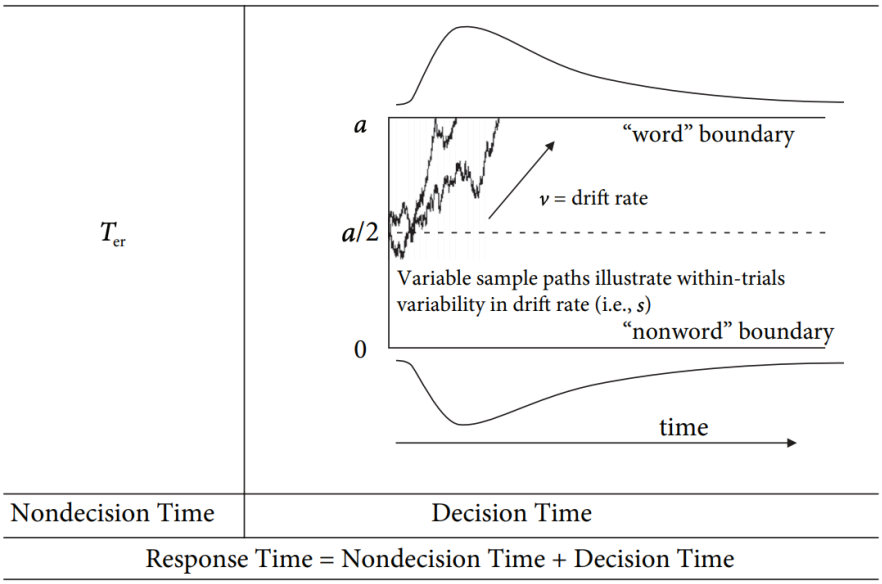


Figure 6.2 The EZ-diffusion drift model, using the application of a lexical-based RT task. As above, the decision is modelled by fitting reaction times to return estimates of non-decision time (perceptual and motor element of decision), boundary threshold (level or boundary to which information must accrue in order to 'push' the choice), and drift rate (efficiency and quality of the drift or decision process). Where a= boundary separation value, $T_{er}$ =non-decision time, and v = drift rate.

The EZ model is a simple model of the DDM, the mathematical basis of which is described in detail in Wagenmakers et al (2007). As shown in Figure 6.2, on the basis that within the EZ model, z (across trial variation in starting point) = a/2, the EZ model estimates boundary separation value using equation 6.2

$$a = \frac{s^2 \operatorname{logit}\left(P_c\right)}{v}, \tag{6.2}$$

Where Pc = proportion correct, and where:

$$\operatorname{logit}\left(P_c\right) \equiv \log\left(\frac{P_c}{1-P_c}\right). \tag{6.3}$$

Drift rate (v) is then calculated as follows (equation 6.4)

$$v = \operatorname{sign}\left(P_c - \frac{1}{2}\right) s \left\{ \frac{\operatorname{logit}\left(P_c\right)\left[P_c^2 \operatorname{logit}\left(P_c\right) - P_c \operatorname{logit}\left(P_c\right) + P_c - \frac{1}{2}\right]}{VRT} \right\}^{\frac{1}{4}} \tag{6.4}$$

Where: VRT = variance of the diffusion process as described in (Wagemakers, Grasman & Molenaar, 2005), and as calculated by equation 6.5

$$VRT = \left[\frac{as^2}{2v^3}\right] \frac{2y\exp\left(y\right) - \exp\left(2y\right) + 1}{\left[\exp\left(y\right)+1\right]^2}, \tag{6.5}$$

Where $y = -va/s^2$. After calculating both v and a, mean decision time (MDT), which refers to the mean time until reaching a response threshold, is determined using equation 6.6

$$MDT = \left(\frac{a}{2v}\right) \frac{1-\exp\left(y\right)}{1+\exp\left(y\right)}, \tag{6.6}$$

Finally, as it is known that mean RT is equal to the mean decision time + non-decision time, non-decision time can be derived.

One practical advantage of the EZ model is that it has been shown to outperform comparative models in the fitting of data from reduced trial numbers (<100; van Ravenzwaaij & Oberauer, 2009). In addition, the EZ model has also been shown to be sensitive to responses which may arise from sources outside the diffusion process assumptions (Ratcliff & McKoon, 2008). These advantages do come at the compromise that EZ does not provide estimation of intertrial variability. However, this is outweighed by the model's

appropriateness in smaller sample sizes with lower trial numbers which is beneficial in my study of age- and DLB-related differences.

DDM evidence in healthy ageing so far suggests that older adults show increased boundary separation values, and prolonged non-decision time, despite no difference in accuracy between groups (Ratcliff et al., 2006; Ratcliff, Thapar, Gomez & McKoon, 2004; Spaniol, Madden & Voss, 2006). Non-decision time has been shown to be slower in older than younger participants across a range of different tasks, including letter discrimination (Thapar et al., 2003), signal detection (Ratcliff et al., 2001), brightness discrimination and recognition memory (Ratcliff et al., 2006b). While some studies did not find any age-related differences in boundary separation (Ben-David et al., 2014), others observed an increase in boundary separation value that may reflect a more cautious decision process at older age (Ratcliff, Thapar & McKoon, 2003; Ratcliff, Thapar, Gomez & McKoon, 2004; Ratcliff, Thapar & McKoon, 2006). This would mean that older adults require more evidence to reach a decision threshold than younger adults, and that older participants try to minimize errors despite this leading to slower RTs (Starns & Ratcliff, 2010). However, it is important to note that the boundary separation value can be influenced by instructions to respond either more accurately or with greater speed**.** Ratcliff, Thapar & McKoon (2004) reported approximately equal boundary separation values between older and younger adults when provided with instructions to prioritise accuracy, suggesting that this measure can be influenced by task instructions and that younger adults adopted a more cautious response strategy which was similar to older adults.

Findings regarding the drift rate are less consistent. Drift rate does not appear to change much with age and if so, modest age-related drift rate lengthening were observed only in tasks requiring memory recall (Ratcliff et al., 2011). For instance, in tasks involving episodic and semantic memory retrieval non-decision time was found to significantly increase in older adults, while only small age-related increases in drift rate was reported (Spaniol, Madden & Voss, 2006). This is also true for performance on perceptual tasks, which show that older adults have longer non-decision elements of processing, and a more conservative decision boundary separation value (Ratcliff, Thapar & McKoon, 2003; Thapar, Ratcliff & McKoon, 2003) but no age-related difference in drift rate. Together these findings seem to suggest that drift rate remains relatively preserved in older adults, and that age-related changes in this measure are more reflective of a shift in response time strategy, in which perceptual encoding and motor response is increased (Ratcliff, Thapar, Gomez & McKoon, 2004).

There are only a few studies that have investigated the microstructural correlates of these age-related changes in DDM parameters. Findings suggest a positive relationship between radial diffusivity in white matter in the corpus callosum and non-decision time (Yang et al., 2015). Evidence has also suggested that a more cautious threshold setting with ageing is related to reduced white matter integrity, as indicated by estimated tract integrity (FA) between the frontal cortex and the corticospinal tract (Forstmann et al., 2011).

These findings are consistent with work demonstrating that functional connectivity of frontoparietal activation, as assessed using fMRI and DTI combined is also related to age-related variability in drift rate (Madden et al., 2010). Moreover, more recent work has also highlighted a relationship between non-decision time and age which was mediated by BOLD signal changes in the fronto-parietal regions (Madden et al., 2020). Despite this, to the best of my knowledge no studies so far have examined the microstructural properties of white matter pathways in brain networks underpinning DDM parameter changes in ageing using more advanced diffusion weighted imaging techniques such as CHARMED. As I have shown in Chapter 4, CHARMED FR provides a more sensitive index of white matter microstructure than conventional DTI indices and hence may be more suitable to study the white matter correlates of age-related decision making and response speed differences. I hypothesised that age-related increases in boundary separation value may be related to reductions in FR particularly in fronto-parietal connections, as these tracts are key in higher visual processing.

Furthermore, although there is some evidence suggesting that metabolic changes, particularly in GABA, are involved in response inhibition and distraction suppression (Kondo et al., 2018; Silveri et al., 2013; Sumner et al., 2010), but to my knowledge the relationship between DDM parameters and brain metabolites in ageing has not been investigated yet. As such, it was hypothesised that lower OCC GABA would be related to lengthened non-decision time respectively, as non-decision time represents the perceptual element of RT and reductions in OCC GABA has been found to be key in age-related impairments in perception (Gao et al., 2013).

In summary, previous literature demonstrates that older adults consistently show changes in boundary separation and non-decision parameters following diffusion modelling, indicating a more cautious approach in the accumulation of sensory evidence in older age. Older adults tend to make slower decisions which avoid errors, in comparison to younger adults who attempt to balance speed and accuracy (Starns & Ratcliff, 2010). Despite this, it remains unclear what age-related processes in the brain may underlie these changes in perceptual decision making with age. Some studies have proposed that age-related deterioration in white matter integrity as well as age-related functional changes in fronto-parietal networks may lead to age-related changes in the decision-making processes that are captures by the drift diffusion parameters.

In previous empirical chapters, I have shown that older adults had longer response latencies than younger adults when completing mid to higher level visual tasks. The objective of the current chapter was to further investigate the nature of this age-related response slowing by applying drift diffusion modelling to assess which decision-making components were subject to age-related differences. In other words, the aim of this chapter was to find out whether any - and if so which - of the DDM elements were affected by ageing and if this could account for the observed response slowing in older people. Importantly, I also aimed to investigate the neurochemical and microstructural correlates of any such age-related differences in model parameters. Based on previous evidence summarised above and my observations of age-related changes in

the speed accuracy trade-off, I anticipated that non-decision time and boundary separation values would be increased in older compared with younger adults and that they would contribute to the overall longer RTs. In addition, based on previous findings of non-decision time being related to fronto-parietal activity in older adults, I hypothesised that age-related reductions in SLF microstructure – notably FR – would account for a slowing in non-decision time. In addition, as boundary separation values represent the threshold of evidence accumulation during a trial it was also hypothesised that ACC metabolites, notably GABA, may be related to boundary separation. This was anticipated as wider boundary separation values have been related to increased inhibitory process (Rawji et al., 2020), which are also associated with GABA in the ACC. It was anticipated that drift rate would be relatively similar between groups.

To investigate these hypotheses, I applied the EZ drift diffusion model to RT data from a modified ANT task and constructed regression models using microstructural and metabolic predictors to determine which neural substrates may underlie DDM parameters. A modified version of the Attention Network Task (ANT) was used to assess attention performance, as has previously been employed in a DDM investigation (O'Callaghan et al., 2017). The ANT was modified for use in the current experiment for two main reasons. Firstly, the modified ANT removed the cueing and spatial conditions typically included in the regular ANT. This was done in order to minimise the potential effect of these conditions (and order of these conditions presented) on DDM parameters. For example, two more 'difficult' cueing conditions presented by chance may result in longer boundary separation value, where this may not be an accurate reflection of performance. In addition, as the spatial and cueing conditions were not required in the calculation of DDM parameters, these were omitted. Secondly, as the ANT used in Chapter 3 was designed for DLB patients' participation and thus limited the number of trials, the current ANT was modified to present more trials in order to maximise RT information from each participant and increase validity of DDM parameter estimation. To establish neural predictors of DDM, metabolite and microstructural measurements were entered as predictors with each DDM parameter entered as dependent variables to mitigate the risk of overfitting. As no evidence with regards to the metabolic underpinnings of drift diffusion parameters exists, I investigated whether metabolic measurements would predict DDM parameters in a linear regression model. I also ran a separate regression model to test whether the microstructural measurements would also predict DDM parameters. Finally, to investigate the group specific relationships between DDM parameters, microstructure, metabolites and SAT performance, individual correlations were conducted.

## 6.2 Methods

### 6.2.1 Participants

Participants from younger (n=25) and older (n=25) control groups who had previously had an MRI scan (Chapter 4) and had taken part in cognitive testing (Chapter 3) were invited back to complete one additional attentional testing session. Participants from the initial study who declined or were unable to attend were a total of 1 older and 3 younger participants. These dropouts were replaced by newly recruited participants,

who completed both visual and attentional testing, further attentional testing, and scanning according to the same protocol. Demographic details of the sample are reported in Table 6.1. For those participants who had previously completed the full cognitive test battery and MRI scanning, only additional informed written consent was sought for completion of the modified ANT. For those participants who had not, full written informed consent was obtained in accordance with the Declaration of Helsinki. For those participants who had not previously been assessed, demographic details and assessments (FRACT, MOCA, ACE, TOPF-UK) were obtained as previously described (Chapter 3). The ANT was then completed, and MRI scanning took place following cognitive testing on the same day.

Table 6.1 Participant demographic information for younger and older adult groups for drift diffusion model (DDM) analysis. F=female

| | Young (N=25) | | Old (N=25) | |
|---|---|---|---|---|
| | **Mean** | **Standard deviation** | **Mean** | **Standard deviation** |
| *Age* | 21.61 | 2.81 | 68.36 | 6.11 |
| *Education* | 21.18 | 2.45 | 20.64 | 4.31 |
| *Sex* | F (14) | | F (15) | |

### 6.2.2 Materials and procedure

#### 6.2.2.1 Modified Attention Network Task (ANT)

The modified ANT stimuli consisted of five horizontal arrows presented on the screen in which participants were instructed to attend to the central arrow as the target. Central arrows were flanked by horizontal lines (neutral condition), arrows facing in different directions to the target (incongruent condition), or arrows facing in the same direction as the target (congruent condition). During this version of the ANT, stimuli were presented in the same central position on the screen following the presentation of a fixation cross. Participants viewed the screen from a seated position, 400mm from the computer screen (details of equipment as in Chapter 3). Participants were instructed to maintain focus on the central fixation point of the screen and respond as quickly and accurately as possible. In accordance with the original study (Fan et al., 2002), these stimuli subtended 3.08° of visual angle. Fixations were presented for a random variable length of time between 400-1600ms and target stimuli were presented for a maximum of 1700ms. Participants completed 96 trials (32 trials per condition) in each block, for a duration of 5 blocks. Between blocks, participants were instructed to rest for 30 seconds, before being given a 5 second count-down into the following block. The entire task totalled 480 trials and took approximately 12-15 minutes to complete.

#### 6.2.2.2 Drift Diffusion Model (DDM)

DDM parameters were calculated using an in-house R based custom script provided by Craig Hedge with consent. Following standard checks for outliers (as described in Chapter 2), raw RT and accuracy data for each participant for congruent, neutral and incongruent trial conditions were input into the script in R Studio (v 1.1.463). The script first calculated means and variances of correct RTs. Incorrect trials were not included in the remainder of the analysis (average retained trials = 469). Following this, the script calculated DDM parameters using the equation provided in Wagenmakers et al., (2007) described above, under the assumption that trial-to-trial variability is zero and the starting point of each decision process is equidistant from the response boundaries (Schmiedek et al., 2007). This resulted in average estimates for non-decision, boundary separation and drift rate for each participant. Details of the mathematical basis for the EZ model can be found in Wagenmakers, Van der Maas & Grasman, (2007).

### 6.2.3 Statistical analyses

Group differences in DDM parameters were assessed using MANOVA. RT, accuracy, RT variance and SAT outcomes were also entered into this MANOVA. Although group differences in metabolites and microstructure are reported in Chapter 4, the group assessed in this chapter consisted of some different participants as described. Therefore, microstructure and metabolites were initially compared between groups to ensure age-related differences were observed using non-parametric Mann-Whitney U tests. DDM parameters were entered into separate linear regression models as dependent variables. Mann-Whitney U tests were used in the assessment of brain measurements as in Chapter 4, due to the non-normal skewed distribution of these parameters in both younger and older groups.

EZ parameters were entered into three separate linear regression models as dependent variables. In the first model, DDM parameters were entered as dependent variables and age, sex, education and metabolites were entered as predictors. The second model followed the same format, however microstructural parameters were entered as predictors in place of metabolite measurements. Following this, non-parametric correlations (Spearman's Rho) were conducted between significant predictors and DDM indices, and DDM parameters and SAT to confirm the directionality and significance of the relationships.

## 6.3 Results

### 6.3.1 Group differences in DDM parameters

A significant omnibus effect of group was present for DDM, RT, accuracy and variance, and SAT outcome measures as listed below in Table 6.2 ($F(16,24)=61.45$, $p=<.001$; Wilk's $\Lambda = 0.215$, partial $\eta^2=.785$). Mean non-decision time and mean boundary separation value were significantly longer in older adults in comparison to younger adults. Significant group differences were present in non-decision time (t) ($F(1,49)=4.857$, $p=.034$) and boundary separation (a) ($F(1,49)=5.341$, $p=.026$), with older participants

having greater values for each parameter. No group difference in drift rate was present (F(1,49)=.001, p=0.971) (Figure 6.3).

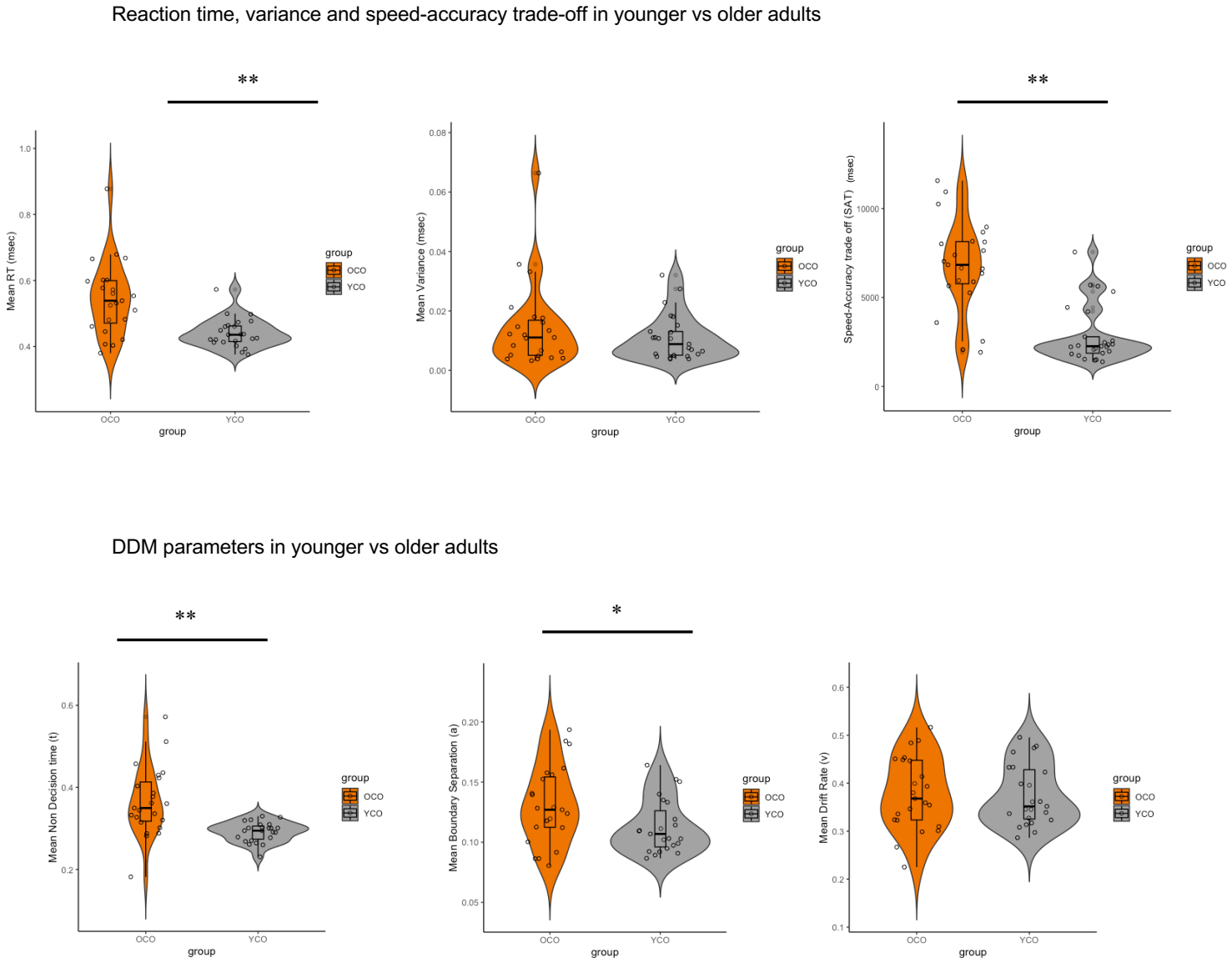


Figure 6.3 Group comparisons between older and younger adults' mean RT, RT variance, SAT performance and DDM parameters. MANOVA results showed mean non-decision time (perceptual and motor processing) and mean boundary separation values (information threshold for decision making) are significantly greater in older adults than younger adults. OCO=older control participants (orange), YCO=younger control participants (grey). **p<.001, *p<.05

Table 6.2 Mean and standard deviation values for age, education, RT and diffusion parameters, and between-subjects effects. RT = reaction time, MOCA = Montreal cognitive assessment **p<.001 *p<.05

| | Young (N=25) | | Old (N=25) | | |
|---|---|---|---|---|---|
| | **Mean** | **Standard deviation** | **Mean** | **Standard deviation** | **MANOVA between-subjects effects** |
| *Age* | 21.61 | 2.81 | 68.36 | 6.11 | F(1,49)=124.6, p<.001** |
| *Education* | 21.18 | 2.45 | 20.64 | 4.31 | F(1,49)=.015, p=.903 |
| *Visual Acuity* | 1.85 | .239 | 1.82 | .309 | F(1,49)=.151, p=.699 |
| *MOCA* | 28.84 | 1.31 | 29 | 1.18 | F(1,49)=.298, p=.588 |
| *Congruent RT* | .441 | .0468 | .537 | .107 | F(1,49)=9.19, p=.004* |
| *Incongruent RT* | .455 | .0463 | .554 | .106 | F(1,49)=9.21, p=.004* |
| *Neutral RT* | .436 | .0461 | .529 | .112 | F(1,49)=8.62, p=.006* |
| *Mean RT* | .444 | .046 | .541 | .108 | F(1,49)=12.133, p=<.001* |
| *Congruent RT variance* | .0112 | .009 | .014 | .014 | F(1,49)=.283, p=.598 |
| *Incongruent RT variance* | .0114 | .008 | .015 | .013 | F(1,49)=1.45, p=.235 |
| *Neutral RT variance* | .0102 | .007 | .013 | .015 | F(1,49)=.878, p=.355 |
| *Mean variance* | .0109 | .007 | .014 | .014 | F(1,49)=1.360, p=.249 |
| *Congruent accuracy* | 96.86% | .052 | 96.5% | .072 | F(1,49)=.001, p=.972 |
| *Incongruent accuracy* | 97.65% | .019 | 99.2% | .011 | F(1,49)=3.68, p=.052 |
| *Neutral accuracy* | 98.35% | .019 | 99.3% | .008 | F(1,49)=2.49, p=.122 |
| *SAT* | 2876.98 | 1627.07 | 6785.53 | 1581.57 | F(1,49)=40.06, p<.001* |
| *Mean Non-decision (t)* | .295 | .048 | .342 | .091 | F(1,49)=4.857, p=.034* |
| *Mean Boundary separation (a)* | .114 | .023 | .162 | .090 | F(1,49)=5.341, p=.026* |
| *Mean Drift rate (v)* | .376 | .068 | .375 | .074 | F(1,49)=.001, p=.971 |

Group differences in brain measurements are described in Table 6.3. Brain measurements are generally consistent with the group comparisons described earlier in the thesis (Chapter 4), with age-related declines in microstructural integrity in many of the selected tracts of interest, and age-related differences in NAA in ACC and PPC, Glx in ACC and PPC and myoinositol in PPC.

Table 6.3 Mean and standard deviation values for metabolites and diffusion parameters, and Mann Whitney U comparisons. Significant group differences are shown in bold text. FA = fractional anisotropy, MD = mean diffusivity, FR = restricted fraction, RD = radial diffusivity, L1 = axial diffusivity, OCC = occipital cortex, ACC = anterior cingulate cortex, PPC = posterior parietal cortex **p<.001 *p<.05

| | **Young Mean (SD)** | **Old Mean (SD)** | **Mann-Whitney** | **Young Mean (SD)** | **Old Mean (SD)** | **Mann-Whitney** |
|---|---|---|---|---|---|---|
| | | *Left* | | | *Right* | |
| ***FA fornix*** | **.423(.0175)** | **.371(.02)** | **U=21, p<.001**** | | | |
| *FA optic radiation* | .470(.037) | .450(.043) | U=197, p=.096 | **.474(.027)** | **.453(.037)** | **U=174, p=.031*** |
| ***FA ILF*** | **.442(.019)** | **.425(.025)** | **U=175, p=.020*** | **.446(.018)** | **.424(.023)** | **U=130, p=.001*** |
| ***FA SLF 1*** | **.470(.047)** | **.425(.031)** | **U=114.5, p<.001**** | .448(.040) | .426(.042) | U=224, p=.190 |
| ***FA SLF 2*** | **.405(.041)** | **.379(.028)** | **U=173, p=.018*** | .426(.040) | .379(.028) | U=195, p=.056 |
| *FA SLF 3* | .443(.050) | .429(.036) | U=206, p=.093 | **.458(.028)** | **.432(.029)** | **U=154, p=.006*** |
| ***MD fornix*** | **.00092(.00003)** | **.0010(.00006)** | **U=60, p<.001**** | | | |
| ***MD optic radiation*** | **.00069(.00001)** | **.00073(.00005)** | **U=117, p=.001*** | **.00069(.00001)** | **.00072(.00004)** | **U=115, p=.001*** |
| *MD ILF* | .00070(.00001) | .00071(.00002) | U=211, p=.114 | **.00070(.00001)** | **.00071(.00002)** | **U=185, p=.034*** |
| *MD SLF 1* | .00067 (.00001) | .00068(.00002) | U=202, p=.078 | **.00065 (.00001)** | **.00067(.00002)** | **U=164, p=.011*** |
| *MD SLF 2* | .00066 (.00001) | .00067(.00001) | U=204, p=.085 | .00042(.00004) | .00040(.00004) | U=195, p=.056 |
| *MD SLF 3* | .00065(.00001) | .00067(.00002) | U=194, p=.054 | **.00065(.00001)** | **.00067(.00002)** | **U=164, p=.011*** |
| ***FR fornix*** | **.248 (.018)** | **.216(.019)** | **U=68, p<.001**** | | | |
| ***FR optic radiation*** | **.360(.031)** | **.334(.037)** | **U=179, p=.041*** | **.366(.022)** | **.334(.042)** | **U=127, p=.002*** |
| *FR ILF* | .315 (.015) | .311(.020) | U=261, p=.584 | **.324(.016** | **.309(.02)** | **U=178, p=.024*** |
| ***FR SLF 1*** | **.386(.034)** | **.357(.031)** | **U=141, p=.002*** | .377(.033) | .309(.022) | U=257, p=.529 |
| ***FR SLF 2*** | **.396(.024)** | **.376(.022)** | **U=157, p=.007*** | **.403(.020)** | **.375(.046)** | **U=165, p=.011*** |
| ***FR SLF 3*** | **.400(.031)** | **.378(.029)** | **U=178.5, p=.024*** | **.410(.019)** | **.387(.029)** | **U=154, p=.006*** |
| ***RD fornix*** | **.00068(.00003)** | **.00079(.00006)** | **U=29, p<.001** | | | |
| ***RD optic radiation*** | **.00049(.00002)** | **.00053(.00004)** | **U=117, p=.001*** | **.00049(.00001)** | **.00052(.00003)** | **U=117, p=.001*** |
| ***RD ILF*** | **.00052(.00001)** | **.00053(.00002)** | **U=169, p=.014*** | **.00051(.00001)** | **.00053(.00002)** | **U=126, p=.001*** |
| ***RD SLF 1*** | **.00048(.00003)** | **.00052(.00002)** | **U=118, p<.001**** | .00050(.00002) | .00052(.00003) | U=167, p=.178 |
| ***RD SLF 2*** | **.00051(.00002)** | **.00053(.00002)** | **U=140, p=.002*** | **.00049(.00002)** | **.00051(.00002)** | **U=163, p=.010*** |
| ***RD SLF 3*** | **.00049(.00002)** | **.00051(.00003)** | **U=183.5, p=.032*** | **.00048(.00001)** | **.00051(.00002)** | **U=124, p=.001*** |
| ***L1 fornix*** | **.0014(.00003)** | **.00147(.00009)** | **U=105, p<.001**** | | | |
| *L1 optic radiation* | .0010(.00005) | .0011(.00008) | U=174.5, p=.052 | .0010(.00004) | .0011(.00008) | U=183, p=.080 |
| *L1 ILF* | .0010(.00003) | .0010(.00004) | U=262, p=.965 | .0010(.00002) | .0010(.00003) | U=259, p=.921 |
| ***L1 SLF 1*** | **.0010(.00003)** | **.0010(.00003)** | **U=143, p=.005*** | **.0010(.00003)** | **.0010(.00002)** | **U=123, p<.001**** |
| *L1 SLF 2* | .00096(.00003) | .00095(.00003) | U=215, p=.201 | .00098(.00004) | .00097(.00004) | U=251, p=.609 |
| *L1 SLF 3* | .00098(.00004) | .00098(.00002) | U=256, p=.685 | .00099(.00002) | .00099(.00002) | U=231, p=.348 |
| *OCC GABA/* $H_20$ | 4.70(.48) | 4.84(.61) | U=251.5, p=.457 | | | |
| *OCC Glx* | 13.67(.87) | 13.76(2.1) | U=256.5, p=.522 | | | |
| *OCC NAA* | 18.11(1.9) | 17.96(2.3) | U=260, p=.956 | | | |
| *OCC myoinositol* | 9.89(1.2) | 9.08(1.86) | U=181, p=.072 | | | |
| *OCC choline* | 1.80(.20) | 1.84(.28) | U=227, p=.434 | | | |
| *OCC creatine* | 10.87(.85) | 10.90(1.42) | U=235.5, p=.552 | | | |
| *ACC GABA/* $H_20$ | 4.14(.28) | 3.96(.43) | U=213, p=.124 | | | |
| ***ACC Glx*** | **15.37(.90)** | **14.46(1.78)** | **U=171.5, p=.017*** | | | |
| ***ACC NAA*** | **14.59(1.07)** | **12.39(2.4)** | **U=100, p<.001**** | | | |
| *ACC myoinositol* | 10.32(1.12) | 9.27(2.44) | U=201, p=.074 | | | |
| *ACC choline* | 2.60(.25) | 2.51(.442) | U=264, p=.628 | | | |
| *ACC creatine* | 10.14(.635) | 9.43(1.42) | U=214, p=.129 | | | |
| *PPC GABA/*$H_20$ | 4.23(.37) | 4.44(.466) | U=212.5, p=.183 | | | |
| ***PPC Glx*** | **14.5(.96)** | **13.71 (1.5)** | **U=177.5, p=.037*** | | | |
| ***PPC NAA*** | **17.16(2.07)** | **15.52 (2.3)** | **U=160, p=.009*** | | | |
| ***PPC myoinositol*** | **10.19(1.25)** | **8.97(2.15)** | **U=180.5, p=.027*** | | | |
| *PPC choline* | 2.10(.23) | 2.14 (.38) | U=254.5, p=.496 | | | |
| *PPC creatine* | 2.10(.22) | 10.15 (1.51) | U=241, p=.337 | | | |

### 6.3.2 Neural predictors of DDM performance

Three separate linear regression models were conducted that entered age, sex and education and all metabolite measurements as predictors to assess how much variance they accounted for in the three DDM parameters of non-decision time, boundary separation and drift rate. Age was also seen to significantly predict non-decision time, boundary separation and drift rate in linear regression models. Mean non-decision time (t) was significantly predicted by age in the first linear regression model (adj $R^2$ = 0.254, beta=0.519, p<.001). NAA in the ACC was also seen to predict mean non-decision time (adj $R^2$=0.058, beta=-0.278, delta $R^2$=0.09, p=0.048). Age also significantly predicted boundary separation value (a) (adj $R^2$=0.410, beta=0.246, p=0.008) but no metabolites were significant. Finally, no entered predictors were shown to significantly predict drift rate.

The same linear regression models as described above were also used to test for microstructural parameters as predictors together with age, sex and education. Non decision time (t) was seen to be significantly predicted by MD in the left SLF 3 (adj $R^2$=0.326, beta=0.553, p=.004), MD in the SLF 2 right (adj $R^2$=0.436, beta=0.484, p<.001), MD in right optic radiation (adj $R^2$=0.529, beta=0.496, p=.002), RD in left SLF 3 (adj $R^2$=0.297, beta=0.394, p=.004). Boundary separation (a) was significantly predicted by age (adj $R^2$=0.101, beta=0.437, p=.002), MD in left optic radiation (adj $R^2$=0.070, beta=-0.763, p<.001), FR in the fornix (adj $R^2$=0.058, beta=-0.836, p<.001), FR in right ILF (adj $R^2$=0.342, beta=0.581, p=.002) and L1 in left optic radiation (adj $R^2$=0.131, beta=-0.540, p<.001). Drift rate was predicted by FA in the left ILF (adj $R^2$=0.062, beta=-0.468, p=.005), MD in left SLF 3 (adj $R^2$=0.058, beta=.498, p=.008), L1 in the right ILF (adj $R^2$=.048, beta=.548, p=.001), and L1 in left ILF (adj $R^2$=.200, beta=-0.314, p=.026), however drift rate did not show any age-related differences.

### 6.3.3 Relationships between DDM parameters, SAT and neural predictors in older and younger adults

Mean DDM parameters were correlated with SAT to determine how these relationships differed between younger and older groups (Figure 6.4).

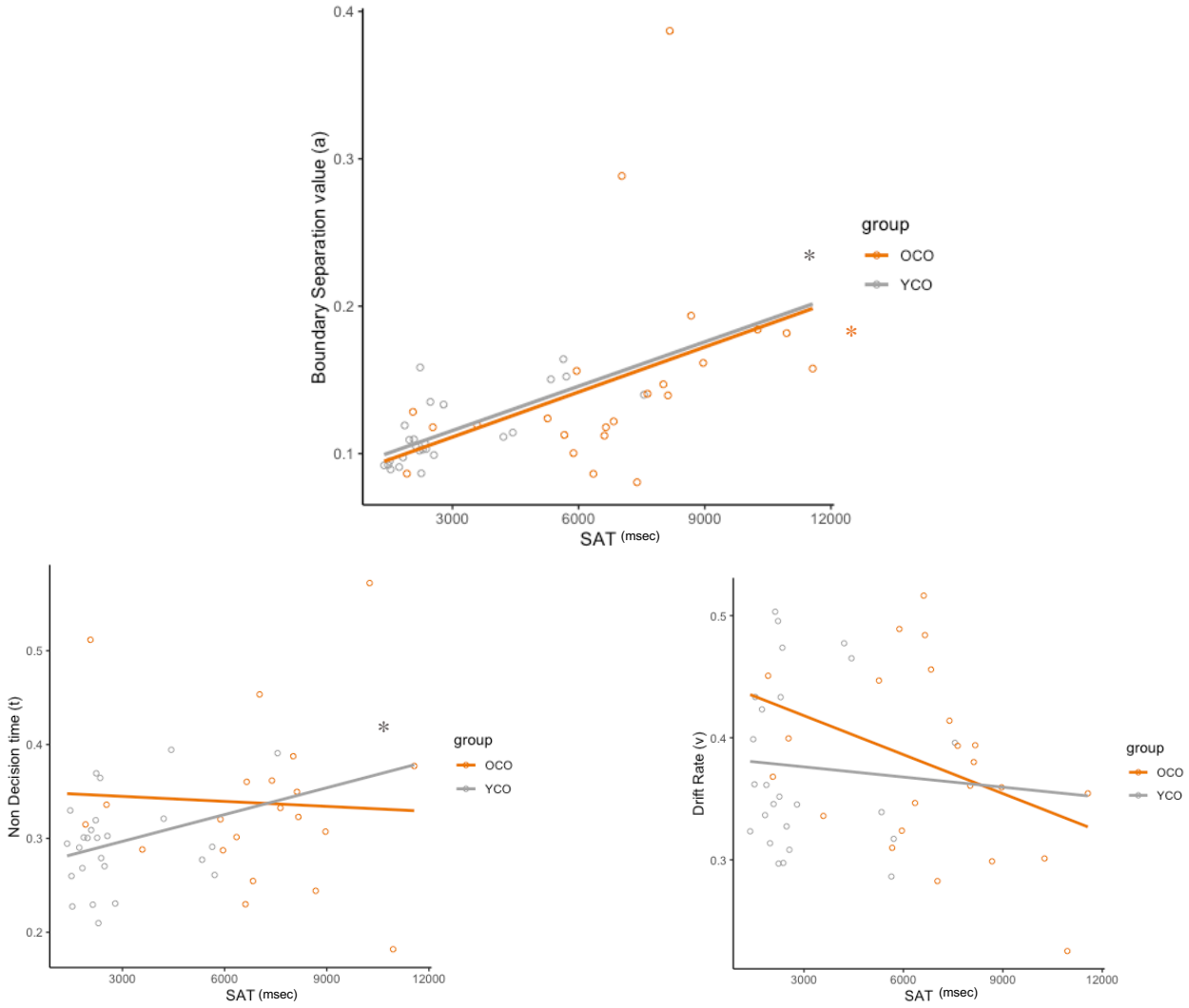


Figure 6.4 Spearman's correlations between mean non-decision time, mean boundary separation, drift rate and speed-accuracy trade-off (SAT) in both younger and older groups. Younger adults show a significant positive correlation between mean non-decision time and SAT, and both groups show a significant positive correlation between SAT and boundary separation **p<.001, *p<.05

In younger adults, SAT was positively correlated with mean boundary (rho=.412, p=.041), and mean non decision time (rho=.388, p=.049) but not mean drift rate (rho=-.373, p=.067). In older adults, SAT was significantly correlated with boundary separation (boundary: rho=.322, p=.04) but not drift rate or non-decision time (drift: rho=.130, p=.535; non-decision: rho=.196, p=.381) (Figure 6.4).

Non-parametric correlations were conducted between predictors which were significant in the linear regression models above and their corresponding DDM parameter to determine directionality and strength of relationship in the two separate age groups. Mean non-decision time and NAA in ACC showed a

significant negative correlation in younger adults (rho=-0.361, p=.009) but no correlations for older adults (rho=.052, p=.823) (Figure 6.5).

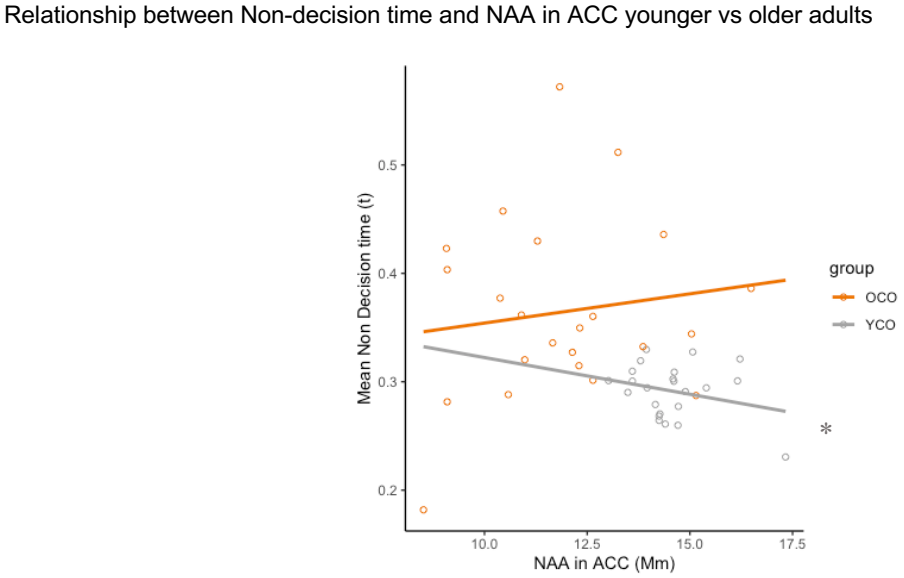


Figure 6.5 Relationship between non-decision time (perceptual and motor processing time) and NAA in ACC. Spearman's correlation between mean non-decision time and NAA in ACC in both younger and older groups. A significant negative correlation was show between NAA in ACC and mean non-decision time in younger adults only **p<.001, *p<.05

Mean non decision time and MD in left SLF 3 (rho=0.492, p=<.001), and RD in left SLF 3 (rho=0.369, p=.008) were also significantly correlated in older adults, but not younger adults (MD SLF3: rho= .298, p=.148; RD in SLF3: rho=.010, p=.962) (Figure 6.6).

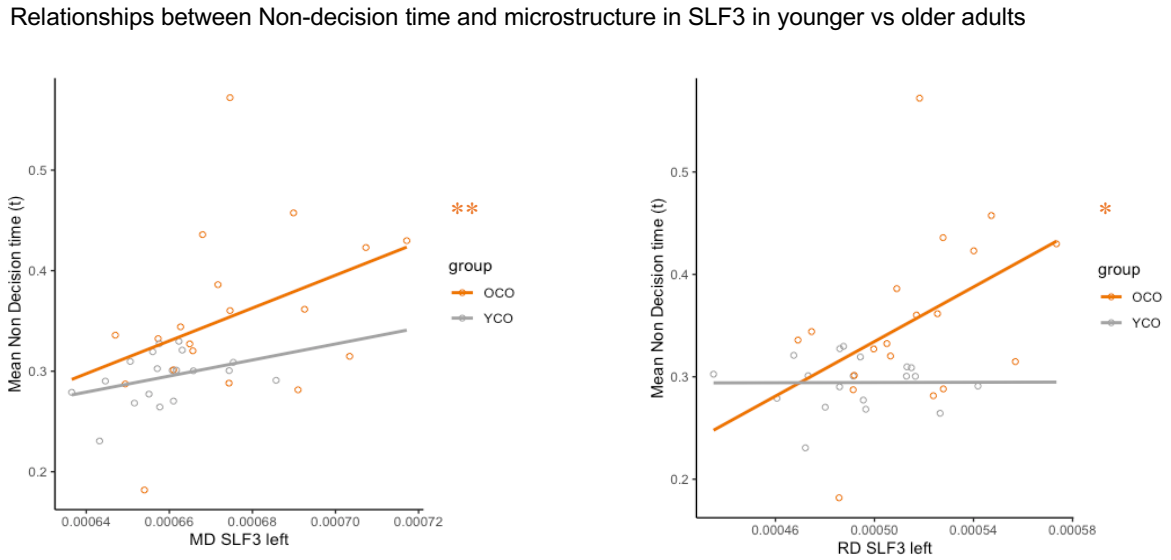


Figure 6.6 Relationship between non-decision time (perceptual and motor processing time) and superior longitudinal fasciculus 3 microstructure. Spearman's correlations between mean non decision time and microstructural tract parameters in both younger and older groups. Significant positive correlations were shown between mean non-decision time and MD/ RD in SLF3 in the older group **p<.001, *p<.05

Mean boundary separation value and L1 left optic radiation (rho=-0.350, p=0.014) were significantly negatively correlated in older adults, but not younger adults (rho=-.157, p=.454) (Figure 6.7).

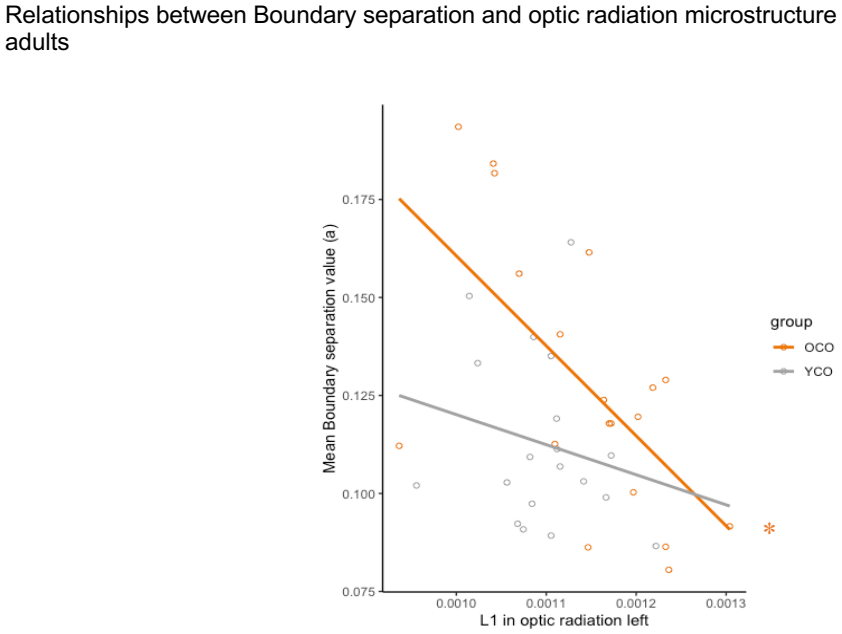


Figure 6.7 Relationship between boundary separation time (information decision threshold) and optic radiation microstructure. Spearman's correlations between mean boundary separation and optic radiations in both younger and older groups. A significant negative correlation between L1 in optic radiation and boundary separation was present in older adults **p<.001, *p<.05.

## 6.4 Discussion

In the current chapter I further investigated the underpinnings of age-related response slowing following on from my findings in Chapter 3 which showed age-related lengthening of RT but maintained accuracy. I investigated this by applying the EZ DDM and assessing any age-related differences in EZ parameters. Furthermore, I explored white matter microstructural and grey matter metabolite predictors of these parameters. Previous DDM research suggested that age-related increases in non-decision time and boundary separation contributed to the overall slowing in RT with ageing (Ratcliff et al., 2012). In addition, some evidence suggested that age-related alterations in the frontoparietal attention network may underlie these changes. However, previous studies primarily adopted standard morphology and DTI based measurements to assess structural brain-function relationships. Instead, I adopted advanced metabolites and diffusion weighted imaging measurements to further probe the neural underpinnings of age-related differences in decision making components that contribute to overall response slowing in ageing (Madden et al., 2009; Madden et al., 2020). Based on previous research, I anticipated that non-decision time and boundary separation values would be larger in older adults compared to younger adults. I also hypothesised that non-decision time would be related to SLF white matter microstructure, as the SLF is the most prominent intra-hemispheric white matter connection between the frontal and the parietal cortices and is

involved in perceptual and attentional processing. I also hypothesised that non-decision time would be related to OCC GABA/$H_20$, as GABA has been shown to play a key role in visual perceptual abilities (Pitchaimuthu et al., 2017). Finally, I expected boundary separation to be related to GABA/$H_20$ in the ACC, due to previous evidence indicating the role of frontal GABA in evidence accumulation (Takacs et al., 2021).

Consistent with my hypotheses I found greater non-decision time and boundary separation values in older adults in comparison to younger adults. This pattern of results suggests a slowing of perceptual and/or motor elements of RT as reflected in larger non-decision time, as well as a higher boundary of information to be accrued before a decision can be reached as reflected in higher boundary separation values. This pattern of DDM parameters may also underpin the typical age-related shift in SAT. An emphasis on accuracy in place of faster speed has previously been shown to result in increased boundary separation in visual perceptual tasks in younger adults (Zhang & Rowe, 2014) and older adults (Starns & Ratcliff, 2010), suggesting that longer SATs are related to increase boundary separation values in both younger and older adults. However, my results indicate that age-related increases in SAT are due to both impairments in lower-level perceptual processing, as indicated by longer non-decision time, and greater boundary separation values. I posited that, as older adults tend to adopt a more cautious approach, this increase in SAT and thus boundary separation values, which was demonstrated in the significant positive correlation between boundary separation and SAT. As I have also shown however, older adults have impaired visual perceptual performance which may then underlie lengthening of non-decision times, however this was not evident in correlation analysis. As such, increased SAT in older adults, leading to the adoption of a slower and more cautious processing strategy, is likely to be the result of by greater boundary separation values, indicating an increased threshold of information required to allow a decision.

Further to this, I sought to determine which brain measurements predicted DDM parameter performance in younger and older adults. Consistent with my hypotheses, I showed that non-decision time was predicted by differences in SLF and optic radiation microstructure in older adults and NAA in ACC in younger adults. Interestingly and not consistent with my prediction, I also showed that boundary separation was predicted by ILF and optic radiation microstructural integrity and drift rate was predicted by ILF and SLF microstructural integrity. Drift rate was significantly predicted by microstructural integrity in ILF and SLF but showed no age-related differences.

Finally, I showed significant negative correlations between non-decision time and NAA in ACC in younger adults, and positive correlations between non-decision time and MD and RD in SLF 3 in older adults. A significant negative correlation was present between boundary separation and L1 in optic radiation in older adults.

### 6.4.1 Age-related differences in non-decision time are predicted by fronto-parietal white matter integrity and anterior cingulate metabolites

Non-decision time was shown to be predicted by microstructural differences in the optic radiation and SLF. Significant positive correlations suggested that greater diffusivity in the SLF was associated with longer non-decision times in older adults. Non-decision time has previously been linked to fronto-parietal fMRI activity in older adults, therefore these observed findings complement and extend these results (Madden et al., 2020). Similarly, age-related increases in variability and reductions in visual functions requiring the suppression of irrelevant perceptual information were associated with individual variability in fronto-parietal white matter microstructure (Chadick et al., 2014). Thus, age-related deterioration in the SLF - a white matter pathway crucial for the effective communication within the fronto-parietal attention network and hence between sensory and motor networks - is likely to contribute to the overall slowing of sensory and/or motor processing components reflected in the non-decision time. In addition, it has also been documented that older adults show reduced functional connectivity in fronto-parietal networks and that this is related to increased distractibility and diminished attentional focus with age (Campbell et al., 2012, Madden et al., 2020). Thus, the observed pattern of associations between age-related variation in non-decision time and SLF microstructure may reflect age-related difficulties in perceptual suppression or inhibition (Chadick et al., 2014) and/or a greater reliance in top-down processing as a response to diminished low-level sensory input (Lai et al., 2020). As top-down processing is thought to occur in the dorsal processing stream in frontal and parietal brain regions (Gilbert & Sigman, 2007), non-decision time may capture elements of both bottom-up and top-down perceptual changes in ageing that are mediated by the dorsal attention processing networks. My results suggest that older adults attempt to rely on top-down processing - due to fronto-parietal tracts showing significant relationships with non-decision time - but that these connections have lower WM integrity and thus result in longer non-decision times. This interpretation of my findings is in line with previous findings of age-related mediation of the relationship between frontoparietal activation and impaired top-down attention (Madden et al., 2014). My findings add to the evidence by demonstrating that such relationships can be identified with a greater sensitivity using advanced multi-shell diffusion imaging. Moreover, this finding is in line with the frontal ageing hypothesis as they show microstructural impairments in fronto-parietal white matter connections that were linked to impairments in non-decision time.

In addition, I found that non-decision time was negatively related to NAA in the ACC in younger adults. As NAA is thought to be a marker for neuronal health and integrity, and the ACC is linked to inhibitory functioning as it is thought to be part of the anterior salience network responsible for conflict monitoring (Dosenbach et al., 2006), it is possible that reductions in neuronal health in the ACC may contribute to longer non-decision time on the basis of poorer inhibition. The relationship between NAA in the ACC and cognitive inhibitory processes has been shown (Grachev et al., 2001) suggesting that NAA in the ACC may play a role in perceptual interference which may be represented by non-decision time. However, as non-

decision time represents both perceptual and motor aspects of the RT, and NAA in the ACC has also been linked to motor inhibition processes (Leland et al., 2008; Paus, 2001; Rubia et al., 2001), it is unclear which element of non-decision time may be predicted by metabolite changes in the ACC.

These findings are also interesting, as in the previous chapter lengthening of SAT in older adults was seen to be predicted by NAA, however the relationship between non-decision time and SAT was only significant in younger adults. This indicates that NAA in ACC may play a crucial role in speed of processing, but that this may not be age group specific. This warrants further investigation to confirm the underlying metabolic correlates of non-decision time.

Finally, lengthened non-decision time was predicted by increased diffusivity in the SLF 3 and in Chapter 5 I also showed that visual contrast was predicted by increased diffusivity in the SLF 3. The SLF 3 has been shown to be responsible in part for automatic capture of visuo-spatial attention by visual targets (De Schotten et al., 2011). Thus, an age-related reduction in microstructural integrity of the SLF may lead to longer non-decision time due to difficulties in such perceptual processes. In older adults, visual contrast performance is poorer and this is predicted by MD in the SLF 3, which also predicts lengthened non-decision time in older adults. To conclude, the relationship between frontal metabolites, fronto-parietal microstructure and SAT is apparent in Chapter 5, and here these predictors are shown to be specifically related to the perceptual element of RT processing, which is lengthened in older adults.

### 6.4.2 Age-related differences in boundary separation are related to temporal, fornix and optic radiation microstructure

I also showed that boundary separation was significantly predicted by microstructural differences in the optic radiation, ILF and fornix. Correlations showed that greater boundary separation values in older adults were related to lower L1 in the optic radiations. No significant correlations were found between boundary separation and neural substrates in younger adults. In contrast and inconsistent with my hypothesis I did not observe any relationships between individual differences in GABA/$H_20$ in the ACC and differences in boundary separation. The findings may be consistent with previous results which have shown that differences in boundary separation were related to striatal activity, of which the fornix is connected (Kühn et al., 2010). However, there are no clear associations in previous literature between white matter integrity in optic radiation and boundary separation in younger or older adults. Estimates of white matter microstructural integrity were also seen to predict SAT performance in younger adults and ANT alerting performance in younger adults, with better performance being predicted by lower levels of diffusivity and higher fractional anisotropy. As such, my findings may support the relationship between faster SAT strategy, boundary separation and optic radiation microstructure, but only in younger adults. It is unclear the role the optic radiations may play in boundary separation estimates, therefore further replications may be required to confirm this finding.

Previous results have identified the role of inferior temporal activity in evidence accumulation during perceptual tasks (Ploran et al., 2007). It has been shown that the inferior temporal cortex is involved in consolidation of the decision (Grossberg & Huang, 2009) represented by reaching a boundary of decision. This may then explain why differences in white matter microstructure in the fornix was shown to be a predictor of age-related differences in boundary separation in the current results. The ILF is also thought to play a crucial role in bottom-up visual processing and in the processing of stimulus saliency (Yuki et al., 2020). Thus, the ILF may be vulnerable to a loss of microstructural integrity with age which may impact on processing of stimulus saliency and thus requires older adults to spend longer accumulating evidence. However, these findings warrant further, more detailed investigation.

### 6.4.3 Drift rate is related to temporal and inferior parietal tract microstructure

Drift rate did not significantly differ between younger and older adults; however, my results showed it to be predicted by FA and L1 in the ILF and MD in the SLF3. Evidence has previously shown that drift rate is related to attentional allocation and general functional connectivity, recruiting numerous brain regions (Madden et al., 2010, 2020). As the SLF 3 has been related to the allocation of visuo-spatial attention (De Schotten et al., 2011) my findings are in line with the literature. However, MD in the SLF 3 was also seen to predict non-decision, therefore further investigation of the role of SLF microstructure in DDM parameters is required to disentangle and clarify these results. As non-decision time is an unspecific parameter which captures sensory and motor processes and the integration of these processes, it may be plausible that overlapping brain regions are involved in different DDM parameters. Moreover, information processing speed, to which drift rate is closely related, is associated with temporal lobe oscillations (Chauvière, 2020) and stimulus-related attention has been associated with neural activity in the inferior temporal cortex (Zhang et al., 2011). This may explain why microstructure in the ILF was shown to predict drift rate in this study.

### 6.4.4 Limitations

Despite the novel approach in the current study, a number of limitations should be acknowledged. Firstly, the application of the DDM selected – the EZ model (Wagenmakers, Van Der Maas & Grasman, 2007)– has been well documented in the literature. The model is designed for application in smaller sample numbers and also limited trial numbers, and therefore was appropriate for the current experiment. However, greater trial numbers would also allow for the application of more complex diffusion models, thus also increasing the validity of parameter estimates. One such model – the hierarchical drift diffusion model (HDDM) – is a more complex Bayesian implementation of the classic diffusion model which requires greater trial numbers but uses Bayesian priors to create more accurate parameter estimations.

Moreover, it should be noted that as the EZ-model assumes no variability in the 'starting point' of the decision process, there may be some limitation in it's application in older adults, as it would be expected

that older adults are more variable in their response. Intraindividual variability of RT has been observed to reliably increase in older age (Kochan et al., 2017) and whilst intraindividual variability was not an DDM outcome measure of interest in the current study, it may be a limitation of the application of EZ model in the current study. By limited trial-to-trial variability, it is possible that the lengthening of DDM parameters observed in older age in my results is not a direct measure of lengthened perceptual processing or boundary separation, but includes a larger degree of intraindividual variability. This also provides further support for the potential implementation of more complex models as discussed above which allow this variability to be altered and considered. Despite this, variability in starting point has been shown to have a small impact on the overall response distribution (Voss et a., 2013), and in some cases models with a variability parameter fixed to zero can be superior to more complex models (Schuch, 2016). Whilst it is suggested that further implementations may use greater trial numbers and more complex modelling, the model implemented in the current experiment was appropriate for the current study in older adults, despite its limitations

Moreover, my results have suggested that microstructural integrity better predicts DDM parameters in older adults. However, it is possible that these findings are the result of ageing in general, in which a reduction in microstructural integrity is particularly notable. As such, microstructural changes may be more abundant and varied in older adults, therefore appearing more readily as predictors in this group. In addition, as has been previously discussed, the older adult group in the current experiment was substantially more heterogeneous than the younger adult group, perhaps lending to increased inter-individual variability and thus presenting different results.

### 6.4.5 Future directions

The current results have demonstrated that fronto-parietal microstructural integrity is important in DDM parameters which vary with age. However, the findings that key brain metabolites may be involved in the prediction of performance in these parameters is novel. More specifically, NAA in the ACC was seen to predict non-decision time performance in younger adults which, to my knowledge, has not previously been shown. This is interesting as NAA has been linked to inhibitory and motor functioning and may then support the concept of non-decision time element – which is composed of perceptual and motor aspects - to RT neurobiologically. As such, this area of interest should be considered in future research.

### 6.4.6 Chapter summary

My results showed that non-decision time was predicted by microstructural measures in the optic radiation and SLF. SLF microstructural integrity was related to non-decision time in older adults. This suggests that older adults experience a reduction in efficiency in this network, resulting in lengthened non-decision time. Younger adults showed a relationship between non-decision time and higher NAA in the ACC, suggesting that metabolites in a region responsible for inhibition also play a role in non-decision processing in younger

adults. In addition, boundary separation value was predicted by white matter microstructure in ILF, optic radiation and fornix, indicating that in older adults a lower sensory processing ability has a subsequent effect on boundary separation, coupled with a decline in stimulus salience ability which is governed by the ILF. Drift rate did not differ between younger and older adults but was related to ILF and SLF microstructural integrity. The current results are consistent with previous findings that older adults show slower RTs, including longer non-decision times and wider decision boundaries. These findings provide insight into the decline in connectivity underlying information processing in older adults and may warrant further investigation. Moreover, I found that these behavioural differences were associated with age-related white matter microstructural and metabolic differences in regions of the fronto-parietal attention network, notably the ACC and the SLF, the most prominent fronto-parietal white matter connection.

# Chapter 7 : Impairments in perceptual encoding are related to visual hallucinations in dementia with Lewy bodies: a drift diffusion analysis

## 7.1 Introduction

As demonstrated in Chapter 6, fitting an EZ DDM RT model provided greater insight into age-related slowing of performance and allowed the assessment of different elements involved in response time. From this analysis I showed that greater non-decision time and boundary separation values underlie age-related slowing of reaction times as part of a more cautious response strategy. In Chapter 3, I also compared this age-related slowing with RT performance in four individuals with DLB, who showed large RT variations compared with each other and with the healthy control group. However, this highly varied performance was not necessarily accompanied by much slower RTs as had been previously reported in the literature (Ballard et al., 2001; Wesnes et al., 2013). Bearing in mind the caveat that only four individuals with DLB could be studied, the inferences that could be drawn in Chapter 3 about DLB patients' vision and attention deficits were limited.

Here, I therefore extended the investigation of DLB patients' RT performance by making use of choice RT data from a larger sample of n = 50 patients from the LewyPro database (Donaghy et al., 2018). More specifically the aim of the present chapter was to investigate the nature of RT slowing and variability in DLB by adopting the EZ DDM model to study disease-related differences in the decision-making components that contribute to highly varied RT performance and hence may potentially underpin clinical symptoms of visual hallucinations and cognitive fluctuation in DLB.

The Lewy-Pro study was established to clarify the clinical and cognitive presentation of mild cognitive impairment (MCI) DLB (MCI-DLB) and contribute to diagnostic guidance for clinically identifying MCI-DLB. Exact details of the full cohort are described in Donaghy et al (2018), however all participants were recruited from memory clinics and had clinically recognised MCI, in addition to at least one core clinical symptom of DLB. MCI refers to the stage between normal ageing and dementia, in which cognitive decline occurs, but activities of daily living are relatively preserved. MCI-DLB specifically refers to individuals experiencing mild cognitive deficits in processing speed, executive dysfunction and visuospatial functions, that are likely to progress to DBL (McKeith et al., 2020).

As previously described, DLB is clinically characterized by frequent cognitive fluctuations and complex visual hallucinations alongside rapid eye movement sleep behaviour disorder (RBD) and Parkinsonism (McKeith et al., 2017) Cognitively, DLB patients experience disproportionate impairment in attention and visual perceptual abilities in comparison to both older adults and patients with Alzheimer's disease (AD) (McKeith et al., 2017). However, it remains unclear how these cognitive and perceptual impairments relate to the clinical symptoms in DLB. For instance, visual hallucinations may arise from bottom up

visuoperceptual and top-down attentional impairments (Collerton et al 2005) and similarly, cognitive fluctuations may be related to attentional deficits (Ballard et al., 2001).

A greater slowing of RTs in DLB compared with AD patients and healthy older controls, particularly in tasks with increasing complexity of cognitive processing such as choice RT tasks has been frequently reported. For instance, as discussed earlier DLB patients may show disproportional slowing in flanker performance, but can exhibit the flanker effect when alerted to the trial (Fuentes et al., 2010). Moreover, as also observed in Chapter 4 of this thesis DLB patients exhibit large intraindividual fluctuation in RT performance, that may underpin cognitive fluctuation (Ballard et al., 2001). However, not all studies have found variability in RT performance to be related to visual or attentional performance, thus this link remains unclear (Elder et al., 2016, Landy et al., 2015). Currently, the nature of RT slowing and variability in DLB and their relationship to clinical symptoms is not well understood. To address this, the present chapter adopted the EZ DDM to gain a better understanding of the nature of RT slowing and response variability in DLB patients.

As previously described in Chapter 6, the DDM (Ratcliff, 1978; Ratcliff & Rouder, 1998) assumes that information which drives a decision is accumulated over time until it reaches one of two response boundaries, which form the ultimate response. Overall processing is segmented into several components which contribute to ultimate performance: first, components of processing which do not include active decision, such as perceptual encoding and response execution, represented by 'non-decision time (t)', second, a criteria threshold that information accumulates to represented by 'boundary separation (a)', the rate at which information accumulates towards a decision, represented by 'drift rate (v)'.

While DDM RT models have not previously been fitted to DLB patient data, they have been applied to the related disorder of PD (O'Callaghan et al., 2017). O'Callaghan et al. (2017) applied DDM modelling to CRT performance of PD patients with hallucinations relative to PD without hallucinations and healthy controls. The authors reported slower drift rates in PD patients with hallucinations, as well as shorter perceptual encoding times in all PD patients compared to controls. This pattern of results suggested that the accumulation of sensory evidence was hindered by a perceptual encoding problem. O'Callaghan et al. (2017) proposed that impaired sensory evidence accumulation may lead to reduced information processing quality and an over-reliance on top-down processing in PD, which in turn may underpin visual hallucinations.

Given that both visual and attentional problems are also characteristic of DLB, assessing RT components in more depth may also aid in illuminating the process deficits that contribute to visual hallucination incidence in DLB. Visual hallucinations in Lewy body disorders are thought to be the product of dysfunctional attentional control networks, and a relationship between impaired sensory input, or visual

processing, and faulty top-down attentional control (Collerton et al., 2005; Shine et al., 2011). According to the Perceptual Attentional Deficit (PAD) model, DLB patients experience bottom-up perceptual deficits, that are then over-compensated by top-down processing (Collerton et al., 2005). Collerton and colleagues propose that this over-compensation of top-down processing may lead to 'inputting' of irrelevant schema or images into a perceptual scene, leading to visual hallucinations. According to predictive coding, attention acts as a mechanism to enhance precision of sensory prediction (Spratling, 2008), allowing more detailed processing of a stimulus. In the instance of visual hallucinations, impaired precision control may be consistent with attentional deficits where sensory evidence is not effectively selected, resulting in a failure to update perceptual inferences (O'Callaghan et al., 2017). Support for the PAD model comes from previous research suggesting that hallucinations may be the result of poorer sensory input resulting in excessive bias of prior beliefs towards expected stimulus features, resulting in visual hallucinations (Horga & Dargham, 2019). In addition, hallucinations in DLB have been associated with altered integration of top-down predictions with sensory evidence, also showing an over-weighting of prior knowledge (Zarkali et al., 2019). Thus, visual hallucinations in DLB may arise due to a failure of the integration of sensory input and attentional processes (Collerton et al., 2005; Diederich et al., 2005).

By employing the DDM to assess elements of RT in DLB patients, I may be able to further investigate the relationship between visual impairments, cognitive slowing and clinical symptoms. More specifically in this context, drift rate may correspond to the precision or certainty of the evidence accumulated, non-decision time refers to the sensory accuracy and boundary separation value to the efficiency of sensory evidence accumulation.

Choice RT data from patients from the Lewy-Pro cohort (Donaghy et al., 2018) who were diagnosed with prodromal DLB were accessed in the current experiment. As DLB patients are diagnosed according to consensus guidelines (McKeith et al., 2017), and are categorised into 'possible' or 'probable' depending on the number of core and/or supportive symptoms present, the Lewy-Pro cohort also categorises patients into MCI possible and MCI probable DLB. Due to the severity of disease and different symptom presentation between possible and probable diagnoses, they were treated as separate groups in the current chapter. The EZ model of DDM (as previously described in Chapter 6) was applied to RTs as it is appropriate for smaller trial numbers which occur in clinical contexts. It was hypothesised that modelling RT performance may result in similar findings as observed in PD patients (O'Callaghan et al., 2017). That means it was hypothesised that MCI-LB patients would show impaired non-decision time and difficulty in accumulating sensory information - as represented by boundary separation value - in comparison to healthy older adults. It was also hypothesised that these parameters would be correlated with the instance of visual hallucinations, and performance in clinical measures of visual perception, such as the MOCA, ACE and NEVHI, as detailed in Chapter 3.

## 7.2 Methods

### 7.2.1 Participants

Participants were part of the Lewy-Pro cohort (Donaghy et al., 2018). The cohort was recruited from memory clinics in the North East of England and Cumbria. Participants were patients with mild cognitive impairment (MCI) over the age of 60 years and were eligible for the study if they presented with at least one DLB symptom, including autonomic symptoms, visual disturbances, and any core or supportive features of DLB. For this investigation, data from a subset of 50 participants described previously by Donaghy et al., (2018) was accessed, including choice RT task data, and clinical assessments detailed below.

A clinical diagnosis was made by trained psychiatrists categorising patients into one of two groups; patients were diagnosed with either possible MCI-LB when one core clinical feature or biomarker was present or with probable MCI-LB when two or more clinical features were present, or one clinical feature plus one biomarker according to the proposed MCI-LB criteria. For the subset of data analyses in the current chapter, all participants were diagnosed with either possible or probable MCI-DLB. One participant (probable DLB) was excluded due to limited RT data for the RT task.

Healthy controls were recruited from the School of Psychology volunteer's panel at Cardiff University, and local age interest groups in Cardiff, South Wales. The control group were identical to the older adult group described in Chapter 6. Healthy control participants had no visual disturbances, no history of psychiatric illness, no current diagnosis of dementia or cognitive impairment, and were over the age of 60. Table 7.1 shows demographic information of the cohort.

Table 7.1 Demographic information of Lewy Pro cohort and control participants. ACE = Addenbrooke's Cognitive Examination, NEVHI = North East Visual Hallucinations Inventory, UPDRS = Unified Parkinson's disease rating scale, CAF= clinical assessment of fluctuation

| | **MCI Probable DLB (n=37)** | **MCI Possible DLB (n=12)** | **Control (n=25)** |
|---|---|---|---|
| *Age* | 72.86 (15.51) | 75.25 (7.3) | 68.36 (6.11) |
| *Sex* | Female = 13 | Female = 3 | Female = 13 |
| *Education* | 11.57 (2.85) | 10.75 (2.09) | 15.12 (2.40) |
| *ACE* | 78.34 (8.88) | 79.33 (14.09) | 93.52 (4.18) |
| *NEVHI* | 3.667 (4.47) | 1 (3.316) | 0 |
| *UPDRS* | 25.21 (15.71) | 15.36 (7.75) | - |
| *CAF* | 2.70 (3.03) | 2.16 (2.48) | 0.32 (0.63) |
| *Cholinesterase Inhibitor* | 18 | 0 | - |
| *Levodopa* | 8 | 0 | - |

### 7.2.2 Materials and Methods

Lewy-Pro participants' general cognitive performance was assessed with the Addenbrooke's Cognitive Exam (ACE-R; Mioshi et al., 2006), verbal fluency was assessed using FAS Verbal Fluency and Graded Naming Tests (Mckenna & Warrington, 1983), executive function assessed using the Trail-making test parts A and B and verbal memory assessed using Rey Auditory Verbal learning test (Rey, 1958). Results from the FAS, Trail-making and Rey auditory verbal learning tasks are reported elsewhere, as they were not used in the current analysis (Donaghy et al., 2018). Participants completed computerised assessments of choice RT, digit vigilance and visual perceptual assessments, in addition to clinical assessments including; Geriatric depression scale (Yesavage, 1988), Clinician Assessment of Fluctuations (CAF; Walker et al., 2000), Dementia cognitive fluctuations scale (Lee et al., 2014), Neuropsychiatric Inventory (NPI; Cummings et al., 1994), North East Visual Hallucinations Interview (NEVHI; Mosimann et al., 2008), Unified Parkinson's disease rating scale (UPDRS; Goetz et al., 2008) and Instrumental activities of daily living scale (ADL; Lawton & Brody et al., 1969). Control participants were also assessed using a computerised assessment of choice RT (described in Chapter 6), the ACE-R, CAF and NEVHI.

### 7.2.3 Procedure

For the Lewy-Pro cohort, RT data for each participant was collected using a 30-trial choice RT flanker task (Ballard et al., 2001). The task consisted of five horizontal arrows presented on the screen. Participants were instructed to attend to the central arrow and respond to the direct of this target, using either left or right keyboard buttons. Central arrows were flanked by arrows facing in different directions (incongruent conditions), the same direction as the central arrow (congruent condition) or by lines (neutral condition). The older control group completed the flanker task, as described in Chapter 6 (section 6.2.2.1). Mean RT, mean accuracy and mean RT variance was generated for each participant across all completed trials. Participants were excluded from the analysis if the task was not completed (n=1 in the Lewy-Pro group). Following this, a simplified version of the original drift diffusion model, the EZ DDM (Wagenmakers, Van der Mass & Grasman, 2007) was fit to the data using the script and method as described in Chapter 6 (section 6.2.2.2) and average drift diffusion outcome variables were estimated for each participant. The EZ DDM (Wagenmakers, Van der Maas & Grasman, 2007) estimated three primary outcome variables (drift rate [v], boundary separation [a], and non-decision time [t]) from mean RT, accuracy (proportion correct), and variance of response times for correct decisions.

### 7.2.4 Statistical analyses

RTs which were over or under 2 standard deviations from the group mean were removed as outliers from the analyses. This led to an exclusion of data from n= 3 participants in the Lewy-Pro group. Following EZ model fitting, one-way ANOVAs were used to test for group differences in mean RT and mean accuracy. A MANOVA was used to assess EZ parameters between control, possible and probable Lewy body groups. For DDM analyses, Tukey post-hoc tests were conducted to assess group comparisons. Following this,

linear hierarchical stepwise regression models were fit to clinical and cognitive data in order to determine the best predictors of DDM parameters between groups.

Finally, patient groups were also categorized on the basis of their NEVHI score, with a high NEVHI indicating greater incidence of visual disturbances. This allowed me to compare drift parameters between those patients who experienced symptoms without visual hallucinations (NEVHI score = 0; NEVHI−, n = 29) and those who experienced symptoms with visual hallucinations (NEVHI score > 1; NEVHI+, n = 20), as per classifications in O'Callaghan et al (2017). In addition, these comparisons were also conducted between patients with clinically rated absence (n = 37) or presence (n = 12) of complex visual hallucinations. Mann–Whitney U tests were used to assess group differences in DDM parameters.

## 7.3 Results

### 7.3.1 Mean RT and accuracy differences between control and Lewy body groups

All analyses were conducted first by comparing control, possible and probable Lewy body groups. Probable DLB patients were significantly older than healthy control participants ($F(2,71)=8.738$, $p=<.001$) and possible DLB and controls significantly differed in age $F(2,71)=8.738$, $p=0.017$). In addition, control participants had significantly more years of education than possible DLB ($F(2,71)=16.9$, $p=<.001$) and probable DLB ($F(2,71)=16.9$, $p<.001$). Mean RT was significantly lower in the older control relative to probable DLB ($F(3,72)=18.72$, $p=<.001$) (Figure 2). Younger participants had significantly lower RT than older controls ($F(2,47)=8.451$, $p=<.001$). Healthy older controls also had higher accuracy scores than possible ($F(3,92)=7.746$, $p=0.05$) and probable DLB patients ($F(3,92)=7.746$, $p=<.001$). However only probable DLB had lower accuracy scores than younger controls ($F(3,92)=7.746$, $p=0.002$) (Figure 7.1).

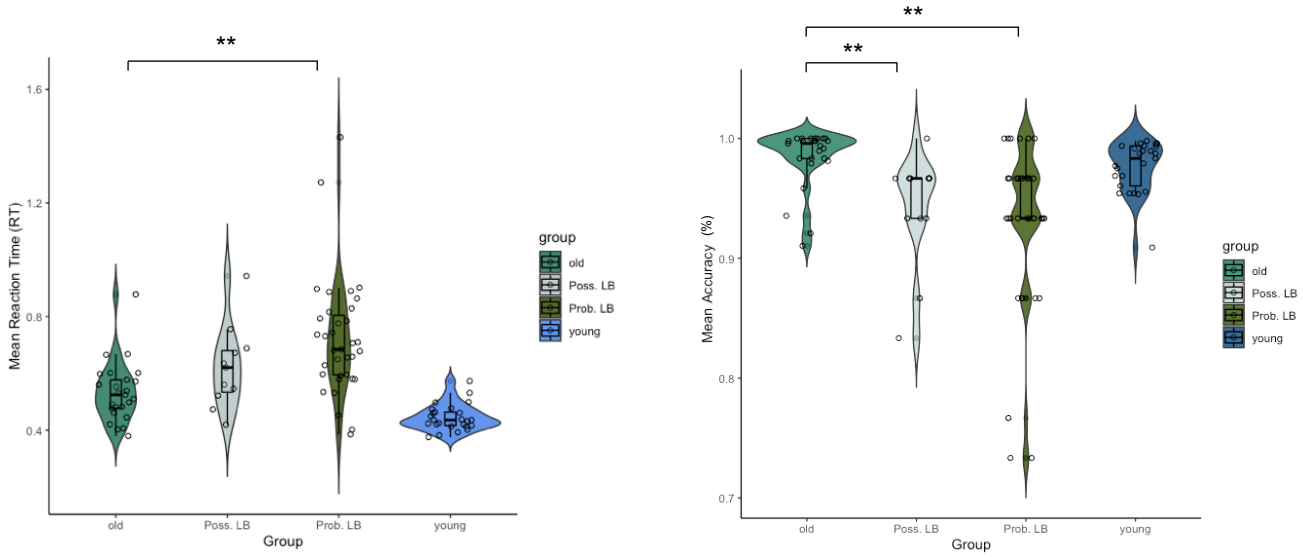


Figure 7.1 Diagnostic group differences in mean accuracy and mean RT between possible Lewy body patients, probable Lewy body patients, older adults and young adults. One-way ANOVAs show mean RT in a flanker attention task was significantly greater in probable DLB compared to older adults. Mean accuracy was significantly lower in both DLB groups in comparison to older adults. Poss LB = MCI-DLB patients with a possible diagnosis, Prob LB = MCI-DLB with a probable diagnosis. **p<.001, *p<.05

### 7.3.2 Non-decision time differs between control and Lewy body groups

Non-decision time was significantly greater in Lewy body patients ($F(2,66)=8.8$, p=.002) with post-hoc analyses revealing a significant difference between probable Lewy body patients and healthy older controls (p=<.001). No significant difference was detected in non-decision time between possible and probable Lewy body patients, or possible Lewy body patients and healthy controls (p=0.707) (Figure 7.2).

No significant difference in boundary separation (F(2,71)=1.077, p=0.346) or drift rate were present between any groups ($F(2,71)=0.503$, p=0.607) (Figure 7.2). Levene's tests of variance showed no statistical significant difference in the variance of mean RT between all groups (F(2,68)=2.191, p=0.119). However, Levene's test of variance showed significantly greater variation in non-decision time (F(2,69)=8.41, p=<.001), boundary separation (F(2,68)=3.26, p=0.041), and drift rate (F(2,71)=9.809, p=<.001) between control participants and the probable DLB group.

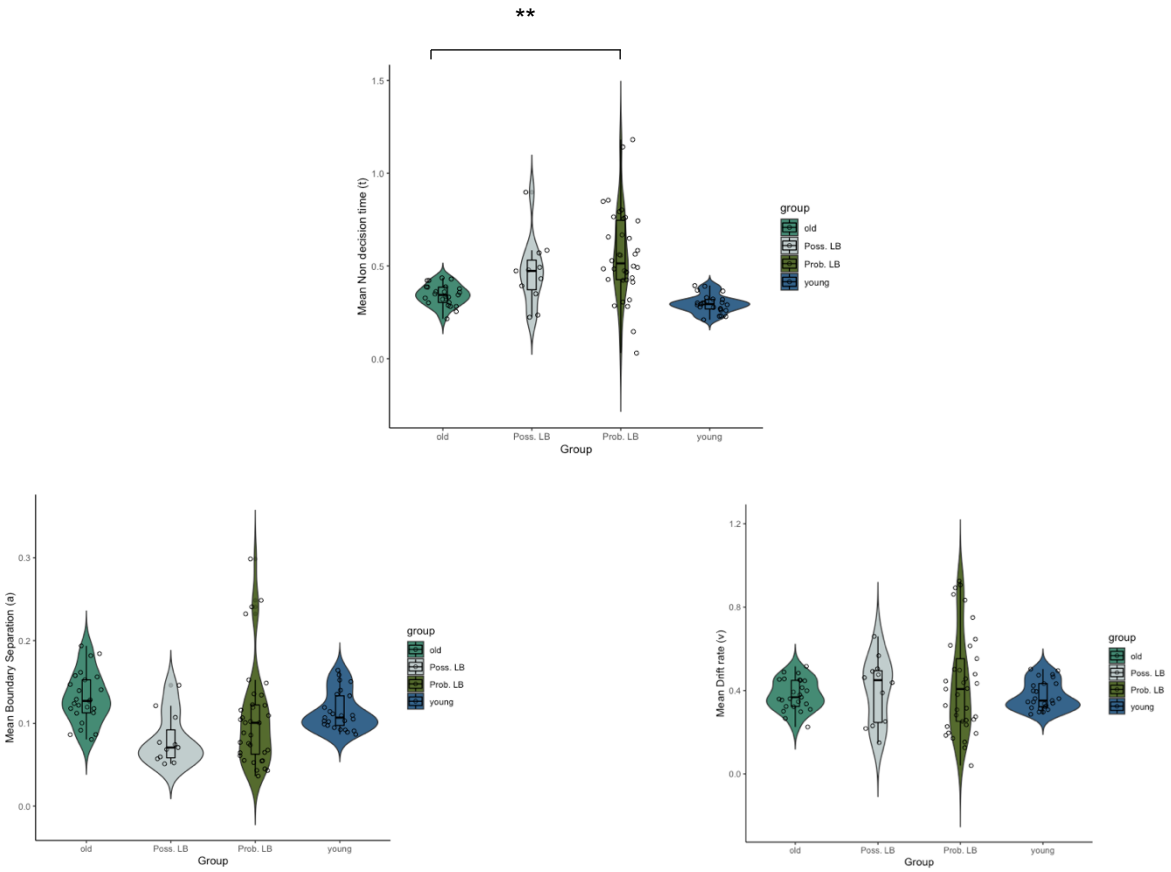


Figure 7.2 Diagnostic group differences in drift diffusion model (DDM) output metrics between possible Lewy body patients, probable Lewy body patients, older adults and young adults. MANOVA results indicate that mean non-decision time (perceptual and motor processing time) was significantly longer in probable LB in comparison to older adults. Poss LB = MCI-DLB patients with a possible diagnosis, Prob LB = MCI-DLB with a probable diagnosis. **p<.001, *p<.05

### 7.3.3 DDM parameters are predicted by clinical assessments of visual perception

Following group comparisons, DDM parameters were fit to separate linear stepwise regression models as predictors, along with demographic information including education, gender and age. ACE subscales, NEVHI, UPDRS and CAF scores were then entered into the model separately as outcome variables.

Non decision time (t) significantly predicted ACE Visuo- spatial subscale score (adj $R^2$=0.198, beta=-0.321, p=0.004), and NEVHI (adj $R^2$=0.062, beta=4.521, p=0.019) in both possible and probable Lewy body groups (Figure 7.3).

Table 7.2 All regression parameters for age, gender and cognitive outcomes of interest. ACE = Addenbrooke's cognitive examination, NEVHI = North East Visual Hallucination Inventory, CAF = clinical assessment of fluctuations. Adjusted $R^2$, beta value and significance (p) are shown.

| **Predictors** | **Non-decision time (t)** | **Boundary separation (a)** | **Drift rate (v)** |
|---|---|---|---|
| Age | Adj $R^2$=.718, beta=.850, p<.001 | Adj $R^2$=.710, beta=.845, p<.001 | Adj $R^2$=.718, beta=.850, p<.001 |
| Gender | Adj $R^2$=.304, beta=.336, p=.057 | Adj $R^2$=.135, beta=.336, p=.261 | Adj $R^2$=.135, beta=.178, p=.558 |
| Education | Adj $R^2$=.646, beta=.042, p=.062 | Adj $R^2$=.689, beta=.009, p=.083 | Adj $R^2$=.806, beta=.035, p=.089 |
| ACE Memory | Adj $R^2$=.701, beta=.042, p=.062 | Adj $R^2$=.747, beta=-.003, p=.241 | Adj $R^2$=.803, beta=-.005, p=.470 |
| ACE Fluency | Adj $R^2$=.701, beta=-.025, p=.052 | Adj $R^2$=.701, beta=-.007, p=.092 | Adj $R^2$=.822, beta=.003, p=.831 |
| ACE Language | Adj $R^2$=.751, beta=.025, p=.214 | Adj $R^2$=.642, beta=.005, p=.122 | Adj $R^2$=.907, beta=.016, p=.116 |
| ACE Visuospatial | Adj $R^2$=.198, beta=.321, p=.004 | Adj $R^2$=.761, beta=.007, p=.206 | Adj $R^2$=.701, beta=.012, p=.452 |
| NEVHI | Adj $R^2$=.062, beta=4.521, p=.019 | Adj $R^2$=.646, beta=-.002, p=.332 | Adj $R^2$=.822, beta=-.007, p=.363 |
| CAF | Adj $R^2$=.761, beta=-.015, p=.301 | Adj $R^2$=.761, beta=.001, p=.831 | Adj $R^2$=.907, beta=-.010, p=.251 |
| UPDRS | Adj $R^2$=.-.017, beta=.112, p=.450 | Adj $R^2$=.-.102, beta=-.109, p=.470 | Adj $R^2$=-.112, beta=-.121, p=.424 |

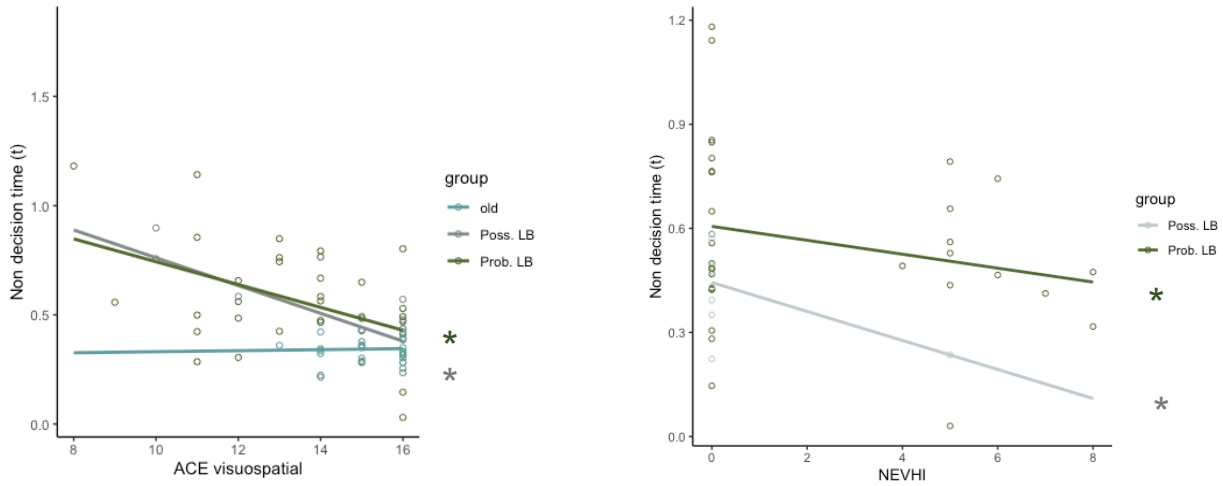


Figure 7.3 Relationships between drift diffusion model (DDM) metrics and clinical visual-related scores in older adults and possible and probable Lewy body patient groups. Linear regressions indicate that non-decision time (t) is negatively related to scores on the Addenbrooke's Cognitive Exam (ACE) Visuospatial subscale in DLB groups (adj $R^2$=0.198, beta=-0.321, p=0.004), and NEVHI in DLB groups (adj $R^2$=0.062, beta=4.521, p=0.019)

### 7.3.4 Clinical measure of visual hallucinations is related to non-decision time

To further investigate the relationship between visual hallucinations (VH) and drift diffusion parameters, group comparisons between those patients with a higher NEVHI score (NEVHI+), and those with a low NEVHI score (NEVHI-) were carried out. There was a significant difference in non-decision time between the NEVHI+ and NEVHI- group (U=183, p=0.024). Boundary separation (p= 0.416) and drift rate (p=0.476) did not differ between groups. Finally, Spearman's Rho correlation showed a significant positive relationship between ACE score and non-decision time in MCI-LB patients in the NEVHI+ (rho=5.412, p=0.013) (Figure 7.4). However, as the NEVHI score is not a direct indicator of the presence of visual hallucinations, we also carried out a comparison between those patients with the presence of complex VH (VH+), as rated by a clinical panel - as per Donaghy et al (2018) - in accordance with DLB criteria (McKeith et al., 2017), and patients with absence of complex VH (VH-). VH+ and VH- patients did not show any significant difference in non-decision time (p=0.625) or drift rate (p=0.659), but VH+ patients had significantly higher boundary separation values (U=90, p=0.002).

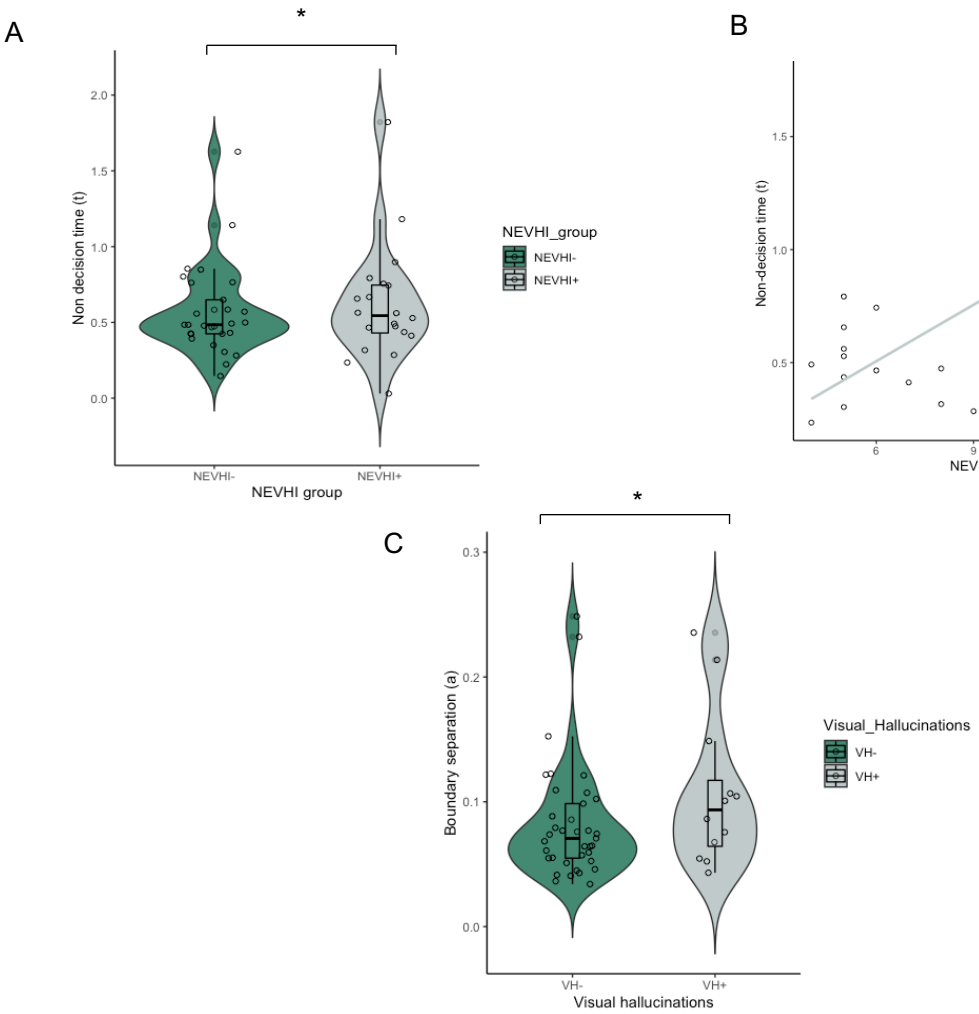


Figure 7.4 Group comparisons between drift diffusion model (DDM) metrics and North East Visual Hallucinations (NEVHI) in patients demonstrating or not presenting with visual hallucinations A) Non-decision time (t) comparisons between NEVHI+ and NEVHI- MCI-LB patients. B) Relationship between visual hallucinations score (NEVHI) and non-decision time in VH group. C) Boundary separation (a) comparisons between VH+ and VH- MCI-LB patients.

## 7.4 Discussion

In the current chapter, I employed the EZ DDM to assess different components of RT in DLB patients in order to study the nature of their slowed and more varied RT performance as well as to observe the relationship between sensory and attentional impairments and visual hallucinations. RT data from MCI-DLB patients were fit to the EZ model of DDM and it was hypothesised that DLB patients would show impaired non-decision time and difficulty accumulating information as evidenced by wider boundary separation values, based on previous findings in PD patients.

### 7.4.1 Non-decision time differs between healthy older adults and prodromal DLB patients

Mean RT was longer in the DLB than in controls, however RT did not differ between possible and probable Lewy body groups. Moreover, accuracy was lower in both Lewy body groups in comparison to controls. These findings are consistent with previous reports of lengthened RTs and reduced accuracy cognitive RT in Lewy body patients (Firbank et al., 2016, 2018). My results showed that older adults had longer non-decision times and greater boundary separation values in comparison to younger adults, which is consistent with previous findings (Ratcliff et al., 2007). Partially consistent with my hypotheses, in MCI-DLB groups compared with the older control group non-decision time values were significantly longer, suggesting that these patients took greater time in the perceptual encoding and/or motor stage of processing during task completion than healthy older controls. Despite this, and not consistent with my hypotheses, drift rates and boundary separation values did not differ between control and patient groups, suggesting that all participants accumulated evidence for a decision at the same rate with the same level of certainty.

It is possible that Lewy body patients experience difficulties at perceptual encoding (non-decision) element of decision making, causing them to take longer in this processing stage. Consistent with previous findings in patients with visual hallucinations (O'Callaghan et at., 2017), DLB patients may struggle to perceptually process information. This may result in a threshold for correct information that is not significantly altered in comparison to older adults but is not sufficiently altered to account for the impairment in non-decision time. As such, it is possible that this pattern of response process results in a potentially incorrect response, in comparison to a more considered yet accurate approach in healthy older controls. Moreover, previous findings have suggested that RT performance in DLB patients is unrelated to clinical motor performance (Ballard et al., 2001) and visual search performance (Cormack et al., 2004). Taken together, these results may then support the role of a primary lower-level perceptual deficit in elongated RTs in DLB patients. These findings are consistent with my results in Chapter 3, which showed patients experienced impairments in lower to mid-level vision, thus suggest a primary perceptual impairment underlies impaired non-decision time in the present results.

However, these results are also not consistent with my hypotheses that boundary separation value would be impaired in DLB patients. I posit that if DLB patients are experiencing longer non-decision times and

they also show lower levels of accuracy, it is possible that their overall evidence accumulation is not significantly altered but is of an overall poorer quality due to impaired perceptual processing. Thus, whereas in healthy older adults RTs are longer due to a deficit in perceptual processing which is rectified by elongating both non-decision time and boundary separation, RTs in DLB may be the product of faulty perceptual processing, leading to longer non-decision times, which is then not rectified by longer time spent accumulating evidence, hence greater levels of inaccuracy. This is also plausible in the context of visual hallucinations, where impaired perceptual processing is not mitigated by any greater time spent accumulating evidence, leading to the incorrect processing of a percept. Consistent with the PAD model (Collerton et al., 2005), this would then lead to an incorrect percept being inserted into the scene, thus forming a visual hallucination. As such, it would be pertinent for future research to examine the underlying mechanisms which may help explain why healthy older adults are able to rectify poorer perceptual processing with increased evidence accumulation, but DLB patients are not. I posit that this is due to the severity of initial perceptual impairment, leading to an inability to accumulate further evidence, in comparison to healthy older adults.

### 7.4.2 Non-decision time is related to clinical visual scores

This may also be supported by the results from the hierarchical stepwise regression fitting in which non-decision values predicted performance in visual clinical tasks. As non-decision time may broadly include aspects of motor response, it should be noted that motor impairment (as measured by UPDRS score) was not a significant predictor of DDM stage differences, further suggesting that differences in DLB patients were of a perceptual nature. The relationship between non-decision time and both ACE visuospatial scores, and NEVHI scores provides further evidence for the hypothesis that DLB patients experience perceptual processing impairments. These findings are also consistent with the results of DDM fitting in PD patients (O'Callaghan et al., 2017) as NEVHI score was seen to predict perceptual encoding ability. The results from hierarchical stepwise regression fitting revealed that mean non-decision values predicted visuo-spatial performance but not NEVHI score. However, further analyses showed that patients in the NEVHI+ had longer non-decision times than NEVHI− and non-decision time correlated positively with higher NEVHI score in this group. As a positive NEVHI score does not necessarily reflect the incidence of visual hallucinations but can be due to other visual problems, I also classified patients on the basis of clinical ratings into those with a history of visual hallucinations and those without. This comparison revealed that individuals with visual hallucinations showed wider boundary separation than those without. The finding of significantly longer non-decision times in the NEVHI+ versus the NEVHI− group suggests that patients who experience visual difficulties including visual hallucinations are prone to difficulties in perceptual encoding and that these encoding problems may contribute to their experience of visual hallucinations. The additional finding that individuals with a history of visual hallucinations showed larger boundary separation than those without, suggests that these individuals experience additional decision-making problems and adopt a more cautious response strategy in light of noisy perceptual input, that may contribute to and/or

reflect the experience of visual hallucinations. Thus, perceptual encoding difficulties appear to be a necessary but not a sufficient condition for the occurrence of visual hallucinations.

The present results would suggest that a primary bottom-up sensory impairment may drive the aetiology of visual hallucinations in DLB. That is, that non-decision time appears to be selectively impaired in DLB patients in comparison to other DDM parameters, and this primary perceptual impairment may lead to incorrect processing and evidence accumulation as indicated by greater levels of inaccuracy in DLB patients. Moreover, impairments in non-decision time are also related to both clinical visuospatial ability and the incidence of visual hallucinations. Previous research has reported a state of underactivity in the visual cortex which is consistent with several aetiological theories of visual hallucination occurrence in DLB patients (Collerton et al., 2005; Fosse et al., 2001). From this, it can be considered that perceptual impairments may lead to an over-reliance on top-down processing, thus leading to visual hallucinations in Lewy body disease, consistent with the PAD model (Collerton et al., 2005).

Another theory of hallucinations in PD patients suggest that perceptual errors arise in the context of impaired signalling between both a task-negative dorsal attention network (DAN) and a stimulus driven ventral attentional network. Usually, perceptual errors would be corrected by the dorsal attention network however in PD it is proposed that a breakdown in frontostriatal circuits may not activate the filtering mechanism necessary to make these corrections (Shine et al., 2011). This may also be reflected in DLB, in which improvement of top-down control and modulation of cortical excitability has been shown in DLB following transcranial direct current stimulation (tDCS) on frontal regions, resulting in improved RT performance (Elder et al., 2016). Moreover, DLB patients also have reduced functional connectivity of the ventral and dorsal attention networks, resulting in longer RTs than control participants (Kobeleva et al., 2017), suggesting that RT performance in DLB may arise as a result of dysfunctional attention network activity. As such, the present results provide some evidence that a primary perceptual deficit in DLB, which is consistent with theories of hallucination in DLB, suggesting that they may arise due to over-activation or compensation of top-down mechanisms (which also experience decline) resulting in both longer RTs and the incidence of abnormal visual experiences.

In addition, visual hallucinations in schizophrenia are considered the occur as a product of disruption to the feedback mechanisms within the visual system, often driven by interruptions in GABAergic inhibition or excitatory processes (Adams et al., 2013). These disruptions in schizophrenia have also been shown to impair predictive coding abilities (Horga et al., 2014). Whilst the clinical presentation and nature of visual hallucinations can differ between schizophrenia and DLB, this does provide some suggestion that disruption to GABAergic processing may be important in the aetiology of visual hallucinations in both disorders. In addition, whilst it was not possible to assess the neural mechanisms underlying DDM performance of DLB patients in the current chapter, my results in Chapter 4 showed parietal GABA to be

raised in all patients. These findings together may suggest that the relationship between parietal GABA and DDM performance could be an important avenue of inquiry in the investigation of visual hallucinations and perceptual impairments in DLB.

### 7.4.3 Limitations

There were also some limitations of the present study. Due to healthy control participants being recruited on an opportunistic basis, the older healthy control participant group were significantly younger on average than probable and possible Lewy body patients, which may have affected some drift diffusion results. Most notably, RT lengthening has been related to increased age, which may underlie average RT differences between groups, as opposed to diagnostic group membership. However, it should be noted that age was not a significant predictor in the linear regression analyses, therefore this may not influence DDM measures significantly. Moreover, a large proportion of the patients within the study were medicated, predominantely with dopaminergic drugs which may significantly impact both movement-related and cognitive outcome measures of the DDM. This may mean that results are both less generalisable to patients with different clinical presentations who are medicated with alternative treatments, but also more generalisable to the Lewy body population more generally as most patients are likely to be medicated with a pharmacological intervention of some form.

In addition, due to recruitment from a University panel, control participants had significantly more years of education than Lewy body groups which may also have influenced performance in some cognitive tests, however these were also not significant in hierarchical linear regressions.

Finally, as data from the Lewy-Pro cohort were accessed it should be noted that patients and healthy controls completed slightly different tasks, however these were as closely matched as possible and followed very similar procedures. It should be noted that healthy older controls completed more trials in the task than DLB patients, which may influence RTs and subsequent calculation of DDM parameters.

### 7.4.4 Chapter summary

The work in this chapter provided a novel approach to studying visual impairment in DLB by applying a drift diffusion model of RT to DLB patients' performance and comparing the outcome parameters with clinical visual scales. My findings showed that DLB patients have longer non-decision times than healthy older adults. I also showed that non-decision time was negatively related to clinical visuospatial performance and visual hallucinations ratings. Taken together, my results suggest that visual hallucinations are related predominantly to impairments in perceptual encoding inabilities in DLB patients. In comparison to my previous results which demonstrate that healthy older adults are able to mitigate impaired perceptual processing with increased evidence accumulation, I show in this chapter than DLB patients do not do so, leading to increased errors. This suggests that a bottom-up sensory impairment is a key element in both the

slowing of RTs and the occurrence of poor perceptual processing possibly leading to visual hallucinations in possible or probable DLB, which is consistent with findings in similar disorders (Dierderich et al., 2005; O'Callaghan et al., 2017).

# Chapter 8 : General Discussion

This chapter will highlight key findings from each experimental chapter in the thesis, discuss the implications of these results in the context of the wider ageing and dementia literature and identify important future directions.

## 8.1 General overview of results

The work in this thesis examined the neural mechanisms underlying visual perception and attention in healthy and pathological ageing. This work investigated cognitive differences between young and older healthy control participants, and between healthy older control participants and DLB patients. Furthermore, the research attempted to link age- and disease-related cognitive differences to neural predictors of white matter microstructural integrity and metabolites in regions associated with visual perception and attention. To achieve this, Chapter 3 characterised the pattern of younger and older adults' visual perceptual and attentional performance and DLB patients' performance using a task battery designed to assess different elements of functioning within the perception and attention hierarchy. Chapter 4 characterised brain differences between younger and older adults in structural, microstructural and neurochemical modalities and compared DLB patients' brain measurements with healthy older adults. Chapter 5 linked cognitive and brain differences in younger and older adults by determining significant neural predictors of cognitive performance between groups across different tasks. Chapter 6 applied a DDM of perceptual decision making in order to determine differences in elements underlying age-related RT slowing and associated brain changes. Finally, Chapter 7 applied this model of perceptual decision making to RT data from MCI-DLB patients from the LewyPro database (Donaghy et al., 2018) to establish potential relationships between changes in DDM parameters and clinical visual impairments.

This thesis identified structural, microstructural and neurochemical correlates of perceptual and attentional differences in older adults. The work in this thesis also found correlations between age-related changes in microstructure and metabolites which have not previously been shown. In addition, neural correlates of age-related compensation, strategy shift and maintenance of cognitive performance were identified. In line with previous literature the empirical work within this thesis also showed slowing of RT in older adults leading to age-related increases in SAT and both replicated and extended findings from decision making modelling in older adults. I also found novel results suggesting that neurochemical differences were related to these RT elements. Finally, my results showed highly varied perceptual and attentional performance in DLB patients with a novel relationship being identified between elements of RT performance in DLB patients and visual hallucinations. My findings provided an insight into the biological basis for perceptual impairment and response slowing in older adults and DLB patients and I suggest a potential mechanism for these changes.

## 8.2 Main findings of the thesis

### 8.2.1 Perception and attention performance differs between younger and older adults, and in DLB patients

Chapter 3 aimed to characterise perceptual and attentional processes in younger and older adults, in addition to assessing these functions in four cases of DLB patients. By developing and employing a bespoke battery of cognitive tasks I was able to assess observers' performance at different stages of the visual processing hierarchy and different elements of the attention network. These tasks were designed to maximise sensitivity to performance by employing psychophysical methodology where appropriate within the constraint that tasks needed to be suitable for individuals with DLB. It was expected that lower-level vision would be maintained in older adults, while age-related decline would become apparent with increasing task complexity, i.e. the increasing requirement to recruit executive and attentional processes. In addition, it was hypothesised that older adults would exhibit slower RT and greater SAT as they adopted a more cautious response strategy in order to maintain accuracy. My results showed that no significant differences in visual acuity were present between younger and older adults, but some low-level age-related visual impairments were observed as visual contrast and visual orientation showed decline in older adults. Findings were mixed at mid-level vision as motion perception was also poorer in older adults, but contour integration ability showed no significant group differences. In higher-level tasks, no group differences were shown in accuracy, but longer RTs and increased SATs were shown demonstrating a shift to a slower but equally accurate response strategy in older adults consistent with my hypothesis. Moreover, no age-related differences were shown in attention network activations.

On the surface, this pattern of results does seem to be consistent with the hypothesis that age-related slowing becomes more apparent in more complex tasks. I found that higher-level tasks and attention tasks do not show poorer accuracy outcomes in older adults, but they did show age-related lengthening of RTs. These results reflect well established work that older adults have longer SATs particularly in non-lexical tasks (Hale et al., 1991). In this way my results support the ageing complexity theory, in that older adults' RT and subsequent SAT was greater in tasks requiring greater cognitive demand and executive control. However, taken together with my findings that show evidence of age-related impairments in lower-level visual functions, these results suggest that age-related slowing in more complex tasks may be a strategy to mitigate impaired bottom-up perceptual processing with age. Previous findings have indicated that where older adults have noisier sensory processing, they sacrifice response speed to preserve performance (Jones et al., 2019). This may suggest that impaired lower-level perceptual processing - as opposed to a specific decline in executive functioning – may underlie age-related slowing.

However, an exception to this pattern of my results was older adults' SAT performance in the motion task which did not show significant age-related differences. I posit that this was most likely due to task-related features of the stimuli duration, meaning that when forced older adults can adopt a faster approach which

is comparable with younger adults, albeit at the expense of lower perceptual thresholds. These findings also demonstrate that where older adults are not able to apply a more cautious, slower strategy they can perform at the same speed as younger adults at the expense of efficient perceptual discrimination. I propose that a decline in effective sensory processing with age may lead to a higher 'load' on top-down cognitive processes, and that a trade-off occurs between compensating this perceptual impairment with a slower response strategy or engaging a faster response strategy but foregoing effective perceptual performance (Roberts & Allen, 2016).

My results also showed no apparent group difference in any ANT network functions as measured by difference scores between alerting, orienting and executive conditions and their respective control conditions. These observations were inconsistent with previous findings that revealed poorer executive network activation in older adults compared to younger adults (Mahoney et al., 2010; Zhou et al., 2011). This again appears to suggest that more complex executive processes are not necessarily impaired with age. However, network effects from the ANT were calculated as a relative difference between two RTs in different task conditions. As such, it needs to be considered that a 'difference' score may not be a reliable measure of the true performance within the context of slower and/or more varied RT in older adults. This is a potential explanation for the absence of group effects in network functioning which have also been previously observed by others and would be anticipated in ageing (Fan et al., 2010).

Four DLB patients were also assessed on this task battery, allowing me to explore visual function in pathological ageing. Previous findings have indicated that very low-level vision is unaffected in DLB, but that visual impairments occur around mid-level of the visual hierarchy (Metzler-Baddeley et al., 2010). Therefore, it was hypothesised that DLB patients would show impairment from contour integration level to higher vision functions. My results from Chapter 3 suggest that visual acuity and orientation were relatively preserved in DLB, with only contour integration ability showing impairments in all participants. Motion coherence performance varied between the DLB patients while all individuals showed greater impairment at higher level performance. As DLB patients showed impairments in functions - particularly in contour integration – which did not differ between younger and older adults, these observations suggest a qualitatively different performance pattern in DLB than healthy ageing. This is of interest as performance in these tasks could aid early diagnosis of DLB. Higher-level visual functions were also impaired in DLB patients, however most patients showed ANT network activation. With regards to RT and SAT in DLB patients, I observed no clear pattern and high variability. Given that only four individuals with DLB could be studied it is difficult to infer any consistent pattern associated with DLB in these tasks. It may also be possible that mean RT may not be a reliable performance measurement in the context of highly variable and slowed and hence noisy RT data. I posit that highly varied RT in DLB may be due to varied individual deposition of pathology throughout the cortex and visual system (Schneider et al., 2012) which can be reflected in the heterogeneity of symptom presentation and disease progression in the individuals included

in this study. Thus, the pattern observed across the four individuals studied here should be interpreted with caution.

In summary, my results suggest that older adults show intact visual acuity but a decline in other lower-level visual functions. My results are somewhat consistent with previous findings showing a complexity effect in ageing, as slowing was apparent in tasks requiring greater processing. However, where older adults were given the chance to be slower and more cautious they were able to perform at the same level as younger adults, thus mitigating lower-level perceptual decline. DLB patients showed a similar level of lower-level visual performance as older adults, but impairments were present predominantly in mid- to higher- level vision although large individual variations were observed. This could perhaps suggest that although DLB patients have the same level of perceptual impairment as older adults, they are not able to consistently compensate their performance by engaging a more cautious strategy as healthy older adults do.

### 8.2.2 Metabolites, microstructure and cortical morphology differ between younger and older adults, and DLB patients

In Chapter 4, I characterised the structural, microstructural and metabolic profile of age-related differences in the brain by firstly assessing regions of interest in an a-priori manner, and then conducting exploratory whole brain analysis of white matter microstructure and grey matter structure. I anticipated that cortical thickness would be reduced in older adults in regions associated with perceptual and attentional functioning, particularly in frontal regions. My results from the a priori analyses showed reduced frontal, temporal and parietal cortical thickness in older adults relative to younger adults. This was supported by my results from the exploratory analysis which also showed widespread reductions in thickness throughout the cortex, in addition to decreased subcortical volume in age. In addition, I predicted that for a priori analysis white matter microstructure in tracts of interest would show age-related decline particularly in the fornix, SLF and ILF. This was supported by my results which showed reductions in FR in the fornix, SLF and optic radiations in older adults. With regards to DTI metrics almost all tracts showed decreased FA and increased MD and RD in older adults. This was apart from L1 which only showed increases in fornix and SLF 1 in older adults. Although FR in the ILF showed high effect sizes (Cohen's $d$ = 0.84), FR was found to be more variable in older and younger groups than DTI indices in the current sample. It is unclear why this may occur but may again be due to low sample size and higher intra-individual variability in addition to diffusion model fitting resulting in unexpected outcomes. This finding has also been reported previously (Zhong et al., 2012) in which age-related reductions in RD were prominent in all regions except for the occipital lobe, but no significant reduction in L1 was present. Thus, my results are consistent with both age-related myelin loss and/or axonal degeneration particularly in the fornix and SLF, suggesting these tracts are particularly vulnerable to age-relate degeneration (Cox et al., 2016; Metzler-Baddeley et al., 2019).

My results from exploratory TBSS analyses were consistent with the findings from the a priori analysis, and demonstrated that age-related reductions in microstructural integrity were not limited to anterior brain

regions but were present in posterior brain regions in older adults, particularly in measurements of FR. This suggests that - consistent with the theory of frontal ageing (Dempster, 1992) - microstructural differences are present in anterior regions in ageing, but differences are not limited to the frontal lobes and occur more globally in the ageing brain. Thus, older adults may be subject to a decline in white matter integrity in early visual cortices, which may potentially underlie the observed decline in lower and mid-level vision, as reported in older adults in Chapter 3.

Based on the preliminary evidence available on metabolic changes in ageing (Haga et al., 2009; Lind et al., 2020), I expected that frontal metabolites would be elevated but that posterior metabolites would show a decline in older adults. I also hypothesised that OCC GABA/$H_20$ would be reduced with age. My results indicated that lower Glx was present in the ACC, and lower NAA was shown in the ACC and PPC with older age. No significant differences in GABA/$H_20$ were reported between groups, with only a trend towards lower GABA/$H_20$ in the ACC in older adults. As Glx and NAA mark mitochondrial functioning and glial health, this suggests that neuronal activity is reduced in more anterior and parietal regions with ageing but that neuronal functioning may be relatively preserved in posterior regions, consistent with my microstructural results. It was anticipated that GABA/$H_20$ in the OCC would be reduced with age as has been previously shown (Gao et al., 2013; Simmonite et al., 2019), but this was not the case in the current results. Methodologically, my study design is consistent with these investigations in older adults including acquisition and post-processing model, however these investigations have assessed GABA as a ratio to creatine, due to its relatively stable concentration in the brain. As discussed in Chapter 2, due to the instability of creatine in pathological ageing raw concentrations were analysed and reported in the current study to ensure comparability with DLB patients. However, it is possible that this may have influenced the present results. Metabolite ratios can aid in the regional susceptibility to variations in concentration and partial volume effects and thus mitigate the influence of individual variation on the conclusions of group comparisons (Li, Wang & Gonen, 2003).

My results indicated that FR had higher effect sizes in comparison to other DTI indices (Cohen's *d*: fornix = 1.72, optic radiation = 1.01, ILF = 0.84, SLF1 = 0.95, SLF2 = 0.84, SLF 3 = 0.98), indicating that it may be a highly sensitive estimate of white matter microstructure (De Santis et al., 2014). On this basis, I examined the relationships between FR and metabolites. My results showed that Glx, myoinositol and NAA in more anterior brain regions were related to FR in the SLF in ageing. Further to this, my results indicated that these metabolites fully mediated the relationship between age and FR, pointing to the potential direction of this relationship. As NAA is a marker of neuronal health and specifically mitochondrial function, these findings further suggest that age-related reductions in neuronal activity may drive age-related white matter microstructural decline, likely activating the Wallerian pathway and potentially leading to axonal and/or myelin degeneration (Loreto et al., 2020). Previous findings have shown relationships between prefrontal glucose and FA in the posterior temporal region in ageing (Kuczynski et al., 2010)

indicating that frontal cortex metabolite concentration may be related to posterior white matter microstructure. The relationship between NAA and intra-axonal compartment parameters from diffusion kurtosis imaging has been previously shown in patients with brain injury, particularly in the corpus callosum (Grossman et al., 2015). However, this relationship has not previously been characterised in healthy ageing and is therefore highly informative with regards to deconstructing the potential mechanisms by which white matter microstructure declines with ageing. Future work should consider observing changes in these regions across several different age groups cross-sectionally or in a longitudinal manner to determine the order of changes within the lifespan.

Finally, in DLB patients my results showed widespread reductions in cortical thickness and impairments in white matter microstructural measures. With regards to metabolites, no clear pattern was present for most measurements between the three patient cases. This is with the exception of consistently raised levels of GABA/$H_20$ in the PPC in all cases. To my knowledge, no previous research has assessed GABA in vivo in DLB patients despite indications from post-mortem studies showing reductions in occipital GABA (Khundakar et al., 2016). The role of the PPC and GABA in inhibitory processes of attention and top-down processing may be of relevance to theories of visual hallucinations. Visual hallucinations in DLB are thought to occur due to overcompensation of top-down processing in response to poor sensory processing (Collerton et al., 2005). My results suggest that GABA/$H_20$ concentrations in the parietal regions involved in the top-down attentional processing stream were raised in DLB. This suggests that greater levels of inhibitory neurotransmitter were present in regions responsible for direction of attention and visual integration. It is possible that this may contribute to the instance of visual hallucinations, as ineffective integration of information in a scene in addition to poor attentional focus and/or orientation would lead to missing or incorrectly processed information. According to the study of visual hallucinations in other disorders, poor or incomplete visual processing may lead to over-reliance on schemata contributing to incorrect objects being inserted into the visual scene (Diederich et al., 2004; Koerts et al., 2010; Onofrj et al., 2013)

In summary, widespread age-related reductions in cortical thickness were present in my results. A-priori analysis showed declines in frontal white matter microstructure in older adults however, exploratory analysis also showed comparable declines in posterior microstructure, thus questioning disproportional age effects on anterior brain regions as proposed by the frontal ageing hypothesis. In older adults, NAA and Glx in the ACC and PPC were significantly reduced, indicating alterations in frontal and parietal neuronal and mitochondrial functioning. These metabolites also mediated the relationship between age and reduced fronto-parietal white matter microstructure. This suggests that brain changes are not solely limited to anterior regions in ageing, and thus it may not be just frontal executive cognitive functions that show predominant decline with age. It also suggests that age-related alterations in frontal and parietal metabolites may underlie age-related reductions in white matter microstructure in frontal-parietal connections,

suggesting that where reduced mitochondrial activity occurs this impacts connective axonal white matter microstructure. DLB patients show widespread reductions in white matter microstructure and cortical thickness as anticipated. Interestingly, all patients showed elevated GABA/$H_20$ in PPC which may play a role in visual or attentional symptoms.

### 8.2.3 Age-related differences in perception and attention are predicted by changes in metabolites and microstructural integrity

The work in this thesis then examined which neural correlates best predicted both age-related differences and age-related maintenance in cognitive performance. In Chapter 5, I used regression models to determine which brain microstructural and metabolic metric from Chapter 4 best predicted the cognitive performance described in Chapter 3 in older and younger adults.

My results revealed that for tasks where no significant group differences in performance were identified (visual acuity, contour threshold, and all ANT network effects), I reported no significant neural predictors. However, for tasks in which older adults' performance was impaired in comparison to younger adults (visual contrast, visual orientation, motion threshold) my results showed that lower-level vision was predicted by declines in optic radiation and SLF microstructure, frontal and parietal metabolites in younger adults, while mid-level vision was predicted by GABA/$H_20$ in the occipital cortex in older adults. Finally, predictors of a 'shift' in performance to a slower SAT in older adults were GABA/$H_20$ and NAA in the PPC and ACC. In contrast, predictors of a faster SAT in younger adults were largely microstructural measurements in the optic radiations and fornix – regions which show decline in older adults.

For tasks where adults showed unimpaired performance, my results showing no significant predictors for either group were unexpected. It was anticipated that optic radiation microstructure may underlie visual acuity performance, GABA may underlie contour integration performance and frontal, temporal and subcortical predictors may underlie ANT performance as previously demonstrated (Fan et al., 2010). I posit that my results may be the product of noise within a small sample – it is possible that larger variability in the older group coupled with limited data may have prevented a clear pattern of neural predictors emerging. This was also reflected in cognitive outcomes of the ANT groups, in which I unexpectedly did not find any age-related group differences thus is likely to be due to methodological limitations such as limited trial numbers to accommodate patients.

With regards to impaired task predictors poorer optic radiation microstructure predicted poorer visual contrast performance in older adults, suggesting that lower-level age-related perceptual processing impairments are in part related to a physical decline of the integrity of white matter in sensory processing tracts. Further to this, predictors of orientation were shown to be frontal and parietal metabolites and SLF microstructure in both younger and older adults. This demonstrates the importance of this fronto-parietal

system in supporting perceptual processing in both older and younger adults. However, my results from Chapter 4 indicated that metabolic differences in older adults mediate the relationship between age and microstructure in the SLF. As such, it is apparent that in older adults the fronto-parietal network (including ACC and PPC metabolites and SLF microstructural parameters) is susceptible to age-related decline. The parietal cortex in particular plays an integral role in the spatial processing element of attentional orientation (Gottlieb & Snyder, 2010), thus impairments to functions within this region may contribute to age-related impairments in orientation ability.

Finally, I observed the neural correlates for the SAT scores which were lengthened in the older adult group. As SAT differences in older adults clearly reflected a slowing in response time but maintenance of accuracy thus highlighting a change in response strategy with age, these outcomes were categorised as being reflective of a 'shift' in performance. A clear distinction was present in my results as in young people, performance was linked to microstructural differences in sensory tract and fornix white matter, which is consistent with the vast literature highlighting the importance of healthy white matter for effective cognitive function. This contrasted with predictors in older adults (where these white matter connections show decline), where longer SAT was related to metabolic markers of neuronal activity in the frontal parietal attention network, suggesting age-related engagement in top-down compensation for the decline in perceptual processing and associated networks. Taken together with my findings from Chapter 4 which indicate that metabolites related to neuronal and mitochondrial functioning mediate the relationship between age and FR in SLF, this suggests that decreased neuronal activity in the frontal and parietal lobes also weaken transmission along the SLF. As such, although older adults recruit this system as a compensatory mechanism in response to the decline in integrity in predictors underlying faster SAT in younger adults, the fronto-parietal system is also impaired which is marked by declines in metabolites. Therefore, processing using this compensatory system may be slowed resulting in longer SAT.

In summary, my results demonstrate that older adults show declines in the biological mechanisms that underlie effective perceptual processing leading to lower and mid-level visual impairments. However, where older adults are able to recruit more cautious strategies, they are able to use the fronto-parietal network and thus increased top-down processing as a mechanism to compensate for impaired low-level perception (i.e. where the task allows longer processing). This is supported by predictors of SAT performance showing that older adults successfully recruit fronto-parietal 'top-down' predictors to maintain accuracy whilst lengthening response time. In contrast, younger adults have faster SAT but use 'bottom-up' predictors with greater microstructural integrity, which are shown to decline with age. In addition, although older adults can recruit this compensatory system it is marked by reductions in neuronal activity, suggesting reduced processing capacity potentially translating to slower response times. This highlights the key neural mechanisms which may underlie the age-related switch to a slower more cautious response strategy.

### 8.2.4 Age-related differences in RT elements are predicted by microstructural changes in older adults and metabolites in younger adults

The neural predictors found in Chapter 5 were seen to indicate a compensatory age-related shift to greater top-down processing systems with increased task complexity, but this warranted further investigation to establish why this switch in strategy may occur. Chapter 6 addressed this by applying a DDM to observers' RTs to investigate model parameters and their underlying neural correlates in ageing. My findings were consistent with previous literature; non-decision time (thus combined perceptual and motor processing time) was found to be longer, and boundary separation values wider in older adults compared to younger adults (Ratcliff et al., 2012). Increased non-decision time was related to reduced SLF microstructural integrity in older adults and NAA in the ACC in younger adults, which supports previous findings that report non-decision time to be related to fronto-parietal functional connectivity (Madden et al., 2020). My results also showed that greater boundary separation in older adults was related to microstructure of the ILF and optic radiation.

These findings are consistent with my interpretation of a compensatory role of the fronto-parietal system in older adults in response to impaired perceptual processing. As the SLF is a key tract involved in top-down processing (D'Andrea, 2019), my results suggest a relationship between the lengthening of the non-decision component of RT and reliance on top-down processing in older adults. Taken together, my results suggest older adults have less efficient non-decision time - thus perceptual processing - which is in line with my findings from Chapter 3 indicating that older adults show some lower-level visual impairments. Consistent with my results from Chapter 5, this poorer perceptual processing - as indicated by lengthened non decision time – may be compensated for by top-down systems in ageing. To my knowledge, no previous research has applied multi-shell DWI to these questions. Hence, my research adds to the existing DTI-based literature of white matter microstructural contributions to perception and attention deficits in ageing showing that novel multi-shell DWI indices can provide more sensitive microstructural estimates than standard DTI measurements (De Santis et al., 2014).

Further, my results also indicated that NAA in the ACC predicted non-decision time in younger adults which, to my knowledge has not previously been shown. These results suggest that in younger adults, effective perceptual-motor mapping within the decision-making process was marked by effective neuronal functioning in the frontal lobe consistent with the literature (Collins & Koechlin, 2012; Domenech & Koechlin, 2015; Rouault, Drugowitsch & Koechlin, 2019). This observation complements my findings in older adults that suggest a contributing role of fronto-parietal networks in perceptual and motor processing. This included the results in Chapter 5 which suggest that longer SAT was marked by reduced neuronal functioning in the ACC in older adults and my results in Chapter 4, demonstrating that individual differences in NAA in ACC mediated the relationship between age and SLF FR. The latter suggests that age-related declines in NAA in ACC may drive a reduction in FR in the SLF, which then contribute to age-

related fronto-parietal impairments. Thus, younger adults may be more efficient in perceptually and motor processing as a result of effective neuronal functioning in the ACC. As the ACC plays an important role in conflict monitoring and guidance of attention (Weissman et al., 2013) it may be that younger adults demonstrate faster non-decision time as a result of intact bottom-up processing and efficient conflict monitoring. In contrast, where older adults attempt to use the fronto-parietal network to compensate for impaired sensory processing - and a reduction in NAA in ACC reducing the efficiency of attentional guidance - a greater level of top-down processing is required to mitigate these age-related impairments, leading to increased non-decision time. However, it should also be noted that non-decision time is also thought to incorporate a motor component, thus these findings cannot be concluded to be related to perceptual processing alone.

My results also indicated a relationship between wider boundary separation and occipital and temporal microstructure. Boundary separation is thought to represent the criterion of evidence accumulation required before a decision is made, and was lengthened in older adults (Ratcliff et al., 2012). As sensory evidence accumulation has been related to temporal integration (Kelly & O'Connell, 2013) and sensory evidence accumulation and integration also require longer processing time in older adults (Jones et al., 2019), this may have underpinned my results. As occipital regions mediate sensory processing and evidence accumulation, key elements of perceptual decision making may happen in these networks in parallel (Koziol et al., 2012).

In summary, my results indicate that older adults adopt more cautious processing strategies as a response to poorer lower-level perceptual processing (as indicated by longer non-decision times). Where younger adults have effective perceptual processing, this is marked by efficient neuronal processing in the ACC, whereas older adults' poorer perceptual processing was related to reduced integrity in the SLF, which I have also shown to be related to age-related declines in neuronal processing in the ACC. The combination of this impaired perceptual processing (non-decision time) and switch to top-down processing may then result in a more cautious response strategy, as indicated by longer boundary separation values (and longer SATs) thus greater evidence accumulation periods in older adults.

### 8.2.5 Non-decision time is altered in DLB patients, and is related to visual hallucinations

Finally, in Chapter 7 I applied the same DDM model of perceptual decision making to RTs in a cohort of MCI-DLB patients. Previous work has applied the DDM to RT in PD patients (O'Callaghan et al., 2017) in which impaired sensory evidence accumulation was found to be related to the incidence of visual hallucinations. It was therefore hypothesised that the DDM model may also provide informative insight into the cognitive basis for visual hallucinations in DLB. Consistent with previous reports of slowed response speed in DLB (Ballard et al., 2001, I found that DLB patients have highly varied and lengthened RTs. Importantly though in this thesis - for the first time - I also found that non-decision time was longer

in DLB patients and that this was related to ACE visuospatial and North East Visual hallucination Inventory (NEVHI) score. However, boundary separation was not found to be any greater in DLB patients.

This pattern of results suggests a primary deficit in perceptual and motor processing, as opposed to a difficulty in accumulating sensory evidence or quality of information processing in DLB. These findings appear consistent with previous findings which have suggested that DLB patients are impaired in initial processing of stimuli, but when attention is re-directed by the researcher to the stimuli the task can be completed with little impairment (Fuentes et al., 2010). My results complement these observations as they suggest that initial perceptual processing is more severely impaired in DLB in comparison to healthy controls. However, unlike in older adults where perceptual impairments are mitigated by longer boundary separation values to result in a more cautious response strategy, DLB patients are unable to do this which leads to greater inaccuracies. Furthermore, as I found that differences in non-decision time were related to differences in the NEVHI scores I posit that this may be a mechanism for the occurrence of visual hallucinations, as poorer accurate processing may subsequently result in an incorrect percept being inserted into the scene consistent with the PAD (Collerton et al., 2005).

Moreover, my findings from the DDM in healthy ageing in Chapter 6 showed that non-decision time was predicted by frontal and parietal brain regions, however the most consistent finding in DLB patients in Chapter 4 was raised GABA/$H_20$ in the PPC. Theories considering the cognitive basis of visual hallucinations in DLB suggest that a primary perceptual deficit results in an over-compensation of top-down processing (Collerton et al., 2001), located in the frontal and parietal brain regions. Therefore, my results may indicate that the relationship between GABA/$H_20$ in the PPC and non-decision time is important as these differences could underlie an inability to engage effective compensatory mechanisms to mitigate perceptual impairment in pathological ageing. Furthermore, due to its inhibitory role it is possible that raised GABA in the PPC acts as a 'gate' in DLB patients, preventing the recruitment of effective compensatory top-down processing. Reduced occipital GABA has been reported to underlie visual hallucinations in Parkinson's disease patients (Firbank et al., 2018), and this has been supported by post-mortem findings in DLB patients (Khundakar et al., 2016) indicating the importance of GABA in visual hallucinations in Lewy body disease. However, the mechanism by which GABA may contribute to hallucinations is yet to be confirmed and the role of GABA/$H_20$ in PPC is speculatory thus requires further investigation to consolidate these results.

### 8.2.6 Summary of main findings

Based on my current results, I propose that the following mechanisms contribute to the neural and cognitive basis for performance in healthy ageing and DLB (Figure 8.1). Taken together, my findings suggest that older adults experience low-level visual impairments independent of visual acuity which is also reflected in longer non-decision times, suggesting a low-level perceptual impairment with age. This is compensated by

both the switch to a more cautious and slower response style, reflected in lengthened SATs and greater boundary separation values. It is possible that older adults may take longer to accumulate information as they do not 'trust' lower-level sensory input, thus a more cautious strategy is engaged voluntarily (Forstmann et al., 2011) or a more cautious strategy is engaged automatically as a response to greater noise in perceptual input. This switch is seen to be mitigated by NAA in the ACC and white matter microstructure in the SLF, suggesting a greater reliance on compensatory top-down processing systems with age. I have also shown that age-related reductions in NAA in the ACC may be the driving factor in age-related reductions in white matter microstructure in connective fibres associated with top-down processing (SLF), meaning this compensatory shift may require greater processing power and/or time, possibly contributing to lengthening of SAT's and response times.

DLB patients also experience an impairment in lower-level perceptual processing and may also experience a 'distrust' in sensory processing ability, as indicated by non-decision time changes. However, it is possible that they do not recruit the top-down compensatory mechanism that older adults do (as indicated by no compensatory widening of boundary separation values), leading to more impaired and varied cognitive outcomes. Alternatively, consistent with the Perception Attention Deficit model (PAD; Collerton et al., 2004), DLB patients may be able to over-recruit top-down mechanisms - as older adults do - but the feedback process of this may be altered in DLB. I suggest that this may be the product of altered GABA/$H_20$ in the PPC (as shown in Chapter 4). The activation of the GABAergic system plays a key role in the prevention of mitochondrial oxidative stress (Surmeier & Schumacker, 2013) and deficits in GABA have been attributed to neuronal loss in PD via this mechanism (Hurley et al., 2013). Moreover, GABA release in the striatum in a mouse model of PD has been shown to mediate α-synuclein – the major aggregated component of the pathological Lewy body (Emmanouilidou et al., 2016) and a decline in GABA control has been seen to initiate pathological processes including weakening of the blood-brain barrier (Blaszczyk, 2016). However, findings have typically suggested that reductions in GABA contribute to these events, therefore further investigation is required to establish whether over-accumulation or faulty regulation of GABA may also contribute to aggregation of Lewy bodies, as per the current results, and then how this may occur.

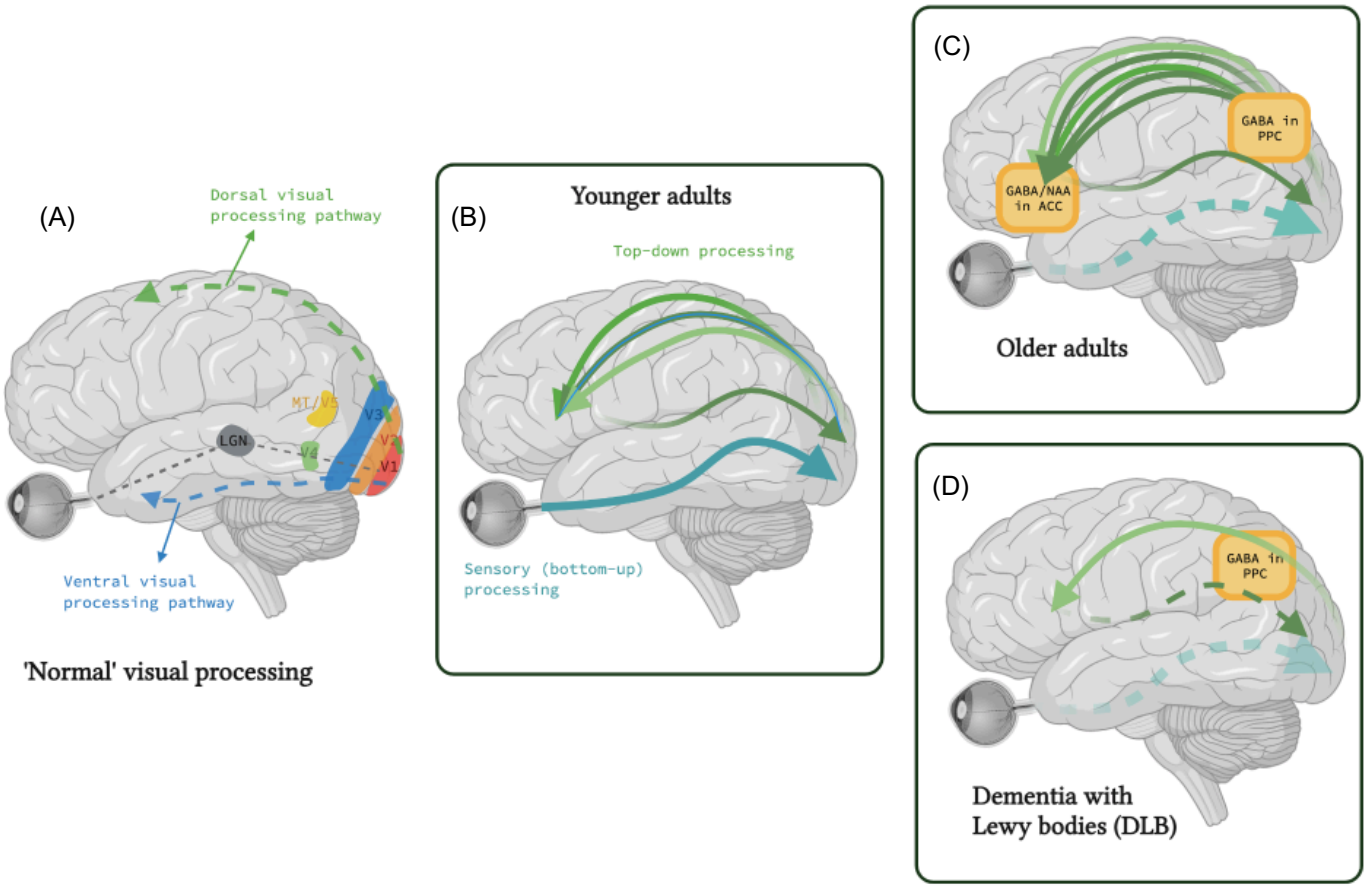


Figure 8.1 Mechanisms of visual perceptual processing in younger and older adults, and dementia with Lewy bodies. (A) Normal visual processing, light information enters the retina, passes through the LGN to primary visual cortex (V1). Visual processing occurs hierarchically following this through V2, V3, V4, V5/MT and dorsal/ ventral processing pathways. (B) Visual processing in younger adults follows this, where bottom-up sensory processing and top-down processing work in synergy to allow accurate and timely responses. (C) Visual processing in older adults is hindered in bottom-up processing pathway and overcompensates with greater top-down processing. This over-compensation is marked by alterations in ACC and PPC metabolites. (D) Visual processing in DLB, where bottom-up processing is impaired, but patients are unable to recruit adequate top-down compensation and/or experience a faulty feedback system, potentially mediated by GABA/$H_20$ in PPC.

## 8.3 Methodological considerations and limitations

### 8.3.1 Statistical analysis and sample

One limitation of the thesis is the statistical approach to regression modelling that was taken due to the high number of variables being assessed. This was done by limiting the number of predictors entered into individual regression models, meaning that predictors were assessed by modality (Chapter 5). This may have had an influence on the predictors appearing as significant, potentially leading to some neural substrates appearing that may be not as strong in the predictive relationship if entered into a model with other variables. To address this, predictors were considered significant at a 1% level with FDR correction across all models to ensure only those with the strongest predictive relationship were found. Moreover, as regression models were conducted for age groups separately, it was possible that predictors which appeared in one age group were also predictors in the other age group. To account for this, Z-score correlation co-

efficient comparisons were conducted to determine the significance of the predictor between the groups (i.e. if the predictor was unique to one age group), in addition to partial correlation in the older group to controlling for the influence of generalised atrophy or white matter damage.

It should also be noted that the sample sizes were relatively small in the thesis in both younger, older and DLB patient groups. Sample size was limited due to rigorous screening for MRI contraindications, recruitment opportunities, feasibility of taking part for both older and patient participants and limitations on scanning hours. As the study was initially designed to assess DLB patients, this impacted the wider recruitment of older, healthier participants due to matching procedures for age and sex, and if the current study were to be replicated or extended a larger sample should be recruited. Despite a power calculation indicating that sample would be adequate for the study, this calculation was based on limited relevant literature which also recruited low sample sizes, thus power is limited for the current study. Both the presence of suitable patients in clinic (in terms of MRI suitability and cognitive ability to partake) and overall number of DLB patients was lacking, highlighting the difficulty of recruiting DLB patients this nature of research study. In addition, a few cases who were suitable to take part and agreed to contact were disheartened by length of the testing session(s) and travel to CUBRIC for MRI scanning. This led to a very limited number of DLB patients recruited over a 2.5-year period. In Chapter 5 particularly, this limitation in sample size may have contributed to the lack of clear pattern in neural predictors for tasks which showed an unimpaired cognitive outcome.

Finally, as has previously been discussed the impact of cognitive and/or brain reserve should be considered within the current sample. Cognitive reserve refers to the ability of individuals to be more flexible or efficient with brain resources than others (Stern et al.,2012). Brain reserve refers to the ability to switch or engage compensatory neural mechanisms to complete a task. In the context of ageing, those individuals with higher cognitive and/or brain reserve are more able to engage compensatory cognitive and neural mechanisms than those with lower cognitive reserve. It is possible that, given the ability of the current older sample to engage readily in a shift in their response strategy, that the older adults recruited have higher cognitive reserve. This therefore would provide them with an advantage in cognitive performance in that they are able to maintain performance, or make a switch to maintain accuracy, where other older adults with lower reserve may not be able to do so as readily. In addition, those tasks in which no performance differences were reported may demonstrate this cognitive reserve and thus may not be representative of performance in the rest of the ageing population. As cognitive and/or brain reserve was not assessed in the present study this cannot be confirmed however it should be noted, and results interpreted with this consideration.

### 8.3.2 MR imaging

Although using advanced MRI techniques has many advantages over traditional clinical MRI or even other methods of measuring brain function such as electroencephalography as discussed in Chapter 2, there are

some limitations that should be discussed. First, there are several limitations associated with MR Spectroscopy in general relating to the human metabolome. MRS is influenced by physiological and external factors such as diet, stress, medications, alcohol or caffeine consumption and menstrual cycle (Tognarelli et al., 2015). Furthermore, sex differences have also been noted in MRS imaging both with regards to the influence of hormones but also levels of creatine in relation to skeletal mass which differs between males and females (Grachev & Apkarian, 2000). Although the sample in the current study was well balanced for gender, it is possible that this may have resulted in over-exaggeration or masking of metabolic patterns. However, due to limitations in the recruitment of suitable participants, dietary and menstrual factors were not controlled for which may have influenced my results in younger adults. Whilst younger and older adult groups were balanced for sex, this was not possible in DLB patients. As metabolic results were found to be particularly important in the current study, future replications or extensions should account for this.

Secondly, there is great potential for contamination during the MRS acquisition. This can be in part due to voxel placement and individual differences in brain structure but also the efficiency of shimming in eliminating field inhomogeneities, as previously discussed. As older adults have relatively reduced cortical thickness and grey matter volume, I accounted for this limitation by controlling for CSF volume within voxels in post-processing and adhering to anatomically guided voxel placement. Moreover, manual shimming was employed to reduce field inhomogeneities.

In addition, GABA contamination and spectral fitting can also be limited depending on the selected model and the method of quality controlling for outliers or poorly fitting data. I addressed this by employing a sensitive post-processing model specific to GABA signal. Quality control was also employed post acquisition as described in Chapter 4.

Finally, as discussed in Chapter 2, the GABA signal also contains concentrations of macromolecules. The editing pulse used to acquire the GABA signal co-edits a macromolecule peak at 1.7ppm meaning that the GABA peak can be contaminated with a macromolecule signal by up to 50% (Bell et al., 2021). Findings have suggested that the relationship between age and GABA+ in 20-50 year olds disappears when macromolecules are suppressed, suggesting that they may be a significant driver in the apparent role of 'GABA' in the brain (Aufhaus et al., 2013). Whilst further editing can be applied in the acquisition of the GABA signal to suppress these macromolecules, this was not introduced in the current study due to time constraints. This should be noted as a limitation in the current results, however GABA+ levels are known to decrease later in life, therefore this effect may not be as apparent in the current cohort.

As previously discussed, typical tractography methods which are based on the tensor model can fail to account for crossing or bending fibres, as only the principal diffusion direction is accounted for (Jones, 2010). In this thesis I acquired HARDI data and applied a spherical deconvolution-based algorithm - the dRL algorithm - to allow for improved fibre tracking in areas with complex fibre architecture and affected

by partial volume. However, while these methods can improve fibre tracking (Jeurissen et al., 2017), it is worth remembering that current shortcomings of diffusion MRI tractography also include an inability to determine the direction of white matter (afferent or efferent) as well as the presence of false positives with CSD approaches.

It should also be noted that there are other advanced imaging techniques which can return indices that are highly sensitive to the biological properties of myelin, which were not accounted for in the current work. Other methods such as quantitative magnetization transfer (qMT) or T1 and T2 relaxometry methods (mcDESPOT; Deoni et al., 2008) could be employed in subsequent work as they are highly sensitive, allowing the characterisation of pathophysiology in the white matter (Makovac et al., 2018). This may be particularly pertinent to consider, as my results suggest that fronto-parietal myelin loss may play a key role in age related slowing and myelin loss in the optic radiation may be related to age related worsening of perceptual processing. However, within this thesis MR acquisition time was limited due to both older adults' and DLB patients' capacity to be in the MR scanner for a prolonged period, and also due to the collection of multiple voxels of MEGA-PRESS data. As such, there was a trade-off between acquiring more advanced imaging and acquiring all the modalities of interest which resulted in the acquisition of multi-shell diffusion data as a measure of white matter microstructure.

### 8.3.3 Cognitive Task limitations

The perceptual and attentional task battery was compiled using tasks which had been shown to assess certain visual functions that were associated with a neuroanatomical region within the visual hierarchy. The task battery was compiled to address the limited literature which has assessed DLB patients' perceptual impairments in a sensitive manner using psychophysical methods. As such, the battery was designed to be accessible to patients. It has been discussed previously in this thesis that this may then have limited the complexity and thus sensitivity of the tasks when assessing control participants. However, arguably some tasks still show group differences between younger and older participants, therefore appeared sufficiently sensitive to detect age-related differences in performance.

Furthermore, the task battery aimed to incorporate psychophysical methods including adjusting stimuli signal using a staircase procedure. This was done to obtain a more sensitive measure of perceptual sensitivity in observers. However, it should be noted that an up-down staircase was employed in this thesis in tasks from low to mid-level. Whilst this can narrow down an estimate of perceptual sensitivity for participants, there are more complex staircases which employ prior knowledge, working on Bayesian inference which may have been employed to return more accurate estimates of perceptual sensitivity (Kontsevich & Tyler, 1999). However, with this comes the need for a greater number of trials therefore a trade-off between the sensitivity of the psychophysical method employed and the number of trials patients and older adults were able to complete (within a larger task battery) lead to a compromise in which the current staircase was used.

Across all tasks trial numbers were also limited to ensure suitability for patients. In addition, trial numbers were limited due to the number of tasks included in the battery, number of assessments used within the testing session and practicality of completing the testing session in both patient and older adult groups.

Finally, motion perception was measured using a random dot kinetogram which assessed coherence sensitivity in participants. However, it should be noted that there are several different elements within motion perception such as biological motion of walking bodies, which are separate to motion coherence perception. These were not assessed within this study, as motion perception alone was not the focus of the task battery and therefore conclusions about motion perception ability are limited to this sub-function only. Moreover, there are some issues with the random dot kinetogram stimuli parameters which in turn influence the function being measured. For example, using dots which are animated in different directions at too slow a speed can be problematic, in that the observer can fixate and use one dot as a reference for motion, as opposed to viewing the stimuli as a whole. Moreover, there have been some age-related differences concerning the direction of motion (Pilz et al., 2017) in that horizontal motion perception is more subject to age-related impairment. To mitigate these limitations, this thesis replicated the stimuli used in Landy et al (2015) which showed reliable age-related changes and was successfully completed by all participants.

### 8.3.4 Issues in investigating cognitive ageing

Given the time constraints of the PhD project, the current study was designed in a cross-sectional manner. However, cross-sectional studies are not ideal in the study of ageing and it has been suggested that they may be misleading, as other factors aside from age may contribute to cognitive performance (Salthouse, 2014). One of the major limitations in the cross-sectional study of ageing is that average trends across individuals regardless of age may upwardly bias certain estimates and thus lead to assumptions that trends with ageing are present (Hofer et al., 2002). Moreover, covariances can result from several sources such as random individual differences, but also cohort effects such as differences in education level between younger and older adults (Hofer et al., 2002). It has been highlighted that the gold standard approach to studying ageing is longitudinal investigation (Huppert et al., 2000), however this was not feasible in the time frame of this thesis and considering concurrent patient recruitment.

In addition, due to the initial design of the study recruiting DLB patients, participants were required to be of capacity to consent and partake in cognitive testing. Therefore, longitudinal design was not possible in this instance, as patients would likely progress in their disease and be unable to partake in the study. The current design was therefore cross-sectional as it was a practical approach but adults from a wider range of ages in both groups were recruited and age was included as a predictor in analyses to mitigate the limitations of the design. As such, my results are limited to the conclusion that they represent group differences between young and old as opposed to age-related changes over time. However, the cross-sectional approach in this thesis was appropriate considering the research questions and practicalities of testing.

## 8.4 Thesis conclusions and future directions

Despite the limitations of the study, this thesis has shown some interesting and novel results which have wider implications in the study of vision and attention in healthy ageing and DLB.

This thesis characterised visual perception and attention in older adults and investigated the age-related brain differences in regions associated with visual and attentional function using MRS and advanced diffusion methods. This thesis also characterised visual perception and attention in DLB patients and related this to associated brain networks, to establish which stage in the visual processing hierarchy processes become impaired in comparison to older adults. Finally, elements of RT and SAT were assessed in both healthy ageing and DLB and associated neural differences were investigated in healthy older adults.

My results show that visual and attentional decline in ageing follow a pattern of maintained visual acuity but a decline in lower-level and mid-level visual abilities. Moreover, older adults did not show impairments in accuracy in tasks requiring greater executive processing, but longer RTs and SATs were required to maintain performance highlighting an age-related 'shift' in strategy. Most notably, the results from this thesis demonstrate the presence of age-related relationships between metabolites in the ACC and microstructural integrity in the SLF and highlight that impairments in these mechanisms may be related to impaired perceptual functions in older adults. Unimpaired performance on mid-level visual tasks were maintained by the same neural predictors in both groups. Furthermore, this thesis demonstrated that metabolites in fronto-parietal regions predicted older adults' shift in strategy to a slower and more cautious response style, highlighting a greater reliance on the top-down network. As older adults also showed reductions in microstructural integrity in lower-level sensory brain regions, it is possible that this reliance on top-down mechanisms occurs as a response to a distrust in lower-level sensory processing. This contrasts with younger adults who showed a faster response style and predictors which were largely related to the microstructural integrity of optic radiations.

To explore this further a DDM was applied to RT in younger and older adults. My findings indicated that longer non-decision time and boundary separation values were related to SLF microstructure in older adults and NAA in ACC in younger adults, further supporting an age-related switch to top-down processing with a more cautious cognitive strategy in response to perceptual processing impairments. Although it has been well established that DDM elements are altered in older adults and reductions in white matter integrity have been linked to this, investigations have not established metabolic or advanced diffusion markers of these changes previously.

These findings have implications in the further study of RT elements in older age but also link brain changes with age to reliable changes in processing speed and decision-making elements. Furthermore, these findings also clarify the biological basis for the abstract elements of RT within the diffusion drift model and confirm the neural processes which underlie this. More generally, these findings have implications for the further

study of cognitive ageing as they do not support the traditional views of generalised cognitive slowing or impaired executive functions with ageing, but show that perceptual elements and the neural mechanisms engaged to support these processes in older adults may be more informative of overall cognitive performance.

The work in this thesis also revealed important novel results with regards to vision, attention and decision-making elements in pathological ageing and their relationship to clinical symptoms in DLB. DLB patients showed some low-level visual impairments and more marked impairments from mid-level visual function to high level vision, but varied RT in comparison to healthy older adults. When examining brain differences, widespread reductions in white matter microstructural integrity were found, but notably all DLB patients also showed consistently raised GABA/$H_20$ levels in the PPC.

Whilst the DDM elements of RT have been investigated in PD patients in relation to visual hallucinations (O'Callaghan et al., 2017), it has not been applied to DLB patients. As visual hallucinations and RT slowing are key features in DLB, my investigation of differences in DDM elements in these patients may provide an indication of the cognitive basis for clinical cognitive symptoms and perceptual decline. My results revealed longer non-decision time only in comparison to older adults suggesting a primary perceptual problem which can't be mitigated by greater evidence accumulation. Moreover, these findings were found to be related to visual performance and the incidence of visual hallucinations. In addition, firstly characterising the neural basis of RT elements in older adults and then showing the profile of these elements in DLB allows some inference to be made on key brain regions which may be important in cognitive decline in these patients.

My results highlight the importance of investigating neural metabolite changes in older age when studying cognition. I demonstrated important relationships between FR and metabolites related to mitochondrial function in the frontal lobe, highlighting potential cellular mechanisms for age-related differences in the brain. Studies which have assessed metabolic changes in relation to cognitive differences in ageing are limited but are starting to become more abundant. The work in this thesis supports the usefulness and importance of this direction of enquiry in the cognitive ageing literature. The results from this thesis also have implications for further study of neural impairments in DLB. My results indicate potential markers of decline in this group which are linked to the incidence of clinical symptoms, which may be useful in the prediction of visual hallucinations.

These results provide the basis for understanding neural processes related to vision, attention and processing speed that change with age. When this research was initially designed, a thorough characterisation of vision and perception in healthy ageing and neural correlates was not available. As this study was initially designed to assess DLB patients' performance, this was problematic, as no comparative in healthy ageing existed from which pathological changes could be measured. Therefore, this work is

important as it provides a platform from which pathological age-related changes in vision and perception and their corresponding brain regions can be explored. As this thesis also assessed the feasibility of adopting a multimodal design in pathological ageing to examining the brain and cognition in a small sample of DLB patients, subsequent work could launch this framework in a larger sample of DLB patients. Moreover, my research has highlighted some important clinical findings such as altered parietal GABA/$H_20$, impaired mid-level vision in DLB patients and poor perceptual processing as a basis for visual hallucinations in DLB. One of the most important future directions of this work would be to investigate the neural correlates of lengthened non-decision time in DLB and the role of parietal GABA in clinical and cognitive presentation. This would help to clarify, with some physiological evidence, the neural mechanisms of perceptual impairment and visual hallucinations in DLB.

# Bibliography


Aarsland, D., Ballard, C., McKeith, I., Perry, R. H., & Larsen, J. P. (2001). Comparison of Extrapyramidal Signs in Dementia With Lewy Bodies and Parkinson's Disease. *The Journal of Neuropsychiatry and Clinical Neurosciences*, *13*(3), 374–379. https://doi.org/10.1176/jnp.13.3.374

Acosta-Cabronero, J., & Nestor, P. J. (2014). Diffusion tensor imaging in Alzheimer's disease: insights into the limbic-diencephalic network and methodological considerations. *Frontiers in aging neuroscience*, *6*, 266.

Agathos, C. P., Bernardin, D., Huchet, D., Scherlen, A.-C., Assaiante, C., & Isableu, B. (2015). Sensorimotor and cognitive factors associated with the age-related increase of visual field dependence: A cross-sectional study. *Age*, *37*(4). https://doi.org/10.1007/s11357-015-9805-x

Agrell, B., & Dehlin, O. (1998). The clock-drawing test. *Age and ageing*, *27*(3), 399-404.

Ala, T. A. (2001). Pentagon copying is more impaired in dementia with Lewy bodies than in Alzheimer's disease. *Journal of Neurology, Neurosurgery & Psychiatry*, *70*(4), 483–488. https://doi.org/10.1136/jnnp.70.4.483

Aldridge, G. M., Birnschein, A., Denburg, N. L., & Narayanan, N. S. (2018). Parkinson's Disease Dementia and Dementia with Lewy Bodies Have Similar Neuropsychological Profiles. *Frontiers in Neurology*, *9*. https://doi.org/10.3389/fneur.2018.00123

Allman, J., Miezin, F., & McGuinness, E. (1985). Stimulus Specific Responses from Beyond the Classical Receptive Field: Neurophysiological Mechanisms for Local-Global Comparisons in Visual Neurons. *Annual Review of Neuroscience*, *8*(1), 407–430. https://doi.org/10.1146/annurev.ne.08.030185.002203

Altmann, C. F., Deubelius, A., & Kourtzi, Z. (2004). Shape saliency modulates contextual processing in the human lateral occipital complex. *Journal of Cognitive Neuroscience*, *16*(5), 794-804.

Amarya, S., Singh, K., & Sabharwal, M. (2018). Ageing process and physiological changes. In *Gerontology*. IntechOpen.

Andersen, G. J. (2012). Aging and vision: Changes in function and performance from optics to perception. *WIREs Cognitive Science*, *3*(3), 403–410. https://doi.org/10.1002/wcs.1167

Andersen, G. J., & Ni, R. (2008). Aging and visual processing: Declines in spatial not temporal integration. *Vision Research*, *48*(1), 109–118. https://doi.org/10.1016/j.visres.2007.10.026

Anderson, J. A., Campbell, K. L., Amer, T., Grady, C. L., & Hasher, L. (2014). Timing is everything: Age differences in the cognitive control network are modulated by time of day. *Psychology and aging*, *29*(3), 648.

Andersson, J. L., Jenkinson, M., & Smith, S. (2007). Non-linear optimisation. FMRIB technical report TR07JA1. *Practice*.

Anstey, K. J., Wood, J., Lord, S., & Walker, J. G. (2005). Cognitive, sensory and physical factors enabling driving safety in older adults. *Clinical Psychology Review*, *25*(1), 45–65. https://doi.org/10.1016/j.cpr.2004.07.008

Armstrong, R. A. (2012). Visual signs and symptoms of dementia with Lewy bodies. *Clinical and Experimental Optometry*, *95*(6), 621–630. https://doi.org/10.1111/j.1444-0938.2012.00770.x

Ashburner, J., & Friston, K. J. (2000). Voxel-based morphometry—the methods. *Neuroimage*, *11*(6), 805-821.

Assaf, Y., & Basser, P. J. (2005). Composite hindered and restricted model of diffusion (CHARMED) MR imaging of the human brain. *NeuroImage*, *27*(1), 48–58. https://doi.org/10.1016/j.neuroimage.2005.03.042

Assaf, Y., Freidlin, R. Z., Rohde, G. K., & Basser, P. J. (2004). New modeling and experimental framework to characterize hindered and restricted water diffusion in brain white matter. *Magnetic Resonance in Medicine*, *52*(5), 965–978. https://doi.org/10.1002/mrm.20274

Auger, M. L., Meccia, J., & Floresco, S. B. (2017). Regulation of sustained attention, false alarm responding and implementation of conditional rules by prefrontal GABA A transmission: comparison with NMDA transmission. *Psychopharmacology*, *234*(18), 2777-2792.

Bach, M. (1996). The Freiburg Visual Acuity Test-automatic measurement of visual acuity. *Optometry and vision science*, *73*(1), 49-53.

Baddeley, A. (2000). The episodic buffer: A new component of working memory? *Trends in Cognitive Sciences*, *4*(11), 417–423. https://doi.org/10.1016/S1364-6613(00)01538-2

Baddeley, A. D., & Hitch, G. (1974). Working Memory. In G. H. Bower (Ed.), *Psychology of Learning and Motivation* (Vol. 8, pp. 47–89). Academic Press. https://doi.org/10.1016/S0079-7421(08)60452-1

Baddely, A. D., Emslie, H., & Nimmo-Smith, I. (1994). The Doors and People Test: A test of visual and verbal recall and recognition. *Bury-St-Edmunds, United Kingdom: Thames Valley Test*.

Bai, X., Edden, R. A. E., Gao, F., Wang, G., Wu, L., Zhao, B., Wang, M., Chan, Q., Chen, W., & Barker, P. B. (2015). Decreased γ-aminobutyric acid levels in the parietal region of patients with Alzheimer's disease. *Journal of Magnetic Resonance Imaging*, *41*(5), 1326–1331. https://doi.org/10.1002/jmri.24665

Bailon, O., Roussel, M., Boucart, M., Krystkowiak, P., & Godefroy, O. (2010). Psychomotor slowing in mild cognitive impairment, Alzheimer's disease and lewy body dementia: mechanisms and diagnostic value. *Dementia and geriatric cognitive disorders*, *29*(5), 388-396.

Ball, K., Owsley, C., Sloane, M. E., Roenker, D. L., & Bruni, J. R. (1993). Visual attention problems as a predictor of vehicle crashes in older drivers. *Investigative Ophthalmology & Visual Science*, *34*(11), 3110–3123.

Ballard, C., O'Brien, J., Morris, C. M., Barber, R., Swann, A., Neill, D., & McKeith, I. (2001). The progression of cognitive impairment in dementia with Lewy bodies, vascular dementia and Alzheimer's disease. *International Journal of Geriatric Psychiatry*, *16*(5), 499–503. https://doi.org/10.1002/gps.381

Ballmaier, M., O'Brien, J. T., Burton, E. J., Thompson, P. M., Rex, D. E., Narr, K. L., ... & Toga, A. W. (2004). Comparing gray matter loss profiles between dementia with Lewy bodies and Alzheimer's disease using cortical pattern matching: diagnosis and gender effects. *Neuroimage*, *23*(1), 325-335.

Baltes, P. B., Cornelius, S. W., Spiro, A., Nesselroade, J. R., & Willis, S. L. (1980). Integration versus differentiation of fluid/crytallized intelligence in old age. *Developmental Psychology*, *16*(6), 625.

Barrick, T. R., Charlton, R. A., Clark, C. A., & Markus, H. S. (2010). White matter structural decline in normal ageing: a prospective longitudinal study using tract-based spatial statistics. *Neuroimage*, *51*(2), 565-577.

Bartzokis, G., Beckson, M., Lu, P. H., Nuechterlein, K. H., Edwards, N., & Mintz, J. (2001). Age-related changes in frontal and temporal lobe volumes in men: a magnetic resonance imaging study. *Archives of general psychiatry*, *58*(5), 461-465.

Bartzokis, G. (2004). Age-related myelin breakdown: a developmental model of cognitive decline and Alzheimer's disease. *Neurobiology of aging*, *25*(1), 5-18.

Basak, C., & Verhaeghen, P. (2011). Aging and Switching the Focus of Attention in Working Memory: Age Differences in Item Availability But Not in Item Accessibility. *The Journals of Gerontology: Series B*, *66B*(5), 519–526. https://doi.org/10.1093/geronb/gbr028

Bashore, T. R., Ridderinkhof, K. R., & van der Molen, M. W. (1997). The decline of cognitive processing speed in old age. *Current Directions in Psychological Science*, *6*(6), 163-169.

Basser, P. J., Mattiello, J., & LeBihan, D. (1994). MR diffusion tensor spectroscopy and imaging. *Biophysical journal*, *66*(1), 259-267.

Basser, P. J. (1995). Inferring microstructural features and the physiological state of tissues from diffusion-weighted images. *NMR in Biomedicine*, *8*(7), 333-344.

Basser, P. J., Pajevic, S., Pierpaoli, C., Duda, J., & Aldroubi, A. (2000). In vivo fiber tractography using DT-MRI data. *Magnetic resonance in medicine*, *44*(4), 625-632.

Basser, P. J., & Jones, D. K. (2002). Diffusion-tensor MRI: theory, experimental design and data analysis–a technical review. *NMR in Biomedicine: An International Journal Devoted to the Development and Application of Magnetic Resonance In Vivo*, *15*(7-8), 456-467.

Bastin, M. E., Maniega, S. M., Ferguson, K. J., Brown, L. J., Wardlaw, J. M., MacLullich, A. M. J., & Clayden, J. D. (2010). Quantifying the effects of normal ageing on white matter structure using unsupervised tract shape modelling. *NeuroImage*, *51*(1), 1–10. https://doi.org/10.1016/j.neuroimage.2010.02.036

Beauchamp, M. S. (2005). See me, hear me, touch me: multisensory integration in lateral occipital-temporal cortex. *Current opinion in neurobiology*, *15*(2), 145-153.

Beaulieu, C., & Allen, P. S. (1994). Determinants of anisotropic water diffusion in nerves. *Magnetic resonance in medicine*, *31*(4), 394-400.

Beck, D., de Lange, A. M. G., Maximov, I. I., Richard, G., Andreassen, O. A., Nordvik, J. E., & Westlye, L. T. (2021). White matter microstructure across the adult lifespan: A mixed longitudinal and cross-sectional study using advanced diffusion models and brain-age prediction. *NeuroImage*, *224*, 117441.

Beck, D., de Lange, A. M. G., Pedersen, M. L., Alnæs, D., Maximov, I. I., Voldsbekk, I., ... & Westlye, L. T. (2021). Cardiometabolic risk factors associated with brain age and accelerate brain ageing. *medRxiv*.

Beck, D. M., Rees, G., Frith, C. D., & Lavie, N. (2001). Neural correlates of change detection and change blindness. *Nature Neuroscience*, *4*(6), 645–650. https://doi.org/10.1038/88477

Bedard, A. C., Nichols, S., Barbosa, J. A., Schachar, R., Logan, G. D., & Tannock, R. (2002). The development of selective inhibitory control across the life span. *Developmental neuropsychology*, *21*(1), 93-111.

Beer, A. L., Plank, T., & Greenlee, M. W. (2020). Aging and central vision loss: Relationship between the cortical macro-structure and micro-structure. *NeuroImage*, *212*, 116670. https://doi.org/10.1016/j.neuroimage.2020.116670

Behrens, T. E. J., Woolrich, M. W., Jenkinson, M., Johansen-Berg, H., Nunes, R. G., Clare, S., Matthews, P. M., Brady, J. M., & Smith, S. M. (2003). Characterization and propagation of uncertainty in diffusion-weighted MR imaging. *Magnetic Resonance in Medicine*, *50*(5), 1077–1088. https://doi.org/10.1002/mrm.10609

Ben-David, B. M., Eidels, A., & Donkin, C. (2014). Effects of Aging and Distractors on Detection of Redundant Visual Targets and Capacity: Do Older Adults Integrate Visual Targets Differently than Younger Adults? *PLOS ONE*, *9*(12), e113551. https://doi.org/10.1371/journal.pone.0113551

Benjamini, Y., & Hochberg, Y. (1995). Controlling the False Discovery Rate: A Practical and Powerful Approach to Multiple Testing. *Journal of the Royal Statistical Society. Series B (Methodological)*, *57*(1), 289–300. JSTOR.

Bennett, I. J., & Madden, D. J. (2014). Disconnected aging: Cerebral white matter integrity and age-related differences in cognition. *Neuroscience*, *276*, 187–205. https://doi.org/10.1016/j.neuroscience.2013.11.026

Bennett, Ilana J., Motes, M. A., Rao, N. K., & Rypma, B. (2012). White matter tract integrity predicts visual search performance in young and older adults. *Neurobiology of Aging*, *33*(2), 433.e21-433.e31. https://doi.org/10.1016/j.neurobiolaging.2011.02.001

Benton, A. L., Varney, N. R., & Hamsher, K. D. (1978). Visuospatial judgment: A clinical test. *Archives of neurology*, *35*(6), 364-367.
Bergfield, K. L., Hanson, K. D., Chen, K., Teipel, S. J., Hampel, H., Rapoport, S. I., Moeller, J. R., & Alexander, G. E. (2010). Age-related networks of regional covariance in MRI gray matter: Reproducible multivariate patterns in healthy aging. *NeuroImage*, *49*(2), 1750–1759. https://doi.org/10.1016/j.neuroimage.2009.09.051
Berggren, N., & Eimer, M. (2019). The roles of relevance and expectation for the control of attention in visual search. *Journal of experimental psychology: human perception and performance*, *45*(9), 1191.
Betts, L. R., Taylor, C. P., Sekuler, A. B., & Bennett, P. J. (2005). Aging reduces center-surround antagonism in visual motion processing. *Neuron*, *45*(3), 361-366.
Betts, L. R., Sekuler, A. B., & Bennett, P. J. (2007). The effects of aging on orientation discrimination. *Vision Research*, *47*(13), 1769–1780. https://doi.org/10.1016/j.visres.2007.02.016
Beyer, M. K., Larsen, J. P., & Aarsland, D. (2007). Gray matter atrophy in Parkinson disease with dementia and dementia with Lewy bodies. *Neurology*, *69*(8), 747–754. https://doi.org/10.1212/01.wnl.0000269666.62598.1c
Bhagwagar, Z., Wylezinska, M., Jezzard, P., Evans, J., Boorman, E., Matthews, P. M., & Cowen, P. J. (2008). Low GABA concentrations in occipital cortex and anterior cingulate cortex in medication-free, recovered depressed patients. *International Journal of Neuropsychopharmacology*, *11*(2), 255–260. https://doi.org/10.1017/S1461145707007924
Billiet, T., Vandenbulcke, M., Mädler, B., Peeters, R., Dhollander, T., Zhang, H., ... & Emsell, L. (2015). Age-related microstructural differences quantified using myelin water imaging and advanced diffusion MRI. *Neurobiology of aging*, *36*(6), 2107-2121.
Billino, J., Bremmer, F., & Gegenfurtner, K. R. (2008). Differential aging of motion processing mechanisms: Evidence against general perceptual decline. *Vision Research*, *48*(10), 1254–1261. https://doi.org/10.1016/j.visres.2008.02.014
Billino, J., & Pilz, K. S. (2019). Motion perception as a model for perceptual aging. *Journal of Vision*, *19*(4), 3–3. https://doi.org/10.1167/19.4.3
Birren, J. E. (1974). Translations in gerontology: From lab to life: Psychophysiology and speed of response. *American Psychologist*, *29*(11), 808.
Bishop, N. A., Lu, T., & Yankner, B. A. (2010). Neural mechanisms of ageing and cognitive decline. *Nature*, *464*(7288), 529–535. https://doi.org/10.1038/nature08983
Blanc, F., Colloby, S. J., Philippi, N., Pétigny, X. de, Jung, B., Demuynck, C., Phillipps, C., Anthony, P., Thomas, A., Bing, F., Lamy, J., Martin-Hunyadi, C., O'Brien, J. T., Cretin, B., McKeith, I., Armspach, J.-P., & Taylor, J.-P. (2015). Cortical Thickness in Dementia with Lewy Bodies and Alzheimer's Disease: A Comparison of Prodromal and Dementia Stages. *PLOS ONE*, *10*(6), e0127396. https://doi.org/10.1371/journal.pone.0127396
Bodammer, N., Kaufmann, J., Kanowski, M., & Tempelmann, C. (2004). Eddy current correction in diffusion-weighted imaging using pairs of images acquired with opposite diffusion gradient polarity. *Magnetic Resonance in Medicine*, *51*(1), 188–193. https://doi.org/10.1002/mrm.10690
Boeve, B. F., Silber, M. H., & Ferman, T. J. (2004). REM Sleep Behavior Disorder in Parkinson's Disease and Dementia with Lewy Bodies. *Journal of Geriatric Psychiatry and Neurology*, *17*(3), 146–157. https://doi.org/10.1177/0891988704267465
Borghesani, P. R., Madhyastha, T. M., Aylward, E. H., Reiter, M. A., Swarny, B. R., Warner Schaie, K., & Willis, S. L. (2013). The association between higher order abilities, processing speed, and age are variably mediated by white matter integrity during typical aging. *Neuropsychologia*, *51*(8), 1435–1444. https://doi.org/10.1016/j.neuropsychologia.2013.03.005
Bossaerts, P., & Murawski, C. (2016). Decision neuroscience: why we become more cautious with age. *Current biology*, *26*(12), R495-R497.
Bottomley, P. A. (1987). Spatial Localization in NMR Spectroscopy in Vivo. *Annals of the New York Academy of Sciences*, *508*(1 Physiological), 333–348. https://doi.org/10.1111/j.1749-6632.1987.tb32915.x
Bowman, A. R., Bruce, V., Colbourn, C. J., & Collerton, D. (2017). Compensatory shifts in visual perception are associated with hallucinations in Lewy body disorders. *Cognitive Research: Principles and Implications*, *2*(1), 26. https://doi.org/10.1186/s41235-017-0063-6
Boy, F., Evans, C. J., Edden, R. A. E., Lawrence, A. D., Singh, K. D., Husain, M., & Sumner, P. (2011). Dorsolateral Prefrontal γ-Aminobutyric Acid in Men Predicts Individual Differences in Rash Impulsivity. *Biological Psychiatry*, *70*(9), 866–872. https://doi.org/10.1016/j.biopsych.2011.05.030
Boy, F., Evans, C. J., Edden, R. A., Singh, K. D., Husain, M., & Sumner, P. (2010). Individual differences in subconscious motor control predicted by GABA concentration in SMA. *Current Biology*, *20*(19), 1779-1785.
Braddick, O. J., O'Brien, J. M. D., Wattam-Bell, J., Atkinson, J., & Turner, R. (2000). Form and motion coherence activate independent, but not dorsal/ventral segregated, networks in the human brain. *Current Biology*, *10*(12), 731–734. https://doi.org/10.1016/S0960-9822(00)00540-6

Bradshaw, J. (2004). Fluctuating cognition in dementia with Lewy bodies and Alzheimer's disease is qualitatively distinct. *Journal of Neurology, Neurosurgery & Psychiatry*, *75*(3), 382–387. https://doi.org/10.1136/jnnp.2002.002576

Braver, T. S., Barch, D. M., Gray, J. R., Molfese, D. L., & Snyder, A. (2001). Anterior cingulate cortex and response conflict: effects of frequency, inhibition and errors. *Cerebral cortex*, *11*(9), 825-836.

Breitve, M. H., Chwiszczuk, L. J., Brønnick, K., Hynninen, M. J., Auestad, B. H., Aarsland, D., & Rongve, A. (2018). A Longitudinal Study of Neurocognition in Dementia with Lewy Bodies Compared to Alzheimer's Disease. *Frontiers in Neurology*, *9*. https://doi.org/10.3389/fneur.2018.00124

Bridge, H., von dem Hagen, E. A., Davies, G., Chambers, C., Gouws, A., Hoffmann, M., & Morland, A. B. (2014). Changes in brain morphology in albinism reflect reduced visual acuity. *Cortex*, *56*, 64-72.

Brown, L. A., & Brockmole, J. R. (2010). The Role of Attention in Binding Visual Features in Working Memory: Evidence from Cognitive Ageing. *Quarterly Journal of Experimental Psychology*, *63*(10), 2067–2079. https://doi.org/10.1080/17470211003721675

Brown, S. D., & Heathcote, A. (2008). The simplest complete model of choice response time: Linear ballistic accumulation. *Cognitive Psychology*, *57*(3), 153–178. https://doi.org/10.1016/j.cogpsych.2007.12.002

Buckner, R. L. (2005). Molecular, Structural, and Functional Characterization of Alzheimer's Disease: Evidence for a Relationship between Default Activity, Amyloid, and Memory. *Journal of Neuroscience*, *25*(34), 7709–7717. https://doi.org/10.1523/JNEUROSCI.2177-05.2005

Buch, H., Vinding, T., & Nielsen, N. V. (2001). Prevalence and causes of visual impairment according to World Health Organization and United States criteria in an aged, urban Scandinavian population: the Copenhagen City Eye Study. *Ophthalmology*, *108*(12), 2347-2357.

Bucur, B., Madden, D. J., Spaniol, J., Provenzale, J. M., Cabeza, R., White, L. E., & Huettel, S. A. (2008). Age-related slowing of memory retrieval: Contributions of perceptual speed and cerebral white matter integrity. *Neurobiology of Aging*, *29*(7), 1070–1079. https://doi.org/10.1016/j.neurobiolaging.2007.02.008

Bugg, J. M., Zook, N. A., DeLosh, E. L., Davalos, D. B., & Davis, H. P. (2006). Age differences in fluid intelligence: Contributions of general slowing and frontal decline. *Brain and Cognition*, *62*(1), 9–16. https://doi.org/10.1016/j.bandc.2006.02.006

Burghaus, L., Eggers, C., Timmermann, L., Fink, G. R., & Diederich, N. J. (2012). Hallucinations in Neurodegenerative Diseases. *CNS Neuroscience & Therapeutics*, *18*(2), 149–159. https://doi.org/10.1111/j.1755-5949.2011.00247.x

Burton, E. J., McKeith, I. G., Burn, D. J., Williams, E. D., & O'Brien, J. T. (2004). Cerebral atrophy in Parkinson's disease with and without dementia: A comparison with Alzheimer's disease, dementia with Lewy bodies and controls. *Brain*, *127*(4), 791–800. https://doi.org/10.1093/brain/awh088

Busemeyer, J. R., & Johnson, J. G. (2004). Computational models of decision making. *Blackwell handbook of judgment and decision making*, 133-154.

Bradshaw, J. M., Saling, M., Anderson, V., Hopwood, M., & Brodtmann, A. (2006). Higher cortical deficits influence attentional processing in dementia with Lewy bodies, relative to patients with dementia of the Alzheimer's type and controls. *Journal of Neurology, Neurosurgery & Psychiatry*, *77*(10), 1129-1135.

By, S., Xu, J., Box, B. A., Bagnato, F. R., & Smith, S. A. (2017). Application and evaluation of NODDI in the cervical spinal cord of multiple sclerosis patients. *NeuroImage: Clinical*, *15*, 333-342.

Cabeza, R. (2002). Hemispheric asymmetry reduction in older adults: The HAROLD model. *Psychology and Aging*, *17*(1), 85–100. https://doi.org/10.1037/0882-7974.17.1.85

Cabeza, R., Albert, M., Belleville, S., Craik, F. I. M., Duarte, A., Grady, C. L., Lindenberger, U., Nyberg, L., Park, D. C., Reuter-Lorenz, P. A., Rugg, M. D., Steffener, J., & Rajah, M. N. (2018). Maintenance, reserve and compensation: The cognitive neuroscience of healthy ageing. *Nat Rev Neurosci*, 701–710.

Cabeza, R., Anderson, N., Locantore, J., & McIntosh, A. (2003). *Aging Gracefully: Compensatory Brain Activity*.

Cacciamani, F., Tandetnik, C., Gagliardi, G., Bertin, H., Habert, M. O., Hampel, H., ... & Vlaincu, M. (2017). Low cognitive awareness, but not complaint, is a good marker of preclinical Alzheimer's disease. *Journal of Alzheimer's Disease*, *59*(2), 753-762.

Cagnin, A., Gnoato, F., Jelcic, N., Favaretto, S., Zarantonello, G., Ermani, M., & Dam, M. (2013). Clinical and cognitive correlates of visual hallucinations in dementia with Lewy bodies. *Journal of Neurology, Neurosurgery & Psychiatry*, *84*(5), 505–510. https://doi.org/10.1136/jnnp-2012-304095

Cagnin, Annachiara, Bussè, C., Jelcic, N., Gnoato, F., Mitolo, M., & Caffarra, P. (2015). High specificity of MMSE pentagon scoring for diagnosis of prodromal dementia with Lewy bodies. *Parkinsonism & Related Disorders*, *21*(3), 303–305. https://doi.org/10.1016/j.parkreldis.2014.12.007

Calderon, J. (2001). Perception, attention, and working memory are disproportionately impaired in dementia with Lewy bodies compared with Alzheimer's disease. *Journal of Neurology, Neurosurgery & Psychiatry*, *70*(2), 157–164. https://doi.org/10.1136/jnnp.70.2.157

Campbell, K. L., Grady, C. L., Ng, C., & Hasher, L. (2012). Age differences in the frontoparietal cognitive control network: Implications for distractibility. *Neuropsychologia*, *50*(9), 2212–2223. https://doi.org/10.1016/j.neuropsychologia.2012.05.025

Cao, M., Wang, J.-H., Dai, Z.-J., Cao, X.-Y., Jiang, L.-L., Fan, F.-M., Song, X.-W., Xia, M.-R., Shu, N., Dong, Q., Milham, M. P., Castellanos, F. X., Zuo, X.-N., & He, Y. (2014). Topological organization of the human brain functional connectome across the lifespan. *Developmental Cognitive Neuroscience*, *7*, 76–93. https://doi.org/10.1016/j.dcn.2013.11.004

Cao, X., Yao, Y., Li, T., Cheng, Y., Feng, W., Shen, Y., Li, Q., Jiang, L., Wu, W., Wang, J., Sheng, J., Feng, J., & Li, C. (2016). The Impact of Cognitive Training on Cerebral White Matter in Community-Dwelling Elderly: One-Year Prospective Longitudinal Diffusion Tensor Imaging Study. *Scientific Reports*, *6*(1), 33212. https://doi.org/10.1038/srep33212

Cappell, K. A., Gmeindl, L., & Reuter-Lorenz, P. A. (2010). Age differences in prefrontal recruitment during verbal working memory maintenance depend on memory load. *Cortex*, *46*(4), 462–473. https://doi.org/10.1016/j.cortex.2009.11.009

Cardinale, F., Chinnici, G., Bramerio, M., Mai, R., Sartori, I., Cossu, M., ... & Ferrigno, G. (2014). Validation of FreeSurfer-estimated brain cortical thickness: comparison with histologic measurements. *Neuroinformatics*, *12*(4), 535-542.

Casco, C., Barollo, M., Contemori, G., & Battaglini, L. (2017). The Effects of Aging on Orientation Discrimination. *Frontiers in Aging Neuroscience*, *9*. https://doi.org/10.3389/fnagi.2017.00045

Cassey, P., Heathcote, A., & Brown, S. D. (2014). Brain and Behavior in Decision-Making. *PLoS Computational Biology*, *10*(7). https://doi.org/10.1371/journal.pcbi.1003700

Catani, M., Cherubini, A., Howard, R., Tarducci, R., Pelliccioli, G., Piccirilli, M., Gobbi, G., Senin, U., & Mecocci, P. (2001). 1H-MR spectroscopy differentiates mild cognitive impairment from normal brain aging. *NeuroReport*, *12*(11), 2315–2317.

Catani, M., Howard, R. J., Pajevic, S., & Jones, D. K. (2002). Virtual in Vivo Interactive Dissection of White Matter Fasciculi in the Human Brain. *NeuroImage*, *17*(1), 77–94. https://doi.org/10.1006/nimg.2002.1136

Cavanagh, J. F., Wiecki, T. V., Cohen, M. X., Figueroa, C. M., Samanta, J., Sherman, S. J., & Frank, M. J. (2011). Subthalamic nucleus stimulation reverses mediofrontal influence over decision threshold. *Nature Neuroscience*, *14*(11), 1462–1467. https://doi.org/10.1038/nn.2925

Cepeda, N. J., Kramer, A. F., & Gonzalez de Sather, J. (2001). Changes in executive control across the life span: examination of task-switching performance. *Developmental psychology*, *37*(5), 715.

Cerella, J., Poon, L. W., & Fozard, J. L. (1981). Mental rotation and age reconsidered. *Journal of Gerontology*, *36*(5), 620-624.

Chabran, E., Roquet, D., Gounot, D., Sourty, M., Armspach, J.-P., & Blanc, F. (2018). Functional Disconnectivity during Inter-Task Resting State in Dementia with Lewy Bodies. *Dementia and Geriatric Cognitive Disorders*, *45*(1–2), 105–120. https://doi.org/10.1159/000486780

Chadick, J. Z., Zanto, T. P., & Gazzaley, A. (2014). Structural and functional differences in medial prefrontal cortex underlie distractibility and suppression deficits in ageing. *Nature Communications*, *5*(1), 4223. https://doi.org/10.1038/ncomms5223

Chahine, L. M., Xie, S. X., Simuni, T., Tran, B., Postuma, R., Amara, A., Oertel, W. H., Iranzo, A., Scordia, C., Fullard, M., Linder, C., Purri, R., Darin, A., Rennert, L., Videnovic, A., Del Riva, P., & Weintraub, D. (2016). Longitudinal changes in cognition in early Parkinson's disease patients with REM sleep behavior disorder. *Parkinsonism & Related Disorders*, *27*, 102–106. https://doi.org/10.1016/j.parkreldis.2016.03.006

Chamberlain, J. D., Gagnon, H., Lalwani, P., Cassady, K. E., Simmonite, M., Foerster, B. R., Petrou, M., Seidler, R. D., Taylor, S. F., Weissman, D. H., Park, D. C., & Polk, T. A. (2019). *GABA levels in ventral visual cortex decline with age and are associated with neural distinctiveness* [Preprint]. Neuroscience. https://doi.org/10.1101/743674

Chan, M. Y., Park, D. C., Savalia, N. K., Petersen, S. E., & Wig, G. S. (2014). Decreased segregation of brain systems across the healthy adult lifespan. *Proceedings of the National Academy of Sciences*, *111*(46), E4997–E5006. https://doi.org/10.1073/pnas.1415122111

Chan, K. C., So, K. F., & Wu, E. X. (2009). Proton magnetic resonance spectroscopy revealed choline reduction in the visual cortex in an experimental model of chronic glaucoma. *Experimental eye research*, *88*(1), 65-70.

Chan, J. S. Y., & Yan, J. H. (2018). Age-Related Changes in Field Dependence–Independence and Implications for Geriatric Rehabilitation: A Review. *Perceptual and Motor Skills*, *125*(2), 234–250. https://doi.org/10.1177/0031512518754422

Chand, G. B., Wu, J., Hajjar, I., & Qiu, D. (2017). Interactions of the Salience Network and Its Subsystems with the Default-Mode and the Central-Executive Networks in Normal Aging and Mild Cognitive Impairment. *Brain Connectivity*, *7*(7), 401–412. https://doi.org/10.1089/brain.2017.0509

Charlton, R. A., McIntyre, D. J. O., Howe, F. A., Morris, R. G., & Markus, H. S. (2007). The relationship between white matter brain metabolites and cognition in normal aging: the GENIE study. *Brain research*, *1164*, 108-116

Chauvière, L. (2020). Potential causes of cognitive alterations in temporal lobe epilepsy. *Behavioural Brain Research*, *378*, 112310. https://doi.org/10.1016/j.bbr.2019.112310

Cheadle, S., Wyart, V., Tsetsos, K., Myers, N., de Gardelle, V., Herce Castañón, S., & Summerfield, C. (2014). Adaptive Gain Control during Human Perceptual Choice. *Neuron*, *81*(6), 1429–1441. https://doi.org/10.1016/j.neuron.2014.01.020

Chen, M., Yan, Y., Gong, X., Gilbert, C. D., Liang, H., & Li, W. (2014). Incremental integration of global contours through interplay between visual cortical areas. *Neuron*, *82*(3), 682-694.

Chen, D. Q., Strauss, I., Hayes, D. J., Davis, K. D., & Hodaie, M. (2015). Age-Related Changes in Diffusion Tensor Imaging Metrics of Fornix Subregions in Healthy Humans. *Stereotactic and Functional Neurosurgery*, *93*(3), 151–159. https://doi.org/10.1159/000368442

Chen, Y., Lv, C., Li, X., Zhang, J., Chen, K., Liu, Z., Li, H., Fan, J., Qin, T., Luo, L., & Zhang, Z. (2019). The positive impacts of early-life education on cognition, leisure activity, and brain structure in healthy aging. *Aging (Albany NY)*, *11*(14), 4923–4942. https://doi.org/10.18632/aging.102088

Cherian, A. K., Kucinski, A., Pitchers, K., Yegla, B., Parikh, V., Kim, Y., ... & Sarter, M. (2017). Unresponsive choline transporter as a trait neuromarker and a causal mediator of bottom-up attentional biases. *Journal of Neuroscience*, *37*(11), 2947-2959.

Chiappelli, J., Rowland, L. M., Wijtenburg, S. A., Muellerklein, F., Tagamets, M., McMahon, R. P., Gaston, F., Kochunov, P., & Hong, L. E. (2015). Evaluation of Myo-Inositol as a Potential Biomarker for Depression in Schizophrenia. *Neuropsychopharmacology*, *40*(9), 2157–2164. https://doi.org/10.1038/npp.2015.57

Chiu, P. W., Mak, H. K. F., Yau, K. K. W., Chan, Q., Chang, R. C. C., & Chu, L. W. (2014). Metabolic changes in the anterior and posterior cingulate cortices of the normal aging brain: proton magnetic resonance spectroscopy study at 3 T. *Age*, *36*(1), 251-264.

Christiansen, P., Toft, P., Larsson, H. B. W., Stubgaard, M., & Henriksen, O. (1993). The concentration of N-acetyl aspartate, creatine+ phosphocreatine, and choline in different parts of the brain in adulthood and senium. *Magnetic resonance imaging*, *11*(6), 799-806.

Christiansen, K., Aggleton, J. P., Parker, G. D., O'Sullivan, M. J., Vann, S. D., & Metzler-Baddeley, C. (2016). The status of the precommissural and postcommissural fornix in normal ageing and mild cognitive impairment: An MRI tractography study. *NeuroImage*, *130*, 35–47. https://doi.org/10.1016/j.neuroimage.2015.12.055

Ciafone, J., Little, B., Thomas, A. J., & Gallagher, P. (2020). The Neuropsychological Profile of Mild Cognitive Impairment in Lewy Body Dementias. *Journal of the International Neuropsychological Society*, *26*(2), 210–225. https://doi.org/10.1017/S1355617719001103

Cleeland, C., Pipingas, A., Scholey, A., & White, D. (2019). Neurochemical changes in the aging brain: A systematic review. *Neuroscience & Biobehavioral Reviews*, *98*, 306–319. https://doi.org/10.1016/j.neubiorev.2019.01.003

Cloak, C. C., Alicata, D., Chang, L., Andrews-Shigaki, B., & Ernst, T. (2011). Age and sex effects levels of choline compounds in the anterior cingulate cortex of adolescent methamphetamine users. *Drug and alcohol dependence*, *119*(3), 207-215.

Coad, B. M., Craig, E., Louch, R., Aggleton, J. P., Vann, S. D., & Metzler-Baddeley, C. (2020). Precommissural and postcommissural fornix microstructure in healthy aging and cognition. *Brain and neuroscience advances*, *4*, 2398212819899316.

Coates, S., Tanna, P., & Scott-Allen, E. (2019). Overview of the UK population: August 2019. *Office for National Statistics: Newport, UK*.

Collerton, D., Burn, D., McKeith, I., & O'Brien, J. (2003). Systematic Review and Meta-Analysis Show that Dementia with Lewy Bodies Is a Visual-Perceptual and Attentional-Executive Dementia. *Dementia and Geriatric Cognitive Disorders*, *16*(4), 229–237. https://doi.org/10.1159/000072807

Collerton, D., Perry, E., & McKeith, I. (2005). Why people see things that are not there: A novel Perception and Attention Deficit model for recurrent complex visual hallucinations. *Behavioral and Brain Sciences*, *28*(06). https://doi.org/10.1017/S0140525X05000130

Colloby, S. J., Elder, G. J., Rabee, R., O'Brien, J. T., & Taylor, J. P. (2017). Structural grey matter changes in the substantia innominata in Alzheimer's disease and dementia with Lewy bodies: a DARTEL-VBM study. *International journal of geriatric psychiatry*, *32*(6), 615-623.

Cook, E., Hammett, S. T., & Larsson, J. (2016). GABA predicts visual intelligence. *Neuroscience Letters*, *632*, 50–54. https://doi.org/10.1016/j.neulet.2016.07.053

Corbetta, M., & Shulman, G. L. (2002). Control of goal-directed and stimulus-driven attention in the brain. *Nature Reviews Neuroscience*, *3*(3), 201–215. https://doi.org/10.1038/nrn755

Cormack, F., Aarsland, D., Ballard, C., & Tovée, M. J. (2004). Pentagon drawing and neuropsychological performance in Dementia with Lewy Bodies, Alzheimer's disease, Parkinson's disease and Parkinson's disease with dementia. *International Journal of Geriatric Psychiatry*, *19*(4), 371–377. https://doi.org/10.1002/gps.1094

Cowell, P. E., Sluming, V. A., Wilkinson, I. D., Cezayirli, E., Romanowski, C. A. J., Webb, J. A., Keller, S. S., Mayes, A., & Roberts, N. (2007). Effects of sex and age on regional prefrontal brain volume in two human cohorts. *European Journal of Neuroscience*, *25*(1), 307–318. https://doi.org/10.1111/j.1460-9568.2006.05281.x

Cox, S. R., Bastin, M. E., Ferguson, K. J., Allerhand, M., Royle, N. A., Maniega, S. M., Starr, J. M., MacLullich, A. M. J., Wardlaw, J. M., Deary, I. J., & MacPherson, S. E. (2015). Compensation or inhibitory failure? Testing

hypotheses of age-related right frontal lobe involvement in verbal memory ability using structural and diffusion MRI. *Cortex*, *63*, 4–15. https://doi.org/10.1016/j.cortex.2014.08.001
Cox, S. R., Ritchie, S. J., Tucker-Drob, E. M., Liewald, D. C., Hagenaars, S. P., Davies, G., ... & Deary, I. J. (2016). Age differences in brain white matter microstructure in UK Biobank (N= 3,513). *bioRxiv*, 051771.
Cox, S. R., Bastin, M. E., Ritchie, S. J., Dickie, D. A., Liewald, D. C., Maniega, S. M., ... & Deary, I. J. (2018). Brain cortical characteristics of lifetime cognitive ageing. *Brain Structure and Function*, *223*(1), 509-518.

Crivello, F., Tzourio-Mazoyer, N., Tzourio, C., & Mazoyer, B. (2014). Longitudinal Assessment of Global and Regional Rate of Grey Matter Atrophy in 1,172 Healthy Older Adults: Modulation by Sex and Age. *PLOS ONE*, *9*(12), e114478. https://doi.org/10.1371/journal.pone.0114478
Cromarty, R. A., Schumacher, J., Graziadio, S., Gallagher, P., Killen, A., Firbank, M. J., Blamire, A., Kaiser, M., Thomas, A. J., O'Brien, J. T., Peraza, L. R., & Taylor, J.-P. (2018). Structural Brain Correlates of Attention Dysfunction in Lewy Body Dementias and Alzheimer's Disease. *Frontiers in Aging Neuroscience*, *10*. https://doi.org/10.3389/fnagi.2018.00347
Csete, G., Szabo, N., Rokszin, A., Toth, E., Braunitzer, G., Benedek, G., ... & Kincses, Z. T. (2014). An investigation of the white matter microstructure in motion detection using diffusion MRI. *Brain research*, *1570*, 35-42.
Culham, J. C., & Kanwisher, N. G. (2001). Neuroimaging of cognitive functions in human parietal cortex. *Current opinion in neurobiology*, *11*(2), 157-163.
Currais, A. (2015). Ageing and inflammation–a central role for mitochondria in brain health and disease. *Ageing research reviews*, *21*, 30-42.
D'Andrea, A., Chella, F., Marshall, T. R., Pizzella, V., Romani, G. L., Jensen, O., & Marzetti, L. (2019). Alpha and alpha-beta phase synchronization mediate the recruitment of the visuospatial attention network through the Superior Longitudinal Fasciculus. *Neuroimage*, *188*, 722-732.
Dagnelie, G. (2013). Age-Related Psychophysical Changes and Low Vision. *Investigative Ophthalmology & Visual Science*, *54*(14), ORSF88–ORSF93. https://doi.org/10.1167/iovs.13-12934
Davis, S. W., & Cabeza, R. (2015). Cross-Hemispheric Collaboration and Segregation Associated with Task Difficulty as Revealed by Structural and Functional Connectivity. *Journal of Neuroscience*, *35*(21), 8191–8200. https://doi.org/10.1523/JNEUROSCI.0464-15.2015
Davis, Simon W., Dennis, N. A., Buchler, N. G., White, L. E., Madden, D. J., & Cabeza, R. (2009). Assessing the effects of age on long white matter tracts using diffusion tensor tractography. *NeuroImage*, *46*(2), 530–541. https://doi.org/10.1016/j.neuroimage.2009.01.068
de Blank, P. M. K., Berman, J. I., Liu, G. T., Roberts, T. P. L., & Fisher, M. J. (2013). Fractional anisotropy of the optic radiations is associated with visual acuity loss in optic pathway gliomas of neurofibromatosis type 1. *Neuro-oncology*, *15*(8), 1088-1095.
de Bruin, A., & Sala, S. D. (2018). Effects of age on inhibitory control are affected by task-specific features. *Quarterly Journal of Experimental Psychology*, *71*(5), 1219–1233. https://doi.org/10.1080/17470218.2017.1311352
de Groot Marius, Verhaaren Benjamin F.J., de Boer Renske, Klein Stefan, Hofman Albert, van der Lugt Aad, Ikram M. Arfan, Niessen Wiro J., & Vernooij Meike W. (2013). Changes in Normal-Appearing White Matter Precede Development of White Matter Lesions. *Stroke*, *44*(4), 1037–1042. https://doi.org/10.1161/STROKEAHA.112.680223
De Santis, S., Drakesmith, M., Bells, S., Assaf, Y., & Jones, D. K. (2014). Why diffusion tensor MRI does well only some of the time: variance and covariance of white matter tissue microstructure attributes in the living human brain. *Neuroimage*, *89*, 35-44.
De Santis, S., Granberg, T., Ouellette, R., Treaba, C. A., Herranz, E., Fan, Q., ... & Toschi, N. (2019). Evidence of early microstructural white matter abnormalities in multiple sclerosis from multi-shell diffusion MRI. *NeuroImage: Clinical*, *22*, 101699.
De Schotten, M. T., Dell'Acqua, F., Forkel, S., Simmons, A., Vergani, F., Murphy, D. G., & Catani, M. (2011). A lateralized brain network for visuo-spatial attention. *Nature Precedings*, 1-1.
de-Wit, L., Huygelier, H., Hallen, R. V. der, Chamberlain, R., & Wagemans, J. (2017). Developing the Leuven Embedded Figures Test (L-EFT): Testing the stimulus features that influence embedding. *PeerJ*, *5*, e2862. https://doi.org/10.7717/peerj.2862
Delahunt, P. B., Hardy, J. L., & Werner, J. S. (2008). The effect of senescence on orientation discrimination and mechanism tuning. *Journal of Vision*, *8*(3), 5–5. https://doi.org/10.1167/8.3.5
Dell'Acqua, F., & Tournier, J.-D. (2019). Modelling white matter with spherical deconvolution: How and why? *NMR in Biomedicine*, *32*(4), e3945. https://doi.org/10.1002/nbm.3945
Delli Pizzi, S., Franciotti, R., Taylor, J.-P., Thomas, A., Tartaro, A., Onofrj, M., & Bonanni, L. (2015). Thalamic Involvement in Fluctuating Cognition in Dementia with Lewy Bodies: Magnetic Resonance Evidences. *Cerebral Cortex*, *25*(10), 3682–3689. https://doi.org/10.1093/cercor/bhu220
Dempster, F. N. (1992). The rise and fall of the inhibitory mechanism: Toward a unified theory of cognitive development and aging. *Developmental Review*, *12*(1), 45–75. https://doi.org/10.1016/0273-2297(92)90003-K

Denburg, N. L., & Hedgcock, W. M. (2015). Age-associated executive dysfunction, the prefrontal cortex, and complex decision making. In *Aging and Decision Making* (pp. 79-101). Academic Press.
Dennis, N. A., Kim, H., & Cabeza, R. (2008). Age-related Differences in Brain Activity during True and False Memory Retrieval. *Journal of Cognitive Neuroscience*, *20*(8), 1390–1402. https://doi.org/10.1162/jocn.2008.20096
Deoni, S. C., Rutt, B. K., Arun, T., Pierpaoli, C., & Jones, D. K. (2008). Gleaning multicomponent T1 and T2 information from steady-state imaging data. *Magnetic resonance in medicine*, *60*(6), 1372–1387. https://doi.org/10.1002/mrm.21704
Desikan, R. S., Ségonne, F., Fischl, B., Quinn, B. T., Dickerson, B. C., Blacker, D., Buckner, R. L., Dale, A. M., Maguire, R. P., Hyman, B. T., Albert, M. S., & Killiany, R. J. (2006). An automated labeling system for subdividing the human cerebral cortex on MRI scans into gyral based regions of interest. *NeuroImage*, *31*(3), 968–980. https://doi.org/10.1016/j.neuroimage.2006.01.021
Diamond, A. (2013). Executive Functions. *Annual Review of Psychology*, *64*(1), 135–168. https://doi.org/10.1146/annurev-psych-113011-143750
Diederich, N. J., Goetz, C. G., & Stebbins, G. T. (2005). Repeated visual hallucinations in Parkinson's disease as disturbed external/internal perceptions: Focused review and a new integrative model. *Movement Disorders*, *20*(2), 130–140. https://doi.org/10.1002/mds.20308
Donaghy, P. C., Taylor, J.-P., O'Brien, J. T., Barnett, N., Olsen, K., Colloby, S. J., Lloyd, J. J., Petrides, G. S., McKeith, I. G., & Thomas, A. J. (2018). Neuropsychiatric symptoms and cognitive profile in mild cognitive impairment with Lewy bodies. *Psychological Medicine*, *48*(14), 2384–2390. https://doi.org/10.1017/S0033291717003956
Donkor, R., Silva, A. E., Teske, C., Wallis-Duffy, M., Johnson, A. P., & Thompson, B. (2021). Repetitive visual cortex transcranial random noise stimulation in adults with amblyopia. *Scientific Reports*, *11*(1), 1-13.
Dorbath, L., Hasselhorn, M., & Titz, C. (2011). Aging and Executive Functioning: A Training Study on Focus-Switching. *Frontiers in Psychology*, *2*. https://doi.org/10.3389/fpsyg.2011.00257
Dosenbach, N. U., Visscher, K. M., Palmer, E. D., Miezin, F. M., Wenger, K. K., Kang, H. C., ... & Petersen, S. E. (2006). A core system for the implementation of task sets. *Neuron*, *50*(5), 799-812.
Drugowitsch, J., Wyart, V., Devauchelle, A.-D., & Koechlin, E. (2016). Computational Precision of Mental Inference as Critical Source of Human Choice Suboptimality. *Neuron*, *92*(6), 1398–1411. https://doi.org/10.1016/j.neuron.2016.11.005
Duma, G. M., Mento, G., Cutini, S., Sessa, P., Baillet, S., Brigadoi, S., & Dell'Acqua, R. (2019). Functional dissociation of anterior cingulate cortex and intraparietal sulcus in visual working memory. *Cortex*, *121*, 277–291. https://doi.org/10.1016/j.cortex.2019.09.009
Duncan, N. W., Wiebking, C., & Northoff, G. (2014). Associations of regional GABA and glutamate with intrinsic and extrinsic neural activity in humans—A review of multimodal imaging studies. *Neuroscience & Biobehavioral Reviews*, *47*, 36–52. https://doi.org/10.1016/j.neubiorev.2014.07.016
Duncan, N. W., Zhang, J., Northoff, G., & Weng, X. (2019). Investigating GABA concentrations measured with macromolecule suppressed and unsuppressed MEGA-PRESS MR spectroscopy and their relationship with BOLD responses in the occipital cortex. *Journal of Magnetic Resonance Imaging*, *50*(4), 1285–1294. https://doi.org/10.1002/jmri.26706
Dutilh, G., Forstmann, B. U., Vandekerckhove, J., & Wagenmakers, E.-J. (2013). A diffusion model account of age differences in posterror slowing. *Psychology and Aging*, *28*(1), 64–76. https://doi.org/10.1037/a0029875
Dye, L., Boyle, N. B., Champ, C., & Lawton, C. (2017). The relationship between obesity and cognitive health and decline. *Proceedings of the Nutrition Society*, *76*(4), 443–454. https://doi.org/10.1017/S0029665117002014
Edden, R. A. E., Muthukumaraswamy, S. D., Freeman, T. C. A., & Singh, K. D. (2009). Orientation Discrimination Performance Is Predicted by GABA Concentration and Gamma Oscillation Frequency in Human Primary Visual Cortex. *Journal of Neuroscience*, *29*(50), 15721–15726. https://doi.org/10.1523/JNEUROSCI.4426-09.2009
Edden, Richard A. E., Puts, N. A. J., Harris, A. D., Barker, P. B., & Evans, C. J. (2014). Gannet: A batch-processing tool for the quantitative analysis of gamma-aminobutyric acid–edited MR spectroscopy spectra. *Journal of Magnetic Resonance Imaging*, *40*(6), 1445–1452. https://doi.org/10.1002/jmri.24478
Elkin-Frankston, S., Rushmore, R. J., & Valero-Cabré, A. (2020). Low frequency transcranial magnetic stimulation of right posterior parietal cortex reduces reaction time to perithreshold low spatial frequency visual stimuli. *Scientific reports*, *10*(1), 1-9.
Elliott, D., Whitaker, D., & MacVeigh, D. (1990). Neural contribution to spatiotemporal contrast sensitivity decline in healthy ageing eyes. *Vision Research*, *30*(4), 541–547. https://doi.org/10.1016/0042-6989(90)90066-T
Ende, G., Cackowski, S., Van Eijk, J., Sack, M., Demirakca, T., Kleindienst, N., ... & Schmahl, C. (2016). Impulsivity and aggression in female BPD and ADHD patients: association with ACC glutamate and GABA concentrations. *Neuropsychopharmacology*, *41*(2), 410-418.
Endrass, T., Schreiber, M., & Kathmann, N. (2012). Speeding up older adults: Age-effects on error processing in speed and accuracy conditions. *Biological Psychology*, *89*(2), 426-432.

Eriksen, B. A., & Eriksen, C. W. (1974). Effects of noise letters upon the identification of a target letter in a nonsearch task. *Perception & Psychophysics*, *16*(1), 143–149. https://doi.org/10.3758/BF03203267
Erskine, D., Taylor, J.-P., Thomas, A., Collerton, D., McKeith, I., Khundakar, A., Attems, J., & Morris, C. (2019). Pathological Changes to the Subcortical Visual System and its Relationship to Visual Hallucinations in Dementia with Lewy Bodies. *Neuroscience Bulletin*, *35*(2), 295–300. https://doi.org/10.1007/s12264-019-00341-4
Esiri, M. M. (2007). Ageing and the brain. *The Journal of Pathology*, *211*(2), 181–187. https://doi.org/10.1002/path.2089
Eyler, L. T., Sherzai, A., Kaup, A. R., & Jeste, D. V. (2011). A Review of Functional Brain Imaging Correlates of Successful Cognitive Aging. *Biological Psychiatry*, *70*(2), 115–122. https://doi.org/10.1016/j.biopsych.2010.12.032
Eylers, V. V., Maudsley, A. A., Bronzlik, P., Dellani, P. R., Lanfermann, H., & Ding, X.-Q. (2016). Detection of Normal Aging Effects on Human Brain Metabolite Concentrations and Microstructure with Whole-Brain MR Spectroscopic Imaging and Quantitative MR Imaging. *American Journal of Neuroradiology*, *37*(3), 447–454. https://doi.org/10.3174/ajnr.A4557
Fan, D., Chaudhari, N. N., Rostowsky, K. A., Calvillo, M., Lee, S. K., Chowdhury, N. F., Zhang, F., O'Donnell, L. J., & Irimia, A. (2019). Post-Traumatic Cerebral Microhemorrhages and their Effects Upon White Matter Connectivity in the Aging Human Brain. *2019 41st Annual International Conference of the IEEE Engineering in Medicine and Biology Society (EMBC)*, 198–203. https://doi.org/10.1109/EMBC.2019.8857921
Fan, J., McCandliss, B. D., Sommer, T., Raz, A., & Posner, M. I. (2002). Testing the Efficiency and Independence of Attentional Networks. *Journal of Cognitive Neuroscience*, *14*(3), 340–347. https://doi.org/10.1162/089892902317361886
Faul, F., Erdfelder, E., Lang, A. G., & Buchner, A. (2007). G* Power 3: A flexible statistical power analysis program for the social, behavioral, and biomedical sciences. *Behavior research methods*, *39*(2), 175-191.
Ferguson, K. J., MacLullich, A. M. J., Marshall, I., Deary, I. J., Starr, J. M., Seckl, J. R., & Wardlaw, J. M. (2002). Magnetic resonance spectroscopy and cognitive function in healthy elderly men. *Brain*, *125*(12), 2743–2749. https://doi.org/10.1093/brain/awf278
Ferman, T. J., Boeve, B. F., Smith, G. E., Lin, S.-C., Silber, M. H., Pedraza, O., Wszolek, Z., Graff-Radford, N. R., Uitti, R., Van Gerpen, J., Pao, W., Knopman, D., Pankratz, V. S., Kantarci, K., Boot, B., Parisi, J. E., Dugger, B. N., Fujishiro, H., Petersen, R. C., & Dickson, D. W. (2011). Inclusion of RBD improves the diagnostic classification of dementia with Lewy bodies. *Neurology*, *77*(9), 875–882. https://doi.org/10.1212/WNL.0b013e31822c9148
Fernandez-Duque, D. (2006). *Attentional Networks in Normal Aging and Alzheimer's Disease*. 12.
Field, D. J., Hayes, A., & Hess, R. F. (1993). Contour integration by the human visual system: evidence for a local "association field". *Vision research*, *33*(2), 173-193.
Firbank, M. J., Blamire, A. M., Krishnan, M. S., Teodorczuk, A., English, P., Gholkar, A., Harrison, R. M., & O'Brien, J. T. (2007). Diffusion tensor imaging in dementia with Lewy bodies and Alzheimer's disease. *Psychiatry Research: Neuroimaging*, *155*(2), 135–145. https://doi.org/10.1016/j.pscychresns.2007.01.001
Firbank, M. J., O'Brien, J. T., & Taylor, J. P. (2018). Long reaction times are associated with delayed brain activity in lewy body dementia: Brain Slowing in Lewy Body Dementia. *Human Brain Mapping*, *39*(2), 633–643. https://doi.org/10.1002/hbm.23866
Firbank, M., Kobeleva, X., Cherry, G., Killen, A., Gallagher, P., Burn, D. J., Thomas, A. J., O'Brien, J. T., & Taylor, J.-P. (2016). Neural correlates of attention-executive dysfunction in lewy body dementia and Alzheimer's disease: Neural Correlates of Attention in Dementia. *Human Brain Mapping*, *37*(3), 1254–1270. https://doi.org/10.1002/hbm.23100
Fischl, B., & Dale, A. M. (2000). Measuring the thickness of the human cerebral cortex from magnetic resonance images. *Proceedings of the National Academy of Sciences*, *97*(20), 11050–11055. https://doi.org/10.1073/pnas.200033797
Fischl, B., Liu, A., & Dale, A. M. (2001). Automated manifold surgery: Constructing geometrically accurate and topologically correct models of the human cerebral cortex. *IEEE Transactions on Medical Imaging*, *20*(1), 70–80. https://doi.org/10.1109/42.906426
Fischl, Bruce. (2012). FreeSurfer. *NeuroImage*, *62*(2), 774–781. https://doi.org/10.1016/j.neuroimage.2012.01.021
Fischl, Bruce, Sereno, M. I., & Dale, A. M. (1999). Cortical Surface-Based Analysis: II: Inflation, Flattening, and a Surface-Based Coordinate System. *NeuroImage*, *9*(2), 195–207. https://doi.org/10.1006/nimg.1998.0396
Fischl, Bruce, van der Kouwe, A., Destrieux, C., Halgren, E., Ségonne, F., Salat, D. H., Busa, E., Seidman, L. J., Goldstein, J., Kennedy, D., Caviness, V., Makris, N., Rosen, B., & Dale, A. M. (2004). Automatically Parcellating the Human Cerebral Cortex. *Cerebral Cortex*, *14*(1), 11–22. https://doi.org/10.1093/cercor/bhg087
Fisher, R. A. (1925). Theory of statistical estimation. In *Mathematical Proceedings of the Cambridge Philosophical Society* (Vol. 22, No. 5, pp. 700-725). Cambridge University Press.

Fjell, A. M., McEvoy, L., Holland, D., Dale, A. M., Walhovd, K. B., & for the Alzheimer's Disease Neuroimaging Initiative. (2013). Brain Changes in Older Adults at Very Low Risk for Alzheimer's Disease. *Journal of Neuroscience*, *33*(19), 8237–8242. https://doi.org/10.1523/JNEUROSCI.5506-12.2013

Fjell, Anders M., & Walhovd, K. B. (2010). Structural Brain Changes in Aging: Courses, Causes and Cognitive Consequences. *Reviews in the Neurosciences*, *21*(3). https://doi.org/10.1515/REVNEURO.2010.21.3.187

Fjell, A. M., Sneve, M. H., Storsve, A. B., Grydeland, H., Yendiki, A., & Walhovd, K. B. (2016). Brain events underlying episodic memory changes in aging: a longitudinal investigation of structural and functional connectivity. *Cerebral cortex*, *26*(3), 1272-1286.

Flanigan, P. M., Khosravi, M. A., Leverenz, J. B., & Tousi, B. (2018). Color Vision Impairment Differentiates Alzheimer Dementia From Dementia With Lewy Bodies. *Journal of Geriatric Psychiatry and Neurology*, *31*(2), 97–102. https://doi.org/10.1177/0891988718767579

Flechsig, L. (1901). Developmental (myelogenetic) localisation of the cerebral cortex in the human subject. *The Lancet*, *158*(4077), 1027-1030.

Flood, D. G., Buell, S. J., Defiore, C. H., Horwitz, G. J., & Coleman, P. D. (1985). Age-related dendritic growth in dentate gyrus of human brain is followed by regression in the 'oldest old'. *Brain research*, *345*(2), 366-368.

Floyer-Lea, A., Wylezinska, M., Kincses, T., & Matthews, P. M. (2006). Rapid Modulation of GABA Concentration in Human Sensorimotor Cortex During Motor Learning. *Journal of Neurophysiology*, *95*(3), 1639–1644. https://doi.org/10.1152/jn.00346.2005

Forstmann, B. U., Tittgemeyer, M., Wagenmakers, E. J., Derrfuss, J., Imperati, D., & Brown, S. (2011). The speed-accuracy tradeoff in the elderly brain: a structural model-based approach. *Journal of Neuroscience*, *31*(47), 17242-17249.

Fosse, R., Stickgold, R., & Hobson, J. A. (2001). Brain-mind states: reciprocal variation in thoughts and hallucinations. *Psychological science*, *12*(1), 30-36.

Frangou, S., Modabbernia, A., Doucet, G. E., Papachristou, E., Williams, S. C., Agartz, I., ... & Serpa, M. H. (2020). Cortical Thickness Trajectories across the Lifespan: Data from 17,075 healthy individuals aged 3-90 years. *BioRxiv*.

Franzmeier, N., Hartmann, J., Taylor, A. N. W., Araque-Caballero, M. Á., Simon-Vermot, L., Kambeitz-Ilankovic, L., Bürger, K., Catak, C., Janowitz, D., Müller, C., Ertl-Wagner, B., Stahl, R., Dichgans, M., Duering, M., & Ewers, M. (2018). The left frontal cortex supports reserve in aging by enhancing functional network efficiency. *Alzheimer's Research & Therapy*, *10*(1), 28. https://doi.org/10.1186/s13195-018-0358-y

Fuentes, L. J., Fernández, P. J., Campoy, G., Antequera, M. M., García-Sevilla, J., & Antúnez, C. (2010). Attention Network Functioning in Patients with Dementia with Lewy Bodies and Alzheimer's Disease. *Dementia and Geriatric Cognitive Disorders*, *29*(2), 139–145. https://doi.org/10.1159/000275672

Gabor, D. (1946). Theory of communication. Part 1: The analysis of information. *Journal of the Institution of Electrical Engineers-Part III: Radio and Communication Engineering*, *93*(26), 429-441.

Gaetz, W., Roberts, T. P., Singh, K. D., & Muthukumaraswamy, S. D. (2012). Functional and structural correlates of the aging brain: Relating visual cortex (V1) gamma band responses to age-related structural change. *Human brain mapping*, *33*(9), 2035-2046.

Gamble, K. R., Howard Jr, J. H., & Howard, D. V. (2014). Not just scenery: viewing nature pictures improves executive attention in older adults. *Experimental aging research*,

Ganis, G., & Kievit, R. (2015). A New Set of Three-Dimensional Shapes for Investigating Mental Rotation Processes: Validation Data and Stimulus Set. *Journal of Open Psychology Data*, *3*. https://doi.org/10.5334/jopd.ai

Gao, F., Edden, R. A. E., Li, M., Puts, N. A. J., Wang, G., Liu, C., Zhao, B., Wang, H., Bai, X., Zhao, C., Wang, X., & Barker, P. B. (2013). Edited magnetic resonance spectroscopy detects an age-related decline in brain GABA levels. *NeuroImage*, *78*, 75–82. https://doi.org/10.1016/j.neuroimage.2013.04.012

Gardener, S. L., Weinborn, M., Sohrabi, H. R., Doecke, J. D., Bourgeat, P., Rainey-Smith, S. R., ... & AIBL Research Group. (2021). Longitudinal trajectories in cortical thickness and volume atrophy: Superior cognitive performance does not protect against brain atrophy in older adults. *Journal of Alzheimer's Disease*, (Preprint), 1-14.

Gaspelin, N., & Luck, S. J. (2018). The Role of Inhibition in Avoiding Distraction by Salient Stimuli. *Trends in Cognitive Sciences*, *22*(1), 79–92. https://doi.org/10.1016/j.tics.2017.11.001

Gazdzinski, S., Millin, R., Kaiser, L. G., Durazzo, T. C., Mueller, S. G., Weiner, M. W., & Meyerhoff, D. J. (2010). BMI and Neuronal Integrity in Healthy, Cognitively Normal Elderly: A Proton Magnetic Resonance Spectroscopy Study. *Obesity*, *18*(4), 743–748. https://doi.org/10.1038/oby.2009.325

Gazzaley, A., Cooney, J. W., Rissman, J., & D'esposito, M. (2005). Top-down suppression deficit underlies working memory impairment in normal aging. *Nature neuroscience*, *8*(10), 1298-1300.

Gazzaley, A., & D'esposito, M. A. R. K. (2007). Top-down modulation and normal aging. *Annals of the New York Academy of Sciences*, *1097*(1), 67-83.

Gazzaley, A., Clapp, W., Kelley, J., McEvoy, K., Knight, R. T., & D'Esposito, M. (2008). Age-related top-down suppression deficit in the early stages of cortical visual memory processing. *Proceedings of the National Academy of Sciences*, *105*(35), 13122-13126.

Gilbert, C. D., & Sigman, M. (2007). Brain States: Top-Down Influences in Sensory Processing. *Neuron*, *54*(5), 677–696. https://doi.org/10.1016/j.neuron.2007.05.019

Giorgio, A., Santelli, L., Tomassini, V., Bosnell, R., Smith, S., De Stefano, N., & Johansen-Berg, H. (2010). Age-related changes in grey and white matter structure throughout adulthood. *NeuroImage*, *51*(3), 943–951. https://doi.org/10.1016/j.neuroimage.2010.03.004

Glanville, N. T., Byers, D. M., Cook, H. W., Spence, M. W., & Palmer, F. B. St. C. (1989). Differences in the metabolism of inositol and phosphoinositides by cultured cells of neuronal and glial origin. *Biochimica et Biophysica Acta (BBA) - Lipids and Lipid Metabolism*, *1004*(2), 169–179. https://doi.org/10.1016/0005-2760(89)90265-8

Gluth, S., Rieskamp, J., & Buchel, C. (2012). Deciding When to Decide: Time-Variant Sequential Sampling Models Explain the Emergence of Value-Based Decisions in the Human Brain. *Journal of Neuroscience*, *32*(31), 10686–10698. https://doi.org/10.1523/JNEUROSCI.0727-12.2012

Goetz, C. G., Tilley, B. C., Shaftman, S. R., Stebbins, G. T., Fahn, S., Martinez-Martin, P., ... & LaPelle, N. (2008). Movement Disorder Society-sponsored revision of the Unified Parkinson's Disease Rating Scale (MDS-UPDRS): scale presentation and clinimetric testing results. *Movement disorders: official journal of the Movement Disorder Society*, *23*(15), 2129-2170.

Goh, J. O., Chee, M. W., Tan, J. C., Venkatraman, V., Hebrank, A., Leshikar, E. D., ... & Park, D. C. (2007). Age and culture modulate object processing and object—scene binding in the ventral visual area. *Cognitive, Affective, & Behavioral Neuroscience*, *7*(1), 44-52.

Gomperts, S. N. (2016). Lewy body dementias: dementia with Lewy bodies and Parkinson disease dementia. *Continuum: Lifelong Learning in Neurology*, *22*(2 Dementia), 435.

Good, C. D., Johnsrude, I. S., Ashburner, J., Henson, R. N. A., Friston, K. J., & Frackowiak, R. S. J. (2001). A voxel-based morphometric study of ageing in 465 normal adult human brains. *NeuroImage*, 21–36.

Gothe, N. P., Keswani, R. K., & McAuley, E. (2016). Yoga practice improves executive function by attenuating stress levels. *Biological Psychology*, *121*, 109–116. https://doi.org/10.1016/j.biopsycho.2016.10.010

Gottlieb, J., & Snyder, L. H. (2010). Spatial and non-spatial functions of the parietal cortex. *Current opinion in neurobiology*, *20*(6), 731-740.

Govenlock, S. W., Taylor, C. P., Sekuler, A. B., & Bennett, P. J. (2009). The effect of aging on the orientational selectivity of the human visual system. *Vision Research*, *49*(1), 164–172. https://doi.org/10.1016/j.visres.2008.10.004

Grachev, I. D., & Apkarian, A. V. (2000). Chemical heterogeneity of the living human brain: a proton MR spectroscopy study on the effects of sex, age, and brain region. *Neuroimage*, *11*(5), 554-563.

Grachev, I. D., Kumar, R., Ramachandran, T. S., & Szeverenyi, N. M. (2001). Cognitive interference is associated with neuronal marker N-acetyl aspartate in the anterior cingulate cortex: An in vivo 1 H-MRS study of the Stroop Color-Word task. *Molecular Psychiatry*, *6*(5), 529–539. https://doi.org/10.1038/sj.mp.4000940

Grady, C. L. (2000). Functional brain imaging and age-related changes in cognition. *Biological Psychology*, *54*(1), 259–281. https://doi.org/10.1016/S0301-0511(00)00059-4

Grady, C., Maisog, J., Horwitz, B., Ungerleider, L., Mentis, M., Salerno, J., Pietrini, P., Wagner, E., & Haxby, J. (1994). Age-related changes in cortical blood flow activation during visual processing of faces and location. *The Journal of Neuroscience*, *14*(3), 1450–1462. https://doi.org/10.1523/JNEUROSCI.14-03-01450.1994

Graff-Radford, J., Murray, M. E., Lowe, V. J., Boeve, B. F., Ferman, T. J., Przybelski, S. A., ... & Kantarci, K. (2014). Dementia with Lewy bodies: basis of cingulate island sign. *Neurology*, *83*(9), 801-809.

Gray, D. T., De La Peña, N. M., Umapathy, L., Burke, S. N., Engle, J. R., Trouard, T. P., & Barnes, C. A. (2020). Auditory and Visual System White Matter Is Differentially Impacted by Normative Aging in Macaques. *The Journal of Neuroscience*, *40*(46), 8913–8923. https://doi.org/10.1523/JNEUROSCI.1163-20.2020

Greene, H. A., & Madden, D. J. (1987). Adult age differences in visual acuity, stereopsis, and contrast sensitivity. *American journal of optometry and physiological optics*, *64*(10), 7

Greenwood, P. (2000). The frontal aging hypothesis evaluated. *Journal of the International Neuropsychological Society : JINS*, *6*, 705–726. https://doi.org/10.1017/S1355617700666092

Greenwood, P. (2007). Functional Plasticity in Cognitive Aging: Review and Hypothesis. *Neuropsychology*, *21*, 657–673. https://doi.org/10.1037/0894-4105.21.6.657

Grimm, O., Pohlack, S., Cacciaglia, R., Winkelmann, T., Plichta, M. M., Demirakca, T., & Flor, H. (2015). Amygdalar and hippocampal volume: a comparison between manual segmentation, Freesurfer and VBM. *Journal of neuroscience methods*, *253*, 254-261.

Grönholm-Nyman, P., Soveri, A., Rinne, J. O., Ek, E., Nyholm, A., Stigsdotter Neely, A., & Laine, M. (2017). Limited Effects of Set Shifting Training in Healthy Older Adults. *Frontiers in Aging Neuroscience*, *9*. https://doi.org/10.3389/fnagi.2017.00069

Grossberg, S., & Huang, T.-R. (2009). ARTSCENE: A neural system for natural scene classification. *Journal of Vision*, *9*(4), 6–6. https://doi.org/10.1167/9.4.6

Grossman, E. J., Kirov, I. I., Gonen, O., Novikov, D. S., Davitz, M. S., Lui, Y. W., ... & Fieremans, E. (2015). N-acetyl-aspartate levels correlate with intra-axonal compartment parameters from diffusion MRI. *Neuroimage*, *118*, 334-343.

Grover, V. P. B., Tognarelli, J. M., Crossey, M. M. E., Cox, I. J., Taylor-Robinson, S. D., & McPhail, M. J. W. (2015). Magnetic Resonance Imaging: Principles and Techniques: Lessons for Clinicians. *Journal of Clinical and Experimental Hepatology*, *5*(3), 246–255. https://doi.org/10.1016/j.jceh.2015.08.001

Gruber, S., Pinker, K., Riederer, F., Chmelík, M., Stadlbauer, A., Bittšanský, M., Mlynárik, V., Frey, R., Serles, W., Bodamer, O., & Moser, E. (2008). Metabolic changes in the normal ageing brain: Consistent findings from short and long echo time proton spectroscopy. *European Journal of Radiology*, *68*(2), 320–327. https://doi.org/10.1016/j.ejrad.2007.08.038

Gu, Y., Manly, J. J., Mayeux, R. P., & Brickman, A. M. (2018). An Inflammation-related Nutrient Pattern is Associated with Both Brain and Cognitive Measures in a Multiethnic Elderly Population. *Current Alzheimer Research*, *15*(5), 493–501. https://doi.org/10.2174/1567205015666180101145619

Gunnlaugsdottir, E., Arnarsson, A., & Jonasson, F. (2008). Prevalence and causes of visual impairment and blindness in Icelanders aged 50 years and older: the Reykjavik Eye Study. *Acta ophthalmologica*, *86*(7), 778-785.

Gutchess, A. H., Welsh, R. C., Hedden, T., Bangert, A., Minear, M., Liu, L. L., & Park, D. C. (2005). Aging and the Neural Correlates of Successful Picture Encoding: Frontal Activations Compensate for Decreased Medial-Temporal Activity. *Journal of Cognitive Neuroscience*, *17*(1), 84–96. https://doi.org/10.1162/0898929052880048

Haga, K. K., Khor, Y. P., Farrall, A., & Wardlaw, J. M. (2009). A systematic review of brain metabolite changes, measured with 1H magnetic resonance spectroscopy, in healthy aging. *Neurobiology of Aging*, *30*(3), 353–363. https://doi.org/10.1016/j.neurobiolaging.2007.07.005

Hájek, M., Dezortová, M., & Komárek, V. (1998). 1H MR spectroscopy in patients with mesial temporal epilepsy. *Magnetic Resonance Materials in Physics, Biology and Medicine*, *7*(2), 95–114.

Halliday, G. M., Song, Y. J. C., & Harding, A. J. (2011). Striatal β-amyloid in dementia with Lewy bodies but not Parkinson's disease. *Journal of Neural Transmission*, *118*(5), 713. https://doi.org/10.1007/s00702-011-0641-6

Happaney, K., Zelazo, P. D., & Stuss, D. T. (2004). Development of orbitofrontal function: Current themes and future directions. *Brain and Cognition*, *55*(1), 1–10. https://doi.org/10.1016/j.bandc.2004.01.001

Harada, M., Miyoshi, H., Otsuka, H., Nishitani, H., & Uno, M. (2001). Multivariate analysis of regional metabolic differences in normal ageing on localised quantitative proton MR spectroscopy. *Neuroradiology*, *43*(6), 448-452.

Harada, C. N., Natelson Love, M. C., & Triebel, K. (2013). Normal Cognitive Aging. *Clinics in Geriatric Medicine*, *29*(4), 737–752. https://doi.org/10.1016/j.cger.2013.07.002

Hardy, J. (2002). The Amyloid Hypothesis of Alzheimer's Disease: Progress and Problems on the Road to Therapeutics. *Science*, *297*(5580), 353–356. https://doi.org/10.1126/science.1072994

Haris, M., Cai, K., Singh, A., Hariharan, H., & Reddy, R. (2011). In vivo mapping of brain myo-inositol. *Neuroimage*, *54*(3), 2079-2085.

Harris, A. D., Puts, N. A. J., & Edden, R. A. E. (2015). Tissue correction for GABA-edited MRS: Considerations of voxel composition, tissue segmentation, and tissue relaxations. *Journal of Magnetic Resonance Imaging*, *42*(5), 1431–1440. https://doi.org/10.1002/jmri.24903

Harris, S. E., & Deary, I. J. (2011). The genetics of cognitive ability and cognitive ageing in healthy older people. *Trends in Cognitive Sciences*, *15*(9), 388–394. https://doi.org/10.1016/j.tics.2011.07.004

Hasher, L., & Zacks, R. T. (1988). Working memory, comprehension, and aging: A review and a new view. *Psychology of learning and motivation*, *22*, 193-225.

Hatanpää, K., Isaacs, K. R., Shirao, T., Brady, D. R., & Rapoport, S. I. (1999). Loss of proteins regulating synaptic plasticity in normal aging of the human brain and in Alzheimer disease. *Journal of neuropathology and experimental neurology*, *58*(6), 637-643.

Hatta, T., Iwahara, A., Hatta, T., Ito, E., Hatta, J., Hotta, C., Nagahara, N., Fujiwara, K., & Hamajima, N. (2015). Developmental trajectories of verbal and visuospatial abilities in healthy older adults: Comparison of the hemisphere asymmetry reduction in older adults model and the right hemi-ageing model. *Laterality: Asymmetries of Body, Brain and Cognition*, *20*(1), 69–81. https://doi.org/10.1080/1357650X.2014.917656

Haueis, P. (2014). Meeting the brain on its own terms. *Frontiers in human neuroscience*, *8*, 815.

Haynes, B. I., Bauermeister, S., & Bunce, D. (2017). A Systematic Review of Longitudinal Associations Between Reaction Time Intraindividual Variability and Age-Related Cognitive Decline or Impairment, Dementia, and Mortality. *Journal of the International Neuropsychological Society*, *23*(5), 431–445. https://doi.org/10.1017/S1355617717000236

Haynes, B. I., Bunce, D., Kochan, N. A., Wen, W., Brodaty, H., & Sachdev, P. S. (2017). Associations between reaction time measures and white matter hyperintensities in very old age. *Neuropsychologia*, *96*, 249–255. https://doi.org/10.1016/j.neuropsychologia.2017.01.021

Head, D., Buckner, R. L., Shimony, J. S., Williams, L. E., Akbudak, E., Conturo, T. E., ... & Snyder, A. Z. (2004). Differential vulnerability of anterior white matter in nondemented aging with minimal acceleration in dementia of the Alzheimer type: evidence from diffusion tensor imaging. *Cerebral cortex*, *14*(4), 410-423.

Hedge, C., Powell, G., & Sumner, P. (20181008). The mapping between transformed reaction time costs and models of processing in aging and cognition. *Psychology and Aging*, *33*(7), 1093. https://doi.org/10.1037/pag0000298

Hedman, A. M., Haren, N. E. M. van, Schnack, H. G., Kahn, R. S., & Pol, H. E. H. (2012). Human brain changes across the life span: A review of 56 longitudinal magnetic resonance imaging studies. *Human Brain Mapping*, *33*(8), 1987–2002. https://doi.org/10.1002/hbm.21334

Heitz, C., Noblet, V., Phillipps, C., Cretin, B., Vogt, N., Philippi, N., Kemp, J., de Petigny, X., Bilger, M., Demuynck, C., Martin-Hunyadi, C., Armspach, J.-P., & Blanc, F. (2016). Cognitive and affective theory of mind in dementia with Lewy bodies and Alzheimer's disease. *Alzheimer's Research & Therapy*, *8*(1), 10. https://doi.org/10.1186/s13195-016-0179-9

Herbet, G., Zemmoura, I., & Duffau, H. (2018). Functional Anatomy of the Inferior Longitudinal Fasciculus: From Historical Reports to Current Hypotheses. *Frontiers in Neuroanatomy*, *12*. https://doi.org/10.3389/fnana.2018.00077

Hermans, L., Leunissen, I., Pauwels, L., Cuypers, K., Peeters, R., Puts, N. A. J., Edden, R. A. E., & Swinnen, S. P. (2018). Brain GABA Levels Are Associated with Inhibitory Control Deficits in Older Adults. *The Journal of Neuroscience*, *38*(36), 7844–7851. https://doi.org/10.1523/JNEUROSCI.0760-18.2018

Hess, R. F., Hayes, A., & Field, D. J. (2003). Contour integration and cortical processing. *Journal of Physiology-Paris*, *97*(2-3), 105-119

Hess, T. M., & Ennis, G. E. (2012). Age differences in the effort and costs associated with cognitive activity. *Journals of Gerontology Series B: Psychological Sciences and Social Sciences*, *67*(4), 447-455.

Hinault, T., Lemaire, P., & Phillips, N. (2016). Aging and sequential modulations of poorer strategy effects: An EEG study in arithmetic problem solving. *Brain Research*, *1630*, 144–158. https://doi.org/10.1016/j.brainres.2015.10.057

Hirst, R. J., Whelan, R., Boyle, R., Setti, A., Knight, S., O'Connor, J., Williamson, W., McMorrow, J., Fagan, A. J., Meaney, J. F., Kenny, R. A., De Looze, C., & Newell, F. N. (2021). Gray matter volume in the right angular gyrus is associated with differential patterns of multisensory integration with aging. *Neurobiology of Aging*, *100*, 83–90. https://doi.org/10.1016/j.neurobiolaging.2020.12.004

Hodgetts, C. J., Postans, M., Shine, J. P., Jones, D. K., Lawrence, A. D., & Graham, K. S. (2015). Dissociable roles of the inferior longitudinal fasciculus and fornix in face and place perception. *ELife*, *4*. https://doi.org/10.7554/eLife.07902

Hofer, S. M., Sliwinski, M. J., & Flaherty, B. P. (2002). Understanding Ageing: Further Commentary on the Limitations of Cross-Sectional Designs for Ageing Research. *Gerontology*, *48*(1), 22–29. https://doi.org/10.1159/000048920

Holtzer, R., Shuman, M., Mahoney, J. R., Lipton, R., & Verghese, J. (2010). Cognitive fatigue defined in the context of attention networks. *Aging, Neuropsychology, and Cognition*, *18*(1), 108-128.

Horga, G., & Abi-Dargham, A. (2019). An integrative framework for perceptual disturbances in psychosis. *Nature Reviews Neuroscience*, *20*(12), 763-778.

Hornak, J., Bramham, J., Rolls, E. T., Morris, R. G., O'Doherty, J., Bullock, P. R., & Polkey, C. E. (2003). Changes in emotion after circumscribed surgical lesions of the orbitofrontal and cingulate cortices. *Brain*, *126*(7), 1691-1712.

Horne, E. D., de Chastelaine, M., & Rugg, M. D. (2021). Neural correlates of post-retrieval monitoring in older adults are preserved under divided attention, but are decoupled from memory performance. *Neurobiology of Aging*, *97*, 106–119. https://doi.org/10.1016/j.neurobiolaging.2020.10.010

Hsieh, S., Liang, Y.-C., & Tsai, Y.-C. (2012). Do age-related changes contribute to the flanker effect? *Clinical Neurophysiology*, *123*(5), 960–972. https://doi.org/10.1016/j.clinph.2011.09.013

Huang, Z., Iv, H. (Hap) D., Yue, Q., Wiebking, C., Duncan, N. W., Zhang, J., Wagner, N.-F., Wolff, A., & Northoff, G. (2015). Increase in glutamate/glutamine concentration in the medial prefrontal cortex during mental imagery: A combined functional mrs and fMRI study. *Human Brain Mapping*, *36*(8), 3204–3212. https://doi.org/10.1002/hbm.22841

Huang, H., Fan, X., Weiner, M., Martin-Cook, K., Xiao, G., Davis, J., ... & Diaz-Arrastia, R. (2012). Distinctive disruption patterns of white matter tracts in Alzheimer's disease with full diffusion tensor characterization. *Neurobiology of aging*, *33*(9), 2029-2045.

Huang, D., Liu, D., Yin, J., Qian, T., Shrestha, S., & Ni, H. (2017). Glutamate-glutamine and GABA in brain of normal aged and patients with cognitive impairment. *European radiology*, *27*(7), 2698-2705.

Hubel, D. H., & Wiesel, T. N. (1962). Receptive fields, binocular interaction and functional architecture in the cat's visual cortex. *The Journal of Physiology*, *160*(1), 106–154. https://doi.org/10.1113/jphysiol.1962.sp006837

Huisman, T. A. G. M. (2010). Diffusion-weighted and diffusion tensor imaging of the brain, made easy. *Cancer Imaging*, *10*(1A), S163–S171. https://doi.org/10.1102/1470-7330.2010.9023

Hultsch, D. F., MacDonald, S. W. S., & Dixon, R. A. (2002). Variability in Reaction Time Performance of Younger and Older Adults. *The Journals of Gerontology: Series B*, *57*(2), P101–P115. https://doi.org/10.1093/geronb/57.2.P101

Huppert, F. A., Brayne, C., Jagger, C., & Metz, D. (2000). Longitudinal studies of ageing: a key role in the evidence base for improving health and quality of life in older adults. *Age and Ageing*, *29*(6), 485-486.

Hutton, C., Draganski, B., Ashburner, J., & Weiskopf, N. (2009). A comparison between voxel-based cortical thickness and voxel-based morphometry in normal aging. *Neuroimage*, *48*(2), 371-380.

Hsieh, S., Liang, Y. C., & Tsai, Y. C. (2012). Do age-related changes contribute to the flanker effect?. *Clinical Neurophysiology*, *123*(5), 960-972.

Iannaccone, S., Cerami, C., Alessio, M., Garibotto, V., Panzacchi, A., Olivieri, S., Gelsomino, G., Moresco, R. M., & Perani, D. (2013). In vivo microglia activation in very early dementia with Lewy bodies, comparison with Parkinson's disease. *Parkinsonism & Related Disorders*, *19*(1), 47–52. https://doi.org/10.1016/j.parkreldis.2012.07.002

Ihara, M., Polvikoski, T. M., Hall, R., Slade, J. Y., Perry, R. H., Oakley, A. E., ... & Kalaria, R. N. (2010). Quantification of myelin loss in frontal lobe white matter in vascular dementia, Alzheimer's disease, and dementia with Lewy bodies. *Acta neuropathologica*, *119*(5), 579-589.

Inano, S., Takao, H., Hayashi, N., Abe, O., & Ohtomo, K. (2011). Effects of Age and Gender on White Matter Integrity. *American Journal of Neuroradiology*, *32*(11), 2103–2109. https://doi.org/10.3174/ajnr.A2785

Ishigami, Y., Eskes, G., Tyndall, A., Longman, R., Drogos, L., & Poulin, M. (2016). The Attention Network Test-Interaction (ANT-I): Reliability and validity in healthy older adults. *Experimental Brain Research*, *234*. https://doi.org/10.1007/s00221-015-4493-4

Jackson, J. D., Balota, D. A., Duchek, J. M., & Head, D. (2012). White matter integrity and reaction time intraindividual variability in healthy aging and early-stage Alzheimer disease. *Neuropsychologia*, *50*(3), 357–366. https://doi.org/10.1016/j.neuropsychologia.2011.11.024

Jang, S. H., Cho, S. H., & Chang, M. C. (2011). Age-related degeneration of the fornix in the human brain: a diffusion tensor imaging study. *International Journal of Neuroscience*, *121*(2), 94-100.

Jansen, J. F. A., Backes, W. H., Nicolay, K., & Kooi, M. E. (2006). 1H MR Spectroscopy of the Brain: Absolute Quantification of Metabolites. *Radiology*, *240*(2), 318–332. https://doi.org/10.1148/radiol.2402050314

Jansen, P., & Kaltner, S. (2014). Object-based and egocentric mental rotation performance in older adults: the importance of gender differences and motor ability. *Aging, Neuropsychology, and Cognition*, *21*(3), 296-316.

Jeurissen, B., Descoteaux, M., Mori, S., & Leemans, A. (2017). Diffusion MRI fiber tractography of the brain. *NMR in Biomedicine*, *32*(4), e3785.

Jernigan, T. L., Archibald, S. L., Fennema-Notestine, C., Gamst, A. C., Stout, J. C., Bonner, J., & Hesselink, J. R. (2001). Effects of age on tissues and regions of the cerebrum and cerebellum. *Neurobiology of Aging*, *22*(4), 581–594. https://doi.org/10.1016/S0197-4580(01)00217-2

Johns, E. K., Phillips, N. A., Belleville, S., Goupil, D., Babins, L., Kelner, N., Ska, B., Gilbert, B., Inglis, G., Panisset, M., de Boysson, C., & Chertkow, H. (2009). Executive functions in frontotemporal dementia and Lewy body dementia. *Neuropsychology*, *23*(6), 765–777. https://doi.org/10.1037/a0016792

Jones, D. K. (2004). The effect of gradient sampling schemes on measures derived from diffusion tensor MRI: a Monte Carlo study. *Magnetic Resonance in Medicine: An Official Journal of the International Society for Magnetic Resonance in Medicine*, *51*(4), 807-815.

Jones, D. K., Horsfield, M. A., & Simmons, A. (1999). Optimal strategies for measuring diffusion in anisotropic systems by magnetic resonance imaging. *Magnetic Resonance in Medicine*, *42*(3), 515–525.

Jones, D. K. (2010). Challenges and limitations of quantifying brain connectivity in vivo with diffusion MRI. *Imaging in Medicine*, *2*(3), 341.

Jones, D. K., Knösche, T. R., & Turner, R. (2013). White matter integrity, fiber count, and other fallacies: The do's and don'ts of diffusion MRI. *NeuroImage*, *73*, 239–254. https://doi.org/10.1016/j.neuroimage.2012.06.081

Jones, S. A., Beierholm, U., Meijer, D., & Noppeney, U. (2019). Older adults sacrifice response speed to preserve multisensory integration performance. *Neurobiology of aging*, *84*, 148-157.

Joubert, C., & Chainay, H. (2018). Aging brain: The effect of combined cognitive and physical training on cognition as compared to cognitive and physical training alone – a systematic review. *Clinical Interventions in Aging*, *13*, 1267–1301. https://doi.org/10.2147/CIA.S165399

Jorge, L., Canário, N., Quental, H., Bernardes, R., & Castelo-Branco, M. (2020). Is the retina a mirror of the aging brain? Aging of neural retina layers and primary visual cortex across the lifespan. *Frontiers in aging neuroscience*, *11*, 360.

Kaiser, L. G., Schuff, N., Cashdollar, N., & Weiner, M. W. (2005). Age-related glutamate and glutamine concentration changes in normal human brain: 1H MR spectroscopy study at 4 T. *Neurobiology of Aging*, *26*(5), 665–672. https://doi.org/10.1016/j.neurobiolaging.2004.07.001

Kamagata, K., Zalesky, A., Hatano, T., Di Biase, M. A., El Samad, O., Saiki, S., ... & Pantelis, C. (2018). Connectome analysis with diffusion MRI in idiopathic Parkinson's disease: Evaluation using multi-shell, multi-tissue, constrained spherical deconvolution. *NeuroImage: Clinical*, *17*, 518-529.

Kantarci, K., Avula, R., Senjem, M. L., Samikoglu, A. R., Zhang, B., Weigand, S. D., Przybelski, S. A., Edmonson, H. A., Vemuri, P., Knopman, D. S., Ferman, T. J., Boeve, B. F., Petersen, R. C., & Jack, C. R. (2010). Dementia with Lewy bodies and Alzheimer disease. *Neurology*, *74*(22), 1814–1821. https://doi.org/10.1212/WNL.0b013e3181e0f7cf

Kantarci, K., Lowe, V., Przybelski, S. A., Senjem, M. L., Weigand, S. D., Ivnik, R. J., Roberts, R., Geda, Y. E., Boeve, B. F., Knopman, D. S., Petersen, R. C., & Jack, C. R. (2011). Magnetic resonance spectroscopy, β-amyloid load, and cognition in a population-based sample of cognitively normal older adults. *Neurology*, *77*(10), 951–958. https://doi.org/10.1212/WNL.0b013e31822dc7e1

Kantarci, K, Petersen, R. C., Boeve, B. F., Knopman, D. S., Tang-Wai, D. F., O'Brien, P. C., Weigand, S. D., Edland, S. D., Smith, G. E., Ivnik, R. J., Ferman, T. J., Tangalos, E. G., & Jack, C. R. (2004). 1H MR SPECTROSCOPY IN COMMON DEMENTIAS. *Neurology*, *63*(8), 1393–1398.

Kaping, D., Vinck, M., Hutchison, R. M., Everling, S., & Womelsdorf, T. (2011). Specific Contributions of Ventromedial, Anterior Cingulate, and Lateral Prefrontal Cortex for Attentional Selection and Stimulus Valuation. *PLOS Biology*, *9*(12), e1001224. https://doi.org/10.1371/journal.pbio.1001224

Kavcic, V., Vaughn, W., & Duffy, C. J. (2011). Distinct visual motion processing impairments in aging and Alzheimer's disease. *Vision Research*, *51*(3), 386–395. https://doi.org/10.1016/j.visres.2010.12.004

Keller, J. B., Hedden, T., Thompson, T. W., Anteraper, S. A., Gabrieli, J. D. E., & Whitfield-Gabrieli, S. (2015). Resting-state anticorrelations between medial and lateral prefrontal cortex: Association with working memory, aging, and individual differences. *Cortex*, *64*, 271–280. https://doi.org/10.1016/j.cortex.2014.12.001

Kelly, S. P., & O'Connell, R. G. (2013). Internal and external influences on the rate of sensory evidence accumulation in the human brain. *Journal of Neuroscience*, *33*(50), 19434-19441.

Kennedy, K. M., & Raz, N. (2009). Aging white matter and cognition: Differential effects of regional variations in diffusion properties on memory, executive functions, and speed. *Neuropsychologia*, *47*(3), 916–927. https://doi.org/10.1016/j.neuropsychologia.2009.01.001

Kennedy, K., & Raz, N. (2015). *Normal Aging of the Brain. In: Arthur W. Toga, editor. Brain Mapping: An Encyclopedic Reference, vol. 3, pp. 603-617. Academic Press: Elsevier.* (pp. 603–617).

Kerchner, G. A., Racine, C. A., Hale, S., Wilheim, R., Laluz, V., Miller, B. L., & Kramer, J. H. (2012). Cognitive Processing Speed in Older Adults: Relationship with White Matter Integrity. *PLOS ONE*, *7*(11), e50425. https://doi.org/10.1371/journal.pone.0050425

Keuken, M. C., Bazin, P.-L., Backhouse, K., Beekhuizen, S., Himmer, L., Kandola, A., Lafeber, J. J., Prochazkova, L., Trutti, A., Schäfer, A., Turner, R., & Forstmann, B. U. (2017). Effects of aging on T1, T2* and QSM MRI values in the subcortex. *Brain Structure and Function*, *222*(6), 2487–2505. https://doi.org/10.1007/s00429-016-1352-4

Khundakar, A. A., Hanson, P. S., Erskine, D., Lax, N. Z., Roscamp, J., Karyka, E., Tsefou, E., Singh, P., Cockell, S. J., Gribben, A., Ramsay, L., Blain, P. G., Mosimann, U. P., Lett, D. J., Elstner, M., Turnbull, D. M., Xiang, C. C., Brownstein, M. J., O'Brien, J. T., … Morris, C. M. (2016). Analysis of primary visual cortex in dementia with Lewy bodies indicates GABAergic involvement associated with recurrent complex visual hallucinations. *Acta Neuropathologica Communications*, *4*(1). https://doi.org/10.1186/s40478-016-0334-3

Kievit, R. A., Davis, S. W., Mitchell, D. J., Taylor, J. R., Duncan, J., & Henson, R. N. A. (2014). Distinct aspects of frontal lobe structure mediate age-related differences in fluid intelligence and multitasking. *Nature Communications*, *5*(1), 5658. https://doi.org/10.1038/ncomms6658

Kiuchi, K., Morikawa, M., Taoka, T., Kitamura, S., Nagashima, T., Makinodan, M., ... & Kishimoto, T. (2011). White matter changes in dementia with Lewy bodies and Alzheimer's disease: a tractography-based study. *Journal of psychiatric research*, *45*(8), 1095-1100.

Kihara, K., Kondo, H. M., & Kawahara, J. I. (2016). Differential contributions of GABA concentration in frontal and parietal regions to individual differences in attentional blink. *Journal of neuroscience*, *36*(34), 8895-8901.

Kim, S. H., Jeon, H. E., & Park, C. H. (2020). Relationship between Visual Perception and Microstructural Change of the Superior Longitudinal Fasciculus in Patients with Brain Injury in the Right Hemisphere: A Preliminary Diffusion Tensor Tractography Study. *Diagnostics*, *10*(9), 641.

Kimoto, A., Iseki, E., Ota, K., Murayama, N., Sato, K., Ogura, N., & Arai, H. (2017). Differences in responses to the Rorschach test between patients with dementia with Lewy bodies and Alzheimer's disease -from the perspective of visuoperceptual impairment. *Psychiatry Research*, *257*, 456–461. https://doi.org/10.1016/j.psychres.2017.08.038

King, B. R., Rumpf, J. J., Verbaanderd, E., Heise, K. F., Dolfen, N., Sunaert, S., & Swinnen, S. P. (2020). Baseline sensorimotor GABA levels shape neuroplastic processes induced by motor learning in older adults. *Human brain mapping*, *41*(13), 3680-3695.

Kingdom, F. A. A., & Prins, N. (2016). *Psychophysics: A Practical Introduction*. Academic Press.

Kiuchi, K., Morikawa, M., Taoka, T., Kitamura, S., Nagashima, T., Makinodan, M., Nakagawa, K., Fukusumi, M., Ikeshita, K., Inoue, M., Kichikawa, K., & Kishimoto, T. (2011). White matter changes in dementia with Lewy bodies and Alzheimer's disease: A tractography-based study. *Journal of Psychiatric Research*, *45*(8), 1095–1100. https://doi.org/10.1016/j.jpsychires.2011.01.011

Kobeleva, X., Firbank, M., Peraza, L., Gallagher, P., Thomas, A., Burn, D. J., O'Brien, J., & Taylor, J.-P. (2017). Divergent functional connectivity during attentional processing in Lewy body dementia and Alzheimer's disease. *Cortex*, *92*, 8–18. https://doi.org/10.1016/j.cortex.2017.02.016

Kochunov, P., Williamson, D. E., Lancaster, J., Fox, P., Cornell, J., Blangero, J., & Glahn, D. C. (2012). Fractional anisotropy of water diffusion in cerebral white matter across the lifespan. *Neurobiology of aging*, *33*(1), 9-20.

Koen, J. D., & Rugg, M. D. (2019). Neural Dedifferentiation in the Aging Brain. *Trends in Cognitive Sciences*, *23*(7), 547–559. https://doi.org/10.1016/j.tics.2019.04.012

Koen, J. D., Srokova, S., & Rugg, M. D. (2020). Age-related neural dedifferentiation and cognition. *Current Opinion in Behavioral Sciences*, *32*, 7–14. https://doi.org/10.1016/j.cobeha.2020.01.006

Koerts, J., Borg, M. A., Meppelink, A. M., Leenders, K. L., van Beilen, M., & van Laar, T. (2010). Attentional and perceptual impairments in Parkinson's disease with visual hallucinations. *Parkinsonism & related disorders*, *16*(4), 270-274.

Kolasinski, J., Logan, J. P., Hinson, E. L., Manners, D., Zand, A. P. D., Makin, T. R., ... & Stagg, C. J. (2017). A mechanistic link from GABA to cortical architecture and perception. *Current Biology*, *27*(11), 1685-1691.

Konar, Y., Bennett, P. J., & Sekuler, A. B. (2013). Effects of aging on face identification and holistic face processing. *Vision Research*, *88*, 38–46. https://doi.org/10.1016/j.visres.2013.06.003

Kondo, H. M., Pressnitzer, D., Shimada, Y., Kochiyama, T., & Kashino, M. (2018). Inhibition-excitation balance in the parietal cortex modulates volitional control for auditory and visual multistability. *Scientific reports*, *8*(1), 1-13.

Konen, C. S., & Kastner, S. (2008). Two hierarchically organized neural systems for object information in human visual cortex. *Nature Neuroscience*, *11*(2), 224–231. https://doi.org/10.1038/nn2036

Kontsevich, L. L., & Tyler, C. W. (1999). Bayesian adaptive estimation of psychometric slope and threshold. *Vision research*, *39*(16), 2729-2737.

Korsch, M., Frühholz, S., & Herrmann, M. (2014). Ageing differentially affects neural processing of different conflict types—An fMRI study. *Frontiers in Aging Neuroscience*, *6*. https://doi.org/10.3389/fnagi.2014.00057

Koscik, T., O'Leary, D., Moser, D. J., Andreasen, N. C., & Nopoulos, P. (2009). Sex differences in parietal lobe morphology: relationship to mental rotation performance. *Brain and cognition*, *69*(3), 451-459.

Kourtzi, Z., & Kanwisher, N. (2001). Representation of perceived object shape by the human lateral occipital complex. *Science*, *293*(5534), 1506-1509.

Kourtzi, Z., & Huberle, E. (2005). Spatiotemporal characteristics of form analysis in the human visual cortex revealed by rapid event-related fMRI adaptation. *Neuroimage*, *28*(2), 440-452.

Kramer, A. F., & Kray, J. (2006). Aging and Attention. In *Lifespan cognition: Mechanisms of change* (pp. 57–69). Oxford University Press. https://doi.org/10.1093/acprof:oso/9780195169539.003.0005

Kuczynski, B., Targan, E., Madison, C., Weiner, M., Zhang, Y., Reed, B., ... & Jagust, W. (2010). White matter integrity and cortical metabolic associations in aging and dementia. *Alzheimer's & dementia*, *6*(1), 54-62.

Kühn, S., Schmiedek, F., Schott, B., Ratcliff, R., Heinze, H.-J., Düzel, E., Lindenberger, U., & Lövden, M. (2010). Brain Areas Consistently Linked to Individual Differences in Perceptual Decision-making in Younger as well as Older Adults before and after Training. *Journal of Cognitive Neuroscience*, *23*(9), 2147–2158. https://doi.org/10.1162/jocn.2010.21564

Lacreuse, A., Moore, C. M., LaClair, M., Payne, L., & King, J. A. (2018). Glutamine/glutamate (Glx) concentration in prefrontal cortex predicts reversal learning performance in the marmoset. *Behavioural Brain Research*, *346*, 11–15. https://doi.org/10.1016/j.bbr.2018.01.025

Lai, L. Y., Frömer, R., Festa, E. K., & Heindel, W. C. (2020). Age-related changes in the neural dynamics of bottom-up and top-down processing during visual object recognition: An electrophysiological investigation. *Neurobiology of Aging*, *94*, 38–49. https://doi.org/10.1016/j.neurobiolaging.2020.05.010

Lai, C. H., & Wu, Y. T. (2014). Alterations in white matter micro-integrity of the superior longitudinal fasciculus and anterior thalamic radiation of young adult patients with depression. *Psychological Medicine*, *44*(13), 2825-2832.

Lalwani, P., Gagnon, H., Cassady, K., Simmonite, M., Peltier, S., Seidler, R. D., Taylor, S. F., Weissman, D. H., & Polk, T. A. (2019). Neural distinctiveness declines with age in auditory cortex and is associated with auditory GABA levels. *NeuroImage*, *201*, 116033. https://doi.org/10.1016/j.neuroimage.2019.116033

Landelle, C., Chancel, M., Blanchard, C., Guerraz, M., & Kavounoudias, A. (2021). Contribution of muscle proprioception to limb movement perception and proprioceptive decline with ageing. *Current Opinion in Physiology*. https://doi.org/10.1016/j.cophys.2021.01.016

Landy, K. M., Salmon, D. P., Galasko, D., Filoteo, J. V., Festa, E. K., Heindel, W. C., Hansen, L. A., & Hamilton, J. M. (2015). Motion discrimination in dementia with Lewy bodies and Alzheimer disease. *Neurology*, *85*(16), 1376–1382. https://doi.org/10.1212/WNL.0000000000002028

Larcombe, S. J., Kennard, C., & Bridge, H. (2018). Increase in MST activity correlates with visual motion learning: a functional MRI study of perceptual learning. *Human brain mapping*, *39*(1), 145-156.

Lawton, M. P., & Brody, E. M. (1969). Assessment of older people: self-maintaining and instrumental activities of daily living. *The gerontologist*, *9*(3_Part_1), 179-186.

Lebedev, A. V., Westman, E., Beyer, M. K., Kramberger, M. G., Aguilar, C., Pirtosek, Z., & Aarsland, D. (2013). Multivariate classification of patients with Alzheimer's and dementia with Lewy bodies using high-

dimensional cortical thickness measurements: An MRI surface-based morphometric study. *Journal of Neurology*, *260*(4), 1104–1115. https://doi.org/10.1007/s00415-012-6768-z
Lee, J. E., Park, B., Song, S. K., Sohn, Y. H., Park, H.-J., & Lee, P. H. (2010). A comparison of gray and white matter density in patients with Parkinson's disease dementia and dementia with Lewy bodies using voxel-based morphometry. *Movement Disorders*, *25*(1), 28–34. https://doi.org/10.1002/mds.22858
Lee, J. S., Kim, S., Yoo, H., Park, S., Jang, Y. K., Kim, H. J., ... & Seo, S. W. (2018). Trajectories of physiological brain aging and related factors in people aged from 20 to over-80. *Journal of Alzheimer's Disease*, *65*(4), 1237-1246.
Lee, S., Kim, E. Y., & Shin, C. (2019). Longitudinal association between brain volume change and gait speed in a general population. *Experimental gerontology*, *118*, 26-30.
Leemans, A., Jeurissen, B., Sijbers, J., & Jones, D. K. (n.d.). *ExploreDTI: a graphical toolbox for processing, analyzing, and visualizing diffusion MR data*. 1.
Leland, D. S., Arce, E., Miller, D. A., & Paulus, M. P. (2008). Anterior cingulate cortex and benefit of predictive cueing on response inhibition in stimulant dependent individuals. *Biological psychiatry*, *63*(2), 184-190.
Lemaire, P. (2010). Cognitive Strategy Variations During Aging. *Current Directions in Psychological Science*, *19*(6), 363–369. https://doi.org/10.1177/0963721410390354
Levar, N., Van Doesum, T. J., Denys, D., & Van Wingen, G. A. (2019). Anterior cingulate GABA and glutamate concentrations are associated with resting-state network connectivity. *Scientific Reports*, *9*(1), 2116. https://doi.org/10.1038/s41598-018-38078-1
Leventhal, A. G., Wang, Y., Pu, M., Zhou, Y., & Ma, Y. (2003). GABA and its agonists improved visual cortical function in senescent monkeys. *Science*.
Lezak, P. of N. P. and N. M. D., Lezak, M. D., Howieson, A. P. of N. and P. D. B., Howieson, D. B., Loring, P. of N. D. W., Loring, D. W., & Fischer, J. S. (2004). *Neuropsychological Assessment*. Oxford University Press.
Li, L., Gratton, C., Fabiani, M., & Knight, R. T. (2013). Age-related frontoparietal changes during the control of bottom-up and top-down attention: an ERP study. *Neurobiology of aging*, *34*(2), 477-488.
Li, B. S., Wang, H., & Gonen, O. (2003). Metabolite ratios to assumed stable creatine level may confound the quantification of proton brain MR spectroscopy. *Magnetic resonance imaging*, *21*(8), 923-928.
Li, A. W. Y., & King, J. (2019). Spatial memory and navigation in ageing: A systematic review of MRI and fMRI studies in healthy participants. *Neuroscience & Biobehavioral Reviews*, *103*, 33–49. https://doi.org/10.1016/j.neubiorev.2019.05.005
Li, F. F., VanRullen, R., Koch, C., & Perona, P. (2002). Rapid natural scene categorization in the near absence of attention. *Proceedings of the National Academy of Sciences*, *99*(14), 9596–9601. https://doi.org/10.1073/pnas.092277599
Liem, F., Mérillat, S., Bezzola, L., Hirsiger, S., Philipp, M., Madhyastha, T., & Jäncke, L. (2015). Reliability and statistical power analysis of cortical and subcortical FreeSurfer metrics in a large sample of healthy elderly. *Neuroimage*, *108*, 95-109.
Lin, F., Heffner, K. L., Ren, P., Tivarus, M. E., Brasch, J., Chen, D. G., ... & Tadin, D. (2016). Cognitive and neural effects of vision-based speed-of-processing training in older adults with amnestic mild cognitive impairment: A pilot study. *Journal of the American Geriatrics Society*, *64*(6), 1293-1298.
Lilja, Y., & Nilsson, D. T. (2015). Strengths and limitations of tractography methods to identify the optic radiation for epilepsy surgery. *Quantitative imaging in medicine and surgery*, *5*(2), 288.
Lind, A., Boraxbekk, C.-J., Petersen, E. T., Paulson, O. B., Siebner, H. R., & Marsman, A. (2020). Regional Myo-Inositol, Creatine, and Choline Levels Are Higher at Older Age and Scale Negatively with Visuospatial Working Memory: A Cross-Sectional Proton MR Spectroscopy Study at 7 Tesla on Normal Cognitive Ageing. *The Journal of Neuroscience*, *40*(42), 8149–8159. https://doi.org/10.1523/JNEUROSCI.2883-19.2020
Lipp, I., Parker, G. D., Tallantyre, E. C., Goodall, A., Grama, S., Patitucci, E., ... & Jones, D. K. (2020). Tractography in the presence of multiple sclerosis lesions. *NeuroImage*, *209*, 116471.
Lloyd, W. K., Morriss, J., Macdonald, B., Joanknecht, K., Nihouarn, J., & Van Reekum, C. M. (2021). Longitudinal change in executive function is associated with impaired top-down frontolimbic regulation during reappraisal in older adults. *NeuroImage*, *225*, 117488.
Lo, C. C., & Wang, X. J. (2006). Cortico–basal ganglia circuit mechanism for a decision threshold in reaction time tasks. *Nature neuroscience*, *9*(7), 956-963.
Lockhart, S. N., Roach, A. E., Luck, S. J., Geng, J., Beckett, L., Carmichael, O., & DeCarli, C. (2014). White matter hyperintensities are associated with visual search behavior independent of generalized slowing in aging. *Neuropsychologia*, *52*, 93–101. https://doi.org/10.1016/j.neuropsychologia.2013.10.011
Logan, J. M., Sanders, A. L., Snyder, A. Z., Morris, J. C., & Buckner, R. L. (2002). Under-recruitment and nonselective recruitment: dissociable neural mechanisms associated with aging. *Neuron*, *33*(5), 827-840.
Long, G. M., & Crambert, R. F. (1990). The nature and basis of age-related changes in dynamic visual acuity. *Psychology and Aging*, *5*(1), 138.

Loreto, A., Hill, C. S., Hewitt, V. L., Orsomando, G., Angeletti, C., Gilley, J., ... & Coleman, M. P. (2020). Mitochondrial impairment activates the Wallerian pathway through depletion of NMNAT2 leading to SARM1-dependent axon degeneration. *Neurobiology of disease*, *134*, 104678.

Lövdén, M., Li, S.-C., Shing, Y. L., & Lindenberger, U. (2007). Within-person trial-to-trial variability precedes and predicts cognitive decline in old and very old age: Longitudinal data from the Berlin Aging Study. *Neuropsychologia*, *45*(12), 2827–2838. https://doi.org/10.1016/j.neuropsychologia.2007.05.005

Lovell, P. G. (2005). Manipulating contour smoothness: Evidence that the association-field model underlies contour integration in the periphery. *Journal of Vision*, *5*(8), 469.

Lu, Z.-H., Chakraborty, G., Ledeen, R. W., Yahya, D., & Wu, G. (2004). N-Acetylaspartate synthase is bimodally expressed in microsomes and mitochondria of brain. *Molecular Brain Research*, *122*(1), 71–78. https://doi.org/10.1016/j.molbrainres.2003.12.002

Lu, Z. L., & Dosher, B. (2013). *Visual psychophysics: From laboratory to theory*. MIT Press.

Lu, Y., Yin, J., Chen, Z., Gong, H., Liu, Y., Qian, L., ... & Wang, W. (2018). Revealing detail along the visual hierarchy: neural clustering preserves acuity from V1 to V4. *Neuron*, *98*(2), 417-428.

Lustig, C., & Jantz, T. (2015). Questions of age differences in interference control: When and how, not if? *Brain Research*, *1612*, 59–69. https://doi.org/10.1016/j.brainres.2014.10.024

Machado, T. H., Fichman, H. C., Santos, E. L., Carvalho, V. A., Fialho, P. P., Koenig, A. M., ... & Caramelli, P. (2009). Normative data for healthy elderly on the phonemic verbal fluency task-FAS. *Dementia & Neuropsychologia*, *3*(1), 55-60.

MacKinnon, J. G., & Magee, L. (1990). Transforming the dependent variable in regression models. *International Economic Review*, 315-339.

MacPherson, S. E., Phillips, L. H., & Della Sala, S. (2002). Age, executive function and social decision making: a dorsolateral prefrontal theory of cognitive aging. *Psychology and aging*, *17*(4), 598.

MacPherson, S. E., Cox, S. R., Dickie, D. A., Karama, S., Starr, J. M., Evans, A. C., Bastin, M. E., Wardlaw, J. M., & Deary, I. J. (2017). Processing speed and the relationship between Trail Making Test-B performance, cortical thinning and white matter microstructure in older adults. *Cortex*, *95*, 92–103. https://doi.org/10.1016/j.cortex.2017.07.021

Madden, D. J., Whiting, W. L., Huettel, S. A., White, L. E., MacFall, J. R., & Provenzale, J. M. (2004). Diffusion tensor imaging of adult age differences in cerebral white matter: relation to response time. *Neuroimage*, *21*(3), 1174-1181.

Madden, D. J. (2007). Aging and Visual Attention. *Current Directions in Psychological Science*, *16*(2), 70–74. https://doi.org/10.1111/j.1467-8721.2007.00478.x

Madden, D. J., Bennett, I. J., & Song, A. W. (2009). Cerebral White Matter Integrity and Cognitive Aging: Contributions from Diffusion Tensor Imaging. *Neuropsychology Review*, *19*(4), 415–435. https://doi.org/10.1007/s11065-009-9113-2

Madden, D. J., Costello, M. C., Dennis, N. A., Davis, S. W., Shepler, A. M., Spaniol, J., Bucur, B., & Cabeza, R. (2010). Adult age differences in functional connectivity during executive control. *NeuroImage*, *52*(2), 643–657. https://doi.org/10.1016/j.neuroimage.2010.04.249

Madden, D. J., Siciliano, R. E., Tallman, C. W., Monge, Z. A., Voss, A., & Cohen, J. R. (2020). Response-level processing during visual feature search: Effects of frontoparietal activation and adult age. *Attention, Perception, & Psychophysics*, *82*(1), 330–349. https://doi.org/10.3758/s13414-019-01823-3

Madden, D. J., Whiting, W. L., Huettel, S. A., White, L. E., MacFall, J. R., & Provenzale, J. M. (2004). Diffusion tensor imaging of adult age differences in cerebral white matter: Relation to response time. *NeuroImage*, *21*(3), 1174–1181. https://doi.org/10.1016/j.neuroimage.2003.11.004

Madhavan, K. M., McQueeny, T., Howe, S. R., Shear, P., & Szaflarski, J. (2014). Superior longitudinal fasciculus and language functioning in healthy aging. *Brain Research*, *1562*, 11–22. https://doi.org/10.1016/j.brainres.2014.03.012

Mahoney, J. R., Holtzer, R., & Verghese, J. (2014). Visual-Somatosensory Integration and Balance: Evidence for Psychophysical Integrative Differences in Aging. *Multisensory Research*, *27*(1), 17–42.

Mahoney, J. R., Verghese, J., Goldin, Y., Lipton, R., & Holtzer, R. (2010). Alerting, orienting, and executive attention in
older adults. *Journal of the International Neuropsychological Society : JINS*, *16*(5), 877–889. https://doi.org/10.1017/S1355617710000767

Mak, E., Su, L., Williams, G. B., & O'Brien, J. T. (2014). Neuroimaging characteristics of dementia with Lewy bodies. *Alzheimer's Research & Therapy*, *6*(2), 18. https://doi.org/10.1186/alzrt248

Makovac, E., Serra, L., Di Domenico, C., Marra, C., Caltagirone, C., Cercignani, M., & Bozzali, M. (2018). Quantitative magnetization transfer of white matter tracts correlates with diffusion tensor imaging indices in predicting the conversion from mild cognitive impairment to Alzheimer's disease. *Journal of Alzheimer's Disease*, *63*(2), 561-575.

Maksimenko, V. A., Runnova, A. E., Zhuravlev, M. O., Makarov, V. V., Nedayvozov, V., Grubov, V. V., Pchelintceva, S. V., Hramov, A. E., & Pisarchik, A. N. (2017). Visual perception affected by motivation

and alertness controlled by a noninvasive brain-computer interface. *PLOS ONE*, *12*(12), e0188700. https://doi.org/10.1371/journal.pone.0188700
Malykhin, N. V., Huang, Y., Hrybouski, S., & Olsen, F. (2017). Differential vulnerability of hippocampal subfields and anteroposterior hippocampal subregions in healthy cognitive aging. *Neurobiology of Aging*, *59*, 121–134. https://doi.org/10.1016/j.neurobiolaging.2017.08.001
Mapstone, M., Logan, D., & Duffy, C. J. (2006). Cue integration for the perception and control of self-movement in ageing and Alzheimer's disease. *Brain*, *129*(11), 2931–2944. https://doi.org/10.1093/brain/awl201
Marchand, D. G., Montplaisir, J., Postuma, R. B., Rahayel, S., & Gagnon, J.-F. (2017). Detecting the Cognitive Prodrome of Dementia with Lewy Bodies: A Prospective Study of REM Sleep Behavior Disorder. *Sleep*, *40*(1). https://doi.org/10.1093/sleep/zsw014
Marenco, S., Meyer, C., van der Veen, J. W., Zhang, Y., Kelly, R., Shen, J., ... & Berman, K. F. (2018). Role of gamma-amino-butyric acid in the dorsal anterior cingulate in age-associated changes in cognition. *Neuropsychopharmacology*, *43*(11), 2285-2291.
Markus, E. J., & Nielsen, M. (1973). Embedded-figures test scores among five samples of aged persons. *Perceptual and motor skills*, *36*(2), 455-459.
Marjańska, M., McCarten, J. R., Hodges, J., Hemmy, L. S., Grant, A., Deelchand, D. K., & Terpstra, M. (2017). Region-specific aging of the human brain as evidenced by neurochemical profiles measured noninvasively in the posterior cingulate cortex and the occipital lobe using 1H magnetic resonance spectroscopy at 7 T. *Neuroscience*, *354*, 168-177.
Martins, M. J. D., Krause, C., Neville, D. A., Pino, D., Villringer, A., & Obrig, H. (2019). Recursive hierarchical embedding in vision is impaired by posterior middle temporal gyrus lesions. *Brain*, *142*(10), 3217–3229. https://doi.org/10.1093/brain/awz242
Masuda-Suzukake, M., Nonaka, T., Hosokawa, M., Oikawa, T., Arai, T., Akiyama, H., Mann, D. M. A., & Hasegawa, M. (2013). Prion-like spreading of pathological α-synuclein in brain. *Brain*, *136*(4), 1128–1138. https://doi.org/10.1093/brain/awt037
Matar, E., Phillips, J. R., Ehgoetz Martens, K. A., Halliday, G. M., & Lewis, S. J. G. (2019). Impaired Color Discrimination-A Specific Marker of Hallucinations in Lewy Body Disorders. *Journal of Geriatric Psychiatry and Neurology*, 891988719845501. https://doi.org/10.1177/0891988719845501
Mathiesen, H. K., Jonsson, A., Tscherning, T., Hanson, L. G., Andresen, J., Blinkenberg, M., ... & Sorensen, P. S. (2006). Correlation of global N-acetyl aspartate with cognitive impairment in multiple sclerosis. *Archives of Neurology*, *63*(4), 533-536.
Maunsell, J., & van Essen, D. (1983). The connections of the middle temporal visual area (MT) and their relationship to a cortical hierarchy in the macaque monkey. *The Journal of Neuroscience*, *3*(12), 2563–2586. https://doi.org/10.1523/JNEUROSCI.03-12-02563.1983
McGinnis, S. M., Brickhouse, M., Pascual, B., & Dickerson, B. C. (2011). Age-Related Changes in the Thickness of Cortical Zones in Humans. *Brain Topography*, *24*(3–4), 279–291. https://doi.org/10.1007/s10548-011-0198-6
McGwin, G., Khoury, R., Cross, J., & Owsley, C. (2010). Vision Impairment and Eye Care Utilization among Americans 50 and Older. *Current Eye Research*, *35*(6), 451–458. https://doi.org/10.3109/02713681003664931
McKeith, I. G. (2006). Consensus guidelines for the clinical and pathologic diagnosis of dementia with Lewy bodies (DLB): Report of the Consortium on DLB International Workshop. *Journal of Alzheimer's Disease*, *9*(s3), 417–423. https://doi.org/10.3233/JAD-2006-9S347
McKeith, I. G., Boeve, B. F., Dickson, D. W., Halliday, G., Taylor, J.-P., Weintraub, D., Aarsland, D., Galvin, J., Attems, J., Ballard, C. G., Bayston, A., Beach, T. G., Blanc, F., Bohnen, N., Bonanni, L., Bras, J., Brundin, P., Burn, D., Chen-Plotkin, A., … Kosaka, K. (2017). Diagnosis and management of dementia with Lewy bodies: Fourth consensus report of the DLB Consortium. *Neurology*, *89*(1), 88–100. https://doi.org/10.1212/WNL.0000000000004058
McKeith, I. G., Ferman, T. J., Thomas, A. J., Blanc, F., Boeve, B. F., Fujishiro, H., ... & prodromal DLB Diagnostic Study Group. (2020). Research criteria for the diagnosis of prodromal dementia with Lewy bodies. *Neurology*, *94*(17), 743-755.
McMorris, T., Mielcarz, G., Harris, R. C., Swain, J. P., & Howard, A. (2007). Creatine Supplementation and Cognitive Performance in Elderly Individuals. *Aging, Neuropsychology, and Cognition*, *14*(5), 517–528. https://doi.org/10.1080/13825580600788100
Menegaux, A., Bäuerlein, F. J., Vania, A., Napiorkowski, N., Neitzel, J., Ruiz-Rizzo, A. L., ... & Finke, K. (2020). Linking the impact of aging on visual short-term memory capacity with changes in the structural connectivity of posterior thalamus to occipital cortices. *NeuroImage*, *208*, 116440.
Mescher, M., Merkle, H., Kirsch, J., Garwood, M., & Gruetter, R. (1998). Simultaneous in vivo spectral editing and water suppression. *NMR in Biomedicine*, *11*(6), 266–272. https://doi.org/10.1002/(sici)1099-1492(199810)
Metzler-Baddeley, Claudia. (2007). A Review of Cognitive Impairments in Dementia with Lewy Bodies Relative to Alzheimer's Disease and Parkinson's Disease with Dementia. *Cortex*, *43*(5), 583–600. https://doi.org/10.1016/S0010-9452(08)70489-1

Metzler-Baddeley, Claudia, Baddeley, R. J., Lovell, P. G., Laffan, A., & Jones, R. W. (2010). Visual impairments in dementia with Lewy bodies and posterior cortical atrophy. *Neuropsychology*, *24*(1), 35–48. https://doi.org/10.1037/a0016834

Metzler-Baddeley, C., Jones, D. K., Belaroussi, B., Aggleton, J. P., & O'Sullivan, M. J. (2011). Frontotemporal connections in episodic memory and aging: a diffusion MRI tractography study. *Journal of Neuroscience*, *31*(37), 13236-13245.

Metzler-Baddeley, C., O'Sullivan, M. J., Bells, S., Pasternak, O., & Jones, D. K. (2012). How and how not to correct for CSF-contamination in diffusion MRI. *Neuroimage*, *59*(2), 1394-1403.

Metzler-Baddeley, C., Mole, J. P., Sims, R., Fasano, F., Evans, J., Jones, D. K., ... & Baddeley, R. J. (2019). Fornix white matter glia damage causes hippocampal gray matter damage during age-dependent limbic decline. *Scientific reports*, *9*(1), 1-14.

Metzler-Baddeley, C., Jones, D. K., Belaroussi, B., Aggleton, J. P., & O'Sullivan, M. J. (2011). Frontotemporal Connections in Episodic Memory and Aging: A Diffusion MRI Tractography Study. *Journal of Neuroscience*, *31*(37), 13236–13245. https://doi.org/10.1523/JNEUROSCI.2317-11.2011

Mijović, B., De Vos, M., Vanderperren, K., Machilsen, B., Sunaert, S., Van Huffel, S., & Wagemans, J. (2014). The dynamics of contour integration: A simultaneous EEG–fMRI study. *Neuroimage*, *88*, 10-21.

Miller, B. L., Changl, L., Booth, R., Ernst, T., Cornford, M., Nikas, D., McBride, D., & Jenden, D. J. (1996). In vivo 1H MRS choline: Correlation with in vitro chemistry/histology. *Life Sciences*, *58*(22), 1929–1935. https://doi.org/10.1016/0024-3205(96)00182-8

Minati, L., Aquino, D., Bruzzone, M. G., & Erbetta, A. (2010). Quantitation of normal metabolite concentrations in six brain regions by in-vivo 1H-MR spectroscopy. *Journal of Medical Physics / Association of Medical Physicists of India*, *35*(3), 154–163. https://doi.org/10.4103/0971-6203.62128

Mioshi, E., Dawson, K., Mitchell, J., Arnold, R., & Hodges, J. R. (2006). The Addenbrooke's Cognitive Examination Revised (ACE-R): A brief cognitive test battery for dementia screening. *International Journal of Geriatric Psychiatry*, *21*(11), 1078–1085. https://doi.org/10.1002/gps.1610

Mishkin, M., & Ungerleider, L. G. (1982). Contribution of striate inputs to the visuospatial functions of parieto-preoccipital cortex in monkeys. *Behavioural Brain Research*, *6*(1), 57–77. https://doi.org/10.1016/0166-4328(82)90081-X

Mishkin, M., Ungerleider, L. G., & Macko, K. A. (1983). Object vision and spatial vision: two cortical pathways. *Trends in neurosciences*, *6*, 414-417.

Mitchell, T., Archer, D. B., Chu, W. T., Coombes, S. A., Lai, S., Wilkes, B. J., ... & Vaillancourt, D. E. (2019). Neurite orientation dispersion and density imaging (NODDI) and free-water imaging in Parkinsonism. *Human brain mapping*, *40*(17), 5094-5107.

Mitolo, M., Hamilton, J. M., Landy, K. M., Hansen, L. A., Galasko, D., Pazzaglia, F., & Salmon, D. P. (2016). Visual Perceptual Organization Ability in Autopsy-Verified Dementia with Lewy Bodies and Alzheimer's Disease. *Journal of the International Neuropsychological Society*, *22*(06), 609–619. https://doi.org/10.1017/S1355617716000436

Moffett, J. R., Arun, P., Ariyannur, P. S., & Namboodiri, A. M. (2013). N-Acetylaspartate reductions in brain injury: Impact on post-injury neuroenergetics, lipid synthesis, and protein acetylation. *Frontiers in Neuroenergetics*, *5*. https://doi.org/10.3389/fnene.2013.00011

Mole, J. P., Fasano, F., Evans, J., Sims, R., Hamilton, D. A., Kidd, E., & Metzler-Baddeley, C. (2020). Genetic risk of dementia modifies obesity effects on white matter myelin in cognitively healthy adults. *Neurobiology of Aging*, *94*, 298-310.

Molina, J. A., Garcia-Segura, J. M., Benito-Leon, J., Gomez-Escalonilla, C., Del Ser, T., Martinez, V., & Viano, J. (2002). Proton magnetic resonance spectroscopy in dementia with Lewy bodies. *European neurology*, *48*(3), 158-163.

Monge, Z. A., Geib, B. R., Siciliano, R. E., Packard, L. E., Tallman, C. W., & Madden, D. J. (2017a). Functional Modular Architecture Underlying Attentional Control in Aging. *NeuroImage*, *155*, 257–270. https://doi.org/10.1016/j.neuroimage.2017.05.002

Monge, Z. A., Geib, B. R., Siciliano, R. E., Packard, L. E., Tallman, C. W., & Madden, D. J. (2017b). Functional modular architecture underlying attentional control in aging. *NeuroImage*, *155*, 257–270. https://doi.org/10.1016/j.neuroimage.2017.05.002

Monteiro, T. S., Zivari Adab, H., Chalavi, S., Gooijers, J., King, B. (Bradley) R., Cuypers, K., Mantini, D., & Swinnen, S. P. (2020). Reduced Modulation of Task-Related Connectivity Mediates Age-Related Declines in Bimanual Performance. *Cerebral Cortex*, *30*(8), 4346–4360. https://doi.org/10.1093/cercor/bhaa021

Mori, E., Ikeda, M., Kosaka, K., & Donepezil-DLB Study Investigators. (2012). Donepezil for dementia with Lewy bodies: A randomized, placebo-controlled trial. *Annals of neurology*, *72*(1), 41-52.

Morrison, J. H., & Hof, P. R. (2007). Life and death of neurons in the aging cerebral cortex. *International review of neurobiology*, *81*, 41-57.

Mosimann, Urs P., Rowan, E. N., Partington, C. E., Collerton, D., Littlewood, E., O'Brien, J. T., Burn, D. J., & McKeith, I. G. (2006). Characteristics of Visual Hallucinations in Parkinson Disease Dementia and

Dementia With Lewy Bodies. *The American Journal of Geriatric Psychiatry*, *14*(2), 153–160. https://doi.org/10.1097/01.JGP.0000192480.89813.80
Mosimann, Urs Peter, Collerton, D., Dudley, R., Meyer, T. D., Graham, G., Dean, J. L., Bearn, D., Killen, A., Dickinson, L., Clarke, M. P., & McKeith, I. G. (2008). A semi-structured interview to assess visual hallucinations in older people. *International Journal of Geriatric Psychiatry*, *23*(7), 712–718. https://doi.org/10.1002/gps.1965
Mukaetova-Ladinska, E. B., Andras, A., Milne, J., Abdel-All, Z., Borr, I., Jaros, E., ... & McKeith, I. G. (2013). Synaptic proteins and choline acetyltransferase loss in visual cortex in dementia with Lewy bodies. *Journal of Neuropathology & Experimental Neurology*, *72*(1), 53-60.
Mulder, M. J., Van Maanen, L., & Forstmann, B. U. (2014). Perceptual decision neurosciences–a model-based review. *Neuroscience*, *277*, 872-884.
Mullins, P. G., McGonigle, D. J., O'Gorman, R. L., Puts, N. A. J., Vidyasagar, R., Evans, C. J., & Edden, R. A. E. (2014). Current practice in the use of MEGA-PRESS spectroscopy for the detection of GABA. *NeuroImage*, *86*, 43–52. https://doi.org/10.1016/j.neuroimage.2012.12.004
Murman, D. L. (2015). The Impact of Age on Cognition. *Seminars in Hearing*, *36*(3), 111–121. https://doi.org/10.1055/s-0035-1555115
Murray, E. A., Wise, S. P., & Graham, K. S. (2017). *the Evolution of Memory Systems: Ancestors, anatomy, and adaptations*. Oxford University Press.
Nakajima, R., Kinoshita, M., Shinohara, H., & Nakada, M. (2019). The superior longitudinal fascicle: reconsidering the fronto-parietal neural network based on anatomy and function. *Brain imaging and behavior*, 1-14.
Nasreddine, Z. S., Phillips, N. A., Bédirian, V., Charbonneau, S., Whitehead, V., Collin, I., ... & Chertkow, H. (2005). The Montreal Cognitive Assessment, MoCA: a brief screening tool for mild cognitive impairment. *Journal of the American Geriatrics Society*, *53*(4), 695-699.
Nazeri, A., Chakravarty, M. M., Rotenberg, D. J., Rajji, T. K., Rathi, Y., Michailovich, O. V., & Voineskos, A. N. (2015). Functional consequences of neurite orientation dispersion and density in humans across the adult lifespan. *Journal of Neuroscience*, *35*(4), 1753-1762.
Newsholme, P., Procopio, J., Lima, M. M. R., Pithon-Curi, T. C., & Curi, R. (2003). Glutamine and glutamate—their central role in cell metabolism and function. *Cell biochemistry and function*, *21*(1), 1-9.
Nilsson, M., Szczepankiewicz, F., van Westen, D., & Hansson, O. (2015). Extrapolation-based references improve motion and eddy-current correction of high B-value DWI data: application in Parkinson's disease dementia. *PloS one*, *10*(11), e0141825.
Noorani, I., & Carpenter, R. H. S. (2011). Full reaction time distributions reveal the complexity of neural decision-making. *European Journal of Neuroscience*, *33*(11), 1948–1951. https://doi.org/10.1111/j.1460-9568.2011.07727.x
Nordahl, C. W., Ranganath, C., Yonelinas, A. P., DeCarli, C., Fletcher, E., & Jagust, W. J. (2006). *White Matter Changes Compromise Prefrontal Cortex Function in Healthy Elderly Individuals*. *18*(3), 19.
Norman, J. F., Clayton, A. M., Shular, C. F., & Thompson, S. R. (2004). Aging and the Perception of Depth and 3-D Shape From Motion Parallax. *Psychology and Aging*, *19*(3), 506–514. https://doi.org/10.1037/0882-7974.19.3.506
Nyberg, L., & Pudas, S. (2019). Successful Memory Aging. *Annual Review of Psychology*, *70*(1), 219–243. https://doi.org/10.1146/annurev-psych-010418-103052
O'Callaghan, C., Hall, J. M., Tomassini, A., Muller, A. J., Walpola, I. C., Moustafa, A. A., Shine, J. M., & Lewis, S. J. G. (2017). Visual Hallucinations Are Characterized by Impaired Sensory Evidence Accumulation: Insights From Hierarchical Drift Diffusion Modeling in Parkinson's Disease. *Biological Psychiatry: Cognitive Neuroscience and Neuroimaging*, *2*(8), 680–688. https://doi.org/10.1016/j.bpsc.2017.04.007
O'Donnell, L. J., & Pasternak, O. (2015). Does diffusion MRI tell us anything about the white matter? An overview of methods and pitfalls. *Schizophrenia Research*, *161*(1), 133–141. https://doi.org/10.1016/j.schres.2014.09.007
O'Donnell, L. J., & Westin, C.-F. (2011). An introduction to diffusion tensor image analysis. *Neurosurgery Clinics of North America*, *22*(2), 185–viii. https://doi.org/10.1016/j.nec.2010.12.004
O'Dowd, S., Schumacher, J., Burn, D. J., Bonanni, L., Onofrj, M., Thomas, A., & Taylor, J.-P. (n.d.). Fluctuating cognition in the Lewy body dementias. *Brain*. https://doi.org/10.1093/brain/awz235
Öhlschläger, S., & Võ, M. L.-H. (2017). SCEGRAM: An image database for semantic and syntactic inconsistencies in scenes. *Behavior Research Methods*, *49*(5), 1780–1791. https://doi.org/10.3758/s13428-016-0820-3
Oishi, Y., Imamura, T., Shimomura, T., & Suzuki, K. (2018). Visual texture agnosia in dementia with Lewy bodies and Alzheimer's disease. *Cortex*, *103*, 277–290. https://doi.org/10.1016/j.cortex.2018.03.018
Oishi, H., Takemura, H., Aoki, S. C., Fujita, I., & Amano, K. (2018). Microstructural properties of the vertical occipital fasciculus explain the variability in human stereoacuity. *Proceedings of the National Academy of Sciences*, *115*(48), 12289-12294.

Onofrj, M., Taylor, J. P., Monaco, D., Franciotti, R., Anzellotti, F., Bonanni, L., ... & Thomas, A. (2013). Visual hallucinations in PD and Lewy body dementias: old and new hypotheses. *Behavioural neurology*, *27*(4), 479-493.

Onofri, E., Mercuri, M., Donato, G., & Ricci, S. (2015). Cognitive fluctuations in connection to dysgraphia: A comparison of Alzheimer's disease with dementia Lewy bodies. *Clinical Interventions in Aging*, *10*, 625–633. https://doi.org/10.2147/CIA.S79679

Oppedal, K., Ferreira, D., Cavallin, L., Lemstra, A. W., Ten Kate, M., Padovani, A., ... & Aarsland, D. (2019). A signature pattern of cortical atrophy in dementia with Lewy bodies: a study on 333 patients from the European DLB consortium. *Alzheimer's & Dementia*, *15*(3), 400-409.

Ortega, R., Carmona, A., Roudeau, S., Perrin, L., Dučić, T., Carboni, E., BOHIC, S., Cloetens, P., & Lingor, P. (2015). α-Synuclein Over-Expression Induces Increased Iron Accumulation and Redistribution in Iron-Exposed Neurons. *Molecular Neurobiology*, *53*. https://doi.org/10.1007/s12035-015-9146-x

Osoba, M. Y., Rao, A. K., Agrawal, S. K., & Lalwani, A. K. (2019). Balance and gait in the elderly: A contemporary review. *Laryngoscope investigative otolaryngology*, *4*(1), 143-153.

Ota, M., Ishikawa, M., Sato, N., Hori, H., Sasayama, D., Hattori, K., ... & Kunugi, H. (2012). Glutamatergic changes in the cerebral white matter associated with schizophrenic exacerbation. *Acta psychiatrica scandinavica*, *126*(1), 72-78.

Ota, K., Murayama, N., Kasanuki, K., Kondo, D., Fujishiro, H., Arai, H., Sato, K., & Iseki, E. (2015). Visuoperceptual Assessments for Differentiating Dementia with Lewy Bodies and Alzheimer's Disease: Illusory Contours and Other Neuropsychological Examinations. *Archives of Clinical Neuropsychology*, *30*(3), 256–263. https://doi.org/10.1093/arclin/acv016

Ota, M., Sato, N., Ogawa, M., Murata, M., Kuno, S., Kida, J., & Asada, T. (2009). Degeneration of dementia with Lewy bodies measured by diffusion tensor imaging. *NMR in Biomedicine*, *22*(3), 280–284. https://doi.org/10.1002/nbm.1321

Owsley, C. (2011). Aging and vision. *Vision Research*, *51*(13), 1610–1622. https://doi.org/10.1016/j.visres.2010.10.020

Pal, A., Biswas, A., Pandit, A., Roy, A., Guin, D., Gangopadhyay, G., & Senapati, A. K. (2016). Study of visuospatial skill in patients with dementia. *Annals of Indian Academy of Neurology*, *19*(1), 83–88. https://doi.org/10.4103/0972-2327.168636

Palejwala, A. H., O'Connor, K. P., Pelargos, P., Briggs, R. G., Milton, C. K., Conner, A. K., ... & Sughrue, M. E. (2020). Anatomy and white matter connections of the lateral occipital cortex. *Surgical and Radiologic Anatomy*, *42*(3), 315-328.

Palombo, M., Shemesh, N., Ronen, I., & Valette, J. (2018). Insights into brain microstructure from in vivo DW-MRS. *Neuroimage*, *182*, 97-116.

Pardo, J. V., Lee, J. T., Sheikh, S. A., Surerus-Johnson, C., Shah, H., Munch, K. R., Carlis, J. V., Lewis, S. M., Kuskowski, M. A., & Dysken, M. W. (2007). Where the brain grows old: Decline in anterior cingulate and medial prefrontal function with normal aging. *NeuroImage*, *35*(3), 1231–1237. https://doi.org/10.1016/j.neuroimage.2006.12.044

Pareek, V., Rallabandi, V. S., & Roy, P. K. (2018). A correlational study between microstructural white matter properties and macrostructural gray matter volume across normal ageing: Conjoint DTI and VBM analysis. *Magnetic resonance insights*, *11*, 1178623X18799926.

Park, J., Carp, J., Kennedy, K. M., Rodrigue, K. M., Bischof, G. N., Huang, C.-M., Rieck, J. R., Polk, T. A., & Park, D. C. (2012). Neural Broadening or Neural Attenuation? Investigating Age-Related Dedifferentiation in the Face Network in a Large Lifespan Sample. *Journal of Neuroscience*, *32*(6), 2154–2158. https://doi.org/10.1523/JNEUROSCI.4494-11.2012

Park, K. W., Kim, H. S., Cheon, S.-M., Cha, J.-K., Kim, S.-H., & Kim, J. W. (2011). Dementia with Lewy Bodies versus Alzheimer's Disease and Parkinson's Disease Dementia: A Comparison of Cognitive Profiles. *Journal of Clinical Neurology*, *7*(1), 19–24. https://doi.org/10.3988/jcn.2011.7.1.19

Parker, G. (2014). *Robust processing of diffusion weighted image data* (Doctoral dissertation, Cardiff University).

Parlatini, V., Radua, J., Dell'Acqua, F., Leslie, A., Simmons, A., Murphy, D. G., & de Schotten, M. T. (2017). Functional segregation and integration within fronto-parietal networks. *Neuroimage*, *146*, 367-375.

Pasternak, O., Sochen, N., Gur, Y., Intrator, N., & Assaf, Y. (2009). Free water elimination and mapping from diffusion MRI. *Magnetic Resonance in Medicine*, *62*(3), 717–730. https://doi.org/10.1002/mrm.22055

Paus, T. (2001). Primate anterior cingulate cortex: where motor control, drive and cognition interface. *Nature reviews neuroscience*, *2*(6), 417-424.

Pehrson, A. L., Bondi, C. O., Totah, N. K., & Moghaddam, B. (2013). The influence of NMDA and GABA A receptors and glutamic acid decarboxylase (GAD) activity on attention. *Psychopharmacology*, *225*(1), 31-39.

Peirce, J. W. (2009). Generating stimuli for neuroscience using PsychoPy. *Frontiers in Neuroinformatics*, *2*. https://doi.org/10.3389/neuro.11.010.2008

Peirce, J. W. (2015). Understanding mid-level representations in visual processing. *Journal of Vision*, *15*(7), 5–5. https://doi.org/10.1167/15.7.5

Penke, L., Maniega, S. M., Murray, C., Gow, A. J., Hernández, M. C. V., Clayden, J. D., ... & Deary, I. J. (2010). A general factor of brain white matter integrity predicts information processing speed in healthy older people. *Journal of Neuroscience*, *30*(22), 7569-7574.

Penke, L., Valdés Hernandéz, M. C., Maniega, S. M., Gow, A. J., Murray, C., Starr, J. M., Bastin, M. E., Deary, I. J., & Wardlaw, J. M. (2012). Brain iron deposits are associated with general cognitive ability and cognitive aging. *Neurobiology of Aging*, *33*(3), 510-517.e2. https://doi.org/10.1016/j.neurobiolaging.2010.04.032

Perceptual decision neurosciences – A model-based review. (2014). *Neuroscience*, *277*, 872–884. https://doi.org/10.1016/j.neuroscience.2014.07.031

Perry, R. H., Irving, D., Blessed, G., Fairbairn, A., & Perry, E. K. (1990). Senile dementia of Lewy body type: A clinically and neuropathologically distinct form of Lewy body dementia in the elderly. *Journal of the Neurological Sciences*, *95*(2), 119–139. https://doi.org/10.1016/0022-510X(90)90236-G

Persson, J., Stening, E., Nordin, K., & Söderlund, H. (2018). Predicting episodic and spatial memory performance from hippocampal resting-state functional connectivity: Evidence for an anterior–posterior division of function. *Hippocampus*, *28*(1), 53–66. https://doi.org/10.1002/hipo.22807

Peters, F., Ergis, A.-M., Gauthier, S., Dieudonné, B., Verny, M., Jolicoeur, P., & Belleville, S. (2012). Abnormal temporal dynamics of visual attention in Alzheimer's disease and in dementia with Lewy bodies. *Neurobiology of Aging*, *33*(5), 1012.e1-1012.e10. https://doi.org/10.1016/j.neurobiolaging.2011.10.019

Peters, R. (2006). Ageing and the brain. *Postgraduate Medical Journal*, *82*(964), 84–88. https://doi.org/10.1136/pgmj.2005.036665

Petrova, M., Pavlova, R., Zhelev, Y., Mehrabian, S., Raycheva, M., & Traykov, L. (2016). Investigation of neuropsychological characteristics of very mild and mild dementia with Lewy bodies. *Journal of Clinical and Experimental Neuropsychology*, *38*(3), 354–360. https://doi.org/10.1080/13803395.2015.1117058

Pichet Binette, A., Gonneaud, J., Vogel, J. W., La Joie, R., Rosa-Neto, P., Collins, D. L., Poirier, J., Breitner, J. C. S., Villeneuve, S., Vachon-Presseau, E., for the Alzheimer's Disease Neuroimaging Initiative, & the PREVENT-AD Research Group. (2020). Morphometric network differences in ageing versus Alzheimer's disease dementia. *Brain*, *143*(2), 635–649. https://doi.org/10.1093/brain/awz414

Pilz, K. S., Miller, L., & Agnew, H. C. (2017). Motion coherence and direction discrimination in healthy aging. *Journal of Vision*, *17*(1), 31–31. https://doi.org/10.1167/17.1.31

Pierpaoli, C., & Basser, P. J. (1996). Toward a quantitative assessment of diffusion anisotropy. *Magnetic resonance in Medicine*, *36*(6), 893-906.

Pitchaimuthu, K., Wu, Q., Carter, O., Nguyen, B. N., Ahn, S., Egan, G. F., & McKendrick, A. M. (2017). Occipital GABA levels in older adults and their relationship to visual perceptual suppression. *Scientific Reports*, *7*(1), 14231. https://doi.org/10.1038/s41598-017-14577-5

Pletnikova, O., West, N., Lee, M. K., Rudow, G. L., Skolasky, R. L., Dawson, T. M., Marsh, L., & Troncoso, J. C. (2005). Aβ deposition is associated with enhanced cortical α-synuclein lesions in Lewy body diseases. *Neurobiology of Aging*, *26*(8), 1183–1192. https://doi.org/10.1016/j.neurobiolaging.2004.10.006

Ploran, E. J., Nelson, S. M., Velanova, K., Donaldson, D. I., Petersen, S. E., & Wheeler, M. E. (2007). Evidence Accumulation and the Moment of Recognition: Dissociating Perceptual Recognition Processes Using fMRI. *Journal of Neuroscience*, *27*(44), 11912–11924. https://doi.org/10.1523/JNEUROSCI.3522-07.2007

Podzebenko, K., Egan, G. F., & Watson, J. D. (2002). Widespread dorsal stream activation during a parametric mental rotation task, revealed with functional magnetic resonance imaging. *Neuroimage*, *15*(3), 547-558.

Porges, E. C., Woods, A. J., Lamb, D. G., Williamson, J. B., Cohen, R. A., Edden, R. A. E., & Harris, A. D. (2017). Impact of tissue correction strategy on GABA-edited MRS findings. *NeuroImage*, *162*, 249–256. https://doi.org/10.1016/j.neuroimage.2017.08.073

Porter, G., Leonards, U., Troscianko, T., Haworth, J., Bayer, A., & Tales, A. (2012). Dealing with Illumination in Visual Scenes: Effects of Ageing and Alzheimer's Disease. *PLOS ONE*, *7*(9), e45104. https://doi.org/10.1371/journal.pone.0045104

Posner, M. I. (1980). Orienting of attention. *The Quarterly Journal of Experimental Psychology*, *32*(1), 3–25.

Posner, Michael I., & Petersen, S. E. (1990). The Attention System of the Human Brain. *Annual Review of Neuroscience*, *13*(1), 25–42. https://doi.org/10.1146/annurev.ne.13.030190.000325

Price, D., Tyler, L. K., Neto Henriques, R., Campbell, K. L., Williams, N., Treder, M. S., Taylor, J. R., & Henson, R. N. A. (2017). Age-related delay in visual and auditory evoked responses is mediated by white- and grey-matter differences. *Nature Communications*, *8*(1), 15671. https://doi.org/10.1038/ncomms15671

Puts, N. A. J., & Edden, R. A. E. (2012). In vivo magnetic resonance spectroscopy of GABA: A methodological review. *Progress in Nuclear Magnetic Resonance Spectroscopy*, *60*, 29–41. https://doi.org/10.1016/j.pnmrs.2011.06.001

Rabbitt, P. (1979). How old and young subjects monitor and control responses for accuracy and speed. *British Journal of Psychology*, *70*(2), 305-311.

Rae, C. D. (2014). A Guide to the Metabolic Pathways and Function of Metabolites Observed in Human Brain 1H Magnetic Resonance Spectra. *Neurochemical Research*, *39*(1), 1–36. https://doi.org/10.1007/s11064-013-1199-5

Raichle, M. E. (2015). The Brain's Default Mode Network. *Annual Review of Neuroscience*, *38*(1), 433–447. https://doi.org/10.1146/annurev-neuro-071013-014030
Ralph, M. A. L. (2001). Semantic memory is impaired in both dementia with Lewy bodies and dementia of Alzheimer's type: A comparative neuropsychological study and literature review. *Journal of Neurology, Neurosurgery & Psychiatry*, *70*(2), 149–156. https://doi.org/10.1136/jnnp.70.2.149
Ramanoël, S., Hoyau, E., Kauffmann, L., Renard, F., Pichat, C., Boudiaf, N., Krainik, A., Jaillard, A., & Baciu, M. (2018). Gray Matter Volume and Cognitive Performance During Normal Aging. A Voxel-Based Morphometry Study. *Frontiers in Aging Neuroscience*, *10*. https://doi.org/10.3389/fnagi.2018.00235
Ratcliff, R. (1978). A theory of memory retrieval. *Psychol. Rev*, *85*(2), 59–108.
Ratcliff, R., & Childers, R. (2015). Individual Differences and Fitting Methods for the Two-Choice Diffusion Model of Decision Making. *Decision (Washington, D.C.)*, *2015*. https://www.ncbi.nlm.nih.gov/pmc/articles/PMC4517692/
Ratcliff, R., & McKoon, G. (2008). The Diffusion Decision Model: Theory and Data for Two-Choice Decision Tasks. *Neural Computation*, *20*(4), 873–922. https://doi.org/10.1162/neco.2008.12-06-420
Ratcliff, R., & Rouder, J. N. (1998). Modeling Response Times for Two-Choice Decisions. *Psychological Science*, *9*(5), 347–356. https://doi.org/10.1111/1467-9280.00067
Ratcliff, R., & Smith, P. L. (2004). A Comparison of Sequential Sampling Models for Two-Choice Reaction Time. *Psychological Review*, *111*(2), 333–367. https://doi.org/10.1037/0033-295X.111.2.333
Ratcliff, R., Thapar, A., & McKoon, G. (2001). The effects of aging on reaction time in a signal detection task. *Psychology and Aging*, *16*(2), 323–341. https://doi.org/10.1037/0882-7974.16.2.323
Ratcliff, R., Thapar, A., & McKoon, G. (2004). A diffusion model analysis of the effects of aging on recognition memory. *Journal of Memory and Language*, *50*(4), 408–424. https://doi.org/10.1016/j.jml.2003.11.002
Ratcliff, R., Thapar, A., & McKoon, G. (2006). Aging and individual differences in rapid two-choice decisions. *Psychonomic Bulletin & Review*, *13*(4), 626–635. https://doi.org/10.3758/BF03193973
Ratcliff, R., Thapar, A., & McKoon, G. (2011). The Effects of Aging and IQ on Item and Associative Memory. *Journal of Experimental Psychology. General*, *140*(3), 464–487. https://doi.org/10.1037/a0023810
Ratcliff, R., & Tuerlinckx, F. (2002). Estimating parameters of the diffusion model: Approaches to dealing with contaminant reaction times and parameter variability. *Psychonomic bulletin & review*, *9*(3), 438-481.
Rawji, V., Rocchi, L., Foltynie, T., Rothwell, J. C., & Jahanshahi, M. (2020). Ropinirole, a dopamine agonist with high D3 affinity, reduces proactive inhibition: a double-blind, placebo-controlled study in healthy adults. *Neuropharmacology*, *179*, 108278.
Rawson, E. S., Lieberman, H. R., Walsh, T. M., Zuber, S. M., Harhart, J. M., & Matthews, T. C. (2008). Creatine supplementation does not improve cognitive function in young adults. *Physiology & Behavior*, *95*(1), 130–134. https://doi.org/10.1016/j.physbeh.2008.05.009
Raz, N. (2001). Ageing and the brain. *e LS*.
Raz, N., Gunning-Dixon, F., Head, D., Rodrigue, K. M., Williamson, A., & Acker, J. D. (2004). Aging, sexual dimorphism, and hemispheric asymmetry of the cerebral cortex: Replicability of regional differences in volume. *Neurobiology of Aging*, *25*(3), 377–396. https://doi.org/10.1016/S0197-4580(03)00118-0
Raz, N., Lindenberger, U., Rodrigue, K. M., Kennedy, K. M., Head, D., Williamson, A., Dahle, C., Gerstorf, D., & Acker, J. D. (2005). Regional Brain Changes in Aging Healthy Adults: General Trends, Individual Differences and Modifiers. *Cerebral Cortex*, *15*(11), 1676–1689. https://doi.org/10.1093/cercor/bhi044
Reddy, P. H., & Beal, M. F. (2008). Amyloid beta, mitochondrial dysfunction and synaptic damage: implications for cognitive decline in aging and Alzheimer's disease. *Trends in molecular medicine*, *14*(2), 45-53.
Reed-Jones, R. J., Solis, G. R., Lawson, K. A., Loya, A. M., Cude-Islas, D., & Berger, C. S. (2013). Vision and falls: A multidisciplinary review of the contributions of visual impairment to falls among older adults. *Maturitas*, *75*(1), 22–28. https://doi.org/10.1016/j.maturitas.2013.01.019
Reid, M. A., White, D. M., Kraguljac, N. V., & Lahti, A. C. (2016). A combined diffusion tensor imaging and magnetic resonance spectroscopy study of patients with schizophrenia. *Schizophrenia Research*, *170*(2), 341–350. https://doi.org/10.1016/j.schres.2015.12.003
Reitan, R. M., & Wolfson, D. (1985). *The Halstead-Reitan neuropsychological test battery: Theory and clinical interpretation* (Vol. 4). Reitan Neuropsychology.
Reuter-Lorenz, P. A., & Cappell, K. A. (2008). Neurocognitive aging and the compensation hypothesis. *Current directions in psychological science*, *17*(3), 177-182.
Reuter, M., Rosas, H. D., & Fischl, B. (2010). Highly accurate inverse consistent registration: A robust approach. *NeuroImage*, *53*(4), 1181–1196. https://doi.org/10.1016/j.neuroimage.2010.07.020
Reutzel, M., Grewal, R., Dilberger, B., Silaidos, C., Joppe, A., & Eckert, G. P. (2020). Cerebral mitochondrial function and cognitive performance during aging: a longitudinal study in NMRI mice. *Oxidative medicine and cellular longevity*, *2020*.
Reyngoudt, H., Achten, E., & Paemeleire, K. (2012). Magnetic resonance spectroscopy in migraine: What have we learned so far? *Cephalalgia*, *32*(11), 845–859. https://doi.org/10.1177/0333102412452048

Reynolds, G., Wilson, M., Peet, A., & Arvanitis, T. N. (2006). An algorithm for the automated quantitation of metabolites in in vitro NMR signals. *Magnetic Resonance in Medicine: An Official Journal of the International Society for Magnetic Resonance in Medicine*, *56*(6), 1211-1219.

Rhodes, R. E., & Katz, B. (2017). Working memory plasticity and aging. *Psychology and aging*, *32*(1), 51.

Richards, O. W. (1977). Effects of luminance and contrast on visual acuity, ages 16 to 90 years. *American journal of optometry and physiological optics*, *54*(3), 178-184.

Riese, F., Gietl, A., Zölch, N., Henning, A., O'Gorman, R., Kälin, A. M., Leh, S. E., Buck, A., Warnock, G., Edden, R. A. E., Luechinger, R., Hock, C., Kollias, S., & Michels, L. (2015). Posterior cingulate γ-aminobutyric acid and glutamate/glutamine are reduced in amnestic mild cognitive impairment and are unrelated to amyloid deposition and apolipoprotein E genotype. *Neurobiology of Aging*, *36*(1), 53–59. https://doi.org/10.1016/j.neurobiolaging.2014.07.030

Ring, H. A., Baron-Cohen, S., Wheelwright, S., Williams, S. C. R., Brammer, M., Andrew, C., & Bullmore, E. T. (1999). Cerebral correlates of preserved cognitive skills in autismA functional MRI study of Embedded Figures Task performance. *Brain*, *122*(7), 1305–1315. https://doi.org/10.1093/brain/122.7.1305

Risacher, S. L., & Saykin, A. J. (2013). Neuroimaging and other biomarkers for Alzheimer's disease: the changing landscape of early detection. *Annual review of clinical psychology*, *9*.

Rizio, A. A., & Diaz, M. T. (2016). Language, aging, and cognition: Frontal aslant tract and superior longitudinal fasciculus contribute to working memory performance in older adults. *Neuroreport*, *27*(9), 689–693. https://doi.org/10.1097/WNR.0000000000000597

Robbins, T. W. (1996). *Dissociating executive functions of the prefrontal cortex*. 9.

Roberts, K. L., & Allen, H. A. (2016). Perception and Cognition in the Ageing Brain: A Brief Review of the Short- and Long-Term Links between Perceptual and Cognitive Decline. *Frontiers in Aging Neuroscience*, *8*. https://doi.org/10.3389/fnagi.2016.00039

Robertson, A. D., Messner, M. A., Shirzadi, Z., Kleiner-Fisman, G., Lee, J., Hopyan, J., Lang, A. E., Black, S. E., MacIntosh, B. J., & Masellis, M. (2016). Orthostatic hypotension, cerebral hypoperfusion, and visuospatial deficits in Lewy body disorders. *Parkinsonism & Related Disorders*, *22*, 80–86. https://doi.org/10.1016/j.parkreldis.2015.11.019

Rosas, H. D., Liu, A. K., Hersch, S. M., Glessner, M., Ferrante, R. J., Salat, D. H., et al. (2002). Regional and progressive thinning of the cortical ribbon in Huntington's disease. Neurology, 58, 695–701.

Roski, C., Caspers, S., Langner, R., Laird, A. R., Fox, P. T., Zilles, K., Amunts, K., & Eickhoff, S. B. (2013). Adult age-dependent differences in resting-state connectivity within and between visual-attention and sensorimotor networks. *Frontiers in Aging Neuroscience*, *5*. https://doi.org/10.3389/fnagi.2013.00067

Ross, A. J., Sachdev, P. S., Wen, W., Valenzuela, M. J., & Brodaty, H. (2005). Cognitive correlates of 1H MRS measures in the healthy elderly brain. *Brain Research Bulletin*, *66*(1), 9–16. https://doi.org/10.1016/j.brainresbull.2005.01.015

Roudaia, E., Bennett, P. J., & Sekuler, A. B. (2008). The effect of aging on contour integration. *Vision Research*, *48*(28), 2767–2774. https://doi.org/10.1016/j.visres.2008.07.026

Roudaia, E., Farber, L. E., Bennett, P. J., & Sekuler, A. B. (2011). The effects of aging on contour discrimination in clutter. *Vision research*, *51*(9), 1022-1032.

Roudaia, E., Bennett, P. J., & Sekuler, A. B. (2013). Contour integration and aging: The effects of element spacing, orientation alignment and stimulus duration. *Frontiers in Psychology*, *4*. https://doi.org/10.3389/fpsyg.2013.00356

Rubia, K., Russell, T., Overmeyer, S., Brammer, M. J., Bullmore, E. T., Sharma, T., ... & Taylor, E. (2001). Mapping motor inhibition: conjunctive brain activations across different versions of go/no-go and stop tasks. *Neuroimage*, *13*(2), 250-261.

Rueckert, D., Clarkson, M. J., Hill, D. L., & Hawkes, D. J. (2000, June). Non-rigid registration using higher-order mutual information. In *Medical Imaging 2000: Image Processing* (Vol. 3979, pp. 438-447). International Society for Optics and Photonics.

Rypma, B., Eldreth, D. A., & Rebbechi, D. (2007). Age-related differences in activation-performance relations in delayed-response tasks: a multiple component analysis. *Cortex*, *43*(1), 65-76.

Saftari, L. N., & Kwon, O. S. (2018). Ageing vision and falls: a review. *Journal of physiological anthropology*, *37*(1), 1-14.

Sala, S., Agosta, F., Pagani, E., Copetti, M., Comi, G., & Filippi, M. (2012). Microstructural changes and atrophy in brain white matter tracts with aging. *Neurobiology of Aging*, *33*(3), 488-498.e2. https://doi.org/10.1016/j.neurobiolaging.2010.04.027

Salat, D. H., Kaye, J. A., & Janowsky, J. S. (2001). Selective Preservation and Degeneration Within the Prefrontal Cortex in Aging and Alzheimer Disease. *Archives of Neurology*, *58*(9), 1403. https://doi.org/10.1001/archneur.58.9.1403

Salonen, L., & Kivelä, S. L. (2012). Eye diseases and impaired vision as possible risk factors for recurrent falls in the aged: a systematic review. *Current gerontology and geriatrics research*, *2012*.

Salthouse, T. A. (1979). Adult age and the speed-accuracy trade-off. *Ergonomics*, *22*(7), 811-821.

Salthouse, T. A. (1996). *The Processing-Speed Theory of Adult Age Differences in Cognition*. 26.

Salthouse, T. A. (2001). Structural models of the relations between age and measures of cognitive functioning. *Intelligence*, *29*(2), 93–115. https://doi.org/10.1016/S0160-2896(00)00040-4
Salthouse, T. A. (2010). Selective review of cognitive aging. *Journal of the International Neuropsychological Society : JINS*, *16*(5), 754–760. https://doi.org/10.1017/S1355617710000706
Sanchez-Castaneda, C., Rene, R., Ramirez-Ruiz, B., Campdelacreu, J., Gascon, J., Falcon, C., Calopa, M., Jauma, S., Juncadella, M., & Junque, C. (2009). Correlations between gray matter reductions and cognitive deficits in dementia with Lewy Bodies and Parkinson's disease with dementia. *Movement Disorders*, *24*(12), 1740–1746. https://doi.org/10.1002/mds.22488
Sarks, S. H. (1976). Ageing and degeneration in the macular region: a clinico-pathological study. *British Journal of Ophthalmology*, *60*(5), 324-341.
Sarter, M., Lustig, C., Blakely, R. D., & Cherian, A. K. (2016). Cholinergic genetics of visual attention: Human and mouse choline transporter capacity variants influence distractibility. *Journal of Physiology-Paris*, *110*(1-2), 10-18.
Sasai-Sakuma, T., Nishio, Y., Yokoi, K., Mori, E., & Inoue, Y. (2017). Pareidolias in REM Sleep Behavior Disorder: A Possible Predictive Marker of Lewy Body Diseases? *Sleep*, *40*(2). https://doi.org/10.1093/sleep/zsw045
Sasson, E., Doniger, G. M., Pasternak, O., Tarrasch, R., & Assaf, Y. (2013). White matter correlates of cognitive domains in normal aging with diffusion tensor imaging. *Frontiers in Neuroscience*, *7*. https://doi.org/10.3389/fnins.2013.00032
Schallmo, M. P., Millin, R., Kale, A. M., Kolodny, T., Edden, R. A., Bernier, R. A., & Murray, S. O. (2019). Glutamatergic facilitation of neural responses in MT enhances motion perception in humans. *NeuroImage*, *184*, 925-931.
Schilling, C., Kühn, S., Paus, T., Romanowski, A., Banaschewski, T., Barbot, A., ... & Gallinat, J. (2013). Cortical thickness of superior frontal cortex predicts impulsiveness and perceptual reasoning in adolescence. *Molecular Psychiatry*, *18*(5), 624-630.
Schmidt-Wilcke, T., Fuchs, E., Funke, K., Vlachos, A., Müller-Dahlhaus, F., Puts, N. A. J., Harris, R. E., & Edden, R. A. E. (2018). GABA—from Inhibition to Cognition: Emerging Concepts. *The Neuroscientist*, *24*(5), 501–515. https://doi.org/10.1177/1073858417734530
Schmiedek, F., Oberauer, K., Wilhelm, O., Süß, H. M., & Wittmann, W. W. (2007). Individual differences in components of reaction time distributions and their relations to working memory and intelligence. *Journal of Experimental Psychology: General*, *136*(3), 414.
Schneider-Garces, N. J., Gordon, B. A., Brumback-Peltz, C. R., Shin, E., Lee, Y., Sutton, B. P., Maclin, E. L., Gratton, G., & Fabiani, M. (2009). Span, CRUNCH, and Beyond: Working Memory Capacity and the Aging Brain. *Journal of Cognitive Neuroscience*, *22*(4), 655–669. https://doi.org/10.1162/jocn.2009.21230
Schuch, S. (2016). Task inhibition and response inhibition in older vs. younger adults: A diffusion model analysis. *Frontiers in psychology*, *7*, 1722.
Schulze, E. T., Geary, E. K., Susmaras, T. M., Paliga, J. T., Maki, P. M., & Little, D. M. (2011, November 16). *Anatomical Correlates of Age-Related Working Memory Declines* [Research Article]. Journal of Aging Research; Hindawi. https://doi.org/10.4061/2011/606871
Scullin, M. K., Trotti, L. M., Wilson, A. G., Greer, S. A., & Bliwise, D. L. (2012). Nocturnal sleep enhances working memory training in Parkinson's disease but not Lewy body dementia. *Brain*, *135*(9), 2789–2797. https://doi.org/10.1093/brain/aws192
Sebastian, A., Jung, P., Neuhoff, J., Wibral, M., Fox, P. T., Lieb, K., Fries, P., Eickhoff, S. B., Tüscher, O., & Mobascher, A. (2016). Dissociable attentional and inhibitory networks of dorsal and ventral areas of the right inferior frontal cortex: A combined task-specific and coordinate-based meta-analytic fMRI study. *Brain Structure & Function*, *221*(3), 1635–1651. https://doi.org/10.1007/s00429-015-0994-y
Segal, M. R. (2004). Machine learning benchmarks and random forest regression.
Ségonne, F., Dale, A. M., Busa, E., Glessner, M., Salat, D., Hahn, H. K., & Fischl, B. (2004). A hybrid approach to the skull stripping problem in MRI. *NeuroImage*, *22*(3), 1060–1075. https://doi.org/10.1016/j.neuroimage.2004.03.032
Sekuler, R., Owsley, C., & Hutman, L. (1982). Assessing spatial vision of older people. *American journal of optometry and physiological optics*, *59*(12), 961-968.
Sexton, C. E., Walhovd, K. B., Storsve, A. B., Tamnes, C. K., Westlye, L. T., Johansen-Berg, H., & Fjell, A. M. (2014). Accelerated Changes in White Matter Microstructure during Aging: A Longitudinal Diffusion Tensor Imaging Study. *Journal of Neuroscience*, *34*(46), 15425–15436. https://doi.org/10.1523/JNEUROSCI.0203-14.2014
Shadlen, M. N., & Newsome, W. T. (2001). Neural Basis of a Perceptual Decision in the Parietal Cortex (Area LIP) of the Rhesus Monkey. *Journal of Neurophysiology*, *86*(4), 1916–1936. https://doi.org/10.1152/jn.2001.86.4.1916
Shepard, S. J., & Metzler, D. (1988). Mental rotation: Effects of dimensionality of objects and type of task. *Journal of Experimental Psychology. Human Perception and Performance*, *14*(1), 3–11. https://doi.org/10.1037//0096-1523.14.1.3

Shimada, H., Hirano, S., Shinotoh, H., Aotsuka, A., Sato, K., Tanaka, N., Ota, T., Asahina, M., Fukushi, K., Kuwabara, S., Hattori, T., Suhara, T., & Irie, T. (2009). Mapping of brain acetylcholinesterase alterations in Lewy body disease by PET. *Neurology*, *73*(4), 273–278. https://doi.org/10.1212/WNL.0b013e3181ab2b58

Shine, J. M., Halliday, G. M., Naismith, S. L., & Lewis, S. J. G. (2011). Visual misperceptions and hallucinations in Parkinson's disease: Dysfunction of attentional control networks? *Movement Disorders*, *26*(12), 2154–2159. https://doi.org/10.1002/mds.23896

Shinoura, N., Suzuki, Y., Yamada, R., Tabei, Y., Saito, K., & Yagi, K. (2009). Damage to the right superior longitudinal fasciculus in the inferior parietal lobe plays a role in spatial neglect. *Neuropsychologia*, *47*(12), 2600-2603.

Sidek, S., Ramli, N., Rahmat, K., Ramli, N. M., Abdulrahman, F., & Tan, L. K. (2014). Glaucoma severity affects diffusion tensor imaging (DTI) parameters of the optic nerve and optic radiation. *European Journal of Radiology*, *83*(8), 1437–1441. https://doi.org/10.1016/j.ejrad.2014.05.014

Silva, M. F., Brascamp, J. W., Ferreira, S., Castelo-Branco, M., Dumoulin, S. O., & Harvey, B. M. (2018). Radial asymmetries in population receptive field size and cortical magnification factor in early visual cortex. *NeuroImage*, *167*, 41-52.

Silveri, M. M., Sneider, J. T., Crowley, D. J., Covell, M. J., Acharya, D., Rosso, I. M., & Jensen, J. E. (2013). Frontal lobe γ-aminobutyric acid levels during adolescence: associations with impulsivity and response inhibition. *Biological psychiatry*, *74*(4), 296-304.

Simard, M. (2000). A Review of the Cognitive and Behavioral Symptoms in Dementia With Lewy Bodies. *Journal of Neuropsychiatry*, *12*(4), 425–450. https://doi.org/10.1176/appi.neuropsych.12.4.425

Simmonite, M., Carp, J., Foerster, B. R., Ossher, L., Petrou, M., Weissman, D. H., & Polk, T. A. (2019). Age-Related Declines in Occipital GABA are Associated with Reduced Fluid Processing Ability. *Academic Radiology*, *26*(8), 1053–1061. https://doi.org/10.1016/j.acra.2018.07.024

Sled, J. G., Zijdenbos, A. P., & Evans, A. C. (1998). A nonparametric method for automatic correction of intensity nonuniformity in MRI data. *IEEE Transactions on Medical Imaging*, *17*(1), 87–97. https://doi.org/10.1109/42.668698

Sled, J. G. (2018). Modelling and interpretation of magnetization transfer imaging in the brain. *Neuroimage*, *182*, 128-135.

Smith, P. F. (2018). On the Application of Multivariate Statistical and Data Mining Analyses to Data in Neuroscience. *Journal of Undergraduate Neuroscience Education*, *16*(2), R20–R32.

Smith, P. F., Ganesh, S., & Liu, P. (2013). A comparison of random forest regression and multiple linear regression for prediction in neuroscience. *Journal of Neuroscience Methods*, *220*(1), 85–91. https://doi.org/10.1016/j.jneumeth.2013.08.024

Smith, S. M. (2002). Fast robust automated brain extraction. *Human Brain Mapping*, *17*(3), 143–155. https://doi.org/10.1002/hbm.10062

Smith, S. M., Jenkinson, M., Johansen-Berg, H., Rueckert, D., Nichols, T. E., Mackay, C. E., Watkins, K. E., Ciccarelli, O., Cader, M. Z., Matthews, P. M., & Behrens, T. E. J. (2006). Tract-based spatial statistics: Voxelwise analysis of multi-subject diffusion data. *NeuroImage*, *31*(4), 1487–1505. https://doi.org/10.1016/j.neuroimage.2006.02.024

Smith, S. M., Jenkinson, M., Woolrich, M. W., Beckmann, C. F., Behrens, T. E. J., Johansen-Berg, H., Bannister, P. R., De Luca, M., Drobnjak, I., Flitney, D. E., Niazy, R. K., Saunders, J., Vickers, J., Zhang, Y., De Stefano, N., Brady, J. M., & Matthews, P. M. (2004). Advances in functional and structural MR image analysis and implementation as FSL. *NeuroImage*, *23*, S208–S219. https://doi.org/10.1016/j.neuroimage.2004.07.051

Snowden, R. J., & Kavanagh, E. (2006). Motion Perception in the Ageing Visual System: Minimum Motion, Motion Coherence, and Speed Discrimination Thresholds. *Perception*, *35*(1), 9–24. https://doi.org/10.1068/p5399

Soares, J., Marques, P., Alves, V., & Sousa, N. (2013). A hitchhiker's guide to diffusion tensor imaging. *Frontiers in Neuroscience*, *7*. https://doi.org/10.3389/fnins.2013.00031

Solé-Padullés, C., Bartrés-Faz, D., Junqué, C., Vendrell, P., Rami, L., Clemente, I. C., Bosch, B., Villar, A., Bargalló, N., Jurado, M. A., Barrios, M., & Molinuevo, J. L. (2009). Brain structure and function related to cognitive reserve variables in normal aging, mild cognitive impairment and Alzheimer's disease. *Neurobiology of Aging*, *30*(7), 1114–1124. https://doi.org/10.1016/j.neurobiolaging.2007.10.008

Song, S. K., Sun, S. W., Ju, W. K., Lin, S. J., Cross, A. H., & Neufeld, A. H. (2003). Diffusion tensor imaging detects and differentiates axon and myelin degeneration in mouse optic nerve after retinal ischemia. *Neuroimage*, *20*(3), 1714-1722.

Song, C., Sandberg, K., Andersen, L. M., Blicher, J. U., & Rees, G. (2017). Human occipital and parietal GABA selectively influence visual perception of orientation and size. *Journal of Neuroscience*, *37*(37), 8929-8937.

Sowell, E. R., Thompson, P. M., & Toga, A. W. (2004). Mapping Changes in the Human Cortex throughout the Span of Life. *The Neuroscientist*, *10*(4), 372–392. https://doi.org/10.1177/1073858404263960

Spaniol, J., Madden, D. J., & Voss, A. (2006). A Diffusion Model Analysis of Adult Age Differences in Episodic and Semantic Long-Term Memory Retrieval. *Journal of Experimental Psychology. Learning, Memory, and Cognition*, *32*(1), 101–117. https://doi.org/10.1037/0278-7393.32.1.101

Spratling, M. W. (2008). Predictive coding as a model of biased competition in visual attention. *Vision research*, *48*(12), 1391-1408.
Spreng, R. N., & Turner, G. R. (2019). The Shifting Architecture of Cognition and Brain Function in Older Adulthood. *Perspectives on Psychological Science*, *14*(4), 523–542. https://doi.org/10.1177/1745691619827511
Stagg, C., & Rothman, D. L. (Eds.). (2013). *Magnetic resonance spectroscopy: tools for neuroscience research and emerging clinical applications*. Academic Press.
Starns, J. J., & Ratcliff, R. (2010). The effects of aging on the speed-accuracy compromise: Boundary optimality in the diffusion model. *Psychology and Aging*, *25*(2), 377–390. https://doi.org/10.1037/a0018022
Starns, J. J., & Ratcliff, R. (2012). Age-related differences in diffusion model boundary optimality with both trial-limited and time-limited tasks. *Psychonomic Bulletin & Review*, *19*(1), 139–145. https://doi.org/10.3758/s13423-011-0189-3
Stejskal, E. O., & Tanner, J. E. (1965). Spin diffusion measurements: spin echoes in the presence of a time-dependent field gradient. *The journal of chemical physics*, *42*(1), 288-292.
Stillman, C. M., Esteban-Cornejo, I., Brown, B., Bender, C. M., & Erickson, K. I. (2020). Effects of Exercise on Brain and Cognition Across Age Groups and Health States. *Trends in Neurosciences*, *43*(7), 533–543. https://doi.org/10.1016/j.tins.2020.04.010
Stolyarova, A., Rakhshan, M., Hart, E. E., O'Dell, T. J., Peters, M. A. K., Lau, H., ... & Izquierdo, A. (2019). Contributions of anterior cingulate cortex and basolateral amygdala to decision confidence and learning under uncertainty. *Nature communications*, *10*(1), 1-14.
Strenziok, M., Greenwood, P. M., Santa Cruz, S. A., Thompson, J. C., & Parasuraman, R. (2013). Differential contributions of dorso-ventral and rostro-caudal prefrontal white matter tracts to cognitive control in healthy older adults. *PloS one*, *8*(12), e81410.
Sugiura, M. (2016). Functional neuroimaging of normal aging: Declining brain, adapting brain. *Ageing Research Reviews*, *30*, 61–72. https://doi.org/10.1016/j.arr.2016.02.006
Sumner, P., Edden, R. A., Bompas, A., Evans, C. J., & Singh, K. D. (2010). More GABA, less distraction: a neurochemical predictor of motor decision speed. *Nature neuroscience*, *13*(7), 825-827.
Tagaris, G. A., Kim, S.-G., Strupp, J. P., & Andersen, P. (1996). Quantitative relations between parietal activation and performance in mental rotation. *Neuroreport: An International Journal for the Rapid Communication of Research in Neuroscience*, *7*(3), 773–776. https://doi.org/10.1097/00001756-199602290-00022
Takacs, A., Stock, A. K., Kuntke, P., Werner, A., & Beste, C. (2021). On the functional role of striatal and anterior cingulate GABA+ in stimulus-response binding. *Human brain mapping*, *42*(6), 1863-1878.
Takeuchi, T., Yoshimoto, S., Shimada, Y., Kochiyama, T., & Kondo, H. M. (2017). Individual differences in visual motion perception and neurotransmitter concentrations in the human brain. *Philosophical Transactions of the Royal Society B: Biological Sciences*, *372*(1714), 20160111
Talairach, J. (1988). Co-Planar Stereotaxic Atlas of the Human Brain-3-Dimensional Proportional System. *An Approach to Cerebral Imaging*. https://ci.nii.ac.jp/naid/10008533708/
Tan, L. P. L., Herrmann, N., Mainland, B. J., & Shulman, K. (2015). Can clock drawing differentiate Alzheimer's disease from other dementias? *International Psychogeriatrics*, *27*(10), 1649–1660. https://doi.org/10.1017/S1041610215000939
Tang, Y., Nyengaard, J. R., Pakkenberg, B., & Gundersen, H. J. G. (1997). Age-induced white matter changes in the human brain: a stereological investigation. *Neurobiology of aging*, *18*(6), 609-615.
Taylor, J.-P., Colloby, S. J., McKeith, I. G., & O'Brien, J. T. (2013). Covariant perfusion patterns provide clues to the origin of cognitive fluctuations and attentional dysfunction in Dementia with Lewy bodies. *International Psychogeriatrics*, *25*(12), 1917–1928. https://doi.org/10.1017/S1041610213001488
Taylor, J.-P., Firbank, M. J., He, J., Barnett, N., Pearce, S., Livingstone, A., Vuong, Q., McKeith, I. G., & O'Brien, J. T. (2012). Visual cortex in dementia with Lewy bodies: Magnetic resonance imaging study. *The British Journal of Psychiatry*, *200*(6), 491–498. https://doi.org/10.1192/bjp.bp.111.099432
Teufel, C., Dakin, S., & Fletcher, P. (2015). Object Knowledge Shapes Properties of Early Feature-Detectors by Top-Down Modulation. *Journal of Vision*, *15*(12), 1029–1029. https://doi.org/10.1167/15.12.1029
Thambisetty, M., Wan, J., Carass, A., An, Y., Prince, J. L., & Resnick, S. M. (2010). Longitudinal changes in cortical thickness associated with normal aging. *NeuroImage*, *52*(4), 1215–1223. https://doi.org/10.1016/j.neuroimage.2010.04.258
Thapar, A., Ratcliff, R., & McKoon, G. (2003). A Diffusion Model Analysis of the Effects of Aging on Letter Discrimination. *Psychology and Aging*, *18*(3), 415–429. https://doi.org/10.1037/0882-7974.18.3.415
Thissen, D., Steinberg, L., & Kuang, D. (2002). Quick and easy implementation of the Benjamini-Hochberg procedure for controlling the false positive rate in multiple comparisons. *Journal of educational and behavioral statistics*, *27*(1), 77-83.
Thomas, A. G., Koumellis, P., & Dineen, R. A. (2011). The fornix in health and disease: an imaging review. *Radiographics*, *31*(4), 1107-1121.
Thompson, D. K., Thai, D., Kelly, C. E., Leemans, A., Tournier, J.-D., Kean, M. J., Lee, K. J., Inder, T. E., Doyle, L. W., Anderson, P. J., & Hunt, R. W. (2014). Alterations in the optic radiations of very preterm children—

Perinatal predictors and relationships with visual outcomes. *NeuroImage: Clinical*, *4*, 145–153. https://doi.org/10.1016/j.nicl.2013.11.007
Toepper, M. (2017). Dissociating Normal Aging from Alzheimer's Disease: A View from Cognitive Neuroscience. *Journal of Alzheimer's Disease*, *57*(2), 331–352. https://doi.org/10.3233/JAD-161099
Tognarelli, J. M., Dawood, M., Shariff, M. I., Grover, V. P., Crossey, M. M., Cox, I. J., ... & McPhail, M. J. (2015). Magnetic resonance spectroscopy: principles and techniques: lessons for clinicians. *Journal of clinical and experimental hepatology*, *5*(4), 320-328.
Toner, C. K., Pirogovsky, E., Kirwan, C. B., & Gilbert, P. E. (2009). Visual object pattern separation deficits in nondemented older adults. *Learning & Memory*, *16*(5), 338–342. https://doi.org/10.1101/lm.1315109
Touroutoglou, A., Hollenbeck, M., Dickerson, B. C., & Feldman Barrett, L. (2012). Dissociable large-scale networks anchored in the right anterior insula subserve affective experience and attention. *NeuroImage*, *60*(4), 1947–1958. https://doi.org/10.1016/j.neuroimage.2012.02.012
Toschi, N., Gisbert, R. A., Passamonti, L., Canals, S., & De Santis, S. (2020). Multishell diffusion imaging reveals sex-specific trajectories of early white matter degeneration in normal aging. *Neurobiology of aging*, *86*, 191-200.
Tseng, B. Y., Gundapuneedi, T., Khan, M. A., Diaz-Arrastia, R., Levine, B. D., Lu, H., Huang, H., & Zhang, R. (2013). White matter integrity in physically fit older adults. *NeuroImage*, *82*, 510–516. https://doi.org/10.1016/j.neuroimage.2013.06.011
Tsvetanov, K. A. (n.d.). *Combining behaviour, fMRI and MR spectroscopy to study selective attention in ageing*. 271.
Tuch, D. S., Reese, T. G., Wiegell, M. R., Makris, N., Belliveau, J. W., & Wedeen, V. J. (2002). High angular resolution diffusion imaging reveals intravoxel white matter fiber heterogeneity. *Magnetic Resonance in Medicine: An Official Journal of the International Society for Magnetic Resonance in Medicine*, *48*(4), 577-582.
Tulving, E., Kapur, S., Markowitsch, H. J., Craik, F. I., Habib, R., & Houle, S. (1994). Neuroanatomical correlates of retrieval in episodic memory: Auditory sentence recognition. *Proceedings of the National Academy of Sciences*, *91*(6), 2012–2015. https://doi.org/10.1073/pnas.91.6.2012
Tumati, S., Martens, S., & Aleman, A. (2013). Magnetic resonance spectroscopy in mild cognitive impairment: Systematic review and meta-analysis. *Neuroscience & Biobehavioral Reviews*, *37*(10, Part 2), 2571–2586. https://doi.org/10.1016/j.neubiorev.2013.08.004
Turken, U., Whitfield-Gabrieli, S., Bammer, R., Baldo, J. V., Dronkers, N. F., & Gabrieli, J. D. E. (2008). Cognitive processing speed and the structure of white matter pathways: Convergent evidence from normal variation and lesion studies. *NeuroImage*, *42*(2), 1032–1044. https://doi.org/10.1016/j.neuroimage.2008.03.057
Turkozer, H. B., Pamir, Z., & Boyaci, H. (2016). Contrast Affects fMRI Activity in Middle Temporal Cortex Related to Center–Surround Interaction in Motion Perception. *Frontiers in Psychology*, *7*. https://doi.org/10.3389/fpsyg.2016.00454
Turner, C. E., & Gant, N. (2013). Chapter 2.2—The Biochemistry of Creatine. In C. Stagg & D. Rothman (Eds.), *Magnetic Resonance Spectroscopy* (pp. 91–103). Academic Press. https://doi.org/10.1016/B978-0-12-401688-0.00007-0
Turner, C. E., & Gant, N. (2014). The biochemistry of creatine. In *Magnetic resonance spectroscopy* (pp. 91-103). Academic Press.
Turner, B. M., van Maanen, L., & Forstmann, B. U. (2015). Informing cognitive abstractions through neuroimaging: The neural drift diffusion model. *Psychological Review*, *122*(2), 312–336. https://doi.org/10.1037/a0038894
Tournier, J. D., Calamante, F., Gadian, D. G., & Connelly, A. (2004). Direct estimation of the fiber orientation density function from diffusion-weighted MRI data using spherical deconvolution. *Neuroimage*, *23*(3), 1176-1185.
Uchiyama, M., Nishio, Y., Yokoi, K., Hirayama, K., Imamura, T., Shimomura, T., & Mori, E. (2012). Pareidolias: Complex visual illusions in dementia with Lewy bodies. *Brain*, *135*(8), 2458–2469. https://doi.org/10.1093/brain/aws126
Uddin, L. Q., Kelly, A. M. C., Biswal, B. B., Castellanos, F. X., & Milham, M. P. (2009). Functional connectivity of default mode network components: Correlation, anticorrelation, and causality. *Human Brain Mapping*, *30*(2), 625–637. https://doi.org/10.1002/hbm.20531
Urenjak, J., Williams, S., Gadian, D., & Noble, M. (1993). Proton nuclear magnetic resonance spectroscopy unambiguously identifies different neural cell types. *The Journal of Neuroscience*, *13*(3), 981–989. https://doi.org/10.1523/JNEUROSCI.13-03-00981.1993
Urger, S. E., De Bellis, M. D., Hooper, S. R., Woolley, D. P., Chen, S. D., & Provenzale, J. (2015). The superior longitudinal fasciculus in typically developing children and adolescents: diffusion tensor imaging and neuropsychological correlates. *Journal of child neurology*, *30*(1), 9-20.
Utsumi, K., Fukatsu, R., Yamada, R., Takamaru, Y., Hara, Y., & Yasumura, S. (2020). Characteristics of initial symptoms and symptoms at diagnosis in probable dementia with Lewy body disease: incidence of symptoms and gender differences. *Psychogeriatrics*, *20*(5), 737-745.
Van Assche, L., Van Aubel, E., Van de Ven, L., Bouckaert, F., Luyten, P., & Vandenbulcke, M. (n.d.). The Neuropsychological Profile and Phenomenology of Late Onset Psychosis: A Cross-sectional Study on the Differential Diagnosis of Very-Late-Onset Schizophrenia-Like Psychosis, Dementia with Lewy Bodies and

Alzheimer's Type Dementia with Psychosis. *Archives of Clinical Neuropsychology*. https://doi.org/10.1093/arclin/acy034
van de Beek, M., van Steenoven, I., van der Zande, J. J., Porcelijn, I., Barkhof, F., Stam, C. J., ... & Lemstra, A. W. (2021). Characterization of symptoms and determinants of disease burden in dementia with Lewy bodies: DEvELOP design and baseline results. *Alzheimer's research & therapy*, *13*(1), 1-13.
van der Leeuw, G., Leveille, S. G., Jones, R. N., Hausdorff, J. M., McLean, R., Kiely, D. K., Gagnon, M., & Milberg, W. P. (2017). Measuring attention in very old adults using the Test of Everyday Attention. *Aging, Neuropsychology, and Cognition*, *24*(5), 543–554. https://doi.org/10.1080/13825585.2016.1226747
van Ravenzwaaij, D., & Oberauer, K. (2009). How to use the diffusion model: Parameter recovery of three methods: EZ, fast-dm, and DMAT. *Journal of Mathematical Psychology*, *53*(6), 463–473. https://doi.org/10.1016/j.jmp.2009.09.004
Van Veen, V., Krug, M. K., & Carter, C. S. (2008). The neural and computational basis of controlled speed-accuracy tradeoff during task performance. *Journal of cognitive neuroscience*, *20*(11), 1952-1965.
van Vugt, M. K., Simen, P., Nystrom, L. E., Holmes, P., & Cohen, J. D. (2012). EEG Oscillations Reveal Neural Correlates of Evidence Accumulation. *Frontiers in Neuroscience*, *6*. https://doi.org/10.3389/fnins.2012.00106
Vann Jones, S. A., & O'Brien, J. T. (2014). The prevalence and incidence of dementia with Lewy bodies: A systematic review of population and clinical studies. *Psychological Medicine*, *44*(04), 673–683. https://doi.org/10.1017/S0033291713000494
Vandierendonck, A. (2017). A comparison of methods to combine speed and accuracy measures of performance: A rejoinder on the binning procedure. *Behavior research methods*, *49*(2), 653-673.
Vaportzis, E., Georgiou-Karistianis, N., & Stout, J. C. (2013). Dual Task Performance in Normal Aging: A Comparison of Choice Reaction Time Tasks. *PLOS ONE*, *8*(3), e60265. https://doi.org/10.1371/journal.pone.0060265
Venkatesh, A., Stark, S. M., Stark, C. E., & Bennett, I. J. (2020). Age-and memory-related differences in hippocampal gray matter integrity are better captured by NODDI compared to single-tensor diffusion imaging. *Neurobiology of Aging*, *96*, 12-21.
Verhaeghen, P., & Basak, C. (2005). Ageing and Switching of the Focus of Attention in Working Memory: Results from a Modified N-Back Task. *The Quarterly Journal of Experimental Psychology Section A*, *58*(1), 134–154. https://doi.org/10.1080/02724980443000241
Veldsman, M., Tai, X. Y., Nichols, T., Smith, S., Peixoto, J., Manohar, S., & Husain, M. (2020). Cerebrovascular risk factors impact frontoparietal network integrity and executive function in healthy ageing. *Nature communications*, *11*(1), 1-10.
Vettel, J. M., Cooper, N., Garcia, J. O., Yeh, F.-C., & Verstynen, T. D. (2001). White Matter Tractography and Diffusion-Weighted Imaging. In John Wiley & Sons Ltd (Ed.), *ELS* (pp. 1–9). John Wiley & Sons, Ltd. https://doi.org/10.1002/9780470015902.a0027162
Volberg, G., & Greenlee, M. W. (2014). Brain networks supporting perceptual grouping and contour selection. *Frontiers in Psychology*, *5*, 264.
Vossel, S., Geng, J. J., & Fink, G. R. (2014). Dorsal and Ventral Attention Systems: Distinct Neural Circuits but Collaborative Roles. *The Neuroscientist*, *20*(2), 150–159. https://doi.org/10.1177/1073858413494269
Wagenmakers, E.-J., Van Der Maas, H. L. J., & Grasman, R. P. P. P. (2007). An EZ-diffusion model for response time and accuracy. *Psychonomic Bulletin & Review*, *14*(1), 3–22. https://doi.org/10.3758/BF03194023
Wakana, S., Caprihan, A., Panzenboeck, M. M., Fallon, J. H., Perry, M., Gollub, R. L., Hua, K., Zhang, J., Jiang, H., Dubey, P., Blitz, A., van Zijl, P., & Mori, S. (2007). Reproducibility of quantitative tractography methods applied to cerebral white matter. *NeuroImage*, *36*(3), 630–644. https://doi.org/10.1016/j.neuroimage.2007.02.049
Walhovd, K. B., Westlye, L. T., Amlien, I., Espeseth, T., Reinvang, I., Raz, N., Agartz, I., Salat, D. H., Greve, D. N., Fischl, B., Dale, A. M., & Fjell, A. M. (2011). Consistent neuroanatomical age-related volume differences across multiple samples. *Neurobiology of Aging*, *32*(5), 916–932. https://doi.org/10.1016/j.neurobiolaging.2009.05.013
Walker, M. P., Ayre, G. A., Perry, E. K., Wesnes, K., McKeith, I. G., Tovee, M., Edwardson, J. A., & Ballard, C. G. (2000). Quantification and Characterisation of Fluctuating Cognition in Dementia with Lewy Bodies and Alzheimer's Disease. *Dementia and Geriatric Cognitive Disorders*, *11*(6), 327–335. https://doi.org/10.1159/000017262
Wang, C. (2005). Responses of Human Anterior Cingulate Cortex Microdomains to Error Detection, Conflict Monitoring, Stimulus-Response Mapping, Familiarity, and Orienting. *Journal of Neuroscience*, *25*(3), 604–613. https://doi.org/10.1523/JNEUROSCI.4151-04.2005
Ward, L. M., Morison, G., Simmers, A. J., & Shahani, U. (2018). Age-related changes in global motion coherence: Conflicting haemodynamic and perceptual responses. *Scientific Reports*, *8*(1), 1-11.
Warrington, E. K., & James, M. (1991). The visual object and space perception battery.
Waskom, M. L., Okazawa, G., & Kiani, R. (2019). Designing and Interpreting Psychophysical Investigations of Cognition. *Neuron*, *104*(1), 100–112. https://doi.org/10.1016/j.neuron.2019.09.016

Wassef, A., Baker, J., & Kochan, L. D. (2003). GABA and schizophrenia: a review of basic science and clinical studies. *Journal of clinical psychopharmacology*, *23*(6), 601-640.
Watanabe, H., Nishio, Y., Mamiya, Y., Narita, W., Iizuka, O., Baba, T., Takeda, A., Shimomura, T., & Mori, E. (2018). Negative mood invites psychotic false perception in dementia. *PLOS ONE*, *13*(6), e0197968. https://doi.org/10.1371/journal.pone.0197968
Watson, A. B., & Pelli, D. G. (1983). QUEST: A Bayesian adaptive psychometric method. *Perception & psychophysics*, *33*(2), 113-120.
Watson, R., Blamire, A. M., Colloby, S. J., Wood, J. S., Barber, R., He, J., & O'Brien, J. T. (2012). Characterizing dementia with Lewy bodies by means of diffusion tensor imaging. *Neurology*, *79*(9), 906–914. https://doi.org/10.1212/WNL.0b013e318266fc51
Watson, R., Blamire, A. M., & O'Brien, J. T. (2009). Magnetic Resonance Imaging in Lewy Body Dementias. *Dementia and Geriatric Cognitive Disorders*, *28*(6), 493–506. https://doi.org/10.1159/000264614
Watson, R., Colloby, S. J., Blamire, A. M., Wesnes, K. A., Wood, J., & O'Brien, J. T. (2017). Does attentional dysfunction and thalamic atrophy predict decline in dementia with Lewy bodies? *Parkinsonism & Related Disorders*, *45*, 69–74. https://doi.org/10.1016/j.parkreldis.2017.10.006
Weaver, K. E., Richards, T. L., Saenz, M., Petropoulos, H., & Fine, I. (2013). Neurochemical changes within human early blind occipital cortex. *Neuroscience*, *252*, 222–233. https://doi.org/10.1016/j.neuroscience.2013.08.004
Wechsler, D. (2011). Test of premorbid functioning. UK version (TOPF UK). *UK: Pearson Corporation*.
Weerasekera, A., Levin, O., Clauwaert, A., Heise, K. F., Hermans, L., Peeters, R., ... & Swinnen, S. P. (2020). Neurometabolic correlates of reactive and proactive motor inhibition in young and older adults: Evidence from multiple regional 1H-MR spectroscopy. *Cerebral Cortex Communications*, *1*(1), tgaa028.
Werner, J. S., Schefrin, B. E., & Bradley, A. (2010). Optics and vision of the aging eye. *Handbook of optics*, *3*, 13-1.
Wesnes, K., Aarsland, D., Ballard, C., & Londos, E. (2013). Memantine improves attention and verbal episodic memory in Parkinson's disease dementia and dementia with Lewy bodies: A double-blind, placebo-controlled multicentre trial. *Alzheimer's & Dementia*, *4(S)*(9), P890. https://doi.org/10.1016/j.jalz.2013.08.252
West, R. L. (1996). An application of prefrontal cortex function theory to cognitive aging. *Psychological Bulletin*, *120*(2), 272–292. https://doi.org/10.1037//0033-2909.120.2.272
Westlye, L. T., Grydeland, H., Walhovd, K. B., & Fjell, A. M. (2011). Associations between Regional Cortical Thickness and Attentional Networks as Measured by the Attention Network Test. *Cerebral Cortex*, *21*(2), 345–356. https://doi.org/10.1093/cercor/bhq101
Wheeler-Kingshott, C. A., & Cercignani, M. (2009). About "axial" and "radial" diffusivities. *Magnetic Resonance in Medicine: An Official Journal of the International Society for Magnetic Resonance in Medicine*, *61*(5), 1255-1260.
Whitson, L. R., Karayanidis, F., Fulham, R., Provost, A., Michie, P. T., Heathcote, A., & Hsieh, S. (2014). Reactive control processes contributing to residual switch cost and mixing cost across the adult lifespan. *Frontiers in Psychology*, *5*, 383.
Whitwell, J. L., Weigand, S. D., Shiung, M. M., Boeve, B. F., Ferman, T. J., Smith, G. E., Knopman, D. S., Petersen, R. C., Benarroch, E. E., Josephs, K. A., & Jack, C. R., Jr. (2007). Focal atrophy in dementia with Lewy bodies on MRI: A distinct pattern from Alzheimer's disease. *Brain*, *130*(3), 708–719. https://doi.org/10.1093/brain/awl388
Williams, R. S., Biel, A. L., Wegier, P., Lapp, L. K., Dyson, B. J., & Spaniol, J. (2016). Age differences in the Attention Network Test: Evidence from behavior and event-related potentials. *Brain and Cognition*, *102*, 65–79. https://doi.org/10.1016/j.bandc.2015.12.007
Winkler, A. M., Ridgway, G. R., Webster, M. A., Smith, S. M., & Nichols, T. E. (2014). Permutation inference for the general linear model. *NeuroImage*, *92*, 381–397. https://doi.org/10.1016/j.neuroimage.2014.01.060
Wittfoth, M., Buck, D., Fahle, M., & Herrmann, M. (2006). Comparison of two Simon tasks: Neuronal correlates of conflict resolution based on coherent motion perception. *NeuroImage*, *32*(2), 921–929. https://doi.org/10.1016/j.neuroimage.2006.03.034
Wolf, W., Hicks, T. P., & Albus, K. (1986). The contribution of GABA-mediated inhibitory mechanisms to visual response properties of neurons in the kitten's striate cortex. *Journal of Neuroscience*, *6*(10), 2779-2795.
Wolfe, J. M., Oliva, A., Horowitz, T. S., Butcher, S. J., & Bompas, A. (2002). Segmentation of objects from backgrounds in visual search tasks. *Vision research*, *42*(28), 2985-3004.
Wood, J. S., Firbank, M. J., Mosimann, U. P., Watson, R., Barber, R., Blamire, A. M., & O'Brien, J. T. (2013). Testing Visual Perception in Dementia with Lewy Bodies and Alzheimer Disease. *The American Journal of Geriatric Psychiatry*, *21*(6), 501–508. https://doi.org/10.1016/j.jagp.2012.11.015
World Health Organization. (2019). *Global status report on alcohol and health 2018*. World Health Organization.
Yang, Y., Bender, A. R., & Raz, N. (2015). Age related differences in reaction time components and diffusion properties of normal-appearing white matter in healthy adults. *Neuropsychologia*, *66*, 246-258.
Yassa, M. A., Mattfeld, A. T., Stark, S. M., & Stark, C. E. L. (2011). Age-related memory deficits linked to circuit-specific disruptions in the hippocampus. *Proceedings of the National Academy of Sciences*, *108*(21), 8873–8878. https://doi.org/10.1073/pnas.1101567108

Yeatman, J. D., Weiner, K. S., Pestilli, F., Rokem, A., Mezer, A., & Wandell, B. A. (2014). The vertical occipital fasciculus: a century of controversy resolved by in vivo measurements. *Proceedings of the National Academy of Sciences*, *111*(48), E5214-E5223.
Yesavage, J. A. (1988). Geriatric depression scale. *Psychopharmacol Bull*, *24*(4), 709-711.
Yochim, B. P., Baldo, J. V., Kane, K. D., & Delis, D. C. (2009). D-KEFS Tower Test performance in patients with lateral prefrontal cortex lesions: The importance of error monitoring. *Journal of Clinical and Experimental Neuropsychology*, *31*(6), 658–663. https://doi.org/10.1080/13803390802448669
Yokoi, K., Nishio, Y., Uchiyama, M., Shimomura, T., Iizuka, O., & Mori, E. (2014). Hallucinators find meaning in noises: Pareidolic illusions in dementia with Lewy bodies. *Neuropsychologia*, *56*, 245–254. https://doi.org/10.1016/j.neuropsychologia.2014.01.017
Yoon, J. H., Lee, J. E., Yong, S. W., Moon, S. Y., & Lee, P. H. (2014). The mild cognitive impairment stage of dementia with Lewy bodies and Parkinson disease: a comparison of cognitive profiles. *Alzheimer Disease & Associated Disorders*, *28*(2), 151-155.
Yoon, J. H., Grandelis, A., & Maddock, R. J. (2016). Dorsolateral Prefrontal Cortex GABA Concentration in Humans Predicts Working Memory Load Processing Capacity. *The Journal of Neuroscience*, *36*(46), 11788–11794. https://doi.org/10.1523/JNEUROSCI.1970-16.2016
Yoshida, T., Tanaka, M., Sotomatsu, A., & Hirai, S. (1995). Activated microglia cause superoxide-mediated release of iron from ferritin. *Neuroscience Letters*, *190*(1), 21–24. https://doi.org/10.1016/0304-3940(95)11490-N
Youn, J.-H., Ryu, S.-H., Lee, J.-Y., Park, S., Cho, S.-J., Kwon, H., Yang, J.-J., Lee, J.-M., Lee, J., Kim, S., Livingston, G., & Yoon, D. H. (2019). Brain structural changes after multi-strategic metamemory training in older adults with subjective memory complaints: A randomized controlled trial. *Brain and Behavior*, *9*(5), e01278. https://doi.org/10.1002/brb3.1278
Yuki, N., Yoshioka, A., Mizuhara, R., & Kimura, T. (2020). Visual hallucinations and inferior longitudinal fasciculus in Parkinson's disease. *Brain and Behavior*, *10*(12), e01883. https://doi.org/10.1002/brb3.1883
Zahr, N. M., Mayer, D., Rohlfing, T., Chanraud, S., Gu, M., Sullivan, E. V., & Pfefferbaum, A. (2013). In vivo glutamate measured with magnetic resonance spectroscopy: Behavioral correlates in aging. *Neurobiology of Aging*, *34*(4), 1265–1276. https://doi.org/10.1016/j.neurobiolaging.2012.09.014
Zanto, T. P., & Gazzaley, A. (2014). Attention and ageing.
Zarahn, E., Rakitin, B., Abela, D., Flynn, J., & Stern, Y. (2007). Age-related changes in brain activation during a delayed item recognition task. *Neurobiology of Aging*, *28*(5), 784–798. https://doi.org/10.1016/j.neurobiolaging.2006.03.002
Zarkali, A., Adams, R. A., Psarras, S., Leyland, L.-A., Rees, G., & Weil, R. S. (2019). Increased weighting on prior knowledge in Lewy body-associated visual hallucinations. *Brain Communications*, *1*(fcz007). https://doi.org/10.1093/braincomms/fcz007
Zeisel, S. H., & da Costa, K.-A. (2009). Choline: An Essential Nutrient for Public Health. *Nutrition Reviews*, *67*(11), 615–623. https://doi.org/10.1111/j.1753-4887.2009.00246.x
Zelazo, P. D., & Cunningham, W. A. (2007). Executive Function: Mechanisms Underlying Emotion Regulation. In *Handbook of emotion regulation* (pp. 135–158). The Guilford Press.
Zelazo, P. D., Craik, F. I., & Booth, L. (2004). Executive function across the life span. *Acta psychologica*, *115*(2-3), 167-183.
Zhang, Y., Brady, M., & Smith, S. (2001). Segmentation of brain MR images through a hidden Markov random field model and the expectation-maximization algorithm. *IEEE Transactions on Medical Imaging*, *20*(1), 45–57. https://doi.org/10.1109/42.906424
Zhang, Y., Meyers, E. M., Bichot, N. P., Serre, T., Poggio, T. A., & Desimone, R. (2011). Object decoding with attention in inferior temporal cortex. *Proceedings of the National Academy of Sciences*, *108*(21), 8850–8855. https://doi.org/10.1073/pnas.1100999108
Zhang, J., & Rowe, J. B. (2014). Dissociable mechanisms of speed-accuracy tradeoff during visual perceptual learning are revealed by a hierarchical drift-diffusion model. *Frontiers in neuroscience*, *8*, 69.
Zhang, H., Menzies, K. J., & Auwerx, J. (2018). The role of mitochondria in stem cell fate and aging. *Development*, *145*(8).
Zhong, W. J., Guo, D. J., Zhao, J. N., Xie, W. B., Chen, W. J., & Wu, W. (2012). Changes of axial and radial diffusivities in cerebral white matter led by normal aging. *Diagnostic and interventional imaging*, *93*(1), 47-52.
Zhou, S. S., Fan, J., Lee, T. M., Wang, C. Q., & Wang, K. (2011). Age-related differences in attentional networks of alerting and executive control in young, middle-aged, and older Chinese adults. *Brain and Cognition*, *75*(2), 205-210.
Zhou, D., Lebel, C., Evans, A., & Beaulieu, C. (2013). Cortical thickness asymmetry from childhood to older adulthood. *Neuroimage*, *83*, 66-74.

# Appendices

## Appendix 1 : Pilot study of visual and attentional tasks in healthy younger and older adults

### Methods

*Participants and Design*

To ensure the battery was effective and accessible, participants from ages 18-30 (n=31) and 50-90 (n=10) were recruited. Younger participants were undergraduates or postgraduates at Cardiff University recruited through the School of Psychology, Cardiff University Experimental Management System (EMS) in exchange for course credits, or via word of mouth. Older participants were recruited through the Community Panel at Cardiff University, which is a database of members of the public interested in partaking in research. Participants were invited to take part if they had normal or normal corrected vision and were fluent English speakers. All participants provided written informed consent. All tasks designed for the project were coded using PsychoPy v 1.85.6 (Pierce 2007; Pierce, 2009) with the exception of the FrACT (Bach, 1996) which was downloaded in its original form, and the TOPF-UK (Weschler, 2011) and Doors and People standardised tasks.

*Materials: Visual Task Battery Development*

A visual task battery was designed in order to assess functions at each stage of visual processing in order to determine a specific level at which visual perception becomes impaired in DLB patients.

Lower-level vision

V1, involved in the lowest levels of visual processing was assessed using measures of visual acuity, visual contrast and orientation. Two tasks were used to determine the functioning of this region, the FrACT (Bach, 1996) which determines level of visual acuity and contrast using a classic Landolt C test. Participants viewed the 'C' shape on the screen and were asked to respond to the 'gap' in the C, which was rotated at random between trials. For the visual acuity paradigm, shapes were reduced in size in response to performance, and for the contrast paradigm the 'faintness' of the shapes was manipulated.

Orientation detection was measured using a Gabor patch paradigm (Peirce, 2007; Peirce, 2009) in which two shapes were presented on the screen with vertical lines down the centre of each shape. The vertical 'line' in the centre of the shape was manipulated in degrees of orientation in one of the shapes on each trial, and participants were asked to identify which shape was oriented exactly vertical. The location of the 'correct' answer was randomly determined for each trial. Each trial increased in difficulty via the level of degrees oriented to find a threshold of contour detection.

Mid-level vision

Mid-level visual perception involves contour detection which was assessed using a Gabor patch paradigm in which participants were asked to detect the outline of a shape within the dot pattern (Metzler-Baddeley et al., 2010). Orientation of the contour Gabor patches was manipulated between 0° and 40° in order to increase difficulty of detection in a 4-forced choice paradigm. Participants responded to the location of the contour which was randomly determined for each trial. A linear staircase selected the difficulty of trials depending on performance on a 3 up 1 down basis. Motion perception was also assessed using a random dot kinetogram, in which participants were asked to determine the direction of the moving dots whilst 'distractor' moved randomly through the animation. Direction of dots was determined at random, and the same linear 3 up 1 down staircase and 4-forced choice task design was employed to manipulate the ratio of uniform to random dots.

Higher-level vision

Figure ground-segregation, the ability to discriminate objects from background The embedded figures test (EFT) involves perceiving information which is integrated into a background, requiring parieto-occipital and frontal cortical regions (Ring et al., 1999; Withkin et al., 1971). The participant is required to separate the figure from the ground in order to perceive the embedded target (de-Wit et al., 2017). The EFT uses stimuli from the Leuven Embedded figures test (L-EFT). Participants view one target line shape at the top of the screen (e.g. triangle), and three line drawings at the bottom of the screen (see Figure 4D). Participants are asked to identify which of the three-line drawings contains the target, embedded into the lines. Number of lines in the target shape, number of lines in the line drawing options, and symmetry of the target shape are manipulated to make the trials more difficult. Trials were presented until response (trials = 62).

Seemingly large changes in a scene, such as the removal of an object, can be missed due to absence of attentional processing to the particular element of the scene. This phenomenon is referred to as 'change blindness'. Objects and elements of the scene are processed by the ventral visual pathway; however, conscious detection of change also relies on dorsal stream activation, thus dorsal-ventral interaction is important in effective visual perception (Beck et al., 2001). Change blindness was assessed in the present study by presenting participants with coloured photographs of household scenes (see Figure 4C), accessed from the SCEGRAM image database (Öhlschläger & Võ, 2017) with permission. Each trial consisted of the presentation of one photograph on the screen (6000ms), followed by a blank screen interval, with a central fixation cross (1000ms), and the subsequent presentation of a second photograph. The second photograph shown was identical to the first, however an element of the image was altered from the first photograph. Following the presentation of images, participants were shown three choices on screen (for example 'plant', 'chair', 'newspaper'), and were prompted to select which of the items they believed had changed (either appeared or disappeared) between the images. Images and items were altered for difficulty by manipulating the size and location of the target in the scene (trials = 20).

Object based visual perception is also considered to be a higher-level visual perceptual process, which involves the ventral stream, including the temporal lobe (Reddy & Kanwisher, 2006). The effective recognition of objects has been assessed by multiple tasks, such as the chimeric non-object task (Lloyd-Jones & Humphreys, 1997). The stimuli used in the task are line-drawings of figures (animals, natural objects, birds, household items) which are either chimeric non-objects or real objects. Chimeric non-objects are formed by parts of 2 objects (Figure B), and real objects are true to form (replicated from Lloyd-Jones and Humphreys (1997) by Gerlach (2017) used with permission). In the present study, participants are presented with 4 line-drawings, at the top, bottom, left and right of the screen, on a white background. Images presented included 3 objects, and 1 chimeric non-object, which was presented at a different position on each trial. Each trial was displayed until a response was made using the corresponding arrows (trials = 20).

*Visual attention and executive tasks*

Visual attention refers to the process in which visual information is located and attended to within a scene (Derrington, 1996). Impairments in visual search tasks can be observed following damage to the occipito-parietal cortex (Atkinson & Braddick, 1989) and have also been observed in DLB patients (Cormack, Gray, et al., 2004). The present task used simple green and red 'T' stimuli in varying rotations, which were presented to participants on a grey background. Participants were presented with the target 'T' prior to the task, which remained the same throughout all trials. Stimuli were presented in two blocks: block one contained 12 trials, each containing 8 stimuli, in which 4 of these trials contained no target, and block two contained 12 trials, each containing 16 stimuli, in which 4 trials contained no target. Trials which contained the target were balanced by location of the target (in four screen quadrants). Trials were altered in difficulty by manipulating the eccentricity of target on the screen from foveation (trials = 52).

Executive function refers to a set of cognitive processes such as judgement, inhibition and cognitive flexibility (Diamond, 2013). The Stroop Colour and Word Test has been extensively used for the assessment of inhibition of cognitive interference (Stroop, 1935) and DLB patients are seen to have poorer performance than AD on this task (Park et al., 2011). As in the classic Stroop task, in the present study participants viewed colour words ('red', 'blue', 'green', 'yellow', 'pink') presented individually at the centre of the screen on a grey background, for 5000ms. Participants were instructed to respond as quickly as possible to the word itself, ignoring the colour ink. Responses were made using colour coded keys (trial =50).

In addition to visual tasks, the Attention Network Task (ANT; Fan et al., 2002), a flanker task integrated with the Posner cueing task (Posner, 1980) was adapted for use in the battery. The task was employed in order to ascertain more detail about the nature of attentional impairments in patient groups and how these may contribute to performance in visual perception tasks. The ANT presents participants with four cue

conditions (spatial, double, centre or no cue) and three flanker conditions (neutral, congruent or incongruent), scores from which can be calculated for individual network performance (orienting, altering and executive). Stimuli consist of a horizontal row of 5 horizontal black lines with arrow heads against a grey background. In accordance with the original study, these stimuli subtended 3.08° of visual angle and, in order to introduce the orienting component, these stimuli were presented variably at 1.06° above or below a central fixation point. Each trial consisted of five events, firstly a fixation period of 400ms. Secondly, in order to introduce an alerting component, one of four 'warning' conditions (star cue; spatial, double, no or centre) were presented at random for 100ms. Next, the stimuli (either congruent, neutral or incongruent) in one of three positions (above, below or on fixation) were presented for response, and disappeared after 1700ms. Excluding two practice trials, the session consisted of 144 trials (4 cue conditions x 3 target locations x 3 flanker conditions x 2 repetitions) which look approximately 10-12 minutes to complete in healthy control subjects.

In order to determine the efficacy and validity of the tasks designed, a pilot study was conducted to assess both younger and older healthy controls' task performance, as well as ease of use and accessibility of tasks for all ages. In addition to the experimental tasks, measures of executive function, intellect, verbal fluency, visual and verbal memory and general visual attention were also included in the task battery.

*Procedure*

Participants were tested individually in cognitive testing rooms in Cardiff University Brain Imaging Research Centre (CUBRIC). Participant information, details and consent forms were completed prior to testing with full consent being obtained from each participant. Computerised tasks were executed using a 15" MacBook Pro 2012 (macOS Sierra v 10.12.6, 2.3 GHz, Intel Core i7, Apple Inc., CA) and projected onto a 24" monitor with a Full HD LED 1920 x 1080 resolution (Iiyama Prolite PI1283h, Mouse Computer Corporation, Tokyo). Participant's responses were recorded using a Bluetooth wireless numeric keypad for Mac OS (BKB-Apple-PM, Cateck Inc., Tokyo) coded and adapted for the study by creating colour and arrow response buttons. Prior to each computerised task, the researcher gave a verbal introduction and explanation to each task procedure and how to respond. Participants were then shown the instructions provided on screen before each task and given practice trials. The researcher ensured that participants were confident in completing the task before proceeding.

Domains of general cognitive functioning were assessed using standardised and validation measures of memory, visual attention and executive function to supplement clinical assessments of cognition from medical information. Memory, specifically visual and verbal recall and recognition was measured using the 'Doors and People Test' (Baddeley, Emslie & Nimmo-Smith, 1994). The test involves memory and delayed

memory recall for names, shapes and images and has been widely used in the dementia population and returned valid results (Green, Baddeley & Hodges, 1996; Clare et al., 2001; Nestor, Fryer & Hodges, 2006). Computerised tasks were completed as described above.

## Results

### Demographic characteristics

Participants in the younger adult group (n=31) had a mean age of 20.89, and in the older group (n=10), mean age was 67.2. Participants did not significantly differ in years of education (F(1,37)=0.127, p=.072), TOPF-UK intelligence score (F(1,37)=0.195, p=.66) or visual acuity (F(1,37)=2.418,p=.0142)

| | Younger M (SD) | Older M (SD) |
|---|---|---|
| Age | 20.89 (3.37) | 67.2 (8.59) |
| Gender | Male (10) Female (21) | Male (3) Female (7) |
| Handedness | Left (3) Right (28) | Left (0) Right (10) |
| Years of education | 20.55 (3.12) | 21 (4.24) |
| TOPF-UK score | 49.64 (11.83) | 51.88 (15.32) |
| Visual acuity (Snellen fraction) | 1.31 (0.37) | 1.77 (0.31) |
| Visual contrast (LogMAR) | 1.01 (0.31) | 1.74 (0.59) |

*General cognitive assessments*

Average lexical fluency performance on the FAS task was 15.01 words per minute (SD=4.23). Doors and People task age scaled verbal forgetting (M=8, SD=2.26) showed no significant group difference ($F(1)=0.853$, $p=0.39$), or visual forgetting (M=10.14, SD=2.53) ($F(1)=0.47$, $p=0.52$).

Stroop task results demonstrated high accuracy of performance (M=95.48%, SD=9.86) and reaction time (M=323 msec, SD=30.5). No significant difference in group performance was present for accuracy ($F(1)=0.608$, $p=0.45$) or speed ($F(1)=3.06$, $p=0.10$). Visual search task accuracy (M=89.81, SD=3.46) and speed of reaction time (M=168.1 msec, SD=61) demonstrated consistent performance between participants, which did not significantly differ between age groups (accuracy: $F(1)=0.003$, $p=0.95$, RT: $F(1)=2.77$, $p=0.117$).

*Low-level visual perceptual tasks*

No significant differences were found between younger and older groups in orientation threshold. No significant group differences in visual acuity or visual contrast were observed

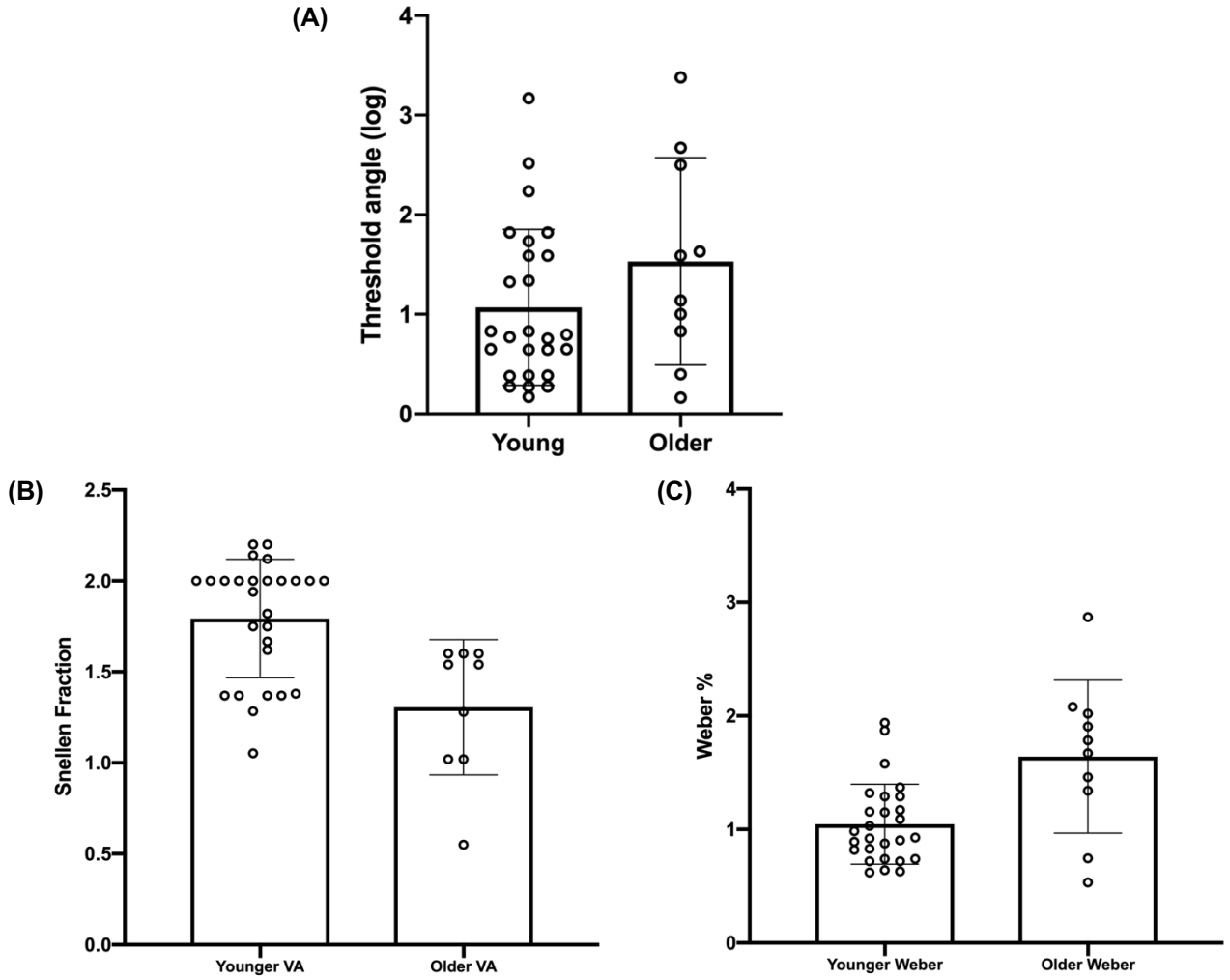


*Mid-level visual perceptual tasks*

No significant differences were found between younger and older groups in contour detection threshold. No significant difference in motion coherence threshold between younger and older groups was present.

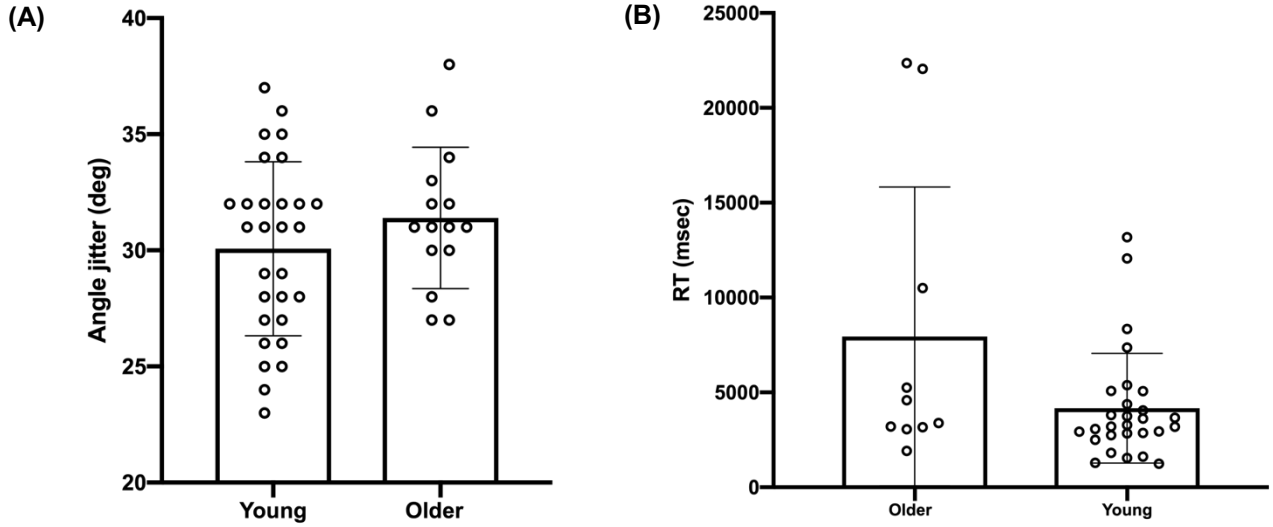

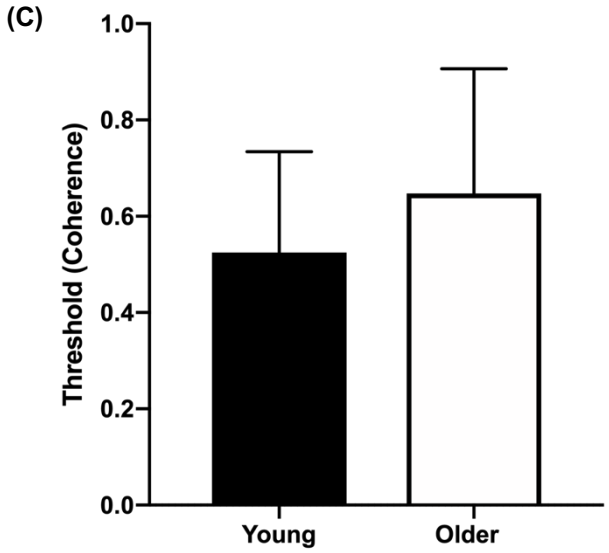


*High-level visual perceptual tasks*

A significant effect of rotation condition was found in the mental rotation task (F=75.643, p=<.001) on reaction time (RT). The effect of rotation condition on RT was also found to be significant within the younger group (F=4.741, p=.003), however this was not present in the older group following correction for multiple comparisons (F=2.93, p=.037). No significant effect of number of cubes per stimuli on RT was detected.

*

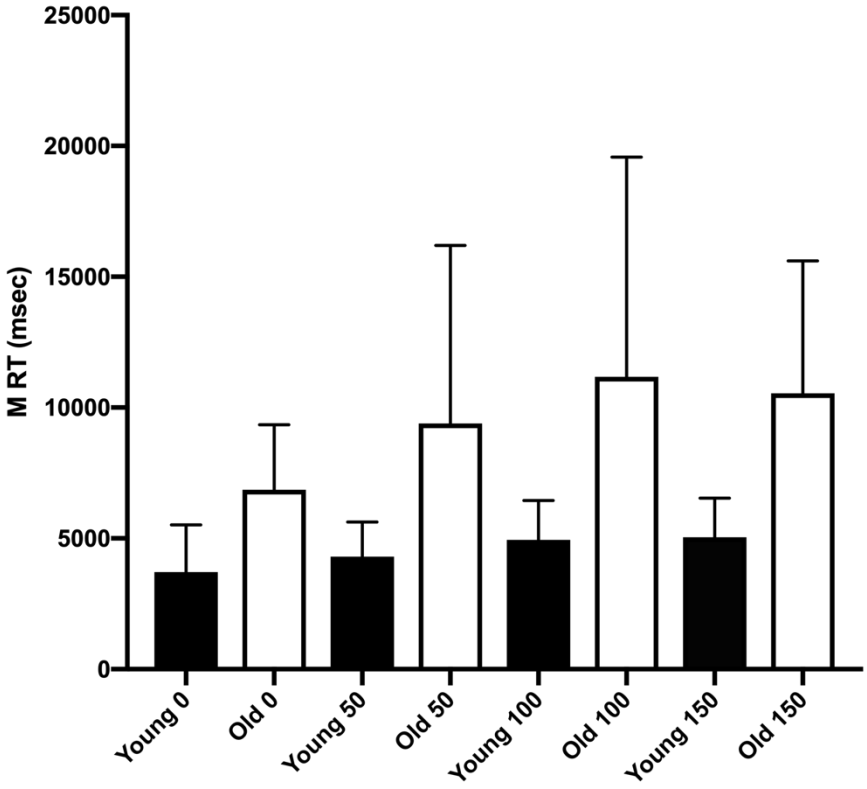

In the change blindness task, a significant effect of object size on reaction time was found in the younger group (r=.201, p=.002). Object location (distance from centre of screen) was also seen to have a significant effect on reaction time in the younger group only (r=-.187, p=.004) (Figure 13).

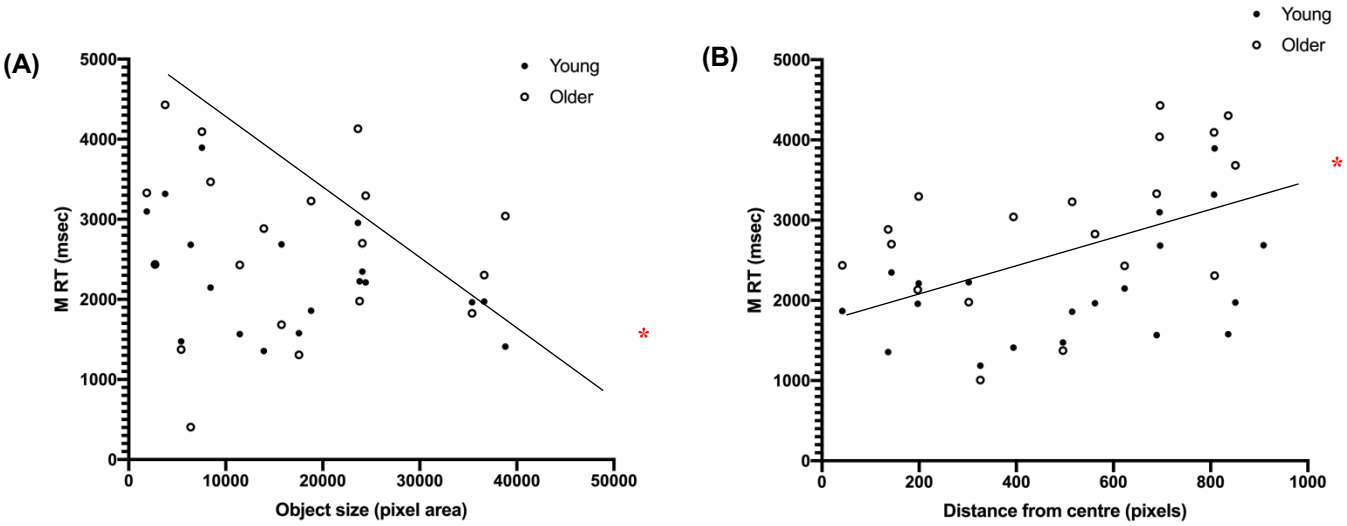


In the embedded figures task, a significant effect of the number of lines in the target shape on reaction time was found, with increasing numbers of lines (2,4,6, 8) resulting in longer RT (F=32.352, p<.001). Interestingly, RT was longer in 6-line condition, and became shorter in the 8-line condition in older groups only. A significant effect of group was found on reaction time (F=12.45, p<.001). No effect of line number in the target patterns on reaction time was found (Figure 14, 15).

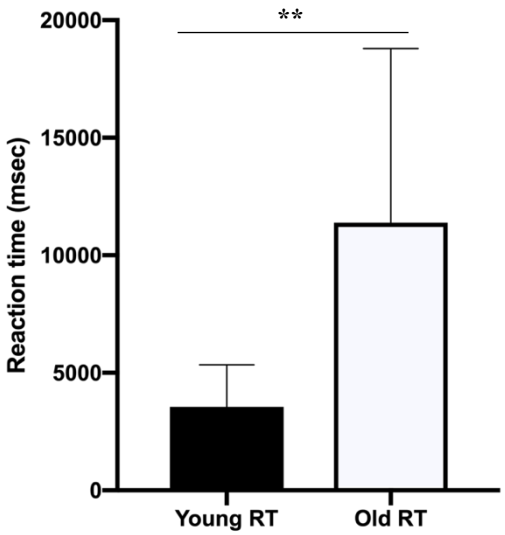

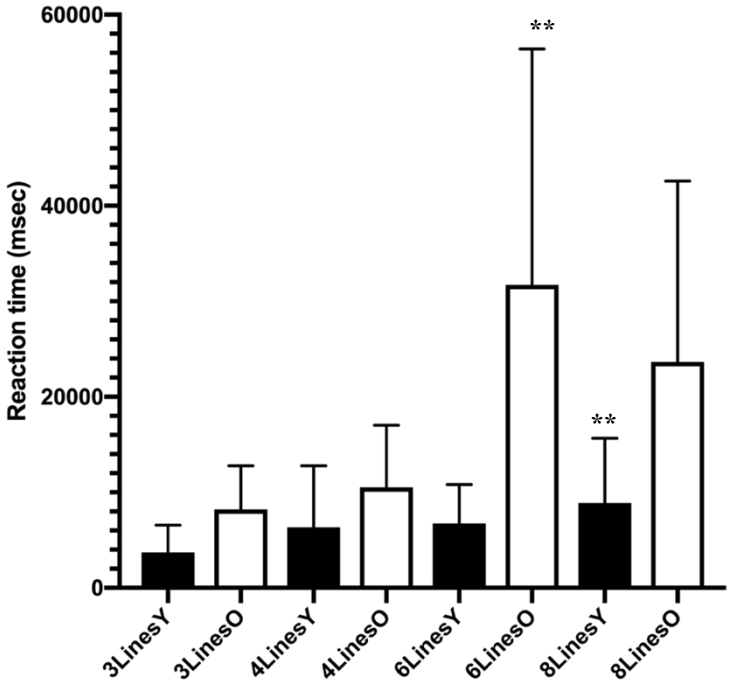


*Visual attention and executive tasks*

The classic Stroop effect was found to be present in the Stroop task, with a significant effect of trial congruency on RT (F=22.311, p<.001). A significant Stroop effect was found in each group (Younger = F=26.147, p=<.001; Older = F=7.098, p=.008). Group differences in overall RT were not significant. In the visual search task, a significant effect of the number of distractor stimuli presented (8, 16) on RT was present (F=12.33, p<.001). A significant group effect on RT was also observed (F=6.771, p<.001).

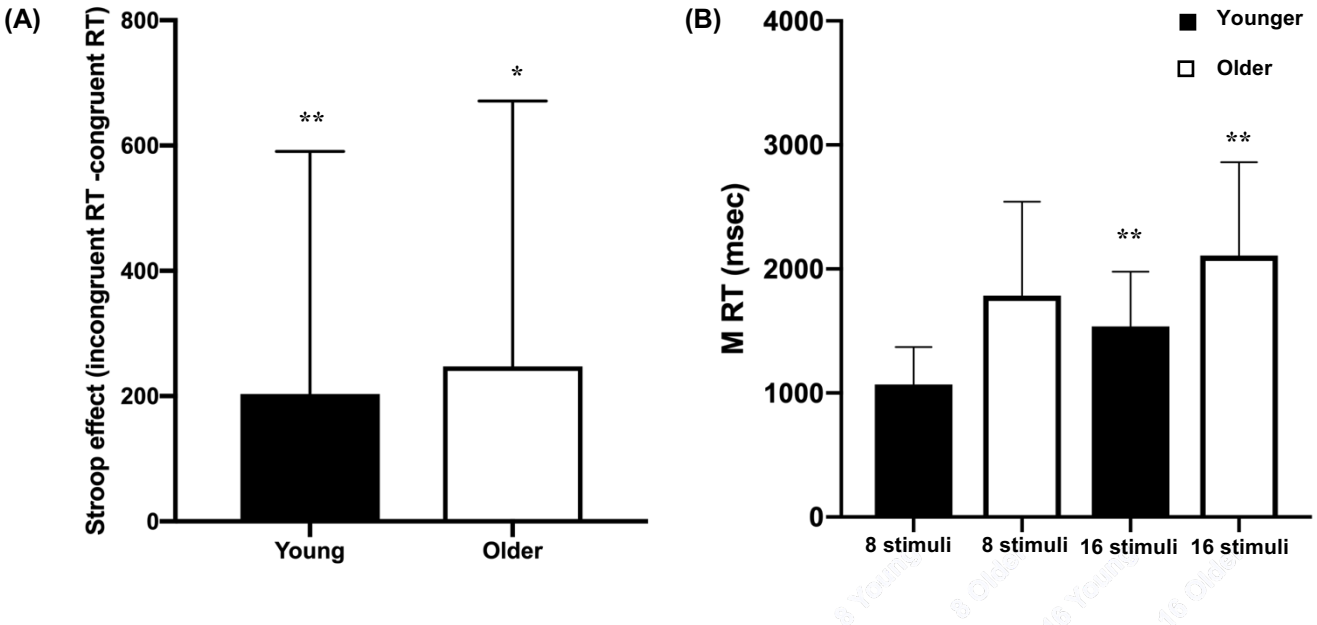

*Attention*

A significant effect of cue condition on reaction time was present in the ANT (F=3.737, p=<.001). Post hoc tests revealed a significant effect of spatial cue vs centre cue on reaction time (p=.004) and approached significance in no cue vs double cue (p=.035). A significant effect of flanker condition on reaction time (F=5.216, p=.006).

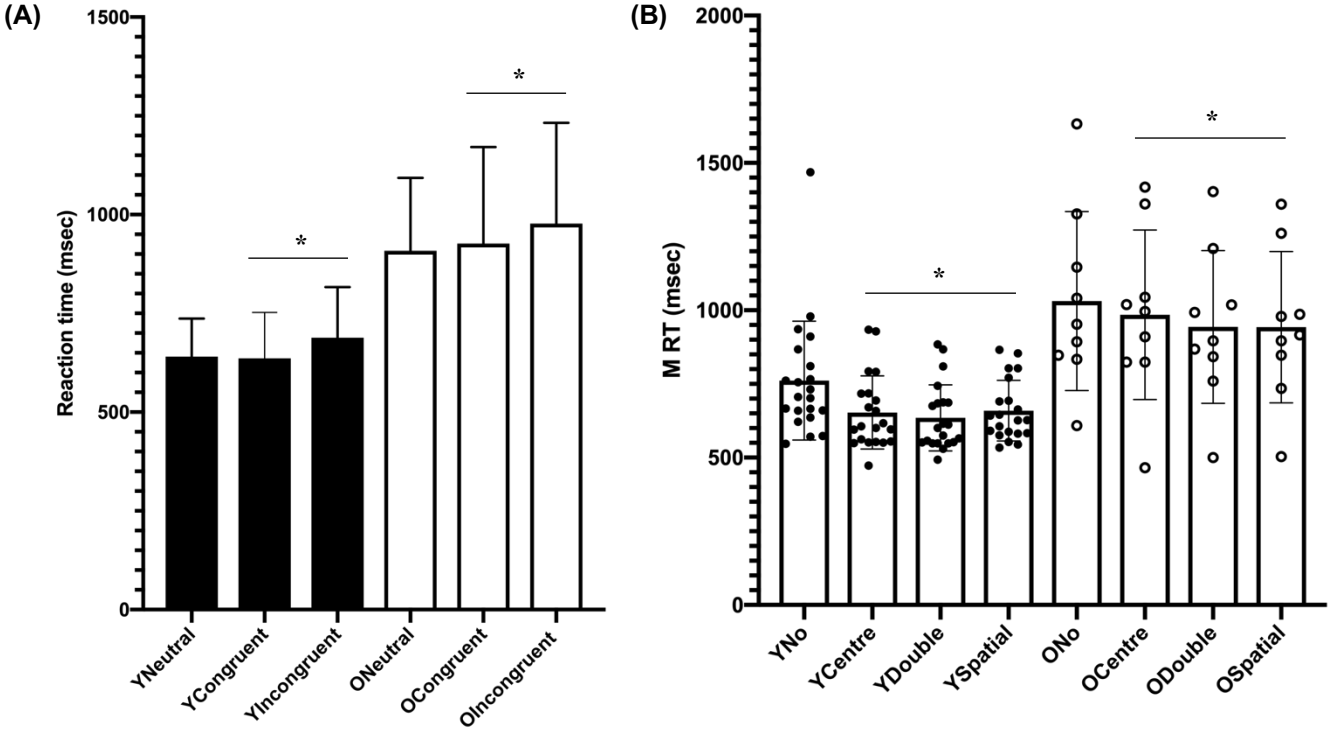


Preliminary results have demonstrated results consistent with previous findings in the majority of tasks. General cognitive assessments demonstrated no differences in performance between older and younger participants, with relatively low variation in both accuracy of performance and speed of reaction time.

Stroop task performance in the present project is consistent with previous investigations which have demonstrated no significant difference in performance on a computerised Stroop task in older and younger healthier groups (Shilling, Chetwynd & Rabbitt, 2002). Data for visual search task indicates variable performance, which are very evident in previous research, and as such, group similarities or differences may not be as clear as in alternative tasks (Ball, Roenker & Bruni, 1990). Tasks assessing lexical fluency are generally predicted by vocabulary size, and lexical access speed (Bolla, Lindgren, Bonaccorsy & Bleecker, 1990), and observation of lexical fluency scores in the present project suggest relationship with TOPF-UK scores, indicating the task may be valid. Previous ANT performance in older adults has demonstrated no difference in performance in orienting or executive networks, and some slight difference in alerting performance (Jennings et al., 2004). The task demonstrated no group differences at present, however the results are consistent with the original ANT experiment (Fan et al., 2002). Performance on tasks of visual orientation have demonstrated results consistent with the current findings (Faust & Balota, 1997), however there is no normative data previously determined for the exact task which was adapted for use from PsychoPy original psychophysics tasks (Peirce, 2007; Peirce, 2009). The task assessing contour integration

was computerised from Metzler-Baddeley et al., (2010), and demonstrated a slightly lower level of difficulty reached in healthy controls. However, this may be due to the computerisation of the task and screen viewing, or co-ordination of viewing and response on keypad. The motion perception task returned little usable data due to an error in the code, which has since been amended for future use. Results which have been returned have indicated that sensitivity of the task may need to be edited in order to provide a more accurate measure of threshold. Embedded figure task was based on stimuli and parameters used in the Leuven Perceptual organisation screening test (L-POST; Vancleef et al, 2014) and L-EFT. Reliability and validity for these measures are high in sensitivity in a large healthy control cohort. Older adults demonstrated longer reaction times yet more variable performance in accuracy, which has been previously demonstrated in cognitive functioning in older adults (Hultsch, MacDonald & Dixon, 2002). Normative scores for the database images used in the object in scene task did appear to be higher in reaction time, however task designs differed significantly between the previous published task and the task at present.

Participants gave some unprompted feedback that they felt they may be 'guessing' on the object recognition task, however mean performance was above average. Some amendments may need to be made to this task to increase ease of completion. From observation and feedback during task participation, all task instructions and use of response keypad were clear to all participants. No participants experienced difficulty in completing tasks and needed minimal reminders in performance on computerised tasks.

It was concluded that amendments to the task battery were required, including the omission of visual search, Stroop, object decision and lexical fluency tasks in the interests of time, and the removal of the doors and people task from the main study. Psychophysical staircases in contour integration task and difficulty level in object recognition task need some revision in order to return more accurate results. Generally, performance on other tasks is consistent with previous literature.

Appendix 2 : Metabolite median (SD), variance and range in older and younger adults

| | | ***Younger*** | | | ***Older*** | |
|---|---|---|---|---|---|---|
| ***OCC*** | **Median (SD)** | **Variance** | **Range** | **Median (SD)** | **Variance** | **Range** |
| *GABA* | 4.69 (.48) | .24 | 2.00 | 4.66 (.61) | .367 | 2.22 |
| *Glx* | 13.9 (.87) | .76 | 3.1 | 13.1 (2.01) | 4.05 | 8.4 |
| *NAA* | 17.8 (2.0) | 4.01 | 7.84 | 17.88 (2.28) | 5.23 | 9.55 |
| *Myoinositol* | 10.07 (1.32) | 1.76 | 5.3 | 9.07 (1.91) | 3.66 | 8.21 |
| *Choline* | 1.79 (.19) | .039 | .901 | 1.88 (.28) | .084 | 1.02 |
| *Creatine* | 11.04 (.95) | .914 | 4.82 | 11.38 (1.45) | 2.13 | 5.27 |
| ***ACC*** | | | | | | |
| *GABA* | 4.07 (.29) | .086 | 1.36 | 3.86 (.43) | .19 | 1.95 |
| *Glx* | 15.4 (.87) | .75 | 4.1 | 13.9 (1.75) | 3.1 | 7.6 |
| *NAA* | 14.27 (1.06) | 1.13 | 4.31 | 12.14 (2.42) | 5.88 | 10.98 |
| *Myoinositol* | 10.28 (1.25) | 1.57 | 5.14 | 8.95 (2.35) | 5.54 | 10.77 |
| *Choline* | 2.59 (.255) | .066 | .97 | 2.56 (.44) | .194 | 1.75 |
| *Creatine* | 10.08 (.65) | .429 | 2.75 | 9.40 (1.44) | 2.07 | 4.99 |
| ***PPC*** | | | | | | |
| *GABA* | 4.24 (.35) | .126 | 1.75 | 4.41 (.45) | .202 | 1.68 |
| *Glx* | 14.25 (.94) | .89 | 3.8 | 13.9 (1.49) | 2.24 | 6.4 |
| *NAA* | 16.9 (2.01) | 4.04 | 8.84 | 15.86 (2.34) | 5.5 | 9.77 |
| *Myoinositol* | 10.45 (1.23) | 1.51 | 5.31 | 9.76 (2.25) | 5.06 | 10.21 |
| *Choline* | 2.03 (.23) | .054 | .926 | 2.17 (.37) | .14 | 1.56 |
| *Creatine* | 10.72 (.94) | .89 | 3.83 | 10.6 (1.57) | 2.48 | 6.74 |

Appendix 3 : Tractography metrics median (SD), variance and range in younger and older adults. Fractional anisotropy (FA), mean diffusivity (MD), restricted fraction (FR), radial diffusivity (RD), axial diffusivity (L1)

| | | ***Younger*** | | | ***Older*** | |
|---|---|---|---|---|---|---|
| | **Median (SD)** | **Variance** | **Range** | **Median (SD)** | **Variance** | **Range** |
| *FA in fornix* | .420 (.02) | .00 | .064 | .374 (.026) | .001 | .114 |
| *FA in optic radiation left* | .471 (.035) | .001 | .171 | .460 (.041) | .002 | .187 |
| *FA in optic radiation right* | .478 (.028) | .001 | .112 | .461 (.036) | .001 | .155 |
| *FA in ILF left* | .442 (.021) | .00 | .084 | .425 (.025) | .001 | .099 |
| *FA in ILF right* | .450 (.018) | .00 | .068 | .423 (.023) | .001 | .109 |
| *FA in SLF1 left* | .478 (.046) | .002 | .218 | .425 (.03) | .010 | .127 |
| *FA in SLF1 right* | .448 (.039) | .002 | .171 | .441 (.041) | .002 | .160 |
| *FA in SLF2 left* | .406 (.04) | .002 | .176 | .382 (.028) | .001 | .106 |
| *FA in SLF2 right* | .424 (.039) | .002 | .185 | .399 (.047) | .002 | .237 |
| *FA in SLF3 left* | .451 (.049) | .002 | .257 | .427 (.036) | .001 | .120 |
| *FA in SLF3 right* | .459 (.027) | .001 | .125 | .435 (.028) | .001 | .109 |
| *MD in fornix* | .00092 (.000035) | .000 | .000145 | .0010 (.000071) | .000 | .00024 |
| *MD in optic radiation left* | .00068 (.000027) | .000 | .000011 | .00071 (.000048) | .000 | .00017 |
| *MD in optic radiation right* | .00068 (.000017) | .000 | .000084 | .00071 (.000046) | .000 | .00021 |
| *MD in ILF left* | .00070 (.000014) | .000 | .000070 | .00072 (.000019) | .000 | .000074 |
| *MD in ILF right* | .00070 (.000013) | .000 | .000069 | .00071 (.000021) | .000 | .000098 |
| *MD in SLF1 left* | .00067 (.000012) | .000 | .000042 | .00067 (.000020) | .000 | .000089 |
| *MD in SLF1 right* | .00065 (.000010) | .000 | .000045 | .00066 (.000021) | .000 | .000079 |
| *MD in SLF2 left* | .00066(.000012) | .000 | .000050 | .00067 (.000018) | .000 | .000061 |
| *MD in SLF2 right* | .424 (.039) | .002 | .185 | .3997 (.047) | .002 | .2376 |
| *MD in SLF3 left* | .00065 (.000011) | .000 | .000049 | .00066 (.000021) | .009 | .000084 |
| *MD in SLF3 right* | .00065 (.000010) | .000 | .000045 | .00069 (.000021) | .000 | .000079 |
| *FR in fornix* | .243 (.017) | .000 | .062 | .213 (.018) | .000 | .087 |
| *FR in optic radiation left* | .357 (.03) | .001 | .116 | .338 (.040) | .002 | .175 |
| *FR in optic radiation right* | .369 (.02) | .000 | .098 | .339 (.036) | .001 | .144 |
| *FR in ILF left* | .317 (.016) | .000 | .060 | .312 (.02) | .000 | .072 |
| *FR in ILF right* | .325 (.016) | .000 | .064 | .314 (.021) | .000 | .103 |
| *FR in SLF1 left* | .395 (.034) | .001 | .146 | .356 (.03) | .001 | .128 |
| *FR in SLF1 right* | .378 (.032) | .001 | .156 | .376 (.033) | .001 | .122 |
| *FR in SLF2 left* | .397 (.023) | .001 | .095 | .372 (.022) | .001 | .083 |
| *FR in SLF2 right* | .403 (.020) | .000 | .082 | .381 (.045) | .002 | .229 |
| *FR in SLF3 left* | .398 (.031) | .001 | .124 | .375 (.029) | .001 | .107 |
| *FR in SLF3 right* | .415 (.019) | .000 | .076 | .00077 (.029) | .001 | .120 |
| *RD in the fornix* | .00068 (.000034) | .000 | .00013 | .00074 (.000066) | .000 | .00022 |
| *RD in optic radiation left* | .00049 (.000026) | .000 | .00012 | .00052 (.000035) | .000 | .00020 |

| | | | | | | |
|---|---|---|---|---|---|---|
| *RD in optic radiation right* | .00048 (.000018) | .000 | .000068 | .000514 (.000035) | .000 | .00012 |
| *RD in ILF left* | .000052 (.000016) | .000 | .000064 | .000538 (.000021) | .000 | .000075 |
| *RD in ILF right* | .000051 (.000015) | .000 | .000067 | .000529 (.000021) | .000 | .000077 |
| *RD in SLF1 left* | .000048 (.000029) | .000 | .00013 | .000518 (.000027) | .000 | .00011 |
| *RD in SLF1 right* | .00050 (.000028) | .000 | .00011 | .00051 (.000034) | .000 | .00012 |
| *RD in the SLF2 left* | .00051 (.000024) | .000 | .000097 | .00053 (.000020) | .000 | .000072 |
| *RD in the SLF2 right* | .00049 (.000023) | .000 | .000098 | .00051 (.000025) | .000 | .000086 |
| *RD in SLF3 left* | .00048 (.000028) | .006 | .00014 | .00052 (.000030) | .000 | .00011 |
| *RD in SLF3 right* | .00048 (.000018) | .000 | .000078 | .00051 (.000025) | .000 | .00010 |
| *L1 in the fornix* | .0014 (.000043) | .000 | .00017 | .0015 (.000089) | .000 | .000424 |
| *L1 in optic radiation left* | .0010 (.00006) | .000 | .00028 | .0011 (.000084) | .000 | .000367 |
| *L1 in optic radiation right* | .0011 (.000047) | .000 | .00019 | .0011 (.000086) | .000 | .0000405 |
| *L1 in ILF left* | .0011 (.000032) | .000 | .00013 | .0011 (.000042) | .000 | .00014 |
| *L1 in ILF right* | .0011 (.000028) | .000 | .00014 | .0010 (.000038) | .000 | .000015 |
| *L1 in SLF1 left* | .0010 (.000037) | .000 | .00017 | .0010 (.000030) | .000 | .000132 |
| *L1 in SLF1 right* | .001 (.000030) | .000 | .00011 | .0010 (.000025) | .000 | .000096 |
| *L1 in SLF2 left* | .00096 (.000033) | .000 | .00014 | .00095 (.000037) | .000 | .000168 |
| *L1 in SLF2 right* | .00098 (.000042) | .000 | .00021 | .00097 (.000046) | .000 | .00022 |
| *L1 in SLF3 left* | .00099 (.000041) | .000 | .00097 | .00099 (.000026) | .000 | .00010 |
| *L1 in SLF3 right* | .0010 (.000019) | .000 | .000076 | .00099 (.000026) | .000 | .000095 |

## Appendix 4 : Correlations between microstructure and metabolites

Summary tables for correlation matrix assessing relationships between all microstructural measurements and metabolites. Tables show p-values for correlation matrix (yellow highlighted = p<.001) and are presented by microstructural measurement separately. Cohen's d for group comparison effect size for each microstructural measurement are also show. High Cohen's D (>0.8) are highlighted in green.

| | fa_fornix | fa_opradleft | fa_opradright | fa_ilfleft | fa_ilfright | fa_slf1left | fa_slf1right | fa_slf2left | fa_slf2right | fa_slf3left | fa_slf3right |
|---|---|---|---|---|---|---|---|---|---|---|---|
| occ_gaba | 0.476450844 | 0.51326082 | 0.40888279 | 0.11355798 | 0.60270634 | 0.33617971 | 0.88595548 | 0.70594825 | 0.85792615 | 0.5369486 | 0.50299503 |
| occ_glx | 0.646961271 | 0.97609033 | 0.64779383 | 0.06710934 | 0.64672737 | 0.83459006 | 0.66278103 | 0.91300727 | 0.87861661 | 0.33502288 | 0.73824506 |
| occ_naa | 0.017512843 | 0.04592118 | 0.04207143 | 0.04322817 | 0.01202102 | 0.5963253 | 0.31467601 | 0.8302054 | 0.09125682 | 0.66530923 | 0.01868965 |
| occ_ins | 0.006646422 | 0.55040496 | 0.48800326 | 0.59311615 | 0.26770162 | 0.27339989 | 0.63070065 | 0.41640423 | 0.88660458 | 0.74370209 | 0.67650153 |
| occ_cho | 0.169967932 | 0.1782835 | 0.24156725 | 0.75817809 | 0.10590821 | 0.75479709 | 0.59246087 | 0.74112814 | 0.8292856 | 0.42471247 | 0.59342593 |
| occ_cr | 0.007664018 | 0.13349186 | 0.06318129 | 0.20426975 | 0.02679409 | 0.83954776 | 0.13025756 | 0.92380289 | 0.94099342 | 0.6259285 | 0.72516151 |
| acc_gaba | 0.196585949 | 0.58956167 | 0.51438363 | 0.11401159 | 0.54740381 | 0.47682449 | 0.75908265 | 0.05380281 | 0.6649962 | 0.17694007 | 0.75978759 |
| acc_glx | 0.008495729 | 0.45295765 | 0.51661174 | 0.70814969 | 0.71513142 | 0.1400697 | 0.34355981 | 0.30316367 | 0.5432505 | 0.9677311 | 0.23175769 |
| acc_naa | 0.000203239 | 0.18332386 | 0.87764541 | 0.74210637 | 0.20511925 | 0.00954413 | 0.07800078 | 0.02708926 | 0.72880717 | 0.24199114 | 0.24484117 |
| acc_ins | 0.065124326 | 0.59083863 | 0.71820785 | 0.69564262 | 0.93973858 | 0.02126835 | 0.00369699 | 0.44218537 | 0.32442501 | 0.4421295 | 0.98767733 |
| acc_cho | 0.013700034 | 0.83059133 | 0.77336794 | 0.33244077 | 0.93955644 | 0.24608808 | 0.06785869 | 0.80610595 | 0.53539004 | 0.61067572 | 0.481992 |
| acc_cr | 0.000254623 | 0.5856093 | 0.55646652 | 0.3781283 | 0.47661655 | 0.08050484 | 0.05941842 | 0.22849535 | 0.48225537 | 0.80703612 | 0.90657657 |
| ppc_gaba | 0.45614706 | 0.07345773 | 0.52420834 | 0.00081792 | 0.26476745 | 0.40938591 | 0.21890115 | 0.1370424 | 0.04119919 | 0.06745217 | 0.00417074 |
| ppc_glx | 0.05078095 | 0.3374423 | 0.26622124 | 0.53890549 | 0.47241427 | 0.1242116 | 0.28942445 | 0.32993514 | 0.63839357 | 0.28564769 | 0.77188815 |
| ppc_naa | 0.007380141 | 0.03007923 | 0.70496739 | 0.49751334 | 0.09159021 | 0.06206169 | 0.31507823 | 0.11236415 | 0.02723691 | 0.59053422 | 0.08753372 |
| ppc_ins | 0.130511621 | 0.95534121 | 0.43604297 | 0.94019424 | 0.33027904 | 0.06433416 | 0.07303054 | 0.54791837 | 0.66094631 | 0.76859413 | 0.60806988 |
| ppc_cho | 0.287398622 | 0.28302248 | 0.90222699 | 0.41734936 | 0.64664435 | 0.5563791 | 0.71878915 | 0.94511652 | 0.327987 | 0.15391756 | 0.63147035 |
| ppc_cr | 0.05023945 | 0.12727704 | 0.87461463 | 0.97957239 | 0.15612309 | 0.24489413 | 0.11257302 | 0.28513583 | 0.301658 | 0.55724826 | 0.74910712 |
| Cohens D (groups) | 2.261386148 | 0.47237854 | 0.58786615 | 0.73264091 | 1.02060948 | 1.15929675 | 0.5254282 | 0.80259289 | 0.62804434 | 0.41353288 | 0.96718536 |

| | md_fornix | md_opradleft | md_opradright | md_ilfleft | md_ilfright | md_slf1left | md_slf1right | md_slf2left | md_slf2right | md_slf3left | md_slf3right |
|---|---|---|---|---|---|---|---|---|---|---|---|
| occ_gaba | 0.2330095 | 0.89652619 | 0.94376359 | 0.59308424 | 0.66604028 | 0.34021975 | 0.99375962 | 0.50872663 | 0.85792615 | 0.68430236 | 0.99375962 |
| occ_glx | 0.223638724 | 0.87529822 | 0.4826847 | 0.88734245 | 0.27465394 | 0.64959936 | 0.72476145 | 0.89165273 | 0.87861661 | 0.24377567 | 0.72476145 |
| occ_naa | 0.406600704 | 0.84505807 | 0.28058832 | 0.1506031 | 0.13137946 | 0.2714609 | 0.24314949 | 0.94248102 | 0.09125682 | 0.52662654 | 0.24314949 |
| occ_ins | 0.000931608 | 0.45716281 | 0.11946297 | 0.25039885 | 0.29006258 | 0.15665271 | 0.82509632 | 0.32579845 | 0.88660458 | 0.60804195 | 0.82509632 |
| occ_cho | 0.196974347 | 0.04196536 | 0.10304585 | 0.79129728 | 0.85284893 | 0.73365434 | 0.52580997 | 0.4314451 | 0.8292856 | 0.5736463 | 0.52580997 |
| occ_cr | 0.00234858 | 0.97579762 | 0.73414197 | 0.16133933 | 0.31057976 | 0.41539876 | 0.45137032 | 0.55174503 | 0.94099342 | 0.79719369 | 0.45137032 |
| acc_gaba | 0.002597338 | 0.34716275 | 0.03412316 | 0.27770126 | 0.53350365 | 0.99801623 | 0.83996819 | 0.27266894 | 0.6649962 | 0.8721047 | 0.83996819 |
| acc_glx | <.001 | 0.12684641 | 0.07470999 | 0.12688663 | 0.49137202 | 0.10947627 | 0.05277431 | 0.04171314 | 0.5432505 | 0.31059528 | 0.05277431 |
| acc_naa | <.001 | 0.01119641 | <.001 | 0.00803583 | 0.02700928 | 0.02335938 | 0.00507655 | 0.00148302 | 0.72880717 | 0.00789525 | 0.00507655 |
| acc_ins | 0.003248751 | 0.01669909 | 0.00342526 | 0.16935571 | 0.26037911 | 0.22403428 | 0.17543681 | 0.02483509 | 0.32442501 | 0.07395418 | 0.17543681 |
| acc_cho | <.001 | 0.0893619 | 0.01862187 | 0.12628494 | 0.45780879 | 0.22263998 | 0.13140215 | 0.07383907 | 0.53539004 | 0.08110772 | 0.13140215 |
| acc_cr | <.001 | 0.01180274 | 0.00147519 | 0.00723127 | 0.2283108 | 0.07122531 | 0.03287715 | 0.00481118 | 0.48225537 | 0.05840479 | 0.03287715 |
| ppc_gaba | 0.619179367 | 0.56022976 | 0.545589 | 0.12422306 | 0.0238933 | 0.29061278 | 0.0458358 | 0.35925725 | 0.04119919 | 0.1061944 | 0.0458358 |
| ppc_glx | 0.006196597 | 0.30545899 | 0.41650659 | 0.57376287 | 0.63251791 | 0.18244314 | 0.63823962 | 0.34817631 | 0.63839357 | 0.54399992 | 0.63823962 |
| ppc_naa | 0.003707494 | 0.06227752 | 0.06650875 | 0.78502016 | 0.24132508 | 0.01818512 | 0.10726462 | 0.04416878 | 0.02723691 | 0.08930572 | 0.10726462 |
| ppc_ins | 0.032801274 | 0.06720421 | 0.00167226 | 0.53420864 | 0.70390182 | 0.2975535 | 0.84698625 | 0.15504649 | 0.66094631 | 0.49071941 | 0.84698625 |
| ppc_cho | 0.161053977 | 0.85749407 | 0.81089396 | 0.40542244 | 0.73507127 | 0.33182323 | 0.59042724 | 0.85600902 | 0.327987 | 0.93636713 | 0.59042724 |
| ppc_cr | 0.002796033 | 0.60693472 | 0.24953975 | 0.80145684 | 0.75813052 | 0.18373126 | 0.87003865 | 0.34939715 | 0.301658 | 0.75833865 | 0.87003865 |
| cohens d (groups) | 1.747776601 | 0.69840069 | 0.63912175 | 0.61398136 | 0.74728956 | 0.72565208 | 0.93627607 | 0.76074132 | 0.62804434 | 0.7955152 | 0.93627607 |

| | fr_fornix | fr_opradleft | fr_opradright | fr_ilfleft | fr_ilfright | fr_slf1left | fr_slf1right | fr_slf2left | fr_slf2right | fr_slf3left | fr_slf3right |
|---|---|---|---|---|---|---|---|---|---|---|---|
| occ_gaba | 0.595964101 | 0.62817732 | 0.8732707 | 0.93812309 | 0.54556094 | 0.33341643 | 0.58748557 | 0.09544905 | 0.46808135 | 0.70297937 | 0.78293 |
| occ_glx | 0.305337129 | 0.58875486 | 0.60792534 | 0.38249223 | 0.4039074 | 0.91390475 | 0.78396479 | 0.86147934 | 0.5700742 | 0.43483332 | 0.93300866 |
| occ_naa | 0.018391074 | 0.12864853 | 0.06649088 | 0.00129327 | 0.0007996 | 0.09549993 | 0.23036503 | 0.08406071 | 0.0091961 | 0.03638907 | 0.00210819 |
| occ_ins | 0.002979774 | 0.38944437 | 0.40554874 | 0.51785803 | 0.14098316 | 0.22805911 | 0.39792951 | 0.21849841 | 0.42405101 | 0.26225729 | 0.19783479 |
| occ_cho | 0.152640333 | 0.75903943 | 0.74005193 | 0.0547979 | 0.31788924 | 0.76256503 | 0.25623845 | 0.32118847 | 0.53130932 | 0.56812313 | 0.34103309 |
| occ_cr | 0.007986591 | 0.3519029 | 0.12011738 | 0.00094525 | 0.059262 | 0.42924183 | 0.06348074 | 0.05952902 | 0.24718135 | 0.43166578 | 0.11646562 |
| acc_gaba | 0.262163292 | 0.96245309 | 0.54158427 | 0.81970458 | 0.82790096 | 0.83859747 | 0.88969809 | 0.25988408 | 0.94149369 | 0.35561061 | 0.66848934 |
| acc_glx | 0.004383229 | 0.69837801 | 0.73475579 | 0.31789554 | 0.54032994 | 0.31049753 | 0.49037649 | 0.22222392 | 0.6816295 | 0.57987649 | 0.13050097 |
| acc_naa | 0.000352816 | 0.02852236 | 0.0197969 | 0.21187146 | 0.05177788 | 0.00041197 | 0.08169641 | 0.00043792 | 0.15340498 | 0.0261495 | 0.01143976 |
| acc_ins | 0.05556035 | 0.06747451 | 0.28045781 | 0.43532232 | 0.57359223 | 0.03407516 | 0.00107949 | 0.00157592 | 0.56441457 | 0.03643936 | 0.1284691 |
| acc_cho | 0.011891387 | 0.20269781 | 0.27157492 | 0.25819146 | 0.53472538 | 0.11823247 | 0.02282459 | 0.0311628 | 0.58282516 | 0.0616461 | 0.06582765 |
| acc_cr | 0.000472317 | 0.08479629 | 0.09697333 | 0.24823465 | 0.28324837 | 0.08086012 | 0.03649333 | 0.01165314 | 0.50482812 | 0.1565195 | 0.07450509 |
| ppc_gaba | 0.534675413 | 0.13398652 | 0.48226833 | 0.13869177 | 0.35783987 | 0.28389587 | 0.23648618 | 0.66513312 | 0.04348394 | 0.40625263 | 0.02035184 |
| ppc_glx | 0.033399745 | 0.94419139 | 0.51083171 | 0.84497031 | 0.66302836 | 0.33663163 | 0.39458521 | 0.40791442 | 0.70927646 | 0.56797029 | 0.55230878 |
| ppc_naa | 0.010478175 | 0.03561071 | 0.13483678 | 0.14941562 | 0.02152425 | 0.00060264 | 0.15381478 | 0.00041541 | 0.31278037 | 0.21959556 | 0.14130874 |
| ppc_ins | 0.161469848 | 0.19906448 | 0.21390172 | 0.79623313 | 0.35642761 | 0.19414926 | 0.00060096 | 0.0805174 | 0.67314568 | 0.25559743 | 0.86084616 |
| ppc_cho | 0.36457375 | 0.5299742 | 0.92478863 | 0.91462155 | 0.44322547 | 0.52583147 | 0.28865739 | 0.70888618 | 0.88685765 | 0.74508592 | 0.81857768 |
| ppc_cr | 0.166619592 | 0.30070716 | 0.36410027 | 0.98641961 | 0.43210387 | 0.54759304 | 0.06768787 | 0.34161731 | 0.78905366 | 0.83531986 | 0.98501811 |
| cohens d (groups) | 1.720671911 | 0.6723105 | 1.00095853 | 0.84648688 | 0.7857896 | 0.95797774 | 0.34325197 | 0.91861324 | 0.84163031 | 0.86328755 | 0.98110461 |

| | rd_fornix | rd_opradleft | rd_opradright | rd_ilfleft | rd_ilfright | rd_slf1left | rd_slf1right | rd_slf2left | rd_slf2right | rd_slf3left | rd_slf3right |
|---|---|---|---|---|---|---|---|---|---|---|---|
| occ_gaba | 0.229856167 | 0.60719599 | 0.64318401 | 0.402021 | 0.53148504 | 0.2692682 | 0.67239003 | 0.57034733 | 0.65265504 | 0.49446365 | 0.58783858 |
| occ_glx | 0.27932318 | 0.81227042 | 0.61653793 | 0.22381977 | 0.30198042 | 0.70124007 | 0.50231133 | 0.78869529 | 0.55825165 | 0.30200754 | 0.63062812 |
| occ_naa | 0.14481492 | 0.1264395 | 0.88097071 | 0.03237273 | 0.02305226 | 0.55876923 | 0.13294968 | 0.97841067 | 0.40183601 | 0.62273647 | 0.0697143 |
| occ_ins | 0.000628512 | 0.31258755 | 0.43073532 | 0.29670483 | 0.19956412 | 0.15220124 | 0.26882511 | 0.13529146 | 0.47343317 | 0.74326247 | 0.78351568 |
| occ_cho | 0.133997091 | 0.5146873 | 0.39160242 | 0.8845229 | 0.30089426 | 0.73708378 | 0.28463369 | 0.67588619 | 0.31562293 | 0.44967172 | 0.94137589 |
| occ_cr | 0.001051394 | 0.30795584 | 0.56060356 | 0.10224174 | 0.04818502 | 0.63925936 | 0.09192669 | 0.74103537 | 0.90789694 | 0.94872416 | 0.59753281 |
| acc_gaba | 0.009056299 | 0.59341483 | 0.12193535 | 0.61173093 | 0.95669285 | 0.48394771 | 0.69585188 | 0.07490515 | 0.28016241 | 0.57218983 | 0.87803785 |
| acc_glx | 4.3023E-05 | 0.07301776 | 0.02945346 | 0.52184269 | 0.52025245 | 0.05185893 | 0.34168301 | 0.04820095 | 0.50656333 | 0.42393238 | 0.0520301 |
| acc_naa | 7.4546E-07 | 0.00590976 | 0.00019 | 0.07265448 | 0.04695544 | 0.00404722 | 0.06670056 | 0.00068923 | 0.02262125 | 0.01504445 | 0.01362768 |
| acc_ins | 0.005235459 | 0.14209581 | 0.00732346 | 0.4638651 | 0.41996086 | 0.02053893 | 0.0021552 | 0.04738349 | 0.27271759 | 0.12776877 | 0.32392444 |
| acc_cho | 0.002098304 | 0.14763496 | 0.01258941 | 0.72835842 | 0.6026061 | 0.1286813 | 0.00645844 | 0.20705082 | 0.19124327 | 0.1608433 | 0.16147386 |
| acc_cr | 1.54632E-09 | 0.02177674 | 0.00080083 | 0.30082698 | 0.21675066 | 0.02601979 | 0.03046448 | 0.01758223 | 0.18014892 | 0.28126974 | 0.14564074 |
| ppc_gaba | 0.819993838 | 0.17702089 | 0.87902802 | 0.00144999 | 0.04933586 | 0.32535288 | 0.57302228 | 0.11768239 | 0.08719645 | 0.10311793 | 0.01327492 |
| ppc_glx | 0.007008281 | 0.14418543 | 0.1710456 | 0.88577203 | 0.90675236 | 0.08098376 | 0.17357096 | 0.18258633 | 0.55511779 | 0.51088077 | 0.53011916 |
| ppc_naa | 0.00225877 | 0.00818769 | 0.06674626 | 0.55287069 | 0.07426082 | 0.02531911 | 0.02572119 | 0.01957961 | 0.00037861 | 0.17004867 | 0.0328495 |
| ppc_ins | 0.042357575 | 0.18988349 | 0.02104984 | 0.89607155 | 0.33779633 | 0.07208565 | 0.00809438 | 0.13282344 | 0.30463953 | 0.46002496 | 0.88324006 |
| ppc_cho | 0.151400965 | 0.46985557 | 0.91803392 | 0.29305185 | 0.95720461 | 0.39607299 | 0.08373372 | 0.81019761 | 0.20949155 | 0.40190253 | 0.63723758 |
| ppc_cr | 0.003863835 | 0.21348101 | 0.24563627 | 0.85805027 | 0.44210594 | 0.13467298 | 0.02016948 | 0.14516935 | 0.05730818 | 0.95328305 | 0.89061687 |
| | | | | | | | | | | | |
| cohens d (groups) | 0.541926262 | 0.58797599 | 0.32644822 | 0.86592905 | 0.6714299 | 1.18439343 | 0.43381336 | 1.07589258 | 0.77566175 | 0.72263315 | 1.17840852 |

| | L1_fornix | L1_opradleft | L1_opradright | L1_ilfleft | L1_ilfright | L1_slf1left | L1_slf1right | L1_slf2left | L1_slf2right | L1_slf3left | L1_slf3right |
|---|---|---|---|---|---|---|---|---|---|---|---|
| occ_gaba | 0.322856092 | 0.72121596 | 0.62337596 | 0.25624807 | 0.9952084 | 0.57952039 | 0.87976474 | 0.91843326 | 0.61747414 | 0.56181642 | 0.187441 |
| occ_glx | 0.23218017 | 0.86184561 | 0.38976928 | 0.09791287 | 0.63631482 | 0.67141303 | 0.54450048 | 0.87251797 | 0.27126131 | 0.90471017 | 0.86346489 |
| occ_naa | 0.222689514 | 0.31172056 | 0.08641003 | 0.77011372 | 0.92145116 | 0.30475259 | 0.61992414 | 0.68451212 | 0.09381943 | 0.82407704 | 0.42004859 |
| occ_ins | 0.035084756 | 0.65485582 | 0.05711188 | 0.24276331 | 0.42633034 | 0.75982673 | 0.21604696 | 0.85227115 | 0.23507148 | 0.68161944 | 0.58717813 |
| occ_cho | 0.907800462 | 0.01069977 | 0.0580139 | 0.99996338 | 0.49373291 | 0.46483957 | 0.41770469 | 0.92350916 | 0.92329466 | 0.61250001 | 0.49341209 |
| occ_cr | 0.079953464 | 0.34958323 | 0.29126663 | 0.82595013 | 0.68620787 | 0.4243308 | 0.79590699 | 0.45741688 | 0.72405945 | 0.5746189 | 0.27283396 |
| acc_gaba | 0.004006335 | 0.23052379 | 0.03472288 | 0.04041298 | 0.17734592 | 0.54243802 | 0.57881066 | 0.5743846 | 0.90967226 | 0.38754564 | 0.49421215 |
| acc_glx | 0.000173372 | 0.33963959 | 0.37756833 | 0.04604551 | 0.44475389 | 0.761212 | 0.14608031 | 0.50744338 | 0.64526005 | 0.69025501 | 0.47505061 |
| acc_naa | 0.000108695 | 0.14454684 | 0.00104541 | 0.01216362 | 0.08885939 | 0.23759748 | 0.43817704 | 0.99275536 | 0.15168653 | 0.95853788 | 0.07793777 |
| acc_ins | 0.016383162 | 0.00881473 | 0.01840935 | 0.05578881 | 0.21380528 | 0.0687082 | 0.28710988 | 0.53483171 | 0.00934699 | 0.84538522 | 0.12360522 |
| acc_cho | 0.003610694 | 0.15891914 | 0.09565603 | 0.01361395 | 0.29734964 | 0.71478793 | 0.27129526 | 0.2963518 | 0.02496243 | 0.75652429 | 0.23217976 |
| acc_cr | 1.83565E-07 | 0.05356055 | 0.0248658 | 0.00153539 | 0.2674596 | 0.52589944 | 0.28899227 | 0.34148431 | 0.01740248 | 0.2543909 | 0.00701472 |
| ppc_gaba | 0.485323007 | 0.60036719 | 0.41678827 | 0.41452955 | 0.19527945 | 0.57570928 | 0.37183887 | 0.23034259 | 0.18325837 | 0.70240175 | 0.4291193 |
| ppc_glx | 0.016403829 | 0.61022269 | 0.86720395 | 0.27159292 | 0.38088671 | 0.64067086 | 0.60683613 | 0.98664809 | 0.09941976 | 0.63988419 | 0.66618063 |
| ppc_naa | 0.053507648 | 0.57633247 | 0.22465723 | 0.97294202 | 0.94792214 | 0.92186152 | 0.49177531 | 0.90447718 | 0.20661744 | 0.68403149 | 0.36790688 |
| ppc_ins | 0.112607485 | 0.05950844 | 0.00290026 | 0.94322907 | 0.72410626 | 0.23401655 | 0.78525599 | 0.83338068 | 0.10711529 | 0.91407519 | 0.71059076 |
| ppc_cho | 0.419661577 | 0.68192219 | 0.74574295 | 0.77430107 | 0.58995682 | 0.82027713 | 0.58866385 | 0.894465 | 0.53261933 | 0.1556616 | 0.96264979 |
| ppc_cr | 0.021150795 | 0.76117262 | 0.46416458 | 0.83028808 | 0.18525984 | 0.8707021 | 0.97527242 | 0.73781023 | 0.58129881 | 0.58936467 | 0.82541629 |
| cohens d (groups) | 0.486229363 | 0.52772958 | 0.50996743 | 0.11566688 | 0.07126419 | 0.78177356 | 0.60921009 | 0.28792327 | 0.23981538 | 0.58288214 | 0.17037902 |

## Appendix 5 : Grey matter and cortical thickness values for healthy adults

Grey matter volume median (SD), variance and range for younger and older adults

| | | ***Younger*** | | | ***Older*** | |
|---|---|---|---|---|---|---|
| | **Median (SD)** | **Variance** | **Range** | **Median (SD)** | **Variance** | **Range** |
| *Left lateral ventricle* | 6121.65(2562.55) | 6566680 | 8866 | 12430.2(8229.57) | 67725838.7 | 32131.9 |
| *Left inferior lateral ventricle* | 339.9(179.52) | 32229.14 | 841.4 | 438.4 (297.05) | 297.05 | 88239.78 |
| *Left cerebellum WM* | 15555.1(1171.62) | 1372697.5 | 6385.5 | 14543.2 (2891.01) | 2891.09 | 8357935.3 |
| *Left cerebellum* | 57427.5 (4975.4) | 24754612.8 | 21460 | 50210.2 (5431.05) | 29496345.6 | 20941.3 |
| *Left thalamus* | 7547.2 (766.28) | 587191.87 | 2925.6 | 6641.3 (573.87) | 329335.11 | 2504.3 |
| *Left caudate* | 3702.9 (383.906) | 147383.89 | 1698.9 | 3450.9 (486.69) | 236868.97 | 2332.3 |
| *Left putamen* | 5264.25 (501.38) | 251385.76 | 2074.3 | 4472.8 (822.13) | 675903.65 | 4252.9 |
| *Left pallidum* | 2025.9 (218.497) | 47741.23 | 911 | 2049.6 (273.17) | 74622.13 | 1803.6 |
| *Left hippocampus* | 1738.85(211.514) | 44738.34 | 1452.9 | 3826.5 (334.33) | 111776.28 | 1439.4 |
| *Left amygdala* | 1738.85 (211.51) | 44738.34 | 974.9 | 1548.5 (166.58) | 27744.69 | 633.7 |
| *Left accumbens* | 537.8 (103.39) | 10689.55 | 510 | 466.7 (66.73) | 4453.86 | 259.5 |
| *Left choroid plexus* | 377.65 (138.79) | 19265.11 | 546.5 | 682.2 (264.06) | 69725.88 | 1077.4 |
| *Right lateral ventricle* | 4752.05 (2674.69) | 7153990.88 | 9603.9 | 12020.6 (6762.24) | 45728001.9 | 25945.3 |
| *Right inferior lateral ventricle* | 295.65 (136.48) | 18626.89 | 622.9 | 391.9 (334.19) | 111687.43 | 1531 |
| *Right cerebellum WM* | 14800.95 (1299.26) | 1688081.89 | 7130.3 | 13481.7 (2075.95) | 4309578.42 | 9174.1 |
| *Right cerebellum* | 58028 (4913.61) | 24143515.6 | 21814 | 51590.5 (5600.07) | 31360823.4 | 19879.9 |
| *Right thalamus* | 7483.05 (792.56) | 628154.97 | 3251.3 | 6525.1 (573.69) | 329124.92 | 2459.2 |
| *Right caudate* | 3855.25 (409.49) | 167687.5 | 1959.4 | 3489.7 (553.85) | 306755.35 | 2300.8 |
| *Right putamen* | 5158.7 (587.26) | 344876.56 | 2219.5 | 4636 (805.19) | 648343.32 | 4216.2 |
| *Right pallidum* | 1905.8 (196.35) | 38554.09 | 931.1 | 1948.2 (290.32) | 84286.79 | 1405 |
| *Right hippocampus* | 4131.35 (395.55) | 156459.6 | 1309.4 | 3956 (341.07) | 116331.91 | 1277.9 |
| *Right amygdala* | 1765 (187.61) | 35199.25 | 654.2 | 1704.3 (165.44) | 27370.881 | 670.6 |
| *Right accumbens* | 611.150(119.49) | 14277.82 | 520.8 | 524.9 (72.01) | 5186.05 | 291.4 |
| *Right choroid plexus* | 433.65(151.72) | 23017.86 | 537.9 | 649.8 (189.04) | 35737.33 | 670.8 |
| *WM hypointensities* | 640.95 (343.08) | 117708.44 | 1408.3 | 2211 (6253.46) | 39105869.9 | 27942.2 |
| *Optic chiasm* | 182.35 (44.32) | 1964.32 | 172.8 | 196.8 (36.71) | 1347.71 | 150.5 |
| *Posterior cortex vol* | 912.5 (99.77) | 9953.83 | 399.6 | 1015.9 (152.02) | 23110.13 | 617.4 |
| *Mid posterior cortex vol* | 521.9 (73.88) | 5458.93 | 276.4 | 499 (92.09) | 8480.87 | 340.6 |
| *Central cortex vol* | 633.05 (115.05) | 13237.89 | 523.2 | 433.6 (105.44) | 11119.2 | 397.3 |

| | | | | | | |
|---|---|---|---|---|---|---|
| *Mid anterior cortex vol* | 529.4 (147.72) | 21821.68 | 538.3 | 448.1 (127.44) | 16239.82 | 516.7 |
| *Anterior cortex vol* | 929.15 (123.96) | 15367.02 | 502.2 | 851.2 (146.26) | 21392.43 | 495.5 |
| *Total Gray vol* | 680829.56(63334.9) | 401180.9 | 242316.11 | 624623.04 (53582.12) | 28714.99 | 176868.15 |

Cortical thickness median (SD), variance and range for younger and older adults

| | ***Younger*** | | | ***Older*** | | |
|---|---|---|---|---|---|---|
| | **Median (SD)** | **Variance** | **Range** | **Median (SD)** | **Variance** | **Range** |
| *Left bank superior temporal sulcus* | 2.65 (.13) | .02 | .516 | 2.46 (.11) | .011 | .461 |
| *Left caudal anterior cingulate* | 2.8 (.21) | .04 | .914 | 2.6 (.23) | .053 | .968 |
| *Left caudal middle frontal* | 2.7 (.17) | .029 | 1.01 | 2.52 (.12) | .014 | .457 |
| *Left cuneus* | 2.08 | .31 | 2.01 | 1.95 (.12) | .015 | .491 |
| *Left entorhinal* | 3.38 (.23) | .05 | 1.08 | 3.28 (.34) | .116 | 1.66 |
| *Left fusiform* | 2.79 (.12) | .015 | .642 | 2.67 (.11) | .010 | .474 |
| *Left inferior parietal* | 2.56 (.11) | .011 | .530 | 2.39 (.08) | .007 | .305 |
| *Left inferior temporal* | 2.77 (.14) | .02 | .75 | 2.66 (.14) | .021 | .74 |
| *Left isthmuscingulate* | 2.43 (.11) | .013 | .507 | 2.18 (.21) | .04 | .79 |
| *Left lateral occipital* | 2.28 (.11) | .013 | .595 | 2.20 (.11) | .01 | .47 |
| *Left lateral orbitofrontal* | 2.72 (.14) | .02 | .697 | 2.56 (.14) | .02 | .75 |
| *Left lingual* | 2.21 (.11) | .012 | .466 | 2.06 (.11) | .01 | .41 |
| *Left medial orbitofrontal* | 2.53 (.12) | .016 | .646 | 2.38 (.09) | .01 | .46 |
| *Left middle temporal* | 2.93 (.11) | .013 | .403 | 2.75 (.14) | .02 | .78 |
| *Left parahippocampal* | 3.01 (.21) | .043 | .86 | 2.75(.27) | .07 | 1.26 |
| *Left paracentral* | 2.53 (.12) | .016 | .475 | 2.45 (0.9) | .008 | .38 |
| *Left parsopercularis* | 2.70 (.09) | .008 | .393 | 2.53(.09) | .009 | .245 |
| *Left parsorbitalis* | 2.81 (.15) | .024 | .573 | 2.60(.17) | .029 | .68 |
| *Left pericalcarine* | 1.88 (.13) | .018 | .569 | 2.41 (.09) | .016 | .528 |
| *Left postcentral thickness* | 2.27 (.11) | .013 | .569 | 2.14 (.09) | .009 | .335 |
| *Left posterior cingulate* | 2.62 (.11) | .011 | .443 | 2.36 (.12) | .015 | .53 |
| *Left precentral* | 2.74 (.12) | .015 | .618 | 2.56 (.12) | .015 | .59 |
| *Left precuneus* | 2.52 (.12) | .015 | .624 | 2.38 (.07) | .07 | .01 |
| *Left rostral ACC* | 2.87 (.17) | .031 | .747 | 2.68 (.18) | .03 | .81 |
| *Left rostral middle frontal* | 2.52 (.11) | .012 | .453 | 2.36 (.06) | .004 | .28 |
| *Left superior frontal* | 2.81 (.15) | .025 | .875 | 2.61 (.11) | .011 | .424 |
| *Left superior parietal* | 2.35 (.16) | .025 | .909 | 2.25 (.07) | .005 | .287 |
| *Left superior temporal* | 2.93 (.12) | .015 | .592 | 2.67 (.14) | .021 | .71 |
| *Left supramarginal* | 2.68(.12) | .014 | .426 | 2.5 (.09) | .01 | .43 |
| *Left frontal pole* | 2.88 (.24) | .059 | 1.28 | 2.64 (.17) | .03 | .846 |
| *Left temporal pole* | 3.48 (.37) | .141 | 1.81 | 3.36 (.48) | .23 | 2.25 |
| *Left transverse temporal* | 2.59 (.17) | .031 | .719 | 2.43 (.16) | .028 | .75 |
| *Left insula* | 2.98 (.15) | .025 | .68 | 2.82 (.17) | .028 | .69 |
| *Left Mean thickness* | 2.60 (.07) | .006 | .31 | 2.44(.06) | .004 | .34. |

| | | | | | | |
|---|---|---|---|---|---|---|
| *Right bank superior temporal sulcus* | 2.67 (.11) | .014 | .389 | 2.51 (.11) | .013 | .445 |
| *Right caudal anterior cingulate* | 2.55 (.18) | .032 | .736 | 2.37 (.201) | .041 | .879 |
| *Right caudal middle frontal* | 2.61 (.11) | .013 | .469 | 2.49 (.109) | .012 | .404 |
| *Right cuneus* | 2.09 (.12) | .016 | .456 | 1.98 (.12) | .013 | .46 |
| *Right entorhinal* | 3.5 (.31) | .098 | 1.29 | 3.4 (.34) | .121 | 1.27 |
| *Right fusiform* | 2.82 (.09) | .010 | .349 | 2.71 (.08) | .008 | .334 |
| *Right inferior parietal* | 2.58 (.11) | .011 | .415 | 2.45 (.10) | .01 | .41 |
| *Right inferior temporal* | 2.82 (.12) | .016 | .487 | 2.63 (.10) | .10 | .36 |
| *Right isthmuscingulate* | 2.48 (.14) | .021 | .552 | 2.30 (.21) | .042 | .96 |
| *Right lateral occipital* | 2.36 (0.7) | .006 | .338 | 2.29 (.10) | .011 | .462 |
| *Right lateral orbitofrontal* | 2.63 (.12) | .017 | .500 | 2.53 (.11) | .012 | .478 |
| *Right lingual* | 2.21 (.11) | .012 | .479 | 2.09 (.08) | .007 | .31 |
| *Right medial orbitofrontal* | 2.53 (0.8) | .007 | .419 | 2.37 (.11) | .01 | .39 |
| *Right middle temporal* | 2.90 (.19) | .015 | .488 | 2.76 (.11) | .01 | .49 |
| *Right parahippocampal* | 2.91 (.19) | .036 | .811 | 2.67 (.22) | .053 | .827 |
| *Right paracentral* | 2.58 (.10) | .010 | .433 | 2.46 (.12) | .014 | .506 |
| *Right parsopercularis* | 2.64 (.11) | .014 | .541 | 2.48 (.10) | .010 | .423 |
| *Right parsorbitalis* | 2.75 (.18) | .033 | .802 | 2.58 (.14) | .021 | .534 |
| *Right pericalcarine* | 1.90 (.11) | .013 | .412 | 2.41 (.07) | .005 | .245 |
| *Right postcentral thickness* | 2.21 (.13) | .016 | .610 | 1.809(.11) | .014 | .532 |
| *Right posterior cingulate* | 2.52 (.11) | .013 | .454 | 2.11 (.11) | .014 | .416 |
| *Right precentral* | 2.65 (.11) | .011 | .474 | 2.32 (.15) | .023 | .615 |
| *Right precuneus* | 2.56 (.09) | .008 | .401 | 2.39(.10) | .012 | .401 |
| *Right rostral ACC* | 2.89 (.17) | .032 | .918 | 2.77 (.19) | .039 | .644 |
| *Right rostral middle frontal* | 2.41 (.09) | .010 | .418 | 2.31 (.06) | .004 | .298 |
| *Right superior frontal* | 2.79 (.12) | .015 | .552 | 2.57 (0.9) | .009 | .411 |
| *Right superior parietal* | 2.36 (.09) | .009 | .33 | 2.25 (.07) | .006 | .357 |
| *Right superior temporal* | 2.92 (0.9) | .009 | .480 | 2.66 (.11) | .012 | .394 |
| *Right supramarginal* | 2.63 (.12) | .014 | .48 | 2.51 (.09) | .009 | .403 |
| *Right frontal pole* | 2.72 (.26) | .071 | 1.104 | 2.66 (.24) | .05 | 1.02 |
| *Right temporal pole* | 3.67 (.31) | .096 | 1.206 | 3.58 (.33) | .11 | 1.53 |
| *Right transverse temporal* | 2.58 (.17) | .029 | .857 | 2.41 (.12) | .015 | .425 |
| *Right insula* | 3.02 (.11) | .011 | .380 | 2.85 (.11) | .014 | .41 |
| *Right Mean thickness* | 2.57 (.08) | .007 | .35 | 2.46 (.05) | .004 | .24 |

## Appendix 6 : DLB patients' metabolites, microstructure, cortical thickness and GM volume and CIs for healthy older controls

Microstructure in DLB and Older adults

| | Left | | | | Right | | | |
|---|---|---|---|---|---|---|---|---|
| | **CI** | **DLB 1** | **DLB 2** | **DLB 3** | **Upper control CI** | **DLB 1** | **DLB 2** | **DLB 3** |
| *FA fornix* | 0.361-0.382 | 0.36 | 0.455 | 0.435 | | | | |
| *FA optic radiations* | 0.434-0.467 | 0.455 | 0.353 | 0.383 | 0.439-0.467 | 0.435 | 0.438 | 0.438 |
| *FA ILF* | 0.440-0.419 | 0.416 | 0.410 | 0.405 | 0.437-0.425 | 0.376 | 0.400 | 0.402 |
| *FA SLF 1* | 0.413-0.437 | 0.464 | 0.401 | 0.431 | 0.412-0.444 | 0.421 | 0.354 | 0.422 |
| *FA SLF 2* | 0.366-0.388 | 0.391 | 0.343 | 0.328 | 0.379-0.416 | 0.426 | 0.342 | 0.334 |
| *FA SLF 3* | 0.414-0.442 | 0.468 | 0.377 | 0.375 | 0.421-0.443 | 0.444 | 0.418 | 0.316 |
| *MD fornix* | 0.00099-0.00105 | 0.00115 | 0.00112 | 0.00114 | | | | |
| *MD optic radiations* | 0.00071-0.00075 | 0.00082 | 0.00073 | 0.00068 | 0.00070-0.00074 | 0.00082 | 0.00075 | 0.00071 |
| *MD ILF* | 0.00071-0.00072 | 0.00075 | 0.00073 | 0.00069 | 0.00070-0.00072 | 0.00073 | 0.00074 | 0.00069 |
| *MD SLF 1* | 0.00067-0.00069 | 0.00066 | 0.00068 | 0.00066 | 0.00066-0.00068 | 0.00068 | 0.00070 | 0.00067 |
| *MD SLF 2* | 0.00066-0.00068 | 0.00066 | 0.00067 | 0.00066 | 0.00063-0.00064 | 0.00063 | 0.00063 | 0.00064 |
| *MD SLF 3* | 0.00066-0.00068 | 0.00067 | 0.00068 | 0.00065 | 0.00066-0.00068 | 0.00068 | 0.00066 | 0.00069 |
| *FR fornix* | 0.20-0.223 | 0.190 | 0.191 | 0.212 | | | | |
| *FR optic radiation* | 0.319-0.351 | 0.309 | 0.288 | 0.367 | 0.321-0.350 | 0.290 | 0.295 | 0.339 |
| *FR ILF* | 0.302-0.318 | 0.277 | 0.283 | 0.331 | 0.301-0.318 | 0.271 | 0.284 | 0.318 |
| *FR SLF 1* | 0.345-0.369 | 0.406 | 0.340 | 0.360 | 0.352-0.378 | 0.365 | 0.308 | 0.360 |
| *FR SLF 2* | 0.366-0.384 | 0.372 | 0.377 | 0.378 | 0.357-0.392 | 0.386 | 0.316 | 0.402 |
| *FR SLF 3* | 0.364-0.387 | 0.389 | 0.322 | 0.247 | 0.376-0.398 | 0.368 | 0.377 | 0.247 |
| *RD fornix* | 0.00076-0.00081 | 0.00090 | 0.00088 | 0.00088 | | | | |
| *RD optic radiation* | 0.00051-0.00055 | 0.00061 | 0.00054 | 0.00050 | 0.00051-0.00053 | 0.00060 | 0.00056 | 0.00053 |
| *RD ILF* | 0.00052-0.00054 | 0.00057 | 0.00055 | 0.00052 | 0.00052-0.00054 | 0.00057 | 0.00057 | 0.00053 |
| *RD SLF 1* | 0.00051-0.00053 | 0.00049 | 0.00053 | 0.00050 | 0.00050-0.00053 | 0.00052 | 0.00057 | 0.00051 |
| *RD SLF 2* | 0.00052-0.00054 | 0.00052 | 0.00055 | 0.00054 | 0.00050-0.00052 | 0.00050 | 0.00054 | 0.00051 |
| *RD SLF 3* | 0.00050-0.00052 | 0.00048 | 0.00055 | 0.00052 | 0.00050-0.00052 | 0.00050 | 0.00051 | 0.00057 |
| *L1 fornix* | 0.000144-0.000151 | 0.000165 | 0.000161 | 0.000168 | | | | |
| *L1 optic radiation* | 0.00110-0.00116 | 0.00126 | 0.00111 | 0.00103 | 0.00108-0.00115 | 0.00124 | 0.00113 | 0.00109 |
| *L1 ILF* | 0.00107-0.00110 | 0.00112 | 0.00109 | 0.00101 | 0.00106-0.00109 | 0.00104 | 0.00109 | 0.00100 |
| *L1 SLF 1* | 0.0009-0.00102 | 0.00100 | 0.00097 | 0.00098 | 0.00099-0.00101 | 0.00100 | 0.00096 | 0.00097 |
| *L1 SLF 2* | 0.00094-0.00097 | 0.00094 | 0.00092 | 0.00088 | 0.00095-0.00099 | 0.00099 | 0.00092 | 0.00090 |
| *L1 SLF 3* | 0.00097-0.00099 | 0.00104 | 0.00096 | 0.00091 | 0.00098-0.0010 | 0.0010 | 0.00096 | 0.00093 |

Metabolites in DLB and Older adults

| | Lower control CI | Upper control CI | DLB 1 | DLB 2 | DLB 3 |
|---|---|---|---|---|---|
| ***OCC*** | | | | | |
| *GABA* | 4.562 | 5.0371 | 4.25 | 4.329 | 5.5 |
| *Glx* | 12.930 | 14.509 | 12.4 | 13.2 | 16 |
| *NAA* | 17.076 | 18.869 | 12.24 | 13.46 | 15.21 |
| *Myoinositol* | 8.412 | 9.911 | 2.287 | 2.11 | 9.242 |
| *Choline* | 1.724 | 1.951 | 1.719 | 1.33 | 1.978 |
| *Creatine* | 10.345 | 11.489 | 9.439 | 9.974 | 9.949 |
| ***ACC*** | | | | | |
| *GABA* | 3.751 | 4.095 | 3.87 | 3.48 | 4.77 |
| *Glx* | 13.68 | 15.054 | 14.2 | 14.8 | 16 |
| *NAA* | 11.235 | 13.136 | 9.89 | 11.24 | 11.17 |
| *Myoinositol* | 8.277 | 10.123 | 2.042 | 3.574 | 9.925 |
| *Choline* | 2.303 | 2.649 | 2.258 | 2.315 | 2.7 |
| *Creatine* | 8.77 | 9.907 | 8.59 | 10.14 | 8.749 |
| ***PPC*** | | | | | |
| *GABA* | 4.261 | 4.614 | 4.9 | 5.06 | 5.02 |
| *Glx* | 13.176 | 14.348 | 14.2 | 12.4 | 18 |
| *NAA* | 14.651 | 16.49 | 16.78 | 11.3 | 12.72 |
| *Myoinositol* | 8.253 | 10.018 | 2.645 | 6.25 | 9.139 |
| *Choline* | 2.007 | 2.301 | 2.541 | 1.76 | 2.224 |
| *Creatine* | 9.649 | 10.886 | 12.41 | 8.127 | 9.86 |

Cortical thickness CI for healthy older adults and DLB patients

| | Left | | | | | Right | | | | |
|---|---|---|---|---|---|---|---|---|---|---|
| | **Lower CI** | **Upper CI** | **DLB 1** | **DLB 2** | **DLB 3** | **Lower CI** | **Upper CI** | **DLB 1** | **DLB 2** | **DLB 3** |
| *Bank STSS* | 2.416 | 5.12342403 | 2.484 | 2.731 | 2.532 | 2.474 | 2.563 | 2.407 | 2.52 | 2.649 |
| *Caudal ACC* | 2.434 | 4.53501549 | 2.341 | 2.652 | 2.87 | 2.278 | 2.436 | 2.564 | 2.64 | 2.257 |
| *Caudal middle frontal* | 2.497 | 4.69753558 | 2.455 | 2.651 | 2.346 | 2.455 | 2.541 | 2.406 | 2.726 | 2.242 |
| *Cuneus* | 1.896 | 3.90988242 | 1.93 | 2.039 | 1.908 | 1.943 | 2.034 | 1.895 | 2.036 | 1.966 |
| *Entorhinal* | 3.174 | 7.3613534 | 3.395 | 3.569 | 3.003 | 3.228 | 3.500 | 3.534 | 3.397 | 4.133 |
| *Fusiform* | 2.644 | 5.4188194 | 2.714 | 2.867 | 2.805 | 2.679 | 2.747 | 2.691 | 2.878 | 2.739 |
| *Inferior parietal* | 2.371 | 4.85597274 | 2.21 | 2.59 | 2.353 | 2.424 | 2.503 | 2.356 | 2.474 | 2.431 |
| *Inferior temporal* | 2.610 | 5.52216429 | 2.473 | 2.829 | 2.678 | 2.633 | 2.712 | 2.579 | 2.716 | 2.889 |
| *Ithmus cingulate* | 2.151 | 4.36754747 | 2.322 | 2.401 | 2.183 | 2.223 | 2.385 | 2.333 | 2.283 | 2.144 |
| *Lateral occipital* | 2.180 | 4.47593286 | 2.036 | 2.32 | 2.188 | 2.252 | 2.3349 | 2.033 | 2.322 | 2.223 |
| *Lateral orbitofrontal* | 2.477 | 5.06238925 | 2.37 | 2.599 | 2.58 | 2.497 | 2.582 | 2.689 | 2.564 | 2.565 |
| *Lingual gyrus* | 2.050 | 4.09978302 | 2.036 | 2.163 | 2.057 | 2.062 | 2.128 | 2.126 | 2.138 | 2.037 |

| | | | | | | | | | | |
|---|---|---|---|---|---|---|---|---|---|---|
| *Medial orbitofrontal* | 2.347 | 5.00440761 | 2.514 | 2.707 | 2.474 | 2.347 | 2.435 | 2.588 | 2.65 | 2.657 |
| *Middle temporal* | 2.680 | 5.51361954 | 2.749 | 2.953 | 2.81 | 2.725 | 2.815 | 2.692 | 2.987 | 2.788 |
| *Parahippocampus* | 2.644 | 5.5399182 | 2.961 | 2.657 | 3.114 | 2.618 | 2.798 | 2.923 | 2.962 | 2.921 |
| *Paracentral* | 2.405 | 4.96518708 | 2.339 | 2.594 | 2.281 | 2.429 | 2.523 | 2.45 | 2.626 | 2.536 |
| *Parsopercularis* | 2.496 | 4.9379576 | 2.496 | 2.712 | 2.535 | 2.468 | 2.548 | 2.517 | 2.572 | 2.469 |
| *Parsorbitalis* | 2.520 | 5.21535179 | 2.507 | 2.624 | 2.63 | 2.520 | 2.633 | 2.328 | 2.612 | 2.695 |
| *Pars triangularis* | 2.382 | 4.75699151 | 2.405 | 2.618 | 2.301 | 2.386 | 2.443 | 2.338 | 2.383 | 2.37 |
| *Pericalcarine* | 1.711 | 3.52211435 | 1.657 | 1.854 | 1.667 | 1.754 | 1.846 | 1.755 | 1.87 | 1.768 |
| *Post central* | 2.123 | 4.18517778 | 2.114 | 2.239 | 2.067 | 2.107 | 2.198 | 2.217 | 2.216 | 2.078 |
| *Posterior cingulate* | 2.311 | 4.7353088 | 2.298 | 2.636 | 2.495 | 2.274 | 2.392 | 2.355 | 2.554 | 2.461 |
| *Precentral* | 2.515 | 4.90380733 | 2.591 | 2.626 | 2.533 | 2.472 | 2.566 | 2.532 | 2.553 | 2.431 |
| *Precuneus* | 2.350 | 4.76350608 | 2.285 | 2.439 | 2.282 | 2.373 | 2.457 | 2.322 | 2.417 | 2.39 |
| *Rostral ACC* | 2.640 | 5.69323881 | 2.698 | 3.133 | 3.115 | 2.696 | 2.850 | 3.01 | 2.882 | 2.997 |
| *Rostral middle frontal* | 2.335 | 4.55251996 | 2.411 | 2.599 | 2.289 | 2.299 | 2.350 | 2.311 | 2.499 | 2.253 |
| *Superior frontal* | 2.576 | 5.16292762 | 2.625 | 2.883 | 2.522 | 2.544 | 2.619 | 2.67 | 2.842 | 2.618 |
| *Superior parietal* | 2.233 | 4.30240286 | 2.128 | 2.404 | 2.203 | 2.213 | 2.274 | 2.106 | 2.271 | 2.089 |
| *Superior temporal* | 2.641 | 5.64898277 | 2.735 | 2.84 | 2.845 | 2.658 | 2.746 | 2.797 | 2.752 | 2.99 |
| *Supramarginal* | 2.463 | 4.94892853 | 2.415 | 2.643 | 2.534 | 2.481 | 2.555 | 2.53 | 2.67 | 2.467 |
| *Frontal pole* | 2.586 | 5.07232206 | 2.813 | 2.677 | 2.619 | 2.603 | 2.792 | 2.621 | 2.807 | 2.469 |
| *Temporal pole* | 3.184 | 7.12445747 | 3.497 | 3.94 | 3.612 | 3.442 | 3.704 | 3.57 | 4.282 | 3.682 |
| *Transverse temporal* | 2.343 | 4.91749383 | 2.322 | 2.54 | 2.225 | 2.388 | 2.484 | 2.34 | 2.419 | 2.529 |
| *Insula* | 2.710 | 5.51453522 | 2.973 | 3.011 | 2.931 | 2.809 | 2.900 | 3.061 | 2.9 | 2.705 |
| *Mean thickness* | 2.427 | 4.87835676 | 2.40228 | 2.60418 | 2.43627 | 2.431 | 2.478 | 2.43141 | 2.53886 | 2.44725 |

Volume values and CIs for healthy older adults and DLB patients

| | Left | | | | | Right | | | | |
|---|---|---|---|---|---|---|---|---|---|---|
| | **Lower CI** | **Upper CI** | **DLB 1** | **DLB 2** | **DLB 3** | **Lower CI** | **Upper CI** | **DLB 1** | **DLB 2** | **DLB 3** |
| *Lateral Ventricle* | 12314.17 | 18766.03 | 11066.2 | 13299.2 | 13301.1 | 11377.98 | 16679.49 | 11569.5 | 9590.3 | 11230.3 |
| *Inferior Lateral Ventricle* | 389.05 | 621.93 | 632.8 | 599.5 | 717.2 | 381.74 | 643.75 | 731.4 | 704.3 | 729.2 |
| *Cerebellum White Matter* | 14029.83 | 16296.34 | 11975.6 | 10505.2 | 10796.7 | 13176.07 | 14803.59 | 11664.5 | 10256.3 | 17328.8 |
| *Cerebellum Cortex* | 48619.31 | 52877.18 | 49729.2 | 48353.9 | 42633.8 | 50137.29 | 54527.66 | 51322.2 | 49109.8 | 39360.1 |
| *Thalamus* | 6490.92 | 6940.83 | 5708.3 | 5463.9 | 6073.9 | 6399.92 | 6849.69 | 5817.8 | 5916.7 | 6241.7 |
| *Caudate* | 3220.44 | 3602.01 | 2879.3 | 2816.8 | 2527 | 3339.56 | 3773.77 | 3134.7 | 2814 | 3038.8 |

| | | | | | | | | | | |
|---|---|---|---|---|---|---|---|---|---|---|
| *Putamen* | 4279.34 | 4923.89 | 3918 | 3750.1 | 4063.4 | 4319.46 | 4950.72 | 3892.9 | 3298.4 | 4154.1 |
| *Pallidum* | 1935.83 | 2149.99 | 1946.7 | 1539.4 | 1691.2 | 1841.19 | 2068.80 | 1816.7 | 1842.9 | 1556 |
| *3rd Ventricle* | 1315.86 | 1786.13 | 2073.4 | 1791.7 | 1804.1 | 3813.44 | 4080.83 | 3502.6 | 3403 | 3656.3 |
| *4th Ventricle* | 1547.69 | 1951.32 | 2590.8 | 1224.1 | 1763.9 | 1613.03 | 1742.73 | 1685.2 | 1450.7 | 1708.3 |
| *Brain Stem* | 19359.73 | 21576.90 | 18178.6 | 17421.4 | 14677.5 | 486.09 | 542.55 | 471.9 | 618.1 | 358.4 |
| *Hippocampus* | 3691.39 | 3953.50 | 3804.4 | 3198.2 | 3537.1 | 3712.72 | 3997.80 | 3588.1 | 3440.2 | 3416.3 |
| *Amygdala* | 1510.88 | 1641.46 | 1509.1 | 1258.2 | 1350.7 | 27.67 | 59.61 | 27 | 12.4 | 23 |
| *CSF* | 1070.99 | 1297.06 | 1220.3 | 877 | 1203.1 | 616.06 | 764.26 | 1094.7 | 705.6 | 546.4 |
| *Accumbens area* | 442.03 | 494.35 | 368.2 | 560 | 329.5 | 11377.98 | 16679.49 | 11569.5 | 9590.3 | 11230.3 |
| *Ventral diencephalon* | 3788.57 | 4110.59 | 3698.3 | 3256.5 | 3494.7 | 381.74 | 643.75 | 731.4 | 704.3 | 729.2 |
| *Vessel* | 31.27 | 56.44 | 64.5 | 21.2 | 63.3 | 13176.07 | 14803.59 | 11664.5 | 10256.3 | 17328.8 |
| *Choroid plexus* | 612.81 | 819.83 | 944.9 | 879.4 | 717.4 | 50137.29 | 54527.66 | 51322.2 | 49109.8 | 39360.1 |
| *Optic chiasm* | 183.10 | 211.88 | 152.8 | 194.8 | 181.5 | | | | | |
| *Cortex vol* | 452050 | 487387 | 416251 | 448395 | 434204 | | | | | |
| *Subcortical grey matter* | 52746 | 56587 | 49187 | 46023 | 48407 | | | | | |

## Appendix 7: Regression model values for each cognitive task for analysis in Chapter 5

**Models are presented by cognitive task category (either unimpaired, impaired or shift). Red text indicates predictors which were significant in hierarchical regression models for respective groups. Values in bold text are those predictors which showed significant z-comparisons (i.e. they were unique predictors in that group). Values in black are corresponding regression outcomes for predictors within the other group as a comparison. *=p<.05, **=p<.001**

**Unimpaired cognitive performance**

| *Visual acuity* | *Young* | | | | | | *Old* | | | | | |
|---|---|---|---|---|---|---|---|---|---|---|---|---|
| **Modality** | Predictor | **$R^2$** | **Adj $R^2$** | **Beta** | **Sig** | **Z test (group)** | Predictor | **$R^2$** | **Adj $R^2$** | **Beta** | **Sig** | **Z test (group)** |
| Tractography | | .112 | .035 | -.076 | .706 | | **L1 in optic radiation** | **.633** | **.572** | **.463** | **.003** | **Z=1.36, p=.017** |
| Metabolites | | .121 | .001 | .095 | .641 | | **Choline in ACC** | **.426** | **.382** | **.739** | **.001** | **Z=1.68, p=.009** |

| *Contour threshold* | *Young* | | | | | | *Old* | | | | | |
|---|---|---|---|---|---|---|---|---|---|---|---|---|
| **Modality** | **Predictor** | **$R^2$** | **Adj $R^2$** | **Beta** | **Sig** | **Z test (group)** | **Predictor** | **$R^2$** | **Adj $R^2$** | **Beta** | **Sig** | **Z test (group)** |
| Tractography | **FA in ILF (right)** | **.225** | **.186** | **-.474** | **<.001** | **Z=1.88, p=0.04** | | .0004 | -0.019 | .001 | 0.88 | |
| | | 0.002 | -0.017 | 1.31 | 0.752 | | RD in SLF 2 (right) | .296 | .249 | .925 | <.001 | Z=0.13, p=0.9 |
| Metabolites | - | - | - | - | - | | **Glx in PPC** | **.292** | **.422** | **-.575** | **.001** | **Z=1.54, p=.005** |
| | | | | | | | GABA in OCC | .654 | .575 | -.391 | .004 | Z=1.87, p=.012 |

| *ANT alerting* | *Young* | | | | | | *Old* | | | | | |
|---|---|---|---|---|---|---|---|---|---|---|---|---|
| **Modality** | **Predictor** | **$R^2$** | **Adj $R^2$** | **Beta** | **Sig** | **Z test (group)** | **Predictor** | **$R^2$** | **Adj $R^2$** | **Beta** | **Sig** | **Z test (group)** |
| *Tractography* | **RD in optic radiation (left)** | **.230** | **.191** | **.480** | **.002** | **Z=2.17, p=.01** | | .028 | -.021 | -.167 | .458 | |
| *Metabolites* | **-** | **-** | **-** | **-** | **-** | **-** | | - | - | - | .- | |

| *ANT orienting* | *Young* | | | | | | *Old* | | | | | |
|---|---|---|---|---|---|---|---|---|---|---|---|---|
| **Modality** | **Predictor** | **$R^2$** | **Adj $R^2$** | **Beta** | **Sig** | **Z test (group)** | **Predictor** | **$R^2$** | **Adj $R^2$** | **Beta** | **Sig** | **Z test (group)** |
| *Tractography* | **L1 in optic radiation (left)** | **.274** | **.237** | **-.626** | **<.001** | **Z=1.9,p=.018** | | .129 | .092 | -.359 | .072 | |
| *Metabolites* | | .029 | -.013 | .171 | .413 | | **Glx in OCC** | **.412** | **.372** | **-.642** | **.005** | **Z=2.75, p<.001**** |

| *ANT executive* | *Young* | | | | | | *Old* | | | | | |
|---|---|---|---|---|---|---|---|---|---|---|---|---|
| **Modality** | **Predictor** | **$R^2$** | **Adj $R^2$** | **Beta** | **Sig** | **Z test (group)** | **Predictor** | **$R^2$** | **Adj $R^2$** | **Beta** | **Sig** | **Z test (group)** |
| Tractography | **MD ILF (right)** | **.202** | **.162** | **.643** | **.002** | **Z=1.24, p=0.02** | | .003 | -.045 | .054 | .808 | |
| | **L1 in optic radiation (right)** | **.446** | **.388** | **-.530** | **.009** | **Z=1.88, p=.03** | | | | | | |
| | | .008 | -.034 | -.088 | .669 | | **FR in SLF2 (right)** | **.810** | **.782** | **-.419** | **.004** | **Z=1.81, p=0.03** |
| Metabolites | - | - | - | - | - | - | | - | - | - | - | |

## Shift in Performance

| *Embedded figures SAT* | *Young* | | | | | | *Old* | | | | | |
|---|---|---|---|---|---|---|---|---|---|---|---|---|
| **Modality** | **Predictor** | **$R^2$** | **Adj $R^2$** | **Beta** | **Sig** | **Z test (group)** | **Predictor** | **$R^2$** | **Adj $R^2$** | **Beta** | **Sig** | **Z test (group)** |
| Tractography | **FA optic radiation (left)** | **.367** | **.337** | **-.606** | **.002** | **Z=-2.106, p=.018** | | .042 | -.018 | -.206 | .413 | |
| | | **.003** | **-.038** | **.056** | **.785** | | FR in SLF 1 (left) | .199 | .157 | .446 | .003 | |
| Metabolites | | - | - | - | - | - | - | - | - | - | - | - |

| *Rotation SAT* | *Young* | | | | | | *Old* | | | | | |
|---|---|---|---|---|---|---|---|---|---|---|---|---|
| **Modality** | **Predictor** | **$R^2$** | **Adj $R^2$** | **Beta** | **Sig** | **Z test (group)** | **Predictor** | **$R^2$** | **Adj $R^2$** | **Beta** | **Sig** | **Z test (group)** |
| Tractography | **L1 in optic radiation (left)** | **.028** | **-.013** | **.166** | **.417** | | | .039 | -.007 | .197 | .368 | |
| | **FR in SLF 2 (left)** | **.491** | **.465** | **-.244** | **.004** | | | .194 | .159 | -.441 | .028 | |
| | | .036 | -.003 | .189 | .346 | | L1 in SLF 1 (right) | .206 | -.164 | -.478 | .003 | |
| | | .072 | .034 | .268 | .177 | | FA in optic radiation (right) | .391 | .323 | -.883 | <.001 | |
| | | .008 | -.031 | .091 | .653 | | FR in SLF 3 (right) | .668 | .609 | .695 | .002 | |
| Metabolites | | .041 | .003 | .203 | .310 | | **NAA in ACC** | **.364** | **.330** | **.603** | **.004** | **Z=1.67, p=.046** |
| | | .036 | -.002 | .190 | .343 | | Choline in ACC | .806 | .785 | -.859 | <.001 | Z=0.87, p=.19 |

| *Change blindness SAT* | *Young* | | | | | | *Old* | | | | | |
|---|---|---|---|---|---|---|---|---|---|---|---|---|
| **Modality** | **Predictor** | **$R^2$** | **Adj $R^2$** | **Beta** | **Sig** | **Z test (group)** | **Predictor** | **$R^2$** | **Adj $R^2$** | **Beta** | **Sig** | **Z test (group)** |
| Tractography | **FA in optic radiation (left)** | **.299** | **.265** | **-.547** | **.007** | **Z=1.826, p=.034** | - | .000 | -.045 | -.002 | .994 | |
| Metabolites | NAA in OCC | .193 | .160 | -.440 | .025 | Z=1.269, p=.102 | | | | | | |
| | | .110 | .075 | .331 | .085 | | **GABA in ACC** | **.284** | **-.246** | **-.533** | **.002** | **Z=2.91, p=.002** |

| *Contour SAT* | *Young* | | | | | | *Old* | | | | | |
|---|---|---|---|---|---|---|---|---|---|---|---|---|
| **Modality** | **Predictor** | **$R^2$** | **Adj $R^2$** | **Beta** | **Sig** | **Z test (group)** | **Predictor** | **$R^2$** | **Adj $R^2$** | **Beta** | **Sig** | **Z test (group)** |

| | | | | | | | | | | | | |
|---|---|---|---|---|---|---|---|---|---|---|---|---|
| Tractography | **MD in fornix** | **.267** | **.230** | **-.517** | **.009** | **Z=-2.44, p=.007** | | .112 | -.037 | .132 | .578 | |
| | **FR in optic radiation (right)** | **.224** | **.185** | **.473** | **.002** | **Z=1.77, p=.04** | | .422 | .361 | .396 | .036 | |
| | **FA in SLF1 (right)** | **.881** | **.830** | **-1.24** | **.003** | **Z=1.87, p=.032** | | .314 | .103 | .286 | .264 | |
| | | .026 | -.021 | .161 | .464 | | **GABA in PPC** | **.253** | **.204** | **-.503** | **.009** | **Z=2.40, p=.008** |

## Impaired performance

| *Visual contrast* | *Young* | | | | | | *Old* | | | | | |
|---|---|---|---|---|---|---|---|---|---|---|---|---|
| **Modality** | **Predictor** | **$R^2$** | **Adj $R^2$** | **Beta** | **Sig** | **Z test (group)** | **Predictor** | **$R^2$** | **Adj $R^2$** | **Beta** | **Sig** | **Z test (group)** |
| Tractography | | .028 | -.013 | .166 | .417 | | **FA in optic radiation (right)** | **.557** | **.509** | **.509** | **.001** | **Z=2.49, p=.01*** |
| Metabolites | | - | - | - | - | | **-** | **-** | **-** | **-** | **-** | |

| *Visual orientation* | *Young* | | | | | | *Old* | | | | | |
|---|---|---|---|---|---|---|---|---|---|---|---|---|
| **Modality** | **Predictor** | **$R^2$** | **Adj $R^2$** | **Beta** | **Sig** | **Z test (group)** | **Predictor** | **R2** | **Adj $R^2$** | **Beta** | **Sig** | **Z test (group)** |
| Tractography | **FR in SLF1 (right)** | **.261** | **.225** | **-.510** | **.013*** | **Z=2.1, p=0.02** | | .277 | .229 | -.547 | .011 | Z=1.14, p=.13 |
| | | .034 | -.046 | -.124 | .555 | | **FA in SLF 2 (right)** | **.916** | **.890** | **-.641** | **<.001** | **Z=1.10, p=.03** |
| | | .094 | .018 | .290 | .155 | | RD in optic radiation (left) | .778 | .738 | .303 | <.001 | Z=0.09, p=.47 |
| Metabolites | **Glx in ACC** | **.442** | **.383** | **.661** | **<.001** | **Z=1.8, p=.03** | | **.552** | **.515** | **.417** | **.03** | |
| | **GABA in PPC** | **.629** | **.567** | **.204** | **.009** | **Z=1.5, p=.04** | | **.343** | **.266** | **.396** | **.060** | |

| *Motion threshold* | *Young* | | | | | | *Old* | | | | | |
|---|---|---|---|---|---|---|---|---|---|---|---|---|
| **Modality** | **Predictor** | **$R^2$** | **Adj $R^2$** | **Beta** | **Sig** | **Z test (group)** | **Predictor** | **$R^2$** | **Adj $R^2$** | **Beta** | **Sig** | **Z test (group)** |
| *Tratography* | | | | | | | L1 in optic radiation (right) | .415 | .342 | .436 | .037* | Z=0.63, p=0.26 |
| *Metabolites* | - | - | - | - | - | - | **GABA in OCC** | **.344** | **.294** | **.777** | **<.001** | **Z=1.85, p=0.03*** |